MASARYK UNIVERSITY

FACULTY OF MEDICINE

DEPARTMENT OF PATHOLOGICAL PHYSIOLOGY

NEW INSIGHTS INTO THE PATHOGENESIS OF PROSTATE CANCER

Habilitation thesis

Brno 2017

RNDr. Michal Masařík, Ph.D.

Acknowledgment

My deepest gratitude and thanks belong to my amazing team for their help, hard work, enormous support and humanity.

I would like to thank all of my past supervisors and mentors who contributed to my scientific education. In particular, I thank Prof. Stanislav Pavelka, Prof. Emil Paleček and Prof. René Kizek, who supervised me during my undergraduate and graduate studies.

Additionally, I would like to thank all of the colleagues and collaborators I had the pleasure to work with for their creativity, excellent work, and inspiring discussions. I would like to thank prof. Anna Vašků and prof. Petr Babula for their support.

My greatest thanks belong to Monika, Magdalénka, Markétka, my parents and sisters for all their help, support and inspiration in my personal and scientific life.

Special thanks belong to my Angels, without whom I would not be where I am…..

א דִּבְרֵי קֹהֶלֶת בֶּן-דָּוִד, מֶלֶךְ בִּירוּשָׁלָם.

ב הֲבֵל הֲבָלִים אָמַר קֹהֶלֶת, הֲבֵל הֲבָלִים הַכֹּל הָבֶל.

ג מַה-יִּתְרוֹן, לָאָדָם: בְּכָל-עֲמָלוֹ--שֶׁיַּעֲמֹל, תַּחַת הַשָּׁמֶשׁ.

יח כִּי בְּרֹב חָכְמָה, רָב-כָּעַס; וְיוֹסִיף דַּעַת, יוֹסִיף מַכְאוֹב.

Book of Ecclesiastes, 1; 1-3,18

Table of contents

Preface

This habilitation work is a compilation of selected scientific publications to which I have contributed as the first author, corresponding author or a co-author in the course of my independent scientific career. These articles were published between 2011 and 2017. All of these publications have a common theme related to prostate cancer. In particular, this habilitation summarizes new findings in the field of biochemistry and pathogenesis of prostate cancer. It has been divided into four parts depending on their specific focus. The first part is devoted to the issue of the zinc ions and their relation to prostate cancer development and progression. Part two deals with the amino acid metabolism in prostate cancer. Part three is dedicated to monitoring of the redox status of the prostate tumour cells and the last part is focused on the newly investigated prostate cancer markers and their determination. The accompanying text highlights my contribution to the field of prostate cancer and also contains a brief introduction to the topic. Comprehensive information on the individual topics can be found in the enclosed original publications.

1 Introduction

Prostate cancers are one of the most frequently occurring malign solid tumours in the Czech Republic and globally as well. The adenocarcinoma arising from epithelial prostate acini cells is the most common histological type of prostate cancer. In the text below, the prostate adenocarcinoma will be understood under the general abbreviation CaP. The adenocarcinoma is usually generated in the peripheral part of the prostate gland (**Fig. 1**) and therefore, at the initial stage, the patient may not have any observable difficulties. Ductal adenocarcinoma, mucinous adenocarcinoma, transitional cell carcinoma, small cell carcinoma, prostate squamous cell carcinoma and a highly malignant sarcomatoid carcinoma occur only rarely [1, 2].

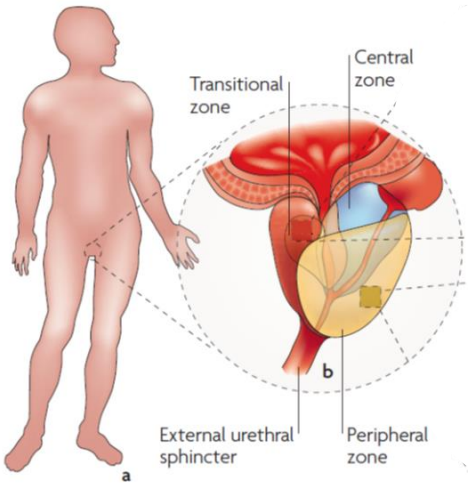

Figure 1 | Anatomy of prostate gland. a) Both benign prostatic hyperplasia (BPH) and prostate cancer are age-related diseases in the male, predominantly occurring later in life. b) The human prostate contains several different tissue zones (recognized by their pathology). BPH typically arises within the transitional zone, whereas prostate cancer predominantly occurs in the peripheral zone [1].

Variability in growth rate is an important characteristic feature of the prostate carcinoma. One part of the prostate adenocarcinomas have a low metastatic potential and slow growth, and therefore they are often revealed only during the autopsy of the persons deceased for the reason other than CaP or during surgical interventions [3, 4]. In the patients, whose tumours are of low

grade and progressive increase in plasma levels of prostate-specific antigen biomarkers does not occur (a latent form of the disease), radical therapy is often not applied, and the active surveillance is chosen instead [5]. In case of progressing tumours or higher-grade tumours, surgical approach or radiotherapy is chosen. Chemotherapy is not a standard treatment for early CaP but is sometimes used when CaP spreads out of the prostate gland and the hormonal therapy does not work [6]. Though the localized CaP is potentially curable (by applying surgery and radiotherapy), metastases or resistance to treatment and progression of the tumour disease develop in about 20% of patients. If prostate carcinoma cells metastasize, the disease can hardly be managed therapeutically and palliation is the only way in many cases. Skeleton is the most frequent site of CaP distant metastases. Metastases, however, often occur also in lungs and liver [7].

In 1941 Charles Huggins revealed benefit of the systemic androgen deprivation therapy (ADT) in the patients with advanced CaP [8]. This finding has led to the application of the androgen deprivation therapy and androgen receptor blockade (AR) as the therapeutic strategy for metastasizing prostate carcinomas. ADT is performed by surgical castration or chemical castration by anti-androgens [9]. Under normal circumstances, survival of healthy prostate tissue and prostate carcinoma cells is dependent directly on stimulation of the androgen receptor (AR), which dihydrotestosterone (DHT) or testosterone is bound to, thus activating the appropriate cellular processes such as proliferation, anti-apoptotic signals, and prostate-specific antigen (PSA) synthesis (**Fig. 2)**. The patients initially respond favourably to androgen deprivation, however, remission of the disease followed by growth of an androgen-independent tumour is often seen [10]. This stage of the disease is referred to as the hormone-refractory prostate cancer (HRPC) or also as the castration-resistant prostate cancer (CRPC). The interval from onset of the hormonal therapy up to the development of HRPC varies considerably in individual cases and ranges from several months to several years, 18–24 months on average. Prognosis of patients, where a tumour passes to the hormone refractory stage, is unfavourable. The androgen-independent proliferation can run in several ways; receptor hypersensitivity, non-androgen ligand bond, or activation of alternative signal pathways is employed [2].

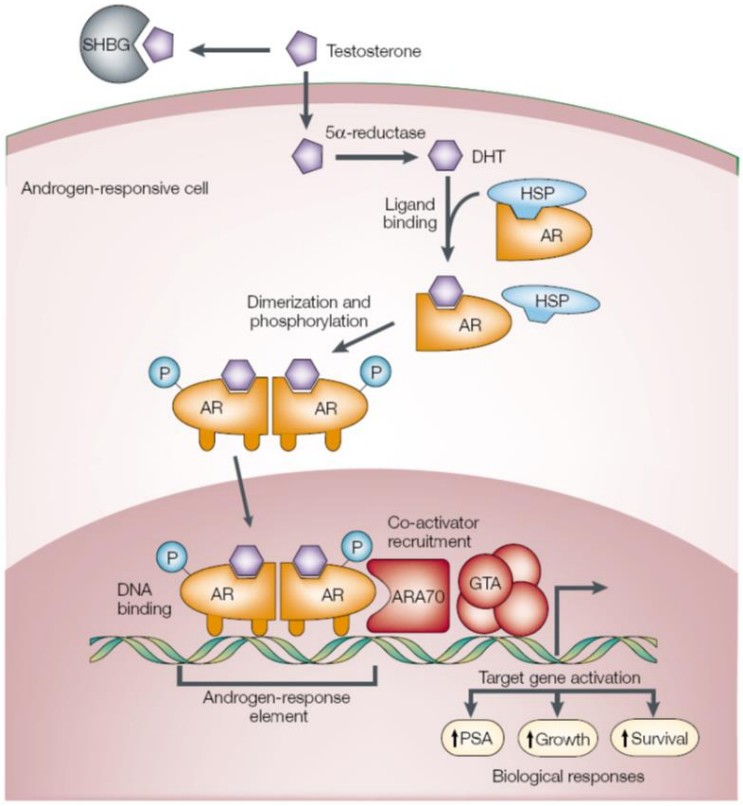

Figure 2 | Androgen action. Testosterone circulates in the blood bound to albumin (not shown) and sex-hormone-binding globulin (SHBG), and exchanges with free testosterone. Free testosterone enters prostate cells and is converted to dihydrotestosterone (DHT) by the enzyme 5α-reductase. Binding of DHT to the androgen receptor (AR) induces dissociation from heat-shock proteins (HSPs) and receptor phosphorylation. The AR dimerizes and can bind to androgen-response elements in the promoter regions of target genes. Activation (or repression) of target genes leads to biological responses including growth, survival and the production of prostate-specific antigen (PSA) [10].

During the last two decades, the number of patients suspected of having CaP has increased significantly. This increase is related directly to the introduction of the prostate-specific antigen (PSA) examination into clinical practice [11, 12]. The prostate-specific antigen (PSA) is a glycoprotein produced exclusively by epithelial prostate tissues. A small PSA fraction enters the bloodstream and can be detected from the blood sample and serve as a biomarker. This marker allowed to identify the presence of tumours that were undetectable by *per rectum* examination. Though the CaP diagnosis has thus been facilitated, the mortality rate declined slightly until 1993 only. After that year, the mortality rate of the CaP patients was no more reduced significantly [13]. The values ranging from 0 to 2.5 ng/ml are considered mostly the normal PSA level. PSA levels in the men suffering from the prostate carcinoma are often relatively high. However, PSA as a marker is neither sensitive nor specific adequately. In 2004 Thompson et al. have proved that CaP may also occur in the patients having low PSA levels. The share of these cases was up to 27% [14]. The high presence of obese men in the monitored group could be the reason.

Obese men usually have decreased PSA levels, though their CaP risk is increased [15]. On the other hand, a lot of men with the PSA level higher than 2.5 ng/ml do not suffer from the prostate carcinoma. The most common process leading to increased PSA value is the benign prostatic hyperplasia, (a common noncancerous prostate enlargement often accompanied by urination problems). Other reasons of elevated PSA levels in the blood can be as follows: prostate inflammation and/or various prostate examination procedures. With respect to the reported disadvantages of PSA, which is the only widely used clinical marker, it is of the great importance to focus on prostate physiology and pathophysiology to find new or complementary markers.

This habilitation work summarizes new findings in the field of biochemistry and pathogenesis of prostate cancer obtained during my CaP research. It has been divided into four parts depending on their specific focus. The first part is devoted to the issue of the zinc ions and their relation to CaP development and progression. Part two deals with the amino acid metabolism in CaP. Part three is dedicated to monitoring of the redox status of the prostate tumour cells and the last part is focused on the newly investigated CaP markers and their detection. It is a set of commented publications.

1.1 Models used in experiments

To investigate the mechanisms playing a role in CaP pathogenesis, biological samples of the CaP patients and four model human prostate cell lines were used. The PNT1A cell line has been derived from normal epithelial prostate cells immortalized with a plasmid containing the SV40 virus genome with a defective origin of replication. The primary culture was obtained from the normal prostate tissue of a 35-year-old man post-mortem. PNT1A is a non-tumour epithelial cell line positive for the tumour suppressor PTEN expressing the common (wild-type; wt) p53 [16]. The 22Rv1 cell line was used as the primary androgen-responsive carcinoma model. It is a human epithelial line derived from the xenograft during serial propagation in mice. The 22Rv1 cell line represents the primary prostatic badly differentiated adenocarcinoma, Gleason score of 9 [17]. The 22Rv1 line shows a significantly lower degree of gene variability and a lower degree of aneuploidy - karyotype 50 XY (trisomy 7,8,12) - DNA index of 1.30 (PC-3 1.84 and LNCaP 2.09), compared with all other lines [18]. The 22Rv1 line expresses the prostate-specific antigen (PSA); its growth is stimulated moderately by testosterone, and lysates of these cells are immunoreactive to antibodies against the androgen receptor (AR). 22Rv1 is PTEN and p53 positive

[19, 20]. The androgen-responsive metastatic cell line is represented by the LNCaP cell line derived from a 50-year-old man's infraclavicular node. LNCaP cells have a mutation in the AR gene. This mutation creates a promiscuous AR that can be bound to different types of steroids. LNCaP is AR-positive, PSA-positive, PTEN negative and express the wild-type p53 [20, 21]. The PC-3 metastatic line derived from grade 4 adenocarcinoma metastasizing to bones was used as a model of aggressive androgen-nonresponsive CaP. The PC-3 line is PTEN-, AR-, PSA and p53-negative [19, 21, 22]. All cell lines used in this study were obtained from HPA Culture Collections (Salisbury, UK).

2 PART I: Zinc, metallothionein and prostate cancer progression

2.1 Theoretical basis

The theoretical basis of the Part I consist of the basic information about the studied topic and of a set of overview papers published by our group regarding this issue.

2.1.1 Zinc ions and their regulation

Zinc ions (Zn^{2+}) are the essential element necessary for proper cell functions. They have four major biological roles, including the structural, signalling, catalytic and regulatory functions [23]. Zn^{2+} are a co-factor of a number of proteins, this being essential for proper functioning of the transcription factors, enzymes and structural proteins. Zn^{2+} are involved in regulation of the immune system, gene expression, energy metabolism, signal transduction and a number of other processes [24].

Zinc concentration in the interstitial fluid ranges from 2–5 μM. However, the free Zn^{2+} level is significantly lower, approximately 200 nM [24]. Most of the zinc content is bound to albumin and α2 macroglobulin. Intracellular Zn^{2+} concentration ranges from 100–500 μM. Most of this content is bound firmly to protein structures (about 90%). Only 10% acts as a releasable reserve form of Zn^{2+}, which is bound to low molecular weight compounds - metallothionein, amino acids (cysteine, histidine, proline) and organic acids (citrate, oxalate) [25, 26]. About 30–40% of Zn^{2+} is present in the nucleus, about 50% in the cytoplasm and organelles (mitochondria, endoplasmic reticulum, Golgi's apparatus, endosomes and lysosomes), and the remaining part is bound to cell membranes [27]. Zinc is included in many types of physiological processes and therefore its levels must be regulated carefully. The high Zn^{2+} levels may have toxic effects [28]. The whole body level of regulation is based on affecting of intestinal absorption and secretion. The cellular zinc level regulation is based on the coordination of the zinc-binding and zinc-transporting proteins [29]. The metal-responsive-element-binding transcription factor-1 (MTF-1) is the key transcription regulator of both the transporters and the Zn^{2+} binding proteins [30].

Zinc is unable to diffuse freely across the membrane and must, therefore, utilize the transport system (**Fig. 3)** [31]. There are two known families of zinc transporters: the first family is represented by Zrt-Irt type proteins (the ZIP family) and the other family is represented by CDF (Cation Diffusion Facilitator) also called the ZnT family. The ZIP family transporters are responsible for the zinc transport to cytoplasm from extracellular space and also play a role in

zinc ions flow out of the cell organelles into the cytoplasm. Members of the ZnT transporter family have a reverse role, they affect export of zinc out of the cell and the translocation of zinc from the cytoplasm into the organelles, thus reducing the concentration of cytosolic zinc effectively [31].

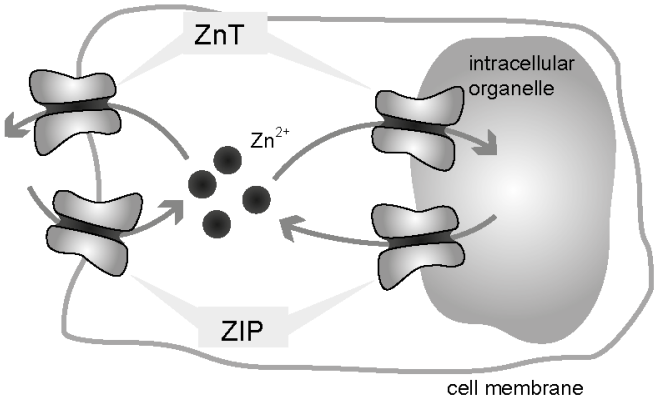

Figure 3 | ZIP carriers are responsible for transport of Zn2+ to the cytoplasm, out of the extracellular environment and out of the organelles. On the contrary, ZnT transporters are responsible for transport out of the cytoplasm, i.e. into the organelles or into the extracellular environment.

Important zinc-binding proteins include metallothioneins (MT). Metallothioneins represent a class of metal-binding polypeptides with high cysteine content (up to 30% of amino acid residues) and a low molecular weight (0.5 to 15 kDa). Up to seven divalent metal ions can be bound to the human MT, and this bond stabilizes the three dimensional MT structure [32]. MT plays an important detoxification role in defence against heavy metals. This protective function is related to the MT ability to capture free radicals. Therefore, MT is highly expressed under oxidative stress conditions [33], which is a common situation inside the tumour tissue. The relationship between the oxidative stress and MT is summarized in the overview paper [33], full text - see page 16 of the habilitation thesis.

Several all-genomic studies have shown that a cluster of MT genes located on chromosome 16 (16q12-22) is an important target in the search for candidate genes playing a role in carcinogenesis [34, 35]. MT functions also affect regulation of apoptosis, where elevated levels of metallothionein have the anti-apoptotic effect. Further, metallothioneins regulate the level, activity and cellular localization of the NF-κB transcription factor, which activates the anti-apoptotic Bcl-2, c-myc and TRAF-1 genes. This anti-apoptotic cascade can be used as a protective mechanism of prostate carcinoma cells against apoptotic signals [36, 37]. Polymorphisms

associated with the onset of the tumour disease have also been identified in genes for MT recently. Influence of polymorphisms in MT on the development of various pathologies, including prostate tumours, is summarized in the overview paper [38] available on page 39.

Author's publications relevant to this chapter

1. Ruttkay-Nedecky, B., L. Nejdl, et al. (2013). "The Role of Metallothionein in Oxidative Stress." International Journal of Molecular Sciences **14**(3): 6044-6066
Available on page 16

2. Raudenska, M., J. Gumulec, et al. (2014). "Metallothionein polymorphisms in pathological processes." Metallomics **6**(1): 55-68.
Available on page 39

Int. J. Mol. Sci. **2013**, *14*, 6044-6066; doi:10.3390/ijms14036044

OPEN ACCESS
International Journal of
Molecular Sciences
ISSN 1422-0067
www.mdpi.com/journal/ijms

Review

The Role of Metallothionein in Oxidative Stress

Branislav Ruttkay-Nedecky [1], Lukas Nejdl [2], Jaromir Gumulec [1,3], Ondrej Zitka [1,2], Michal Masarik [1,3], Tomas Eckschlager [4], Marie Stiborova [5], Vojtech Adam [1,2] and Rene Kizek [1,2,*]

[1] Central European Institute of Technology, Brno University of Technology, Technicka 3058/10, CZ-616 00 Brno, Czech Republic; E-Mails: brano.ruttkay@seznam.cz (B.R.-N.); lukasnejdl@gmail.com (L.N.); j.gumulec@gmail.com (J.G.); zitkao@seznam.cz (O.Z.); masarik@med.muni.cz (M.M.); vojtech.adam@mendelu.cz (V.A.)

[2] Department of Chemistry and Biochemistry, Faculty of Agronomy, Mendel University in Brno, Zemedelska 1, CZ-613 00 Brno, Czech Republic

[3] Department of Pathological Physiology, Faculty of Medicine, Masaryk University, Kamenice 5, CZ-612 00 Brno, Czech Republic

[4] Department of Paediatric Haematology and Oncology, 2nd Faculty of Medicine, Charles University and University Hospital Motol, V Uvalu 84, CZ-150 06 Prague 5, Czech Republic; E-Mail: tomas.eckschlager@fnmotol.cz

[5] Department of Biochemistry, Faculty of Science, Charles University, Albertov 2030, CZ-128 40 Prague 2, Czech Republic; E-Mail: stiborov@natur.cuni.cz

* Author to whom correspondence should be addressed; E-Mail: kizek@sci.muni.cz; Tel.: +420-5-4513-3350; Fax: +420-5-4521-2044.

Received: 14 January 2013; in revised form: 14 February 2013 / Accepted: 20 February 2013 / Published: 15 March 2013

Abstract: Free radicals are chemical particles containing one or more unpaired electrons, which may be part of the molecule. They cause the molecule to become highly reactive. The free radicals are also known to play a dual role in biological systems, as they can be either beneficial or harmful for living systems. It is clear that there are numerous mechanisms participating on the protection of a cell against free radicals. In this review, our attention is paid to metallothioneins (MTs) as small, cysteine-rich and heavy metal-binding proteins, which participate in an array of protective stress responses. The mechanism of the reaction of metallothioneins with oxidants and electrophilic compounds is discussed. Numerous reports indicate that MT protects cells from exposure to oxidants and electrophiles, which react readily with sulfhydryl groups. Moreover, MT plays a key

Int. J. Mol. Sci. **2013**, *14* **6045**

role in regulation of zinc levels and distribution in the intracellular space. The connections between zinc, MT and cancer are highlighted.

Keywords: metallothionein; free radicals; cellular oxidative stress; zinc; transcription factor; cancer

1. Introduction

Free radicals are chemical particles containing one or more unpaired electrons, which may be part of the molecule. They cause the molecule to become highly reactive [1]. Free radicals (a) can be generated during UV irradiation, X-ray or gamma radiation, (b) are the products of reactions catalyzed by metals, (c) are present in the air as pollutants, (d) are produced by neutrophils and macrophages during inflammation and (e) are by-products of the mitochondrial respiratory chain [2]. Free radicals are known to play a dual role in biological systems, because they can be considered as beneficial or deleterious [3]. The beneficial effects of free radicals are in the immune response to infection and that they are a part of many cellular signaling systems. In contrast, at high concentrations of free radicals, they may be important mediators of damage to cell structures, including lipids and membranes, proteins and nucleic acids, when oxidative stress occurs [4].

The harmful effects of free radicals are balanced by the antioxidant action of antioxidant enzymes and non-enzymatic antioxidants [5]. Despite the presence of the antioxidant defense system, which protects cells from oxidative damage originating from free radicals, oxidative damage accumulates during the lifecycle and, with radicals related damage of DNA, proteins and lipids, plays a key role in the development of diseases, such as cancer, atherosclerosis, arthritis and neurodegenerative diseases [6–8]. The most important free radicals in aerobic organisms are oxygen reactive species (ROS) [3] and nitrogen reactive species (RNS) [9]. An overview of the most important reactive oxygen and nitrogen reactive species is summarized in (Table 1). In this review, our attention is aimed at the mutual relations of metallothionein and zinc(II) ions.

Table 1. Summary of reactive oxygen and nitrogen species [10,11].

Reactive Oxygen Species				Reactive Nitrogen Species			
Free Radicals		**Other Substances**		**Free Radicals**		**Other Substances**	
Superoxide anion radical	$O_2^{\bullet-}$	Hydrogen peroxide	H_2O_2	Nitric oxide radical	NO•	Peroxynitrite	$ONOO^-$
Hydroxyl radical	HO•	Hypochlorous acid	HOCl	Nitric dioxide radical	NO_2•	Nitrites	NO_2^-
Alkoxyl radical	RO•	Ozone	O_3			Nitrates	NO_3^-
Peroxyl radical	ROO•	Singlet oxygen	$^1O_2$			Nitrosyl	NO^+

2. Metallothioneins

Metallothioneins (MTs) belong to the group of intracellular cysteine-rich, metal-binding proteins that have been found in bacteria, plants, invertebrates and vertebrates [12–14]. These proteins were discovered in 1957 as cadmium-binding proteins isolated from horse kidney [15]. Since their

Int. J. Mol. Sci. **2013**, *14* **6046**

discovery, these low molecular weight cysteine-rich proteins have been continuously studied in all aspects, including physical, chemical and biochemical properties. Mammalian MTs may contain 61–68 amino acids, and among them 20 are cysteines [16,17]. These unique proteins are involved in diverse intracellular functions [18], but their role in the detoxification of heavy metals and in the maintaining of essential metal ion homeostasis, which is due to their high affinity for these metals, is mostly investigated [19,20]. For mammals, MTs bind zinc [21], but with excess copper or cadmium, zinc can be easily replaced by these metals [22]. Cells that contain excessive amounts of MTs are resistant to cadmium toxicity [23], while cell lines that cannot synthesize MTs are sensitive to cadmium [24]. Genetic studies using transgenic or knockout mouse models are further evidence of the role of MTs in protection against cadmium toxicity [25,26]. Based on structural models, it can be assumed that the MT molecule is composed of two binding domains, α and β, which are composed of cysteine clusters. Covalent binding of metal atoms involves sulfhydryl cysteine residues (Figure 1). The *N*-terminal part of the peptide is designated as β-domain and has three binding sites for divalent ions, and the C-terminal part (the α-domain) has the ability to bind four divalent metal ions.

Figure 1. Metallothionein (MT) structure. Model of two binding sites of metallothionein. Red big beads are metal atoms (e.g., Zn), and small yellow beads are sulfur atoms. Adopted and modified according to [27].

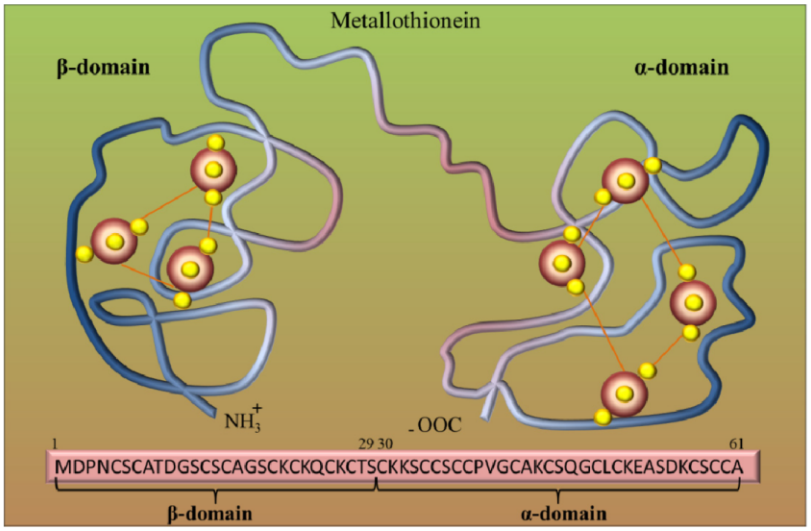

Four mammalian MT isoforms (MT-1–MT-4) and 13 MT-like human proteins were identified [28]. The differences of constituent forms come mainly from post-translational modifications, small changes in primary structure, type of incorporated metal ion and speed of degradation. Despite the physical-chemical similarity of the forms, their roles and occurrence in tissues vary significantly [29]. MT-1 and MT-2 are present almost in all types of soft tissues [30–32], MT-3 is expressed mostly in brain tissue, but also in heart, kidneys and reproductive organs [33,34] and the MT-4 gene was detected in stratified squamous epithelial cells associated with oral epithelia, esophagus, upper stomach, tail, footpads and neonatal skin. [35]. In humans, the MT genes are located on chromosome 16 in a cluster and involve 16 identified genes, from which five are pseudogenes [36]. Although the MT-II, MT-III and MT-IV proteins are encoded by a single gene, the MT-I protein comprises many

Int. J. Mol. Sci. **2013**, *14* **6047**

subtypes encoded by a set of 13 MT-I genes. The known active MT-I genes are MT-IA,-IB, -IE, -1F, -IG, -IH,-IM and -IX. The rest of the MT-I genes (MT-1C,-1D,-1I,-1J and 1L) are pseudogenes that are not expressed in humans [36].

3. Zinc as Signaling Compound and Antioxidant

Given that a number of MT functions are due to its close interaction with zinc ions, it is appropriate to mention zinc and metallothionein roles for easier comprehension separately. However, it should be noted that a separate description is too "textbook-styled", while *in vivo* systems operate both systems simultaneously. The role of zinc has been extensively studied in recent years, and thus, the insight into this issue distinctly has changed during the last decade. Originally, the mere perception of zinc(II) as a structural component and an integral component of cytoskeletal structures significantly expanded, and these ions are considered as an important signaling component necessary for the physiological function of all cells [37–40]. These include influence on redox state, enzyme activity, gene transcription, energetic metabolism, cell cycle, cell migration and invasivity, apoptosis and proliferation [41–45]. Not surprisingly, disbalance in the levels of zinc, and thereby causing interference in these systems, has important consequences, including the development of cancers and other diseases [46]. The importance of zinc(II) might be illustrated by the consequences of the near-complete chelation of cellular zinc content. A potent zinc(II) chelator, TPEN (*N*,*N*,*N*',*N*'-tetrakis[2-pyridylmethyl]ethylenediamine), for instance, induces cell death [47,48]. In contrast, cell death may be prevented by zinc(II) treatment and, thus, restore these unphysiological levels [46].

Due to the fact that zinc can't freely pass through the membranes, the crucial role in the maintenance of intracellular zinc level is provided by zinc-transporting proteins, ZIPs (Zrt-Irt-like protein or Zinc Iron permease) and ZnTs (Zinc transporters) [49,50]. A concept of overall zinc signaling, either on the regulation of transcription or antioxidant acting, can be generalized to a scheme, where various stimuli (cell stress) lead to the increase in ROS/RNS and other oxidants, which subsequently release zinc(II) from a pool (usually MT), and this free zinc(II) fraction influences the target structures. In addition, a direct interaction between MT and apo-zinc binding peptides during the process of zinc transfer has been demonstrated in a cell-free system [51].

With regard to energetic metabolism, zinc(II) has inhibitory effects on the mitochondrial enzyme, aconitase, which catalyzes the conversion of citrate to isocitrate and, thus, enables the utilization of citrate in the Krebs cycle. This cascade is prostate-specific, and due to inhibition of this enzyme, prostate cells act as zinc-accumulating [52]. Also, the proapoptic effects of zinc are well-described. Zinc(II) facilitates the formation of BAX pores on the mitochondrial membrane and, thus, increases the BAX/Bcl-2 ratio. As a result, cytochrome c moves to the cytoplasm and triggers a caspase cascade, resulting in apoptosis [53,54]. Nevertheless, these aspects of zinc(II) are the subject of many comprehensive reviews [55–57], but the aim of this review lies in zinc's relation to oxidative stress.

Although zinc(II) itself has no redox capacity, it is considered a potent and important antioxidant agent [45]. Cellular zinc decrease was associated with an increase in oxidants and oxidation parameters in several studies [58–61]. Its antioxidant properties are due to both the direct and indirect interference with target structures. These include induction of metallothionein expression and glutathione synthesis,

regulation of oxidant production, association with cysteines (with concomitant release by other oxidants) and regulation of redox signaling.

Zinc(II) itself causes an increase in the major zinc-binding protein metallothionein. The induction of MT expression is induced through metal regulatory transcription factor 1 (MTF-1), a 753 amino acid transcription factor, which directly responds to increased levels of free zinc(II) [62]. Thus, MTF-1 binds the metal-responsive element of the *MT* gene and initiates MT transcription [63]. This autoregulatory loop maintains narrow optimal limits of intracellular zinc(II) and helps to reduce generated oxidative stress, as mentioned below.

In addition to zinc-metallothionein interactions widely discussed in this review, zinc(II) is an important regulator of glutathione (GSH) synthesis. The importance of zinc in the metabolism of glutathione underscores the finding that, as zinc deficiency is accompanied by oxidant increase, many studies reveal a deficiency of glutathione under such conditions [59,60]. Glutamate-cysteine ligase (GCL) was identified as a link in these conditions. GCL is a key regulatory enzyme in the synthesis of glutathione. It catalyzes a reaction of glutamate and cysteine to gamma-L-glutamyl-L-cysteine in glutathione and glutamate metabolism [64]. As shown on primary rat endothelial cells exposed to H_2O_2, zinc supplementation protects from peroxide-induced cell death via increasing the transcription of the GCLC and the concentrations of glutathione (GSH). Conversely, zinc depletion significantly decreased the expression of GCLC and the cellular GSH levels [65].

In addition, zinc deficiency was associated with indirect regulation of oxidant production. Although little is known, it was demonstrated that zinc(II) deficiency increased the level of NO and superoxide anion by the inhibition of the *N*-methyl-D-aspartate receptor (NMDAR) [45] As described on PC12 cells, NMDAR activation leads to an increase in cytoplasmic calcium levels and, thus, to increased ROS [66].

It is worth mentioning that zinc(II) is an integral part of up to 10% of all human proteins [67]. These proteins include zinc fingers, domains consisting mostly of cysteine and histidine able to interact with DNA specific bases [68]. The function of zinc fingers consists not only in DNA recognition and transcriptional activation, but also in RNA packaging, protein folding and apoptosis, whose regulation is important not only in development of tissues, but also in neoplastic transformation and proliferation [69,70]. For instance, zinc exchange between MT and zinc finger transcription factors [17,71,72] serves as a mechanism for the regulation of gene expression through activation or inhibition of DNA binding by estrogen receptors [73], SP1[71,74], TFIIIA [72,75], Gal4 [76] or tramtrack [77]. The above mentioned MTF-1-mediated MT expression is another *de facto* example of zinc finger transcriptional activity.

In addition to those "traditional" effects, Kröncke *et al.* attributed another function to zinc fingers; these structures act as redox-sensitive molecular switches. Similarly, as ROS or RNS cause the release of zinc(II) form metallothionein, it leads to a release of zinc(II) from these structures, causing not only a loss of zinc-finger function, but also an increase in cytoplasmic or nuclear free zinc(II) that may, in turn, stimulate and interfere with cellular signaling cascades [78].

4. Zinc and MT

The binding of zinc to MTs has proven to be a physiologically relevant. Several studies have produced strong evidence to support the idea that MTs function as zinc chaperones for the regulation

Int. J. Mol. Sci. **2013**, *14* **6049**

of gene expression and activity of proteins, such as metalloproteins and metal-dependent transcription factors, as shown in Figure 2 and discussed in the following papers [79,80]. The binding of zinc to MTs is thermodynamically stable, which makes MTs an ideal zinc reservoir *in vivo*. The question is how MTs make zinc available for other molecules, including transcription factors and metalloproteins.

Figure 2. Overview of metallothionein (MT) gene regulation and function. The MT promoter has many response elements that upregulate transcription. These include the following: (1) metal response elements (MRE), which are activated by the metal-responsive transcription factor (MTF-1) after zinc occupancy, which is a function of the dietary zinc supply; (2) glucocorticoid response elements (GRE); (3) elements activated by STAT (signal transducers and activators of transcription) proteins through cytokine signaling; and 4) the antioxidant (or electrophile) response element (ARE), activated in response to redox status. Methylation may downregulate expression in some tumor cells. Cellular zinc pools are influenced by dietary zinc intake and zinc transporter activity and serve as the source of zinc bound to MT. Zinc bound to MT exhibits high thermodynamic stability. Apo-MT (thionein) and Zn_7-MT (all coordination sites occupied) may serve to abstract or donate zinc, respectively, from/to zinc metalloproteins. Apo-MT is more rapidly degraded than Zn_7-MT. The numerous zinc coordination sites of proteins (including transcription factors, signaling molecules and adapter molecules that use zinc fingers for protein-protein interaction) provide the opportunity for the cellular MT level to influence key processes, including gene regulation, cell proliferation and differentiation, signal transduction and apoptosis, as well as influence oxidative damage caused by oxidative stress and electrophiles. Adopted and modified according to [18].

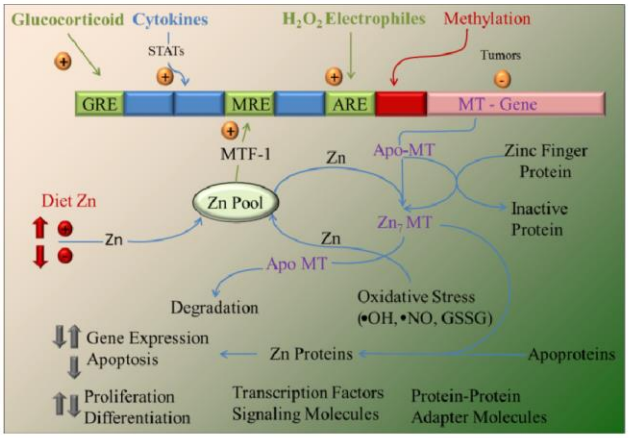

Maret *et al.* [76] showed that there is fast zinc exchange between MT isoforms 1 and 2 and also between MT2 and the zinc cluster in the Gal4 transcription factor [76]. Moreover, Jacob *et al.* found zinc transfer between MT and the apo-forms of zinc proteins *E. coli* alkaline phosphatase and bovine carboxypeptidase A [80]. Reduced glutathione (GSH) and glutathione disulfide (GSSG) are critical modulators of both the rate of zinc transfer and the ultimate number of zinc atoms transferred [79,81,82]. GSH inhibits zinc release in the absence of GSSG, indicating that MT is stabilized at relatively high cellular GSH concentrations. The presence of GSSG results in zinc release [81].

Under stress conditions, zinc release from MT occurs when the levels of nitric oxide or reactive oxygen species increase [83–86]. Treatment of lung fibroblasts with the NO donor, S-nitrosocysteine, resulted in an increase in intracellular labile zinc, as detected by a zinc-specific fluorophore, Zinquin, in wild-type, but not MT-null, fibroblasts [84]. Additional data obtained in sheep pulmonary artery endothelial cells suggested a role for the apo form of MT, thionein (T), as a Zn^{2+}-binding protein in intact cells [84]. Collectively, these data showed that MT mediates NO-induced changes in intracellular Zn(II). Furthermore, in another study, Pearce *et al.* have shown that, in cultured pulmonary artery endothelial cells, a MT-green fluorescent fusion protein (FRET-MT) undergoes conformational changes in the presence of NO [87]. These conformational changes are consistent with the release of metals from the thiolate clusters of MT [88–90].

5. The Role of MT in Cancer and Apoptosis

MT can be activated by a variety of stimuli, including metal ions, cytokines and growth factors [91–93], as shown in Figure 3. In a number of experiments, the synthesis of MT was shown to be increased by several-fold during oxidative stress [94,95] to protect the cells against cytotoxicity [96,97], radiation and DNA damage [98–100]. The stimuli that induce MT and the downstream effects of MT overexpression are summarized in Figure 3. A lot of studies have shown an increased expression of MT in various human tumors of the breast, colon, kidney, liver, lung, nasopharynx, ovary, prostate, salivary gland, testes, thyroid and urinary bladder [91]. MT expression in tumor tissues is mainly correlated with the proliferative capacity of tumor cells [101]. However, there are few exceptional cases, like downregulation of MT-I and -II in hepatocellular carcinoma [102] and also a reduced level of intracellular zinc, resulting in the increase of granulocytes, but a decreased number of lymphocytes [103]. Hence, the expression of MT is not universal to all human tumors, but may depend on the differentiation status and proliferative index of tumors, along with other tissue factors and gene mutations. Downregulation of MT synthesis in hepatic tumors may be related to hypermethylation of the MT-promoter or mutation of other genes, such as the p53 tumor suppressor gene. Mao *et al.* [104] identified a member of the MT family, termed *MT1M*, which is expressed in various normal tissues, with the highest level in the liver. However, *MT1M* expression markedly decreased in human hepatocellular carcinoma specimens. A methylation profiling analysis indicated that the MT1M promoter is methylated in the majority of hepatocellular carcinoma tumors examined. Moreover, restored expression of *MT1M* in the hepatocellular carcinoma cell line, Hep3B, which lacks endogenous *MT1M* expression, suppressed cell growth *in vitro* and *in vivo* and augmented apoptosis induced by tumor necrosis factor [104]. Similarly, Yan *et al.* [105] observed downregulation of *MT1F* by loss of heterozygosity in colon cancer tissue. Furthermore, exogenous *MT1F* expression increased colon cancer cell line (RKO) apoptosis and inhibited RKO cell migration, invasion and adhesion, as well as *in vivo* tumorigenicity. From this study, it could be concluded that *MT1F* is a putative tumor suppressor gene in colon carcinogenesis [105]. In another study, Faller *et al.* [106] observed DNA methylation in *MT1E* in malignant melanoma, which suggests that *MT1E* is also a potential tumor suppressor gene.

Int. J. Mol. Sci. **2013**, *14* **6051**

Figure 3. Schematic presentation of the stimuli that induce MT and the downstream effects of MT overexpression. MT can be activated by a variety of stimuli, including metal ions, cytokines, growth factors, oxidative stress and radiation. Downstream effects of MT overexpression are modulation of transcription of both tumor suppressor protein p53 and nuclear transcription factor NF-κB. Another downstream effect of MT overexpression is free radical scavenging activity. All these downstream MT effects influence cell survival, cell growth, drug resistance and differentiation. Adopted and modified according to [107].

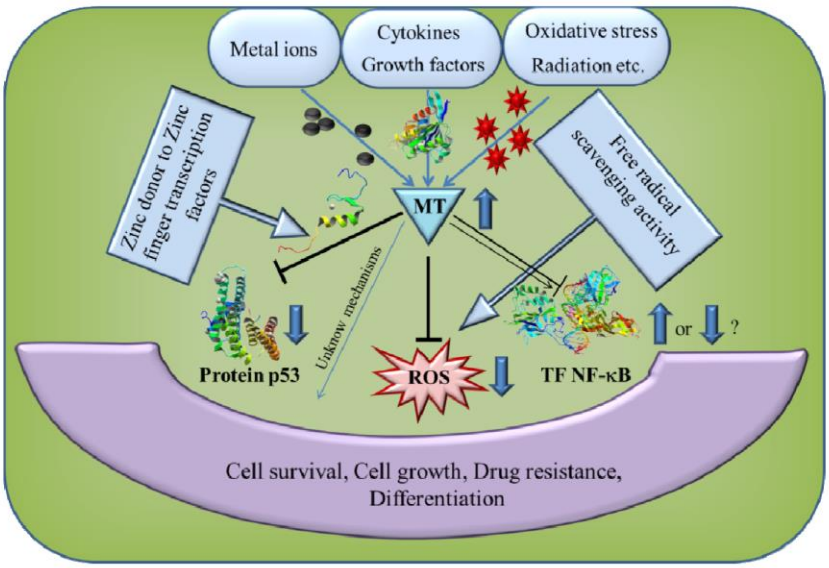

MTs can also help cancer cells to survive by inhibition of apoptosis [108,109]. Apoptosis, or programmed cell death, is a mechanism for the elimination of unnecessary or damaged cells [110]. This process involves the activation of cysteine proteases caspases and, subsequently, of nuclear endonucleases. These events later lead to nuclear DNA damage and to ceasing of all biosynthetic processes in the cell [111]. During apoptosis, in contrast to necrosis, the rupture and spillage of cell content, which would cause inflammation, does not occur, but cells undergo condensation, DNA fragmentation and disintegration of the cell into small parts that can be easily phagocytosed [112,113]. Deregulation of apoptosis is essential for pathogenic mechanisms in many diseases, such as neurodegenerative disorders, autoimmune disease and cancers [113–115].

MT plays two important roles in the regulation of apoptosis. The first role of MT is regulation of intracellular zinc concentration, and the second role is interaction of MT with some proteins involved in apoptosis. MT protects against apoptosis by distributing cellular Zn. Zinc is an intracellular mediator of apoptosis, which can interfere with the action of Ca^{2+}. Zinc addition prevents DNA fragmentation and inhibits many proteins connected to apoptosis, such as caspases and calcium-magnesium–dependent proteases [116]. Increased apoptosis *in vivo* may occur as a direct or indirect consequence of a decrease in intracellular Zn concentration [117,118]. Therefore, cellular Zn is described as an inhibitor of apoptosis, while its depletion induces death in many cell lines [119]. This Zn depletion activates caspases-3, -8 and -9, responsible for the proteolysis of several target proteins, like poly (ADP-ribose) polymerase or transcription factors [120]. Moreover, zinc is involved in structural stabilization and activation of the p53 that appears to be an important component of the

apoptotic process by inducing a transcription of the p53 gene, with increased expression of p53 mRNA and protein [121].

The tumor suppressor p53 protein is a metal-binding transcription factor, which binds DNA through a structurally complex domain stabilized by a zinc atom [122,123]. The nuclear accumulation of MT may be important for supplying zinc or other metals to target molecules, including enzymes, zinc-finger transcription factors and tumor suppressor gene products, such as p53 [31,73,122–125]. Meplan *et al.* [123] demonstrated that zinc incorporation is required for the stabilization of wild-type recombinant p53 in a form capable of binding specifically to DNA. They also showed that human recombinant thionein, the metal-free form of MT, reported to remove zinc from zinc finger transcription factors Sp1, thereby abrogating their transcriptional activity [74,75], inhibited binding of p53 to a specific consensus sequence *in vitro*. Supplementation of thionein with equimolar amounts of zinc prior to incubation with p53 abrogated this effect. Further, recombinant MT, a metal-chelator protein, was found to modulate p53 conformation *in vitro*. In cultured cells, overexpression of MT by transfection could modulate p53 transcriptional activity [123]. Analysis of human cancer patients also showed interesting correlations between p53 and MT gene expressions. In pancreatic serous cystadenomas, the increased expressions of MTs and p53 were observed in the less-differentiated tumors [126]. Similarly, in oral squamous cell carcinoma, frequent localization of MTs in nuclei was associated with the increased expression of the p53 gene [127].

One of the most important MT interactions with proteins involved in apoptosis is the regulation of NF-κB activity. Nuclear factor-κB (NF-κB) is a transcription factor that is involved in the regulation of cell death. Overexpression of NF-κB renders cancer cells resistant to chemotherapeutic agents [128,129], and it has been suggested that the antiapoptotic proteins IAP, IEX-1L and the Bcl-2 family are regulated by NF-κB transcription [130–132]. MT-1 and MT-2 regulate the level, activity and cellular location of the transcription factor, NF-κB [133–136]. In fact, MT interacts with the p50 subunit of NF-κB to increase the transactivation of NF-κB [135]. In another study, MT overexpression was found to upregulate NF-κB DNA binding [137]. Those interactions are important for the growth of some tumors, e.g., activation of NF-κB may mediate the antiapoptotic effect of MT.

6. Antioxidant Function of MT

The most critical advance in MTs research is the demonstration of the redox regulation of Zn-S interaction and the coupling of zinc and redox metabolism [88]. The cluster structure of Zn-MT provides a chemical basis by which the cysteine ligand can induce oxidoreductive properties [89]—what constitutes a MT redox cycle (Figure 4). The hypothesis that MT functions as an antioxidant against reactive oxygen and nitrogen species has received extensive experimental support from many *in vitro* studies. Studies using a cell-free system have demonstrated the ability of MT as a free radical scavenger [138–140]. Metallothionein has been shown to scavenge hydroxyl radicals *in vitro*, because of its cysteinyl thiolate groups [94] Thornalley and Vasak [138] showed that the rabbit liver metallothionein-1, which contains zinc and/or cadmium ions, appeared to scavenge free hydroxyl (•OH) and superoxide (O^{2-}•) radicals produced by the xanthine/xanthine oxidase reaction. All 20 cysteine sulfur atoms are involved in the radical quenching process, and the rate constant for the reaction of hydroxyl radical with MT is about 340-fold higher than that with GSH [138].

Int. J. Mol. Sci. **2013**, *14* **6053**

Figure 4. Metallothionein scavenging of reactive oxygen species. Presence of redox metals, such as Cu and Fe, in a cell can produce reactive oxygen species (ROS), leading to damaging of DNA and cell structures. The cell protects itself using various molecules as scavengers of the radicals. One of the most crucial cell pathways to scavenge the radicals is the glutathione redox complex. However, free –SH moieties of MT can be also involved in the scavenging of ROS in the MT redox cycle. Under physiologic conditions, zinc bound to MT is released through oxidation of the thiolate cluster when the environment becomes oxidized. Formation of MT-disulfide would be subjected to degradation; however, when the oxidized environment became reduced—through, for example, an increase in the glutathione (GSH)/glutathione disulfide (GSSG) ratio—MT disulfide is reduced to MT-thiol. This reduction process is greatly enhanced in the presence of selenium catalyst. In the presence of zinc, MT is quickly reconstituted. This process constitutes the MT redox cycle, which plays a crucial role in the biologic function of MT. Adopted and modified according to [141] and [93].

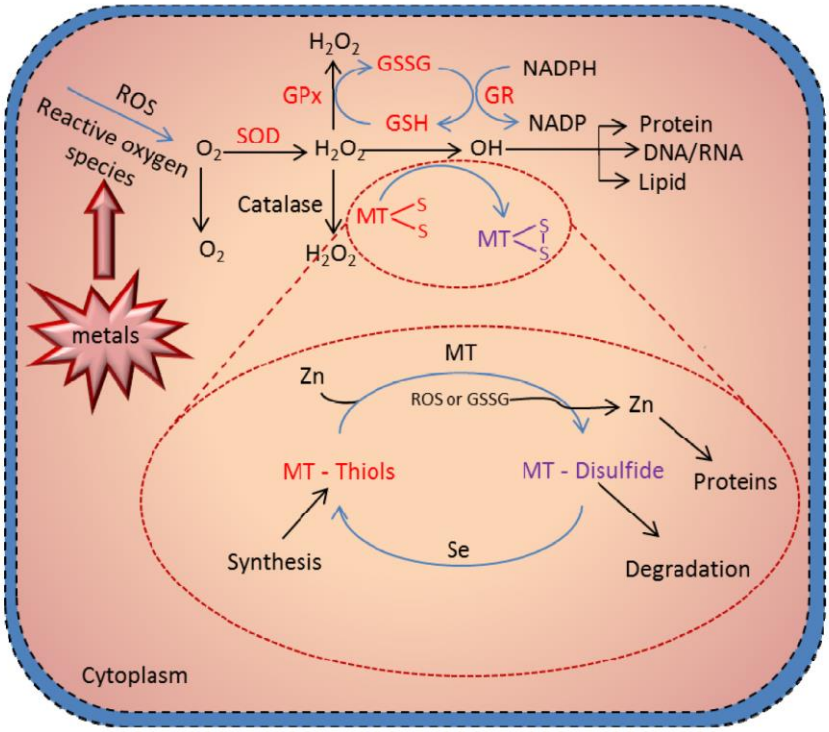

Studies using cultured cells and intact animal models have provided further evidence supporting the antioxidant function of MT [95,100,142–147]. Quesada *et al.* [148] examined the reaction of the sulfhydryl groups in metallothionein with hydrogen peroxide in human promyelocytic leukemia cells (HL-60). Zinc-metallothionein (Zn-MT) was induced by 24-h treatment of HL-60 cells with $ZnCl_2$.The ratio of H_2O_2 concentrations needed to reduce HL-60 cell survival by 50% in Zn-MT-induced cells compared to normal cells was 1.65 to 1. So, the Zn-MT-induced cells were more resistant to oxidative stress caused by hydrogen peroxide than normal cells. In the other paper Chubatsu *et al.* [149] investigated the role of MT in protection against oxidative damage to DNA on V79 Chinese hamster cells. An increase in MT content of V79 Chinese hamster cells was induced by zinc without

Int. J. Mol. Sci. **2013**, *14* **6054**

concomitant increase in the GSH level. These induced cells were more resistant to the production of DNA-strand scission by H_2O_2 than the parental cells. Conversely, cells rendered partially deprived of MT, by transfection with a plasmid vector in which the MT-I cDNA is antisense oriented in relation to a simian virus 40 promoter, became more susceptible to the DNA-damaging action of H_2O_2 [149]. In another study, Schwarz *et al.* [142] examined the sensitivity of NIH 3T3 cells transfected with a plasmid containing mouse metallothionein-I gene (NIH3T3/MT) to the membrane permeant oxidant, tert-butyl hydroperoxide. NIH3T3/MT cells had a four-fold increase in intracellular metallothionein, as compared to cells transfected with a plasmid containing an inverted gene (NIH3T3/TM). NIH3T3/MT cells were six-times more resistant than NIH3T3/TM cells to the cytotoxic effects of tert-butyl hydroperoxide. Furthermore, homogenates of NIH3T3/MT cells were more capable of scavenging *in vitro*-generated phenoxyl radicals, as quantified by electron spin resonance detection.

MT is primarily localized in the cytoplasm [150]. The highest cytoplasmic concentration of MT was found in the late G1 and G1/S cell cycle phase [151]. Depending on the cell cycle phase, cell differentiation or in the case of toxicity, MT-1 and MT-2 are rapidly translocated to the nucleus, as seen in oxidative stress and during the early S-phase [151–153]. It has been reported that hydrogen peroxide induces the nuclear localization of MT in culturing BALB 3T3 cells, depending on the cell cycle [154,155]. Karyophilic MT induced by H_2O_2 treatment was suggested to play the role of nuclear antioxidant [156]. Moreover, Ogra *et al.* [157] reported that nitric oxide enhances the nuclear localization of MT in digitonin-permeabilized semi-intact HeLa cells. The results suggest that MT can scavenge NO using the sulfhydryl groups of cysteines in its molecule to form nitrosothiol, thereby reducing nuclear and cytoplasmic damage by NO. In the next study, Du *et al.* [143] examined the role of reactive oxygen metabolites and the protective effect of zinc-induced MT synthesis on gentamicin nephrotoxicity in rats, both *in vivo* and *in vitro*. In the *in vivo* study, MT content of the renal cortex of the zinc preinjected rats was significantly increased, and proximal tubular necrosis and acute renal failure caused by injection of gentamicin were ameliorated. In suspended proximal tubules (PT), Na^+-K^+-ATPase activity and DNA synthesis were suppressed by the addition of gentamicin, but in zinc-pretreated rats' PT, these were not suppressed by the addition of gentamicin. In addition, malondialdehyde and hydroxyl radical production in Zn-preinjected rats' PT were significantly lower than those in the normal and saline-preinjected rats' PT. In another study, Sato *et al.* [158] determined dose-dependent changes in the concentration of metallothionein-I (MT-I) in rat tissues following subcutaneous administration of paraquat (PQ), a superoxide radical-generating agent. Twenty four hours after injection, MT-I concentrations in the lung increased linearly with PQ dose. Concentrations in the liver increased with dose, until a plateau was reached at a dose of 30 mg/kg body wt. In the kidneys, MT-I concentrations did not increase, even at high doses of PQ. Zn was the principal metal bound to MT in the liver. The same authors [159] studied the roles of cytokines tumor necrosis factor (TNF) and interleukin 6 (IL-6) in MT synthesis induced by the superoxide generator, paraquat (PQ). They came to the conclusion that MT synthesis induced by oxidative stress may be, at least partly, mediated through cytokines, because pretreatment of rat with dexamethasone, an inhibitor of cytokine production, prevented MT synthesis induced by paraquat.

In addition, MT was reported to be induced by radiation. Shiraishi *et al.* [160] measured hepatic and renal MT contents in rats following whole-body X-irradiation. When compared with control rats, the hepatic MT-Zn content increased five-fold, and MT protein content increased 15-fold by 18 h

following irradiation. Similar results were reported from Koropatnick *et al.* [161]. They observed that whole-body X irradiation of mice induces MT-1 mRNA transcription and protein expression and accumulation in liver, but not in kidney or spleen. Similarly, Shibuya *et al.* [162] examined the accumulation of MT in the Meth-A tumor (mouse fibrosarcoma cells) transplanted into mice exposed to whole-body X irradiation. The MT content in the tumor cells was increased by X irradiation in a dose-dependent manner. Matsubara *et al.* [163,164] found a striking radioresistance in mice, which were subjected to various pretreatments to induce MT synthesis in the liver prior to irradiation. The normal level of MT in mouse liver is 20 μg/g tissue. This level increased up to 70 μg/g tissue following irradiation at 6.3 Gy. Among irradiated mice, MT levels in the liver increased approximately 200%–800% after cadmium, manganese or zinc injection, compared to levels of irradiated mice without pretreatment. The observed results suggest that the body's protective mechanism against radiation strongly correlates with the biosynthesis of MT or MT itself acting as a scavenger of radiation-induced peroxides. On the other hand, MT-transgenic mice, which carried 56 copies of the MT-I transgene and had higher tissue MT concentrations, were not protected against the toxic effects produced by gamma-radiation [165].

The most convincing evidence for the antioxidant action of MT was generated from genetically manipulated mouse model studies. Using MT-overexpressing transgenic or MT-null mice, many studies have shown MT protection against oxidative injuries induced by a diversity of oxidative conditions, including doxorubicin cardiotoxicity, ischemia/reperfusion, diabetes and alcohol administration [166–170].

Sun *et al.* [166] investigated the effect of overexpression of MT on doxorubicin chronic cardiotoxicity in mice, since MT is a potent antioxidant and oxidative stress is critically involved in doxorubicin-induced heart injury. As compared with nontransgenic controls, doxorubicin-induced cardiac hypertrophy was significantly inhibited in the transgenic mice. Light microscopic examination revealed that doxorubicin-induced myocardial morphological changes were markedly suppressed or almost eliminated in the transgenic mice. In the next study using also a cardiac-specific MT-overexpressing transgenic mouse model, Kang *et al.* [167] demonstrated that MT suppresses ischemia/reperfusion-induced myocardial apoptosis through, at least in part, the inhibition of the cytochrome c-mediated caspase-3 activation pathway. The antiapoptotic effect of MT likely results from the suppression of oxidative stress and correlates with the inhibition of myocardial infarction. Another study with the same transgenic mice model was performed to test whether inhibition of nitrosative damage is involved in MT prevention of diabetic cardiomyopathy [168]. Cardiac-specific MT-overexpressing transgenic mice and wild-type controls were treated with streptozotocin by a single intraperitoneal injection, and both developed diabetes. However, the development of diabetic cardiomyopathy, revealed by histopathological and ultrastructural examination, serum creatine phosphokinase and cardiac hemodynamic analysis, was significantly observed only in the wild-type, but not in MT-overexpressing transgenic, diabetic mice. Formations of superoxide and 3-nitrotyrosine, a marker for peroxynitrite-induced protein damage, were detected only in the heart of wild-type diabetic mice [168]. These results thus suggest that MT prevention of diabetic cardiomyopathy is mediated, at least in part, by suppression of superoxide generation and associated nitrosative damage. In addition, Wang *et al.* [169] showed that MT-null mice are more prone to develop cardiac hypertrophy and fibrosis after feeding an alcohol-containing liquid diet for two months than the wild-type control mice.

In another study, Zhou *et al.* [171] evaluated MT-mediated cardioprotection from angiotensin II-induced pathologic remodeling in both the nondiabetic and diabetic heart. The acute and chronic cardiac effects of angiotensin II were examined in MT-overexpressing transgenic and wild-type mice, and the signaling pathways of angiotensin II-induced cardiac cell death were examined in neonatal mouse cardiomyocytes. Acute angiotensin II administration to wild-type mice or neonatal cardiomyocytes increased cardiac apoptosis, nitrosative damage and membrane translocation of the nicotinamide adenine dinucleotide phosphate oxidase (NOX) isoform p47 (phox). These effects were abrogated in MT-overexpressing transgenic mice and MT-overexpressing transgenic cardiomyocytes. In addition, prolonged administration of angiotensin II also induced apoptosis and nitrosative damage in both diabetic and nondiabetic wild-type hearts, but not in diabetic and nondiabetic MT-overexpressing transgenic hearts.

An interesting result came from a study with a MT gene family knockout in *Drosophila melanogaster*. Egli *et al.* [172] reported the generation of viable flies with targeted disruption of all four MT genes (MtnA, MtnB, MtnC and MtnD). These flies were highly sensitive to copper, cadmium and, to a lesser extent, zinc load during development. MT expression was particularly important for male viability. While copper load during development affected males and females equally, adult males lacking MTs displayed a severely reduced life span, possibly due to copper-mediated oxidative stress. Another finding of the study was that MTs are expressed in a tissue-specific manner, notably at sites of metal accumulation. Binding of copper to MTs leads to an orange luminescence of copper accumulated in copper cells of the midgut. Once heavy metal is bound in such a manner, it no longer triggers the activation of MT genes, thus generating a negative feedback on MT gene expression [172].

7. Conclusions

Oxidative or nitrosative stress can cause a release of zinc from proteins containing zinc-fingers and cluster motifs and its re-distribution, thereby altering the functions of those proteins from which it is released and/or to which it binds. Based on the above mentioned facts, MTs belong to the important maintainers of the zinc pool and, also, can be associated with scavenging of free radicals. It is clear that the potential of MT as a scavenger of reactive species is not fully understood, but the published data show that this protein could be selected as a target for some treatment strategies, mainly in the case of tumor diseases. In addition to this, MT overexpression could be used as a predictive marker of worse prognosis and a sign of a higher grade in selected tumors [173].

Acknowledgments

Financial support from GA CR P301/10/0356, DOC CEITEC.02/2012, CEITEC CZ.1.05/1.1.00/02.0068 and the project for conceptual development of research organization 00064203 is highly acknowledged.

Conflict of Interest

The authors declare no conflict of interest.

References

1. Halliwell, B.; Gutteridge, J.M.C. Oxygen free-radicals and iron in relation to biology and medicine—Some problems and concepts. *Arch. Biochem. Biophys.* **1986**, *246*, 501–514.
2. Cadenas, E. Biochemistry of oxygen-toxicity. *Annu. Rev. Biochem.* **1989**, *58*, 79–110.
3. Valko, M.; Izakovic, M.; Mazur, M.; Rhodes, C.J.; Telser, J. Role of oxygen radicals in DNA damage and cancer incidence. *Mol. Cell. Biochem.* **2004**, *266*, 37–56.
4. Poli, G.; Leonarduzzi, G.; Biasi, F.; Chiarpotto, E. Oxidative stress and cell signalling. *Curr. Med. Chem.* **2004**, *11*, 1163–1182.
5. Halliwell, B. Antioxidants in human health and disease. *Annu. Rev. Nutr.* **1996**, *16*, 33–50.
6. Gutteridge, J.M.C.; Halliwell, B. Comments on review of free-radicals in biology and medicine *Free Radic. Biol. Med.* **1992**, *12*, 93–95.
7. Niki, E. Free radicals in biology and medicine: Good, unexpected, and uninvited friends. *Free Radic. Biol. Med.* **2010**, *49*, S2.
8. Halliwell, B.; Gutteridge, J.M.C. *Free-Radicals in Biology and Medicine*; Clarendon Press: Gloucestershire, UK, 1985.
9. Pacher, P.; Beckman, J.S.; Liaudet, L. Nitric oxide and peroxynitrite in health and disease. *Physiol. Rev.* **2007**, *87*, 315–424.
10. Ramalingam, M.; Kim, S.J. Reactive oxygen/nitrogen species and their functional correlations in neurodegenerative diseases. *J. Neural Transm.* **2012**, *119*, 891–910.
11. Pourova, J.; Kottova, M.; Voprsalova, M.; Pour, M. Reactive oxygen and nitrogen species in normal physiological processes. *Acta Physiol.* **2010**, *198*, 15–35.
12. Vasak, M. Advances in metallothionein structure and functions. *J. Trace Elements Med Biol.* **2005**, *19*, 13–17.
13. Henkel, G.; Krebs, B. Metallothioneins: Zinc, cadmium, mercury, and copper thiolates and selenolates mimicking protein active site features—Structural aspects and biological implications. *Chem. Rev.* **2004**, *104*, 801–824.
14. Coyle, P.; Philcox, J.C.; Carey, L.C.; Rofe, A.M. Metallothionein: The multipurpose protein. *Cell. Mol. Life Sci.* **2002**, *59*, 627–647.
15. Margoshes, M.; Vallee, B.L. A cadmium protein from equine kidney cortex *J. Am. Chem. Soc.* **1957**, *79*, 4813–4814.
16. Kagi, J.H.R.; Schaffer, A. Biochemistry of metallothionein. *Biochemistry* **1988**, *27*, 8509–8515.
17. Romero-Isart, N.; Vasak, M. Advances in the structure and chemistry of metallothioneins. *J. Inorg. Biochem.* **2002**, *88*, 388–396.
18. Davis, S.R.; Cousins, R.J. Metallothionein expression in animals: A physiological perspective on function. *J. Nutr.* **2000**, *130*, 1085–1088.
19. Klaassen, C.D.; Liu, J.; Diwan, B.A. Metallothionein protection of cadmium toxicity. *Toxicol. Appl. Pharmacol.* **2009**, *238*, 215–220.
20. Templeton, D.M.; Cherian, M.G. Toxicological significance of metallothionein. *Methods Enzymol.* **1991**, *205*, 11–24.
21. Kagi, J.H.R. Overview of metallothionein. *Methods Enzymol.* **1991**, *205*, 613–626.

22. Shaw, C.F.; Savas, M.M.; Petering, D.H. Ligand substitution and sulfhydryl reactivity of metallothionein. *Methods Enzymol.* **1991**, *205*, 401–414.
23. Karin, M.; Cathala, G.; Nguyenhuu, M.C. Expression and regulation of a human metallothionein gene carried on an autonomously replicating shuttle vector. *Proc. Natl. Acad. Sci. USA* **1983**, *80*, 4040–4044.
24. Enger, M.D.; Tesmer, J.G.; Travis, G.L.; Barham, S.S. Clonal variation of cadmium response in human-tumor cell-lines. *Am. J. Phys.* **1986**, *250*, C256–C263.
25. Liu, Y.P.; Liu, J.; Iszard, M.B.; Andrews, G.K.; Palmiter, R.D.; Klaassen, C.D. Transgenic mice that overexpress metallothionein-I are protected from cadmium lethality and hepatotoxicity. *Toxicol. Appl. Pharmacol.* **1995**, *135*, 222–228.
26. Masters, B.A.; Kelly, E.J.; Quaife, C.J.; Brinster, R.L.; Palmiter, R.D. Targeted disruption of metallothionein-I and metallothionein-II genes increases sensitivity to cadmium. *Proc. Natl. Acad. Sci. USA* **1994**, *91*, 584–588.
27. Petrlova, J.; Potesil, D.; Mikelova, R.; Blastik, O.; Adam, V.; Trnkova, L.; Jelen, F.; Prusa, R.; Kukacka, J.; Kizek, R. Attomole voltammetric determination of metallothionein. *Electrochim. Acta* **2006**, *51*, 5112–5119.
28. Simpkins, C.O. Metallothionein in human disease. *Cell. Mol. Biol.* **2000**, *46*, 465–488.
29. Hamer, D.H. Metallothionein—An Overview. *Mar. Environ. Res.* **1988**, *24*, 171–171.
30. Masters, B.A.; Quaife, C.J.; Erickson, J.C.; Kelly, E.J.; Froelick, G.J.; Zambrowicz, B.P.; Brinster, R.L.; Palmiter, R.D. Metallothionein-III is expressed in neurons that sequester zinc in synaptic vesicles. *J. Neurosci.* **1994**, *14*, 5844–5857.
31. Moffatt, P.; Denizeau, F. Metallothionein in physiological and physiopathological processes. *Drug Metab. Rev.* **1997**, *29*, 261–307.
32. Searle, P.F.; Davison, B.L.; Stuart, G.W.; Wilkie, T.M.; Norstedt, G.; Palmiter, R.D. Regulation, linkage, and sequence of mouse metallothionein-I and metallothionein-II genes. *Mol. Cell. Biol.* **1984**, *4*, 1221–1230.
33. Moffatt, P.; Seguin, C. Expression of the gene encoding metallothionein-3 in organs of the reproductive system. *DNA Cell. Biol.* **1998**, *17*, 501–510.
34. Uchida, Y.; Takio, K.; Titani, K.; Ihara, Y.; Tomonaga, M. The growth inhibitory factor that is deficient in the Alzheimers-disease brain is a 68-amino acid metallothionein-like protein. *Neuron* **1991**, *7*, 337–347.
35. Quaife, C.J.; Findley, S.D.; Erickson, J.C.; Froelick, G.J.; Kelly, E.J.; Zambrowicz, B.P.; Palmiter, R.D. Induction of a new metallothionein isoform (Mt-Iv) occurs during differentiation of stratified squamous epithelia. *Biochemistry* **1994**, *33*, 7250–7259.
36. Moleirinho, A.; Carneiro, J.; Matthiesen, R.; Silva, R.M.; Amorim, A.; Azevedo, L. Gains, losses and changes of function after gene duplication: Study of the metallothionein family. *PLoS One* **2011**, *6*, e18487.
37. Vallee, B.L. The function of metallothionein. *Neurochem. Int.* **1995**, *27*, 23–33.
38. Wong, C.P.; Ho, E. Zinc and its role in age-related inflammation and immune dysfunction. *Mol. Nutr. Food Res.* **2012**, *56*, 77–87.
39. Chasapis, C.T.; Loutsidou, A.C.; Spiliopoulou, C.A.; Stefanidou, M.E. Zinc and human health: An update. *Arch. Toxicol.* **2012**, *86*, 521–534.

40. Plum, L.M.; Rink, L.; Haase, H. The essential toxin: Impact of zinc on human health. *Int. J. Environ. Res. Public Health* **2010**, *7*, 1342–1365.
41. Biswas, S.K.; Rahman, I. Environmental toxicity, redox signaling and lung inflammation: The role of glutathione. *Mol. Aspects Med.* **2009**, *30*, 60–76.
42. Franklin, R.B.; Costello, L.C. The important role of the apoptotic effects of zinc in the development of cancers. *J. Cell. Biochem.* **2009**, *106*, 750–757.
43. MacDonald, R.S. The role of zinc in growth and cell proliferation. *J. Nutr.* **2000**, *130*, 1500S–1508S.
44. Prasad, A.S. Zinc—An overview. *Nutrition* **1995**, *11*, 93–99.
45. Oteiza, P.I. Zinc and the modulation of redox homeostasis. *Free Radic. Biol. Med.* **2012**, *53*, 1748–1759.
46. Costello, L.C.; Franklin, R.B. Cytotoxic/tumor suppressor role of zinc for the treatment of cancer: An enigma and an opportunity. *Expert Rev. Anticancer Ther.* **2012**, *12*, 121–128.
47. Carraway, R.E.; Dobner, P.R. Zinc pyrithione induces ERK- and PKC-dependent necrosis distinct from TPEN-induced apoptosis in prostate cancer cells. *Biochim. Biophys. Acta* **2012**, *1823*, 544–557.
48. Guo, B.L.; Yang, M.W.; Liang, D.; Yang, L.; Cao, J.J.; Zhang, L. Cell apoptosis induced by zinc deficiency in osteoblastic MC3T3-E1 cells via a mitochondrial-mediated pathway. *Mol. Cell. Biochem.* **2012**, *361*, 209–216.
49. Kambe, T.; Yamaguchi-Iwai, Y.; Sasaki, R.; Nagao, M. Overview of mammalian zinc transporters. *Cell. Mol. Life Sci.* **2004**, *61*, 49–68.
50. Hogstrand, C.; Kille, P.; Nicholson, R.I.; Taylor, K.M. Zinc transporters and cancer: A potential role for ZIP7 as a hub for tyrosine kinase activation. *Trends Mol. Med.* **2009**, *15*, 101–111.
51. Hathout, Y.; Fabris, D.; Fenselau, C. Stoichiometry in zinc ion transfer from metallothionein to zinc finger peptides. *Int. J. Mass Spectrom.* **2001**, *204*, 1–6.
52. Costello, L.C.; Liu, Y.Y.; Franklin, R.B.; Kennedy, M.C. Zinc inhibition of mitochondrial aconitase and its importance in citrate metabolism of prostate epithelial cells. *J. Biol. Chem.* **1997**, *272*, 28875–28881.
53. Coffey, R.N.T.; Watson, R.W.G.; Hegarty, N.J.; O'Neill, A.; Gibbons, N.; Brady, H.R.; Fitzpatrick, J.M. Thiol-Mediated apoptosis in prostate carcinoma cells. *Cancer* **2000**, *88*, 2092–2104.
54. Feng, P.; Liang, J.Y.; Li, T.L.; Guan, Z.X.; Zou, J.; Franklin, R.B.; Costello, L.C. Zinc induces mitochondria apoptogenesis in prostate cells. *Mol. Urol.* **2000**, *4*, 31–36.
55. Costello, L.C.; Fenselau, C.C.; Franklin, R.B. Evidence for operation of the direct zinc ligand exchange mechanism for trafficking, transport, and reactivity of zinc in mammalian cells. *J. Inorg. Biochem.* **2011**, *105*, 589–599.
56. Vallee, B.L.; Falchuk, K.H. The biochemical basis of zinc physiology. *Physiol. Rev.* **1993**, *73*, 79–118.
57. Gumulec, J.; Masarik, M.; Krizkova, S.; Adam, V.; Hubalek, J.; Hrabeta, J.; Eckschlager, T.; Stiborova, M.; Kizek, R. Insight to Physiology and pathology of zinc(II) ions and their actions in breast and prostate carcinoma. *Curr. Med. Chem.* **2011**, *18*, 5041–5051.

58. Aimo, L.; Cherr, G.N.; Oteiza, P.I. Low extracellular zinc increases neuronal oxidant production through nadph oxidase and nitric oxide synthase activation. *Free Radic. Biol. Med.* **2010**, *48*, 1577–1587.
59. Kojima-Yuasa, A.; Umeda, K.; Olikita, T.; Kennedy, D.O.; Nishiguchi, S.; Matsui-Yuasa, I. Role of reactive oxygen species in zinc deficiency-induced hepatic stellate cell activation. *Free Radic. Biol. Med.* **2005**, *39*, 631–640.
60. Kraus, A.; Roth, H.P.; Kirchgessner, M. Supplementation with vitamin C, vitamin E or beta-carotene influences osmotic fragility and oxidative damage of erythrocytes of zinc-deficient rats. *J. Nutr.* **1997**, *127*, 1290–1296.
61. Oteiza, P.I.; Olin, K.L.; Fraga, C.G.; Keen, C.L. Zinc-Deficiency causes oxidative damage to proteins, lipids and DNA in rat testes. *J. Nutr.* **1995**, *125*, 823–829.
62. Wang, M.H.; Yang, F.; Zhang, X.Z.; Zhao, H.B.; Wang, Q.S.; Pan, Y.C. Comparative analysis of MTF-1 binding sites between human and mouse. *Mamm. Genome* **2010**, *21*, 287–298.
63. Andrews, G.K. Regulation of metallothionein gene expression by oxidative stress and metal ions. *Biochem. Pharmacol.* **2000**, *59*, 95–104.
64. Soltaninassab, S.R.; Sekhar, K.R.; Meredith, M.J.; Freeman, M.L. Multi-faceted regulation of gamma-glutamylcysteine synthetase. *J. Cell. Physiol.* **2000**, *182*, 163–170.
65. Cortese, M.M.; Suschek, C.V.; Wetzel, W.; Kroncke, K.D.; Kolb-Bachofen, V. Zinc protects endothelial cells from hydrogen peroxide via Nrf2-dependent stimulation of glutathione biosynthesis. *Free Radic. Biol. Med.* **2008**, *44*, 2002–2012.
66. Westbrook, G.L.; Mayer, M.L. Micromolar concentrations of Zn^{2+} antagonize NMDA and GABA responses of hippocampal-neurons. *Nature* **1987**, *328*, 640–643.
67. Maret, W.; Li, Y. Coordination dynamics of zinc in proteins. *Chem. Rev.* **2009**, *109*, 4682–4707.
68. Zitka, O.; Kukacka, J.; Krizkova, S.; Huska, D.; Adam, V.; Masarik, M.; Prusa, R.; Kizek, R. Matrix metalloproteinases. *Curr. Med. Chem.* **2010**, *17*, 3751–3768.
69. Yan, W.; Imanishi, M.; Futaki, S.; Sugiura, Y. Alpha-Helical linker of an artificial 6-zinc finger peptide contributes to selective DNA binding to a discontinuous recognition sequence. *Biochemistry* **2007**, *46*, 8517–8524.
70. Krishna, S.S.; Majumdar, I.; Grishin, N.V. Structural classification of zinc fingers. *Nucleic Acids Res.* **2003**, *31*, 532–550.
71. Posewitz, M.C.; Wilcox, D.E. Properties of the SP1 zinc-finger-3 peptide-coordination chemistry, redox reactions, and metal-binding competition with metallothionein *Chem. Res. Toxicol.* **1995**, *8*, 1020–1028.
72. Huang, M.; Shaw, C.F.; Petering, D.H. Interprotein metal exchange between transcription factor IIIa and apo-metallothionein. *J. Inorg. Biochem.* **2004**, *98*, 639–648.
73. CanoGauci, D.F.; Sarkar, B. Reversible zinc exchange between metallothionein and the estrogen receptor zinc finger. *FEBS Lett.* **1996**, *386*, 1–4.
74. Zeng, J.; Heuchel, R.; Schaffner, W.; Kagi, J.H.R. Thionein (apometallothionein) can modulate DNA-binding and transcriptional activation by zinc finger containing factor-SP1. *FEBS Lett.* **1991**, *279*, 310–312.
75. Zeng, J.; Vallee, B.L.; Kagi, J.H.R. Zinc transfer from transcription factor-IIIA fingers to thionein clusters. *Proc. Natl. Acad. Sci. USA* **1991**, *88*, 9984–9988.

76. Maret, W.; Larsen, K.S.; Vallee, B.L. Coordination dynamics of biological zinc "clusters" in metallothioneins and in the DNA-binding domain of the transcription factor Gal4. *Proc. Natl. Acad. Sci. USA* **1997**, *94*, 2233–2237.
77. Roesijadi, G.; Bogumil, R.; Vasak, M.; Kagi, J.H.R. Modulation of DNA binding of a tramtrack zinc finger peptide by the metallothionein-thionein conjugate pair. *J. Biol. Chem.* **1998**, *273*, 17425–17432.
78. Kroncke, K.D.; Klotz, L.O. Zinc fingers as biologic redox switches? *Antioxid. Redox Signal.* **2009**, *11*, 1015–1027.
79. Maret, W. Metallothionein disulfide interactions, oxidative stress, and the mobilization of cellular zinc. *Neurochem. Int.* **1995**, *27*, 111–117.
80. Jacob, C.; Maret, W.; Vallee, B.L. Control of zinc transfer between thionein, metallothionein, and zinc proteins. *Proc. Natl. Acad. Sci. USA* **1998**, *95*, 3489–3494.
81. Jiang, L.J.; Maret, W.; Vallee, B.L. The glutathione redox couple modulates zinc transfer from metallothionein to zinc-depleted sorbitol dehydrogenase. *Proc. Natl. Acad. Sci. USA* **1998**, *95*, 3483–3488.
82. Maret, W. Oxidative metal release from metallothionein via zinc thiol-disulfide interchange. *Proc. Natl. Acad. Sci. USA* **1994**, *91*, 237–241.
83. Kroncke, K.D.; Fehsel, K.; Schmidt, T.; Zenke, F.T.; Dasting, I.; Wesener, J.R.; Bettermann, H.; Breunig, K.D.; Kolbbachofen, V. Nitric-oxide destroys zinc-sulfur clusters inducing zinc release from metallothionein and inhibition of the zinc finger-type yeast transcription activator LAC9. *Biochem. Biophys. Res. Commun.* **1994**, *200*, 1105–1110.
84. St Croix, C.M.; Wasserloos, K.J.; Dineley, K.E.; Reynolds, I.J.; Levitan, E.S.; Pitt, B.R. Nitric oxide-induced changes in intracellular zinc homeostasis are mediated by metallothionein/thionein. *Am. J. Physiol.* **2002**, *282*, L185–L192.
85. Spahl, D.U.; Berendji-Grun, D.; Suschek, C.V.; Kolb-Bachofen, V.; Kroncke, K.D. Regulation of zinc homeostasis by inducible NO synthase-derived NO: Nuclear translocation and intranuclear metallothionein Zn^{2+} release. *Proc. Natl. Acad. Sci. USA* **2003**, *100*, 13952–13957.
86. Malaiyandi, L.M.; Dineley, K.E.; Reynolds, I.J. Divergent consequences arise from metallothionein overexpression in astrocytes: Zinc buffering and oxidant-induced zinc release. *Glia* **2004**, *45*, 346–353.
87. Pearce, L.L.; Gandley, R.E.; Han, W.P.; Wasserloos, K.; Stitt, M.; Kanai, A.J.; McLaughlin, M.K.; Pitt, B.R.; Levitan, E.S. Role of metallothionein in nitric oxide signaling as revealed by a green fluorescent fusion protein. *Proc. Natl. Acad. Sci. USA* **2000**, *97*, 477–482.
88. Maret, W. Zinc and sulfur: A critical biological partnership. *Biochemistry* **2004**, *43*, 3301–3309.
89. Maret, W.; Vallee, B.L. Thiolate ligands in metallothionein confer redox activity on zinc clusters. *Proc. Natl. Acad. Sci. USA* **1998**, *95*, 3478–3482.
90. Maret, W. Redox biochemistry of mammalian metallothioneins. *J. Biol. Inorg. Chem.* **2011**, *16*, 1079–1086.
91. Cherian, M.G.; Jayasurya, A.; Bay, B.H. Metallothioneins in human tumors and potential roles in carcinogenesis. *Mutat. Res.* **2003**, *533*, 201–209.
92. Ebadi, M.; Leuschen, M.P.; ElRefaey, H.; Hamada, F.M.; Rojas, P. The antioxidant properties of zinc and metallothionein. *Neurochem. Int.* **1996**, *29*, 159–166.

93. Kang, Y.J. Metallothionein redox cycle and function. *Exp. Biol. Med.* **2006**, *231*, 1459–1467.
94. Sato, M.; Bremner, I. Oxygen free-radicals and metallothionein. *Free Radic. Biol. Med.* **1993**, *14*, 325–337.
95. Iszard, M.B.; Liu, J.; Klassen, C.D. Effect of several metallothionein inducers on oxidative stress defense mechanisms in rats. *Toxicology* **1995**, *104*, 25–33.
96. Aschner, M.; Conklin, D.R.; Yao, C.P.; Allen, J.W.; Tan, K.H. Induction of astrocyte metallothioneins (MTs) by zinc confers resistance against the acute cytotoxic effects of methylmercury on cell swelling, Na^+ uptake, and K^+ release. *Brain Res.* **1998**, *813*, 254–261.
97. Namdarghanbari, M.; Wobig, W.; Krezoski, S.; Tabatabai, N.M.; Petering, D.H. Mammalian metallothionein in toxicology, cancer, and cancer chemotherapy. *J. Biol. Inorg. Chem.* **2011**, *16*, 1087–1101.
98. Cai, L.; Koropatnick, J.; Cherian, M.G. Metallothionein protects DNA from copper-induced but not iron-induced cleavage *in vitro*. *Chem. Biol. Interact.* **1995**, *96*, 143–155.
99. Shibuya, K.; Nishimura, N.; Suzuki, J.S.; Tohyama, C.; Naganuma, A.; Satoh, M. Role of metallothionein as a protective factor against radiation carcinogenesis. *J. Toxicol. Sci.* **2008**, *33*, 651–655.
100. Schwarz, M.A.; Lazo, J.S.; Yalowich, J.C.; Allen, W.P.; Whitmore, M.; Bergonia, H.A.; Tzeng, E.; Billiar, T.R.; Robbins, P.D.; Lancaster, J.R. *et al.* Metallothionein protects against the cytotoxic and DNA-damaging effects of nitric-oxide. *Proc. Natl. Acad. Sci. USA* **1995**, *92*, 4452–4456.
101. Kondo, Y.; Rusnak, J.M.; Hoyt, D.G.; Settineri, C.E.; Pitt, B.R.; Lazo, J.S. Enhanced apoptosis in metallothionein null cells. *Mol. Pharmacol.* **1997**, *52*, 195–201.
102. Tao, X.; Zheng, J.M.; Xu, A.M.; Chen, X.F.; Zhang, S.H. Downregulated expression of metallothionein and its clinicopathological significance in hepatocellular carcinoma. *Hepatol. Res.* **2007**, *37*, 820–827.
103. Fraker, P.J.; King, L.E. A distinct role for apoptosis in the changes in lymphopoiesis and myelopoiesis created by deficiencies in zinc. *FASEB J.* **2001**, *15*, 2572–2578.
104. Mao, J.; Yu, H.X.; Wang, C.J.; Sun, L.H.; Jiang, W.; Zhang, P.Z.; Xiao, Q.Y.; Han, D.B.; Saiyin, H.; Zhu, J.D. *et al.* Metallothionein MT1M is a tumor suppressor of human hepatocellular carcinomas. *Carcinogenesis* **2012**, *33*, 2568–2577.
105. Yan, D.W.; Fan, J.W.; Yu, Z.H.; Li, M.X.; Wen, Y.G.; Li, D.W.; Zhou, C.Z.; Wang, X.L.; Wang, Q.; Tang, H.M. *et al.* Downregulation of Metallothionein 1F, a putative oncosuppressor, by loss of heterozygosity in colon cancer tissue. *Biochim. Biophys. Acta* **2012**, *1822*, 918–926.
106. Faller, W.J.; Rafferty, M.; Hegarty, S.; Gremel, G.; Ryan, D.; Fraga, M.F.; Esteller, M.; Dervan, P.A.; Gallagher, W.M. Metallothionein 1E is methylated in malignant melanoma and increases sensitivity to cisplatin-induced apoptosis. *Melanoma Res.* **2010**, *20*, 392–400.
107. Takahashi, S. Molecular functions of metallothionein and its role in hematological malignancies. *J. Hematol. Oncol.* **2012**, *5*, 1–8.
108. Dutsch-Wicherek, M.; Sikora, J.; Tomaszewska, R. The possible biological role of metallothionein in apoptosis. *Front. Biosci.* **2008**, *13*, 4029–4038.
109. McGee, H.M.; Woods, G.M.; Bennett, B.; Chung, R.S. The two faces of metallothionein in carcinogenesis: Photoprotection against UVR-induced cancer and promotion of tumour survival. *Photochem. Photobiol. Sci.* **2010**, *9*, 586–596.

110. Chaabane, W.; User, S.D.; El-Gazzah, M.; Jaksik, R.; Sajjadi, E.; Rzeszowska-Wolny, J.; Los, M.J. Autophagy, apoptosis, mitoptosis and necrosis: Interdependence between those pathways and effects on cancer. *Arch. Immunol. Ther. Exp.* **2013**, *61*, 43–58.
111. Ouyang, L.; Shi, Z.; Zhao, S.; Wang, F.T.; Zhou, T.T.; Liu, B.; Bao, J.K. Programmed cell death pathways in cancer: A review of apoptosis, autophagy and programmed necrosis. *Cell. Prolif.* **2012**, *45*, 487–498.
112. Nath, R.; Kumar, D.; Li, T.M.; Singal, P.K. Metallothioneins, oxidative stress and the cardiovascular system. *Toxicology* **2000**, *155*, 17–26.
113. Wyllie, A.H. Apoptosis: An overview. *Br. Med. Bull.* **1997**, *53*, 451–465.
114. Thornberry, N.A.; Lazebnik, Y. Caspases: Enemies within. *Science* **1998**, *281*, 1312–1316.
115. Wyllie, A.H.; Bellamy, C.O.C.; Bubb, V.J.; Clarke, A.R.; Corbet, S.; Curtis, L.; Harrison, D.J.; Hooper, M.L.; Toft, N.; Webb, S. *et al.* Apoptosis and carcinogenesis. *Br. J. Cancer* **1999**, *80*, 34–37.
116. Dhawan, D.K.; Chadha, V.D. Zinc: A promising agent in dietary chemoprevention of cancer. *Indian J. Med. Res.* **2010**, *132*, 676–682.
117. Telford, W.G.; Fraker, P.J. Preferential induction of apoptosis in mouse CD4(+)CD8(+)alpha-beta-tcr(lo)CD3-epsilon(lo) thymocytes by zinc. *J. Cell. Physiol.* **1995**, *164*, 259–270.
118. Perry, D.K.; Smyth, M.J.; Stennicke, H.R.; Salvesen, G.S.; Duriez, P.; Poirier, G.G.; Hannun, Y.A. Zinc is a potent inhibitor of the apoptotic protease, caspase-3—A novel target for zinc in the inhibition of apoptosis. *J. Biol. Chem.* **1997**, *272*, 18530–18533.
119. Stefanidou, M.; Maravelias, C.; Dona, A.; Spiliopoulou, C. Zinc: A multipurpose trace element. *Arch. Toxicol.* **2006**, *80*, 1–9.
120. Seve, M.; Chimienti, F.; Favier, A. Role of intracellular zinc in programmed cell death. *Pathol. Biol.* **2002**, *50*, 212–221.
121. Fan, L.Z.; Cherian, M.G. Potential role of p53 on metallothionein induction in human epithelial breast cancer cells. *Br. J. Cancer* **2002**, *87*, 1019–1026.
122. Meplan, C.; Verhaegh, G.; Richard, M.J.; Hainaut, P. Metal ions as regulators of the conformation and function of the tumour suppressor protein p53: Implications for carcinogenesis. *Proc. Nutr. Soc.* **1999**, *58*, 565–571.
123. Meplan, C.; Richard, M.J.; Hainaut, P. Metalloregulation of the tumor suppressor protein p53: zinc mediates the renaturation of p53 after exposure to metal chelators *in vitro* and in intact cells. *Oncogene* **2000**, *19*, 5227–5236.
124. Maret, W.; Jacob, C.; Vallee, B.L.; Fischer, E.H. Inhibitory sites in enzymes: Zinc removal and reactivation by thionein. *Proc. Natl. Acad. Sci. USA* **1999**, *96*, 1936–1940.
125. Woo, E.S.; Kondo, Y.; Watkins, S.C.; Hoyt, D.G.; Lazo, J.S. Nucleophilic distribution of metallothionein in human tumor cells. *Exp. Cell. Res.* **1996**, *224*, 365–371.
126. Sliwinska-Mosson, M.; Milnerowicz, H.; Rabczynski, J.; Milnerowicz, S. Immunohistochemical localization of metallothionein and p53 protein in pancreatic serous cystadenomas. *Arch. Immunol. Ther. Exp.* **2009**, *57*, 295–301.
127. Cardoso, S.V.; Silveira, J.B.; Machado, V.D.; De-Paula, A.M.B.; Loyola, A.M.; de Aguiar, M.C.F. Expression of metallothionein and p53 antigens are correlated in oral squamous cell carcinoma. *Anticancer Res.* **2009**, *29*, 1189–1193.

128. Baldwin, A.S. Control of oncogenesis and cancer therapy resistance by the transcription factor NF-kappa B. *J. Clin. Invest.* **2001**, *107*, 241–246.
129. Karin, M.; Cao, Y.X.; Greten, F.R.; Li, Z.W. NF-Kappa B in cancer: From innocent bystander to major culprit. *Nat. Rev. Cancer* **2002**, *2*, 301–310.
130. Wang, C.Y.; Mayo, M.W.; Korneluk, R.G.; Goeddel, D.V.; Baldwin, A.S. NF-kappa B antiapoptosis: Induction of TRAF1 and TRAF2 and c-IAP1 and c-IAP2 to suppress caspase-8 activation. *Science* **1998**, *281*, 1680–1683.
131. Wang, C.Y.; Guttridge, D.C.; Mayo, M.W.; Baldwin, A.S. NF-kappa B induces expression of the Bcl-2 homologue A1/Bfl-1 to preferentially suppress chemotherapy-induced apoptosis. *Mol. Cell. Biol.* **1999**, *19*, 5923–5929.
132. Wu, M.X.; Ao, Z.H.; Prasad, K.V.S.; Wu, R.L.; Schlossman, S.F. IEX-1L, an apoptosis inhibitor involved in NF-kappa B-mediated cell survival. *Science* **1998**, *281*, 998–1001.
133. Butcher, H.L.; Kennette, W.A.; Collins, O.; Zalups, R.K.; Koropatnick, J. Metallothionein mediates the level and activity of nuclear factor kappa B in murine fibroblasts. *J. Pharmacol. Exp. Therapeutics* **2004**, *310*, 589–598.
134. Kim, C.H.; Kim, J.H.; Lee, J.; Ahn, Y.S. Zinc-Induced NF-kappa B inhibition can be modulated by changes in the intracellular metallothionein level. *Toxicol. Appl. Pharmacol.* **2003**, *190*, 189–196.
135. Abdel-Mageed, A.B.; Agrawal, K.C. Activation of nuclear factor kappa B: Potential role in metallothionein-mediated mitogenic response. *Cancer Res.* **1998**, *58*, 2335–2338.
136. Wang, C.Y.; Cusack, J.C.; Liu, R.; Baldwin, A.S. Control of inducible chemoresistance: Enhanced anti-tumor therapy through increased apoptosis by inhibition of NF-kappa B. *Nat. Med.* **1999**, *5*, 412–417.
137. Kanekiyo, M.; Itoh, N.; Kawasaki, A.; Tanaka, J.; Nakanishi, T.; Tanaka, K. Zinc-induced activation of the human cytomegalovirus major immediate-early promoter is mediated by metallothionein and nuclear factor-kappa B. *Toxicol. Appl. Pharmacol.* **2001**, *173*, 146–153.
138. Thornalley, P.J.; Vasak, M. Possible role for metallothionein in protection against radiation-induced oxidative stress—Kinetics and mechanism of its reaction with superoxide and hydroxyl radicals. *Biochim. Biophys. Acta* **1985**, *827*, 36–44.
139. Abel, J.; Deruiter, N. Inhibition of hydroxyl-radical-generated DNA-degradation by metallothionein *Toxicol. Lett.* **1989**, *47*, 191–196.
140. Cai, L.; Klein, J.B.; Kang, Y.J. Metallothionein inhibits peroxynitrite-induced DNA and lipoprotein damage. *J. Biol. Chem.* **2000**, *275*, 38957–38960.
141. Schwarz, M.A.; Lazo, J.S.; Yalowich, J.C.; Reynolds, I.; Kagan, V.E.; Tyurin, V.; Kim, Y.M.; Watkins, S.C.; Pitt, B.R. Cytoplasmic metallothionein overexpression protects NIH 3T3 cells from tert-butyl hydroperoxide toxicity. *J. Biol. Chem.* **1994**, *269*, 15238–15243.
142. Du, X.H.; Yang, C.L. Mechanism of gentamicin-nephrotoxicity in rats and the protective effect of zinc-induced metallothionein synthesis. *Nephrol. Dial. Transplant.* **1994**, *9*, 135–140.
143. Yang, C.L.; Du, X.H.; Zhao, J.H.; Chen, W.; Han, Y.X. Zinc-Induced metallothionein synthesis could protect from gentamicin-nephrotoxicity in suspended proximal tubules of rats. *Renal Fail.* **1994**, *16*, 61–69.

144. Hart, B.A.; Eneman, J.D.; Gong, Q.; DurieuxLu, C.C. Increased oxidant resistance of alveolar epithelial type II cells. Isolated from rats following repeated exposure to cadmium aerosols. *Toxicol. Lett.* **1995**, *81*, 131–139.
145. Satoh, M.; Kondo, Y.; Mita, M.; Nakagawa, I.; Naganuma, A.; Imura, N. Prevention of carcinogenicity of anticancer drugs by metallothionein induction. *Cancer Res.* **1993**, *53*, 4767–4768.
146. Satoh, M.; Naganuma, A.; Imura, N. Effect of preinduction of metallothionein on paraquat toxicity in mice. *Arch. Toxicol.* **1992**, *66*, 145–148.
147. Quesada, A.R.; Byrnes, R.W.; Krezoski, S.O.; Petering, D.H. Direct reaction of H_2O_2 with sulfhydryl groups in HL-60 cells: Zinc-metallothionein and other sites. *Arch. Biochem. Biophys.* **1996**, *334*, 241–250.
148. Chubatsu, L.S.; Meneghini, R. Metallothionein protects DNA from oxidative damage. *Biochem. J.* **1993**, *291*, 193–198.
149. Banerjee, D.; Onosaka, S.; Cherian, M.G. Immunohistochemical localization of metallothionein in cell-nucleus and cytoplasm of rat-liver and kidney. *Toxicology* **1982**, *24*, 95–105.
150. Nagel, W.W.; Vallee, B.L. Cell-Cycle regulation of metallothionein in human colonic-cancer cells. *Proc. Natl. Acad. Sci. USA* **1995**, *92*, 579–583.
151. Ghoshal, K.; Jacob, S.T. Regulation of metallothionein gene expression. *Prog. Nucl. Res. Mol. Biol.* **2001**, *66*, 357–384.
152. Tsujikawa, K.; Imai, T.; Kakutani, M.; Kayamori, Y.; Mimura, T.; Otaki, N.; Kimura, M.; Fukuyama, R.; Shimizu, N. Localization of metallothionein in nuclei of growing primary cultured adult-rat hepatocytes. *FEBS Lett.* **1991**, *283*, 239–242.
153. Takahashi, Y.; Ogra, Y.; Ibata, K.; Suzuki, K.T. Role of metallothionein in the cell cycle: Protection against the retardation of cell proliferation by endogenous reactive oxygen species. *J. Health Sci.* **2004**, *50*, 154–158.
154. Takahashi, Y.; Ogra, Y.; Suzuki, K.T. Synchronized generation of reactive oxygen species with the cell cycle. *Life Sci.* **2004**, *75*, 301–311.
155. Takahashi, Y.; Ogra, Y.; Suzuki, K.T. Nuclear trafficking of metallothionein requires oxidation of a cytosolic partner. *J. Cell. Physiol.* **2005**, *202*, 563–569.
156. Ogra, Y.; Onishi, S.; Kajiwara, A.; Hara, A.; Suzuki, K.T. Enhancement of nuclear localization of metallothionein by nitric oxide. *J. Health Sci.* **2008**, *54*, 339–342.
157. Eckschlager, T.; Adam, V.; Hrabeta, J.; Figova, K.; Kizek, R. Metallothioneins and cancer. *Curr. Protein Peptide Sci.* **2009**, *10*, 360–375.
158. Sato, M. Dose-Dependent increases in metallothionein synthesis in the lung and liver of paraquat-treated rats. *Toxicol. Appl. Pharmacol.* **1991**, *107*, 98–105.
159. Sato, M.; Sasaki, M.; Hojo, H. Antioxidative roles of metallothionein and manganese superoxide-dismutase induced by tumor-necrosis-factor-alpha and interleukin-6. *Arch. Biochem. Biophys.* **1995**, *316*, 738–744.
160. Shiraishi, N.; Yamamoto, H.; Takeda, Y.; Kondoh, S.; Hayashi, H.; Hashimoto, K.; Aono, K. Increased metallothionein content in rat-liver and kidney following X-irradiation. *Toxicol. Appl. Pharmacol.* **1986**, *85*, 128–134.
161. Koropatnick, J.; Leibbrandt, M.; Cherian, M.G. Organ-specific metallothionein induction in mice by X-irradiation. *Radiat. Res.* **1989**, *119*, 356–365.

Int. J. Mol. Sci. **2013**, *14* **6066**

162. Shibuya, K.; Satoh, M.; Muraoka, M.; Watanabe, Y.; Oida, M.; Shimizu, H. Induction of metallothionein synthesis in transplanted murine tumors by X-irradiation. *Radiat. Res.* **1995**, *143*, 54–57.
163. Matsubara, J.; Tajima, Y.; Karasawa, M. Promotion of radioresistance by metallothionein induction prior to irradiation. *Environ. Res.* **1987**, *43*, 66–74.
164. Matsubara, J. Metallothionein induction—A measure of radioprotective action. *Health Phys.* **1988**, *55*, 433–436.
165. Liu, J.; Kimler, B.F.; Liu, Y.P.; Klaassen, C.D. Metallothionein-I transgenic mice are not protected from gamma-radiation. *Toxicol. Lett.* **1999**, *104*, 183–187.
166. Sun, X.H.; Zhou, Z.X.; Kang, Y.J. Attenuation of doxorubicin chronic toxicity in metallothionein-overexpressing transgenic mouse heart. *Cancer Res.* **2001**, *61*, 3382–3387.
167. Kang, Y.J.; Li, Y.; Sun, X.C.; Sun, X.H. Antiapoptotic effect and inhibition of ischemia/reperfusion-induced myocardial injury in metallothionein-overexpressing transigenic mice. *Am. J. Pathol.* **2003**, *163*, 1579–1586.
168. Cai, L.; Wang, J.X.; Li, Y.; Sun, X.H.; Wang, L.P.; Zhou, Z.X.; Kang, Y.J. Inhibition of superoxide generation and associated nitrosative damage is involved in metallothionein prevention of diabetic cardiomyopathy. *Diabetes* **2005**, *54*, 1829–1837.
169. Wang, L.P.; Zhou, Z.X.; Saari, J.T.; Kang, Y.J. Alcohol-Induced myocardial fibrosis in metallothionein-null mice—Prevention by zinc supplementation. *Am. J. Pathol.* **2005**, *167*, 337–344.
170. Merten, K.E.; Feng, W.K.; Zhang, L.; Pierce, W.; Cai, J.; Klein, J.B.; Kang, Y.J. Modulation of cytochrome c oxidase-Va is possibly involved in metallothionein protection from doxorubicin cardiotoxicity. *J. Pharmacol. Exp. Ther.* **2005**, *315*, 1314–1319.
171. Zhou, G.H.; Li, X.K.; Hein, D.W.; Xiang, X.L.; Marshall, J.P.; Prabhu, S.D.; Cai, L. Metallothionein suppresses angiotensin II-Induced nicotinamide adenine dinucleotide phosphate oxidase activation, nitrosative stress, apoptosis, and pathological remodeling in the diabetic heart. *J. Am. Coll. Cardiol.* **2008**, *52*, 655–666.
172. Egli, D.; Yepiskoposyan, H.; Selvaraj, A.; Balamurugan, K.; Rajaram, R.; Simons, A.; Multhaup, G.; Mettler, S.; Vardanyan, A.; Georgiev, O.; *et al.* A family knockout of all four *Drosophila metallothioneins* reveals a central role in copper homeostasis and detoxification. *Mol. Cell. Biol.* **2006**, *26*, 2286–2296.
173. Krizkova, S.; Ryvolova, M.; Hrabeta, J.; Adam, V.; Stiborova, M.; Eckschlager, T.; Kizek, R. Metallothioneins and zinc in cancer diagnosis and therapy. *Drug Metab. Rev.* **2012**, *44*, 287–301.

Metallomics

TUTORIAL REVIEW

Metallothionein polymorphisms in pathological processes

Cite this: *Metallomics*, 2014, 6, 55

Martina Raudenska,[ab] Jaromir Gumulec,[ab] Ondrej Podlaha,[c] Marketa Sztalmachova,[ad] Petr Babula,[e] Tomas Eckschlager,[f] Vojtech Adam,[bd] Rene Kizek[bd] and Michal Masarik*[ab]

Received 24th April 2013,
Accepted 2nd September 2013

DOI: 10.1039/c3mt00132f

www.rsc.org/metallomics

Metallothioneins (MTs) are a class of metal-binding proteins characterized by a high cysteine content and low molecular weight. MTs play an important role in metal metabolism and protect cells against the toxic effects of radiation, alkylating agents and oxygen free radicals. The evidence that individual genetic characteristics of MTs play an important role in physiological and pathological processes associated with antioxidant defense and detoxification inspired targeted studies of genetic polymorphisms in a clinical context. In recent years, common MT polymorphisms were identified and associated with, particularly, western lifestyle diseases such as cancer, complications of atherosclerosis, and type 2 diabetes mellitus along with related complications. This review summarizes all evidence regarding MT polymorphisms of major human MTs (MT1, MT2, MT3 and MT4), their relation to pathological processes, and outlines specific applications of MTs as a set of genetic markers for certain pathologies.

1 Introduction

Living organisms constantly need to cope with harmful environmental conditions such as heavy metal load, UV radiation, and oxidative stress. It is well known that the toxicity levels of metals and reactive oxygen species (ROS) vary considerably between, as well as within, species.[1] Differential expression and function of metal binding proteins, such as metallothioneins (MTs), might be one of the reasons for this variation.[2] In several genome-wide association studies a cluster of MT genes located on chromosome 16 (16q12-22) was found to be an important target in candidate gene finding. Lee *et al.* associated this gene cluster with obesity[3] and Seibold *et al.* with breast cancer risk.[4] Furthermore, promoter methylation and differential gene expression of *MT1G*, an MT gene paralog, was identified as a novel marker in melanoma in a genome-wide study.[5] Notable changes in the expression of a variety of metallothionein genes, with a number of them being clearly upregulated, were identified in the pancreatic beta-cells from type 2 diabetes mellitus (T2DM) patients. These include the metallothioneins 1E, 1G, 1M, 1X and 2A.[6] Expression of MTs may be also influenced by different external and internal factors, such as single nucleotide polymorphisms (SNPs).[7] The evidence that individual genetic characteristics play an important role in physiological and pathological processes associated with antioxidant defense and detoxification resulted in numerous follow-up studies of genetic polymorphisms in the clinical settings.

In this review we discuss the role of MTs and report all relevant single nucleotide polymorphisms (SNPs) in humans, including their locations along the gene sequence. Subsequently, we summarize the evidence regarding the association of MT SNPs with various pathological conditions. To date, no comprehensive review and only one genome-wide association study[4] with regard to human MT polymorphisms have been published. Moreover, although numerous studies in the last three decades have described the association of MT SNPs with various pathological conditions, the nomenclature is riddled with inconsistency and inaccuracy. The novelty of this review lies in the synthesis of all studies related to MT polymorphisms, the nomenclature standardization according to the latest recommendations,[8] and the exhaustive comparison across multiple databases.

1.1 How SNPs affect protein function

Single nucleotide polymorphisms (SNPs) are the most common source of variation in the human genome.[9] Given their location,

[a] *Department of Pathological Physiology, Faculty of Medicine, Masaryk University, Kamenice 5, CZ-625 00 Brno, Czech Republic. E-mail: masarik@med.muni.cz; Fax: +420-5-4949-4340; Tel: +420-5-4949-3631*
[b] *Central European Institute of Technology, Brno University of Technology, Technicka 3058/10, CZ-616 00 Brno, Czech Republic*
[c] *Department of Biostatistics and Computational Biology, Dana-Farber Cancer Institute, and Department of Biostatistics, Harvard School of Public Health, Boston, MA 02115, USA*
[d] *Department of Chemistry and Biochemistry, Mendel University in Brno/Zemedelska 1, CZ-613 00 Brno, Czech Republic*
[e] *Department of Natural Drugs, Faculty of Pharmacy, University of Veterinary and Pharmaceutical Sciences, Palackeho 1-3, CZ-612 42 Brno, Czech Republic*
[f] *Department of Paediatric Haematology and Oncology, 2nd Faculty of Medicine Charles University and University Hospital Motol, V Uvalu 84, CZ-150 06 Prague 5, Czech Republic*

SNPs can be divided into coding and non-coding region SNPs. A SNP in the coding region may affect the amino acid composition in two different ways:

(a) Non-synonymous SNPs (nsSNPs) result in an alteration of the coded amino acid. NsSNPs may lead to missense and nonsense types of mutation. A missense mutation changes one codon into another, thereby causing a change in the resulting amino acid, whereas nonsense mutation results in a misplaced termination codon. NsSNPs usually have a significant effect on the structure or function of the encoded protein. The functional effects caused by nsSNPs can be divided into several categories: SNPs affecting protein structure (protein aggregation, stability, flexibility, functional sites, and protein folding); reaction kinetics and its dependence on the environmental parameters; subcellular protein localization; mRNA stability and protein expression; and finally, interactions with other molecules.[10]

(b) Due to the redundant nature of the RNA triplet code, many coding region SNPs will not cause an amino acid change of the encoded protein. Such SNPs are called synonymous or silent, but it cannot be said with certainty that they have no effect.[11] Synonymous polymorphisms appear to influence the kinetics of translation and protein folding (possibly *via* translational pausing during the recruitment of rare tRNAs).[12] Synonymous polymorphisms also affect the mRNA structure and stability. Furthermore, SNPs in coding as well as in intron regions play a role in alternative splicing.[13]

SNPs found in promoters and other regulatory regions affect the amount or timing of protein production.

2 Materials and methods

2.1 Identification of relevant studies

MEDLINE (PubMed; 1968 to January 2013), EMBASE (1977 to January 2013), Cochrane Library (1953 to January 2013) and Web of Science (Science citation index expanded 1945 to January 2013) were searched using common keywords related to metallothionein and polymorphisms. The keywords were as follows: ''polymorphism'', ''SNP'', or ''genetic variation'' and ''metallothionein''. Cited references of found studies were analyzed to find additional articles. Date of publication and language were not a restriction. Database search in the National Center for Biotechnology Information's Gene database (NCBI gene, www.ncbi.nlm.nih.gov/gene) was used to identify all human MT genes. Subsequently, database search was performed in the NCBI Short Genetic Variations database (NCBI dbSNP, www.ncbi.nlm.nih.gov/projects/SNP) and in Boston Children's Hospital's Informatics Program's SNPper database (http://snpper.chip.org) to identify relevant MT polymorphisms and their position within genes.

2.2 SNP nomenclature

SNPs localized in 5′ untranslated regions of a gene (5′UTR), in the coding sequence, in introns and in 3′ untranslated regions of a gene (3′UTR) were only taken into account. SNPs localized near gene regions are not included. The data acquisition process is shown in Fig. 1. SNP names are listed in the NCBI rs format. The SNP position within the gene sequence is depicted by SNP nomenclature according to the Human genome variation society' recommendations for the description of DNA sequence variants v2.0 only,[8] previous designations, genomic reference sequence, mRNA and protein positions are not listed.

Martina Raudenska

Martina Raudenska, PhD, is a genetic specialist at the Department of Pathological Physiology, Faculty of Medicine, Masaryk University in Brno. Her research is mainly focused on analysis of selected genes important in carcinogenesis and association of specific single nucleotide polymorphisms with grave diseases.

Jaromir Gumulec

Jaromir Gumulec, MD, is a PhD student at the Department of Pathological Physiology, Faculty of Medicine, Masaryk University in Brno and a holder of the prestigious PhD grant from the Central European Institute of Technology, Brno University of Technology. His research is mainly focused on analysis of molecular mechanisms of zinc ions and cytotoxic agents in prostate tumor cells.

Michal Masarik

Michal Masarik, PhD, is assistant professor at the Department of Pathological Physiology, Faculty of Medicine, Masaryk University in Brno and a senior scientist in the Research group of Submicron Systems and Nanodevices in the Central European Institute of Technology, Brno University of Technology. His research is mainly focused on prostate cancer development, analysis of tumor biomarkers and effect of selected cytostatic drugs and metal ions on tumor cell lines.

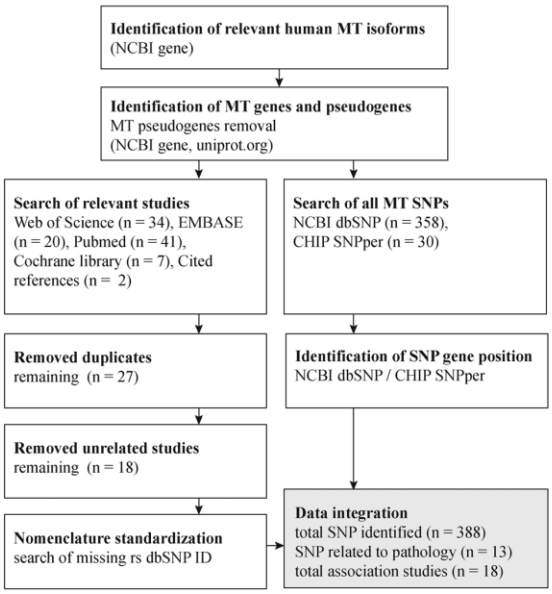

Fig. 1 Data acquisition process. Flow diagram for identification of metallothionein (MT) genes, MT single nucleotide polymorphisms (SNPs) and relevant studies.

According to this nomenclature, nucleotide +1 is the first in the coding sequence (the first nucleotide of the exon). SNPs in the untranslated region at the 5′ end of the gene (5′UTR) are numbered in relation to this first coding nucleotide, for example, substitution of the 12th G to A before the first coding nucleotide, as follows: c.-12G>A. Likewise, SNPs in the coding region (*e.g.* C to G substitution of the third nucleotide) are designated as follows: c.3G>C. Intron SNPs are designated relative to its 5′ or 3′ end, giving priority to the closer end. For instance, T to G substitution of the second nucleotide in the intron (88 + 2) positioned between coding DNA nucleotides 88 and 89 is as follows: c.88+2T>G. Variants in the 3′ untranslated region of the gene are designated in relation to the termination codon as follows: T to A substitution 70 nucleotides downstream of the termination codon: c.*70T>A.

3 Metallothionein gene family

Metallothioneins (MTs) are a class of metal-binding proteins characterized by high cysteine content (up to 30% of the amino acid residues) and low molecular weight (0.5–15 kDa). Up to seven divalent metal ions can be bound to human MTs and this binding stabilizes the three-dimensional structure of MTs.[14] MTs play an important detoxification role in the defense against excessive essential metals; this protective function is related to the ability of MTs to scavenge free radicals.[15] Therefore, MTs are highly expressed when exposed to oxidative stress or toxic factors.[2a,16]

Metallothioneins (MTs) can be found in most eukaryotes. Whereas the structure, physiology, and pathophysiology of MTs exhibit differences between individual species, the claims mentioned herein relate only to the human MTs and cannot be generalized to all organisms. There are four main gene subfamilies of MTs expressed in humans: MT1, MT2, MT3, and MT4. In humans, this cluster of genes is located on chromosome 16 (16q12-22).[17] MT1 and MT2 consist of nine functional (MT1A, MT1B, MT1E, MT1F, MT1G, MT1H, MT1M (also called MT1K), MT1X, and MT2A) and seven nonfunctional (MT1C, MT1D, MT1I, MT1J, MT1L, PT1P, and MT2B) paralogs.[18] Whereas MT1 and MT2 are expressed ubiquitously, MT3 expression appears to be restricted to the brain[19] and metallothionein 4 (MT4) was found to be specifically expressed in stratified squamous epithelia.[20]

The ubiquitously expressed MT1 and MT2 isoforms are inducible in mammalian cells by heavy metals. In contrast, MT3 seems to be not inducible by heavy metals, although its gene contains metal responsive elements (MREs) in its promoter.[21] Additionally, the status of the MT4 inducibility is still unclear. The early induction of MTs by metals also makes these proteins a potential biomarker useful to assess the ecotoxicological significance of non-essential (Cd, Pb) and essential, but potentially toxic, (Cu) metals.[22] A significant association between the metal levels, MTs expression, and diseases was shown in various tissues[2c,23] including breast,[24] renal,[25] and prostate cancers.[26] The overexpression of MT2A is frequently observed in invasive human breast tumors and was linked with more aggressive breast cancers.[24b] Experimental studies have also shown both enhanced and reduced neuronal protection against a variety of oxidative stress-induced damages in MT-overexpressing and MT-knockout mice, respectively.[27] However, mice with targeted deletion of both the MT1 and MT2 genes do not exhibit an altered phenotype under normal laboratory conditions.[28] Nevertheless, when exposed to cadmium, these mice showed an increased sensitivity to intoxication and a dramatically reduced myotonic reflex of mesenteric arteries.[29] Mice with defective genes for MT were ten times more sensitive to Cd toxicity than wild type strains.[23a]

MT2A seems to be the most expressed MT in the human body.[26d] The difference in expression between MT2A and other metallothioneins is attributed to the binding ability of enhancers in the *MT2A* promoter region.[30]

Under physiological conditions, MTs primarily bind zinc, but at the same time they have a particularly high affinity for potentially toxic heavy metals. In a study performed by Waalkes and co-workers, the order of binding affinity of MTs was determined as follows, Cd > Pb > Cu > Hg > Zn > Ag > Ni > Co;[31] thus MTs are capable of binding Cd and Pb more strongly than Zn.

3.1 Regulation of MT expression

MT expression is controlled mainly at the transcriptional level.[23d] It could be induced by many different stimuli, such as metal exposure, oxidative stress, glucocorticoids, and changes in pH.[16c,d,32] MT expression control elements can be functionally subdivided into two categories: basal and inducible. There are several distinct basal sequences, which include the TATA-box, GC-box, and at least two basal level enhancer (BLE) sequences.[33] MT genes also respond to induction by heavy metals, antioxidants, and steroid hormones through the action of metal

regulatory elements (MRE), antioxidant responsive elements (AREs), and glucocorticoid responsive elements (GRE) in the 5′-regulatory regions.[34]

The main transcription factor involved in the metal regulation of expression is MRE-binding transcription factor-1 (MTF-1).[35] On exposure to various heavy metals and under conditions of oxidative stress MTF-1 is activated and binds to MRE regions with the consensus sequence TGCRCNC and initializes the gene transcription.[36] A recent study has shown that antioxidant response element-mediated expression of MTs is preferentially activated by nuclear respiratory factor 1 (Nrf1).[37]

4 MT1A polymorphisms

In terms of human MT1A polymorphisms, according to the NCBI database of polymorphisms (http://www.ncbi.nlm.nih.gov/snp/), 41 human SNPs are identified in the *MT1A* gene region (from the 5′ untranslated region (5′UTR) to the 3′ untranslated region (3′UTR)). According to this database, one is located in the 5′UTR, 6 in the coding sequence, 27 in introns, and 7 in 3′UTR. Of these, three polymorphisms were mentioned in the literature to have a significant impact on physiological and pathophysiological processes (as of January 2013)[38] (Fig. 2).

4.1 MT1A polymorphism rs11640851

rs11640851 is a c.80C>A single nucleotide polymorphism (80 nucleotides from the beginning of the exon) located in the *MT1A* coding region. It leads to an amino acid change (Thr27Asn), and can therefore be described as non-synonymous (two different polypeptide sequences can be produced). This polymorphism was associated with longevity in the Italian population and the A allele carriers were predisposed to longevity.[38a] In contrast, C allele carriers were predisposed to the development of cardiovascular disease and type 2 diabetes (T2DM).[38b] Concomitantly, older women with the CC genotype showed higher zinc release by MT (detected by a Zinpyr-1 fluorescent probe in the presence of a nitric oxide donor), reduced MT levels and low IL-6 plasma concentrations. MTs induction and zinc metabolism are essential for keeping the inflammatory status under control and for achieving healthy longevity.[38b]

4.2 MT1A polymorphism rs8052394

This is a non-synonymous polymorphism of the *MT1A* gene, which is located 152 nucleotides from the first codon (ATG) (c.152A>G) and leads to an amino acid change Lys51Arg. Frequency of the rs8052394 G allele was significantly associated with the incidence of the type 2 diabetes mellitus (T2DM).[38c] Significant differences in the distribution of genotypes and allelic frequencies between T2DM patients and controls were found. Frequency of GA or GG carriers in T2DM groups compared with the control was increased.[38c] Serum superoxide dismutase (SOD) activity was significantly lower in GG or GA carriers than in AA carriers in diabetic patients.[38c] SOD catalyzes the conversion of superoxide into oxygen and hydrogen peroxide and represents an important antioxidant defense mechanism against oxidative stress. DM patients overproduce superoxide and their antioxidant system is usually weakened. As a result, damage in multiple organs, such as renal injuries or diabetic cardiomyopathy, occurs.[39] Furthermore, the rs8052394 A allele was associated with an increased risk of oral squamous cell carcinoma (OSCC). The AA genotype is associated with alteration of homeostasis of zinc and copper, which may affect molecules containing one of those metals, such as p53. The abnormal expression of MT may also affect its antioxidant role.[38d] Furthermore Wang *et al.* found, that rs8052394 GA and GG carriers with increased methylmercury (MeHg) intake had lower levels of mercury in their hair compared to subjects with the AA genotype.[38e]

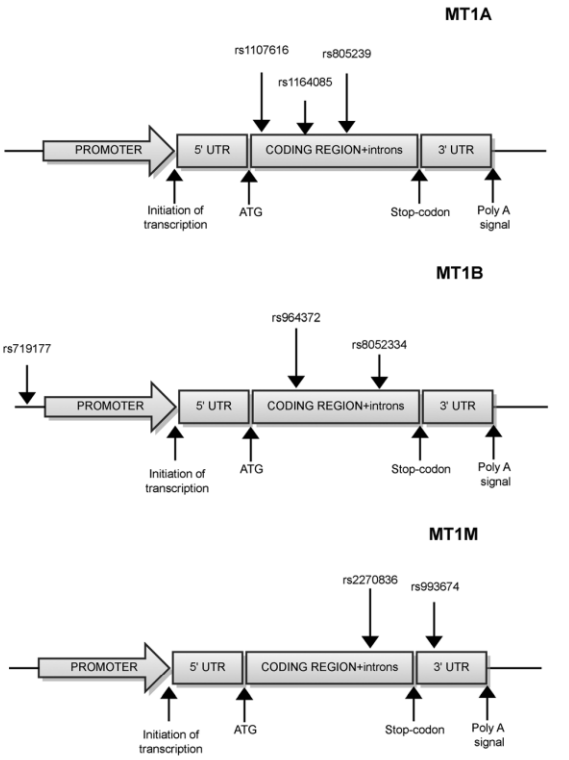

Fig. 2 Metallothionein-1 polymorphisms. Localization of clinically relevant single nucleotide polymorphisms (SNPs) in MT genes. SNP names according to NCBI dbSNP. UTR – untranslated region, ATG – start codon.

4.3 MT1A polymorphism rs11076161

This SNP (c. 29-28A>G) is a polymorphism in the first intron of *MT1A*. Yang *et al.* found that rs11076161 is significantly related to the occurrence of diabetic neuropathy in the T2DM patients and is explained by the decreased neuronal protection against oxidative stress.[38c] rs11076161 A allele carriers also showed a protective trend against oral squamous cell carcinoma (OSCC, odds ratio (OR) = 0.53).[38d]

5 MT1B polymorphisms

55 human SNPs were identified in the *MT1B* gene region according to the NCBI database (as of January 2013). Of these,

two are located in the 5′UTR, 15 in the coding sequence, 27 in introns, and 11 in the 3′UTR region. Three of these polymorphisms (rs964372, rs8052394, and rs7191779) have a significant association with diseases (see below)[38c,d,40] (Fig. 2).

5.1 MT1B polymorphism rs964372

This SNP is located in the *MT1B* intron 1 (c.28+137C>G). Significant association was observed between this SNP and decreased utilization of fatty acids in T2DM patients.[38c] These carriers were characterized by hyperlipidemia with increased serum triglycerides and neuropathy. Furthermore, a protective trend was observed between OSCC and rs964372 C allele carriers (OR = 0.49).[38d] Increased risk of hepatocellular carcinoma was also observed in individuals carrying haplotype AGT of the *MT1A* rs8052394 A allele, the *MT1B* rs964372 G allele, and the *MT1B* rs8052334 T allele (2.25-fold) compared to the most common ACT haplotype.[40] In particular, this risk was highlighted in smokers carrying the AGT haplotype (a 6.72-fold increased risk of HCC development). A possible explanation is the different efficiency of individual MT1Bs in coping with oxidative stress induced by smoking.[40]

5.2 MT1B polymorphism rs8052334

This SNP is located in the *MT1B* intron 2 (c.95-68T>C). As indicated above, increased risk of hepatocellular carcinoma was observed in individuals carrying haplotype AGT of the *MT1A* rs8052394 A allele, the *MT1B* rs964372 G allele, and the *MT1B* rs8052334 T allele in smokers.[40]

5.3 MT1B polymorphism rs7191779

This SNP is located upstream of the *MT1B* gene region on chromosome 16 (c.-1975C>G). Similarly, rs7191779 C allele carriers also showed a protective trend against OSCC (OR = 0.36).[38d]

6 MT1M polymorphisms

MT1M, another MT superfamily gene is transcriptionally regulated by both heavy metals and glucocorticoids. The *MT1M* gene was shown to induce changes of the cell cycle and activate the NF-κB pathway in Hep-G2 cells.[41] In total, 29 SNPs were identified, two of which are located in the 5′UTR, 10 in the coding sequence, 12 in introns, and 5 in the 3′UTR region. Two of them were associated with a disease[38e] (Fig. 2).

6.1 MT1M polymorphism rs2270836

rs2270836 is an intron 2 SNP in the *MT1M* gene (c.95-49G>A). Wang *et al.* found a significant effect of the minor homozygote genotype AA of *MT1M* (rs2270836) on urinary Hg levels. Multivariate regression analysis showed that subjects with the AA genotype had lower urinary mercury levels than those with the GG genotype because the binding of heavy metals varies depending on the molecular structures of MTs.[38e]

6.2 MT1M polymorphism rs9936741

This is a 3′UTR single nucleotide polymorphism at the 327th position of the *MT1M* mRNA sequence (c.*31T>C). As reported by Wang *et al.*, subjects with the TT genotype had lower hair mercury levels than subjects with TC and CC genotypes, respectively, after controlled MeHg intake.[38e]

7 Other functional MT1 polymorphisms

We found a high level of inconsistency between databases with regard to MT1 polymorphisms. Hence, the data from NCBI dbSNP are reported in this review. In case no polymorphisms are indexed in the NCBI dbSNP database, the SNPper database entry is mentioned. To date, there is no evidence of polymorphisms other than those mentioned to be associated with any given pathological condition. However, the number of polymorphisms without known effects was identified for MT1s. There were 13 coding, 4 in 5′UTR, 19 intron and 2 in 3′UTR in the *MT1F* gene (according to NCBI), 3 coding, 3 in 5′UTR, 10 intron and 14 in 3′UTR in the *MT1G* gene (according to SNPper, no information in NCBI), 19 coding, 3 in 5′UTR, 29 intron and 8 in 3′UTR in the *MT1H* gene (according to NCBI), and 6 coding, 3 in 5′UTR, 34 intron and 8 in 3′UTR in the *MT1X* gene (according to NCBI).

8 MT2A polymorphisms

According to NCBI (dbSNP), 24 human SNPs were identified in the *MT2A* gene region, 4 of them are located in the 5′UTR, 7 in the coding sequence, 9 in introns and 4 in the 3′UTR region (January 2013). Three *MT2A* polymorphisms with significant impact on the physiological and pathophysiological processes were mentioned in recent publications[23c,38a,c,e,42] (Fig. 3).

8.1 MT2A polymorphism rs28366003

rs28366003 is an A/G substitution located in the center of the MREa-like consensus sequence TGCACTC (c.-77A>G). This polymorphism was studied in Japanese, Polish, and Turkish populations. The genotype frequencies of AA, AG, and GG were identified in these studies as follows: 82%, 17%, and 0.9% in the Japanese, 88.9%, 10.6%, and 0.5% in the Polish, and 87%, 12.3%, and 0.7% in the Turkish population.[42a–c] McElroy *et al.* determined the frequency of the A and G alleles in Caucasian and Afro-American females in the Midwestern United States. The frequency of the G allele was 1.1% in Afro-Americans and 6.4% in Caucasians, which was less frequent than the Japanese and Turkish populations.[43] The exact effect of this polymorphism is still not fully understood. Since this SNP position is located in the 5′ regulation region, it is possible that the A/G substitution produces allele-specific *MT2A* gene expression. Using reporter-gene assay with HEK293 cells, Kita *et al.* observed that this SNP inhibits the binding of nuclear proteins to the core promoter region of the *MT2A* gene. As a result, this polymorphism should decrease the induction of gene transcription. It was confirmed that this SNP reduced

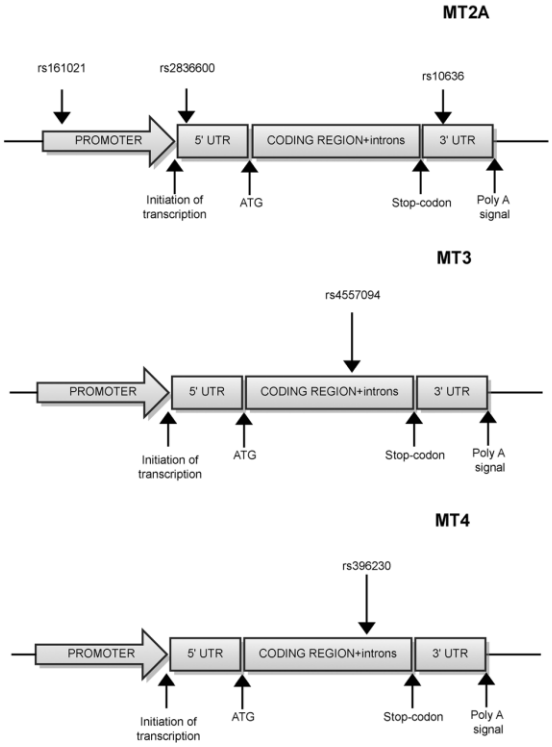

Fig. 3 Metallothionein-2, -3 and -4 polymorphisms. Localization of clinically relevant single nucleotide polymorphisms (SNPs) in MT genes. SNP names according to NCBI dbSNP. UTR – untranslated region, ATG – start codon.

cadmium-induced transcription of the *MT2A* gene in the HEK293cells.[42a]

Kayaalti *et al.* in the study of metal levels in kidney autopsies found considerably high accumulation of Cd in individuals having AG and GG genotypes compared with individuals having the AA genotype.[38a] Furthermore, the G allele carriers also had higher blood levels of cadmium and lead and lower levels of zinc.[23c] The critical tissue level of cadmium is 200 μg g^{-1} and exceeding this limit may cause renal dysfunction.[44] Absorption of the Cd and Pb is also associated with a decrease in Zn, as a result of the antagonistic relationships between these elements.[23b] Consequently, rs28366003 SNP could become a promising indicator of increased risk of diseases associated with the exposure to Cd and ROS. Nevertheless, an association between *MT2A* promoter polymorphisms and sporadic amyotrophic lateral sclerosis (ALS) in a Japanese population was not confirmed although reactive oxygen species (ROS) are assumed to be involved in the pathogenesis of ALS.[45]

As was shown in another study, maternal blood Cd levels were statistically higher in women with the AG genotype compared to the AA genotype. In contrast, placental Cd levels were significantly higher in mothers with the AA rather than the AG genotype.[42d] Another study suggested that blood lead levels of the heterozygote genotype (AG) in pregnant women were statistically higher than those of the homozygote genotype (AA) ($P < 0.05$).[46]

8.1.1 rs28366003 and ageing. The remodeling capacity of the immune responses during stress (named immune plasticity) is fundamental to reaching successful ageing. Zinc and MT homeostasis is crucial in conferring immune plasticity, taking also into account that satisfactory zinc ion bioavailability is observed in human centenarians. MT expression, stimulated *via* IL-6 and glucocorticoids, seems to be one of the markers of immunosenescence.[42e] Recent studies show the link between the rs28366003 polymorphism and longevity in the Turkish population. These data support that the AA genotype may be more beneficial for longevity.[38a,42b]

8.1.2 rs28366003 and cancer risk. Several lines of evidence indicate that MTs play a role in carcinogenesis and chemoresistance of cancer cells.[47] Although the role of MTs in cancer remains controversial, their overexpression is suggested to increase metastatic potency, resistance to therapy, and a poor prognosis at least in some malignancies.[26a,e,48]

Since the rs28366003 SNP is located in the center of the MRE consensus sequence, the A/G substitution might alter *MT2A* gene expression. As a result, the MT protein level could decrease, and differences in cancer development and prognosis might be expected in these allele carriers.

The association between rs28366003 and prostate cancer was shown in a study of the Polish population.[42c] Compared to homozygous common allele carriers, heterozygous carriers had a significantly increased risk of prostate cancer (OR = 2.30). The association between SNP in *MT2A* and clinicopathological parameters, such as the prostate-specific antigen (PSA) level, Gleason score (histological grading), tumour stage, and prostate volume, was analyzed. The statistically significant association was only found between rs28366003 and the Gleason score. The AG genotype and the G allele were more frequently found in patients with Gleason score >7 tumors.[42c]

8.2 MT2A polymorphism rs1610216

Polymorphism rs1610216 is located in the promoter region of the *MT2A* gene (c.-284C>T). The genotype frequencies of AA, AG, and GG are 90.5%, 0.0%, and 9.5%, respectively, as shown in the healthy Bulgarian population.[42k] Because of the position in the promoter, this SNP could influence the level of MT expression. Overexpression of MT in various metabolic organs was shown to reduce hyperglycemia-induced oxidative stress, organ specific diabetic complications like diabetic cardiomyopathy,[49] nephropathy,[50] and DNA damage in diabetic experimental animals, as shown in comparison to MT-knockout mice.[51]

According to Giacconi *et al.*, the AA, rather than the AG, genotype of the rs1610216 polymorphism is associated with chronic inflammation (higher plasma levels of IL-6), hyperglycaemia, enhanced glycosylated hemoglobin (HbA1c), and marked zinc deficiency in atherosclerosis patients. AA patients are at higher risk of developing type 1 DM in association with atherosclerosis (OR = 2.6) and related complications, such as ischaemic cardiomyopathy (OR = 12.6). Nevertheless, no association between this polymorphism and hypertension has been found.[42h]

Conversely, in the Bulgarian cohort, the G allele (compared to the AA-genotype) was identified as an independent predictor for the development of diabetes without cardiovascular complications (OR = 7.56).[42k]

8.3 MT2A polymorphism rs10636

This is a 3′ untranslated region *MT2A* single nucleotide polymorphism (c.*77G>C). The genotype frequencies are 58.3%, 33.3%, and 8.3% for the GG, GC, and CC alleles in the Caucasian population, respectively.[42g]

Yang *et al.* found that rs10636 is significantly related to the occurrence of diabetic neuropathy and hyperlipidemia in the T2DM patients.[38c] An earlier study compared rs10636 *MT2A* polymorphisms in 288 patients with atherosclerosis and 218 healthy elderly controls. The GG carriers had a higher risk of atherosclerosis than controls. Furthermore, a significant decrease in intracellular zinc, decreased serum zinc and copper levels, and increased inflammatory cytokines were shown in (C–) carriers. A major incidence of soft carotid plaques was also significantly associated with this allele. This MT2A polymorphism influences inflammatory status, zinc availability, NK cell cytotoxicity, and trace element levels, all of which may promote plaque development.[42i]

In another research, Gundacker and co-workers[42g] studied the association between the rs10636 in *MT2A* and Pb levels. They found a negative association between non-wild type variants and blood lead.[42g] According to the work of Giacconi *et al.*,[42i] the C allele of rs10636 is also associated with decreased NK cell cytotoxicity and increased MCP-1 (monocyte chemotactic protein-1) levels in patients suffering from carotid artery stenosis. Zinc deficiency may be responsible for decreased NK cell activity and enhanced plasma concentrations of MCP-1. MCP-1 was increased in atherosclerotic lesions in humans as well as in animal models.[42i] Chen *et al.* identified a weak association of blood cadmium levels and the rs10636 allele variant in females living in the densely polluted conditions.[42j] Multivariate regression analysis showed that subjects with the rsl0636 CC genotype had lower urinary mercury levels than those with the GG genotype.[38e]

9 MT3 polymorphisms

MT3 (also called the growth inhibitory factor, GIF, GIFB or GRIF) is expressed primarily in the central nervous system and small amounts of protein can also be traced in the pancreas and intestines.[16b] MT3 binds Zn and Cd ions more weakly than MT2.[52] MT3 functions as a growth inhibitory factor. It plays a major role in the organization and apoptosis of brain cells, and, compared to other MT superfamily members, plays unique biological roles in various neuropathological disorders.[19,53]

Inter alia, MT3 was revealed as a neuron outgrowth inhibitor in Alzheimer's disease.[53,54] In total, 32 human SNPs were identified according to the NCBI, 3 of which are located in the 5′UTR region, 4 in the coding sequence, 15 in introns, and 10 in the 3′UTR region. Only one relevant *MT3* polymorphism with a significant impact on the physiological and pathophysiological processes was mentioned in recent publications[55] (Fig. 3).

9.1 MT3 polymorphism rs45570941

This polymorphism, which is an intron 2 SNP in the *MT3* gene (c.97+377G>C), was studied in a Chinese population of autistic children. Significant differences in the frequencies of rs45570941 genotypes and alleles between autistic children and controls were found[55b] (χ^2 = 13.569, $P < 0.05$ and χ^2 = 6.89, $P < 0.05$, respectively). Heavy metal toxicity was proposed as a hypothetical cause of autism. More specifically, the dysfunction of the MT synthesis and activity may be the major driver of this disorder. Numerous heavy metals, including mercury, lead, and arsenic, were linked with symptoms that resemble the neurological symptoms of autism.[55a]

10 MT4 polymorphisms

The MT4 gene is located about 20 kb upstream from the MT3 gene and is expressed solely in the epithelia of upper parts of the digestive tract, in the footpads, and in the neonatal skin.[56] Histologically, *MT4* mRNA was detected in the differentiating spinous layer of cornified epithelia, whereas in the basal layer MT1 expression prevailed.[56] Furthermore, MT4 showed better Cu binding properties than MT1.[57]

According to NCBI dbSNP, two polymorphisms are located in the coding sequence and 55 in introns. Of these, only one *MT4* polymorphism (rs396230) is known to have a significant impact on the physiological and pathophysiological processes[58] (Fig. 3).

10.1 MT4 polymorphism rs396230

This is an intron 2 SNP (c.98-137 A>G) in the *MT4* gene. Since MT4 is involved in the detoxification of lead, rs396230 genotypes and renal functions were investigated. Serum creatinine, urea,

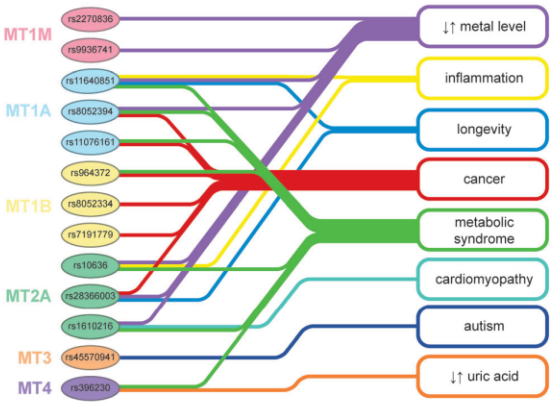

Fig. 4 Association of metallothionein polymorphisms with pathological conditions and laboratory changes. See the distinct relation between polymorphisms, metal level change, and disease occurrence. Polymorphism names are in the rs NCBI format. Clinical/laboratory conditions and MT genes are color-coded. Most frequent linkage includes metabolic syndrome-related pathologies (including diabetes and its complications, atherosclerosis, high blood pressure and dyslipoproteinaemia), disbalance of various metal levels, and cancers. For a more detailed view, see Table 1. ↑↓ – alteration of concentration.

Table 1 Metallothionein polymorphisms associated with diseases. Metallothionein single nucleotide polymorphism names according to the NCBI SNP database. Association with pathological conditions and cited references are listed below. OSCC – oral squamous cell carcinoma, T2DM – type 2 DM, HCC – hepatocellular carcinoma

Gene	NCBI rs number	SNP	Associated with	Ref.
MT1A	rs11640851	Non-synonymous in the coding region	Longevity	38*a*
			Cardiovascular disease	38*b*
			T2DM	38*b*
			MT levels	38*b*
			IL-6 plasma concentrations	38*b*
	rs8052394	Non-synonymous in the coding region	T2DM	38*c*
			Serum superoxide dismutase	38*c*
			OSCC	38*d*
			Hair mercury levels	38*e*
			HCC	40
	rs11076161	In intron	Diabetic neuropathy	38*c*
			OSCC	38*d*
MT1B	rs964372	In intron	Hyperlipidemia	38*c*
			Diabetic neuropathy	38*c*
			OSCC	38*d*
			HCC	40
	rs8052334	In intron	HCC	40
	rs7191779	Upstream gene region	OSCC	38*d*
MT1M	rs2270836	In intron	Urinary Hg level	38*e*
	rs9936741	In 3′UTR	Hair Hg levels	38*e*
MT2A	rs28366003	In the 5′UTR regulatory region	Cd blood levels	23*c*
			Pb blood levels	23*c*
			Zn blood levels	23*c*
			Autopsy kidney Cd levels	38*a*
			Maternal blood Cd levels	42*d*
			Placental Cd levels	42*d*
			Maternal blood Pb levels	46
			Longevity	59
			Prostate cancer	42*c*
	rs10636	In 3′UTR	Diabetic neuropathy	38*c*
			Hyperlipidemia in T2DM	38*c*
			Atherosclerosis	42*i*
			Intracellular Zn availability	42*i*
			Serum Zn and Cu levels	42*i*
			Inflammatory cytokines levels	42*i*
			Soft carotid plaques incidence	42*i*
			Pb blood levels	42*g*
			NK cell cytotoxicity	42*i*
			Monocyte chemotactic protein-1	42*i*
			Urinary Hg levels	38*e*
			Cd blood levels	42*j*
	rs1610216	In the promoter region	Chronic inflammation	42*h*
			Hyperglycaemia	42*h*
			Glycated hemoglobin	42*h*
			Zinc deficiency	42*h*
			NIDDM	42*h*
			Ischaemic cardiomyopathy	42*h*
			Development of diabetes	42*k*
MT3	rs45570941	In intron	Autism in children	55*b*
MT4	rs396230	In intron	Blood pressure	58
			Serum uric acid	58

and uric acid levels were measured by Chen *et al.* as indicators of renal function in a cohort of lead battery-recycling factory workers (65.5% had AA, 15.9% AG, and 18.6% GG genotypes). Workers with the AG genotype had higher serum creatinine and urea levels. Furthermore, after adjusting potential confounders, blood pressure and serum uric acid values showed a positive correlation with AA, AG, and GG genotypes (AA genotype strongest). Workers with the G allele had blood pressures more than 10 mmHg higher than those with the AA genotype.[58]

11 Conclusion

MTs play an important role in the cell transportation and management of metals and have a crucial role in the

detoxification processes. MTs expression and their ability to bind metals can be influenced by changes at the DNA level, such as SNPs. In addition to changes in metal levels, some single nucleotide polymorphisms (SNPs) were found to be associated with predisposition to various diseases including cancer, cardiovascular diseases, and faster aging, confirming the key role of MTs in organisms against oxidative stress and toxic metals (Fig. 4).

Although there are numerous association studies investigating the effects of MT polymorphisms in humans, the large level of nomenclature inaccuracy causes an unprecedented degree of confusion in the literature. In addition, the classification of MTs with a clear separation between functional genes and pseudogenes is lacking. Using a systematic approach, we identified in total 388 MT SNPs, of which 18 studies linked 13 MT SNPs in 6 MT paralogs with various pathological conditions. Of these, the most frequent linkage includes metabolic syndrome-related pathologies (including diabetes and its complications, atherosclerosis, high blood pressure and dyslipoproteinaemia) and disbalance of various metal levels, each associated with 7 SNPs. These disorders were followed by cancers, associated with 6 SNPs. The largest numbers of associations have been demonstrated in MT1A and MT2A. These findings emphasize the role of MT in the development and progression of a number of pathological conditions. In addition, the possibility of using MT polymorphisms as risk indicators for a large spectrum of diseases is obvious. However, it is worth noting that because some studies show associations in the laboratory setting only, while others investigate true clinical conditions, there are still missing pieces of the puzzle that would allow a more comprehensive understanding of the issue. Thus, association studies with a more systematic approach are highly desirable.

Conflict of interest

The authors declare they have no competing interests as defined by *Metallomics*, or other interests that might be perceived to influence the results and discussion reported in this paper.

Acknowledgements

Financial support from CEITEC CZ.1.05/1.1.00/02.0068, doc CEITEC.02/2012 (JG), and project for conceptual development of research organization 00064203 is greatly acknowledged.

References

1 (*a*) J. Busciglio and B. A. Yankner, Apoptosis and increased generation of reactive oxygen species in Downs-syndrome neurons in-vitro, *Nature*, 1995, **378**, 776–779, DOI: 10.1038/378776a0; (*b*) J. C. A. Marr, H. L. Bergman, J. Lipton and C. Hogstrand, Differences in relative sensitivity of naive and metals-acclimated brown and rainbow-trout exposed to metals representative of the clark-fork river, montana, *Can. J. Fish. Aquat. Sci.*, 1995, **52**, 2016–2030, DOI: 10.1139/f95-793; (*c*) S. Silver, Bacterial resistances to toxic metal ions – a review, *Gene*, 1996, **179**, 9–19, DOI: 10.1016/s0378-1119(96)00323-x; (*d*) T. K. S. Janssens, D. Roelofs and N. M. van Straalen, Molecular mechanisms of heavy metal tolerance and evolution in invertebrates, *Insect Sci.*, 2009, **16**, 3–18, DOI: 10.1111/j.1744-7917.2009.00249.x.

2 (*a*) V. Adam, I. Fabrik, T. Eckschlager, M. Stiborova, L. Trnkova and R. Kizek, Vertebrate metallothioneins as target molecules for analytical techniques, *TrAC, Trends Anal. Chem.*, 2010, **29**, 409–418, DOI: 10.1016/j.trac.2010.02.004; (*b*) V. Adam, J. Petrlova, J. Wang, T. Eckschlager, L. Trnkova and R. Kizek, Zeptomole electrochemical detection of metallothioneins, *PLoS One*, 2010, **5**, e11441, DOI: 10.1371/journal.pone.0011441; (*c*) S. Krizkova, I. Fabrik, V. Adam, P. Hrabeta, T. Eckschlager and R. Kizek, Metallothionein – a promising tool for cancer diagnostics, *Br. Med. J.*, 2009, **110**, 93–97.

3 B. Y. Lee, D. H. Shin, S. Cho, K. S. Seo and H. Kim, Genome-wide analysis of copy number variations reveals that aging processes influence body fat distribution in Korea Associated Resource (KARE) cohorts, *Hum. Genet.*, 2012, **131**, 1795–1804, DOI: 10.1007/s00439-012-1203-1.

4 P. Seibold, R. Hein, P. Schmezer, P. Hall, J. J. Liu, N. Dahmen, D. Flesch-Janys, O. Popanda and J. Chang-Claude, Polymorphisms in oxidative stress-related genes and postmenopausal breast cancer risk, *Int. J. Cancer*, 2011, **129**, 1467–1476, DOI: 10.1002/ijc.25761.

5 Y. Koga, M. Pelizzola, E. Cheng, M. Krauthammer, M. Sznol, S. Ariyan, D. Narayan, A. M. Molinaro, R. Halaban and S. M. Weissman, Genome-wide screen of promoter methylation identifies novel markers in melanoma, *Genome Res.*, 2009, **19**, 1462–1470, DOI: 10.1101/gr.091447.109.

6 L. Marselli, J. Thorne, S. Dahiya, D. C. Sgroi, A. Sharma, S. Bonner-Weir, P. Marchetti and G. C. Weir, Gene expression profiles of beta-cell enriched tissue obtained by laser capture microdissection from subjects with type 2 diabetes, *PLoS One*, 2010, **5**, e11499, DOI: 10.1371/journal.pone.0011499.

7 M. Hlavna, M. Raudenska, K. Hudcova, J. Gumulec, M. Sztalmachova, V. Tanhauserova, P. Babula, V. Adam, T. Eckschlager, R. Kizek and M. Masarik, MicroRNAs and zinc metabolism-related gene expression in prostate cancer cell lines treated with zinc(II) ions, *Int. J. Oncol.*, 2012, **41**, 2237–2244, DOI: 10.3892/ijo.2012.1655.

8 J. T. den Dunnen and S. E. Antonarakis, Mutation nomenclature extensions and suggestions to describe complex mutations: a discussion, *Hum. Mutat.*, 2000, **15**, 7–12, DOI: 10.1002/(SICI)1098-1004(200001)15:1<7::AID-HUMU4>3.0.CO;2-N.

9 F. S. Collins, L. D. Brooks and A. Chakravarti, A DNA polymorphism discovery resource for research on human genetic variation, *Genome Res.*, 1998, **8**, 1229–1231.

10 (*a*) E. Alexov, Numerical calculations of the pH of maximal protein stability – the effect of the sequence composition and three-dimensional structure, *Eur. J. Biochem.*, 2004, **271**, 173–185, DOI: 10.1046/j.1432-1033.2003.03917.x; (*b*) V. Chelliah, L. Chen, T. L. Blundell and S. C. Lovell, Distinguishing structural and functional restraints in evolution in order to identify interaction sites, *J. Mol. Biol.*, 2004, **342**, 1487–1504, DOI: 10.1016/j.jmb.2004.08.022; (*c*) D. Gilis and M. Rooman,

Predicting protein stability changes upon mutation using database-derived potentials: solvent accessibility determines the importance of local *versus* non-local interactions along the sequence, *J. Mol. Biol.*, 1997, **272**, 276–290, DOI: 10.1006/jmbi.1997.1237.

11 J. V. Chamary, J. L. Parmley and L. D. Hurst, Hearing silence: non-neutral evolution at synonymous sites in mammals, *Nat. Rev. Genet.*, 2006, **7**, 98–108, DOI: 10.1038/nrg1770.

12 H. Akashi, Synonymous codon usage in *Drosophila-melanogaster* – natural-selection and translational accuracy, *Genetics*, 1994, **136**, 927–935.

13 (*a*) Y. Xing and C. Lee, Assessing the application of *K*a/*K*s ratio test to alternatively spliced exons, *Bioinformatics*, 2005, **21**, 3701–3703, DOI: 10.1093/bioinformatics/bit613; (*b*) A. G. Nackley, S. A. Shabalina, I. E. Tchivileva, K. Satterfield, O. Korchynskyi, S. S. Makarov, W. Maixner and L. Diatchenko, Human catechol-*O*-methyltransferase haplotypes modulate protein expression by altering mRNA secondary structure, *Science*, 2006, **314**, 1930–1933, DOI: 10.1126/science.1131262.

14 (*a*) C. C. Chang and P. C. Huang, Semi-empirical simulation of Zn/Cd binding site preference in the metal binding domains of mammalian metallothionein, *Protein Eng.*, 1996, **9**, 1165–1172, DOI: 10.1093/protein/9.12.1165; (*b*) M. Fedurco and I. Sestakova, Adsorption of Cd,Zn-metallothionein on covered Hg electrodes and its voltammetric determination, *Bioelectrochem. Bioenerg.*, 1996, **40**, 223–232, DOI: 10.1016/0302-4598(96)01914-9; (*c*) X. L. Yu, M. Wojciechowski and C. Fenselau, Assessment of metals in reconstituted metallothioneins by electrospray mass-spectrometry, *Anal. Chem.*, 1993, **65**, 1355–1359, DOI: 10.1021/ac00058a010.

15 (*a*) J. Abel and N. Deruiter, Inhibition of hydroxyl-radical-generated DNA-degradation by metallothionein, *Toxicol. Lett.*, 1989, **47**, 191–196, DOI: 10.1016/0378-4274(89)90075-1; (*b*) L. Cai, J. B. Klein and Y. J. Kang, Metallothionein inhibits peroxynitrite-induced DNA and lipoprotein damage, *J. Biol. Chem.*, 2000, **275**, 38957–38960, DOI: 10.1074/jbc.C000593200; (*c*) P. J. Thornalley and M. Vasak, Possible role for metallothionein in protection against radiation-induced oxidative stress – kinetics and mechanism of its reaction with superoxide and hydroxyl radicals, *Biochim. Biophys. Acta*, 1985, **827**, 36–44, DOI: 10.1016/0167-4838(85)90098-6.

16 (*a*) P. Babula, M. Masarik, V. Adam, T. Eckschlager, M. Stiborova, L. Trnkova, H. Skutkova, I. Provaznik, J. Hubalek and R. Kizek, Mammalian metallothioneins: properties and functions, *Metallomics*, 2012, **4**, 739–750, DOI: 10.1039/c2mt20081c; (*b*) E. Tokuda, S. I. Ono, K. Ishige, A. Naganuma, Y. Ito and T. Suzuki, Metallothionein proteins expression, copper and zinc concentrations, and lipid peroxidation level in a rodent model for amyotrophic lateral sclerosis, *Toxicology*, 2007, **229**, 33–41, DOI: 10.1016/j.tox.2006.09.011; (*c*) J. W. Bauman, J. Liu, Y. P. Liu and C. D. Klaassen, Increase in metallothionein produced by chemicals that induce oxidative stress, *Toxicol. Appl. Pharmacol.*, 1991, **110**, 347–354, DOI: 10.1016/s0041-008x(05)80017-1; (*d*) G. K. Andrews, Regulation of metallothionein gene expression by oxidative stress and metal ions, *Biochem. Pharmacol.*, 2000, **59**, 95–104, DOI: 10.1016/s0006-2952(99)00301-9.

17 M. Karin, R. L. Eddy, W. M. Henry, L. L. Haley, M. G. Byers and T. B. Shows, Human metallothionein genes are clustered on chromosome-16, *Proc. Natl. Acad. Sci. U. S. A.*, 1984, **81**, 5494–5498, DOI: 10.1073/pnas.81.17.5494.

18 (*a*) F. A. Stennard, A. F. Holloway, J. Hamilton and A. K. West, Characterization of 6 additional human metallothionein genes, *Biochim. Biophys. Acta, Gene Struct. Expression*, 1994, **1218**, 357–365, DOI: 10.1016/0167-4781(94)90189-9; (*b*) A. K. West, R. Stallings, C. E. Hildebrand, R. Chiu, M. Karin and R. I. Richards, Human metallothionein genes – structure of the functional locus at 16q13, *Genomics*, 1990, **8**, 513–518, DOI: 10.1016/0888-7543(90)90038-v; (*c*) Z. M. Liu, G. G. Chen, C. K. Y. Shum, A. C. Vlantis, M. G. Cherlan, J. Koropatnick and C. A. van Hasselta, Induction of functional MT1 and MT2 isoforms by calcium in anaplastic thyroid carcinoma cells, *FEBS Lett.*, 2007, **581**, 2465–2472, DOI: 10.1016/j.febslet.2007.04.049.

19 Y. Uchida, F. Gomi, T. Masumizu and Y. Miura, Growth inhibitory factor prevents neurite extension and the death of cortical neurons caused by high oxygen exposure through hydroxyl radical scavenging, *J. Biol. Chem.*, 2002, **277**, 32353–32359, DOI: 10.1074/jbc.M111263200.

20 G. Meloni, K. Zovo, J. Kazantseva, P. Palumaa and M. Vasak, Organization and assembly of metal-thiolate clusters in epithelium-specific metallothionein-4, *J. Biol. Chem.*, 2006, **281**, 14588–14595, DOI: 10.1074/jbc.M601724200.

21 R. Faraonio, P. Moffatt, O. LaRochelle, H. M. Schipper, R. S-Arnaud and C. Seguin, Characterization of *cis*-acting elements in the promoter of the mouse metallothionein-3 gene – activation of gene expression during neuronal differentiation of P19 embryonal carcinoma cells, *Eur. J. Biochem.*, 2000, **267**, 1743–1753, DOI: 10.1046/j.1432-1327.2000.01167.x.

22 (*a*) Z. Y. Huang, Q. Zhang, J. Chen, Z. X. Zhuang and X. R. Wang, Bioaccumulation of metals and induction of metallothioneins in selected tissues of common carp (*Cyprinus carpio* L.) co-exposed to cadmium, mercury and lead, *Appl. Organomet. Chem.*, 2007, **21**, 101–107, DOI: 10.1002/aoc.1167; (*b*) M. F. McAleer and R. S. Tuan, Metallothionein overexpression in human trophoblastic cells protects against cadmium-induced apoptosis, *In Vitro Mol. Toxicol.*, 2001, **14**, 25–42.

23 (*a*) Y. P. Liu, J. Liu, S. M. Habeebu, M. P. Waalkes and C. D. Klaassen, Metallothionein-I/II null mice are sensitive to chronic oval cadmium-induced nephrotoxicity, *Toxicol. Sci.*, 2000, **57**, 167–176, DOI: 10.1093/toxsci/57.1.167; (*b*) A. U. R. Memon, T. G. Kazi, H. I. Afridi, M. K. Jamali, M. B. Arain, N. Jalbani and N. Syed, Evaluation of zinc status in whole blood and scalp hair of female cancer patients, *Clin. Chim. Acta*, 2007, **379**, 66–70, DOI: 10.1016/j.cca.2006.12.009; (*c*) Z. Kayaalti, V. Aliyev and T. Soylemezogiu, The potential effect of metallothionein 2A-5 A/G single nucleotide polymorphism on blood

cadmium, lead, zinc and copper levels, *Toxicol. Appl. Pharmacol.*, 2011, **256**, 1–7, DOI: 10.1016/j.taap.2011.06.023; (*d*) T. Eckschlager, V. Adam, J. Hrabeta, K. Figova and R. Kizek, Metallothioneins and cancer, *Curr. Protein Pept. Sci.*, 2009, **10**, 360–375, DOI: 10.2174/138920309788922243.

24 (*a*) H. Goulding, B. Jasani, H. Pereira, A. Reid, M. Galea, J. A. Bell, C. W. Elston, J. F. Robertson, R. W. Blamey, R. A. Nicholson, K. W. Schmid and I. O. Ellis, Metallothionein expression in human breast-cancer, *Br. J. Cancer*, 1995, **72**, 968–972, DOI: 10.1038/bjc.1995.443; (*b*) H. G. Kim, J. Y. Kim, E. H. Han, Y. P. Hwang, J. H. Choi, B. H. Park and H. G. Jeong, Metallothionein-2A overexpression increases the expression of matrix metalloproteinase-9 and invasion of breast cancer cells, *FEBS Lett.*, 2011, **585**, 421–428, DOI: 10.1016/j.febslet.2010.12.030.

25 J. I. Izawa, M. Moussa, M. G. Cherian, G. Doig and J. L. Chin, Metallothionein expression in renal cancer, *Urology*, 1998, **52**, 767–772, DOI: 10.1016/s0090-4295(98)00323-9.

26 (*a*) J. Gumulec, M. Masarik, S. Krizkova, M. Hlavna, P. Babula, R. Hrabec, A. Rovny, M. Masarikova, J. Sochor, V. Adam, T. Eckschlager and R. Kizek, Evaluation of alpha-methylacyl-CoA racemase, metallothionein and prostate specific antigen as prostate cancer prognostic markers, *Neoplasma*, 2012, **59**, 191–200, DOI: 10.4149/neo_2012_025; (*b*) H. Wei, M. M. Desouki, S. Lin, D. Xiao, R. B. Franklin and P. Feng, Differential expression of metallothioneins (MTs) 1, 2, and 3 in response to zinc treatment in human prostate normal and malignant cells and tissues, *Mol. Cancer*, 2008, **7**, DOI: 10.1186/1476-4598-7-7; (*c*) J. Gumulec, M. Masarik, S. Krizkova, V. Adam, J. Hubalek, J. Hrabeta, T. Eckschlager, M. Stiborova and R. Kizek, Insight to physiology and pathology of zinc(II) ions and their actions in breast and prostate carcinoma, *Curr. Med. Chem.*, 2011, **18**, 5041–5051, DOI: 10.2174/092986711797636126; (*d*) M. Masarik, J. Gumulec, M. Hlavna, M. Sztalmachova, P. Babula, M. Raudenska, M. Pavkova-Goldbergova, N. Cernei, J. Sochor, O. Zitka, B. Ruttkay-Nedecky, S. Krizkova, V. Adam and R. Kizek, Monitoring of the prostate tumour cells redox state and real-time proliferation by novel biophysical techniques and fluorescent staining, *Integr. Biol.*, 2012, **4**, 672–684, DOI: 10.1039/c2ib00157h; (*e*) M. Masarik, J. Gumulec, M. Sztalmachova, M. Hlavna, P. Babula, S. Krizkova, M. Ryvolova, M. Jurajda, J. Sochor, V. Adam and R. Kizek, Isolation of metallothionein from cells derived from aggressive form of high-grade prostate carcinoma using paramagnetic antibody-modified microbeads off-line coupled with electrochemical and electrophoretic analysis, *Electrophoresis*, 2011, **32**, 3576–3588, DOI: 10.1002/elps.201100301; (*f*) S. Krizkova, M. Ryvolova, J. Hrabeta, V. Adam, M. Stiborova, T. Eckschlager and R. Kizek, Metallothioneins and zinc in cancer diagnosis and therapy, *Drug Metab. Rev.*, 2012, **44**, 287–301, DOI: 10.3109/03602532.2012.725414; (*g*) V. Pekarik, J. Gumulec, M. Masarik, R. Kizek and V. Adam, Prostate cancer, miRNAs, metallothioneins and resistance to cytostatic drugs, *Curr. Med. Chem.*, 2013, **20**, 534–544, DOI: 10.2174/092986713804910102; (*h*) J. K. Choi, U. S. Yu, O. J. Yoo and S. Kim, Differential coexpression analysis using microarray data and its application to human cancer, *Bioinformatics*, 2005, **21**, 4348–4355, DOI: 10.1093/bioinformatics/bti722.

27 (*a*) S. Suemori, M. Shimazawa, K. Kawase, M. Satoh, H. Nagase, T. Yamamoto and H. Hara, Metallothionein, an endogenous antioxidant, protects against retinal neuron damage in mice, *Invest. Ophthalmol. Visual Sci.*, 2006, **47**, 3975–3982, DOI: 10.1167/iovs.06-0275; (*b*) K. Wakida, M. Shimazawa, I. Hozumi, M. Satoh, H. Nagase, T. Inuzuka and H. Hara, Neuroprotective effect of erythropoietin, and role of metallothionein-1 and -2, in permanent focal cerebral ischemia, *Neuroscience*, 2007, **148**, 105–114, DOI: 10.1016/j.neuroscience.2007.04.063; (*c*) M. Penkowa, S. Florit, M. Giralt, A. Quintana, A. Molinero, J. Carrasco and J. Hidalgo, Metallothionein reduces central nervous system inflammation, neuro degeneration, and cell death following kainic acid-induced epileptic seizures, *J. Neurosci. Res.*, 2005, **79**, 522–534, DOI: 10.1002/jnr.20387.

28 A. E. Michalska and K. H. A. Choo, Targeting and germ-line transmission of a null mutation at the metallothionein I-loci and II-loci in mouse, *Proc. Natl. Acad. Sci. U. S. A.*, 1993, **90**, 8088–8092, DOI: 10.1073/pnas.90.17.8088.

29 (*a*) B. A. Masters, E. J. Kelly, C. J. Quaife, R. L. Brinster and R. D. Palmiter, Targeted disruption of metallothionein-I and metallothionein-II genes increases sensitivity to cadmium, *Proc. Natl. Acad. Sci. U. S. A.*, 1994, **91**, 584–588, DOI: 10.1073/pnas.91.2.584; (*b*) L. L. Pearce, R. E. Gandley, W. P. Han, K. Wasserloos, M. Stitt, A. J. Kanai, M. K. McLaughlin, B. R. Pitt and E. S. Levitan, Role of metallothionein in nitric oxide signaling as revealed by a green fluorescent fusion protein, *Proc. Natl. Acad. Sci. U. S. A.*, 2000, **97**, 477–482, DOI: 10.1073/pnas.97.1.477; (*c*) J. Carrasco, M. Penkowa, H. Hadberg, A. Molinero and J. Hidalgo, Enhanced seizures and hippocampal neurodegeneration following kainic acid-induced seizures in metallothionein-I plus II-deficient mice, *Eur. J. Neurosci.*, 2000, **12**, 2311–2322, DOI: 10.1046/j.1460-9568.2000.00128.x.

30 (*a*) Y. Y. Yang, P. D. Robbins and J. S. Lazo, Differential transactivation of human metallothionein-IIa in cisplatin-resistant and -sensitive cells, *Oncol. Res.*, 1998, **10**, 85–98; (*b*) M. Karin, A. Haslinger, A. Heguy, T. Dietlin and T. Cooke, Metal-responsive elements act as positive modulators of human metallothionein-IIA enhancer activity, *Mol. Cell. Biol.*, 1987, **7**, 606–613.

31 M. P. Waalkes, M. J. Harvey and C. D. Klaassen, Relative in vitro affinity of hepatic metallothionein for metals, *Toxicol. Lett.*, 1984, **20**, 33–39, DOI: 10.1016/0378-4274(84)90179-6.

32 (*a*) R. D. Palmiter, Regulation of metallothionein genes by heavy-metals appears to be mediated by a zinc-sensitive inhibitor that interacts with a constitutively active transcription factor, MTF-1, *Proc. Natl. Acad. Sci. U. S. A.*, 1994, **91**, 1219–1223, DOI: 10.1073/pnas.91.4.1219; (*b*) L. J. Hager and R. D. Palmiter, Transcriptional regulation of mouse-liver

metallothionein-I gene by glucocorticoids, *Nature*, 1981, **291**, 340–342, DOI: 10.1038/291340a0.

33 W. Lee, A. Haslinger, M. Karin and R. Tjian, Activation of transcription by two factors that bind promoter and enhancer sequences of the human metallothionein gene and SV40, *Nature*, 1987, **325**, 368–372, DOI: 10.1038/325368a0.

34 A. Haslinger and M. Karin, Upstream promoter element of the human metallothionein-IIA gene can act like an enhancer element, *Proc. Natl. Acad. Sci. U. S. A.*, 1985, **82**, 8572–8576, DOI: 10.1073/pnas.82.24.8572.

35 F. Otsuka, A. Iwamatsu, K. Suzuki, M. Ohsawa, D. H. Hamer and S. Koizumi, Purification and characterization of a protein that binds to metal-responsive elements of the human metallothionein II(A) gene, *J. Biol. Chem.*, 1994, **269**, 23700–23707.

36 (*a*) M. Karin, A. Haslinger, H. Holtgreve, R. I. Richards, P. Krauter, H. M. Westphal and M. Beato, Characterization of DNA-sequences through which cadmium and glucocorticoid hormones induce human metallothionein-IIa gene, *Nature*, 1984, **308**, 513–519, DOI: 10.1038/308513a0; (*b*) K. Suzuki and S. Koizumi, Individual metal responsive elements of the human metallothionein-IIA gene independently mediate responses to various heavy metal signals, *Ind. Health*, 2000, **38**, 87–90, DOI: 10.2486/indhealth.38.87.

37 M. Ohtsuji, F. Katsuoka, A. Kobayashi, H. Aburatani, J. D. Hayes and M. Yamamoto, Nrf1 and Nrf2 Play distinct roles in activation of antioxidant response element-dependent genes, *J. Biol. Chem.*, 2008, **283**, 33554–33562, DOI: 10.1074/jbc.M804597200.

38 (*a*) Z. Kayaalti, G. Mergen and T. Soylemezoglu, Effect of metallothionein core promoter region polymorphism on cadmium, zinc and copper levels in autopsy kidney tissues from a Turkish population, *Toxicol. Appl. Pharmacol.*, 2010, **245**, 252–255, DOI: 10.1016/j.taap.2010.03.007; (*b*) C. Cipriano, M. Malavolta, L. Costarelli, R. Giacconi, E. Muti, N. Gasparini, M. Cardelli, D. Monti, E. Mariani and E. Mocchegiani, Polymorphisms in MT1a gene coding region are associated with longevity in Italian central female population, *Biogerontology*, 2006, **7**, 357–365, DOI: 10.1007/s10522-006-9050-x; (*c*) L. Yang, H. Y. Li, T. Yu, H. J. Zhao, M. G. Cherian, L. Cai and Y. Liu, Polymorphisms in metallothionein-1 and -2 genes associated with the risk of type 2 diabetes mellitus and its complications, *Am. J. Physiol.: Endocrinol. Metab.*, 2008, **294**, E987–E992, DOI: 10.1152/ajpendo.90234.2008; (*d*) A. I. Zavras, A. J. Yoon, M. K. Chen, C. W. Lin and S. F. Yang, Metallothionein-1 genotypes in the risk of oral squamous cell carcinoma, *Ann. Surg. Oncol.*, 2011, **18**, 1478–1483, DOI: 10.1245/s10434-010-1431-3; (*e*) Y. Wang, J. M. Goodrich, B. Gillespie, R. Werner, N. Basu and A. Franzblau, An investigation of modifying effects of metallothionein single-nucleotide polymorphisms on the association between mercury exposure and biomarker levels, *Environ. Health Perspect.*, 2012, **120**, 530–534, DOI: 10.1289/ehp.1104079.

39 (*a*) F. R. DeRubertis, P. A. Craven and M. F. Melhem, Acceleration of diabetic renal injury in the superoxide dismutase knockout mouse: effects of tempol, *Metab., Clin. Exp.*, 2007, **56**, 1256–1264, DOI: 10.1016/j.metabol.2007.04.024; (*b*) T. Nishikawa, D. Edelstein, X. L. Du, S. Yamagishi, T. Matsumura, Y. Kaneda, M. A. Yorek, D. Beebe, P. J. Oates, H. P. Hammes, I. Giardino and M. Brownlee, Normalizing mitochondrial superoxide production blocks three pathways of hyperglycaemic damage, *Nature*, 2000, **404**, 787–790, DOI: 10.1038/35008121; (*c*) V. Elangovan, E. Shohami, I. Gati and R. Kohen, Increased hepatic lipid soluble antioxidant capacity as compared to other organs of streptozotocin-induced diabetic rats: a cyclic voltammetry study, *Free Radical Res.*, 2000, **32**, 125–134, DOI: 10.1080/10715760000300131.

40 R. H. Wong, C. H. Huang, C. B. Yeh, H. S. Lee, M. H. Chien and S. F. Yang, Effects of metallothionein-1 genetic polymorphism and cigarette smoking on the development of hepatocellular carcinoma, *Ann. Surg. Oncol.*, 2012, **20**, 2088–2095, DOI: 10.1245/s10434-012-2456-6.

41 L. Sun, X. Zhang, Y. Kong and L. Yu, Effect of MT1M gene on the cell cycle and signaling pathway of Hep-G2, *Int. J. Androl.*, 2004, **10**, 932–934.

42 (*a*) K. Kita, N. Miura, M. Yoshida, K. Yamazaki, T. Ohkubo, Y. Imai and A. Naganuma, Potential effect on cellular response to cadmium of a single-nucleotide A → G polymorphism in the promoter of the human gene for metallothionein IIA, *Hum. Genet.*, 2006, **120**, 553–560, DOI: 10.1007/s00439-006-0238-6; (*b*) Z. Kayaalti and T. Soylemezoglu, The polymorphism of core promoter region on metallothionein 2A-metal binding protein in Turkish population, *Mol. Biol. Rep.*, 2010, **37**, 185–190, DOI: 10.1007/s11033-009-9586-3; (*c*) E. Forma, A. Krzeslak, J. Wilkosz, P. Jozwiak, A. Szymczyk, W. Rozanski and M. Brys, Metallothionein 2A genetic polymorphisms and risk of prostate cancer in a Polish population, *Cancer Genet.*, 2012, **205**, 432–435, DOI: 10.1016/j.cancergen.2012.05.005; (*d*) D. Tekin, Z. Kayaalti, V. Aliyev and T. Soylemezoglu, The effects of metallothionein 2A polymorphism on placental cadmium accumulation: is metallothionein a modifiying factor in transfer of micronutrients to the fetus?, *J. Appl. Toxicol.*, 2012, **32**, 270–275, DOI: 10.1002/jat.1661; (*e*) E. Mocchegiani, R. Giacconi, C. Cipriano, M. Muzzioli, N. Gasparini, R. Moresi, R. Stecconi, H. Suzuki, E. Cavalieri and E. Mariani, MtmRNA gene expression, *via* IL-6 and glucocorticoids, as potential genetic marker of immunosenescence: lessons from very old mice and humans, *Exp. Gerontol.*, 2002, **37**, 349–357, DOI: 10.1016/s0531-5565(01)00202-9; (*f*) M. G. Cherian, A. Jayasurya and B. H. Bay, Metallothioneins in human tumors and potential roles in carcinogenesis, *Mutat. Res., Fundam. Mol. Mech. Mutagen.*, 2003, **533**, 201–209, DOI: 10.1016/j.mrfmmm.2003.07.013; (*g*) C. Gundacker, K. J. Wittmann, M. Kukuckova, G. Komarnicki, I. Hikkel and M. Gencik, Genetic background of lead and mercury metabolism in a group of medical students in Austria, *Environ. Res.*, 2009, **109**, 786–796, DOI: 10.1016/j.envres.2009.05.003; (*h*) R. Giacconi, C. Cipriano, E. Muti, L. Costarelli, C. Maurizio, V. Saba, N. Gasparini, M. Malavolta and E. Mocchegiani, Novel-209A/G MT2A

polymorphism in old patients with type 2 diabetes and atherosclerosis: relationship with inflammation (IL-6) and zinc, *Biogerontology*, 2005, **6**, 407–413, DOI: 10.1007/s10522-005-4907-y; (*i*) R. Giacconi, E. Muti, M. Malavolta, C. Cipriano, L. Costarelli, G. Bernardini, N. Gasparini, E. Mariani, V. Saba, G. Boccoli and E. Mocchegiani, The +838 C/G MT2A polymorphism, metals, and the inflammatory/immune response in carotid artery stenosis in elderly people, *Mol. Med.*, 2007, **13**, 388–395, DOI: 10.2119/2007-00045.Giacconi; (*j*) X. Chen, L. J. Lei, L. T. Tian, G. Y. Zhu and T. Y. Jin, Bone mineral density and polymorphisms in metallothionein 1A and 2A in a Chinese population exposed to cadmium, *Sci. Total Environ.*, 2012, **423**, 12–17, DOI: 10.1016/j.scitotenv.2012.02.020; (*k*) R. Kozarova, A. Postadzhiyan, B. Finkov and M. Apostolova, Association of copy number variations and single nucleotide polymorphisms in metallothionein genes with pathogenesis of diabetes and coronary artery disease, *Atheroscler. Suppl.*, 2011, **12**, 107, DOI: 10.1016/S1567-5688(11)70504-9.

43 J. A. McElroy, E. C. Bryda, S. D. McKay, R. D. Schnabel and J. F. Taylor, Genetic variation at a metallothionein 2A promoter single-nucleotide polymorphism in white and black females in midwestern United States, *J. Toxicol. Environ. Health, Part A*, 2010, **73**, 1283–1287, DOI: 10.1080/15287394.2010.485067.

44 N. Miura, Individual susceptibility to cadmium toxicity and metallothionein gene polymorphisms: with references to current status of occupational cadmium exposure, *Ind. Health*, 2009, **47**, 487–494.

45 Y. Hayashi, T. Hashizume, K. Wakida, M. Satoh, Y. Uchida, K. Watabe, Z. Matsuyama, A. Kimura, T. Inuzuka and I. Hozumi, Association between metallothionein genes polymorphisms and sporadic amyotrophic lateral sclerosis in a Japanese population, *Amyotrophic Lateral Scler. Other Mot. Neuron Disord.*, 2006, **7**, 22–26, DOI: 10.1080/14660820600618766.

46 Z. Kayaalti, D. Tekin and T. Soylemezoglu, Role of metallothionein 2A polymorphism on lead metabolism: are pregnant women with a heterozygote genotype for metallothionein 2A polymorphism and their newborns at risk of having higher blood lead levels?, *Toxicol. Lett.*, 2011, **205**, S106, DOI: 10.1016/j.toxlet.2011.05.383.

47 (*a*) K. Shibuya, N. Nishimura, J. S. Suzuki, C. Tohyama, A. Naganuma and M. Satoh, Role of metallothionein as a protective factor against radiation carcinogenesis, *J. Toxicol. Sci.*, 2008, **33**, 651–655, DOI: 10.2131/jts.33.651; (*b*) M. P. Waalkes, J. Liu, K. S. Kasprzak and B. A. Diwan, Minimal influence of metallothionein over-expression on nickel carcinogenesis in mice, *Toxicol. Lett.*, 2004, **153**, 357–364, DOI: 10.1016/j.toxlet.2004.06.003; (*c*) J. Zeng, B. L. Vallee and J. H. R. Kagi, Zinc transfer from transcription factor-IIIA fingers to thionein clusters, *Proc. Natl. Acad. Sci. U. S. A.*, 1991, **88**, 9984–9988, DOI: 10.1073/pnas.88.22.9984; (*d*) R. Shimoda, W. E. Achanzar, W. Qu, T. Nagamine, H. Takagi, M. Mori and M. P. Waalkes, Metallothionein is a potential negative regulator of apoptosis, *Toxicol. Sci.*, 2003, **73**, 294–300, DOI: 10.1093/toxsci/kfg095; (*e*) B. Werynska, B. Pula, B. Muszczynska-Bernhard, A. Gomulkiewicz, A. Jethon, M. Podhorska-Okolow, R. Jankowska and P. Dziegiel, Expression of metallothionein-III in patients with non-small cell lung cancer, *Anticancer Res.*, 2013, **33**, 965–974.

48 (*a*) A. M. L. Janssen, W. van Duijn, F. Kubben, G. Griffioen, C. Lamers, J. van Krieken, C. J. H. van de Velde and H. W. Verspaget, Prognostic significance of metallothionein in human gastrointestinal cancer, *Clin. Cancer Res.*, 2002, **8**, 1889–1896; (*b*) M. Moussa, D. Kloth, G. Peers, M. G. Cherian, J. V. Frei and J. L. Chin, Metallothionein expression in prostatic carcinoma: correlation with Gleason grade, pathologic stage, DNA content and serum level of prostate-specific antigen, *Clin. Invest. Med.*, 1997, **20**, 371–380.

49 Q. R. Liang, E. C. Carlson, R. V. Donthi, P. M. Kralik, X. Shen and P. N. Epstein, Overexpression of metallothionein reduces diabetic cardiomyopathy, *Diabetes*, 2002, **51**, 174–181.

50 S. R. Zheng, E. C. Carlson, L. Yang, P. M. Kralik, Y. Huang and P. N. Epstein, Podocyte-specific overexpression of the antioxidant metallothionein reduces diabetic nephropathy, *J. Am. Soc. Nephrol.*, 2008, **19**, 2077–2085, DOI: 10.1681/asn.2007080967.

51 M. D. Apostolova, K. H. A. Choo, A. E. Michalska and C. Tohyama, Analysis of the possible protective role of metallothionein in streptozotocin-induced diabetes using metallothionein-null mice, *J. Trace Elem. Med. Biol.*, 1997, **11**, 1–7.

52 P. Palumaa, I. Tammiste, K. Kruusel, L. Kangur, H. Jornvall and R. Sillard, Metal binding of metallothionein-3 *versus* metallothionein-2: lower affinity and higher plasticity, *Biochim. Biophys. Acta, Proteins Proteomics*, 2005, **1747**, 205–211, DOI: 10.1016/j.bbapap.2004.11.007.

53 J. Hidalgo, M. Aschner, P. Zatta and M. Vasak, Roles of the metallothionein family of proteins in the central nervous system, *Brain Res. Bull.*, 2001, **55**, 133–145, DOI: 10.1016/s0361-9230(01)00452-x.

54 (*a*) A. K. Sewell, L. T. Jensen, J. C. Erickson, R. D. Palmiter and D. R. Winge, Bioactivity of metallothionein-3 correlates with its novel beta-domain sequence rather than metal-binding properties, *Biochemistry*, 1995, **34**, 4740–4747, DOI: 10.1021/bi00014a031; (*b*) Y. Manso, J. Carrasco, G. Comes, G. Meloni, P. A. Adlard, A. I. Bush, M. Vasak and J. Hidalgo, Characterization of the role of metallothionein-3 in an animal model of Alzheimer's disease, *Cell. Mol. Life Sci.*, 2012, **69**, 3683–3700, DOI: 10.1007/s00018-012-1047-9; (*c*) M. C. Amoureux, D. Van Gool, M. T. Herrero, R. Dom, F. C. Colpaert and P. J. Pauwels, Regulation of metallothionein-III (GIF) mRNA in the brain of patients with Alzheimer disease is not impaired, *Mol. Chem. Neuropathol.*, 1997, **32**, 101–121, DOI: 10.1007/bf02815170.

55 (*a*) D. A. Drum, Are toxic biometals destroying your children's future?, *Biometals*, 2009, **22**, 697–700, DOI: 10.1007/s10534-009-9212-9; (*b*) H. Fusheng, X. Feiyan, X. Han and Z. Fang, Study on the relationship between gene polymorphism of metallothionein 3 and childhood autism, *Chin. J. Clin.*, 2011, **5**, 2559–2562.

56 C. J. Quaife, S. D. Findley, J. C. Erickson, G. J. Froelick, E. J. Kelly, B. P. Zambrowicz and R. D. Palmiter, Induction of a new metallothionein isoform (MT-IV) occurs during differentiation of stratified squamous epithelia, *Biochemistry*, 1994, **33**, 7250–7259, DOI: 10.1021/bi00189a029.

57 L. Tio, L. Villarreal, S. Atrian and M. Capdevila, Functional differentiation in the mammalian metallothionein gene family – metal binding features of mouse MT4 and comparison with its paralog MT1, *J. Biol. Chem.*, 2004, **279**, 24403–24413, DOI: 10.1074/jbc.M401346200.

58 H. I. Chen, Y. W. Chiu, Y. K. Hsu, W. F. Li, Y. C. Chen and H. Y. Chuang, The association of metallothionein-4 gene polymorphism and renal function in long-term lead-exposed workers, *Biol. Trace Elem. Res.*, 2010, **137**, 55–62, DOI: 10.1007/s12011-009-8564-x.

59 Z. Kayaalti, L. Sahiner, M. E. Durakoglugil and T. Soylemezoglu, Distributions of interleukin-6 (IL-6) promoter and metallothionein 2A (MT2A) core promoter region gene polymorphisms and their associations with aging in Turkish population, *Arch. Gerontol. Geriatr.*, 2011, **53**, 354–358, DOI: 10.1016/j.archger.2011.01.001.

2.1.2 Unique role of zinc in the prostatic tissue

The prostate is involved in the formation of 30% of the seminal fluid volume, where prostaglandins, a number of enzymes, zinc ions (Zn^{2+}) and citrate are released by the prostate epithelial cells [39]. Metabolism of these substances, especially Zn^{2+} and citrate, differs in the prostatic cells compared with a number of other tissues. Citrate is processed routinely in the Krebs cycle producing a large amount of ATP. To avoid entry of citrate into this cycle and its subsequent degradation, the mitochondrial enzyme aconitase, converting citrate into isocitrate, has to be blocked in epithelial prostate cells [40]. Aconitase is blocked by the zinc ions, accumulated by prostate to a higher extent (up to ten times higher compared with other tissues) [41, 42]. Thanks to inhibition of the mitochondrial aconitase by zinc, prostate loses a substantial portion of the energy in the form of ATP [39]. In most mammalian cells, the total zinc concentration in the cells ranges from 100 to 500 μM. However, the zinc concentration in healthy prostate epithelial cells is much higher, ranging from 800 to 1500 μM; the zinc content accumulating in prostatic mitochondria is 20 times higher. The concentration of zinc in the prostatic fluid is 500 times higher than the concentration in the blood plasma. Citrate level in the peripheral prostate zone is 30 to 80 times higher than that of other soft tissues. Even more pronounced is an increase of citrate concentration in the prostatic fluid, which is about 1000 times higher than the concentration in the blood plasma [43]. Zn^{2+} accumulation is likely to involve zinc transporters and zinc-binding proteins. In addition to direct effects on mitochondrial aconitase, zinc also has other effects, namely induction of apoptosis by cytochrome C (zinc ions increase formation of BAX pores on the mitochondrial membrane, thereby inducing the cytochrome c (CytC)/caspase (Casp) -mediated apoptosis) and regulation of expression of a number of genes through kinases [44].

Irreversible loss of ability to accumulate Zn^{2+} is a typical feature for prostate carcinoma [45, 46]. This leads to a reduction of the pro-apoptotic effect and to loss of ability to produce citrate for seminal fluid [47]. The inhibitory effect of zinc on the enzyme aconitase, which is observable in healthy prostate cells, vanishes (see **Fig. 4**). Citrate can thus enter the Krebs cycle, and the carcinoma cells gain the advantage of being able to gain more energy [41, 42]. Inhibition of the ZIP1 transporter through increased activity of the Ras-Raf-Mek-Erk cascade is one of the assumed mechanisms. ZIP1 has been identified in prostate cells as the functionally most important zinc importer [43, 48].

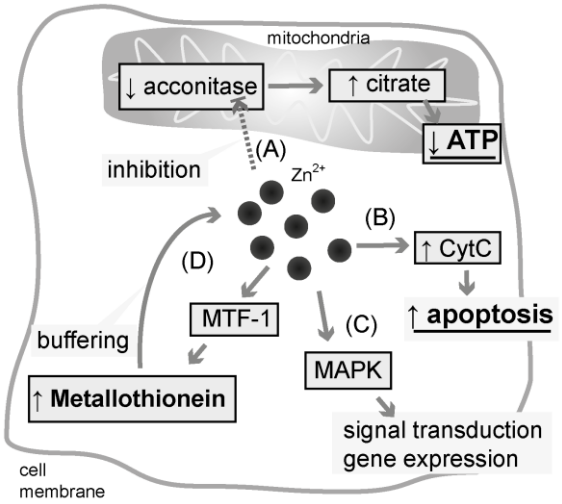

Figure 4 | Zinc ions cause accumulation of citrate (and hence change in energy metabolism of the cells) by (a) inhibiting the mitochondrial aconitase which converts citrate into isocitrate. Prostatic cells thus produce significantly less ATP; (b) Zn2+ has pro-apoptotic effect due to increased release of cytochrome C (CytC) out of mitochondria; (c) Zn2+ functions as a signal molecule and effects, in particular, gene expression by action on mitogen-activated protein kinases (MAPK); (d) Zn2 + induces expression of metallothionein (MT) through its metal-regulatory transcription factor-l (MTF-l), and MT thus affects intracellular level of free Zn2+.

In the previous chapter "Zinc ions and their regulation", the basic mechanisms of zinc ion impact in the non-tumour prostate and in the transformed tissues were mentioned. In the following overview paper, Gumulec et al. on page 55, the zinc ion impact mechanisms are presented in details [48]. Changes in expression of zinc transporters and their pathophysiological associations are shown here as well.

Author's publication relevant to this chapter

Gumulec J, Masarik M, Krizkova S, et al. Insight to Physiology and Pathology of Zinc(II) Ions and Their Actions in Breast and Prostate Carcinoma. Current Medicinal Chemistry. 2011;18(33):5041-5051.

Available on page 55

Current Medicinal Chemistry, **2011**, *18*, 5041-5051 5041

Insight to Physiology and Pathology of Zinc(II) Ions and Their Actions in Breast and Prostate Carcinoma

J. Gumulec[1], M. Masarik[1,2], S. Krizkova[2,3], V. Adam[2,3], J. Hubalek[2,4], J. Hrabeta[5], T. Eckschlager[5], M. Stiborova[6] and R. Kizek*[,2,3]

[1]*Department of Pathological Physiology, Faculty of Medicine, Masaryk University, Kamenice 5, CZ-625 00 Brno, Czech Republic-European Union*

[2]*Central European Institute of Technology, Brno University of Technology, Technicka 3058/10, CZ-616 00 Brno, Czech Republic-European Union*

[3]*Department of Chemistry and Biochemistry, Faculty of Agronomy, Mendel University in Brno, Zemedelska 1, CZ-613 00 Brno, Czech Republic-European Union*

[4]*Department of Microelectronics, Faculty of Electrical Engineering and Communication, Brno University of Technology, Technicka 10, CZ-616 00 Brno, Czech Republic-European Union*

[5]*Department of Paediatric Haematology and Oncology, 2nd Faculty of Medicine and University Hospital Motol, Charles University, V Uvalu 84, CZ-150 06 Prague 5, Czech Republic-European Union*

[6]*Department of Biochemistry, Faculty of Science, Charles University, Albertov 2030, CZ-128 40 Prague 2, Czech Republic-European Union*

Abstract: Zinc(II) ions contribute to a number of biological processes e.g. DNA synthesis, gene expression, enzymatic catalysis, neurotransmission, and apoptosis. Zinc(II) dysregulation, deficiency and over-supply are connected with various diseases, particularly cancer. 98 % of human body zinc(II) is localized in the intracellular compartment, where zinc(II) is bound with low affinity to metallothionein (MT). Zinc transporters ZIP and ZnT maintain transmembrane transport from/to cells or organelles. Imbalance of their regulation is described in cancers, particularly prostate (down-regulated zinc transporters ZIP1, 2, 3 and ZnT-2) and breast, notably its high-risk variant (up-regulated ZIP6, 7, 10). As a result, intracellular and even blood plasma zinc(II) levels are altered. MT protects cells against oxidative stress, because it cooperates with reduced glutathione (GSH). Recent studies indicate elevated serum level of MT in a number of malignancies, among others in breast, and prostate. MT together with zinc(II) affect apoptosis and proliferation, thus together with its antioxidative effects it may affect cancer. To date, only little is known about the influence of zinc(II) and MT on cancer, while these compounds may play an important role in pathogenesis. This review concludes current data regarding the impact of zinc(II) on the pathogenesis of breast and prostate cancers with potential outlines of new, targeted therapy and prevention. Moreover, blood plasma zinc(II) and MT levels and dietary zinc(II) intake are discussed in relation to breast and prostate cancer risk.

Keywords: Zinc, Cancer, Prostate Carcinoma, Breast Carcinoma, Homeostasis, Low Molecular Mass Thiols, Metallothionein, Glutathione, Zinc Intake, Apoptosis, ZnT and ZIP transporters.

1. INTRODUCTION

Zinc(II) is involved in numerous key intra- and extracellular processes including proliferation, differentiation and apoptosis [1,2], its regulation is important not only in development and proliferation of tissues, but also in neoplastic transformation [3,4]. To date, nearly 5,000 studies meeting the criteria of keywords "zinc" and "cancer" are indexed in Web of Knowledge portal, while the amount of papers increased 2.5-fold during the last decade. The effects of zinc(II) are both cancerogenic and protective and seems to be very complex and manifest in cancer-dependent manner. This review aims to summarize current associations between zinc(II) and cancers of prostate and breast, most common cancers, whose association with zinc has been studied most extensively.

Prostate cancer is the second most frequently diagnosed cancer and the sixth leading cause of cancer death in males, accounting for 14% (903,500) of the total new cancer cases and 6% (258,400) of the total cancer deaths in males in 2008. Incidence rates vary by more than 25-fold worldwide, with the highest rates recorded primarily in the developed countries of Oceania, Europe, and North America, largely because of the wide utilization of prostate-specific antigen testing that detects clinically important tumors as well as other slow-growing cancers that might otherwise escape diagnosis [5]. The prevalence of prostate cancer increases with age [6]. Hence, prostate cancer is a disease that predominantly affects older men. It does, however, usually respond to treatment and, if localized, may be curable. The rate of tumor growth varies from very slow to moderately rapid, and some patients may have prolonged survival, even after the cancer has metastasized to distant sites.

Breast cancer is the most frequently diagnosed cancer and the leading cause of cancer death in females worldwide, accounting for 23% (1.38 million) of the total new cancer cases and 14% (458,400) of the total cancer deaths in 2008. About half the breast cancer cases and 60% of the deaths are estimated to occur in economically developing countries. In general, incidence rates are high in Western and Northern Europe, Australia/New Zealand, and North America; intermediate in South America, the Caribbean, and Northern Africa; and low in sub-Saharan Africa and Asia [5]. Breast cancer is an acquired or inherited genetic disorder influenced by environmental, behavioral, and reproductive factors. The most significant risk factors are gender (being a woman) and age (growing older) [7]. Two distinct forms of the disease are identified as hereditary forms of cancers, which are often related to mutations in two high-penetrance susceptibility genes referred to as BRCA-1 and BRCA-2 [8] and sporadic forms account for 90–95% of cases and are consequences of a somatic mutation over the lifetime without any hereditary predisposition [9-11].

The major challenge in the management of prostate, breast and other types of cancers is the understanding biochemical pathways, where zinc metabolism is very interesting. In general, relation to zinc(II) and tumours can be regarded from the perspective of

*Address correspondence to this author at the Department of Chemistry and Biochemistry, Mendel University in Brno, Czech Republic-European Union; Tel: +420-5-4513-3350; Fax: +420-5-4521-2044; E-mail: kizek@sci.muni.cz

dysregulation of their intracellular and blood serum zinc(II) levels and from the perspective of abundant or deficient dietary zinc(II) income and thus resulting alteration of its biochemical roles. Thus, we believe, it is important to study the role of zinc(II) in relation to cancer.

2. MOLECULAR AND CELLULAR BIOLOGY OF ZINC(II)

Most of the zinc (II) in human body, approx. 98%, is localized in the intracellular compartment [12]. Its total intracellular concentration is in a range within hundreds of micromoles, thus it is approx. 10-fold higher compared to serum levels [13-16]. Most of the intracellular zinc(II) is bound to or at least associated with proteins and peptides [17]. Thereof, app. 90 % is tightly bound and the rest (10 %) is bound with relatively low affinities, forming reactive zinc(II) pool able to interact with other intracellular substances and compartments [18]. The last, very small fraction (approx. < 0.01 ‰ of total cellular zinc(II), ranging from pM to single digit nM) includes free zinc(II) ions [16]. The tightly bound zinc(II) ions occur mainly in metalloproteins, metalloenzymes and nucleoproteins and acts as a structural component of these biomolecules or as an enzyme cofactor. This fraction can be considered as an immobile nonreactive zinc(II) pool [1,16]. The rest of zinc(II) ions fraction, which acts as a mobile reactive form [19,20], is bound to low molecular weight compounds (amino acids as cysteine, histidine, proline), protein metallothionein or organic acids (citrate, oxalate) [21]. If there is a focus on cellular functions of zinc(II), determination of total cellular zinc(II) concentration is not of such importance as the determination of mobile reactive zinc(II) [18].

From the point of view of cell compartments, zinc(II) is not uniformly distributed. Approximately 30–40 % is in the nucleus, about 50 % in the cytoplasm and in organelles such as mitochondria, endoplasmic reticulum, Golgi apparatus, endosomes and lysosomes, and the rest is bound to cell membranes [12]. In addition to the ubiquitous conventional organelles, zinc(II) ions were also found in the specialized organelles such as synaptic vesicles, secretory granules and lysosome like structures [22].

Zinc(II) concentration varies within the range 200–400 nmols/gram wet weight tissue in most tissues [23]. However, tissues with physiologically significantly higher zinc(II) content have been described. These include beta cells of the pancreas, secretory cells of the pineal gland, lymphocytes, cells of the salivary glands, cells of retina and epithelial cells of prostate [24]. In prostate, particularly in its peripheral zone, which is the major site of malignancy initiation, zinc(II) is accumulated in approx. tenfold higher concentration compared to other tissues [25], within 3,000–4,500 nmols/gram wet weight tissue [23]. This is because of tissue-specific zinc(II) functions in prostate (Fig. **1**). First, prostatic tissue produces zinc-rich portion of semen; zinc(II) is necessary for proper movement of sperms [12,26]. Second, prostate contributes to high content of citrate in semen [27]. Prostate-specific citrate production is zinc-mediated: Zinc(II) inhibits mitochondrial enzyme aconitase, responsible for conversion of citrate to isocitrate, following its utilization in Krebs cycle. Due to this inhibition citrate is not utilized in Krebs cycle, is accumulated in prostatic cells and may be released into the seminal fluid [28]. Its prostatic intracellular concentration is 12 μmol/g wet tissue, more than 30-fold higher compared to other tissues [23]. However, this causes prostatic tissue less efficient in ATP production: one mol of glucose generates 14 moles of ATP compared to 38 moles in case of complete citrate oxidation [18].

In addition to zinc(II) levels in normal prostatic tissue, its levels are increased in benign prostate hypertrophy, and radically decreased in prostate cancer. In peripheral zone of neoplastic prostate, its levels ranges within 400–800 nmols/gram wet weight tissue, thus 5-fold lower compared to healthy prostate tissue, however still 2-fold higher compared to most other tissues [23]. In terms of zinc(II) level in breast cancer tissue, results of studies are inconsistent. Based on study by Cui *et al.* on 500 US participants, significantly higher zinc(II) content was found in breast cancer tissue compared to controls. In addition, high levels of zinc(II) may be associated with a modest increase of risk of subsequent breast cancer in benign breast tissue [29]. Similarly, based on a study on 36 participants in India, significant elevation (> 2-fold) of tissue zinc(II) was observed in tumor tissue [30]. However, in study presented by Majewska *et al.*, significant differences in tissue samples obtained from breast cancer and benign lesions were not observed [31]. Thus, it can be expected that zinc(II) may play an important role in prostate cancer pathogenesis and apparently also in breast cancer, however probably by other mechanisms due to the fact that its level is higher compared to healthy tissue.

Based on the involvement of zinc(II) in the complex regulatory network, precise mechanisms to maintain intracellular zinc(II) level exist (Fig. **1**). Zinc(II) pool is maintained by two types of proteins: (a) zinc-binding proteins (mostly by metallothionein), which act as buffer and donor of zinc(II) for intracellular processes, and (b) zinc transporters, which are responsible for zinc fluxes into/from cells and organelles. A key regulator of intracellular free zinc level is metal regulatory transcription factor 1 (MTF-1, also called MRE-binding factor) [32]. This 753 amino acids transcription factor directly responds to the elevated zinc(II) level and induces the transcription of metallothionein and main zinc transporter responsible for its export, ZnT-1 (discussed below) [33-35]. This autoregulatory loop maintains narrow optimal limits of intracellular zinc(II): when the level of metallothionein and ZnT-1 is elevated, more free zinc(II) may be buffered (i.e. bound to metallothionein) and more zinc may leave cells (through larger amount of membrane transporters).

2.1. Zinc Transport

Zinc(II) cannot freely pass through membranes, thus, special membrane transporters have developed in a cell. Zinc(II) transporters are transmembrane proteins, which transfer zinc(II) ions through cellular membranes [36]. Most of them are localized both on plasmatic and on organelle's membranes. There are two zinc transporter families: Zinc-Iron Permease transporter (ZIP), also called Zrt-Irt-like protein, or solute-linked carrier 39 (SLC39) family and Zinc transporter (ZnT, SLC30) family. ZIP transporter family is responsible for the influx of zinc(II) ions to the cytoplasm, in other words for transporting zinc(II) ions from extracellular compartments or from intracellular organelles to the cytoplasm. ZnTs are responsible for opposite action, i.e. the efflux of zinc(II) ions from cytoplasm (transport from cytoplasm to the organelles or to the extracellular matrix) [37].

Transport mechanisms of those proteins are not fully understood, however, it is expected there is ATP-independent facilitated diffusion, secondary active transport or symport mechanism [38]. Regulation of expression of both transporter families is not yet fully clear, however, in general, zinc(II) has antagonistic effect on transporters: whereas low zinc(II) load induces expression of zinc importers – ZIPs, high zinc(II) level induces expression of zinc exporters – ZnTs [37]. In the following chapter, transporters associated with breast and prostate cancers or transporters expected to play a role in those cancers are displayed only.

2.1.1. ZIP Transporter Family

ZIP transporter family is responsible for energy-independent zinc(II) influx [39]. In humans, fourteen members of these proteins have been found and denominated ZIP1 – 14 [36]. The proteins are introduced in Table **1**. This family can be divided into subfamilies I, II, LIV-1 and gufA [40]. Most members of the ZIP family consist of 220–650 amino acids residues with eight putative

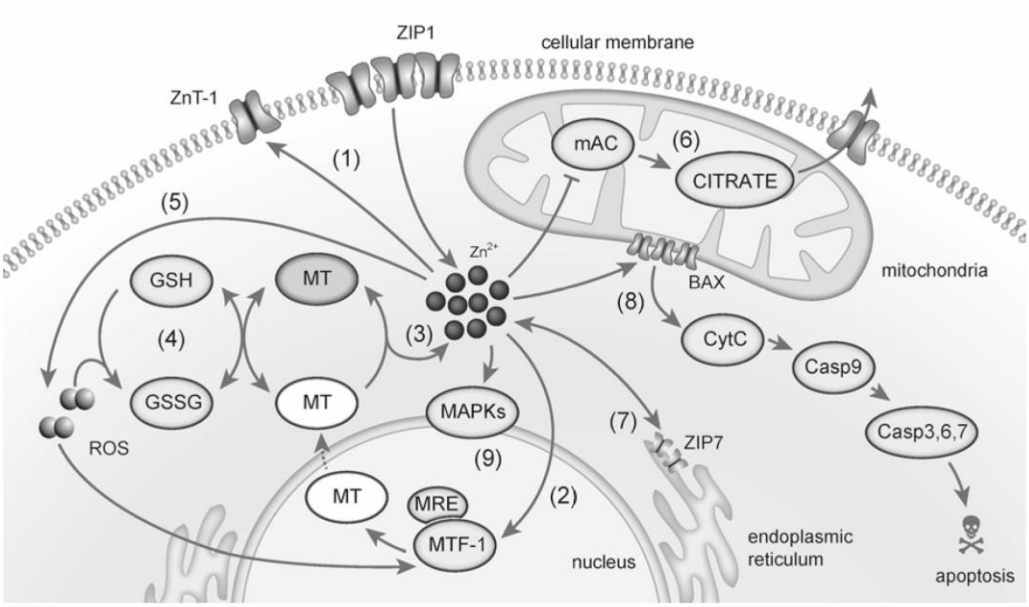

Fig. (1). Zinc in healthy prostate. ZIP and ZnT transporters maintain intracellular zinc transport **(1)**; ZIP1 is a major zinc(II) importer, ZnT-1 is the only export transporter [41,67]. Intracellular free zinc(II) induce metallothionein (MT) expression through metal regulatory transcription factor-1 (MTF-1), which binds to metal regulatory element (MRE) region of MT gene [32] **(2)**. Consequently, zinc(II) is bound by MT [16] **(3)** (white MT represents reduced/metal-free form, grey MT represents oxidized/metal-bound form). High zinc(II) load induces oxidative stress (ROS), **(5)**, which is reduced by glutathione system in cooperation with MT **(4)** [82]; MT convert glutathione to its reduced form while being oxidized [83-86]. Endoplasmic reticulum may serve as the intracellular zinc(II) pool and regulates cytoplasmic free zinc(II) level by ZIP7 transporter, which increase zinc(II) content in cytoplasm **(7)** [43]. Free zinc(II) affect gene expression through mitogen-activated protein kinase cascade (MAPKs, **9**) [3,4]. In prostate, high zinc(II) level inhibit mitochondrial aconitase (mAC), thus citrate is accumulated **(6)** and released in high level [25]. Zinc induces a prostate-specific BAX pore formation **(8)** causing cytochrome C (CytC) release from mitochondria and subsequent caspase-mediated apoptosis [18].

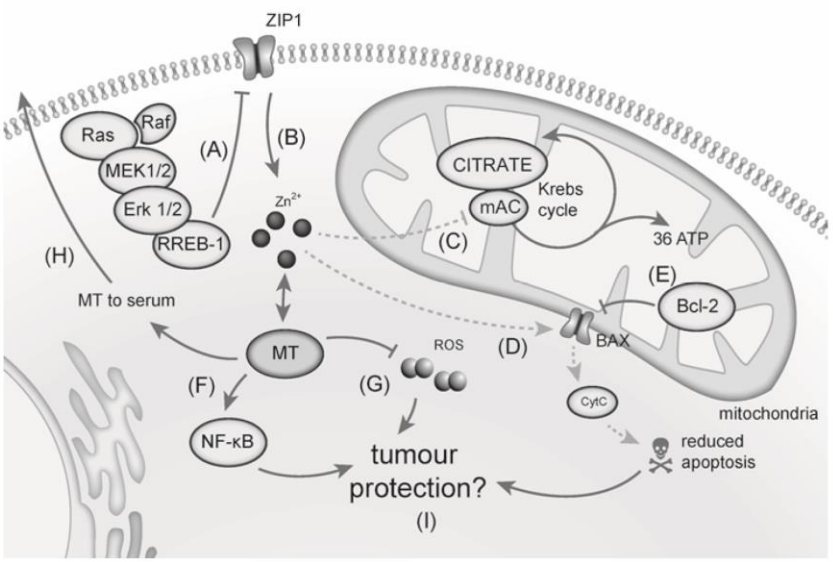

Fig. (2). Zinc in prostate cancer. (A) ZIP1 zinc(II) transporter is down-regulated due to up-regulated Ras-Raf-MEK-ERK cascade in prostate cancer [44]. This causes **(B)** lower zinc(II) influx and thus lower intracellular zinc(II) in prostate cancer cells [25]. Lower zinc(II) **(C)** abolish mitochondrial aconitase (mAC) inhibition, causes citrate utilization in Krebs [25]. **(D)** Abolished formation of BAX pores on outer mitochondria membrane together with **(E)** upregulated Bcl-2 decrease cytochrome-C release that causes reduced apoptosis [18]. MT has tumor cell-protective mechanisms through **(F)** NF-κB activation and **(G)** reactive oxygen species reduction. **(F,G,D)**. Therefore, MT may be a prostate cancer-specific tumor-protective mechanism **(I)**. Similarly to prostate specific antigen (PSA), MT **(H)** leaves tumor cells to circulation (thus possible tumor marker) [83].

Table 1. ZIP Transporters Associated with Cancers

Transporter (gene names)	Subfamily	Tissue localization	Cellular localization	Function	Association with disease	Ref.
ZIP1 (SLC39A1, IRT1, ZIRTL, CGI-08, CGI-71)	II	ubiquitous	plasma membrane,	Zn uptake	decreased expression in PCa	[20]
ZIP2 (SLC39A2)	II	uterus, prostate, monocytes, optic nerve	plasma membrane	Zn, Co Cd, Cu, Mn uptake	decreased expression in PCa	[38,39,54,57]
ZIP3 (SLC39A3)	II	ubiquitous, higher in bone marrow, spleen	plasma membrane	Zn uptake, mammary gland Zn secretion pathway	decreased expression in PCa	[55-57]
ZIP6 (SLC39A6, LIV1)	LIV-1	ubiquitous	plasma membrane	Zn uptake. positively regulated by estrogen	highly expressed in high-risk BCa, highly expressed in cervix ca and lung ca	[58,65]
ZIP7 (SLC39A7, HKE4, RING5)	LIV-1	ubiquitous	ER, Golgi	transport Zn from organelles to cytosol, Zn signalling	elevation in tamoxifen-resistant BCa	[43]
ZIP10 (SLC39A10, KIAA1265)	LIV-1	ubiquitous	plasma membrane	imports Zn to Sertoli cells and spermatocytes	highly expressed in high-risk BCa, reduced level associated with impaired spermatogenesis	[60,149]

Description of the localization and function of ZIP transporter family genes associated or expected to be associated with prostate or breast tumours. Association with cancers described with particular trend. The table was prepared according to Kambe *et al.* [37] and Hogstrand *et al.* [43]. Gene and protein names and variants according to uniprot.org. Abbreviations: PCa – prostate cancer, BCa – breast cancer, ca – cancer.

transmembrane units. Long and variable-in-composition loop rich in histidine, which is probably responsible for metal binding is placed between units 3 and 4. Based on actual studies, six of these fourteen ZIP transporters are reported to be associated with breast or prostate tumors: ZIP1, 2, 3, 6, 7 and ZIP-10.

ZIP1 transporter, the major zinc(II) importer [41], belongs to subfamily II. ZIP1 is encoded by SLC39A1 gene, which is located on a chromosome 1 and the protein itself consists of 324 amino acids (Table **1**). This transporter is ubiquitously and consistently expressed at the plasma membrane of most cells [41]. It is known that the prostate, mainly epithelial cells, accumulates very high levels of zinc(II), up to 4,500 nmols/gram wet weight tissue [25]. Accumulated zinc(II) is then secreted into the seminal fluid. ZIP1 contributes significantly to this accumulation because it is responsible for zinc uptake from the circulation [42]. Prolactin and testosterone induces expression of ZIP1. Therefore, administration of prolactin and testosterone results in enhanced expression ZIP1 and, therefore, increased capacity of zinc(II) accumulation by these cells [21]. This has been demonstrated on the prostate cell lines in the study by Costello *et al.* Authors found that ZIP1 was elevated in androgen-responsive cell line LNCaP, not in androgen nonresponsive PC-3, when exposed to testosterone [21]. One may speculate that testosterone administration may be beneficial in androgen-responsive prostate tumors. However, this topic needs further research. High levels of zinc(II) in diet leads to the reduction of the expression of this protein. In prostate cancer, the ZIP1 expression is reduced. Due to the fact that ZIP1 serves as a main zinc(II) importer, prostate tumor cells have a reduced ability to accumulate zinc(II) ions [23,43]. Reduced intracellular zinc(II) level causes a series of metabolic transformations such as increased proliferation and altering of sensitivity to apoptotic signals (Fig. **2**). It is known that decreased expression of ZIP1 is not caused by deletion or mutation, but by down regulation which is caused by "Ras-responsive element-binding protein 1" (RREB-1) [44]. RREB-1 is a transcription factor containing zinc(II) finger domains with both activation and inactivation potential, whereas activation or inactivation preference is driven by promotor preference [45]. RREB-1 is activated by cascade RAS-RAF-MEK-ERK [46]. Notably, this cascade is up-regulated in prostate cancer [47]. However, RREB-1 is not the only transcription factor with ability to regulate ZIP1 expression. There have been detected other regions in ZIP1 promotor with ability to down-regulate ZIP1 expression [44]. One may speculate that restoration of the expression of ZIP1 or increase of zinc(II) levels in prostate cancer cells might be the new possible therapeutic approach in prostate cancer [25]. Cultivation of prostate cancer cell line LNCaP in medium with high zinc(II) content reduced their proliferation. Intracellular zinc(II) increase go along with increase of VHR phosphatase, ZAP-70 kinase, and p-ERK 1 and 2 [48,49]. Selective zinc(II) deficiency induced by chelator activate NF-κB causes overexpression of the proangiogenic and prometastatic cytokines VEGF, IL-6 and IL-8 in prostate cancer cell lines [50]. Similar effect was described in androgen-independent prostate cancer cell line PC-3, where addition of 50 μM of zinc(II) to medium (approx. 3 times higher compared to blood plasma level) significantly reduce the proliferation compared to PNT1A cell line derived from healthy prostate cells [51]. The importance of ZIP1 transporter in prostate cancer is emphasized by finding that this transporter does uptake the majority of zinc(II) from the circulation and its increased expression reduces the ability of prostate cancer cells to metastasize [52]. However, 50 μM zinc(II) is distinctly higher compared to serum level and thus rather than mere zinc(II) supplementation targeted procedures leading to elevation of ZIP1 expression can provide a significant prospective therapeutic benefit.

Transporter ZIP2 (also called 6A1 or Eti-1) also belongs to subfamily II. This 309 amino acids protein is encoded by SLC39A2 gene, located on chromosome 14 [38]. Compared to ZIP1, it is detected only in certain cells and tissues (uterus, prostate, to a lesser extent also in monocytes and in optic nerve) and it is expressed in lower levels [40,53]. It is localized on the plasmatic membrane solely, not on the organelles' ones. Its localization follows its function, because ZIP2 is also zinc importer. Like ZIP1, ZIP2 expression is increased under low zinc(II) concentrations [54] and conversely, zinc supplementation leads to ZIP2 down-regulation suggesting role in zinc(II) homeostasis [38]. ZIP2 shows a dramatic induction in normal epithelial cells contact inhibition. Loss of its expression may play a role in tumorigenesis [40]. Similar to ZIP1, reduced expression of ZIP2 is associated in prostate cancer [43].

Another transporter ZIP3, also belongs to subfamily II. Its gene is localized on chromosome 19 and encodes 314 amino acids'

product. ZIP3 is ubiquitously localized, however higher expression was found in bone marrow and spleen and lower levels were in small intestine and liver [55]. This transporter plays important role in mammary gland in secretion of zinc(II) into the milk [56]. Like ZIP1 and ZIP2, its expression is also decreased in prostate carcinoma [43,57].

Another ZIP transporter, ZIP6, alternatively named Estrogen-regulated protein LIV-1 (LIV1) or Solute carrier family 39 member 6 (SLC39A6) is a 755 amino acid protein localized on a cell membrane. ZIP6 is highly expressed in the breast, prostate, placenta, kidney, pituitary and corpus callosum and weakly expressed in heart and intestine [58]. Above that, elevated expression of ZIP6, together with ZIP7 and ZIP10 were demonstrated in the high-risk breast cancer with metastatic potential [43,59-61]. In addition, ZIP6 is positively regulated by estrogen suggesting that aberrant estrogen receptor signaling might modulate zinc(II) metabolism [59,62].

ZIP7 (also called Histidine-rich membrane protein Ke4 or Solute carrier family 39 member 7) is a 496 amino acid protein. Although ZIP7 is localized ubiquitously, elevated expression was described in placenta, lung, kidney and pancreas [58]. ZIP7 transporter is localized on the endoplasmic reticulum (ER) membrane [63], which may serve as reservoir of intracellular zinc(II) [43]. ZIP7 has, thus, an important role in zinc signaling. Release of zinc(II) from ER induces zinc-based signals with following signal transduction *via* protein-tyrosine phosphatases signaling [43]. Based on this mechanism, antiapoptotic or cell proliferation mechanisms can be influenced. Tamoxifen-resistant breast cancer cells has increased intracellular zinc(II) levels compared with sensitive cancer cells. This observation corresponds with the high expression of ZIP7 and epidermal growth factor receptor (EGFR) activation that is sign of worse prognosis [64,65]. Together with the finding that elevated expression of ZIP7 was found in high risk breast cancer one may suggest that ZIP7 play important role in its pathogenesis.

ZIP10 (SLC39A10) is 831 amino acid protein. Its high levels of expression are correlated with invasiveness in several breast cancer lines. Significantly higher levels were found in MDA-MB-231 and MDA-MB-435S breast cancer cell lines with high metastatic potential compared to MCF7, T47D, ZR75-1 and ZR75-30 breast cancer cell lines with lower metastatic potential [60]. Expression of ZIP10 mRNA in breast cancer samples positively correlated with the presence of node metastasis [60]. These data suggest that ZIP10 is a potential marker of breast cancer invasivity and potential target of therapeutic strategy [60]. In conclusion ZIP 6, 7 and 10 are overexpressed in breast cancer particularly in those with high metastatic potential and ZIP 1 and 2 are downregulated in prostate cancer.

2.1.2. ZnT Transporter Family

This transporter family, also called "cation diffusion facilitator" (CDF), takes the opposite function compared to ZIP transporters. The proteins belonging to this family transport zinc(II) from cytoplasm to the extracellular environment and to the organelles, i.e. protects cells against toxic levels of zinc(II). ZnT transporters can be divided into subfamilies I, II and III, but only II and III were found in mammals [40]. Nine transporters of this family, called the zinc transporter (ZnT) 1 to 9, have been identified in mammals (Table **2**). Like in ZIP, ZnT contains the histidine rich loop between transmembrane domains 4 and 5, which is responsible for binding of metals [36]. Transport mechanism remains still unclear, but it is considered to antiport mechanism of zinc(II)/potassium(I) and/or zinc(II)/hydrogen(I) [36,66]. The expression of these transporters is regulated by the cytosolic level of zinc(II). Higher zinc(II) level increases the expression of ZnT compared to ZIP, in which excess of zinc(II) ions causes the opposite effect [37]. This induction was described in ZnT-1 and ZnT-2 transporters. The expression of ZnT-1 is regulated by transcription factor MTF-1, which directly responds to increased intracellular free zinc(II) concentration [37].

ZnT-1 is the only transporter in mammals responsible for zinc efflux from cells and therefore the only transporter with protective function against toxic levels of zinc(II) [67]. ZnT-1 is a 507 amino acid protein encoded by SLC30A1 gene. It occurs in many types of cells and together with metallothionein plays a key role in intracellular zinc(II) level regulation [67,68]. In addition, ZnT-1 is involved in zinc efflux from enterocytes across the basolateral membrane into circulation and therefore, its function is complementary in dietary zinc(II) absorption to ZIP4, which is localized on the apical side of enterocytes [69]. Beside altered expression of ZIPs, increased excretion of zinc(II) out of cancer cells may theoretically be another mechanism of decreased intracellular zinc(II) level. To date there is no evidence of ZnT-1 expression in prostate cancer. Altered expression is associated with Alzheimer's disease (AD) suggesting that zinc(II) play a role in AD pathogenesis [70]. However, we have determined significantly elevated level of mRNA of both ZIP1 and ZnT-1 in prostate cancer cell line 22Rv1 and no significant elevation in tumor PC-3 cell line compared to cell line PNT1A derived from healthy tissue [71].

Transporter ZnT-2 (SLC30A2) has two isoforms. Canonical isoform 1 is 323 amino acid protein responsible for the transport of zinc(II) to the endosomes [72]. Its 372 amino acid isoform 2 was found on the lysosome membrane [73]. ZnT-2 occurs in the small intestine, kidney, seminal vesicles, testes, placenta, mammary gland and prostate. Large amount of ZnT-2 mRNA was found in the lateral and dorsal prostate lobes in rat, but none in ventral lobe [74,75]. This is consistent with the finding that these locations accumulate high zinc(II) levels [34]. It can be expected that ZnT-2 plays a role not only in prostatic zinc(II) redistribution but also in prostatic pathology like a benign hyperplasia and cancer [74,75]. As described above, information about ZnT transporters expression in malignant tumors are only limited and it should be subject of further studies.

Table 2. ZnT Transporters Associated with Cancers

Transporter (gene names)	Subfamily	Tissue localization	Cellular localization	Function	Association with disease	Ref.
ZnT-1 (SLC30A1)	II	ubiquitous	plasma membrane	Zn removal from the cytoplasm	decreased in AD, increased in lung ca	[67,68,70]
ZnT-2 (SLC30A2)	III	small intestine, kidney, testes, placenta, prostate, mammary gland	endosomes	transport Zn vesicles and lysosomes; Zn secretory pathway in prostate, breast	role in PCa	[75,150,151 109]
ZnT-4 (SLC30A4)	III	ubiquitous, especially mammary gland	endosome, Golgi apparatus	transport Zn to vesicles, Zn secretion pathway in breast	increased in AD, lung ca	[70]

Description of the tissue and cellular localization and function of ZnT transporter family genes associated or expected to be associated with prostate or breast tumours. Association with cancers described with particular trend. The table was prepared according to Kambe *et al.* [37] and Hogstrand *et al.* [43]. Gene and protein names and variants according to uniprot.org. Abbreviations: AD – Alzheimer's disease, ca – cancer.

2.2. Thiol Compounds

Metallothioneins are a group of mostly intracellular proteins belonging to the metalloprotein family. They are widespread in the animals, however, similar types of proteins have been found in bacteria, fungi and plants. Mammalians metallothioneins were firstly found in horse kidney by Margoshes and Vallee in 1957 [76]. They are low molecular weight (app. 6 kDa) and consist of 60–62 amino acids. In organism, metallothioneins occur in four isoforms; MT-1, MT-2, MT-3 and MT-4 [77]. MTs have atypical primary structure with lack of aromatic amino acids and with un-obviously high content of cysteine, because this amino acid is almost one third of all amino acids. Due to cysteine residues, metallothioneins have an ability to bind metals. One molecule of metallothionein consists of two domains, α and β, whereas both of these include cysteine clusters capable to bind up to 7 divalent or 12 monovalent ions [19,78]. Experiments on MT found significant differences in zinc-binding affinities of cysteine clusters [79]. Affinity varies in nanomolar to picomolar range of zinc(II) concentration, i.e. in at least three orders of magnitude [16]. In addition, there were published papers studying the influence of oxidation on polymerizing of metallothionein and its capacity to bind zinc(II) ions [80,81].

Metallothioneins play a key role in metabolism, transport and storage of heavy metals, particularly zinc(II) [16,82]. When zinc(II) ions get into a cytosol through zinc transporters, it is immediately buffered by metallothioneins, thus the free zinc(II) ion level is maintained on very low level, in picomolar to nanomolar range [16]. Due to signaling roles of free zinc(II) ions, metallothioneins play an important role in this process because of its level regulation (Fig. **1**). Whether zinc(II) level exceeds the buffering capacity of metallothioneins, it is being eliminated out of cells by ZnT-1 exporter and subsequently, zinc(II) induces expression of metallothionein and ZnT-1 by binding to transcription factor MTF-1 that binds to metal responsive elements (MREs) which regulate metallothionein expression (Fig. **1**).

Metallothioneins also protect cells against oxidative stress [82], because they cooperate with reduced glutathione (GSH) [83]. Due to these features it is not surprising that metallothioneins are overexpressed under conditions with increased risk of reactive oxygen species formation such as cell proliferation or embryonic development [83-86]. A lot of recent studies indicate elevated serum levels of metallothioneins in number of malignancies such as breast, bronchial, urogenital, colorectal, prostate carcinomas, melanoma and several lymphoma [82,87-91]. In prostate carcinoma, metallothionein serum levels are up to three times higher compared to healthy controls [83,92]. Metallothioneins that are detected by immunohistochemistry are localized in the nuclei of epithelial cells in a benign prostatic lesion, whereas in the adenocarcinoma they occurred mainly in the cytoplasm [82]. Methods for detection and determination of metallothioneins were recently reviewed [93,94].

As a consequence of higher zinc(II) content in breast cancer cells, metallothionein mRNA and protein levels are significantly increased [61]. Moreover, metallothionein level is positively correlated with more aggressive and higher-grade tumors [64]. Metallothioneins seem to be possible tumor markers in some tumors including breast cancer. More studies are needed to explore effects of anti-hormone therapies on zinc(II) transporter regulation, because these processes are endocrinologically regulated and hormonal therapy is the conventional treatment of breast cancer that express hormonal receptors [59].

Although the cause and the mechanism is not clear, it is considered that its increased level is responsible for protecting cancer cells from apoptosis, for increasing proliferation and the ability to metastasize [82]. This finding leads to several outputs (Fig. **2**). (A) If the serum level of metallothionein is elevated in the malignancies with the highest possible sensitivity, metallothionein could be used as a new tumor marker after further research, because many questions are still unanswered e.g. how metallothioneins levels correlate with age, or how MT levels can be influenced by viral or bacterial infection, or how MT levels change with physical activity. (B) Elevated serum level reflects altered metallothionein metabolism of tumor. Zinc(II) fluxes are tightly bound with metallothioneins, also zinc(II) metabolism and zinc(II) transport mechanisms are altered in cancer patients [95]. Metallothioneins also play important role in resistance to cytostatic drugs, particularly platinum compounds. Transfer of platinum from cisplatin or carboplatin to MTs result in inactivation of these drugs [96]. Thus, pre-treatment of zinc(II) results in MT induction and thus reduction of cisplatin or carboplatin cytotoxicity [97] [82]. Therefore, targeted pharmacological inhibition of MTs may reverse resistance to such cytostatics. These findings however need to be confirmed on large data set.

2.3. Molecular Biology of Zinc(II)

Zinc(II) as the only transition metal lacking redox activity is an essential part of app. 10 % human proteins [1,2]. Zinc(II) acts mainly as a cofactor of these proteins. Due to great portion of the zinc-depending proteins it is not surprising that zinc(II) is involved (through these proteins) in numerous key intra- and extracellular processes including proliferation, differentiation and apoptosis. Zinc-dependent enzymes can be found in all classes of enzymes, i.e. oxidoreductases, transferases, hydrolases, lyases, isomerases and ligases [16,98]. These enzymes include so-called zinc finger domains, repetitive sequences with ability to bind zinc(II) ions. Those domains consist of mostly histidine and/or cysteine. Zinc fingers are able to form complex with DNA based on interactions between α-helix of the zinc finger and DNA specific bases [99]. Function of zinc fingers consists not only in DNA recognition and transcriptional activation, but also in RNA packaging, protein folding and apoptosis, which regulation is important not only in development of tissues, but also in neoplastic transformation and proliferation [3,4].

Zinc(II) is necessary for all stages of cell cycle. Its higher level was described during G1 phase and G1/S phase transition [100]. There was identified influence of MT-1 on ATM/Chk2/cdc25A pathway during the G1/S phase transition [101]. Furthermore, induction of cyclin D3 and E is zinc-dependent, therefore, zinc(II) is required for proper S phase process and consequent G2/M transition [102]. It is expected, that high levels of zinc are required for nuclear functions during the early stage of differentiation of some cell systems [17].

Zinc(II) also play important role in regulation of apoptosis. Effects of zinc on apoptosis are cell specific and very complex. Depending on type of cells, concentration of other compounds and conditions zinc(II) ions can cause and/or counteract apoptotic effects [18]. Apoptotic effects of zinc(II) can be direct, through influence on nucleus/mitochondria, or indirect, through modulating cellular apoptotic signaling factors/pathways [18]. In general, zinc(II) acts as an antiapoptotic agent. It was demonstrated that zinc(II) deficiency induces apoptosis. Antiapoptotic properties of zinc(II) manifest in two ways [103]. First, it protects cells against oxidative damage [104]. Second, it directly inhibits activation of caspase 3 [105,106]. Its antioxidative properties may be mediated through activation of MTF-1 (and thus elevation of MTs and GSH) [19,33,35] and most likely also through activation of Cu,Zn superoxide dismutase (Cu,Zn SOD), a primary defence system involved in the antioxidant response [107-109]. On the other hand, zinc(II) may act as a pro-apoptotic agent in prostatic and neuronal cells [18,110,111]. High zinc(II) content affects apoptosis through the synthesis and formation of BAX pores on the outer mitochondrial membrane (Fig. **1**). Cytochrome-C can further be

released from mitochondria and can trigger cascade of caspases resulting in apoptosis [111].

In terms of apoptosis and proliferation of prostate cancer cells, due to decreased zinc(II) level, BAX-Cytochrome C apoptotic cascade is significantly silenced [18]. In addition, overexpression of Bcl-2 was observed. Antiapoptotic gene Bcl-2 is overexpressed in 30–60 % of prostate cancers within the luminal epithelium in high-grade PIN lesions, but is absent in most low-to-intermediate grade carcinomas [112,113]. Bcl-2 inhibits caspase activity either by preventing the release of Cytochrome C from the mitochondria and/or by binding to the apoptosis-activating factor (APAF-1).

Compared to healthy prostate as a result of down-regulation of zinc(II) in prostate cancer cells, apoptotic/antiapoptotic balance and energetic metabolism is changed in favor of the reduction of apoptosis [25]. Furthermore, because zinc(II) level is decreased, the inhibitory effect of zinc(II) on aconitase is abolished, citrate can enter the Krebs cycle, and cancer cells can then become more energy-efficient compared to healthy "energy inefficient" prostate cells [25]. This "energetic turnover" can also support prostate cancer cells growth (Fig. **2**). If so, it should lead to a speculation that the resumption of the inhibitory effect on mitochondrial aconitase by some inhibitors e.g. fluoroacetate (which is metabolized into fluorocitrate) may have tumor-suppressor effects. Unfortunately, fluoroacetate is not specific for prostate cells and therefore is toxic to most mammalian cells [25].

Furthermore, zinc(II) has a role as a signaling compound. It was demonstrated that concentration of free cytosolic zinc(II) ions could be increased by various intracellular or extracellular stimuli e.g. by reactive oxidation species or nitric oxide [37,43,114,115]. A pool of zinc(II) ions is released from cellular organelles such as endoplasmic reticulum, Golgi's apparatus or special vesicles – "zincosomes" [17,43]. Zincosomes play most likely role in endocytosis of zinc(II), however, their nature is not completely clear to date and needs further research [116]. Free zinc(II) level thereby fluctuates and has therefore downstream effects on cell signaling. All levels of signaling can be affected, from receptor level, through second messengers to transcription factors. Zinc(II) also interferes with the signaling cascades of cyclic nucleotides, tyrosine kinases and protein kinase C [117]. When dysregulated in cancers, activation of various oncogenic genes, e.g., Fos, Akt1, Jak3 and PI3K, was described [118].

3. WHOLE BODY ZINC(II) STATUS

3.1. Blood Plasma Level

Blood plasma zinc(II) concentration ranges within 12–20 μM [23,119,120]. In blood plasma, most of zinc(II) is bound with low affinity to albumin (approx. 60%). Approx. 10% is bound to transferrin and the remainder forms free fraction [121]. Albumin plays important role in blood plasma zinc(II) "buffering" [122]. It participates in the transport of newly absorbed zinc(II) from intestine to liver, it assist the transfer of zinc(II) to target sites [123], it promotes zinc(II) uptake by endothelial cells [124]. However, mechanisms of zinc(II) transfer from albumin are not completely understood. To date, only limited evidence on albumin zinc(II) binding sites exists [122].

Whereas zinc(II) is particularly intracellular ion, its serum level does not reflect total zinc status in humans [123]. However, it has been demonstrated in number of studies, that serum zinc(II) significantly differs in patients suffering from cancer. In United States Mortality Study of the Second national Health and Nutrition Examination Survey (NHANES II) was performed on 6,244 participants with complete history data. Except others, risk of serum zinc(II) and other metals was analyzed in terms of overall cancer mortality. It was concluded that the relation of serum zinc(II) and cancer mortality is nonlinear and the risk is significantly reduced for people with serum zinc between 13.2 to 15.8 μM compared to subjects with serum zinc 10.7 to 13.0 μM. This protective trend is more significant in men compared to women (RR = 0.56 for men vs. 0.79 for women) [125]. Based on similar follow-up study performed in Europe on 4,035 participants, subjects with a combination of low serum zinc(II) and high copper(II) values had increased cancer mortality risks [120].

In terms of serum zinc(II) level in prostate cancer patients, studies performed by Adaramoye *et al.* and Goel *et al.* revealed significantly lower ($p < 0.05$) level in patients of all PSA levels [126,127]. Similar reduction was observed in group of 41 participants using whole blood analysis of zinc(II) level [128]. However, Park *et al.* did not observe any difference and association between serum zinc level and prostate cancer risk in cancer and control group of 1,175 US participants [129]. In terms of serum level in breast cancer patients, decrease in zinc(II) was described by Borella *et al.* [130]. Gupta *et al.* found similar results, however, in the advanced stages of disease only [131]. Significant reduction of whole blood zinc(II) level was furthermore observed by Memon *et al.* on the 80 participants [132].

3.2. Zinc(II) in Diet

In terms of inadequate dietary zinc(II) income, on average, daily zinc(II) intake varies within the range from 8 to 14 mg/day in developed countries, and slightly less in developing countries, app. 5–11 mg/day [115]. The usually recommended zinc(II) intake is 15 mg/day [133], while its upper limit of daily intake is around 50 mg [134]. According to results from epidemiological study National Health and Nutrition Examination Study (NHANES III), zinc(II) intake may be critical in older population [135]. Based on more recent study, "Zinc and Health: Current Status and Future Directions" the zinc(II) intake is significantly inadequate in 12 % of Americans [136] and one may speculate that similar situation is in other developed countries. Deficiency in such a daily dose, leading to a serum zinc(II) concentration is less than 10 μM [119]. Zinc(II) deficiency could disrupt the function of both signaling molecules and proteins directly involved in DNA replication and repair [137-139]. Moreover, zinc(II) affect function of anti-tumor gene p53 – as demonstrated in the rat glioma C6 cells – zinc(II) deficiency up-regulates expression of p53. Furthermore, low intracellular zinc(II) impairs DNA-binding ability of p53, NF-κB and activator protein-1 transcription factor (AP-1) [140,141]. Zinc(II) deficiency may support tumorigenesis also through angiogenesis: endostatin, an angiogenesis inhibitor, require zinc(II) to be bound for its activity. In conditions of zinc(II) deficiency, its antiangiogenic potential is significantly reduced [142]. Such conditions may contribute to the development of cancer. More specifically, in terms of dietary zinc(II) intake and prostate cancer risk, several studies were performed. Kristal *et al.* found protective effect of zinc(II) supplementation on 697 US participants (relative risk 0.55 in higher zinc intake group) [143]. Conversely, based on a study performed on 46,974 US men participating in the Health Professionals Follow-Up Study during 14 years of follow-up from 1986 through 2000, no significant relative risk change was observed in group consuming < 100 mg/day. However, significant increase of risk prostate cancer was observed (relative risk 2.29 at $p < 0.003$) in patients with intake higher than 100 mg/day. Similarly, men taking supplemental zinc for 10 or more years had a relative risk of 2.37 ($p < 0.001$) [144]. Although results are not consistent, data suggest, that there is an ambivalent effect of zinc supplementation: In recommended daily dosage 15 mg/day there might be a protective effect [133]. However, in tenfold higher dosage (higher than 150 mg/day) zinc(II) can promote tumorigenesis. In breast cancer, study performed by Adzersen *et al.* in Germany on 653 participants concluded significantly reduced breast cancer risk (Relative risk 0.35 at $p = 0.01$) in patients with dietary zinc(II) income higher than 13.2 mg/day [145]. However, short-term high levels of zinc(II) are

relatively non-toxic compared to other metals. Many effects of so-called "zinc toxicity" are mostly due to the interference of zinc(II)-copper(II) metabolism, which results in copper(II) deficiency [146]. This phenomenon is most likely due to a competitive mechanism in enterocytes with participation of metal-binding protein metallothionein (MT). Due to competition between zinc(II) and copper(II) and displacing of copper(II) by zinc(II) ions, MT forms with copper(II) complexes which are excreted. Therefore, long-term overdosing with zinc(II) causes reduced absorption of copper [146]. Copper deficiency can then cause, among others, decreased activities of superoxide dismutase and cytochrome-C [147,148]. Hence, studies describing an increased incidence of prostate cancer when long-term over-supplemented with zinc(II) are more likely related with secondary copper deficiency rather than with primary effects of zinc(II).

4. SUMMARY AND CONCLUSIONS

According to recent studies, zinc(II) ions are not only a passive structural component of different cellular compartments, but also have regulatory effects on important cellular and subcellular processes such as regulation of proliferation, differentiation, apoptosis, neurotransmission and many others. The regulation of zinc(II) level is therefore important and its aberrancies may lead to various diseases, particularly cancers. Zinc(II) fluxes are tightly bound with metallothionein and together with finding that both compounds have effects on apoptosis and proliferation, it is naturally predictable that the misbalance of their regulation could affect cancer pathogenesis. However, many questions still exist. Currently, it is known that zinc(II) misbalance in some cancers, particularly in prostate cancer, is caused by alteration of ZIP1 transport mechanism. It is known that RREB-1 down-regulates ZIP1 expression in prostate cancer. However, also other potential pathways for ZIP1 down-regulation in prostate cancer cells may exist. This condition is most likely reversible and, therefore, this pathway may have therapeutic effect on prostate cancer. However, even if ZIP1 play a key role in zinc(II) intake, also other transporters' expression is somehow altered. Therefore, this prostate cancer-specific zinc(II) dysregulation is still not fully clarified and needs further research that leads to a more complex view on zinc(II) fluxes.

Similarly, only a little is known about zinc(II) status in breast cancer. ZIP6, 7 and 10 are identified to be highly expressed in high-risk forms of breast cancer. It has been also demonstrated that ZIP6 is positively regulated by estrogens and depletion of ZIP10 transporter inhibits the migration of highly metastatic breast cancer [60]. These data suggest a potential path to regulate metastatic potential of breast cancer. Further objectives are needed to be focused on (A) identifying of all other mechanisms leading to zinc(II) deregulation, (B) finding other mechanisms leading to zinc/metallothionein misbalance, (C) detailed identification of all effects on prostate and breast cancer pathogenesis. One may speculate that restoring of the expression of these transporters to the physiological levels and understanding of complex zinc(II) effects may lead to new, targeted therapy and prevention.

ACKNOWLEDGEMENTS

We highly acknowledge the support from grants GACR 301/09/P436, IGA MZ NS 10200-3, GA AV IAA40199070, NANOSEMED GA AV KAN208130801 and CEITEC CZ.1.05/1.1.00/02.0068.

ABBREVIATIONS

AD = Alzheimer's disease

ATZ = 3'-azido-3'-deoxythymidine

BAX = Bcl-2-like protein 4

Bcl-2 = B-cell CLL/lymphoma 2

CDF = cation diffusion facilitator

ER = endoplasmic reticulum

GIT = gastrointestinal tract

GSH = reduced glutathione

IL = interleukin

MT = metallothionein

MTF-1 = metal regulatory transcription factor 1

NF-κB = nuclear factor kappa-B

PSA = prostate specific antigen

RREB-1 = Ras-responsive element-binding protein 1

SLC = solute-linked carrier

ZIP = zinc-iron permease (or Zrt Irt-like protein)

ZnT = zinc transporter

REFERENCES

[1] Maret W.; Li Y. Coordination dynamics of zinc in proteins. *Chem. Rev.*, **2009**, *109*, 4682-4707.

[2] Andreini C.; Banci L.; Bertini I.; Rosato A. Counting the zinc-proteins encoded in the human genome. *J. Proteome Res.*, **2006**, *5*, 196-201.

[3] Yan W.; Imanishi M.; Futaki S.; Sugiura Y. alpha-helical linker of an artificial 6-zinc finger peptide contributes to selective DNA binding to a discontinuous recognition sequence. *Biochemistry*, **2007**, *46*, 8517-8524.

[4] Krishna S.S.; Majumdar I.; Grishin N.V. Structural classification of zinc fingers. *Nucleic Acids Res.*, **2003**, *31*, 532-550.

[5] Jemal A.; Bray F.; Center M.M.; Ferlay J.; Ward E.; Forman D. Global cancer statistics. *CA-Cancer J. Clin.*, **2011**, *61*, 69-90.

[6] Bono A.V. The global state of prostate cancer: epidemiology and screening in the second millennium. *Bju International*, **2004**, *94*, 1-2.

[7] Galvao E.; Martins L.M.S.; Ibiapina J.O.; Andrade H.M.; Monte S.J.H. Breast cancer proteomics: a review for clinicians. *J. Cancer Res. Clin. Oncol.*, **2011**, *137*, 915-925.

[8] King M.C.; Marks J.H.; Mandell J.B.; New York Breast Canc Study G. Breast and ovarian cancer risks due to inherited mutations in BRCA1 and BRCA2. *Science*, **2003**, *302*, 643-646.

[9] Mitrunen K.; Hirvonen A. Molecular epidemiology of sporadic breast cancer - The role of polymorphic genes involved in oestrogen biosynthesis and metabolism. *Mutat. Res.-Rev. Mutat. Res.*, **2003**, *544*, 9-41.

[10] Weiss J.M.; Goode E.L.; Ladiges W.C.; Ulrich C.M. Polymorphic variation in hOGG1 and risk of cancer: A review of the functional and epidemiologic literature. *Mol. Carcinog.*, **2005**, *42*, 127-141.

[11] Zhang Y.W.; Newcomb P.A.; Egan K.M.; Titus-Ernstoff L.; Chanock S.; Welch R.; Brinton L.A.; Lissowska J.; Bardin-Mikolajczak A.; Peplonska B.; Szeszenia-Dabrowska N.; Zatonski W.; Garcia-Closas M. Genetic Polymorphisms in base-excision repair pathway genes and risk of breast cancer. *Cancer Epidemiol. Biomarkers Prev.*, **2006**, *15*, 353-358.

[12] Vallee B.L.; Falchuk K.H. The biochemical basis of zinc physiology. *Physiol. Rev.*, **1993**, *73*, 79-118.

[13] Colvin R.A.; Bush A.I.; Volitakis I.; Fontaine C.P.; Thomas D.; Kikuchi K.; Holmes W.R. Insights into Zn2+ homeostasis in neurons from experimental and modeling studies. *Am. J. Physiol.-Cell Physiol.*, **2008**, *294*, C726-C742.

[14] Krezel A.; Maret W. Zinc-buffering capacity of a eukaryotic cell at physiological pZn. *J. Biol. Inorg. Chem.*, **2006**, *11*, 1049-1062.

[15] Palmiter R.D.; Findley S.D. Cloning and functional-characterization of a mammalian zinc transporter that confers resistance to zinc. *EMBO J.*, **1995**, *14*, 639-649.

[16] Colvin R.A.; Holmes W.R.; Fontaine C.P.; Maret W. Cytosolic zinc buffering and muffling: Their role in intracellular zinc homeostasis. *Metallomics*, **2010**, *2*, 306-317.

[17] Beyersmann D.; Haase H. Functions of zinc in signaling, proliferation and differentiation of mammalian cells. *Biometals*, **2001**, *14*, 331-341.

[18] Franklin R.B.; Costello L.C. The important role of the apoptotic effects of zinc in the development of cancers. *J. Cell. Biochem.*, **2009**, *106*, 750-757.

[19] Coyle P.; Philcox J.C.; Carey L.C.; Rofe A.M. Metallothionein: The multipurpose protein. *Cell. Mol. Life Sci.*, **2002**, *59*, 627-647.

[20] Franklin R.B.; Feng P.; Milon B.; Desouki M.M.; Singh K.K.; Kajdacsy-Balla A.; Bagasra O.; Costello L.C. hZIP1 zinc uptake transporter down regulation and zinc depletion in prostate cancer. *Mol. Cancer*, **2005**, *4*, 1-13.

[21] Costello L.C.; Liu Y.Y.; Zou J.; Franklin R.B. Evidence for a zinc uptake transporter in human prostate cancer cells which is regulated by prolactin and testosterone. *J. Biol. Chem.*, **1999**, *274*, 17499-17504.

[22] Frederickson C.J.; Suh S.W.; Silva D.; Thompson R.B. Importance of zinc in the central nervous system: The zinc-containing neuron. *J. Nutr.*, **2000**, *130*, 1471S-1483S.

[23] Costello L.C.; Franklin R.B. Zinc is decreased in prostate cancer: an established relationship of prostate cancer! *J. Biol. Inorg. Chem.*, **2011**, *16*, 3-8.

[24] Chimienti F.; Favier A.; Seve M. ZnT-8, a pancreatic beta-cell-specific zinc transporter. *Biometals*, **2005**, *18*, 313-317.

[25] Costello L.C.; Franklin R.B. The clinical relevance of the metabolism of prostate cancer; zinc and tumor suppression: connecting the dots. *Mol. Cancer*, **2006**, *5*, 1-13.

[26] Bjorndahl L.; Kvist U. Human sperm chromatin stabilization: a proposed model including zinc bridges. *Mol. Hum. Reprod.*, **2010**, *16*, 23-29.

[27] Medrano A.; Fernandez-Novell J.M.; Ramio L.; Alvarez J.; Goldberg E.; Rivera M.M.; Guinovart J.J.; Rigau T.; Rodriguez-Gil J.E. Utilization of citrate and lactate through a lactate dehydrogenase and ATP-regulated pathway in boar spermatozoa. *Mol. Reprod. Dev.*, **2006**, *73*, 369-378.

[28] Costello L.C.; Liu Y.Y.; Franklin R.B.; Kennedy M.C. Zinc inhibition of mitochondrial aconitase and its importance in citrate metabolism of prostate epithelial cells. *J. Biol. Chem.*, **1997**, *272*, 28875-28881.

[29] Cui Y.; Vogt S.; Olson N.; Glass A.G.; Rohan T.E. Levels of zinc, selenium, calcium, and iron in benign breast tissue and risk of subsequent breast cancer. *Cancer Epidemiol. Biomarkers Prev.*, **2007**, *16*, 1682-1685.

[30] Raju G.J.N.; Sarita P.; Kumar M.R.; Murty G.; Reddy B.S.; Lakshminarayana S.; Vijayan V.; Lakshmi P.; Gavarasana S.; Reddy S.B. Trace elemental correlation study in malignant and normal breast tissue by PIXE technique. *Nucl. Instrum. Methods Phys. Res. Sect. B-Beam Interact. Mater. Atoms*, **2006**, *247*, 361-367.

[31] Majewska U.; Banas D.; Braziewicz J.; Gozdz S.; Kubala-Kukus A.; Kucharzewski M. Trace element concentration distributions in breast, lung and colon tissues. *Phys. Med. Biol.*, **2007**, *52*, 3895-3911.

[32] Wang Q.S.; Wang M.H.; Yang F.; Zhang X.Z.; Zhao H.B.; Pan Y.C. Comparative analysis of MTF-1 binding sites between human and mouse. *Mamm. Genome*, **2010**, *21*, 287-298.

[33] Andrews G.K. Regulation of metallothionein gene expression by oxidative stress and metal ions. *Biochem. Pharmacol.*, **2000**, *59*, 95-104.

[34] Hasumi M.; Suzuki K.; Matsui H.; Koike H.; Ito K.; Yamanaka H. Regulation of metallothionein and zinc transporter expression in human prostate cancer cells and tissues. *Cancer Lett.*, **2003**, *200*, 187-195.

[35] Laity J.H.; Andrews G.K. Understanding the mechanisms of zinc-sensing by metal-response element binding transcription factor-1 (MTF-1). *Arch. Biochem. Biophys.*, **2007**, *463*, 201-210.

[36] Eide D.J. Zinc transporters and the cellular trafficking of zinc. *Biochim. Biophys. Acta-Mol. Cell Res.*, **2006**, *1763*, 711-722.

[37] Kambe T.; Yamaguchi-Iwai Y.; Sasaki R.; Nagao M. Overview of mammalian zinc transporters. *Cell. Mol. Life Sci.*, **2004**, *61*, 49-68.

[38] Liuzzi J.P.; Cousins R.J. Mammalian zinc transporters. *Annu. Rev. Nutr.*, **2004**, *24*, 151-172.

[39] Gaither L.A.; Eide D. Functional expression of the human hZIP2 zinc transporter. *Faseb J.*, **2000**, *14*, A228-A228.

[40] Gaither L.A.; Eide D.J. Eukaryotic zinc transporters and their regulation. *Biometals*, **2001**, *14*, 251-270.

[41] Franklin R.B.; Ma J.; Zou J.; Guan Z.; Kukoyi B.I.; Feng P.; Costello L.C. Human ZIP1 is a major zinc uptake transporter for the accumulation of zinc in prostate cells. *J. Inorg. Biochem.*, **2003**, *96*, 435-442.

[42] Johnson L.A.; Kanak M.A.; Kajdacsy-Balla A.; Pestaner J.P.; Bagasra O. Differential zinc accumulation and expression of human zinc transporter 1 (hZIP1) in prostate glands. *Methods*, **2010**, *52*, 316-321.

[43] Hogstrand C.; Kille P.; Nicholson R.I.; Taylor K.M. Zinc transporters and cancer: a potential role for ZIP7 as a hub for tyrosine kinase activation. *Trends Mol. Med.*, **2009**, *15*, 101-111.

[44] Milon B.C.; Agyapong A.; Bautista R.; Costello L.C.; Franklin R.B. Ras responsive element binding protein-1 (RREB-1) down-regulates hZIP1 expression in prostate cancer cells. *Prostate*, **2010**, *70*, 288-296.

[45] Ray S.K.; Nishitani J.; Petry M.W.; Fessing M.Y.; Leiter A.B. Novel transcriptional potentiation of BETA2/NeuroD on the secretin gene promoter by the DNA-binding protein Finb/RREB-1. *Mol. Cell. Biol.*, **2003**, *23*, 259-271.

[46] Thiagalingam A.; DeBustros A.; Borges M.; Jasti R.; Compton D.; Diamond L.; Mabry M.; Ball D.W.; Baylin S.B.; Nelkin B.D. RREB-1, a novel zinc finger protein, is involved in the differentiation response to ras in human medullary thyroid carcinomas. *Mol. Cell. Biol.*, **1996**, *16*, 5335-5345.

[47] Gioeli D. Signal transduction in prostate cancer progression. *Clin. Sci.*, **2005**, *108*, 293-308.

[48] Wong P.F.; Abubakar S. Comparative transcriptional study of the effects of high intracellular zinc on prostate carcinoma cells. *Oncol. Rep.*, **2010**, *23*, 1501-1516.

[49] Wong P.F.; Abubakar S. High intracellular Zn2+ ions modulate the VHR, ZAP-70 and ERK activities of LNCaP prostate cancer cells. *Cell. Mol. Biol. Lett.*, **2008**, *13*, 375-390.

[50] Golovine K.; Uzzo R.G.; Makhov P.; Crispen P.L.; Kunkle D.; Kolenko V.M. Depletion of intracellular zinc increases expression of tumorigenic cytokines VEGF, IL-6 and IL-8 in prostate cancer cells *via* NF-kappa B-dependent pathway. *Prostate*, **2008**, *68*, 1443-1449.

[51] Masarik M.; Gumulec J.; Kuchtickova S.; Kudlackova V.; Jurajda M.; Pavlik D.; Rovny A.; Hrabec R.; Krizkova S.; Kizek R. Determination of novel tumor markers in prostate carcinoma. *Febs J.*, **2010**, *277*, 188-188.

[52] Golovine K.; Makhov P.; Uzzo R.G.; Shaw T.; Kunkle D.; Kolenko V.M. Overexpression of the zinc uptake transporter hZIP1 inhibits nuclear factor-kappa B and reduces the malignant potential of prostate cancer cells *in vitro* and *in vivo*. *Clin. Cancer Res.*, **2008**, *14*, 5376-5384.

[53] Gaither L.A.; Eide D.J. The human ZIP1 transporter mediates zinc uptake in human K562 erythroleukemia cells. *J. Biol. Chem.*, **2001**, *276*, 22258-22264.

[54] Cao J.; Bobo J.A.; Liuzzi J.P.; Cousins R.J. Effects of intracellular zinc depletion on metallothionein and ZIP2 transporter expression and apoptosis. *J. Leukoc. Biol.*, **2001**, *70*, 559-566.

[55] Dufner-Beattie J.; Langmade S.J.; Wang F.D.; Eide D.; Andrews G.K. Structure, function, and regulation of a subfamily of mouse zinc transporter genes. *J. Biol. Chem.*, **2003**, *278*, 50142-50150.

[56] Kelleher S.L.; Lonnerdal B. ZIP3 plays a major role in zinc uptake into mammary epithelial cells and is regulated by prolactin. *Am. J. Physiol.-Cell Physiol.*, **2005**, *288*, C1042-C1047.

[57] Desouki M.M.; Geradts J.; Milon B.; Franklin R.B.; Costello L.C. hZIP2 and hZIP3 zinc transporters are down regulated in human prostate adenocarcinomatous glands. *Mol. Cancer*, **2007**, *6*, 1-7.

[58] Taylor K.M.; Morgan H.E.; Johnson A.; Hadley L.J.; Nicholson R.I. Structure-function analysis of LIV-1, the breast cancer-associated protein that belongs to a new subfamily of zinc transporters. *Biochem. J.*, **2003**, *375*, 51-59.

[59] Kelleher S.L.; Seo Y.A.; Lopez V. Mammary gland zinc metabolism: regulation and dysregulation. *Genes Nutr.*, **2009**, *4*, 83-94.

[60] Kagara N.; Tanaka N.; Noguchi S.; Hirano T. Zinc and its transporter ZIP10 are involved in invasive behavior of breast cancer cells. *Cancer Sci.*, **2007**, *98*, 692-697.

[61] Schlag P.; Seeling W.; Merkle P.; Betzler M. Changes of serum-zinc in breast-cancer. *Langenbecks Arch. Chirurg.*, **1978**, *346*, 129-133.

[62] Manning D.L.; Daly R.J.; Lord P.G.; Kelly K.F.; Green C.D. Effects of estrogen on the expression of a 4.4 kb messenger-RNA in the zr-75-1 human-breast cancer cell-line. *Mol. Cell. Endocrinol.*, **1988**, *59*, 205-212.

[63] Taylor K.M.; Morgan H.E.; Smart K.; Zahari N.M.; Pumford S.; Ellis I.O.; Robertson J.F.; Nicholson R.I. The emerging role of the LIV-1 subfamily of zinc transporters in breast cancer. *Mol. Med.*, **2007**, *13*, 396-406.

[64] Bay B.H.; Jin R.X.; Huang J.X.; Tan P.H. Metallothionein as a prognostic biomarker in breast cancer. *Exp. Biol. Med.*, **2006**, *231*, 1516-1521.

[65] Lopez V.; Kelleher S.L. ZIP6-attenuation promotes epithelial-to-mesenchymal transition in ductal breast tumor (T47D) cells. *Exp. Cell Res.*, **2010**, *316*, 366-375.

[66] Arcangeli A.; Crociani O.; Lastraioli E.; Masi A.; Pillozzi S.; Becchetti A. Targeting ion channels in cancer: A novel frontier in antineoplastic therapy. *Curr. Med. Chem.*, **2009**, *16*, 66-93.

[67] Urani C.; Melchioretto P.; Gribaldo L. Regulation of metallothioneins and ZnT-1 transporter expression in human hepatoma cells HepG2 exposed to zinc and cadmium. *Toxicol. Vitro*, **2010**, *24*, 370-374.

[68] Jayaraman A.K.; Jayaraman S. Increased level of exogenous zinc induces cytotoxicity and up-regulates the expression of the ZnT-1 zinc transporter gene in pancreatic cancer cells. *J. Nutr. Biochem.*, **2011**, *22*, 79-88.

[69] Wang X.X.; Zhou B. Dietary zinc absorption: A play of ZIPs and ZnTs in the gut. *IUBMB Life*, **2010**, *62*, 176-182.

[70] Lyubartseva G.; Smith J.L.; Markesbery W.R.; Lovell M.A. Alterations of zinc transporter proteins ZnT-1, ZnT-4 and ZnT-6 in preclinical Alzheimer's disease brain. *Brain Pathol.*, **2010**, *20*, 343-350.

[71] Masarik M.; Gumulec J.; Sztalmachova M.; Hlavna M.; Babula P.; Krizkova S.; Ryvolova M.; Jurajda M.; Sochor J.; Adam V.; Kizek R. Isolation of metallothionein from cells derived from aggressive form of high grade prostate carcinoma using paramagnetic microbeads immunoassay off-line coupled with electrochemical and electrophoretic determination. *Electrophoresis*, **2011**, *in press*.

[72] Kobayashi T.; Beuchat M.H.; Lindsay M.; Frias S.; Palmiter R.D.; Sakuraba H.; Parton R.G.; Gruenberg J. Late endosomal membranes rich in lysobisphosphatidic acid regulate cholesterol transport. *Nat. Cell Biol.*, **1999**, *1*, 113-118.

[73] Schroder B.; Wrocklage C.; Pan C.; Jager R.; Kosters B.; Schafer H.; Elsasser H.P.; Mann M.; Hasilik A. Integral and associated lysosomal membrane proteins. *Traffic*, **2007**, *8*, 1676-1686.

[74] Sorensen M.B.; Stoltenberg M.; Juhl S.; Danscher G.; Ernst E. Ultrastructural localization of zinc ions in the rat prostate: an autometallographic study. *Prostate*, **1997**, *31*, 125-130.

[75] Iguchi K.; Usui S.; Inoue T.; Sugimura Y.; Tatematsu M.; Hirano K. High-level expression of zinc transporter-2 in the rat lateral and dorsal prostate. *J. Androl.*, **2002**, *23*, 819-824.

[76] Margoshes M.; Vallee B.L. A cadmium protein from equine kidney cortex. *J. Am. Chem. Soc.*, **1957**, *79*, 4813-4814.

[77] Miles A.T.; Hawksworth G.M.; Beattie J.H.; Rodilla V. Induction, regulation, degradation, and biological significance of mammalian metallothioneins. *Crit. Rev. Biochem. Mol. Biol.*, **2000**, *35*, 35-70.

[78] Kilic G.A.; Kutlu M. Effects of exogenous metallothionein against thallium-induced oxidative stress in rat liver. *Food Chem. Toxicol.*, **2010**, *48*, 980-987.

[79] Krizkova S.; Adam V.; Petrlova J.; Zitka O.; Stejskal K.; Zehnalek J.; Sures B.; Trnkova L.; Beklova M.; Kizek R. A suggestion of electrochemical

biosensor for study of platinum(II)-DNA interactions. *Electroanalysis*, **2007**, *19*, 331-338.
[80] Krizkova S.; Adam V.; Kizek R. Study of metallothionein oxidation by using of chip CE. *Electrophoresis*, **2009**, *30*, 4029-4033.
[81] Krizkova S.; Masarik M.; Eckschlager T.; Adam V.; Kizek R. Effects of redox conditions and zinc(II) ions on metallothionein aggregation revealed by chip capillary electrophoresis. *J. Chromatogr. A*, **2010**, *1217*, 7966-7971.
[82] Eckschlager T.; Adam V.; Hrabeta J.; Figova K.; Kizek R. Metallothioneins and Cancer. *Curr. Protein Pept. Sci.*, **2009**, *10*, 360-375.
[83] Krizkova S.; Fabrik I.; Adam V.; Hrabeta P.; Eckschlager T.; Kizek R. Metallothionein - a promising tool for cancer diagnostics. *Bratisl. Med. J.-Bratisl. Lek. Listy*, **2009**, *110*, 93-97.
[84] Lindeque J.Z.; Levanets O.; Louw R.; van der Westhuizen F.H. The involvement of metallothioneins in mitochondrial function and disease. *Curr. Protein Pept. Sci.*, **2010**, *11*, 292-309.
[85] Kadota Y.; Suzuki S.; Ideta S.; Fukinbara Y.; Kawakami T.; Imai H.; Nakagawa Y.; Sato M. Enhanced metallothionein gene expression induced by mitochondrial oxidative stress is reduced in phospholipid hydroperoxide glutathione peroxidase-overexpressed cells. *Eur. J. Pharmacol.*, **2010**, *626*, 166-170.
[86] Verrax J.; Pedrosa R.C.; Beck R.; Dejeans N.; Taper H.; Calderon P.B. In situ modulation of oxidative stress: A novel and efficient strategy to kill cancer cells. *Curr. Med. Chem.*, **2009**, *16*, 1821-1830.
[87] Krizkova S.; Masarik M.; Majzlik P.; Kukacka J.; Kruseova J.; Adam V.; Prusa R.; Eckschlager T.; Stiborova M.; Kizek R. Serum metallothionein in newly diagnosed patients with childhood solid tumours. *Acta Biochim. Pol.*, **2010**, *57*, 561-566.
[88] Adam V.; Baloun J.; Fabrik I.; Trnkova L.; Kizek R. An electrochemical detection of metallothioneins at the zeptomole level in nanolitre volumes. *Sensors*, **2008**, *8*, 2293-2305.
[89] Fabrik I.; Krizkova S.; Huska D.; Adam V.; Hubalek J.; Trnkova L.; Eckschlager T.; Kukacka J.; Prusa R.; Kizek R. Employment of electrochemical techniques for metallothionein determination in tumour cell lines and patients with a tumor disease. *Electroanalysis*, **2008**, *20*, 1521-1532.
[90] Krizkova S.; Fabrik I.; Adam V.; Kukacka J.; Prusa R.; Chavis G.J.; Trnkova L.; Strnadel J.; Horak V.; Kizek R. Utilizing of adsorptive transfer stripping technique Brdicka reaction for determination of metallothioneins level in melanoma cells, blood serum and tissues. *Sensors*, **2008**, *8*, 3106-3122.
[91] Krizkova S.; Fabrik I.; Huska D.; Adam V.; Babula P.; Hrabeta J.; Eckschlager T.; Pochop P.; Darsova D.; Kukacka J.; Prusa R.; Trnkova L.; Kizek R. An adsorptive transfer technique coupled with Brdicka reaction to reveal the importance of metallothionein in chemotherapy with platinum based cytostatics. *Int. J. Mol. Sci.*, **2010**, *11*, 4826-4842.
[92] Knipp M. Metallothioneins and Platinum(II) Anti-Tumor Compounds. *Curr. Med. Chem.*, **2009**, *16*, 522-537.
[93] Adam V.; Fabrik I.; Eckschlager T.; Stiborova M.; Trnkova L.; Kizek R. Vertebrate metallothioneins as target molecules for analytical techniques. *TRAC-Trends Anal. Chem.*, **2010**, *29*, 409-418.
[94] Ryvolova M.; Krizkova S.; Adam V.; Beklova M.; Trnkova L.; Hubalek J.; Kizek R. Analytical methods for metallothionein detection. *Curr. Anal. Chem.*, **2011**, *7*, 243-261.
[95] Adam V.; Petrlova J.; Wang J.; Eckschlager T.; Trnkova L.; Kizek R. Zeptomole electrochemical detection of metallothioneins. *Plos One*, **2010**, *5*, e11441.
[96] Andrews P.A.; Murphy M.P.; Howell S.B. Metallothionein-mediated cisplatin resistance in human ovarian-carcinoma cells. *Cancer Chemother. Pharmacol.*, **1987**, *19*, 149-154.
[97] Choi C.H.; Cha Y.J.; An C.S.; Kim K.J.; Kim K.C.; Moon S.P.; Lee Z.H.; Min Y.D. Molecular mechanisms of heptaplatin effective against cisplatin-resistant cancer cell lines: less involvement of metallothionein. *Cancer Cell. Int.*, **2004**, *4*, 1-12.
[98] Vallee B.; Auld D. Short and long spacer sequences and other structural features of zinc binding sites in zinc enzymes. *FEBS Lett.*, **1989**, *257*, 138-140.
[99] Zitka O.; Kukacka J.; Krizkova S.; Huska D.; Adam V.; Masarik M.; Prusa R.; Kizek R. Matrix Metalloproteinases. *Curr. Med. Chem.*, **2010**, *17*, 3751-3768.
[100] Nagel W.W.; Vallee B.L. Cell-cycle regulation of metallothionein in human colonic-cancer cells. *Proc. Natl. Acad. Sci. U. S. A.*, **1995**, *92*, 579-583.
[101] Lim D.; Jocelyn K.M.X.; Yip G.W.C.; Bay B.H. Silencing the Metallothionein-2A gene inhibits cell cycle progression from G1-to S-phase involving ATM and cdc25A signaling in breast cancer cells. *Cancer Lett.*, **2009**, *276*, 109-117.
[102] Li Y.; Maret W. Transient fluctuations of intracellular zinc ions in cell proliferation. *Exp. Cell Res.*, **2009**, *315*, 2463-2470.
[103] John E.; Laskow T.C.; Buchser W.J.; Pitt B.R.; Basse P.H.; Butterfield L.H.; Kalinski P.; Lotze M.T. Zinc in innate and adaptive tumor immunity. *J. Transl. Med.*, **2010**, *8*, 1-16.
[104] Eibl J.K.; Abdallah Z.; Ross G.M. Zinc-metallothionein: a potential mediator of antioxidant defence mechanisms in response to dopamine-induced stress. *Can. J. Physiol. Pharmacol.*, **2010**, *88*, 305-312.
[105] Truong-Tran A.Q.; Ho L.H.; Chai F.; Zalewski P.D. Cellular zinc fluxes and the regulation of apoptosis/gene-directed cell death. *J. Nutr.*, **2000**, *130*, 1459S-1466S.
[106] Truong-Tran A.Q.; Grosser D.; Ruffin R.E.; Murgia C.; Zalewski P.D. Apoptosis in the normal and inflamed airway epithelium: role of zinc in epithelial protection and procaspase-3 regulation. *Biochem. Pharmacol.*, **2003**, *66*, 1459-1468.
[107] Magalova T.; Bella V.; Brtkova A.; Beno I.; Kudlackova M.; Volkovova K. Copper, zinc and superoxide dismutase in precancerous, benign diseases and gastric, colorectal and breast cancer. *Neoplasma*, **1999**, *46*, 100-104.
[108] Valko M.; Rhodes C.J.; Moncol J.; Izakovic M.; Mazur M. Free radicals, metals and antioxidants in oxidative stress-induced cancer. *Chem.-Biol. Interact.*, **2006**, *160*, 1-40.
[109] Zuo X.L.; Chen J.M.; Zhou X.; Li X.Z.; Mei G.Y. Levels of selenium, zinc, copper, and antioxidant enzyme activity in patients with leukemia. *Biol. Trace Elem. Res.*, **2006**, *114*, 41-53.
[110] Weiss J.H.; Jiang D.M.; Sullivan P.G.; Sensi S.L.; Steward O. Zn2+ induces permeability transition pore opening and release of pro-apoptotic peptides from neuronal mitochondria. *J. Biol. Chem.*, **2001**, *276*, 47524-47529.
[111] Feng P.; Li T.L.; Guan Z.X.; Franklin R.B.; Costello L.C. The involvement of bax in zinc-induced mitochondrial apoptogenesis in malignant prostate cells. *Mol. Cancer*, **2008**, *7*, 1-6.
[112] Humbert L.; Chevrette M. Somatic Molecular Genetics of Prostate Cancer, in: W.D. Foulkes and K.A. Cooney (Eds.), Male Reproductive Cancers Epidemiology, Pathology and Genetics, Springer Verlag, New York, Dordrecht, Heidelberg, London, **2009**, pp. 345.
[113] DiPaola R.S.; Patel J.; Rafi M.M. Targeting apoptosis in prostate cancer. *Hematol. Oncol. Clin. North Am.*, **2001**, *15*, 509-524.
[114] Hirano T.; Murakami M.; Fukada T.; Nishida K.; Yamasaki S.; Suzuki T. Roles of zinc and zinc signaling in immunity: Zinc as an intracellular signaling molecule. *Adv.Immunol.*, **2008**, 149-176.
[115] Oteiza P.I.; Mackenzie G.G. Zinc, oxidant-triggered cell signaling, and human health. *Mol. Asp. Med.*, **2005**, *26*, 245-255.
[116] Ballestin R.; Molowny A.; Marin M.P.; Esteban-Pretel G.; Romero A.M.; Lopez-Garcia C.; Renau-Piqueras J.; Ponsoda X. Ethanol reduces zincosome formation in cultured astrocytes. *Alcohol Alcohol.*, **2011**, *46*, 17-25.
[117] Haase H.; Maret W. Intracellular zinc fluctuations modulate protein tyrosine phosphatase activity in insulin/insulin-like growth factor-1 signaling. *Exp. Cell Res.*, **2003**, *291*, 289-298.
[118] Lin S.F.; Wei H.; Maeder D.; Franklin R.B.; Feng P. Profiling of zinc-altered gene expression in human prostate normal vs. cancer cells: a time course study. *J. Nutr. Biochem.*, **2009**, *20*, 1000-1012.
[119] Tubek S. Zinc supplementation or regulation of its homeostasis: Advantages and threats. *Biol. Trace Elem. Res.*, 2007, *119*, 1-9.
[120] Leone N.; Courbon D.; Ducimetiere P.; Zureik M. Zinc, copper, and magnesium and risks for all-cause, cancer, and cardiovascular mortality. *Epidemiology*, **2006**, *17*, 308-314.
[121] Rink L.; Gabriel P. Zinc and the immune system. *Proc. Nutr. Soc.*, **2000**, *59*, 541-552.
[122] Blindauer C.A.; Harvey I.; Bunyan K.E.; Stewart A.J.; Sleep D.; Harrison D.J.; Berezenko S.; Sadler P.J. Structure, properties, and engineering of the major zinc binding site on human albumin. *J. Biol. Chem.*, **2009**, *284*, 23116-23124.
[123] Cousins R.J. Toward a molecular understanding of zinc-metabolism. *Clin. Phys. Biochem.*, **1986**, *4*, 20-30.
[124] Rowe D.J.; Bobilya D.J. Albumin facilitates zinc acquisition by endothelial cells. *Proc. Soc. Exp. Biol. Med.*, **2000**, *224*, 178-186.
[125] Wu T.J.; Sempos C.T.; Freudenheim J.L.; Muti P.; Smith E. Serum iron, copper and zinc concentrations and risk of cancer mortality in US adults. *Ann. Epidemiol.*, **2004**, *14*, 195-201.
[126] Adaramoye O.A.; Akinloye O.; Olatunji I.K. Trace elements and Vitamin E status in Nigerian patients with prostate cancer. *Afr. Health Sci.*, **2010**, *10*, 2-8.
[127] Goel T.; Sankhwar S.N. Comparative study of zinc levels in benign and malignant lesions of the prostate. *Scand. J. Urol. Nephrol.*, **2006**, *40*, 108-112.
[128] Ozmen H.; Erulas F.A.; Karatas F.; Cukurovali A.; Yalcin O. Comparison of the concentration of trace metals (Ni, Zn, Co, Cu and Se), Fe, vitamins A, C and E, and lipid peroxidation in patients with prostate cancer. *Clin. Chem. Lab. Med.*, **2006**, *44*, 175-179.
[129] Park S.Y.; Kolonel L. Serum zinc and prostate cancer risk in the multiethnic cohort study. *Epidemiology*, **2009**, *20*, S131-S131.
[130] Borella P.; Bargellini A.; Caselgrandi E.; Piccinini L. Observations on the use of plasma, hair and tissue to evaluate trace element status in cancer. *J. Trace Elem. Med. Biol.*, **1997**, *11*, 162-165.
[131] Gupta S.K.; Shukla V.K.; Vaidya M.P.; Roy S.K.; Gupta S. Serum trace elements and Cu/Zn ratio in breast cancer patients. *J. Surg. Oncol.*, **1991**, *46*, 178-181.
[132] Memon A.U.R.; Kazi T.G.; Afridi H.I.; Jamali M.K.; Arain M.B.; Jalbani N.; Syed N. Evaluation of zinc status in whole blood and scalp hair of female cancer patients. *Clin. Chim. Acta*, **2007**, *379*, 66-70.
[133] Tapiero H.; Tew K.D. Trace elements in human physiology and pathology: zinc and metallothioneins. *Biomed. Pharmacother.*, **2003**, *57*, 399-411.
[134] Hambidge M. Human zinc deficiency. *J. Nutr.*, **2000**, *130*, 1344S-1349S.
[135] Alaimo K.; McDowell M.A.; Briefel R.R.; Bischof A.M.; Caughman C.R.; Loria C.M.; Johnson C.L. Dietary intake of vitamins, minerals, and fiber of persons ages 2 months and over in the United States: Third National Health and Nutrition Examination Survey, Phase 1, 1988-91. *Advance Data*, 19941.

[136] Song Y.; Elias V.; Loban A.; Scrimgeour A.G.; Ho E. Marginal zinc deficiency increases oxidative DNA damage in the prostate after chronic exercise. *Free Radic. Biol. Med.*, **2010**, *48*, 82-88.

[137] Dhawan D.K.; Chadha V.D. Zinc: A promising agent in dietary chemoprevention of cancer. *Indian J. Med. Res.*, **2010**, *132*, 676-682.

[138] Chiaverini N.; De Ley M. Protective effect of metallothionein on oxidative stress-induced DNA damage. *Free Radic. Res.*, **2010**, *44*, 605-613.

[139] Banudevi S.; Elumalai P.; Arunkumar R.; Senthilkumar K.; Gunadharini D.N.; Sharmila G.; Arunakaran J. Chemopreventive effects of zinc on prostate carcinogenesis induced by N-methyl-N-nitrosourea and testosterone in adult male Sprague-Dawley rats. *J. Cancer Res. Clin. Oncol.*, **2011**, *137*, 677-686.

[140] Ho E.; Ames B.N. Low intracellular zinc induces oxidative DNA damage, disrupts p53, NF kappa B, and AP1 DNA binding, and affects DNA repair in a rat glioma cell line. *Proc. Natl. Acad. Sci. U. S. A.*, **2002**, *99*, 16770-16775.

[141] Schetter A.J.; Heegaard N.H.H.; Harris C.C. Inflammation and cancer: interweaving microRNA, free radical, cytokine and p53 pathways. *Carcinogenesis*, **2010**, *31*, 37-49.

[142] Boehm T.; O'Reilly M.S.; Keough K.; Shiloach J.; Shapiro R.; Folkman J. Zinc-binding of endostatin is essential for its antiangiogenic activity. *Biochem. Biophys. Res. Commun.*, **1998**, *252*, 190-194.

[143] Kristal A.R.; Stanford J.L.; Cohen J.H.; Wicklund K.; Patterson R.E. Vitamin and mineral supplement use is associated with reduced risk of prostate cancer. *Cancer Epidemiol. Biomarkers Prev.*, **1999**, *8*, 887-892.

Received: June 07, 2011 **Revised: August 01, 2011** **Accepted: August 03, 2011**

[144] Leitzmann M.F.; Stampfer M.J.; Wu K.N.; Colditz G.A.; Willett W.C.; Giovannucci E.L. Zinc supplement use and risk of prostate cancer. *J. Natl. Cancer Inst.*, **2003**, *95*, 1004-1007.

[145] Adzersen K.H.; Jess P.; Freivogel K.W.; Gerhard I.; Bastert G. Raw and cooked vegetables, fruits, selected micronutrients, and breast cancer risk: a case-control study in Germany. *Nutr. Cancer*, **2003**, *46*, 131-137.

[146] Plum L.M.; Rink L.; Haase H. The essential toxin: Impact of zinc on human health. *Int. J. Environ. Res. Pub. Health*, **2010**, *7*, 1342-1365.

[147] Prohaska J.R. Biochemical-changes in copper deficiency. *J. Nutr. Biochem.*, **1990**, *1*, 452-461.

[148] Sandstead H.H. Requirements and toxicity of essential trace-elements, illustrated by zinc and copper. *Am. J. Clin. Nutr.* , **1995**, *61*, S621-S624.

[149] Croxford T.P.; McCormick N.H.; Kelleher S.L. Moderate zinc deficiency reduces testicular ZIP6 and ZIP10 abundance and impairs spermatogenesis in mice. *J. Nutr.*, **2011**, *141*, 359-365.

[150] Guo L.; Lichten L.A.; Ryu M.S.; Liuzzi J.P.; Wang F.D.; Cousins R.J. STAT5-glucocorticoid receptor interaction and MTF-1 regulate the expression of ZnT2 (Slc30a2) in pancreatic acinar cells. *Proc. Natl. Acad. Sci. U. S. A.*, **2010**, *107*, 2818-2823.

[151] Seo Y.A.; Kelleher S.L. Functional analysis of two single nucleotide polymorphisms in SLC30A2 (ZnT2): implications for mammary gland function and breast disease in women. *Physiol. Genomics*, **2010**, *42A*, 219-227.

2.1.3 Prostate cancer and microRNA action

MicroRNAs (miRNAs) are short, non-coding regulatory RNAs of about 20 nucleotides in size. MiRNAs bind to the target mRNA with the complementary sequence, induce its degradation or block translation of the given mRNA. The single miRNA can target up to hundreds of different mRNAs. MiRNAs are involved in a variety of different cellular signalling pathways at many levels. These small molecules are associated with the development of many diseases, including tumours. Each miRNA has the ability to interact with a number of cellular signalling pathways, and changes in the expression of a relatively low number of miRNAs may reflect deregulation of a wide variety of cellular processes that may be decisive for the development of a tumour disease. MiRNAs also play an important regulatory role in developing resistance to the commonly used therapeutic procedures such as radiotherapy and chemotherapy and affect tumour progression [49]. MiRNAs represent an attractive target in research of new non-invasive biomarkers as they are relatively resistant to RNase degradation and are therefore relatively stable in plasma, serum and tissue samples [50]. Based on bioinformatics database outputs and based on a wide range of published studies, it is evident that miRNAs affect significantly the genes associated with zinc regulation and CaP development. The following overview paper by Pekarik et al. on page 67 [51] summarizes the importance of the miRNAs in the regulation of metallothionein and zinc transporters. These findings are presented in the clinical-pathological context.

Author's publication relevant to this chapter

Pekarik V, Gumulec J, Masarik M, Kizek R, Adam V. Prostate Cancer, miRNAs, Metallothioneins and Resistance to Cytostatic Drugs. Current Medicinal Chemistry. 2013;20(4):534-544. Available on page 67

Send Orders of Reprints at bspsaif@emirates.net.ae

534 *Current Medicinal Chemistry*, 2013, *20*, 534-544

Prostate Cancer, miRNAs, Metallothioneins and Resistance to Cytostatic Drugs

V. Pekarik[1], J. Gumulec[2], M. Masarik[2], R. Kizek[3,4] and V. Adam*[,3,4]

[1]*Department of Cellular and Molecular Neurobiology, Central European Technology Institute, Masaryk University, Kamenice 735/3, CZ-625 00 Brno, Czech Republic, European Union;* [2]*Department of Pathological Physiology, Faculty of Medicine, Masaryk University, Kamenice 5, CZ-625 00 Brno, Czech Republic, European Union;* [3]*Department of Chemistry and Biochemistry, Faculty of Agronomy, Mendel University in Brno, Zemedelska 1, CZ-613 00 Brno, Czech Republic, European Union;* [4]*Central European Institute of Technology, Brno University of Technology, Technicka 3058/10, CZ-616 00 Brno, Czech Republic, European Union*

Abstract: MicroRNAs (miRNAs) translationally repressing their target messenger RNAs due to their gene-regulatory functions play an important but not unexpected role in a tumour development. More surprising are the findings that levels of various miRNAs are well correlated with presence of specific tumours and formation of metastases. Moreover, these small regulatory molecules play a role in the resistance of cancer cells to commonly used anti-cancer drugs, such as cisplatin, anthracyclines, and taxanes. In that respect, miRNAs become very attractive target for potential therapeutic interventions. Improvements in the sensitivity of miRNAs detection techniques led to discovery of circulating miRNAs which became very attractive non-invasive biomarker of cancer with a substantial predictive value. In this review, the authors focus on i) oncogenic and anti-tumour acting miRNAs, ii) function of miRNAs in tumour progression, iii) possible role of miRNAs in resistance to anticancer drugs, and iv) diagnostic potential of miRNAs for identification of cancer from circulating miRNAs with special emphasis on prostate cancer. Moreover, relationship between miRNAs and expression of metallothionein is discussed as a possible explanation of resistance against platinum based drugs.

Keywords: Prostate carcinoma, markers, miRNA, circulating miRNAs, metallothionein, anti-cancer drugs, platinum based cytostatics, zinc, resistance, metastases.

INTRODUCTION

Cancer is the leading cause of mortality in Western countries and the second leading cause of death in developing countries [1]. The burden of cancer is rising in economically developing countries: their population is growing and aging and it adopts cancer-associated lifestyle choices including smoking, physical inactivity, and "westernized" diets [2].

Prostate cancer (PCa) is the second most frequently diagnosed cancer and the sixth leading cause of cancer death in males. The prevalence of prostate cancer increases with age. It does, however, usually respond to treatment and, if localized, may be curable. The rate of tumour growth varies from very slow to moderately rapid, and some patients may have prolonged survival, even after the cancer has metastasized to distant sites. Prostate tissue responds to steroid hormones; the prostate cancer is likewise characterised by transition from androgen dependent (AD) stage - where anti-androgen therapy (often castration) can be applied - to androgen independent (AI) stage, where the therapeutical prognosis rapidly declines. Androgen receptor (AR), also known as NR3C4, is cytoplasmatically located receptor which after binding its ligand testosterone or dihydrotestosterone translocates to the nucleus and activates specific gene expression there.

A change from healthy cell to cancer one is often characterised by a loss of E-cadherin, a cell adhesion molecule important for the maintenance of tissue integrity. The loss of E-cadherin permits cells to detach from the original niche, form a tumour mass and/or invade blood or lymphatic system. This biochemical and morphological change is known as epithelial-to-mesenchymal transition (EMT). Migrating cells can re-express cadherins in other tissues or organs where they home and thus form secondary lesions. Gene expression of E-cadherins is regulated by promoter methylation of CpG island, which is induced by transcriptional repressors.

Other extracellular matrix interacting or cell adhesion molecules such as integrins [3] are involved in transition from healthy to transformed cell and can become targets of pharmaceutical intervention [4]. Tumour formation has been analysed from various aspects (genome, transcriptome, metabolone, and other -omes). In this review, two aspects of prostate cancer are discussed - zinc metabolism and function of miRNAs, and the focus is given on the role of these factors in response to chemotherapy and acquired resistance to anticancer drugs.

*Address correspondence to this author at the Department of Chemistry and Biochemistry, Mendel University in Brno, Zemedelska 1, CZ-613 00 Brno, Czech Republic; Tel: +420-5-4513-3350; Fax: +420-5-4521-2044; E-mail: vojtech.adam@mendelu.cz

ZINC METABOLISM AND METALLOTHIONEINS

Among other characteristics, healthy and particularly tumorous prostate tissue is unique in its relation to zinc ions Fig. (**1**). Healthy prostate is highly specialized in zinc accumulating processes: intracellular zinc level ranges in up to tenfold concentrations compared to most other tissues [5]. In contrast, a significant decrease of intracellular zinc concentration has been observed already from early stages of tumorigenesis [6-9]. Although some conflicting results were reported [10], the decrease of prostate's tissue zinc may be considered as well evidenced and established [11]. Due to the fact that zinc cannot freely pass through the membranes, the crucial role in the maintenance of intracellular zinc level is provided by zinc-transporting proteins, ZIPs (Zrt- Irt like protein or Zinc Iron permease) and ZnTs (Zinc transporters). Zinc transport has been discussed in detail in several recent reviews [12, 13]; this review emphasises in particular the decrease of cellular zinc in prostate cancer notably caused by down-regulation of zinc transporter ZIP1 expression [11, 14, 15]. Mechanisms causing the down-regulation of ZIP1 and other transporters in prostate cancer have been addressed recently [16]. Since no mutations have been identified in the zinc transporters' genes [12, 14], the attention focused on epigenetic processes and association of silenced activator protein AP-2α and ZIPs have been studied on *in situ* model [17]. ZIP1 is very likely down-regulated by Ras Responsive Element Binding Protein-1 (RREB-1) which was shown to be up-regulated in prostate cancer due to Ras-Raf-MEK-ERK cascade [18]. Mihelich *et al.* also report a possible regulatory role of miRNA on zinc transporters: a miRNA cluster miR-183-96-182 (miR-96 and miR-183 are expressed as a cluster with miR-182) was found overexpressed in prostate tissue [19]. The overexpression of this cluster was associated with suppression of multiple zinc transporters, including ZIP1.

The reduction of the cellular zinc in prostate cancer is not only a minor consequence of wide myriad of genetic aberrations, but rather an important step in the pathogenesis. It has been experimentally demonstrated that the loss of zinc accumulation *in situ* is es-

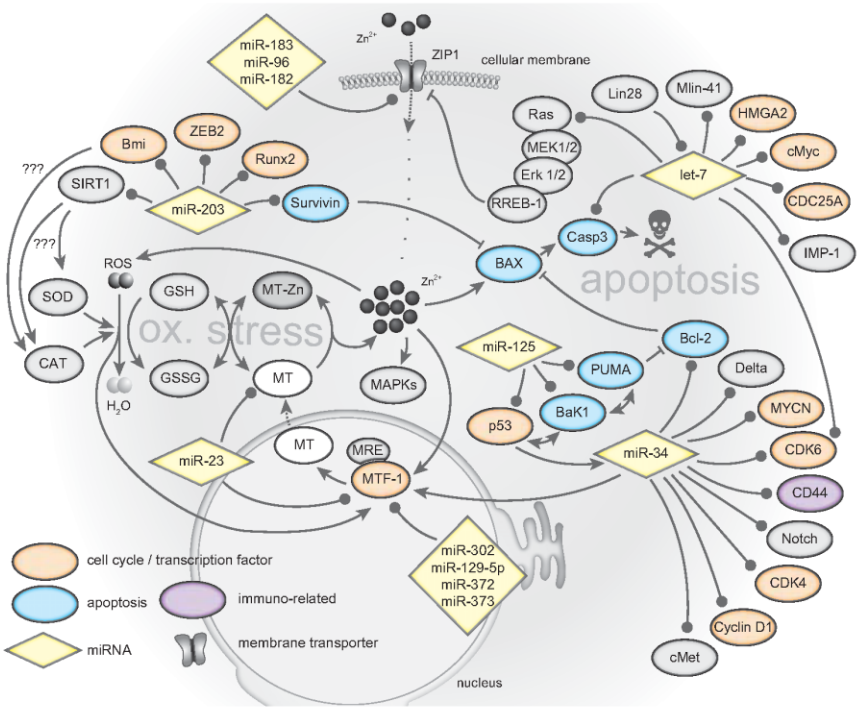

Fig. (1). Zinc- and oxidative stress-related roles of miRNA in prostate cancer. Zinc gets into the cell through zinc transporters (ZIP1), is bound by metallothionein (MT); (white MT represents reduced/metal-free form, grey MT represents oxidized/metal-bound form) and induces its expression *via* metal regulatory transcription factor-1 (MTF-1). Consequently, high zinc(II) load induces oxidative stress (ROS), which is reduced by Superoxid dismutase (SOD), Catalase (CAT) and glutathione system (GSH/GSSG) in cooperation with MT. Free zinc(II) affect gene expression through mitogen-activated protein kinase cascade (MAPKs) and induces BAX-mediated apoptosis. miR-23 affects MT and MT expression *via* MTF-1 together with miR-302, 129-5p, 372, 373 and 34. miR-34, 125 and 203 affect apoptosis *via* altering the expression of p53, BaK1, PUMA, Survivin and Bcl-2 genes. Downstream, let-7 affects the expression of Caspase 3 (Casp3), the effector caspase of apoptosis pathway. let-7 in addition affect Ras gene, further responsible for ZIP-1 down-regulation and thus reduction of intracellular zinc. ZIP1 is in addition down-regulated by miRNA cluster miR-183-96-182. miR-203 in addition affect expression of SIRT1 and Bmi genes further responsible for induction of SOD and CAT by yet unknown mechanisms and thus for reduction of ROS.

sential for prostate cancerogenesis [20]. Thus, the complex understanding of the intracellular zinc, respectively ZIP1 regulation, is of high importance with particular application in targeted therapies.

Recently, the role of zinc has been extensively studied. Possible impacts of zinc in cancer development include influence on gene transcription, energetic metabolism, cell migration and invasivity, and cell cycle [21-24]. Interestingly, conflicting results were published regarding various tumours. Zinc may promote cancer proliferation in some cancers, while in others it exerts an opposite effect. These carcinogenic/protective effects of zinc(II) seem to be very complex and they manifest in cancer-dependent manner [22].

The impact of zinc on energetic metabolism of prostatic cells is well-established. Zinc has inhibitory effects on mitochondrial enzyme aconitase which catalyses the conversion of citrate to isocitrate and thus enables the utilization of citrate in Krebs cycle. Due to aconitase inhibition, prostate cells cannot fully utilise citrate oxidation [25]. As an opposite, because zinc(II) level is decreased in cancer, the inhibitory effect of zinc(II) on aconitase is abolished, citrate can enter the Krebs cycle, and cancer cells can then become more energy-efficient [5, 26]. One may speculate that this "energetic turnover" may provide prostate cancer cells with growth advantage over healthy counterparts.

Zinc is also known to play an important role in apoptosis induction. Increased intracellular concentration of zinc induces release of cytochrome C, which initiates caspase cascade leading to apoptosis [27, 28]. However, the apoptogenic effects of zinc are cell-specific and in other cell types zinc can play a protective role against apoptosis induced by other factors [22, 29].

As a result of disturbances in zinc homeostasis in prostate tumours, several studies reported changes in the serum zinc(II) level in prostate cancer patients. Studies performed by Adaramoye *et al.* and Goel *et al.* revealed significantly lower level in patients of all PSA levels [30, 31]. Similar reduction was observed in group of 41 participants using whole blood analysis of zinc(II) level [32]. However, a study on larger set of participants (1,175 US participants) by Park *et al.* did not observe any difference and no association between serum zinc level and prostate cancer risk in cancer and control groups [33].

The disturbances of zinc homeostasis can be reflected in the activity of transcriptional networks through many regulatory proteins containing zinc in their catalytic centre or in their structure. It is estimated that about 1 % of human genome is coding for zinc-finger proteins. This further emphasises importance of this class of transcription factors for regulation of gene expression. Zinc fingers are small structural protein motifs accommodating one or two zinc atoms that help to stabilise protein folding.

Micro-RNAs (miRNAs) are another factor often connected with tumour development. In this review, we demonstrate that zinc homeostasis and miRNAs are in prostate carcinoma part of mutually interlinked network where these factors might influence each other Fig. (**1**).

One of the proteins with zinc-finger domains plausible connecting miRNA metabolism with zinc homeostasis is Lin28 homolog B. This protein is overexpressed in hepatocellular carcinoma and ovarian primitive germ cell tumours [34]. Lin28 was found to inhibit the biogenesis of let-7 miRNAs through a special domain that contains motif zinc-knuckle and specifically binds to the terminal loop of pre-let-7 [35]. Similarly, miR-138 was found to regulate the epithelial-to-mesenchymal transition *via* direct targeting of zinc finger E-box-binding homeobox 2 in head and neck squamous cell carcinoma and thus promote cancer progression [36].

Conversely, there were also miRNAs identified with the ability to down-regulate the expression of proteins with zinc fingers domains. Using the bioinformatic approach, miR-181a inhibits the expression of large number of zinc fingers proteins by directly targeting their coding sequences [37]. These inhibitory effects might be due to multiple target sites mostly located in the regions coding for the ZNF C2H2 domain within the ZNF gene [37]. As one of these mechanisms, promyelocytic leukaemia zinc finger (PLZF) was identified as a repressor of miR-221 and miR-222 by direct binding to their putative regulatory region [38]. Through this pathway, the progression of melanoma may be controlled.

Alongside to zinc fingers, miRNAs may regulate the expression of other zinc-related proteins associated with tumours – matrix metalloproteases (MMPs). The expression of this large family of zinc endopeptidases is under the control of multiple signalling pathways responding to various hormones, cytokines, and growth factors. MMPs are also regulated post-transcriptionally by controlling mRNA stability, protein translation, and recently by miRNAs [39]. For instance, matrix metalloprotease-2 was found to be regulated by miR-21 in a model of myocardial infarction. MiR-21 directly targets PTEN and through this pathway regulates an increase of MMP-2 in infarct area [40].

miRNA

Among all previously described factors involved in the initiation and development of prostate cancer another element interconnecting several cellular processes may be traced. This element is represented by microRNAs (miRNAs), short non-coding regulatory molecules involved in multitude of processes in eukaryotic cells. They play a role in virtually each step of tumour formation and progression [41-43]. miRNAs networks affect apoptotic pathways, cellular growth, responsiveness to growth factors and anticancer drugs, inhibit expression of tumour suppressor genes or permit expression of oncogenes Fig. (**2**). Classical textbooks refer to carcinogenesis as a harmonic process caused by a loss of function of tumour suppressor genes and simultaneous activation of oncogenic genes. Recent progress in miRNAs function studying did not change this definition substantially; it only extended our understanding of regulation of this intrinsic network by miRNAs which can be likewise characterised as oncogenic miRNAs and antitumour miRNAs. Oncogenic miRNAs are those that directly or indirectly suppress gene expression of tumour suppressors or proapoptotic genes and vice versa anti-tumorigenic miRNAs are those that reduce expression of oncogenic proteins. miRNAs are involved in nearly all types of cancer studied so far and they target

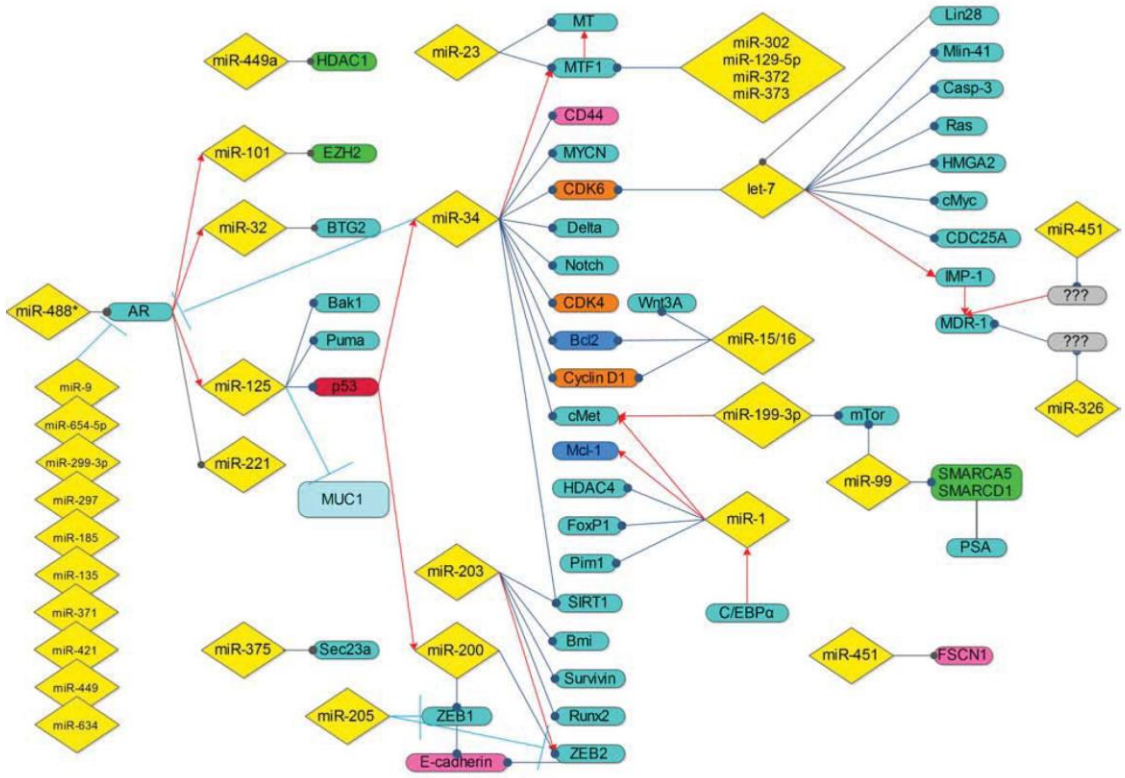

Fig. (2). Mutual relationships of miRNAs and interacting mRNAs with processes connected with development and growth of a tumour.

classical oncological pathways. However, certain miRNAs were specifically associated with defined tumour types suggesting that they are involved in specific processes related to a cancer type or a tissue of origin.

With regard to the number of genes regulated by miRNAs it is not surprising that these small regulatory molecules play a role also in the resistance of cancer cells to various anti-cancer drugs. In that respect, miRNAs become very attractive target for potential therapeutic interventions. Recent research has revealed existence of miRNAs circulating in human blood serum. More surprisingly, it was found that levels of various miRNAs are altered in response to various physiological changes and some of these changes are well correlated with tumour existence. This makes circulating miRNAs a very attractive non-invasive cancer biomarker.

ROLE OF miRNAs IN TUMORIGENESIS

Loss of Tumour Suppressors

Cellular transformation is usually initiated by aberrant expression or function of genes affecting cell cycle and/or cell proliferation. These changes can be caused by a mutation in the coding sequence of tumour suppressors, by deletion of gene loci or altered regulation of gene expression. Genes for miRNAs, which are often located inside introns of structural genes or are independent mono- or polycistronic units, are subject to the same changes. Chromosomal rearrangements leading to deletion of large DNA segments lead to deletions of genes for miRNAs suppressing expression of oncogenic proteins. Chromosomal translocations or retroviral insertions place miRNA genes to the vicinity of promoter and activate transcription of miRNAs which reduce levels of tumour suppressor genes. Under physiological conditions, abnormal proliferation or cell cycle regulation initiates process of apoptosis. High levels of miRNAs targeting pro-apoptotic genes will allow cells to escape this regulatory feedback and further promote cancer development.

Importance of miRNAs is underscored by the fact that nearly half of the genes coding miRNAs are located at fragile sites or at regions with lost homozygozity [44]. For example, a loss of p-arm of chromosome 1 is a common finding in sporadic colon carcinomas. Among many genes associated with DNA repair, checkpoint functions, tumour suppressors, etc. are also multiple miRNAs [45]. The most critical is miR-34a, directly regulated by tumour suppressor gene p53 [46] and classified now as tumour suppressor itself. Ectopic miR-34a expression induces apoptosis and a cell cycle arrest in G1 phase. Downstream targets of miR-34 are Bcl2, MYCN [47], NOTCH1, Delta1, CDK4 and 6, Cyclin D1, Cyclin E2, c-Met, SIRT1 [48], and E2F3, all the genes involved in apoptosis or proliferation and cell growth control Fig. (**2**).

In the case of prostate and miRNAs, prostate cancer stem cells (CSC) with enhanced clonogenic and tumour-initiating and metastatic capacities are characterised by expression of CD44 surface antigen Fig. (**2**). CD44 is a glycoprotein receptor for hyaluronic acid involved in cell-cell interaction, adhesion and migration. Liu *et al.* [49] has shown that miR-34a directly represses CD44 and thus inhibits growth and metastasis of prostate cancer. These experiments were confirmed by knock-down of CD44 which phenocopied miR-34a overexpression. Functional significance of miR-34 loss in cancer was further verified by analysis of genomic sequences of miR-34a and miR-34b/c promoters. In majority of studied cancer lines or histological preparations, methylation of CpGs in promoter regions of the miRNA genes was identified [50]. Methylation of CpG dinucleotide is generally associated with gene expression silencing and epigenetic inactivation.

Another locus (13q14) often deleted specifically in prostate cancer contains miR-15a-miR-16-1 cluster [51]. The same locus is frequently deleted also in non-small cell lung carcinoma [52] where expression of miR-15/16 inversely correlates with the expression of cyclin D1. On the other hand, a cell cycle arrest caused by miR15/16 is dependent on retinoblastoma (Rb) gene. In absence of Rb these miRNAs are unable to induce cell cycle arrest [52]. In prostate tumours, the miR-15-mir-16 locus targets several oncogenic activities, namely anti-apoptotic proto-oncogene BCL2 [53], cyclin D1, and WNT3A [54].

Another often downregulated or lost miRNA is miR-145. Ectopic expression of miR-145 in prostate cancer cell lines inhibited cell proliferation, migration and invasion in study of Fuse *et al.* [55]. The authors have found that miR-145 directly regulates fascin homolog 1 (FSCN1). The FSCN1 los-of-function assay confirmed that cell growth, invasion and migration were inhibited. Other frequently downregulated miRNAs in PC are miR-99 family (miR-99a, -99b, and -100). Three direct targets of miR-99 family were identified [56] – chromatin-remodelling factors SMARCA5 and SMARCD1 and the growth regulatory kinase mTOR. SMARCA5 was shown to regulate the expression of PSA (prostate specific antigen).

miRNA family implicated in early stages of carcinogenesis is let-7, one of the first identified miRNAs originally found in *C. elegans* where it specifies the timing of developmental events [57]. In general, this miRNA is absent in embryonic stem cells and early during embryonic development and its upregulation is strongly associated with differentiation. Let-7 family comprises 13 family members located on 9 chromosomes. Identified let-7 targets are cell cycle regulators (CDC25A, CDK6), oncogenes promoting cells growth and proliferation (cMyc, RAS) and many early embryonic genes (HMGA2, Mlin-41, and IMP-1). Still, it is difficult to imagine that misregulation of gene transcription of let-7 initiates carcinogenesis due to a presence of multiple independently regulated genes coding individual members of the family. Failure of regulation of one gene will be most likely compensated by other family members. More likely, the reduced expression of let-7 is an early consequence of cell transformation. However, intracellular let-7 concentration can be affected by post-transcriptional regulation of let-7. LIN28 is a protein expressed in embryonic stem cells and was also effectively used to generate induced pluripotent stem cells. This protein binds pre-let-7 and prevents pre-miRNA processing by Dicer. Reduced levels of let-7 can lead to increased expression of cMYC, RAS and other proteins promoting carcinogenesis Fig. (**2**).

Carcinogenesis of various tumours, including prostate cancer, is associated with epithelial-to-mesenchymal transition (EMT). It is a process of dedifferentiation important for many embryonic processes and wound healing. This process is associated with changes in epithelial cell morphology and gene expression. These cells might gain invasive properties associated with metastasis caused by loss of cell adhesion molecules such as E-cadherin or by increased expression of mesenchymal markers. Among most often studied regulators of mesenchymal phenotype belongs a family of E-box binding proteins (Snail, Slug, ZEB1, and ZEB2). In cells undergoing EMT transition the expression of miR-200 family (miR-200a, -200b, -200c, -141, and -429) was markedly reduced. These microRNAs cooperatively regulate expression of the E-cadherin transcriptional repressors ZEB1 (also known as deltaEF1) and ZEB2 (also known as SIP1), factors previously implicated in EMT and tumour metastasis. Inhibition of the microRNAs was sufficient to induce EMT in a process requiring up-regulation of ZEB1 and/or SIP1. Conversely, ectopic expression of these microRNAs in mesenchymal cells initiated mesenchymal to epithelial transition (MET) [58]. The regulatory loop comprises also p53, repressing EMT by direct activation of miR-200 and -192 transcription [59]. Another miRNA often attenuated in human carcinomas is miR-199a-3p. Fornari *et al.* [60] has found that miR-199a-3p target of mammalian rapamycin (mTOR) and c-Met (Hepatocyte Growth Factor Receptor). Restoring levels of miR-199a-3p in hepatocellular carcinoma led to G1-phase cell cycle arrest, reduced invasive capability, and enhanced sensitivity to doxorubicin-induced apoptosis.

Increase of Oncogenic miRNAs

There are certain miRNAs, which can suppress carcinogenesis, but others can facilitate the process of malignant transformation and tumour development. These miRNAs are characterised as oncogenic miRNAs, actively acting on 3´UTRs of p53, pro-apoptotic genes or other tumour suppressor genes. In the case of prostate cancer, the androgen receptor (AR) became an interesting therapeutic target.

3´UTR of AR is much longer than originally assumed (~ 6 kb) and contains many binding sites for miRNAs. Thirteen miRNAs (miR-135b, miR-185, miR-297, miR-299-3p, miR-34a, miR-34c, miR-371-3p, miR-421, miR-449a, miR-449b, miR-634, miR-654-5p, and miR-9) were validated to regulate this UTR [61]. Fifteen miRNAs binding AR mRNAs decreased androgen-induced proliferation of prostate cancer cells. In particular, analysis of prostate cancers confirmed a negative correlation of miR-34a and miR-34c expression with AR levels.

A strategy to down-regulate AR level in combination with antiandrogen therapy may prevent or delay the development of androgen-independent (AI) stage. miRNA mimetics targeting AR 3´UTR are good candidates for such approach. Sikand *et al.* [62] demonstrated that over-expression of miR-488* downregulates transcriptional activity of AR in androgen-dependent AD as well as in AI cells and blocks the proliferation and induces apoptosis in PCa cells.

Another miRNA upregulated in prostate cancer is miR-375 with approximately 9 fold increased level as compared to non-cancerous tissue [63]. MiR-375 negatively regulates Sec23A protein, a mammalian homolog of yeast Sec23, involved in endoplasmic reticulum / Golgi trafficking. In cancer cells with high level of miR-375, Sec23A is expressed at low level. It was shown that ectopic expression of Sec23a reduces cell growth; therefore, it is reasonable to assume that reduced levels of Sec23A may speed up cell growth. However, the exact mechanism of such action is so far unclear.

Some of miRNAs do not have clearly defined position in carcinogenesis process. For example, miR-125b is an oncogenic miRNA directly inhibiting expression of tumour suppressor p53 or pro-apoptotic genes Puma and Bak1 [64]. Though, in certain cases it was found to be downregulated in multiple samples of various PC [56]. These discrepancies may be biologically relevant or may reflect experimental bias indigenous to the experimental system. The studies are often performed on cell lines derived from primary tumours but the expansion in non-physiological conditions can lead to irrevocable changes in gene expression patterns. Comparison of primary tissue samples with cell lines can lead to inconclusive results.

miRNA AND FORMATION OF METASTASES

Advanced prostate cancer tends to form metastases predominantly localised in bones. Current understanding of the molecular mechanism remains incomplete. So far it is clear that epithelial-to-mesenchymal transition associated with the loss of attachment and migration of cells is mediated by a loss of E-cadherin. There are two main repressors of E-cadherin expression – ZEB-1 and ZEB-2. Both proteins form a repressor complex with histone deacetylase (HDAC) which reduces histone acetylation and thus leads to DNA methylation and transcription inactivation of target genes.

Saini *et al.* has identified miR-203 as one of important regulators of the metastatic process in prostate cancer [65]. The miRNA is specifically attenuated in bone metastases and ectopic expression of miR-203 reduces development of metastases in bone metastatic model of prostate cancer. This is achieved *via* inhibition of several critical steps of the metastatic cascade including epithelial-to-mesenchymal transition, invasion and motility. MiR-203 regulates several pro-metastatic genes including ZEB2, Bmi, Survivin, and Runx2. Tryndiak *et al.* [66] found that increase of miR-200b and -200c upregulates expression of E-cadherin through direct targeting of ZEB-1 and -2.

Additionally, a cooperative action of miR-203 on downregulation of SIRT1 histone deacetylase and disruption of ZEB1 complex by miR-200b up-regulates proapoptotic genes in the p53 pathway. This process results in increased sensitivity of cancer cells to chemotherapeutic agent doxorubicin.

miRNAs – THERAPEUTICAL TARGET

It is apparent from previous statements that miRNAs represent an interesting therapeutical target or they may become therapeuticals on their own. Downregulation of oncogenic miRNAs could counteract their tumorigenic properties or improve the sensitivity of lesions to chemotherapy. This was clearly proven by experiments carried out by Blower *et al.* [64] who tested the response to several anti-cancer drugs in multiple cancer cell lines transfected with precursors and inhibitors of miRNAs previously implicated in cancer biology (let-7i, miR-16, and mir-21) [67]. Changing the cellular levels of miRNAs affected the potencies of number of the anticancer agents by up to 4-fold. The effects differed for various miRNAs and they were also in opposite directions depending on the compound class. These results suggest that pharmacological interactions of miRNAs and individual drugs are very complex. In following text, we attempt to dissect direct links between individual miRNAs and their identified or putative targets and the impact on drug sensitivity.

Introduction of anti-miR-125b into androgen-independent cds2 cells together with GCP (isoflavone enriched fermentation product having anti-prostate cancer activity [68]) resulted in significant inhibition of the cancer cells as compared to using GCP itself. Similarly, combination of anti-miR-125b with 5 μM cisplatin increased the number of PC cells that entered apoptosis in the presence of androgens [64]. Interestingly, that is not the only example. In lung cancer, reduced expression of miRNA-1 was identified which is normally expressed in bronchial epithelial cells and is downregulated as a consequence of low expression of tumour suppressor C/EBPα, frequently suppressed in cancer cells. Ectopic expression of miRNA-1 in tumour cell lines reversed their tumorigenic properties, such as growth, replication, motility, migration, and clonogenic survival. This is probably a consequence of miR-1 action on oncogenic targets (MET = RTK, Pim-1= Ser/Thr kinase, FoxP1, and HDAC4). Introduction of miR-1 into the cells also induced apoptosis in response to doxorubicin, probably mediated by activation of caspases 3 and 7, and depletion of anti-apoptotic gene Mcl-1 [63]. The effects caused by re-introduction of miR-1 into cancer cells are relatively broad and might suggest that introduction of miR-1 into another types of tumour could have similar antitumour effects. Though, one should be cautious since miR-1 is closely associated with muscle development (mesodermal tissue) and this way it might facilitate EMT.

Interesting relationship between the function of miRNA and response to anti-cancer drugs was identified for let-7. Tumour cells acquire resistance to drugs through various mechanisms including metabolic drug inactivation, drug accumulation in cellular compartments (where the drug is ineffective), and translocating drugs from intra- to extra-cellular spaces. One of such transporters is MDR1 (multi-drug resistance-1), a member of ABC transport family (ATP binding cassette transporters) coding for membrane transporter P-glycoprotein. Substrates for MDR-1 include anthracyclines and taxanes, microtubule targeting drugs. MDR-1 expression is postranscriptionaly regulated by IMP-1 (insulin-like growth factor mRNA binding protein 1). Members of this protein family bind mRNA of various genes and stabilise it from the mRNA degradation. IMP-1 has classic oncofoetal expression pattern and re-

expression occurs in many cancers; it also belongs among proteins which are strongly suppressed by let-7. Downregulation of let-7 leads to activation of protein synthesis of IMP-1 from suppressed mRNA pool which in turn stabilises mRNA for MDR1 and concomitantly increases levels of MDR1 protein in cancer cells. Boyerinas *et al.* has experimentally shown that let-7g selectively affects the sensitivity of a drug-resistant ovarian cancer cells to taxanes by targeting IMP-1, which in turn causes destabilisation of MDR1 at the mRNA and protein level, and this increases sensitivity of multidrug-resistant cancer cells to taxanes [69]. Other miRNAs directly influencing expression of P-glycoprotein (P-gp) are miR-27a and miR-451 [70]. These miRNAs are upregulated in multidrug resistant cell lines and miRNA mimetics increased level of P-gp in non-resistant cell lines. Treatment of resistant cells with antagomirs reduced level of P-gp. These results suggest that targeting miR-27a and miR-451 can be a therapeutic strategy for modulating MDR in cancer cells.

Another study was looking at miRNA expression changes after transition of primary tumour cells into multidrug resistant population. Head and neck squamous cell carcinoma cell lines UMSCC-1 and SQ20B were treated with docetaxel at increasing concentrations to develop resistant cell lines. Parental and resistant cells were treated with cisplatin, 5-fluorouracil, paclitaxel, methotrexate, and doxorubicin to confirm cross-resistance. The miRNA pattern of resistant cells was then compared with their parental cells. Docetaxel treatment successfully induced primary resistance and multidrug cross-resistance. Resistant cells showed significant downregulation of miR-100, miR-130a, and miR-197, and upregulation in miR-101, miR-181b, miR-181d, and miR-195 expression as compared to their parent cells. Real-time polymerase chain reaction (PCR) analysis confirmed statistically significant downregulation in miR-100 and miR-130a and upregulation in miR-181d expressions [71]. However, the question whether any of identified miRNAs can be used as therapeutic target remains to be resolved.

Doxorubicin is an anticancer drug commonly used for treatment of a number of diverse malignant tumours such as acute leukaemia, non-Hodgkin's and Hodgkin's lymphoma and several solid tumours, including neuroblastoma. Despite extensive clinical use, the mechanisms of action of anthracyclines in cancer cells remain a matter of controversy. The following mechanisms were considered: 1) intercalation into DNA, leading to inhibited synthesis of macromolecules; 2) generation of free radicals, leading to DNA damage or lipid peroxidation; 3) DNA binding and alkylation; 4) DNA cross-linking; 5) interference with DNA unwinding or DNA strand separation and helicase activity; 6) direct membrane effects; and 7) inhibition of topoisomerase II [72]. Likewise, with other drugs tumour cells can develop resistance to doxorubicin; manipulation of intracellular miRNAs has a potential to overcome this acquired resistance. Abovementioned work has shown that increase of miR-199a-3p in hepatocellular carcinoma can, among other effects, lead to improved sensitivity to doxorubicin [60].

CISPLATIN RESISTANCE, METALLOTHIONEINS AND miRNAs

Platinum based drugs, namely cisplatin, carboplatin and oxaliplatin became nearly indispensable in our arsenal of anti-cancer drugs nevertheless the fact that cancer cells develop resistance to these compounds Fig. (**3**). Kumar *et al.* have compared miRNA signature of cisplatin-resistant versus cisplatin-sensitive ovarian cancer cell lines [73]. From 1500 analysed miRNAs, 11 up- or downregulated miRNAs have been identified. Moreover, the authors have used Ingenuity Pathway Analysis (IPA) which has identified potential pathways and networks involved in cisplatin resistance.

Alternatively, a key element of the drug – which is platinum atom – can be a focus of interest. A possible way how to acquire resistance to heavy metal containing drugs is an expression of proteins with very high affinity for metal forming active centre of the compound. The most commonly present proteins important for intracellular management of cations such as Zn, Cd, As or Pt belong to the family of metallothioneins (MTs). These are very small proteins rich in cysteine, under physiological conditions binding predominantly zinc; however, the affinity of MTs for platinum exceeds the affinity for zinc by several orders of magnitude [74]. It was shown that increased expression of MTs has marked impact on sensitivity of cancer cells to the treatment with cisplatin, however, the mechanism is still unclear but intensively investigated [75-81]. Can miRNAs participate here? There are no data available but our laboratory has used bioinformatic approach and with the aid of TargetScan software (release 6.1) (http://www.targetscan.org/) has identified multiple binding sites for several different miRNAs in 3´UTRs of mRNAs for MT-1 and MT-2 [82]. Yet another miRNA binding sites were extracted from the microRNA.org database [83] as it is shown in Fig. (**4**).

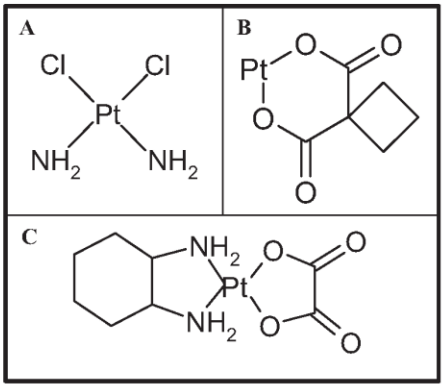

Fig. (3). Structures of (**A**) cisplatin, (**B**) carboplatin and (**C**) oxaliplatin.

The precise relationships between levels of metallothioneins at different stages of PCa progression are yet a bit unclear. Tissue zinc(II) levels are increased in benign hypertrophy of prostate; however, in prostatic cancer these ions´ levels are reduced again. This cannot preclude the possibility of gain a growth advantage and expansion in drug resistant fashion in cells with elevated levels of MTs after the use of cisplatin drugs.

A computer analysis has shown that MT-1 and -2 have redundant binding sites for many miRNAs, including miR-23a and -23b which were found to be downregulated in prostate cancer [84]. Downregulation of miR-23 might elevate levels of MTs which in turn reduce effectivity of cisplatin. Another miRNA predicted to interact with MTs mRNA is miR-224 which was found to be upregulated in perineuronal invading (PNI) PCa cells [85] and potentially reduces MTs levels Fig. (**1**). Surprisingly, downregulation of multiple MTs genes in PNI cancer cells was shown. It is also important to note that not all tumours upregulate miRNA-224 and downregulate MTs. It is tempting to speculate that these two markers can have predictive value in respect to the potential of development of resistance to cisplatin.

Another way to control levels of MTs in cells and the way how platinum based drugs are sequestered is through regulators of MTs expression. A key regulator of intracellular free zinc level is metal regulatory transcription factor 1 (MTF-1, also called MRE-binding factor) [86]. This 753 amino acids transcription factor directly responds to the elevated zinc(II) level and induces the transcription of MT and main zinc transporter responsible for its export, ZnT-1 [87-89]. This autoregulatory loop maintains narrow optimal limits of intracellular zinc(II): when the level of MT and ZnT-1 is elevated, more free zinc(II) and cisplatin may be buffered (i.e. bound to MT)

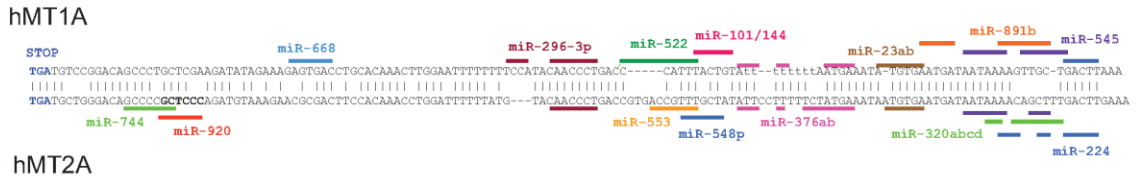

Fig. (4). Alignment of 3′ untranslated regions (BLAST) of human MT1A and MT2A. The sequence alignment starts with termination codon of metallothionein ORF. Predictive software TargetScan and software provided by microRNA.org were used for identification of miRNAs binding sites. Interestingly, both 3′UTRs are very short, but they still contain substantial amount of miRNA binding sites which can have profound impact on cellular levels of proteins and general capabilities to regulate zinc content in cells.

and more zinc may leave cells (through larger amount of membrane transporters). MTF1 has rather (over 5 kb) long 3′-UTR and perhaps not surprisingly miRDB software has predicted over 45 miRNAs interacting with this mRNA. It is reasonable to speculate that elevated expression of MTs in cisplatin resistant cancer can be at least partially related to mis-regulation of miRNAs targeting MTs or MTF1. It can be also assumed that introduction of miRNAs binding MTs mRNA may have a beneficial effect on sensitivity of cells to the treatment with platinum compounds.

EPIGENETIC CONTROL OF miRNAs EXPRESSION

Epigenetic regulation is a common mechanism to control gene expression. Gene silencing is often accompanied by methylation of CpG dinucleotide; it takes place in so-called CpG islands inside or in the vicinity of gene promoters and leads to changes in chromatin structure. Modification of chromatin includes histone modification permitting or prohibiting gene transcription. The transcriptional control is executed by several enzymes, including DNA methyltransferases (DNMTs), histone acetyltransferases (HATs), histone deacetylases (HDACs), histone methyltransferases (HMTs), and histone demethylases (HDMTs) [90, 91]. Function and activity of individual enzymes is regulated by chromatin remodelling complexes such as polycomb group (PcG) proteins. Epigenetic regulation is commonly subject to alteration in process of malignant transformation. Chromatin remodelling enzymes can be themselves targets of miRNAs. One such example is regulation of enhancer of zeste homolog 2 (EZH2), a histone methyltransferase and part of the PcG complex. It was demonstrated that in PCa cells EZH2 acts as an oncogene and is directly regulated by miR-101 and miR-26a [92]. Interestingly, there are androgen receptor binding sites in miR-101 promoter and AR binding activates miR-101 expression. This indicates that miR-101 can be therapeutic target to reduce PCa cells growth and invasiveness. This idea is further supported by the finding that genomic loss of miR-101 negatively correlates with an increased expression of EZH2 in PCa [93]. Another miRNA directly connected with the regulation of epigenetic state of cell is miR-449a; it controls expression of histone deacetylase (HDAC1) in PCa cells [94]. Histone deacetylases are frequently overexpressed in a broad range of cancer and they promote cell proliferation and survival. Noon *et al.* have found that miR-449a is downregulated in PCa and its re-introduction into cancer cells causes cell cycle arrest, apoptosis, and senescent-like phenotype.

Alternatively miRNAs themselves can be subject of epigenetic regulation. Formosa *et al.* has applied demethylation agent 5-aza-2′-deoxycytidine (azaC) to normal prostate epithelial and carcinoma cells and subsequently examined changes in expression of miRNAs [95]. Multiple miRNAs had modified their expression in the presence of azaC. Moreover, analysis of CpG islands present in miRNA promoters revealed changes in DNA methylation. The authors showed that in prostate cancer miR-132 is silenced by DNA methylation. Another study by Hulf *et al.* has identified miR-205, miR-21, and miR-196b to be epigenetically repressed, and miR-615 epigenetically activated in prostate cancer [96].

CIRCULATING miRNAs

Development of new highly sensitive methods of miRNA detection led to identification of miRNAs circulating in blood. Circulating miRNAs are present in bloodstream in a very stable extracellular form resistant to RNA digestion by ubiquitously present RNAases. The mechanism of miRNA release from cells to extracellular space is unknown as well as it is unclear whether it is an active secretion mechanism or a by-product of non-apoptotic or apoptotic cell death. It is also not clear whether the circulating miRNAs have any physiological function, such as translating information to neighbouring cells or even distant organs. Current assumption is that miRNAs are encapsulated in membrane vesicles such as exosomes; however, recent research suggests that this assumption is false or at least incomplete. Arroyo *et al.* [97] has demonstrated that miRNAs circulating in human plasma form a RNA-ase resistant complex with Argonaute2 protein, the key factor of miRNA mediated silencing and part of the RISC complex.

Regardless of present lack of knowledge of their physiological function, several studies have shown that circulating miRNAs reveal the health status of the body and thus pathological or physiological changes are reflected in a signature of circulating miRNAs. For example, several miRNAs were found to be upregulated in pregnant women. Altered levels of several other miRNAs were identified in human serum; they can be good and early indicators of tumours as well as prognostic markers for prospective therapy. Tumour specific dysregulation of miRNAs was described first in 2008 by Lawrie *et al.* who identified altered expression profile of miRNAs in serum of patients suffering from diffuse large B-cell lymphoma [98].

The major advantage of miRNAs as prognostic marker is their easy isolation from blood serum. Moreover, high sensitivity of analytical methods allows identification of asymptomatic individuals with early stage of lung cancer [99]. Furthermore, a specific miRNA signature can also identify the type of tumour. Nevertheless, it is important to notice that circulating miRNAs are correlated with histopathological parameters and not directly associated with patient's outcome in certain malignancies. Brase *et al.* [100] studied circulating miRNAs in serum of patients with different types of prostate cancer. He found that in sera of patients with aggressive metastatic cancer miR-141 and miR-375 were more abundant and that their concentration well correlated with prostate tumour progression. Both miRNAs were also highly upregulated in cancer tissue. On the other hand, Mahn *et al.* [101] correlated miRNAs -26a, -16, and -195 with various types and stages of prostate cancer. Gonzales *et al.* [102] identified miR-141 as clinically valuable diagnostic biomarker. However, it is hard to speculate at present which of miRNAs will be clinically useful as tumour marker.

In case of lung cancer, miR-486, miR-30d, miR-1, and miR-499 were identified as significant biomarkers of non-small cell lung carcinoma and were associated with overall survival [103]. Surprisingly, this study has shown that several miRNAs previously identified in cancer tissue were not identified in serum by Solexa se-

quencing. Therefore, the predictive role of serum miRNAs might be important. However, miRNAs identified in serum do not have to be necessarily the same as miRNAs expressed in tumour tissue. It should be taken in consideration that circulating miRNAs probably reflect more general health status and might not be explicitly linked to a specific gene expression pattern in individual tumour cells. In the abovementioned study, clear and significant associations between miRNA signatures from serum and lung cancer prognosis, potentially useful in clinical practice, were found, but the found mechanism needs additional exploration [103].

Many laboratories generate vast quantity of data on mRNA or miRNA expression in various types of cancer and/or healthy tissues. Extraction of biologically relevant information belongs among the most demanding tasks of contemporary bioinformatics. MicroRNAs are important regulators of signalling pathways. Therefore it is important to take into consideration whether expression of studied miRNAs correspond to identified signalling pathways. A web resource allowing analysis of functional significance of miRNAs in various tissues is now available under the name miTALOS [104]. As a novel feature, this software considers the tissue specific expression signatures of miRNAs and target transcripts to improve the analysis of miRNA regulation in biological pathways. Though, one must be very careful in comparing methods of microRNAs detection regarding their sensitivity and clinical information value. There is a big variation among techniques using quantitative real time PCR based on different systems and comparing data of global expression profiles based on chip hybridisation techniques or with massive parallel sequencing techniques. Only standardised techniques and large patient cohorts will reveal which results are statistically significant, however biologically irrelevant, which are simply false based on applied technique of miRNA isolation or analysis, and those which are truly relevant and will become standards in future diagnostics of tumours.

CONCLUSION

Recent scientific discoveries clearly demonstrate that miRNAs are probably as important in cancer biology as protein coding genes. Moreover, miRNAs were shown to be differently expressed in tumours that had acquired resistance to chemotherapy. On the other side, different levels of intracellular miRNAs can change responsiveness of cells to various cytostatic compounds. Further research is required to identify correlations among specific miRNA expression levels and drug classes. Such research is necessary for future progress toward personalised therapy based on gene expression profile of tumour in a given patient and for rational design of treatment regime.

Many questions remain unanswered. The very complex nature of regulatory networks (including miRNAs, protein expression, modifications and interactions) obscures truly relevant interplays. On the other hand, oversimplification can preclude an understanding of important synergies among players. The scientists have to eternally balance on the edge between these two extremes and perhaps then, answers relevant for future treatment and therapy might be found.

CONFLICT OF INTEREST

The author(s) confirm that this article content has no conflicts of interest.

ACKNOWLEDGEMENTS

Financial support from NanoBioTECell GA CR P102/11/1068, NANOSEMED GA AV KAN208130801 and CEITEC CZ.1.05/1.1.00/02.0068 is greatly acknowledged.

ABBREVIATIONS

3´UTR	=	3´ Untranslated Region
ABC	=	ATP Binding Cassette Transporters
AD	=	Androgen Dependent
AI	=	Androgen Independent
AP-2α	=	Activator Protein 2α
AR	=	Androgen Receptor
azaC	=	5-aza-2´-Deoxycytidine
CDC25	=	Cell Division Cycle 25 – Phosphatise Activating CDK1
CDK	=	Cyclin Dependent Kinase
cMET	=	Hepatocyte Growth Factor Receptor
CSC	=	Cancer Stem Cells
DNMT	=	DNA Methyltransferase
EMT	=	Epithelial-to-Mesenchymal Transition
EZH2	=	Enhancer of Zeste Homolog 2
GCP	=	Isoflavone Enriched Fermentation Product
HAT	=	Histone Acetyltransferase
HDAC	=	Histone Deacetylase
HDMT	=	Histone Demethylase
HMT	=	Histone Methyltransferase
IMP-1	=	Insulin-Like Growth Factor mRNA Binding Protein 1
IPA	=	Ingenuity Pathway Analysis
MDR1	=	Multi-Drug Resistance-1
MET	=	Mesenchymal-to-Epithelial Transition
MMPs	=	Matrix Metalloproteinases
MT	=	Metallothionein
MTF-1	=	Metal Regulatory Transcription Factor 1
PCa	=	Prostate Cancer
PcG	=	Polycomb Group
P-gp	=	P Glycoprotein
PLZF	=	Promyelocytic Leukaemia Zinc Finger
PNI	=	Perinuclear Invasion
PSA	=	Prostate Specific Antigen
Rb	=	Retinoblastoma
RISC	=	RNA-Induced Silencing Complex
RREB-1	=	Ras Responsive Element Binding Protein-1
RTK	=	Receptor Tyrosine Kinase
ZIP	=	Zrt- Irt Like Protein or Zinc Iron Permease
ZNF	=	Zinc Finger
ZnT	=	Zinc Transporters

REFERENCES

[1] Jemal A.; Bray F.; Center M.M.; Ferlay J.; Ward E.; Forman D. Global Cancer Statistics. *CA-Cancer J. Clin.*, **2011**, *61*, 69-90.

[2] Freedland S.J. Screening, Risk Assessment, and the Approach to Therapy in Patients With Prostate Cancer. *Cancer*, **2011**, *117*, 1123-1135.

[3] Goel H.L.; Alam N.; Johnson I.N.; Languino L.R. Integrin signaling aberrations in prostate cancer. *Am. J. Transl. Res.*, **2009**, *1*, 211-220.

[4] Perdih A.; Dolenc M.S. Small Molecule Antagonists of Integrin Receptors. *Curr. Med. Chem.*, **2010**, *17*, 2371-2392.

[5] Costello L.C.; Franklin R.B. The clinical relevance of the metabolism of

prostate cancer; zinc and tumor suppression: connecting the dots. *Mol. Cancer*, **2006**, *5*, 1-13.

[6] Hoare R.; Delory G.E.; Penner D.W. Zinc and acid phosphatase in the human prostate. *Cancer*, **1956**, *9*, 721-726.

[7] Jafa A.; Mahendra N.M.; Chowdhury A.R.; Kamboj V.P. Trace elements in prostatic tissue and plasma in prostatic diseases of man. *Indian J. Cancer*, **1980**, *17*, 34-37.

[8] Schrodt G.R.; Hall T.; Whitmore W.F. The concentration of zinc in diseased human prostate glands. *Cancer*, **1964**, *17*, 1555-1566.

[9] Zaichick V.Y.; Sviridova T.V.; Zaichick S.V. Zinc in human prostate gland: Normal, hyperplastic and cancerous. *J. Radioanal. Nucl. Chem.*, **1997**, *217*, 157-161.

[10] Banas A.M.; Banas K. Response to commentary "Zinc is decreased in prostate cancer: an established relationship of prostate cancer!". *J. Biol. Inorg. Chem.*, **2011**, *16*, 9-13.

[11] Costello L.C.; Franklin R.B.; Zou J.; Feng P.; Bok R.; Swanson M.G.; Kurhanewicz J. Human prostate cancer ZIP1/zinc/citrate genetic/metabolic relationship in the TRAMP prostate cancer animal model. *Cancer Biol. Ther.*, **2011**, *12*, 1078-1084.

[12] Kambe T.; Yamaguchi-Iwai Y.; Sasaki R.; Nagao M. Overview of mammalian zinc transporters. *Cell. Mol. Life Sci.*, **2004**, *61*, 49-68.

[13] Hogstrand C.; Kille P.; Nicholson R.I.; Taylor K.M. Zinc transporters and cancer: a potential role for ZIP7 as a hub for tyrosine kinase activation. *Trends Mol. Med.*, **2009**, *15*, 101-111.

[14] Franklin R.B.; Ma J.; Zou J.; Guan Z.; Kukoyi B.I.; Feng P.; Costello L.C. Human ZIP1 is a major zinc uptake transporter for the accumulation of zinc in prostate cells. *J. Inorg. Biochem.*, **2003**, *96*, 435-442.

[15] Johnson L.A.; Kanak M.A.; Kajdacsy-Balla A.; Pestaner J.P.; Bagasra O. Differential zinc accumulation and expression of human zinc transporter 1 (hZIP1) in prostate glands. *Methods*, **2010**, *52*, 316-321.

[16] Gumulec J.; Masarik M.; Krizkova S.; Adam V.; Hubalek J.; Hrabeta J.; Eckschlager T.; Stiborova M.; Kizek R. Insight to physiology and pathology of zinc(II) ions and their actions in breast and prostate carcinoma. *Curr. Med. Chem.*, **2011**, *18*, 5041-5051.

[17] Makhov P.B.; Golovine K.V.; Kutikov A.; Canter D.J.; Rybko V.A.; Roshchin D.A.; Matveev V.B.; Uzzo R.G.; Kolenko V.M. Reversal of epigenetic silencing of AP-2alpha results in increased zinc uptake in DU-145 and LNCaP prostate cancer cells. *Carcinogenesis*, **2011**, *32*, 1773-1781.

[18] Zou J.; Milon B.C.; Desouki M.M.; Costello L.C.; Franklin R.B. hZIP1 Zinc Transporter Down-Regulation in Prostate Cancer Involves the Overexpression of Ras Responsive Element Binding Protein-1 (RREB-1). *Prostate*, **2011**, *71*, 1518-1524.

[19] Mihelich B.L.; Khramtsova E.A.; Arva N.; Vaishnav A.; Johnson D.N.; Giangreco A.A.; Martens-Uzunova E.; Bagasra O.; Kajdacsy-Balla A.; Nonn L. miR-183-96-182 Cluster Is Overexpressed in Prostate Tissue and Regulates Zinc Homeostasis in Prostate Cells. *J. Biol. Chem.*, **2011**, *286*, 44503-44511.

[20] Costello L.C.; Franklin R.B. The intermediary metabolism of the prostate: a key to understanding the pathogenesis and progression of prostate malignancy. *Oncology*, **2000**, *59*, 269-282.

[21] Beyersmann D.; Haase H. Functions of zinc in signaling, proliferation and differentiation of mammalian cells. *Biometals*, **2001**, *14*, 331-341.

[22] Franklin R.B.; Costello L.C. The Important Role of the Apoptotic Effects of Zinc in the Development of Cancers. *J. Cell. Biochem.*, **2009**, *106*, 750-757.

[23] MacDonald R.S. The role of zinc in growth and cell proliferation. *J. Nutr.*, **2000**, *130*, 1500S-1508S.

[24] Prasad A.S. Zinc - An overview. *Nutrition*, **1995**, *11*, 93-99.

[25] Costello L.C.; Liu Y.Y.; Franklin R.B.; Kennedy M.C. Zinc inhibition of mitochondrial aconitase and its importance in citrate metabolism of prostate epithelial cells. *J. Biol. Chem.*, **1997**, *272*, 28875-28881.

[26] Costello L.C.; Franklin R.B. Novel role of zinc in the regulation of prostate citrate metabolism and its implications in prostate cancer. *Prostate*, **1998**, *35*, 285-296.

[27] Feng P.; Li T.L.; Guan Z.X.; Franklin R.B.; Costello L.C. The involvement of bax in zinc-induced mitochondrial apoptogenesis in malignant prostate cells. *Mol. Cancer*, **2008**, *7*, 1-6.

[28] Coffey R.N.T.; Watson R.W.G.; Hegarty N.J.; O'Neill A.; Gibbons N.; Brady H.R.; Fitzpatrick J.M. Thiol-mediated apoptosis in prostate carcinoma cells. *Cancer*, **2000**, *88*, 2092-2104.

[29] DiPaola R.S.; Patel J.; Rafi M.M. Targeting apoptosis in prostate cancer. *Hematol. Oncol. Clin. North Am.*, **2001**, *15*, 509-524.

[30] Adaramoye O.A.; Akinloye O.; Olatunji I.K. Trace elements and Vitamin E status in Nigerian patients with prostate cancer. *Afr. Health Sci.*, **2010**, *10*, 2-8.

[31] Goel T.; Sankhwar S.N. Comparative study of zinc levels in benign and malignant lesions of the prostate. *Scand. J. Urol. Nephrol.*, **2006**, *40*, 108-112.

[32] Ozmen H.; Erulas F.A.; Karatas F.; Cukurovali A.; Yalcin O. Comparison of the concentration of trace metals (Ni, Zn, Co, Cu and Se), Fe, vitamins A, C and E, and lipid peroxidation in patients with prostate cancer. *Clin. Chem. Lab. Med.*, **2006**, *44*, 175-179.

[33] Park S.Y.; Kolonel L. Serum Zinc and Prostate Cancer Risk in the Multiethnic Cohort study. *Epidemiology*, **2009**, *20*, S131-S131.

[34] Xue D.B.; Peng Y.; Wang F.H.; Allan R.W.; Cao D.F. RNA-binding protein LIN28 is a sensitive marker of ovarian primitive germ cell tumours. *Histopathology*, **2011**, *59*, 452-459.

[35] Loughlin F.E.; Gebert L.F.R.; Towbin H.; Brunschweiger A.; Hall J.; Allain F.H.T. Structural basis of pre-let-7 miRNA recognition by the zinc knuckles of pluripotency factor Lin28. *Nat. Struct. Mol. Biol.*, **2012**, *19*, 84-U105.

[36] Liu X.Q.; Wang C.; Chen Z.J.; Jin Y.; Wang Y.; Kolokythas A.; Dai Y.; Zhou X.F. MicroRNA-138 suppresses epithelial-mesenchymal transition in squamous cell carcinoma cell lines. *Biochem. J.*, **2011**, *440*, 23-31.

[37] Huang S.L.; Wu S.Q.; Ding J.; Lin J.; Wei L.; Gu J.R.; He X.H. MicroRNA-181a modulates gene expression of zinc finger family members by directly targeting their coding regions. *Nucleic Acids Res.*, **2010**, *38*, 7211-7218.

[38] Felicetti F.; Errico M.C.; Bottero L.; Segnalini P.; Stoppacciaro A.; Biffoni M.; Felli N.; Mattia G.; Petrini M.; Colombo M.P.; Peschle C.; Care A. The promyelocytic leukemia zinc finger-microRNA-221/-222 pathway controls melanoma progression through multiple oncogenic mechanisms. *Cancer Res.*, **2008**, *68*, 2745-2754.

[39] Fanjul-Fernandez M.; Folgueras A.R.; Cabrera S.; Lopez-Otin C. Matrix metalloproteinases: Evolution, gene regulation and functional analysis in mouse models. *Biochim. Biophys. Acta-Mol. Cell Res.*, **2010**, *1803*, 3-19.

[40] Roy S.; Khanna S.; Hussain S.R.A.; Biswas S.; Azad A.; Rink C.; Gnyawali S.; Shilo S.; Nuovo G.J.; Sen C.K. MicroRNA expression in response to murine myocardial infarction: miR-21 regulates fibroblast metalloprotease-2 via phosphatase and tensin homologue. *Cardiovasc. Res.*, **2009**, *82*, 21-29.

[41] He M.L.; Luo M.X.M.; Lin M.C.; Kung H.F. MicroRNAs: Potential diagnostic markers and therapeutic targets for EBV-associated nasopharyngeal carcinoma. *Biochim. Biophys. Acta-Rev. Cancer*, **2012**, *1825*, 1-10.

[42] Heusschen R.; van Gink M.; Griffioen A.W.; Thijssen V.L. MicroRNAs in the tumor endothelium: Novel controls on the angioregulatory switchboard. *Biochim. Biophys. Acta-Rev. Cancer*, **2010**, *1805*, 87-96.

[43] Wittmann J.; Jack H.M. Serum microRNAs as powerful cancer biomarkers. *Biochim. Biophys. Acta-Rev. Cancer*, **2010**, *1806*, 200-207.

[44] Calin G.A.; Sevignani C.; Dan Dumitru C.; Hyslop T.; Noch E.; Yendamuri S.; Shimizu M.; Rattan S.; Bullrich F.; Negrini M.; Croce C.M. Human microRNA genes are frequently located at fragile sites and genomic regions involved in cancers. *Proc. Natl. Acad. Sci. U. S. A.*, **2004**, *101*, 2999-3004.

[45] Payne C.M.; Crowley-Skillicorn C.; Bernstein C.; Holubec H.; Bernstein H. Molecular and cellular pathways associated with chromosome 1p deletions during colon carcinogenesis. *Clin. Exp. Gastroenterol.*, **2011**, *4*, 75-119.

[46] Tarasov V.; Jung P.; Verdoodt B.; Lodygin D.; Epanchintsev A.; Menssen A.; Meister G.; Hermeking H. Differential regulation of microRNAs by p53 revealed by massively parallel sequencing: miR-34a is a p53 target that induces apoptosis and G1-arrest. *Cell Cycle*, **2007**, *6*, 1586-1593.

[47] Cole K.A.; Attiyeh E.F.; Mosse Y.P.; Laquaglia M.J.; Diskin S.J.; Brodeur G.M.; Maris J.M. A functional screen identifies miR-34a as a candidate neuroblastoma tumor suppressor gene. *Mol. Cancer Res.*, **2008**, *6*, 735-742.

[48] Kojima K.; Fujita Y.; Nozawa Y.; Deguchi T.; Ito M. MiR-34a attenuates paclitaxel-resistance of hormone-refractory prostate cancer PC3 cells through direct and indirect mechanisms. *Prostate*, **2010**, *70*, 1501-1512.

[49] Liu C.; Kelnar K.; Liu B.G.; Chen X.; Calhoun-Davis T.; Li H.W.; Patrawala L.; Yan H.; Jeter C.; Honorio S.; Wiggins J.F.; Bader A.G.; Fagin R.; Brown D.; Tang D.A.G. The microRNA miR-34a inhibits prostate cancer stem cells and metastasis by directly repressing CD44. *Nat. Med.*, **2011**, *17*, 211-U105.

[50] Vogt M.; Munding J.; Grüner M.; Liffers S.T.; Verdoodt B.; Hauk J.; Steinstraesser L.; Tannapfel A.; Hermeking H. Frequent concomitant inactivation of miR-34a and miR-34b/c by CpG methylation in colorectal, pancreatic, mammary, ovarian, urothelial, and renal cell carcinomas and soft tissue sarcomas. *Virchows Arch.*, **2011**, *458*, 313-322.

[51] Porkka K.P.; Ogg E.L.; Saramaki O.R.; Vessella R.L.; Pukkila H.; Lahdesmaki H.; van Weerden W.M.; Wolf M.; Kallioniemi O.P.; Jenster G.; Visakorpi T. The miR-15a-miR-16-1 Locus is Homozygously Deleted in a Subset of Prostate Cancers. *Gene Chromosomes Cancer*, **2011**, *50*, 499-509.

[52] Bandi N.; Zbinden S.; Gugger M.; Arnold M.; Kocher V.; Hasan L.; Kappeler A.; Brunner T.; Vassella E. miR-15a and miR-16 Are Implicated in Cell Cycle Regulation in a Rb-Dependent Manner and Are Frequently Deleted or Down-regulated in Non-Small Cell Lung Cancer. *Cancer Res.*, **2009**, *69*, 5553-5559.

[53] Cimmino A.; Calin G.A.; Fabbri M.; Iorio M.V.; Ferracin M.; Shimizu M.; Wojcik S.E.; Aqeilan R.I.; Zupo S.; Dono M.; Rassenti L.; Alder H.; Volinia S.; Liu C.G.; Kipps T.J.; Negrini M.; Croce C.M. miR-15 and miR-16 induce

apoptosis by targeting BCL2. *Proc. Natl. Acad. Sci. U. S. A.*, **2005**, *102*, 13944-13949.

[54] Bonci D.; Coppola V.; Musumeci M.; Addario A.; Giuffrida R.; Memeo L.; D'Urso L.; Pagliuca A.; Biffoni M.; Labbaye C.; Bartucci M.; Muto G.; Peschle C.; De Maria R. The miR-15a-miR-16-1 cluster controls prostate cancer by targeting multiple oncogenic activities. *Nat. Med.*, **2008**, *14*, 1271-1277.

[55] Fuse M.; Nohata N.; Kojima S.; Sakamoto S.; Chiyomaru T.; Kawakami K.; Enokida H.; Nakagawa M.; Naya Y.; Ichikawa T.; Seki N. Restoration of miR-145 expression suppresses cell proliferation, migration and invasion in prostate cancer by targeting FSCN1. *Int. J. Oncol.*, **2011**, *38*, 1093-1101.

[56] Sun D.D.; Lee Y.S.; Malhotra A.; Kim H.K.; Matecic M.; Evans C.; Jensen R.V.; Moskaluk C.A.; Dutta A. miR-99 Family of MicroRNAs Suppresses the Expression of Prostate-Specific Antigen and Prostate Cancer Cell Proliferation. *Cancer Res.*, **2011**, *71*, 1313-1324.

[57] Reinhart B.J.; Slack F.J.; Basson M.; Pasquinelli A.E.; Bettinger J.C.; Rougvie A.E.; Horvitz H.R.; Ruvkun G. The 21-nucleotide let-7 RNA regulates developmental timing in Caenorhabditis elegans. *Nature*, **2000**, *403*, 901-906.

[58] Gregory P.A.; Bert A.G.; Paterson E.L.; Barry S.C.; Tsykin A.; Farshid G.; Vadas M.A.; Khew-Goodall Y.; Goodall G.J. The mir-200 family and mir-205 regulate epithelial to mesenchymal transition by targeting ZEB1 and SIP1. *Nat. Cell Biol.*, **2008**, *10*, 593-601.

[59] Kim T.; Veronese A.; Pichiorri F.; Lee T.J.; Jeon Y.J.; Volinia S.; Pineau P.; Marchio A.; Palatini J.; Suh S.S.; Alder H.; Liu C.G.; Dejean A.; Croce C.M. p53 regulates epithelial-mesenchymal transition through microRNAs targeting ZEB1 and ZEB2. *J. Exp. Med.*, **2011**, *208*, 875-883.

[60] Fornari F.; Milazzo M.; Chieco P.; Negrini M.; Calin G.A.; Grazi G.L.; Pollutri D.; Croce C.M.; Bolondi L.; Gramantieri L. MiR-199a-3p Regulates mTOR and c-Met to Influence the Doxorubicin Sensitivity of Human Hepatocarcinoma Cells. *Cancer Res.*, **2010**, *70*, 5184-5193.

[61] Ostling P.; Leivonen S.K.; Aakula A.; Kohonen P.; Makela R.; Hagman Z.; Edsjo A.; Kangaspeska S.; Edgren H.; Nicorici D.; Bjartell A.; Ceder Y.; Perala M.; Kallioniemi O. Systematic Analysis of MicroRNAs Targeting the Androgen Receptor in Prostate Cancer Cells. *Cancer Res.*, **2011**, *71*, 1956-1967.

[62] Sikand K.; Slaibi J.E.; Singh R.; Slane S.D.; Shukla G.C. miR 488(star) inhibits androgen receptor expression in prostate carcinoma cells. *Int. J. Cancer*, **2011**, *129*, 810-819.

[63] Szczyrba J.; Nolte E.; Wach S.; Kremmer E.; Stohr R.; Hartmann A.; Wieland W.; Wullich B.; Grasser F.A. Downregulation of Sec23A Protein by miRNA-375 in Prostate Carcinoma. *Mol. Cancer Res.*, **2011**, *9*, 791-800.

[64] Shi X.B.; Xue L.; Ma A.H.; Tepper C.G.; Kung H.J.; White R.W. miR-125b promotes growth of prostate cancer xenograft tumor through targeting pro-apoptotic genes. *Prostate*, **2011**, *71*, 538-549.

[65] Saini S.; Majid S.; Yamamura S.; Tabatabai L.; Suh S.O.; Shahryari V.; Chen Y.; Deng G.R.; Tanaka Y.; Dahiya R. Regulatory Role of mir-203 in Prostate Cancer Progression and Metastasis. *Clin. Cancer Res.*, **2011**, *17*, 5287-5298.

[66] Tryndyak V.P.; Beland F.A.; Pogribny I.P. E-cadherin transcriptional down-regulation by epigenetic and microRNA-200 family alterations is related to mesenchymal and drug-resistant phenotypes in human breast cancer cells. *Int. J. Cancer*, **2010**, *126*, 2575-2583.

[67] Blower P.E.; Verducci J.S.; Lin S.L.; Zhou J.; Chung J.H.; Dai Z.Y.; Liu C.G.; Reinhold W.; Lorenzi P.L.; Kaldjian E.P.; Croce C.M.; Weinstein J.N.; Sadee W. MicroRNA expression profiles for the NCI-60 cancer cell panel. *Mol. Cancer Ther.*, **2007**, *6*, 1483-1491.

[68] Bemis D.L.; Capodice J.L.; Desai M.; Buttyan R.; Katz A.E. A concentrated aglycone isoflavone preparation (GCP) that demonstrates potent anti-prostate cancer activity *in vitro* and *in vivo*. *Clin. Cancer Res.*, **2004**, *10*, 5282-5292.

[69] Boyerinas B.; Park S.M.; Murmann A.E.; Gwin K.; Montag A.G.; Zillhardt M.; Hua Y.J.; Lengyel E.; Peter M.E. Let-7 modulates acquired resistance of ovarian cancer to Taxanes via IMP-1-mediated stabilization of multidrug resistance 1. *Int. J. Cancer*, **2012**, *130*, 1787-1797.

[70] Zhu H.; Wu H.; Liu X.; Evans B.R.; Medina D.J.; Liu C.G.; Yang J.M. Role of MicroRNA miR-27a and miR-451 in the regulation of MDR1/P-glycoprotein expression in human cancer cells. *Biochem Pharmacol*, **2008**, *76*, 582-588.

[71] Dai Y.M.; Xie C.H.; Neis J.P.; Fan C.Y.; Vural E.; Spring P.M. MicroRNA expression profiles of head and neck squamous cell carcinoma with docetaxel-induced multidrug resistance. *Head Neck-J. Sci. Spec. Head Neck*, **2011**, *33*, 786-791.

[72] Kizek R.; Adam V.; Hrabeta J.; Eckschlager T.; Smutny S.; Burda J.V.; Frei E.; Stiborova M. Anthracyclines and ellipticines as DNA-damaging anticancer drugs; Recent advances. *Pharmacol. Ther.*, **2011**, *133*(2), 26-39.

[73] Kumar S.; Kumar A.; Shah P.P.; Rai S.N.; Panguluri S.K.; Kakar S.S. MicroRNA signature of cis-platin resistant vs. cis-platin sensitive ovarian cancer cell lines. *J. Ovarian Res.*, **2011**, *4*, 1-11.

[74] Krizkova S.; Adam V.; Petrlova J.; Zitka O.; Stejskal K.; Zehnalek J.; Sures B.; Trnkova L.; Beklova M.; Kizek R. A suggestion of electrochemical biosensor for study of platinum(II)-DNA interactions. *Electroanalysis*, **2007**, *19*, 331-338.

[75] Babula P.; Masarik M.; Adam V.; Eckschlager T.; Stiborova M.; Trnkova L.; Skutkova H.; Provaznik I.; Hubalek J.; Kizek R. Mammalian metallothioneins: properties and functions. *Metallomics*, **2012**, *4*, 739-750.

[76] Eckschlager T.; Adam V.; Hrabeta J.; Figova K.; Kizek R. Metallothioneins and Cancer. *Curr. Protein Pept. Sci.*, **2009**, *10*, 360-375.

[77] Galluzzi L.; Senovilla L.; Vitale I.; Michels J.; Martins I.; Kepp O.; Castedo M.; Kroemer G. Molecular mechanisms of cisplatin resistance. *Oncogene*, **2012**, *31*, 1869-1883.

[78] Knipp M. Metallothioneins and Platinum(II) Anti-Tumor Compounds. *Curr. Med. Chem.*, **2009**, *16*, 522-537.

[79] Krizkova S.; Fabrik I.; Huska D.; Adam V.; Babula P.; Hrabeta J.; Eckschlager T.; Pochop P.; Darsova D.; Kukacka J.; Prusa R.; Trnkova L.; Kizek R. An Adsorptive Transfer Technique Coupled with Brdicka Reaction to Reveal the Importance of Metallothionein in Chemotherapy with Platinum Based Cytostatics. *Int. J. Mol. Sci.*, **2010**, *11*, 4826-4842.

[80] Takahashi S. Molecular functions of metallothionein and its role in hematological malignancies. *J. Hematol. Oncol.*, **2012**, *5*, 1-8.

[81] Krizkova S.; Fabrik I.; Adam V.; Hrabeta J.; Eckschlager T.; Kizek R. Metallothionein – a promising tool for cancer diagnostics. *Bratisl. Med. J.-Bratisl. Lek. Listy*, **2009**, *110*, 93-97.

[82] Lewis B.P.; Shih I.H.; Jones-Rhoades M.W.; Bartel D.P.; Burge C.B. Prediction of mammalian microRNA targets. *Cell*, **2003**, *115*, 787-798.

[83] Betel D.; Wilson M.; Gabow A.; Marks D.S.; Sander C. The microRNA.org resource: targets and expression. *Nucleic Acids Res.*, **2008**, *36*, D149-D153.

[84] Tong A.W.; Fulgham P.; Jay C.; Chen P.; Khalil I.; Liu S.; Senzer N.; Eklund A.C.; Han J.; Nemunaitis J. MicroRNA profile analysis of human prostate cancers. *Cancer Gene Ther.*, **2009**, *16*, 206-216.

[85] Prueitt R.L.; Yi M.; Hudson R.S.; Wallace T.A.; Howe T.M.; Yfantis H.G.; Lee D.H.; Stephens R.M.; Liu C.G.; Calin G.A.; Croce C.M.; Ambs S. Expression of microRNAs and protein-coding genes associated with perineural invasion in prostate cancer. *Prostate*, **2008**, *68*, 1152-1164.

[86] Wang M.H.; Yang F.; Zhang X.Z.; Zhao H.B.; Wang Q.S.; Pan Y.C. Comparative analysis of MTF-1 binding sites between human and mouse. *Mamm. Genome*, **2010**, *21*, 287-298.

[87] Andrews G.K. Regulation of metallothionein gene expression by oxidative stress and metal ions. *Biochem. Pharmacol.*, **2000**, *59*, 95-104.

[88] Hasumi M.; Suzuki K.; Matsui H.; Koike H.; Ito K.; Yamanaka H. Regulation of metallothionein and zinc transporter expression in human prostate cancer cells and tissues. *Cancer Lett.*, **2003**, *200*, 187-195.

[89] Laity J.H.; Andrews G.K. Understanding the mechanisms of zinc-sensing by metal-response element binding transcription factor-1 (MTF-1). *Arch. Biochem. Biophys.*, **2007**, *463*, 201-210.

[90] Rando O.J. Combinatorial complexity in chromatin structure and function: revisiting the histone code. *Curr. Opin. Genet. Dev.*, **2012**, *22*, 148-155.

[91] Bannister A.J.; Kouzarides T. Regulation of chromatin by histone modifications. *Cell Res.*, **2011**, *21*, 381-395.

[92] Cao P.; Deng Z.Y.; Wan M.M.; Huang W.W.; Cramer S.D.; Xu J.F.; Lei M.; Sui G.C. MicroRNA-101 negatively regulates Ezh2 and its expression is modulated by androgen receptor and HIF-1 alpha/HIF-1 beta. *Mol. Cancer*, **2010**, *9*, 1-12.

[93] Varambally S.; Cao Q.; Mani R.S.; Shankar S.; Wang X.S.; Ateeq B.; Laxman B.; Cao X.H.; Jing X.J.; Ramnarayanan K.; Brenner J.C.; Yu J.D.; Kim J.H.; Han B.; Tan P.; Kumar-Sinha C.; Lonigro R.J.; Palanisamy N.; Maher C.A.; Chinnaiyan A.M. Genomic Loss of microRNA-101 Leads to Overexpression of Histone Methyltransferase EZH2 in Cancer. *Science*, **2008**, *322*, 1695-1699.

[94] Noonan E.J.; Place R.F.; Pookot D.; Basak S.; Whitson J.M.; Hirata H.; Giardina C.; Dahiya R. miR-449a targets HDAC-1 and induces growth arrest in prostate cancer. *Oncogene*, **2009**, *28*, 1714-1724.

[95] Formosa A.; Lena A.M.; Markert E.K.; Cortelli S.; Miano R.; Mauriello A.; Croce N.; Vandesompele J.; Mestdagh P.; Finazzi-Agrò E.; Levine A.J.; Melino G.; Bernardini S.; Candi E. DNA methylation silences miR-132 in prostate cancer. *Oncogene*, **2012**, *in press, doi: 10.1038/onc.2012.14*.

[96] Hulf T.; Sibbritt T.; Wiklund E.D.; Bert S.; Strbenac D.; Statham A.L.; Robinson M.D.; Clark S.J. Discovery pipeline for epigenetically deregulated miRNAs in cancer: integration of primary miRNA transcription. *BMC Genomics*, **2011**, *12*, 1-9.

[97] Arroyo J.D.; Chevillet J.R.; Kroh E.M.; Ruf I.K.; Pritchard C.C.; Gibson D.F.; Mitchell P.S.; Bennett C.F.; Pogosova-Agadjanyan E.L.; Stirewalt D.L.; Tait J.F.; Tewari M. Argonaute2 complexes carry a population of circulating microRNAs independent of vesicles in human plasma. *Proc. Natl. Acad. Sci. U. S. A.*, **2011**, *108*, 5003-5008.

[98] Lawrie C.H.; Gal S.; Dunlop H.M.; Pushkaran B.; Liggins A.P.; Pulford K.; Banham A.H.; Pezzella F.; Boultwood J.; Wainscoat J.S.; Hatton C.S.R.; Harris A.L. Detection of elevated levels of tumour-associated microRNAs in serum of patients with diffuse large B-cell lymphoma. *Br. J. Haematol.*, **2008**, *141*, 672-675.

[99] Bianchi F.; Nicassio F.; Marzi M.; Belloni E.; Dall'Olio V.; Bernard L.; Pelosi G.; Maisonneuve P.; Veronesi G.; Di Fiore P.P. A serum circulating miRNA diagnostic test to identify asymptomatic high-risk individuals with early stage lung cancer. *EMBO Mol. Med.*, **2011**, *3*, 495-503.

[100] Brase J.C.; Johannes M.; Schlomm T.; Falth M.; Haese A.; Steuber T.; Beissbarth T.; Kuner R.; Sultmann H. Circulating miRNAs are correlated with tumor progression in prostate cancer. *Int. J. Cancer*, **2011**, *128*, 608-616.

[101] Mahn R.; Heukamp L.C.; Rogenhofer S.; von Ruecker A.; Müller S.C.; Ellinger J. Circulating microRNAs (miRNA) in serum of patients with prostate cancer. *Urology*, **2011**, *77*, 1265.e1269-1216.

[102] Gonzales J.C.; Fink L.M.; Goodman O.B.; Symanowski J.T.; Vogelzang N.J.; Ward D.C. Comparison of Circulating MicroRNA 141 to Circulating Tumor Cells, Lactate Dehydrogenase, and Prostate-Specific Antigen for Determining Treatment Response in Patients With Metastatic Prostate Cancer. *Clin. Genitourin. Cancer*, **2011**, *9*, 39-45.

[103] Hu Z.B.; Chen X.; Zhao Y.; Tian T.; Jin G.F.; Shu Y.Q.; Chen Y.J.; Xu L.; Zen K.; Zhang C.Y.; Shen H.B. Serum MicroRNA Signatures Identified in a Genome-Wide Serum MicroRNA Expression Profiling Predict Survival of Non-Small-Cell Lung Cancer. *J. Clin. Oncol.*, **2010**, *28*, 1721-1726.

[104] Kowarsch A.; Preusse M.; Marr C.; Theis F.J. miTALOS: Analyzing the tissue-specific regulation of signaling pathways by human and mouse microRNAs. *RNA-Publ. RNA Soc.*, **2011**, *17*, 809-819.

Received: July 23, 2012 **Revised: November 07, 2012** **Accepted: November 12, 2012**

2.2 Hypotheses verified under PART I

The following hypotheses have been formulated, based on the theoretical starting points outlined above:

Hypothesis 1: Zinc ions and their transporters and binding proteins or peptides interfere with prostate carcinoma pathogenesis significantly. As a result, zinc and metallothionein levels should reflect the formation of CaP both within the prostate cell lines and within a broader framework of clinical samples.

Hypothesis 2: Increasing zinc concentrations should alter expression of genes and miRNAs involved in CaP carcinogenesis significantly. In the cells derived from the primary prostate tumour, higher cell resistance to apoptosis induced by zinc ions can be expected. This higher resistance should be reflected by changes in expression of pro- and anti-apoptotic genes. This resistance can be diminished in the cells derived from metastases because they do not meet high zinc concentrations in prostate anymore, and therefore adaptation to high zinc concentration in the environment may disappear.

Hypothesis 3: Prostate carcinoma is characterized by a long-term reduction in zinc ion accumulation. By creating prostate tumour cells capable of accumulating zinc, the tumour phenotype should be adjusted towards the normal state.

2.2.1 Findings related to the hypothesis 1

***Hypothesis 1*: Zinc ions and their transporters and binding proteins or peptides interfere with prostate carcinoma pathogenesis significantly. As a result, zinc and metallothionein levels should reflect the formation of CaP both within the prostate cell lines and within a broader framework of clinical samples.**

It has been proved that loss of ability to accumulate zinc is necessary for carcinogenesis, namely at the early stages of CaP development [26]. This hypothesis has been confirmed also in our experimentally used prostate cell lines PNT1A (benign line), 22Rv1 (a primary tumour) and PC-3 (bone metastasis derived from CaP). Whilst PNT1A contained 125.9 μg/g of intracellular zinc, the tumour cell lines contained significantly less, 107.75 μg/g, and 75.85 μg/g respectively [52, 53]. However, the experimental studies analyzing the amount of zinc in biological samples of the patients suffering from CaP and in other solid tumours often diverged in their results. The relationship between the clinical-pathological characteristics of CaP patients and the zinc levels was also unclear. This is why meta-analysis (114 studies with a total number of 22,737 patients and controls) has been created, Gumulec et al. on page 80 [54]. A significant decrease of zinc ion concentration in serum was demonstrated in almost all studied malignancies, including CaP,

apparently due to the depletion of zinc reserves in consequence of the immune system burdening by a tumour, and therefore this marker is not usable in the specific CaP diagnostics. More specific behaviour was observed in the tissue zinc concentration. Decreased zinc concentration in the tumour tissue was demonstrated in CaP, thyroid tumours, hepatocellular tumours and non-small cell lung carcinomas. By contrast, the zinc concentration was increased consistently in breast carcinomas. In none of the tumours, meta-regression demonstrated a relationship between the zinc level and the tumour stage and grade.

The significance of metallothionein concentration was assessed by applying a similar methodology [55], see page 91. With respect to a wide range of approaches, by which it is possible to determine this protein in tissue samples and to the resulting heterogeneity of the data, only the studies based on immunohistochemical detection were included in the meta-analysis. In total, 77 works were included (4631 tumour tissue samples and 3384 control tissue samples) into the study. Types of tumours that show a significant increase in metallothionein include ovarian carcinomas and spinocellular head and neck carcinomas. The decrease in MT was demonstrated in hepatocellular carcinomas. In CaP, no significant difference in MT concentration was proved compared with the control tissue. MT was associated neither with CaP staging nor CaP grading; however, patients with higher MT concentrations exhibited generally a lower survival rate.

Conclusion: In CaP, decreased concentration of zinc was demonstrated both in the model tumour cell line [52, 53] and in the patients' tumour tissue [54]. This reduction was not accompanied by a decrease in the concentration of zinc-binding metallothionein [55]. On the other hand, patients with higher MT levels experienced a worse survival rate, which fact is most probably associated with the antioxidant and protective role of MT in tumour cells that will be dealt in the following block of experiments (Part III). Gene and protein expression of the most frequently represented MT form, i.e. MT2A, was increased in the prostate tumour lines compared to the non-tumour line PNT1A [53, 56]. Based on zinc and MT concentrations it is possible to say that the selected prostate tumour cell lines are a relatively good model of the real CaP status.

Author's publications relevant to this chapter

1. Gumulec J, Masarik M, Adam V, Eckschlager T, Provaznik I, Kizek R. Serum and Tissue Zinc in Epithelial Malignancies: A Meta-Analysis. Plos One. 2014;9(6).
   Available on page 80
2. Gumulec, J., M. Raudenska, et al. (2014). "Metallothionein - Immunohistochemical Cancer Biomarker: A Meta-Analysis." Plos One **9**(1).
   Available on page 91

OPEN ACCESS Freely available online

PLOS ONE

Serum and Tissue Zinc in Epithelial Malignancies: A Meta-Analysis

Jaromir Gumulec[1,2], Michal Masarik[1,2]*, Vojtech Adam[2,3], Tomas Eckschlager[4], Ivo Provaznik[5], Rene Kizek[2,3]

1 Department of Pathological Physiology, Faculty of Medicine, Masaryk University, Brno, Czech Republic, **2** Central European Institute of Technology, Brno University of Technology, Brno, Czech Republic, **3** Department of Chemistry and Biochemistry, Mendel University in Brno, Brno, Czech Republic, **4** Department of Paediatric Haematology and Oncology, 2nd Faculty of Medicine and University Hospital Motol, Charles University, Prague, Czech Republic, **5** Department of Biomedical Engineering, Faculty of Electrical Engineering and Communication, Brno University of Technology, Brno, Czech Republic

Abstract

Background and Objectives: Current studies give us inconsistent results regarding the association of neoplasms and zinc(II) serum and tissues concentrations. The results of to-date studies using meta-analysis are summarized in this paper.

Methods: Web of Science (Science citation index expanded), PubMed (Medline), Embase and CENTRAL were searched. Articles were reviewed by two evaluators; quality was assessed by Newcastle-Ottawa scale; meta-analysis was performed including meta-regression and publication bias analysis.

Results: Analysis was performed on 114 case control, cohort and cross-sectional studies of 22737 participants. Decreased serum zinc level was found in patients with lung (effect size = −1.04), head and neck (effect size = −1.43), breast (effect size = −0.93), liver (effect size = −2.29), stomach (effect size = −1.59), and prostate (effect size = −1.36) cancers; elevation was not proven in any tumor. More specific zinc patterns are evident at tissue level, showing increase in breast cancer tissue (effect size = 1.80) and decrease in prostatic (effect size = −3.90), liver (effect size = −8.26), lung (effect size = −3.12), and thyroid cancer (effect size = −2.84). The rest of the included tumors brought ambiguous results, both in serum and tissue zinc levels across the studies. The association between zinc level and stage or grade of tumor has not been revealed by meta-regression.

Conclusion: This study provides evidence on cancer-specific tissue zinc level alteration. Although serum zinc decrease was associated with most tumors mentioned herein, further – prospective - studies are needed.

Citation: Gumulec J, Masarik M, Adam V, Eckschlager T, Provaznik I, et al. (2014) Serum and Tissue Zinc in Epithelial Malignancies: A Meta-Analysis. PLoS ONE 9(6): e99790. doi:10.1371/journal.pone.0099790

Editor: Marcia E Lopes. Consolaro, State University of Maringá/Universidade Estadual de Maringá, Brazil

Received February 6, 2014; **Accepted** May 18, 2014; **Published** June 18, 2014

Funding: Financial support from Central European Institute of Technology CZ.1.05/1.1.00/02.0068 and Internal Grant Agency of Ministry of Health of the Czech Republic (IGA MH NT14337-3/2013) is highly acknowledged. The funders had no role in study design, data collection and analysis, decision to publish, or preparation of the manuscript.

Competing Interests: The authors have declared that no competing interests exist.

* Email: masarik@med.muni.cz

Introduction

Zinc(II) plays a role in several intracellular signalling pathways. It is also a cofactor of numerous enzymes [1]. Its dysregulation is present in various cancers. Imbalance of zinc transporters causing intracellular and serum zinc(II) levels alteration was described in prostate and breast cancers. [2–5]. Questions were raised whether these associations have clinical applications. Studies focusing on zinc content in biological materials in cancer patients provide inconsistent results. Zinc levels in tumor tissues of prostate [6], liver [7], and lung [8] and its serum levels in breast, lung, stomach, and prostate cancer patients were reviewed previously [9].

We investigated the associations of serum and cellular zinc(II) levels with carcinomas via meta-analysis.

Methods

Literature Search

Search was performed in Web of science (Science citation index expanded 1945 to April 2013), PubMed (Medline 1968 to April 2013), Embase (1977 to April 2013), and Cochrane Library (CENTRAL 1953 to April 2013); keywords are shown in Figure 1. Moreover, cited references of found articles were analyzed.

Selection Criteria

Diagram (Fig. 1) shows acquisition process. Among published articles, the search was done for clinical trials, case-control and cohort studies investigating the associations between carcinoma and tissues and serum zinc levels. Because no difference in zinc(II) level between serum and plasma was found [10], both materials were referred as "serum". Studies with full texts available were

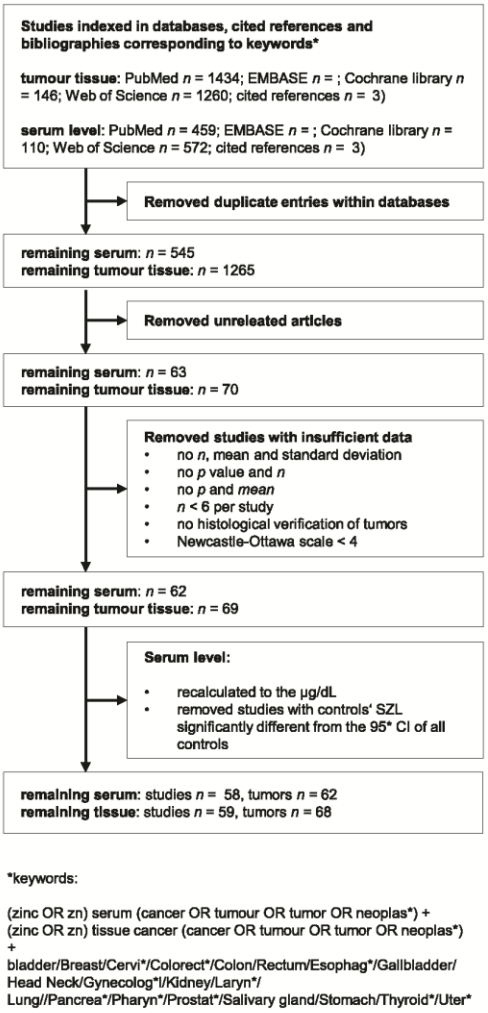

Figure 1. Flow diagram for identification of relevant studies.
doi:10.1371/journal.pone.0099790.g001

included only. Only the studies where the data were displayed in the following ways were accepted: (1) sample size, means and standard deviations, or (2) sample size, means, P values and statistical test type (one- or two-tailed). If similar data were found in more studies by the same group, study with most data was included.

The eligibility of the studies for meta-analysis was evaluated by J.G. and V.A., discrepancies were discussed with R.K and M.M.

Assessment of Methodological Quality

The quality of studies was assessed by the Newcastle-Ottawa Scale (NOS) [11]. NOS ranges from 0 to 9 stars. The studies with <4 stars were excluded, with >6 stars were considered as high quality; the mean was 5.6 stars.

Main and Subgroup Analyses

First, differences of the serum and tissue zinc levels between overall tumors and controls were analysed (Table 1). Then, analyses by tumor type, histology, and methodological quality were performed (Table 2). To meet conditions of between-study independence, zinc level was averaged in studies with multiple tumors, forming age groups or detecting gender separately in case of the summary. For comparison of individual tumors, the tumor was taken as a unit of analysis unless violated between-study independence.

Statistical Analyses

To express the differences in serum and tissue concentrations, standardized difference in means (Cohen's d) was used. To assess heterogeneity across studies, Higgins I^2 (describes percentage of variability) was calculated [12]. Random effects model meta-analysis was employed when $I^2>50\%$; otherwise, fixed model was used. Publication bias was evaluated using funnel plots and two-sided Egger tests in groups with >3 studies. Funnel plots of studies with Egger's test $p<0.05$ are asymmetric (Table S1). There was performed meta-regression using unrestricted maximum likehood method of studies reporting stage or grade if number of studies with corresponding moderators was >10 [13,14]. Comprehensive Meta-analysis Version 2 software (Biostat, Englewood, NJ) was used for analysis.

Results

Identification of Relevant Studies and their Characteristics

Total of 3201 articles were found. After excluding articles not meeting the criteria (Fig. 1) and duplicates, 114 articles studying 130 tumors were included (several studies studied more tumors, Table S2).

Overall 114 studies including 22737 participants (8584 cases, 14153 controls) were analyzed. From studies reporting age, sex and ethnicity, the mean age was 54.5±12.3 (male) and 49.6±12.2 (female); male were included 49.5% and 51.0% in "tumor" and control groups. Publication date ranged within 1952–2012. Caucasians, Asians, Hispanics, and Afro-Americans were reported in 52%, 45%, 1%, and 2%, respectively. Characteristics of studies are summarized in Table S2. Two clinical, 4 cohort, 6 cross-sectional, and 102 case control studies were included.

Overall Zinc Level in Sera and Tumors

Serum level. As shown on Fig. 2 and Table 1, serum zinc level is significantly decreased in patients with tumors (effect size = −1.08; 95% confidence interval, CI, −1.33 to −0.82) using random effects model of 58 studies (6223 cases, 10364 controls). This is consistent with subgroup of 26 high-quality studies (effect size = −1.30; 95% CI, −1.72 to −0.88). High level of heterogeneity is observed (Higgins $I^2 = 96.71\%$). Meta-regression did not reveal that stage, grade, and age or publication year affect effect size (Table S1). Six studies analyzed serum zinc level in group of patients with malignant tumor without other specification (516 cases, 3871 controls), and significant decrease was found (Fig. 2) [15–20].

Tissue level. There was a significant decrease in tissue zinc level using random effects model meta-analysis of 59 studies (2361 cases, 3789 controls) with effect size −1.44 (CI−1.93 to −0.95). However, publication bias was observed at $p = 0.01$ and no significance found in 24 high-quality studies. Meta-regression did not reveal any moderators to affect global effect size.

Bladder

Significant decrease of serum zinc level was observed (−1.24; 95% CI, −1.77 to −0.77) using random effects model of two studies [21,22] (86 cases, 92 controls); both were "high-quality".

Table 1. Overall results of meta-analysis by tumor type and statistical model used.

Tumor	No. of studies	Point estimate	95% CI of point estimate	Heterogeneity, I^2	Model used
Bladder - serum	2	−1.24	−1.77 to −0.71	61.74	random
Breast serum	12	−0.93	−1.68 to −0.17	96.16	random
Breast tissue	15	1.80	1.17 to 2.42	94.89	random
Colorectal serum	5	0.04	−2.57 to 2.64	98.98	random
Colorectal tissue	7	0.37	−0.97 to 1.72	96.23	random
Esophageal serum	4	−2.17	−3.23 to −1.11	86.46	random
Esophageal tissue	3	−1.57	−3.17 to 0.03	94.72	random
Gallbladder - serum	1	−2.31	−2.96 to −1.65		-
Gallbladder - tissue	2	−1.25	−1.73 to −0.77	0.00	fixed
Gynecological serum	3	−0.39	−0.6 to −0.17	49.48	fixed
Gynecological tissue	4	−0.70	−1.85 to 0.45	91.40	random
Head and neck tissue	2	3.11	−5.96 to 12.17	98.75	random
Head Neck serum	5	−1.43	−2.17 to −0.68	77.46	random
Kidney - tissue	4	−2.23	−3.89 to −0.57	89.51	random
Liver - serum	3	−2.29	−5.21 to 0.63	97.64	random
Liver - tissue	7	−8.26	−11.02 to −5.49	98.49	random
Lung - serum	13	−1.04	−1.53 to −0.56	92.94	random
Lung - tissue	6	−3.12	−4.57 to −1.67	96.76	random
Prostate serum	7	−1.36	−1.97 to −0.75	97.93	random
Prostate tissue	12	−3.90	−5.26 to −2.54	94.67	random
Stomach serum	4	−1.59	−3.14 to −0.03	98.24	random
Stomach tissue	3	−0.79	−1.44 to −0.14	60.85	random
Thyroid serum	3	−0.62	−3.04 to 1.79	97.69	random
Thyroid tissue	3	−2.84	−5.39 to −0.29	97.56	random
Overall - serum	58	−1.08	−1.33 to −0.82	96.71	random
Overall - tissue	59	−1.44	−1.93 to −0.95	97.08	random

CI, confidence interval.

doi:10.1371/journal.pone.0099790.t001

Breast

Serum. There was significant decrease (−0.93; 95% CI, −1.68 to −0.17) using random effects model meta-analysis of 12 studies (604 cases, 663 controls) [20,23–33] (Fig. 3, Table 1). However, no significant change was observed in six studies [20,23,25,27,30,31] and significantly increased level in one [24]. No publication bias was observed (Begg's funnel plot was symmetrical, Egger's 2-tailed test p = 0.086). Subgroup meta-analysis by methodological quality of study revealed significant decrease in nine low-quality studies (− 1.32, CI–2.23 to–0.42) using random effects model, but no significant change in three high-quality studies using fixed effects model [25,27,31]. With regard to stage, Yucel *et al.* found no difference between stages [33]; in contrary, studies by Gupta *et al.* and Kuo *et al.* showed a decrease in advanced cancer in comparison to early stages [26] and significantly decreasing trend in relation to stage [29].

Tissue level. Significant elevation was determined using random effects model of 15 studies (635 cases, 714 controls), effect size = 1.80 (95% CI, 1.17 to 2.42) [29,34–47]. However, two studies show insignificant changes [42,46]. The highest levels were observed in study by Ng *et al.*, which include ductal cancers only [35]. Publication bias was observed on p = 0.018. Significant elevation was found in both low- and high- quality studies, while the levels were higher in 9 high-quality studies (2.33; CI, 1.46 to 3.21). Farquharson *et al.* reported significantly decreased tissue zinc concentration in estrogen receptor negative tumors [42]. Kuo *et al.* found no trend [29] in relation to grade, while Farquharson *et al.* showed significant decrease in grade II-III vs. grade I [42].

Gynecological Tumors (Uterine Corpus, Cervix and Ovarian)

Serum. Among ovarian and cervical cancers, there was a significant decrease found (−0.39; CI−0.60 to −0.17) using fixed effects model of three studies (164 cases, 171 controls) [20,48,49]. No publication bias was observed. When subgroup meta-analysis by histological type was done, significant decrease was found in cervical [48], insignificant changes in ovarian cancer [49]. There were no significant trends in relation to stage and grade [49].

Tissue level. No significant difference between uterine corpus and cervix cancers was determined using random-effects model of 4 studies (80 cases, 123 controls) [37,48,50,51]. No publication bias was determined. Significant decrease was reported in two studies [48,51]. Results of high-quality studies did not show a significant trend.

Digestive System Tumors (Esophageal, Stomach, Colorectal, Liver, Gallbladder and Pancreatic Carcinoma)

Esophageal, serum. All four studies included in this analysis (93 cases, 80 controls) [52–55] show significant reduction (−2.17;

Table 2. Subgroup analysis by study quality and histological type.

Subgroup	Tumor	Factor	No. of studies	Point estimate (95% CI)	Heterogeneity, I^2	Model used
Study quality						
	Breast serum	high	3	0.22 (−0.08 to 0.51)	0.00	fixed
	Breast serum	low	9	−1.32 (−2.23 to −0.42)	97.06	random
	Breast tissue	high	9	2.33 (1.46 to 3.21)	95.88	random
	Breast tissue	low	6	1.11 (0.08 to 2.14)	91.22	random
	Colorectal tissue	high	2	−0.50 (−2.84 to 1.85)	81.73	random
	Colorectal tissue	low	5	0.80 (−0.84 to 2.43)	96.55	random
	Esophageal serum	high	2	−1.56 (−3.23 to 0.10)	72.04	random
	Esophageal serum	low	2	−2.99 (−4.79 to −1.19)	93.50	random
	Esophageal tissue	high	2	−1.60 (−3.86 to 0.65)	97.29	random
	Esophageal tissue	low	1	−1.52 (−2.56 to −0.47)		-
	Gynecological tissue	high	3	−0.14 (−1.02 to 0.75)	82.33	random
	Gynecological tissue	low	1	−2.49 (−3.31 to −1.66)		-
	Head Neck serum	high	2	−0.88 (−1.26 to −0.49)	3.16	fixed
	Head Neck serum	low	3	−1.59 (−2.08 to −1.10)	86.60	random
	Kidney - tissue	high	2	−1.03 (−1.80 to −0.26)	22.30	fixed
	Kidney - tissue	low	2	−3.12 (−6.49 to 0.25)	96.07	random
	Liver - tissue	high	2	−8.03 (−15.12 to −0.94)	98.00	random
	Liver - tissue	low	5	−12.29 (−17.08 to −7.51)	98.84	random
	Lung - serum	high	7	−1.01 (−1.69 to −0.33)	95.95	random
	Lung - serum	low	6	−1.09 (−1.84 to −0.34)	70.97	random
	Prostate serum	high	5	−2.07 (−3.82 to −0.32)	98.59	random
	Prostate serum	low	2	−0.34 (−3.07 to 2.39)	78.33	random
	Prostate tissue	high	3	−6.25 (−9.71 to −2.78)	98.02	random
	Prostate tissue	low	9	−3.59 (−5.34 to −1.85)	92.34	random
	Stomach serum	high	1	−0.13 (−0.32 to 0.06)		-
	Stomach serum	low	3	−2.09 (−4.14 to −0.04)	97.68	random
	Stomach tissue	high	2	−1.14 (−1.55 to −0.73)	0.00	fixed
	Stomach tissue	low	1	−0.26 (−0.96 to 0.45)		-
	Overall - serum	high	26	−1.30 (−1.72 to −0.88)	96.62	random
	Overall - serum	low	32	−0.92 (−1.3 to −0.54)	96.77	random
	Overall - tissue	high	23	−0.42 (−1.23 to 0.38)	97.38	random
	Overall - tissue	low	36	−2.12 (−2.77 to −1.47)	96.95	random
Histological type						
	Gynecological serum	Ovary	1	−0.07 (−0.47 to 0.32)		-
	Gynecological serum	Uterine cervix	1	−0.49 (−0.77 to −0.21)		-
	Head Neck serum	Larynx	4	−1.52 (−2.35 to −0.69)	81.96	random
	Head Neck serum	Oral Cavity	2	−0.95 (−1.38 to −0.53)	0.00	fixed
	Lung - serum	adenocarcinoma	2	0.02 (−1.49 to 1.54)	95.48	random
	Lung - serum	large cell	2	−0.78 (−1.32 to −0.23)	0.00	fixed
	Lung - serum	NSCLC	4	−0.94 (−1.36 to −0.53)	58.87	random
	Lung - serum	small cell	2	−1.42 (−3.05 to 0.21)	88.46	random
	Lung - serum	squamous cell	2	−1.23 (−2.75 to 0.29)	97.01	random
	Lung - tissue	adenocarcinoma	2	−0.89 (−2.96 to 1.19)	92.20	random
	Lung - tissue	large cell	1	−1.22 (−2.22 to −0.23)		-
	Lung - tissue	NSCLC	2	−0.62 (−1.88 to 0.65)	88.90	random
	Lung - tissue	small cell	2	−0.52 (−0.80 to −0.23)	0.00	fixed
	Lung - tissue	squamous cell	2	−0.48 (−2.54 to 1.58)	92.14	random
	Thyroid serum	folicular	2	−1.86 (−4.83 to 1.11)	96.81	random

Table 2. Cont.

Subgroup	Tumor	Factor	No. of studies	Point estimate (95% CI)	Heterogeneity, I^2	Model used
	Thyroid serum	papillary	2	−1.48 (−4.43 to 1.48)	96.38	random
	Thyroid tissue	folicular	1	0.00 (−0.59 to 0.59)		-
	Thyroid tissue	papillary	1	−0.50 (−1.09 to 0.09)		-

Note low is for Newcastle-Ottava scale <6, high for NOS >6. Random and fixed effect meta-analysis. NSCLC, non-small cell lung cancer, CI, confidence interval.
doi:10.1371/journal.pone.0099790.t002

95% CI, −3.23 to 1.11) and it was one of the highest decreases. Publication bias was identified (p = 0.04) and insignificant decrease was observed in two high-quality studies.

Esophageal, tissue. No significant change was identified using meta-analysis of three studies (104 cases, 116 controls) [52,56,57] due to high variability among studies, even among two high-quality ones [56,57]. No publication bias was observed.

Stomach, serum. Significant decrease was observed (effect size = −1.59; 95% CI, −3.14 to −0.03) without publication bias. However, high variability was present in the four studies (290 cases, 474 controls) [28,30,58,59] and significant decrease was reported in two studies only [28,59]. No significant change was observed in one high-quality study [58].

Stomach, tissue. Significant decrease was determined (−0.79; 95% CI, −1.44 to −0.14) in three studies (71 cases, 67 controls) [37,59,60] and one study showed significant decrease [59]. No publication bias was identified.

Colorectal cancer, serum. No significant difference was determined. No study fulfilled criteria of "high-quality". Five studies were included (313 cases, 216 controls) [28,30,61–63] and no publication bias was detected. However, two studies showed significant decrease [28,62], one study showed significant elevation [61], and thus, high serum zinc level variances were associated with colorectal cancer. Of studies reporting stage, one showed significantly decreasing trend on Dukes stage [62], whereas other showed no significant changes related to TNM stage [61].

Colorectal cancer, tissue. No significant difference was observed using meta-analysis of seven studies (233 cases, 159 controls) [34,37,46,62,64–66] and no publication bias was observed. None of the high quality studies revealed significant differences. One of the largest variation among tissue levels was observed (effect size = 0.37; 95% CI, −0.97 to 1.72). Two studies showed significant decrease [62,64] while another two significant elevation [46,66]. One study including grade did not show significant trend [64].

Gallbladder, serum. one high-quality study (30 cases, 30 controls), that showed significant decrease, was identified [67].

Gallbladder, tissue. Significant decrease was determined in two studies [68,69] (39 cases, 40 controls) using fixed effects model (−1.25; 95% CI, −1.73 to −0.77). No study analyzed further classifications.

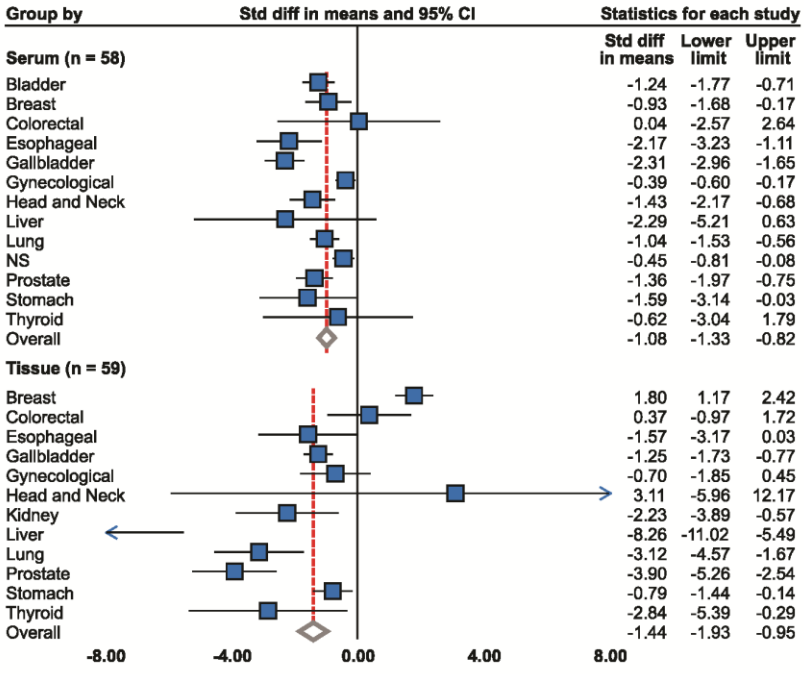

Figure 2. Level of zinc in sera and tissues by tumor type. Summary of individual meta-analyses. For model used and heterogeneity, see Table 1.
doi:10.1371/journal.pone.0099790.g002

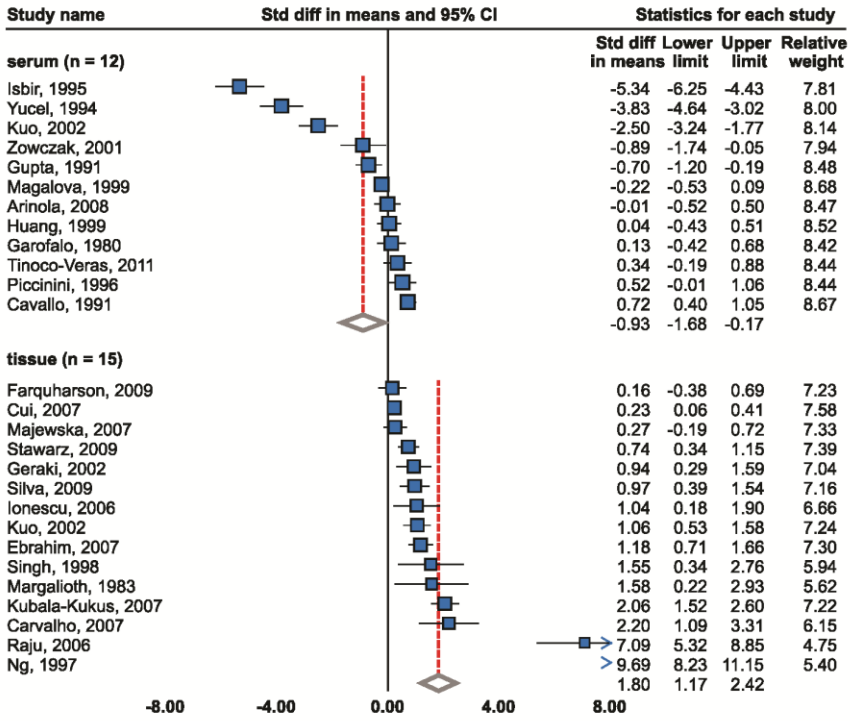

Figure 3. Zinc level in sera and tissues of breast cancer patients. Random effects model meta-analysis. Studies sorted by standardized mean difference.
doi:10.1371/journal.pone.0099790.g003

Liver, serum. No significant change was observed in three studies [70–72] (149 cases, 121 controls) and no publication bias was observed. Two high-quality studies [71,72] are in accordance, showing fixed serum zinc level. One study showed no significant trend in relation to stage [70].

Liver, tissue. Significant decrease was observed in all 7 studies analysed [70,73–78] (269 cases, 329 controls), effect size = −8.26 (95% CI, −11.02 to −5.49). Two high-quality studies [73,76] provided consistent results (−8.03; 95% CI, −15.12 to −0.93). Publication bias was observed (p = 0.04).

Prostate

Serum. Significant decrease was observed (effect size = −1.36; 95% CI, −1.97 to −0.75) using random effects model-meta-analysis of 7 studies [79–85] (2985 cases, 3539 controls, Fig. 4).

Insignificant changes were observed in large sample studies – cohort from French SuViMax study (4961 cases and controls) [82] and Multiethnic Cohort study (1175 cases and controls) [85]. Subgroup meta-analysis found significant decrease in high quality studies (−2.07; 95 CI, −3.82 to −0.32). No publication bias was observed.

Tissue. Random effects model meta-analysis of 12 studies (240 cases, 226 controls) [86–97] detected a significant decrease (effect size = −3.90; 95% CI, −5.26 to −2.54). Only one study showed insignificant decrease [86]. Most significant decrease was observed in study by Guntupalli et al. [89]. High level of publication bias was observed among studies (p = 0.0007). Results are in agreement with more distinct effect size in high-quality studies (−6.03; 95% CI, −9.39 to −2.67). Trend was not observed in one study relating to stage and grade [6].

Head and Neck

Serum. Five studies including cancers of oral cavity [98,99] and larynx [98,100–102] (159 cases, 228 controls) showed significant decrease (random effects model −1.43; 95% CI, −2.17 to −0.68). No publication bias was observed – all studies, including 2 high-quality ones, showed significant decrease [98,99]. No significant trend was observed between stage and serum zinc level [100].

Tissue. Two studies (45 cases, 27 controls) [103,104] were included in the analysis. Findings of these studies were contradictory: one showed significant elevation [103] while the other - significant decrease [104]. Random effects model did not show any trend. No significant trend between grade and zinc level was observed in one study [104].

Thyroid

Serum. No significant difference was observed using random effects model of three studies (131 cases, 93 controls) [105–107]. One study showed significant elevation [107], the other showed significant decrease [105] and third, ranked as high quality [106], found no significant differences. No publication bias was observed. Subgroup analysis by histological type does not highlight significant difference between papillary and follicular cancer. Medullar carcinoma was not included in meta-analysis.

Tissue. Statistically significant decrease was observed using random effects model (effect size = −2.84; 95% CI, −5.39 to −0.29) of three studies (109 cases, 123 controls) [105,108,109]. However, one study reported insignificant results [105], another included papillary, follicular, medullar cancers and reticulosarcoma [108] and the third did not specify histological types. No

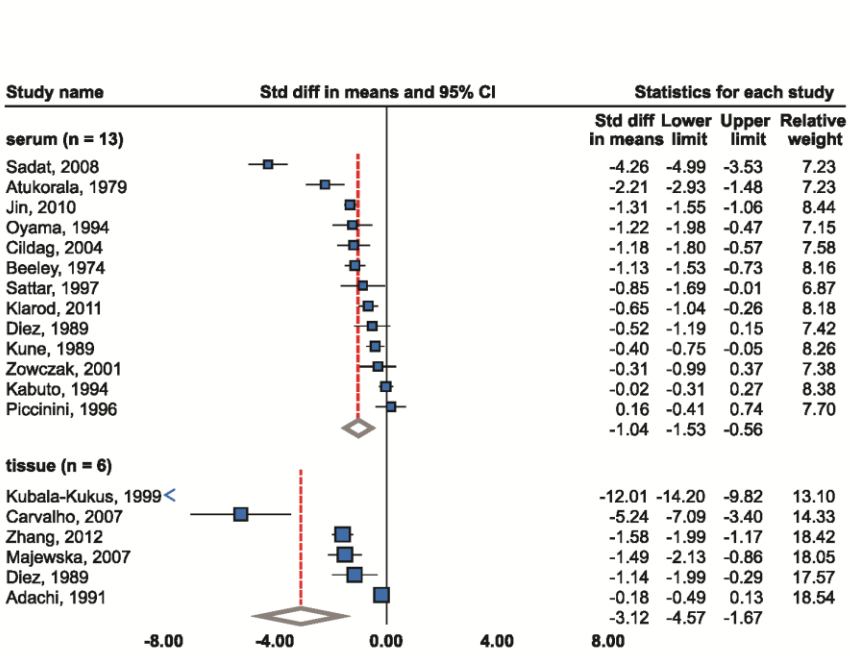

Figure 4. Zinc level in sera and tissues of prostate cancer patients. Random effects model meta-analysis. Studies sorted by standardized mean difference.
doi:10.1371/journal.pone.0099790.g004

publication bias was present. One study determined no significant difference between papillary and follicular cancers [105].

Kidney

Tissue. Significant decrease was observed using random effects model (−2.23; 95% CI, −3.89 to −0.57) of 4 studies (66 cases, 45 controls). Results agree with 2 high quality studies [37,110]. All studies showed significant decrease [37,110–112] and no publication bias was detected.

Lung

Serum. Significant decrease (−1.04; 95% CI, −1.53 to −0.56) was identified using random effect model of 13 studies [20,31,58,113–122] (703 cases, 786 controls, Fig. 5); four of them showed insignificant changes [20,31,58,115]. No publication bias was observed ($p = 0.38$). Analysis of only high-quality studies provided similar results. Subgroup analysis according to histology detected significant decrease in non-small cell lung cancer using random effects model in four studies. Two studies dealt with histological classification [115,116]: no significant difference was observed in adenocarcinoma and squamous cell carcinoma using random effects and significant decrease in large cell carcinoma using fixed effects (−0.78; 95% CI, −1.32 to −0.23). serum zinc level and stage was analyzed in two studies [114,116]. Klarod *et al.* determined significantly lower serum zinc level in advanced compared to low stages [114]. Similarly, descending trend was observed between stages T1, T2, and T3 [116]. Negative correlation between serum zinc level and grade was determined [116].

Tissue. Significant decrease was determined using random effects model (−3.12; 95% CI, −4.57 to −1.67) of six studies, all ranked as low-quality [34,46,115,123–125] (470 cases, 1820 controls). However, publication bias was observed ($p = 0.03$). Insignificant change was observed in one study [123]. Significant decrease was determined in small cell lung cancer (−0.52; 95% CI, −0.80 to −0.23) using fixed model and no significant decrease was identified in non-small cell lung cancer using random effects model. No significant trend was observed in squamous and adenocarcinomas. Large cell cancer showed significant decrease in one study [115].

Discussion

Decreased serum zinc level was found in patients with lung, head and neck, breast, liver, stomach, and prostate cancers. The elevation was not proven in any tumor. More specific zinc patterns are evident in tumors. Unequivocal increase was observed in breast cancer tissue only and decrease in prostatic, liver, lung, and thyroid cancer. The rest of the studied tumors brought ambiguous results, both in serum and tissue zinc levels across the studies. It cannot be confirmed that the serum zinc level does not change except of the abovementioned tumors. Serum and tissue zinc level reduction was evident to certain extent in majority of tumors. Although insignificant differences were found, the analysis indicates that none of the tumors clearly disproves that the zinc levels remained unchanged. Variation of serum zinc level were found in esophageal cancer patients, in cell zinc content in liver cancer and both in serum and tissue zinc level in stomach, colorectal, and thyroid cancers.

Number of studies point to decreasing trend in tumors of higher grades or stages. Nevertheless, meta-regression could not be performed on the majority of tumors due to limited number of studies reporting stage/grade or to inconsistency in the scale used. Regression analysis of all tumors, however, did not show dependence on these parameters. Thus, this meta-analysis fails to explain the sources of high heterogeneity between the studies.

Although serum zinc level decrease in lung, head and neck, and breast carcinomas was shown by meta-analysis, it is unclear, whether hypozincaemia is a consequence of tumor, chronic stress or of a combination of both these effects. Stress, infection or chronic diseases lead to redistribution of zinc(II) between body compartments, and thus reduce zincaemia [126]. In addition, chronic inflammation is a common hallmark of cancer, and thus might be important mechanism of serum zinc level decrease.

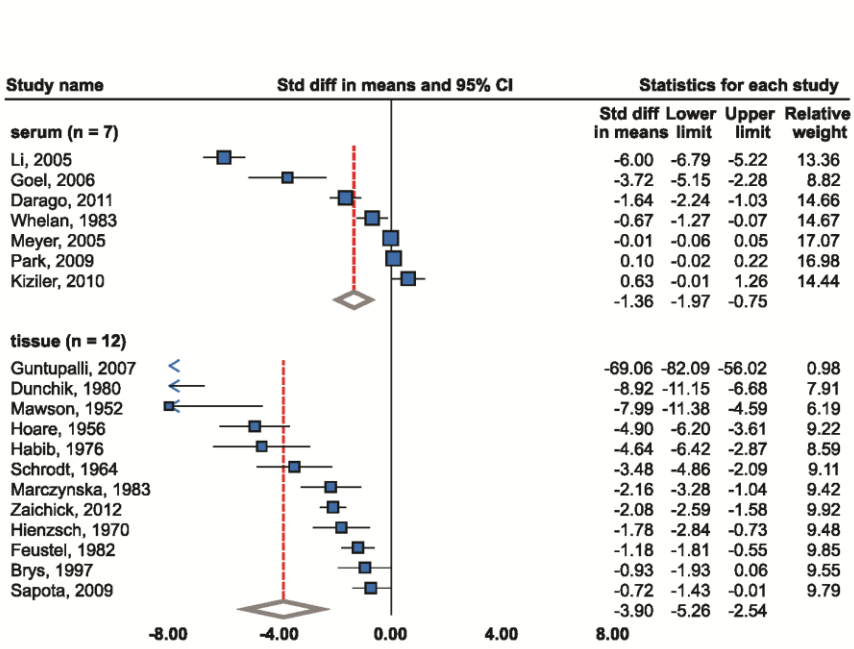

Figure 5. Zinc level in sera and tissues of lung cancer patients. Random effects model meta-analysis. Studies sorted by standardized mean difference.
doi:10.1371/journal.pone.0099790.g005

The association of tissue zinc level and prostate [6], liver [7], and lung [8] cancers serum zinc level and risk of breast, lung, stomach, and prostate cancers [9] were in scope of several reviews. Decrease in prostate cancer tissue zinc level is well-evidenced [127]. Also review by Zaichick *et al.* show decrease of zinc in prostate cancer tissue as compared with benign hyperplasia [6]. A review by Catalani, focusing on zinc content in lung tumors, is the only to date meta-analysis. However, its results did not allow summarizing the significance of tissue metals. No relationship among tissue zinc level and histotype or stage was found. Zinc decrease in liver cancer tissues were reviewed by Gurusamy *et al.* They declared that meta-analytic approach is impossible because of heterogeneity of analyzed studies. All mentioned reviews concluded that there is poor data agreement between studies determining tissue zinc level. This fact – combined with the low metal concentrations – calls for the standardization of methods. Catalani *et al.* propose standardization of sample collection, storage, and analysis. Previous reviews were performed only on specific tumors, with limited number of studies and/or statistic approaches were missing. Our meta-analytical analysis was done on all identified carcinomas, serum and tissue levels were analyzed together, publication bias was assessed and meta-regression was performed when case sufficient data were present. To reduce selection and publication biases, prospective cohort study with defined conditions separating the influence of inflammation is needed. Interest should be focused on the relation of zinc level in each histological type, stage, and grade.

There are limitations in this study caused by features of individual studies: sample sizes, subjects' characteristics, sampling, storage and detection methods, and different tumors classification. Serum zinc level has a limited predictive value, because it is particularly intracellular ion and it fluctuates in circadian rhythm.

This meta-analysis shows a decrease of zincaemia in lung, head and neck, and breast carcinoma, increase of tissue zinc in breast cancer and its decrease in prostate, liver, and lung cancers. However, this analysis does not provide conclusive data with regard to stage and grade, and thus does not clarify heterogeneity in values between the studies.

Supporting Information

Checklist S1 Prisma 2009 checklist.
(DOC)

Table S1 Meta-regression analysis of overall results using mixed effects model (unrestricted maximum likehood). SMD, standardized mean difference.
(XLSX)

Table S2 Source data set extracted from studies used for analysis. Including methodological quality of studies based on Newcastle-Ottawa scale, study design, and information regarding matching cases and controls. NS, not specified, NOS, Newcastle-Ottawa scale, stdev, standard deviation.
(XLSX)

Author Contributions

Conceived and designed the experiments: JG VA MM RK. Performed the experiments: JG VA MM RK. Analyzed the data: JG IP TE. Contributed reagents/materials/analysis tools: RK MM IP. Wrote the paper: JG MM VA TE IP RK.

References

1. Maret W, Li Y (2009) Coordination Dynamics of Zinc in Proteins. Chem Rev 109: 4682–4707.
2. Gumulec J, Masarik M, Krizkova S, Adam V, Hubalek J, et al. (2011) Insight to Physiology and Pathology of Zinc(II) Ions and Their Actions in Breast and Prostate Carcinoma. Curr Med Chem 18: 5041–5051.
3. Eckschlager T, Adam V, Hrabeta J, Figova K, Kizek R (2009) Metallothioneins and Cancer. Curr Protein Pept Sci 10: 360–375.
4. Hogstrand C, Kille P, Nicholson RI, Taylor KM (2009) Zinc transporters and cancer: a potential role for ZIP7 as a hub for tyrosine kinase activation. Trends Mol Med 15: 101–111.

5. Plum LM, Rink L, Haase H (2010) The Essential Toxin: Impact of Zinc on Human Health. Int J Environ Res Public Health 7: 1342–1365.
6. Zaichick VY, Sviridova TV, Zaichick SV (1997) Zinc in human prostate gland: Normal, hyperplastic and cancerous. J Radioanal Nucl Chem 217: 157–161.
7. Gurusamy K (2007) Trace element concentration in primary liver cancers - A systematic review. Biol Trace Elem Res 118: 191–206.
8. Catalani S, De Palma G, Mangili A, Apostoli P (2008) Metallic elements in lung tissues: results of a meta-analysis. Acta Biomed 79: 52–63.
9. Silvera SAN, Rohan TE (2007) Trace elements and cancer risk: a review of the epidemiologic evidence. Cancer Causes Control 18: 7–27.
10. Hess SY, Peerson JA, King JC, Brown KH (2007) Use of serum zinc concentration as an indicator of population zinc status. Food Nutr Bull 28: S403–S429.
11. Wells GA, Shea B, O'Connell D, Peterson J, Welch V, et al. (2014) The Newcastle-Ottawa Scale (NOS) for assessing the quality of nonrandomised studies in meta-analyses.
12. Higgins JPT, Thompson SG (2002) Quantifying heterogeneity in a meta-analysis. Stat Med 21: 1539–1558.
13. Littell JH, Corcoran J, Pillai V (2008) Assessing Bias and Variations in Effects. In: Tripodi T, editor. Systematic Reviews and Meta-Analysis: Oxford University Press, USA. pp. 351.
14. Higgins JPT, Green S (2011) Cochrane Handbook for Systematic Reviews of Interventions Version 5.1.0. In: Higgins JPT, Green S, editors: The Cochrane Collaboration.
15. Boz A, Evliyaoglu O, Yildirim M, Erkan N, Karaca B (2005) The value of serum zinc, copper, ceruloplasmin levels in patients with gastrointestinal tract cancers. Turk J Gastroenterol 16: 81–84.
16. Federico A, Iodice P, Federico P, Del Rio A, Mellone MC, et al. (2001) Effects of selenium and zinc supplementation on nutritional status in patients with cancer of digestive tract. Eur J Clin Nutr 55: 293–297.
17. Chen H, Tan C, Wu T (2011) Ensemble Modeling Coupled with Six Element Concentrations in Human Blood for Cancer Diagnosis. Biol Trace Elem Res 143: 143–152.
18. Kok FJ, Van Duijn CM, Hofman A, Van der Voet GB, De Wolff FA, et al. (1988) Serum copper and zinc and the risk of death from cancer and cardiovascular disease. Am J Epidemiol 128: 352–359.
19. Leone N, Courbon D, Ducimetiere P, Zureik M (2006) Zinc, copper, and magnesium and risks for all-cause, cancer, and cardiovascular mortality. Epidemiology 17: 308–314.
20. Zowczak M, Iskra M, Torlinski L, Cofta S (2001) Analysis of serum copper and zinc concentrations in cancer patients. Biol Trace Elem Res 82: 1–8.
21. Gecit I, Kavak S, Demir H, Gunes M, Pirincci N, et al. (2011) Serum Trace Element Levels in Patients with Bladder Cancer. Asian Pac J Cancer Prev 12: 3409–3413.
22. Mazdak H, Yazdekhasti F, Movahedian A, Mirkheshti N, Shafieian M (2010) The comparative study of serum iron, copper, and zinc levels between bladder cancer patients and a control group. Int Urol Nephrol 42: 89–93.
23. Arinola OG, Charles-Davies MA (2008) Micronutrient levels in the plasma of Nigerian females with breast cancer. Afr J Biotechnol 7: 1620–1623.
24. Cavallo F, Gerber M, Marubini E, Richardson S, Barbieri A, et al. (1991) Zinc and copper in breast cancer. A joint study in northern Italy and southern France. Cancer 67: 738–745.
25. Garofalo JA, Ashikari H, Lesser ML, Menendezbotet C, Cunninghamrundles S, et al. (1980) Serum Zinc, Copper, and the Cu-Zn Ratio in Patients with Benign and Malignant Breast-Lesions. Cancer 46: 2682–2685.
26. Gupta SK, Shukla VK, Vaidya MP, Roy SK, Gupta S (1991) Serum trace elements and Cu/Zn ratio in breast cancer patients. J Surg Oncol 46: 178–181.
27. Huang Y-L, Sheu J-Y, Lin T-H (1999) Association between oxidative stress and changes of trace elements in patients with breast cancer. Clin Biochem 32: 131–136.
28. Isbir T, Tamer L, Erkisi M, Kekec Y, Doran F, et al. (1995) Copper, Zinc and Magnesium in Serum and Tissues from Patients with Carcinoma of Breast, Stomach and Colon. Trace Elem Electrolytes 12: 113–115.
29. Kuo HW, Chen SF, Wu CC, Chen DR, Lee JH (2002) Serum and tissue trace elements in patients with breast cancer in Taiwan. Biol Trace Elem Res 89: 1–11.
30. Magalova T, Bella V, Brtkova A, Beno I, Kudlackova M, et al. (1999) Copper, zinc and superoxide dismutase in precancerous, benign diseases and gastric, colorectal and breast cancer. Neoplasma 46: 100–104.
31. Piccinini L, Borella P, Bargellini A, Medici CI, Zoboli A (1996) A case-control study on selenium, zinc, and copper in plasma and hair of subjects affected by breast and lung cancer. Biol Trace Elem Res 51: 23–30.
32. Tinoco-Veras CM, Sousa MSB, da Silva BB, Cozzolino SMF, Pires LV, et al. (2011) Analysis of plasma and erythrocyte zinc levels in premenopausal women with breast cancer. Nutr Hosp 26: 293–297.
33. Yucel I, Arpaci F, Ozet A, Doner B, Karayilanoglu T, et al. (1994) Serum copper and zinc levels and copper/zinc ratio in patients with breast cancer. Biol Trace Elem Res 40: 31–38.
34. Carvalho ML, Magalhaes T, Becker M, von Bohlen A (2007) Trace elements in human cancerous and healthy tissues: A comparative study by EDXRF, TXRF, synchrotron radiation and PIXE. Spectroc Acta Pt B-Atom Spectr 62: 1004–1011.
35. Ng KH, Bradley DA, Looi LM (1997) Elevated trace element concentrations in malignant breast tissues. Br J Radiol 70: 375–382.
36. Raju GJN, Sarita P, Kumar MR, Murty G, Reddy BS, et al. (2006) Trace elemental correlation study in malignant and normal breast tissue by PIXE technique. Nucl Instrum Methods Phys Res Sect B-Beam Interact Mater Atoms 247: 361–367.
37. Margalioth EJ, Schenker JG, Chevion M (1983) Copper and Zinc Levels in Normal and Malignant-Tissues. Cancer 52: 868–872.
38. Singh V, Garg AN (1998) Trace element correlations in the blood of Indian women with breast cancer. Biol Trace Elem Res 64: 237–245.
39. Ebrahim AM, Eltayeb MAH, Shaat MK, Mohmed MA, Eltayeb EA, et al. (2007) Study of selected trace elements in cancerous and non-cancerous human breast tissues from Sudanese subjects using instrumental neutron activation analysis. Sci Total Environ 383: 52–58.
40. Silva MP, Tomal A, Perez CA, Ribeiro-Silva A, Poletti ME (2009) Determination of Ca, Fe, Cu and Zn and their correlations in breast cancer and normal adjacent tissues. X-Ray Spectrom 38: 103–111.
41. Geraki K, Farquharson MJ, Bradley DA (2002) Concentrations of Fe, Cu and Zn in breast tissue: a synchrotron XRF study. Phys Med Biol 47: 2327–2339.
42. Farquharson MJ, Al-Ebraheem A, Geraki K, Leek R, Harris AL (2009) Zinc presence in invasive ductal carcinoma of the breast and its correlation with oestrogen receptor status. Phys Med Biol 54: 4213–4223.
43. Stawarz R, Formicki G, Zakrzewski M, Rys J, Rozmus M (2009) Distribution of Heavy Metals and Trace Elements in Human Breast Cancer Tissues and in Adjacent Normal Tissues of Women in Poland. Fresen Environ Bull 18: 182–188.
44. Kubala-Kukus A, Banas D, Braziewicz J, Gozdz S, Majewska U, et al. (2007) Analysis of elemental concentration censored distributions in breast malignant and breast benign neoplasm tissues. Spectroc Acta Pt B-Atom Spectr 62: 695–701.
45. Ionescu JG, Novotny J, Stejskal V, Latsch A, Blaurock-Busch E, et al. (2006) Increased levels of transition metals in breast cancer tissue. Neuroendocrinol Lett 27: 36–39.
46. Majewska U, Banas D, Braziewicz J, Gozdz S, Kubala-Kukus A, et al. (2007) Trace element concentration distributions in breast, lung and colon tissues. Phys Med Biol 52: 3895–3911.
47. Cui Y, Vogt S, Olson N, Glass AG, Rohan TE (2007) Levels of zinc, selenium, calcium, and iron in benign breast tissue and risk of subsequent breast cancer. Cancer Epidemiol Biomarkers Prev 16: 1682–1685.
48. Han CZ, Jing JX, Zhao ZW, Guo JG, Zheng SM, et al. (2003) Serum and tissue levels of six trace elements and copper/zinc ratio in patients with cervical cancer and uterine myoma. Biol Trace Elem Res 94: 113–122.
49. Shobeiri MJ, Tabrizi AD, Atashkhoei S, Sayyah-Melli M, Ouladsahebmadarek E, et al. (2011) Serum levels of Copper, Zinc and Copper/Zinc Ratio in Patients with Ovarian Cancer. Pak J Med Sci 27: 561–565.
50. Nasiadek M, Krawczyk T, Sapota A (2005) Tissue levels of cadmium and trace elements in patients with myoma and uterine cancer. Hum Exp Toxicol 24: 623–630.
51. Zhong HH, Tan MJ, Fu YL, Huang JQ, Tang ZF (1999) Determination of trace elements in tissue of human uterine cancer by instrumental neutron activation analysis. Biol Trace Elem Res 71–2: 569–574.
52. Lin HJ, Chan WC, Fong YY, Newberne PM (1977) Zinc Levels in Serum, Hair and Tumors from Patients with Esophageal Cancer. Nutr Rep Int 15: 635–643.
53. Goyal M, Kalwar A, Vyas R, Bhati A (2006) A study of serum zinc, selenium and copper levels in carcinoma of esophagus patients. Ind J Clin Biochem 21: 208–210.
54. Mellow MH, Layne EA, Lipman TO, Kaushik M, Hostetler C, et al. (1983) Plasma zinc and vitamin a in human squamous carcinoma of the esophagus. Cancer 51: 1615–1620.
55. Salehifar E, Khorasani G, Shokrzade M, Asadi M, Shabankhani B, et al. (2008) Comparison of plasma levels of zinc and lead in esophageal cancer patients with normal subjects. Trace Elem Electrolytes 25: 165–168.
56. Abnet CC, Lai B, Qiao YL, Vogt S, Luo XM, et al. (2005) Zinc concentration in esophageal biopsy specimens measured by x-ray fluorescence and esophageal cancer risk. J Natl Cancer Inst 97: 301–306.
57. Sun ZG, Song GM, Zhang M, Wang Z (2011) Clinical study on zinc, copper and manganese levels in patients with esophageal squamous cell cancer. Trace Elem Electrolytes 28: 116–120.
58. Kabuto M, Imai H, Yonezawa C, Neriishi K, Akiba S, et al. (1994) Prediagnostic serum selenium and zinc levels and subsequent risk of lung and stomach cancer in Japan. Cancer Epidemiol Biomarkers Prev 3: 465–469.
59. Narang APS, Wani NA (1991) Levels of Copper and Zinc in Serum and Tissues of Patients with Gastric-Carcinoma. Trace Elem Med 8: 15–18.
60. Yaman M, Kaya G, Yekeler H (2007) Distribution of trace metal concentrations in paired cancerous and non-cancerous human stomach tissues. World J Gastroenterol 13: 612–618.
61. Milde D, Machacek J, Stuzka V (2007) Evaluation of colon cancer elements contents in serum using statistical methods. Chem Pap 61: 348–352.
62. Gupta SK, Shukla VK, Vaidya MP, Roy SK, Gupta S (1993) Serum and tissue trace elements in colorectal cancer. J Surg Oncol 52: 172–175.
63. Zowczak-Drabarczyk M, Torlinska T, Iskra M, Mielcarz G, Matylla G, et al. (2004) Serum zinc concentration in patients with colorectal cancer. Trace Elem Electrolytes 21: 236–239.
64. Kim ES, Lim CS, Chun HJ, Keum B, Seo YS, et al. (2012) Detection of Cu(I) and Zn(II) ions in colon tissues by multi-photon microscopy: novel marker of antioxidant status of colon neoplasm. J Clin Pathol 65: 882–887.

65. Hornik P, Milde D, Trenz Z, Vyslouzil K, Stuzka V (2006) Colon tissue concentrations of copper, iron, selenium, and zinc in colorectal carcinoma patients. Chem Pap-Chem Zvesti 60: 297–301.
66. Kucharzewski M, Braziewicz J, Majewska U, Gozdz S (2003) Selenium, copper, and zinc concentrations in intestinal cancer tissue and in colon and rectum polyps. Biol Trace Elem Res 92: 1–10.
67. Shukla VK, Adukia TK, Singh SP, Mishra CP, Mishra RN (2003) Micronutrients, antioxidants, and carcinoma of the gallbladder. J Surg Oncol 84: 31–35.
68. Gupta SK, Singh SP, Shukla VK (2005) Copper, zinc, and Cu/Zn ratio in carcinoma of the gallbladder. J Surg Oncol 91: 204–208.
69. Rautray TR, Vijayan V, Sudarshan M, Panigrahi S (2009) Analysis of blood and tissue in gallbladder cancer. Nucl Instrum Methods Phys Res Sect B-Beam Interact Mater Atoms 267: 2878–2883.
70. Nagasue N, Kohno H, Chang YC, Nakamura T (1989) Iron, Copper and Zinc Levels in Serum and Cirrhotic Liver of Patients with and without Hepatocellular-Carcinoma. Oncology 46: 293–296.
71. Poo JL, Rosas-Romero R, Montemayor AC, Isoard F, Uribe M (2003) Diagnostic value of the copper/zinc ratio in hepatocellular carcinoma: a case control study. J Gastroenterol 38: 45–51.
72. Kolachi NF, Kazi TG, Afridi HI, Kazi NG, Khan S (2012) Investigation of essential trace and toxic elements in biological samples (blood, serum and scalp hair) of liver cirrhotic/cancer female patients before and after mineral supplementation. Clin Nutr 31: 967–973.
73. Ebara M, Fukuda H, Hatano R, Yoshikawa M, Sugiura N, et al. (2003) Metal contents in the liver of patients with chronic liver disease caused by hepatitis C virus - Reference to hepatocellular carcinoma. Oncology 65: 323–330.
74. Kew MC, Mallett RC (1974) Hepatic zinc concentrations in primary cancer of the liver. Br J Cancer 29: 80–83.
75. Liaw KY, Lee PH, Wu FC, Tsai JS, LinShiau SY (1997) Zinc, copper, and superoxide dismutase in hepatocellular carcinoma. Am J Gastroenterol 92: 2260–2263.
76. Maeda T, Shimada M, Harimoto N, Tsujta E, Maehara S, et al. (2005) Role of tissue trace elements in liver cancers and non-cancerous liver parenchyma. Hepato-Gastroenterol 52: 187–190.
77. Okuno T, Shimamura Y, Mizuno M, Miyata S, Miyake T, et al. (1988) Trace-Elements in Hepatoma Tissue. Trace Elem Med 5: 130–136.
78. Tashiro H, Kawamoto T, Okubo T, Koide O (2003) Variation in the distribution of trace elements in hepatoma. Biol Trace Elem Res 95: 49–63.
79. Darago A, Sapota A, Matych J, Nasiadek M, Skezypinska-Gawrysiak M, et al. (2011) The correlation between zinc and insulin-like growth factor 1 (IGF-1), its binding protein (IGFBP-3) and prostate-specific antigen (PSA) in prostate cancer. Clin Chem Lab Med 49: 1699–1705.
80. Goel T, Sankhwar SN (2006) Comparative study of zinc levels in benign and malignant lesions of the prostate. Scand J Urol Nephrol 40: 108–112.
81. Kiziler AR, Aydemir B, Guzel S, Alici B, Ataus S, et al. (2010) May the level and ratio changes of trace elements be utilized in identification of disease progression and grade in prostatic cancer? Trace Elem Electrolytes 27: 65–72.
82. Meyer F, Galan P, Douville P, Bairati I, Kegle P, et al. (2005) Antioxidant vitamin and mineral supplementation and prostate cancer prevention in the SU.VI.MAX trial. Int J Cancer 116: 182–186.
83. Whelan P, Walker BE, Kelleher J (1983) Zinc, Vitamin A and Prostatic Cancer. Br J Urol 55: 525–528.
84. Li XM, Zhang L, Li J, Li Y, Wang HL, et al. (2005) Measurement of serum zinc improves prostate cancer detection efficiency in patients with PSA levels between 4 ng/mL and 10 ng/mL. Asian J Androl 7: 323–328.
85. Park SY, Kolonel L (2009) Serum Zinc and Prostate Cancer Risk in the Multiethnic Cohort study. Epidemiology 20: S131–S131.
86. Brys M, Nawrocka AD, Miekos E, Zydek C, Foksinski M, et al. (1997) Zinc and cadmium analysis in human prostate neoplasms. Biol Trace Elem Res 59: 145–152.
87. Dunchik VN, Zherbin EA, Zaichick VY, Leonov AI, Sviridova TV (1980) Method for differential diagnostics of malignant and benign prostate tumors. Discoveries, Inventions, Commercial Models, Trade Marks 35: 1–13.
88. Feustel A, Wennrich R, Steiniger D, Klauss P (1982) Zinc and cadmium concentration in prostatic carcinoma of different histological grading in comparison to normal prostate tissue and adenofibromyomatosis (BPH). Urol Res 10: 301–303.
89. Guntupalli JNR, Padala S, Gummuluri A, Muktineni RK, Byreddy SR, et al. (2007) Trace elemental analysis of normal, benign hypertrophic and cancerous tissues of the prostate gland using the particle-induced X-ray emission technique. Eur J Cancer Prev 16: 108–115.
90. Habib FK, Hammond GL, Lee IR, Dawson JB, Mason MK, et al. (1976) Metal-androgen interrelationships in carcinoma and hyperplasia of the human prostate. J Endocrinol 71: 133–141.
91. Marczynska A, Kulpa J, Lenko J (1983) The concentration of zinc in relation to fundamental elements in the diseased human prostate. Int Urol Nephrol 15: 257–265.
92. Mawson CA, Fischer MI (1952) The occurrence of zinc in the human prostate gland. Can J Med Sci 30: 336–339.
93. Sapota A, Darago A, Taczalski J, Kilanowicz A (2009) Disturbed homeostasis of zinc and other essential elements in the prostate gland dependent on the character of pathological lesions. Biometals 22: 1041–1049.
94. Schrodt GR, Hall T, Whitmore WF (1964) The concentration of zinc in diseased human prostate glands. Cancer 17: 1555–1566.
95. Zaichick S, Zaichick V (2012) Trace elements of normal, benign hypertrophic and cancerous tissues of the human prostate gland investigated by neutron activation analysis. Appl Radiat Isot 70: 81–87.
96. Hienzsch E, Schneider H, Anke M (1970) Vergleichende Untersuchungen zurn Mengenund Spurenelernentgehalt der normalen Prostata, des Prostataadenoms und des Prostatakarzinorns. Zsehr Urol 63: 543–546.
97. Hoare R, Delory GE, Penner DW (1956) Zinc and acid phosphatase in the human prostate. Cancer 9: 721–726.
98. Garofalo JA, Erlandson E, Strong EW, Lesser M, Gerold F, et al. (1980) Serum zinc, serum copper, and the Cu/Zn ratio in patients with epidermoid cancers of the head and neck. J Surg Oncol 15: 381–386.
99. Jayadeep A, Pillai KR, Kannan S, Nalinakumari KR, Mathew B, et al. (1997) Serum levels of copper, zinc, iron and ceruloplasmin in oral leukoplakia and squamous cell carcinoma. J Exp Clin Cancer Res 16: 295–300.
100. Taysi S, Akcay F, Uslu C, Dogru Y, Gulcin I (2003) Trace elements and some extracellular antioxidant protein levels in serum of patients with laryngeal cancer. Biol Trace Elem Res 91: 11–18.
101. Akcil E, Caylakli F, Akiner M, Kocak M (2004) Trace element concentrations and superoxide dismutase and catalase activities in benign and malignant larynx tumors. Biol Trace Elem Res 101: 193–201.
102. Drozdz M, Gierek T, Jendryczko A, Piekarska J, Pilch J, et al. (1989) Zinc, Vitamin-a and Vitamin-E, and Retinol-Binding Protein in Sera of Patients with Cancer of the Larynx. Neoplasma 36: 357–362.
103. Durak I, Kavutcu M, Canbolat O, Isik AU, Akyol O (1994) Concentrations of Some Major and Minor Elements in Larynx Tissues with and without Cancer. Biometals 7: 45–48.
104. Yigitbasi OG, Haghighi N, Dogan P, Saraymen R, Balkani S, et al. (1998) Differences of tissue Cu and Zn levels in larynx squamous cell carcinomas. Trace Elem Electrolytes 15: 90–93.
105. Al-Sayer H, Mathew TC, Asfar S, Khourshed M, Al-Bader A, et al. (2004) Serum changes in trace elements during thyroid cancers. Mol Cell Biochem 260: 1–5.
106. Przybylik-Mazurek E, Zagrodzki P, Kuzniarz-Rymarz S, Hubalewska-Dydejczyk A (2011) Thyroid Disorders-Assessments of Trace Elements, Clinical, and Laboratory Parameters. Biol Trace Elem Res 141: 65–75.
107. Leung PL, Li XL (1996) Multielement analysis in serum of thyroid cancer patients before and after a surgical operation. Biol Trace Elem Res 51: 259–266.
108. Zaichick VY, Tsyb AF, Vtyurin BM (1995) Trace elements and thyroid cancer. Analyst 120: 817–821.
109. Kucharzewski M, Braziewicz J, Majewska U, Gozdz S (2003) Copper, zinc, and selenium in whole blood and thyroid tissue of people. with various thyroid diseases. Biol Trace Elem Res 93: 9–18.
110. Homma S, Sasaki A, Nakai I, Sagai M, Koiso K, et al. (1993) Distribution of Copper, Selenium, and Zinc in Human Kidney Tumors by Nondestructive Synchrotron-Radiation X-Ray-Fluorescence Imaging. J Trace Elem Exp Med 6: 163–170.
111. Dobrowolski Z, Drewniak T, Kwiatek W, Jakubik P (2002) Trace elements distribution in renal cell carcinoma depending on stage of disease. Eur Urol 42: 475–480.
112. Kwiatek WM, Drewniak T, Lekka M, Wajdowicz A (1996) Investigation of trace elements in cancer kidney tissues by SRIXE and PIXE. Nucl Instrum Methods Phys Res Sect B-Beam Interact Mater Atoms 109: 284–288.
113. Atukorala S, Basu TK, Dickerson JW, Donaldson D, Sakula A (1979) Vitamin A, zinc and lung cancer. Br J Cancer 40: 927–931.
114. Klarod K, Hongsprabhas P, Khampitak T, Wirasorn K, Kiertiburanakul S, et al. (2011) Serum antioxidant levels and nutritional status in early and advanced stage lung cancer patients. Nutrition 27: 1156–1160.
115. Diez M, Arroyo M, Cerdan FJ, Munoz M, Martin MA, et al. (1989) Serum and tissue trace metal levels in lung cancer. Oncology 46: 230–234.
116. Oyama T, Matsuno K, Kawamoto T, Mitsudomi T, Shirakusa T, et al. (1994) Efficiency of serum copper/zinc ratio for differential diagnosis of patients with and without lung cancer. Biol Trace Elem Res 42: 115–127.
117. Beeley JM, Darke CS, Owen GCR (1974) Serum zinc, bronchiectasis, and bronchial carcinoma. Thorax 29: 21–25.
118. Cildag O, Altinisik M, Kozaci D, Karadag F, Kiter G, et al. (2004) Alterations in trace elements and oxidative stress in lung cancer. Trace Elem Electrolytes 21: 23–27.
119. Kune GA, Kune S, Watson LF, Pierce R, Field B, et al. (1989) Serum levels of beta-carotene, vitamin A, and zinc in male lung cancer cases and controls. Nutr Cancer 12: 169–176.
120. Sadat AFMN, Hossain MI, Hossain MK, Reza MS, Nahar Z, et al. (2008) Serum trace elements and immunoglobulin profile in lung cancer patients. J Appl Res 8: 24–33.
121. Jin Y, Zhang C, Xu H, Xue S, Wang Y, et al. (2010) Combined effects of serum trace metals and polymorphisms of CYP1A1 or GSTM1 on non-small cell lung cancer: A hospital based case-control study in China. Cancer Epidemiol 35: 182–187.
122. Sattar N, Scott HR, McMillan DC, Talwar D, O'Reilly DS, et al. (1997) Acute-phase reactants and plasma trace element concentrations in non-small cell lung cancer patients and controls. Nutr Cancer 28: 308–312.

123. Adachi S, Takemoto K, Ohshima S, Shimizu Y, Takahama M (1991) Metal concentrations in lung tissue of subjects suffering from lung cancer. Int Arch Occup Environ Health 63: 193–197.
124. Kubala-Kukus A, Braziewicz J, Banas D, Majewska U, Gozdz S, et al. (1999) Trace element load in cancer and normal lung tissue. Nucl Instrum Methods Phys Res Sect B-Beam Interact Mater Atoms 150: 193–199.
125. Zhang LL, Lv JG, Sun SK (2012) Elements in Lung Tissues of Patients from a High Lung Cancer Incidence Area of China. Biol Trace Elem Res 148: 7–10.
126. Cousins RJ, Liuzzi JP, Lichten LA (2006) Mammalian zinc transport, trafficking, and signals. J Biol Chem 281: 24085–24089.
127. Costello LC, Franklin RB (2011) Zinc is decreased in prostate cancer: an established relationship of prostate cancer! J Biol Inorg Chem 16: 3–8.

OPEN ACCESS Freely available online

PLOS ONE

Metallothionein – Immunohistochemical Cancer Biomarker: A Meta-Analysis

Jaromir Gumulec[1,2], Martina Raudenska[1,2], Vojtech Adam[2,3], Rene Kizek[2,3], Michal Masarik[1,2]*

1 Department of Pathological Physiology, Masaryk University, Brno, Czech Republic, **2** Central European Institute of Technology, Brno University of Technology, Brno, Czech Republic, **3** Department of Chemistry and Biochemistry, Mendel University in Brno, Brno, Czech Republic

Abstract

Metallothionein (MT) has been extensively investigated as a molecular marker of various types of cancer. In spite of the fact that numerous reviews have been published in this field, no meta-analytical approach has been performed. Therefore, results of to-date immunohistochemistry-based studies were summarized using meta-analysis in this review. Web of science, PubMed, Embase and CENTRAL databases were searched (up to April 30, 2013) and the eligibility of individual studies and heterogeneity among the studies was assessed. Random and fixed effects model meta-analysis was employed depending on the heterogeneity, and publication bias was evaluated using funnel plots and Egger's tests. A total of 77 studies were included with 8,015 tissue samples (4,631 cases and 3,384 controls). A significantly positive association between MT staining and tumors (vs. healthy tissues) was observed in head and neck (odds ratio, OR 9.95; 95% CI 5.82–17.03) and ovarian tumors (OR 7.83; 1.09–56.29), and a negative association was ascertained in liver tumors (OR 0.10; 0.03–0.30). No significant associations were identified in breast, colorectal, prostate, thyroid, stomach, bladder, kidney, gallbladder, and uterine cancers and in melanoma. While no associations were identified between MT and tumor staging, a positive association was identified with the tumor grade (OR 1.58; 1.08–2.30). In particular, strong associations were observed in breast, ovarian, uterine and prostate cancers. Borderline significant association of metastatic status and MT staining were determined (OR 1.59; 1.03–2.46), particularly in esophageal cancer. Additionally, a significant association between the patient prognosis and MT staining was also demonstrated (hazard ratio 2.04; 1.47–2.81). However, a high degree of inconsistence was observed in several tumor types, including colorectal, kidney and prostate cancer. Despite the ambiguity in some tumor types, conclusive results are provided in the tumors of head and neck, ovary and liver and in relation to the tumor grade and patient survival.

Citation: Gumulec J, Raudenska M, Adam V, Kizek R, Masarik M (2014) Metallothionein – Immunohistochemical Cancer Biomarker: A Meta-Analysis. PLoS ONE 9(1): e85346. doi:10.1371/journal.pone.0085346

Editor: Renato Franco, Istituto dei tumori Fondazione Pascale, Italy

Received August 23, 2013; **Accepted** December 4, 2013; **Published** January 8, 2014

Funding: Financial support from Central European Institute of Technology (CEITEC CZ.1.05/1.1.00/02.0068) and Internal Grant Agency of Ministry of Health of the Czech Republic (IGA MH NT14337-3/2013) is acknowledged. The funders had no role in study design, data collection and analysis, decision to publish, or preparation of the manuscript.

Competing Interests: The authors have declared that no competing interests exist.

* E-mail: masarik@med.muni.cz

Introduction

Metallothioneins (MTs) are cysteine-rich low-molecular-mass intracellular proteins occurring in a wide variety of eukaryotes and constituting the major fraction of intracellular protein thiols [1]. The MT gene family consists of four subfamilies designated as MT-1 through to MT-4 in mammals. MTs are involved in many physiological and pathophysiological processes such as intracellular storage, transport and metabolism of metal ions, whereas they regulate essential trace metal homeostasis and play a protective role in heavy metal detoxification reactions [2,3]. They can protect cells against UV/ionic radiation [4,5] as well as cytotoxic alkylating agents including chemotherapeutics [6–9], modulate oxygen free radicals and nitric oxide, and inhibit apoptosis [10–12].

MTs are usually expressed at low levels, but they are inducible [13–16]. The synthesis of MT was shown to be increased during oxidative stress [17,18] to protect the cells against cytotoxicity [19,20], radiation and DNA damage [21–23]. Many studies have shown an increased expression of MT in human tumors of breast, colon, kidney, liver, lung, nasopharynx, ovary, prostate, salivary gland, testes, thyroid and urinary bladder [14]. MT expression in tumor tissues is mainly correlated with the proliferative capacity of tumor cells [24]. However, there are few exceptional cases, e.g. down-regulation of MT in hepatocellular carcinoma [25]. Nevertheless, these case-control and cohort studies give us inconsistent results regarding the association of MTs and tumor histology, staging, grading, prognosis, and survival. Although there is a number of good systematic reviews [2,3,11,13,14,26–28,29,] with particular interest in breast tumors [30,31], a meta-analytic approach has not been employed yet. Thus, the aim of this study is to evaluate the associations between immunohistochemical MT staining and clinicopathological conditions, tumor type, stage, grade, prognosis, and survival using the meta-analysis.

Materials and Methods

Literature search

Search was performed in Web of science (Science citation index expanded 1945 to April 2013), PubMed (Medline 1968 to April 2013) search engines and in bibliographies of cited references. The following keywords were used: histo* OR immunohisto* OR IHC;

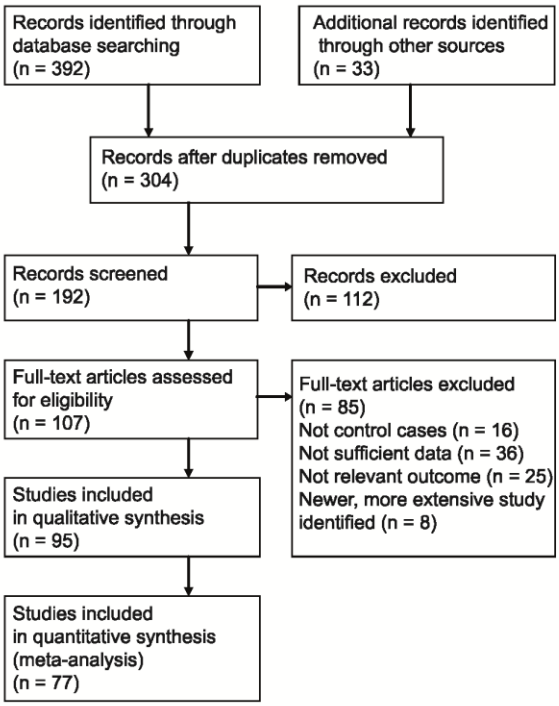

Figure 1. Flow chart showing the number of citations retrieved by database searching.
doi:10.1371/journal.pone.0085346.g001

metallothionein; cancer OR tumor OR tumour OR neoplas*; melanoma. The date of publishing and language were not restricting

Selection criteria

Case-control and cohort studies regarding the associations between malignant neoplasms and metallothionein immunohistochemical staining were searched. Full text articles were included only. Following information were extracted from the studies: (1) MT level in malignant tumors and healthy/benign tissues, (2) MT level regarding the tumor stage, (3) tumor grade, (4) age and sex of patients, and (5) MT level and survival. The following data formats were accepted: (1) means, standard deviation and sample size, (2) sample size, means, P values and type of statistical test type (one- or two-tailed), and (3) sample size, P values, statistical test type and effect direction for continuous data and (1) odds ratios and 95% confidence intervals (CI), (2) 2×2 tables, and (3) Chi-squared and effect directions for dichotomous data. Continuous and dichotomous outcomes were combined. Cox proportional hazard model was used for survival meta-analysis. Univariate model of overall survival was used, hazard ratio and 95% CI was extracted from the studies. Studies with the sample size <6 participants and without histological verification of tumor were not included. If similar data was found in more than one study, studies with more extensive data set were used for the analysis. The eligibility of the studies for meta-analysis was evaluated by two authors (J.G. and M.R.).

Coding of categorical variables

Since different scales regarding MT IHC staining were used across the studies, the following rules were applied: (1) when MT staining was encoded as positive/negative, no change was applied; (2) when percentage data was included, staining >10% was considered positive and vice versa; (3) when no percentage data was identified and data were encoded by 0–2 or 0–3 points, 0–1 was considered negative. Because >2 categories are used in grading/staging scales, Grades 2–3 were grouped and compared with Grade 1; stages 3–4 and 1–2 were grouped in a similar way.

Statistical analysis

Odds ratios with 95% intervals were used as point estimates except for the survival analysis. For the survival analysis, hazard ratios with 95% confidence intervals were used. To assess heterogeneity across the studies, Higgins I^2, describing the percentage of variability in point estimates was calculated [32]. The random effects model meta-analysis using the DerSimonian and Laird method was employed when a distinct heterogeneity was observed [33] (I^2 more than 50.0%), otherwise, a fixed model was used. The model selection is based on a study by Borenstein et al. [34]. In that study, key assumptions of each model and mathematical bases are explained, and differences between the models are outlined; therefore, they will not be discussed in this paper. Subgroups were combined using the fixed effects. Within-subgroup estimates of tau-squared were not pooled. When the number of studies within the groups exceeded 4, the publication bias was evaluated using funnel plots and two-sided Egger's tests. Funnel plots of subgroups whose Egger's test $p<0.05$, are asymmetric. Comprehensive Meta-analysis Version 2 software (Biostat, Englewood, NJ) was used for the analysis.

Results and Discussion

Identification and characteristics of relevant studies

The acquisition process of studies is depicted in Fig. 1. A total of 77 articles were included in the final analysis after eliminating articles unsatisfying the selection criteria and duplicates. The set of 77 studies includes 8,015 tissue samples (4,631 cases and 3,384 controls). On average 95.2 patients were included per study, 1270 cases and controls were included in the largest study [35] and 12 cases and controls were included in the smallest study [36]. The date of publication ranged from 1987–2013 with the median of year 2002. In total, 51 North American and European studies, 20 Asian, 2 South American studies and one African study were included.

MT isoform characteristics

Monoclonal antibody clone E9 was used in a majority of studies; this antibody shows affinity for both MT-1 and 2 isoforms. Anti-MT3 antibody was only used by Sens et al. in bladder cancer [37]. Strong positive associations of MT3 staining with the tumor grade were determined. Therefore, with the exception of Sens et al., all following analyzes concern the MT-1 and 2 isoforms.

MT and patient characteristics

Patient age. First, the association of MT immunoreactivity and patient's age was analyzed. No significant association was determined using the fixed effects model meta-analysis (odds ratio, OR = 1.07; 95% confidence interval, CI, 0.48 to 0.628). No publication bias was identified (Egger's 2-tailed test p = 0.12). In total, 9 studies with 1,069 patients were included [25,38–45]. The following tumors were included: bladder, breast, colorectal, hepatocellular, head and neck, and stomach.

This is a generally expected finding, no correlation of MT immunoreactivity and age was already reported in breast cancer

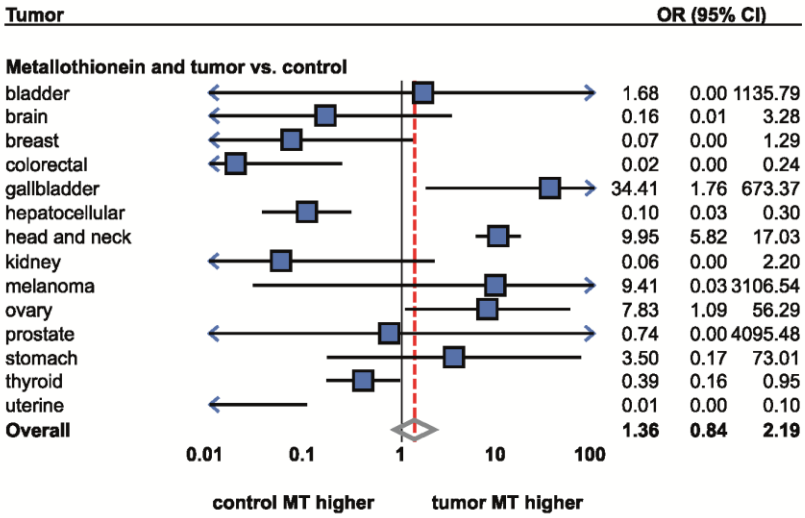

Figure 2. Forrest plot showing associations between metallothionein staining and tumors (tumors versus healthy controls). The result of meta-analysis for particular tumor types displayed instead of individual studies. For more detailed results see Table 1 and 2. Sorted alphabetically by tumor types. Forrest plot displayed as odds ratio and 95% confidence intervals. Red dashed line indicates the result for all tumor types together. OR, odds ratio; CI, confidence interval.
doi:10.1371/journal.pone.0085346.g002

patients [46-49]. No such age-dependent association is beneficial from the perspective of potential diagnostic use.

Patient gender. Consequently, the role of gender was analyzed. No publication bias was observed (p = 0.61) and no significant trend was detected using the fixed effect meta-analysis (OR = 0.99; 95% CI, 0.74 to 1.34). The analysis was performed on 9 studies reporting gender (944 patients). The following tumor types were included: bladder [44], colorectal [38,39,50], head and neck [41,51], hepatocellular [25], and stomach [43]. Similarly as in the patients' age, no significance was expected. Such gender-independence is advantageous for appropriate tumor biomarker.

Metallothionein as cancer biomarker

Consequently, the association of MT staining and tumor presence was analyzed. A total number of 31 studies were included (2,454 cases and healthy individuals). A high degree of heterogeneity was identified (Higgins $I^2 = 89.6\%$) when the meta-analysis was performed on all tumor types together (Fig. 2, Table 1). Therefore, no significant association between MT staining and tumor presence was identified using the random effects model (OR = 1.19; 95% CI, 0.47 to 3.01). No publication bias was identified. The high degree of heterogeneity between the studies calls for explanation. Therefore, a subgroup analysis by tumor types was performed.

Table 1. Association of MT staining and clinicopatological factors. Tumor type not taken into account.

Factor	Number of studies	Number of participants	OR/HR* (95% CI)	Heterogeneity		Publication bias	Model
				P-value	I^2 (%)	P-value	
Age	9	1069	1.07 (0.82–1.39)	0.679	0.00	0.117	Fixed effects
Gender	9	944	0.99 (0.74–1.34)	0.393	5.08	0.611	Fixed effects
Tumor vs. control	31	2454	1.19 (0.47–3.01)	0.000	89.58	0.236	Random effects
Tumor stage	19	1237	1.15 (0.74–1.77)	0.000	60.83	0.987	Random effects
Tumor size	6	1962	1.37 (0.45–4.13)	0.000	90.88	0.194	Random effects
Tumor grade	33	2504	1.58 (1.08–2.30)	0.000	66.57	0.886	Random effects
Metastases, nodal + distant	21	1987	1.59 (1.03–2.46)	0.000	71.68	0.039	Random effects
Metastases, distant	6	741	1.56 (0.56–4.37)	0.014	64.82	0.075	Random effects
Metastases, nodal	15	1246	1.62 (0.98–2.68)	0.000	72.92	0.201	Random effects
Overall survival	10	2041	2.04 (1.47–2.81)	0.000	97.69	0.572	Random effects

Heterogeneity of studies analyzed using Cochran's Q-test (p-value displayed) and using I^2. Egger's two-tailed test used for publication bias analysis (p-value displayed). * effect measure is odds ratio, OR, except for survival analysis using hazard ratio, HR. CI, confidence interval
doi:10.1371/journal.pone.0085346.t001

Head and neck cancer. Head and neck tumors were analyzed most extensively, five studies were identified (Table 2). Tumors in the following locations were included: oral cavity [41], tongue [52], pharynx [53], and larynx [54,55]. Except for Sundelin et al., all studies showed a significant increase of MT levels in tumorous tissues (OR = 9.95; 95% CI, 5.82 to 17.03). The fixed effects model meta-analysis was used due to low heterogeneity, $I^2 = 34.5$. This is in agreement with our study based on voltammetric MT detection [56].

Ovarian cancer. A total of four studies were identified [57–60]. All studies except for Tan et al. reported a significant increase [59]. Using the random effects meta-analysis, significantly higher MT staining was identified in tumors as compared with healthy tissues (OR = 7.83; 95% CI, 1.09 to 56.30). These results are in agreement with Murphy et al. using Hg-binding assay and with Germain et al. [61,62].

Thyroid tumors. Three studies were identified [63–65]. The following histological types were analyzed: papillary, follicular and medullar. When the histological type was not considered as a unit of analysis, non-significant differences were determined when compared with non-malignant tissues by the random effects model meta-analysis.

The subgroup meta-analysis by histological types revealed the sources of heterogeneous results; significantly higher MT levels were determined in follicular cancer (OR = 2.27; 95% CI, 1.11 to 4.62) using the fixed effects, no change in papillary cancer and a significant decrease in medullar cancer (OR = 0.10; 95% CI, 0.03 to 0.39). However, medullar cancer was only dealt with in one study [64]. Apart from IHC technique, contradictory results were demonstrated by mRNA expression analysis, decreased MT expression was demonstrated in papillary cancer and no expression change was demonstrated in follicular cancer [66].

Prostate cancer. No significant associations between MT staining and tumor presence were determined using the random effects model. Results observed in this tumor were contradictory. While one study showed significantly lower MT in the tumorous tissue [67], the other identified a significantly increased MT level [68]. The study by Wei et al., however, used benign prostatic hyperplasia as a control instead of healthy tissue [67].

While the alteration of zinc-metallothionein metabolism is an early sign of prostate cancer progression [69], the benign tissue is not an adequate biological sample for such analyzes. In addition, a study based on radioimmunoanalysis revealed a non-significantly decreased MT level in the tumorous tissue [70]. Although prostate cancer is unique regarding the zinc and MT metabolism [71,72], no conclusive findings were provided by this meta-analysis and more studies are therefore needed.

Hepatocellular cancer. Three studies were identified. Although lower MT levels in the tumorous tissue were reported in all studies [73–75], only Lu et al. reported a significant decrease [75]. Despite this fact, the fixed model analysis revealed significantly lower MT levels (OR = 0.10; 95% CI, 0.04 to 0.30). Nevertheless, Lu et al. used specifically the MT1F isoform antibody instead of nonselective MT1-2, which was used by a majority of study groups.

The decreased MT level in the hepatocellular tumor is a well-established finding. Apart from immunohistochemistry, decreased expression of MT1F [75], MT1G [76,77] and MT1X [25] was determined. ELISA-based detection also showed a decrease [78]. No change in MT levels was determined in one HPLC-based study [79]

Stomach cancer. Contradictory results were evident in three identified studies. While two research groups reported increased levels in tumorous tissues [80,81], the study by Tuccari et al. demonstrated a significant increase in MT levels [43]. While all groups used the E9 antibody clone and included both early and advanced tumors, these contradictory results call for a further explanation by another study. However, contradictory results were shown using other approaches. Apart from IHC analyses, inconclusive results are provided also in gene expression- and radioimmunoanalysis-based methods. Elevation of MT1, 2, and 3 mRNA was determined in an RT-PCR-based study [80] and decrease of MT1 and 2 protein was determined in a radioimmunoanalysis-based study [82].

Bladder cancer. Two studies regarding bladder cancer were identified [83,84]. Using the random effects model, no significant difference was identified. Contradictory results of studies were observed, while a positive association was demonstrated by Zhou et al. and a negative trend was reported by Saika et al. This contradiction may perhaps be explained by the use of benign tissues as controls instead of healthy individuals by Zhou et al. In addition to MT1 and 2 isoforms, Sens et al. demonstrated MT3 to be significantly up-regulated in tumorous tissues, and suggested its use as a potential biomarker for bladder cancer [37].

Kidney cancer. Two studies were identified [83,85]. Although both of them show a decrease, the level of significance is achieved in one study only [85]. As a result, no significance is observed using the random effects model meta-analysis. While both IHC studies used the E9 antibody clone, differential affinity to MT-1 and 2 is not expected. Additionally to IHC determination, down-regulated MT1A, 1F, 1H, and 1G and up-regulated MT2A expression were observed also in other studies [14,86,87]. On a protein level, decreased MT levels were determined in the HPLC-based study [88].

Melanoma. MT levels in melanoma tissues were analyzed in two studies [89,90]. Of those, a significant increase is presented only by Zelger et al. [90] and so a non-significant change in MT levels is observed using the random effects model.

Other tumor types. As compared with the previous chapter, only one study per tumor type was identified for several tumor types. Therefore, no meta-analytical approach was used. This applied to the following tumor types: breast, colon and rectum, gallbladder and uterine corpus.

Compared to non-malignant tissues, significantly higher MT staining was identified in gallbladder cancer [91], a significant decrease in colorectal [92] and cervical [93] tumors and no associations were observed in ductal breast tumors [94] and glioblastomas [95]. Immunohistochemical-based studies of other tumors were not identified.

While El Sharkarvy described non-significant changes in breast cancer tissues, other studies regarding breast cancer described intensive staining in the ductal type, while small or no staining was observed in lobular and papillary cancer [14,46,96]. There are number of reviews regarding MT expression in tumorous tissues. Pedersen, for instance, points to the issue of discrepancy between the MT expression in various tumors and the lack of overall consensus regarding the precise role of MT in human neoplasms [26]. According to these researchers, the enhanced expression is associated with the rapid proliferation or regeneration of normal cells and even with the aggressiveness and drug resistance of neoplasms [26]. This applies to the following tumors: kidney, breast, lung, nasopharynx, salivary gland, ovary, testes, urinary bladder, leukemia, and non-Hodgkin's lymphoma [14,27,97]. However, this meta-analysis only shows an agreement in ovarian and nasopharyngeal cancer while the rest of tumors did not exhibit any alterations of MT levels. On the other hand, the decrease of MT expression is associated with the poor prognosis namely of prostatic, hepatic, thyroid, brain and testicular tumors

Table 2. Association of MT staining and clinicopathological factors – individual tumor types taken into account.

Tumor	Factor	Number of studies	OR/HR* (95% CI)	Heterogeneity		Model
				P-value	I^2 (%)	
bladder	Tumor vs. control	2	1.68 (0–1135.79)	0.002	89.89	Random effects
	Tumor stage	3	1.56 (0.77–3.16)	0.354	3.64	Fixed effects
	Tumor grade	3	0.96 (0.21–4.33)	0.027	72.24	Random effects
	Metastases, nodal + distant	3	1.78 (0.57–5.51)	0.070	62.44	Random effects
	Metastases, nodal	2	1.96 (0.40–9.66)	0.022	80.89	Random effects
	Metastases, distant	1	1.31 (0.21–8.27)	-	-	-
	Overall survival	1	2.06 (1.26–3.37)	-	-	-
breast	Tumor vs. control	1	0.07 (0.00–1.29)	-	-	-
	Tumor stage	1	1.20 (0.59–2.43)	-	-	-
	Tumor size	1	1.73 (0.68–4.40)	-	-	-
	Tumor grade	5	1.85 (1.22–2.82)	0.096	49.19	Fixed effects
	Metastases, nodal + distant	3	2.57 (0.59–11.26)	0.001	86.55	Random effects
	Metastases, nodal	3	2.57 (0.59–11.26)	0.001	86.55	Random effects
colorectal	Tumor vs. control	1	0.02 (0.00–0.24)	-	-	-
	Tumor stage	5	1.27 (0.51–3.16)	0.000	83.09	Random effects
	Tumor size	2	0.71 (0.32–1.56)	0.299	7.15	Fixed effects
	Tumor grade	6	2.32 (0.86–6.29)	0.000	77.64	Random effects
	Metastases, nodal + distant	6	1.11 (0.38–3.24)	0.001	75.84	Random effects
	Metastases, nodal	4	1.12 (0.30–4.16)	0.001	82.13	Random effects
	Metastases, distant	2	1.04 (0.07–15.17)	0.050	73.87	Random effects
	Overall survival	1	1.05 (1.00–1.10)	-	-	-
esophageal	Metastases, nodal + distant	2	2.89 (1.17–7.15)	0.464	0.00	Fixed effects
	Metastases, nodal	1	2.30 (0.77–6.85)			Fixed effects
	Metastases, distant	1	4.78 (0.94–24.33)	-	-	-
gallbladder	Tumor vs. control	1	34.41 (1.76–673.37)	-	-	-
	Tumor grade	1	2.25 (0.37–13.71)	-	-	-
hepatocellular	Tumor vs. control	3	0.10 (0.03–0.30)	0.548	0.00	Fixed effects
	Tumor stage	1	3.53 (0.36–34.18)			-
	Tumor size	2	1.04 (0.12–9.42)	0.023	80.53	Random effects
	Tumor grade	2	0.47 (0.28–0.80)	0.832	0.00	Fixed effects
	Metastases, nodal + distant	1	0.62 (0.39–0.98)	-	-	-
	Metastases, distant	1	0.62 (0.39–0.98)	-	-	-
head and neck	Tumor vs. control	5	9.95 (5.82–17.03)	0.191	34.56	Fixed effects
	Tumor stage	2	2.02 (0.36–11.27)	0.123	58.04	Random effects
	Tumor grade	4	0.72 (0.22–2.40)	0.091	53.68	Random effects
	Metastases, nodal + distant	2	3.49 (0.25–48.04)	0.036	77.24	Random effects
	Metastases, nodal	2	3.49 (0.25–48.04)	0.036	77.24	Random effects
	Overall survival	2	3.14 (1.61–6.15)	0.826	0.00	Fixed effects
kidney	Tumor vs. control	2	0.06 (0.00–2.20)	0.043	75.47	Random effects
	Tumor stage	2	0.38 (0.07–2.13)	0.086	66.00	Random effects
	Tumor grade	2	1.74 (0.66–4.59)	0.001	90.91	Fixed effects
lung	Tumor grade	1	0.92 (0.05–18.12)	-	-	-
	Overall survival	2	1.03 (0.63–1.67)	0.622	0.00	Fixed effects
lung, adenoca.	Tumor grade	1	5.77 (0.29–116.67)	-	-	-
lung, squamous cell	Tumor grade	1	0.15 (0.01–2.81)	-	-	-
melanoma	Tumor vs. control	2	9.41 (0.03–3106.54)	0.000	93.39	Random effects
	Tumor size	1	4.85 (3.51–6.70)	-	-	-
	Metastases, nodal + distant	2	2.47 (1.30–4.70)	0.336	0.00	Fixed effects

Table 2. Cont.

Tumor	Factor	Number of studies	OR/HR* (95% CI)	Heterogeneity		Model
				P-value	I^2 (%)	
	Metastases, nodal	1	2.23 (1.14–4.39)	-	-	-
	Metastases, distant	1	6.63 (0.81–54.61)	-	-	-
	Overall survival	1	7.16 (4.71–10.89)	-	-	-
ovary	Tumor vs. control	4	7.83 (1.09–56.29)	0.003	78.82	Random effects
	Tumor grade	2	3.08 (1.38–6.88)	0.616	0.00	Fixed effects
	Overall survival	1	1.58 (1.01–2.47)	-	-	-
prostate	Tumor vs. control	2	0.74 (0–4095.48)	0.000	95.32	Random effects
	Tumor grade	4	2.09 (0.86–5.07)	0.365	5.64	Fixed effects
	Gleason Grade	2	1.40 (0.47–4.14)	0.238	28.06	Fixed effects
	Overall survival	1	1.86 (1.79–1.94)	-	-	-
stomach	Tumor vs. control	3	3.50 (0.17–73.01)	0.000	95.71	Random effects
	Tumor stage	1	0.73 (0.33-1.63)	-	-	-
	Tumor grade	1	1.45 (0.67–3.14)	-	-	-
	Metastases, nodal + distant	1	0.59 (0.27–1.28)	-	-	-
	Metastases, nodal	1	0.59 (0.27–1.28)	-	-	-
	Overall survival	1	4.23 (1.8–9.94)	-	-	-
testes	Tumor stage	2	0.33 (0.10–1.03)	0.301	6.54	Fixed effects
thyroid	Tumor vs. control	3	0.39 (0.16–0.95)	0.182	41.39	Fixed effects
thyroid, follicular	Tumor vs. control	3	2.27 (1.11–4.63)	0.212	35.59	Fixed effects
thyroid, medullar	Tumor vs. control	1	0.11 (0.03–0.39)	-	-	-
thyroid, papillary	Tumor vs. control	3	0.23 (0.02–2.85)	0.026	72.64	Random effects
uterine	Tumor vs. control	1	0.01 (0.00–0.10)	-	-	-
	Tumor stage	2	1.53 (0.61–3.86)	0.538	0.00	Fixed effects
	Tumor grade	2	2.81 (1.17–6.8)	0.569	0.00	Fixed effects
	Metastases, nodal + distant	1	1.01 (0.27–3.79)	-	-	-
	Metastases, nodal	1	1.01 (0.27–3.79)	-	-	-

Heterogeneity of studies analyzed using Cochran's Q-test (p-value displayed) and using I^2. Egger's two-tailed test used for publication bias analysis (p-value displayed). * effect measure is odds ratio, OR, except for survival analysis using hazard ratio, HR. No heterogeneity test and no model indicated when 1 study per factor analyzed. CI, confidence interval.

doi:10.1371/journal.pone.0085346.t002

[14,25,26,66,98–102]. An agreement is found in hepatic cancer only by this analysis.

Apart from differences between the individual tumor types, contradictory results were found even within particular histological types. According to the meta-analysis, such contradictions were observed in prostate, melanoma, and stomach tumors. While the high MT levels are associated with rapid proliferation and drug resistance and the low levels are associated with poor prognosis, it is likely that the MT levels change during the tumor progression. It is known that the zinc and metallothionein metabolism is being altered during early stages of tumorigenesis in prostate cancer, [69,103,104]; a similar tendency is expected in other histological types. Thus, a careful selection of controls is crucial; benign controls are therefore not an optimal biological material to demonstrate changes in MT/zinc levels. Additionally, it was reported that healthy tissues adjacent to a tumor vary distinctly as compared with the healthy tissues (i.e. tissues of patients without tumors) regarding zinc and MT levels. Considering the fact that MT is tightly related to oxidative stress buffering [11], the increase in oxidative stress affects the MT expression. Therefore, radiation, cytostatic drug therapy, or long-term stress must be taken into account when evaluating the MT levels.

Tumor stage

Although there are outlines that poor prognosis is associated with the higher MT expression in some tumors, for example breast tumors [30,40,49], no significant associations were determined by this meta-analysis (OR = 1.15; 95% CI, 0.74 to 1.77). No publication bias was observed (Egger's 2-tailed p = 0.99) and a vast majority of studies did not reveal any significant trends. In total, 1,237 samples were analyzed (Fig. 3).

Subsequently, the perspective of individual tumor types was taken into account. A colorectal cancer pT staging of two included studies did not reveal any significance using the meta-analysis [38,105]; however, conflicting results were determined in colorectal cancer evaluating the Dukes staging. While a negative association (i.e. lower MT staining in higher stages) was revealed by one study [38], a positive association was determined by another study [106] and non-significant association was determined in another study [39]. Rather confusing was a study using radioimmunoanalysis with a positive association of MT staining and Dukes stage but no association to TNM staging [82].

Using the meta-analysis, no association of MT staining and tumor stage was observed in bladder [44,83,107], endometrial [108,109], testicular [6,98], kidney [110,111], and head and neck

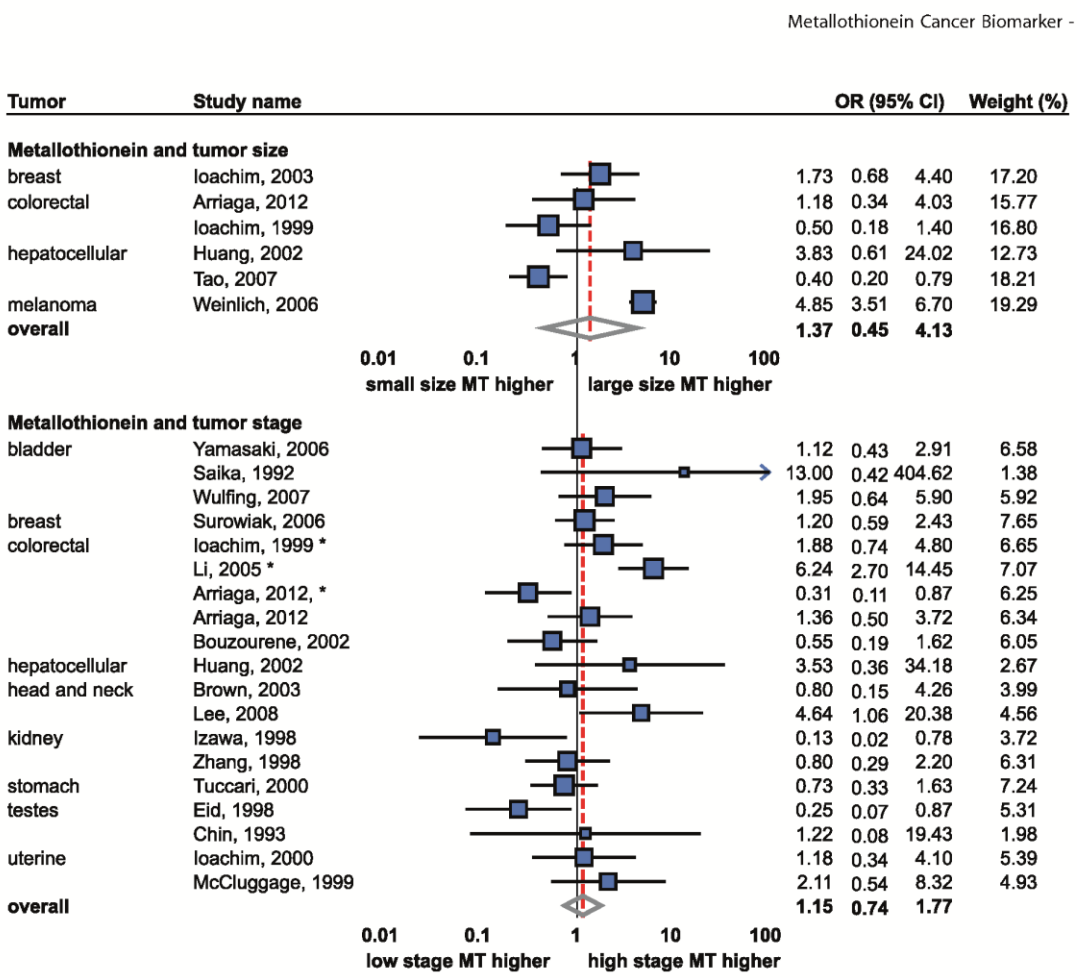

Figure 3. Forrest plot of studies reporting the association of metallothionein staining and tumor size and stage. Random effects model used for both outcomes, Relative weight of individual studies displayed in %. * indicates studies using Dukes staging system. For more detailed results see Table 1 and 2. Sorted alphabetically by tumor types. Forrest plot displayed as odds ratio and 95% confidence intervals. Red dashed line indicates the result for all studies together. OR, odds ratio; CI, confidence interval.
doi:10.1371/journal.pone.0085346.g003

cancer [41,51]. There are also studies regarding tumors of breast [45], liver [74], and stomach [43] showing no significant association between MT staining and the tumor stage (Table 2). Nevertheless, each tumor was represented only by one study and no meta-analytical approach was applied. Therefore, more studies are needed.

Tumor size

The association of MT staining and tumor size was a further subject of the meta-analysis. Six studies were included (1,962 samples); no association was observed using the random effects model and no publication bias was determined (Fig. 3).

When individual tumor types were evaluated separately, no significant trends were observed in colorectal cancer using the fixed effects and in hepatocellular cancer using the random effects model. Breast cancers and melanomas were identified in one study, with the only positive association found in melanoma. Additionally to IHC, no correlation of MT immunopositivity and tumor size was described by other researchers either [40,46–49,112]. Thus, according to our results and previous studies, MT staining is considered tumor size independent.

Tumor grade

The association of MT staining with the histological grade was studied most extensively; a total of 32 studies (2,504 samples) were identified (Fig. 4). Although a relatively high degree of heterogeneity between the studies was observed ($I^2 = 67.2\%$), still a significant positive association (i.e. higher MT in higher-grade tumors) was detected using the random effects model (OR = 1.61; 1.107–2.35). No publication bias was observed (p = p = 0.74).

Consequently, this association was analyzed in particular tumor types. Colorectal cancer was studied most with six studies being included [38,39,50,105,106,113]. A positive trend was observed in only two studies [106,113]. Thus, the random effects meta-analysis revealed no association between IHC staining of MT and the tumor grade.

Contrarily, a strong positive association was determined in breast tumors using the fixed effects model (OR = 1.85; 95% CI, 1.22–2.82). A total number of five studies of this tumor type were found [40,45,114–116] and through the established positive association, a significant trend was observed in two studies only [114,116]. These IHC-based results are in agreement with findings based on other techniques, a similarly positive association was observed by numerous authors [46,47,49,112,117–119].

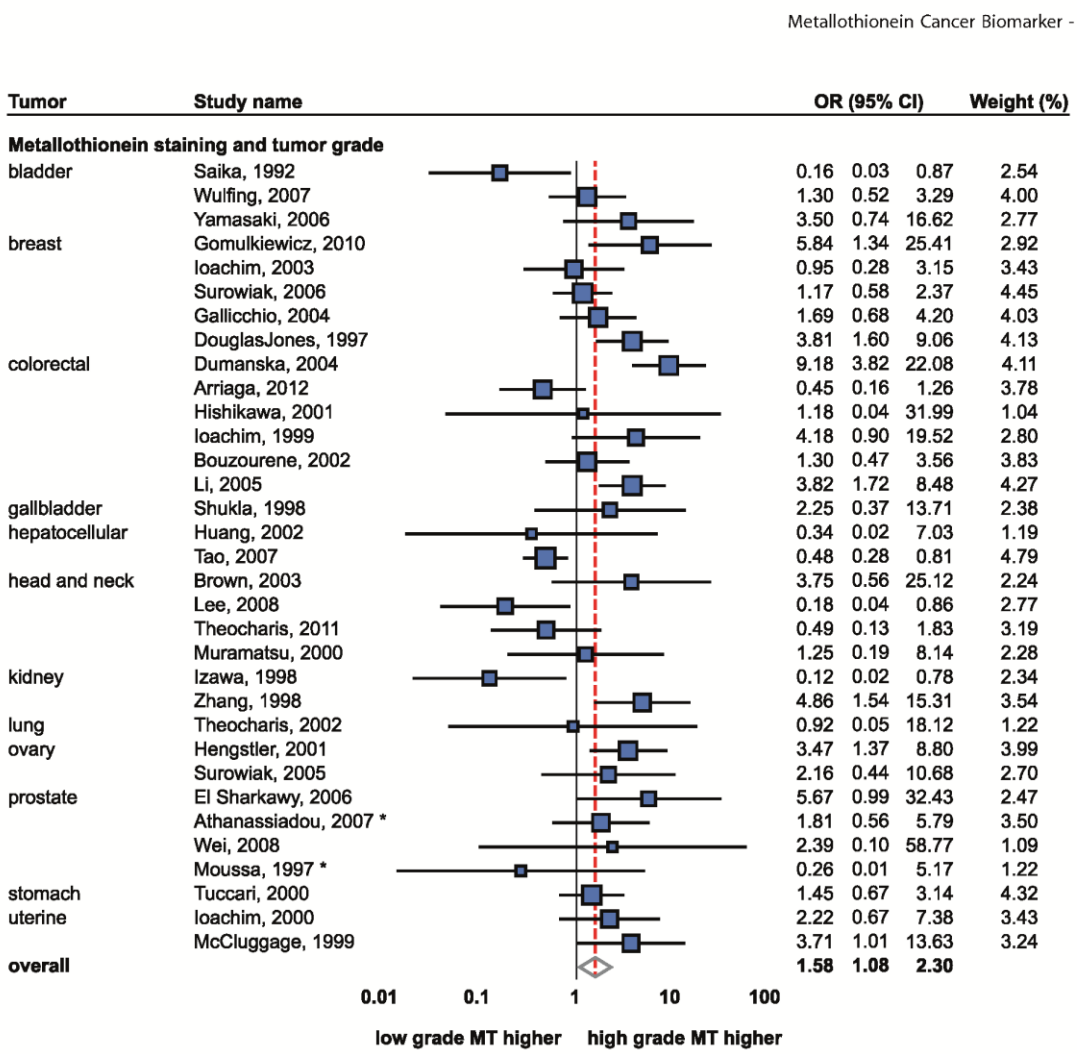

Figure 4. Forrest plot of studies reporting the association of metallothionein staining and tumor grading. Random effects model used. Relative weight of individual studies displayed in %. For more detailed results see Table 1 and 2. * indicates studies using Gleason grading. Sorted alphabetically by tumor types. Forrest plot displayed as odds ratio and 95% confidence intervals. Red dashed line indicates the result for all studies together. OR, odds ratio; CI, confidence interval.
doi:10.1371/journal.pone.0085346.g004

Four studies regarding head and neck tumors were included [41,42,51,120]. However, a significant trend was observed only in one study [41]. Thus, no significant association was observed the using random effects model.

Prostate cancer is particularly interesting from the perspective of MT immunostaining. Four studies were included in total [67,121–123]. Athanassiadou and Moussa used Gleason scale as a measure of tumor grading. When the grading scale was not taken into account, no trend was identified using the fixed effects model. However, the analysis suggests, that only Gleason scale shows no association; by contrast, the tumor grading was positively associated with MT staining (OR = 4.65; 1.01–21.52) using the fixed effects.

Using the fixed effects model, a positive association with the tumor grade was also determined in two studies of ovarian (OR = 3.08; 1.38–6.88) [124,125] and two studies of endometrial cancers (OR = 2.82; 1.17–6.80). However, no MT-grading association was determined in ovarian cancer using Hg-binding assay [61].

On the other hand, a negative association of tumor staging was observed in hepatocellular cancer using the fixed effects, (OR = 0.43; 0.28–0.80). Thus, HCC is considered as the only histological type showing lower MT staining in higher tumor grades. However, only two studies were included and this is why the finding is still of a limited predictive value [25,74].

Inconsistent results were observed in bladder and kidney cancers. While a non-significant association was identified in both tumor types, both positive [111] and negative [110] associations was determined in the case of renal cancer. In terms of bladder cancer, a negative association was demonstrated by Saika et al. [83], while non-significant trends were observed by other two studies [44,107]. Additionally, a decreased MT3 gene expression was associated with higher-grade tumors [37].

Stomach [43], lung [126] and gallbladder [91] tumors were represented by only one study each, but non-significant associations between the tumor grade and MT staining were determined in all these studies. Lung tumors were studied by their histological type; however, non-significant associations were described either

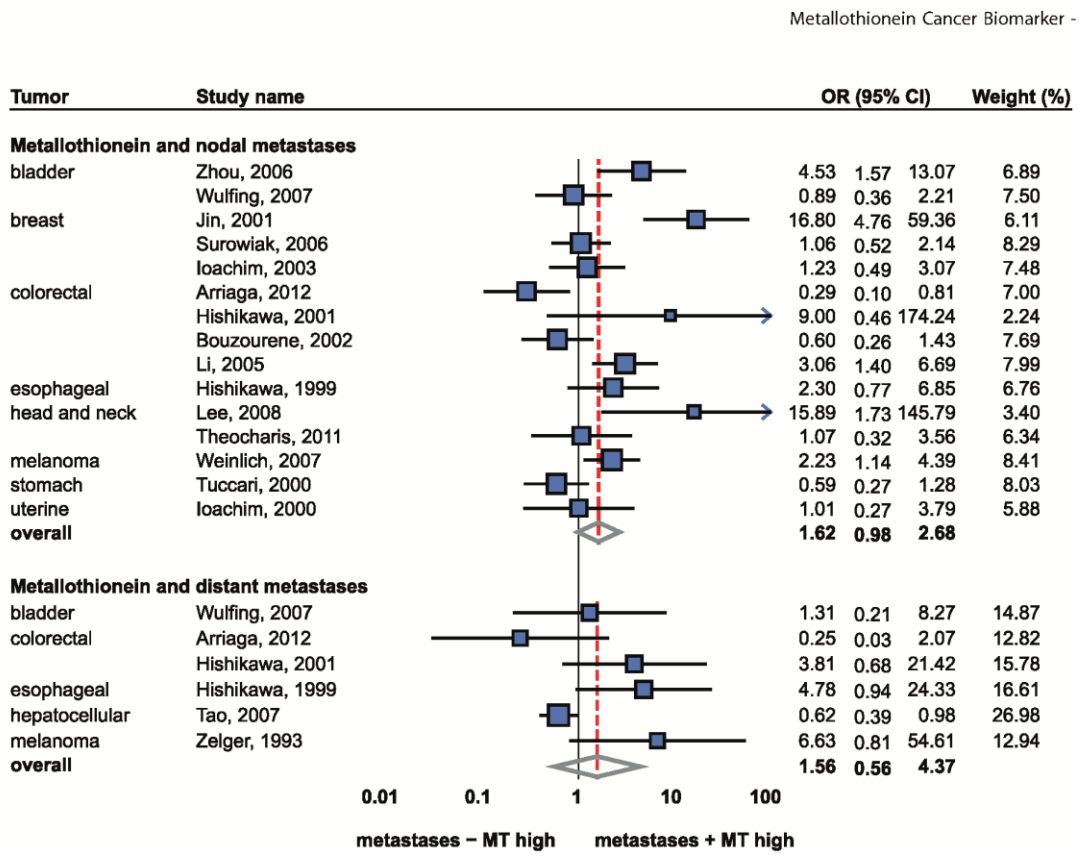

Figure 5. Forrest plot of studies reporting the association of metallothionein staining and nodal and distant metastases. Random effects model used for both outcomes, Relative weight of individual studies displayed in %. For more detailed results see Table 1 and 2. Sorted alphabetically by tumor types. Forrest plot displayed as odds ratio and 95% confidence intervals. Red dashed line indicates the result for all studies together. OR, odds ratio; CI, confidence interval.
doi:10.1371/journal.pone.0085346.g005

in adenocarcinomas or squamous cell carcinomas [126]. Other histological types were not included.

Taking into account the described relations of MT immunostaining with the increased proliferation and cytostatic resistance [14,27,97], it is not surprising that the associations of MT levels with tumor grading were studied to high extent. Meta-analysis results indicate a positive association. However, the results of this meta-analysis also indicate that the MT-grading associations are tumor specific. While a positive association was determined in most tumors, a negative trend was determined in hepatocellular cancer and inconsistent results were found in colorectal, bladder and kidney tumors. While a more or less distinct pattern is evident in all tumors, data are still lacking to prove whether the general positive association of MT staining and tumor grade may be generalized for these tumor types. While the low MT levels are associated with a worse prognosis and the high MT levels with increased proliferation [26], the MT levels vary during the disease progression. It is likely that the heterogeneity observed in some tumor types is a consequence of this phenomenon. Therefore, a precise understanding of MT level fluctuation in individual tumor types during the progression of disease is needed. Understanding the temporal changes will provide better comprehension of cellular tumor mechanisms and may predict a possible development of cytostatic resistance.

Lymph node and metastatic status

Consequently, the association of the metastatic status and MT staining was taken as a subject of the meta-analysis. Included were 15 studies comparing nodal metastases and 6 studies comparing distant metastases (Fig. 5). Using the random effects model meta-analysis, a positive association of the metastatic status and MT staining was observed (OR = 1.59; 95% CI, 1.03–2.46). However, a high degree of heterogeneity between the studies ($I^2 = 71.68\%$) and publication bias were observed (p = 0.04). Nevertheless, when nodal and distant metastases were analyzed separately, no significant trends were observed either in nodal or distant metastases.

Consequently, individual tumor type was considered as a unit of the analysis. A significant association was observed in esophageal cancer (OR = 2.89; 1.17 to 7.15) [127], melanoma (OR = 2.47; 1.30 to 4.70) [90,128] and hepatocellular cancer (OR = 0.62; 0.39 to 0.98) [25]. Notably, only one study per tumor type was included regarding esophageal and hepatocellular cancers.

Tumors of colon and rectum brought ambiguous results. While no association was identified by the meta-analysis, still one study demonstrated a negative association [38], two studies demonstrated a positive association [50,106] and one study did not reveal a significant trend [105]. The remaining tumor types, including bladder [84,107], breast [40,45,119], head and neck [41,42], stomach [43], and uterine cancers [108] indicated no significant association between MT immunostaining and the presence of tumor metastases. However, it must be taken into account that the power of the meta-analysis for individual tumor types is limited due to the limited number of studies. Hence, by combining the tumor types the power of the analysis increases and the combined

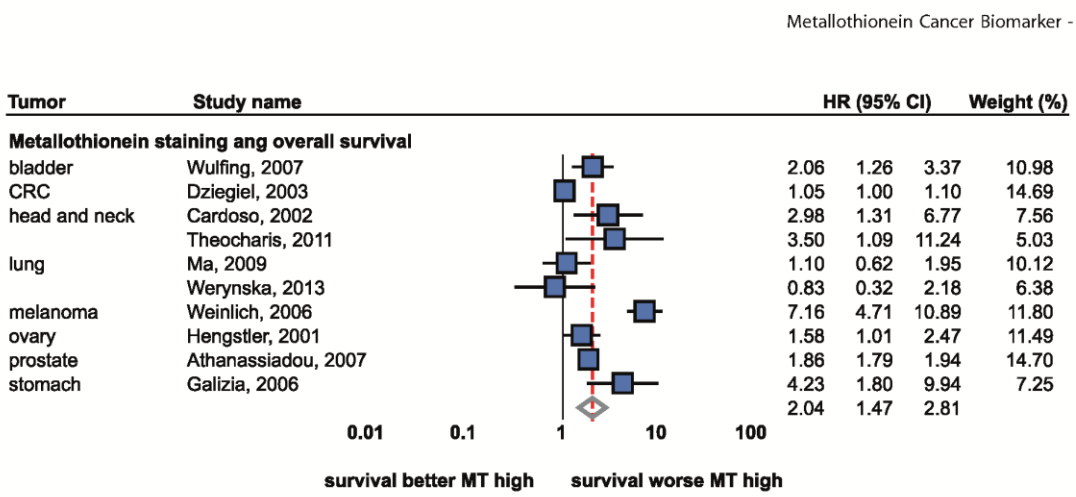

Figure 6. Forrest plot of studies reporting the association of metallothionein staining and the overall survival. Analysis based on Cox-proportional hazard model. Random effects model used. Relative weight of individual studies displayed in %. For more detailed results see Table 1 and 2. Sorted alphabetically by tumor types. Forrest plot displayed as hazard ratio and 95% confidence intervals. Red dashed line indicates the result for all studies together. HR, hazard ratio; CI, confidence interval.
doi:10.1371/journal.pone.0085346.g006

result indicates a significant positive association. However, there is still a lack of IHC data to make conclusive remarks on all tumor types.

Apart from the immunohistochemical analysis, no correlation between the lymph node status and the metastatic potential was described in breast cancer by several investigators [46–49,112]. A significant association between the lymph node status and metastases was observed in one study only [129]. Schmid et al. suggest a higher probability of MT-positive tumors to develop metastases [130]. With regard to non-small cell lung cancer, no difference in the expression of all functional MT-1 and 2 isoforms was determined in another study [131].

Survival analysis

The association of MT immunostaining and patient prognosis was evaluated by several researchers. However, various approaches were used. Univariate Cox proportional hazard model was included in the analysis. Unless noted otherwise, overall survival was used. Additionally, odds ratios, which reported the associations of MT staining with cancer-specific deaths, were also included. Median survival-based data were not evaluable by the meta-analysis and thus were not included.

Firstly, studies describing Cox proportional hazard model were analyzed. A total of 10 studies were included dealing with bladder, colorectal, head and neck, lung, melanoma, ovarian, prostate and stomach tumors (Fig. 6). A significant positive association (i.e. up-regulated MT associated with a worse prognosis) was determined using the random effects model (HR = 2.04; 95% CI, 1.47 to 2.81). No publication bias was determined (p = 0.57).

The significant positive association was determined in head and neck cancers (HR = 3.14; 95% CI, 1.61 to 6.15, fixed effects) [42,132] while no association was determined in lung tumors [131,133]. Both small cell and non-small cell tumors were included. Other tumor types were included in one study. The significant positive association was determined in the cancers of stomach [81], head and neck [42], prostate [121], bladder [107], head and neck [132], ovary [124], colon and rectum [134], and melanoma [35]. No association was identified in kidney tumors [135]. In addition to IHC analyses, poorer prognosis was associated with the higher MT1F and MT2A gene expression in non-small cell lung cancer in a qRT-PCR based study [131] and with higher MT protein levels in colorectal cancer in a radio-immunoanalysis-based study [82].

In addition to Cox model, retrospective studies reporting the following survival-related outcomes were analyzed: cancer-specific death, disease-free survival, short-term survival. While different outcomes were analyzed, the meta-analytical approach was limited in these studies. High MT expression was associated with poorer survival (OR = 3.42; 1.06 to 11.04) in melanoma patients, while an inverse effect was identified in patients with colon and rectum tumors. In those patients, lower MT levels were associated with a worse prognosis (OR = 0.41; 0.18 to 0.95). Univariable analysis of cancer-specific death was a subject of four studies. The following tumor types were included: breast [45], esophagus [136], head and neck [51], and stomach [43]. Neither any of the studies nor the result of the meta-analysis showed an association between cancer-specific death and MT staining. According to Joseph et al., no association was observed between MT staining and short-term survival [137]. Disease-free survival was analyzed in one study [36], which demonstrated a positive association in gastrointestinal stromal tumors (OR = 6.12; 1.12 to 33.52) and no association in leiomyosarcomas.

Conclusions

The associations of immunohistochemical MT staining and various clinicopathological conditions of patients with tumors were analyzed using the meta-analytical approach. To date, it is the first meta-analysis regarding MT in pathological conditions. This meta-analysis was conducted only in studies based on immunohistochemical detection due to indubitable advantages of this method, which clearly identifies tumorous tissues. Therefore, effects of adjacent tissues on gene expression measurements are eliminated. In addition, the largest number of studies was based on immunohistochemistry. Therefore, the IHC-based results are of great statistical power.

More intensive MT staining in tumorous tissues compared to healthy tissues was observed in head and neck and ovarian tumors and a negative association was determined in liver tumors. No significant associations were identified in breast, colorectal, prostate, thyroid, stomach, bladder, kidney, gallbladder, and uterine cancers and in melanoma. However, more studies are

needed in tumors showing insignificant results to confirm or disprove finding that the MT level remains unchanged. Most "insignificant" tumors is often represented by only two studies, which are often conflicting.

While no associations were identified between MT and tumor staging, a positive association was identified with the tumor grade. In particular, strong associations were observed in breast, ovarian, uterine and prostate cancers. Conversely, a negative association between MT staining and hepatocellular tumors was determined in this analysis. Borderline significant association of metastatic status and MT staining was determined in all tumors, in esophageal cancer in particular. Significant association between patient's prognosis and MT staining was also demonstrated.

However, this study has several limitations. Despite the mentioned advantages of immunohistochemistry, the semi-quantitative analysis is to a certain extent always subjective. Moreover, antibodies show affinity to a broad spectrum of MT1 and 2 isoforms. Nevertheless, gene expression-based studies indicate that MT level alterations are confined to certain isoforms. Such differences between isoforms may cause between-study discrepancies, which was evident in several tumor types, including colorectal, kidney, and prostate cancers. Therefore, techniques capable to distinguish MT isoforms on the protein level are desirable, e.g. capillary-based electrophoresis [138]. Despite this fact, such heterogeneity might also be due to MT fluctuation during the development of cancers, high levels being associated with the high rate of proliferation and cytostatic resistance, and low levels being associated with poorer prognoses. Therefore, precise understanding of MT level fluctuation in individual tumor types during the progression of disease is needed. Understanding the temporal changes will provide better comprehension of cellular tumor mechanisms and may predict possible development of cytostatic resistance. Moreover, the association of MT staining was investigated by researchers in certain tumor types more than in others. Therefore, the overall results (i.e. without taking into account the specific type of tumor) are biased toward more published tumor types and a cautious interpretation of the overall results is therefore necessary.

Despite these drawbacks, conclusive results are provided in some tumor types and in relation to tumor grade and patient survival by this meta-analysis. It is however still necessary to clarify the ambiguity of the association between MT staining and colorectal, lung, kidney, and prostate tumors.

Supporting Information

Checklist S1 Prisma 2009 checklist.
(DOC)

Figure S1 Prisma 2009 flow diagram showing the number of citations retrieved by database searching.
(DOC)

Author Contributions

Conceived and designed the experiments: JG MM. Analyzed the data: JG MR VA MM. Contributed reagents/materials/analysis tools: VA RK MM. Wrote the paper: JG MR VA RK MM.

References

1. Nordberg M, Nordberg GF (2000) Toxicological aspects of metallothionein. Cellular and Molecular Biology 46: 451–463.
2. Miles AT, Hawksworth GM, Beattie JH, Rodilla V (2000) Induction, regulation, degradation, and biological significance of mammalian metallothioneins. Critical Reviews in Biochemistry and Molecular Biology 35: 35–70.
3. Krizkova S, Ryvolova M, Hrabeta J, Adam V, Stiborova M, et al. (2012) Metallothioneins and zinc in cancer diagnosis and therapy. Drug Metabolism Reviews 44: 287–301.
4. Hanada K, Sawamura D, Tamai K, Baba T, Hashimoto I, et al. (1998) Novel function of metallothionein in photoprotection: Metallothionein-null mouse exhibits reduced tolerance against ultraviolet B injury in the skin. Journal of Investigative Dermatology 111: 582–585.
5. Reeve VE, Nishimura N, Bosnic M, Michalska AE, Choo KHA (2000) Lack of metallothionein-I and -II exacerbates the immunosuppressive effect of ultraviolet B radiation and cis-urocanic acid in mice. Immunology 100: 399–404.
6. Chin JL, Banerjee D, Kadhim SA, Kontozoglou TE, Chauvin PJ, et al. (1993) Metallothionein in testicular germ-cell tumors and drug-resistance - clinical correlation. Cancer 72: 3029–3035.
7. Fuertes MA, Alonso C, Perez JM (2003) Biochemical modulation of cisplatin mechanisms of action: Enhancement of antitumor activity and circumvention of drug resistance. Chemical Reviews 103: 645–662.
8. Sunada F, Itabashi M, Ohkura H, Okumura T (2005) p53 negativity, CDC25B positivity, and metallothionein negativity are predictors of a response of esophageal squamous cell carcinoma to chemoradiotherapy. World Journal of Gastroenterology 11: 5696–5700.
9. Kelley SL, Basu A, Teicher BA, Hacker MP, Hamer DH, et al. (1988) Overexpression of metallothionein confers resistance to anticancer drugs. Science 241: 1813–1815.
10. Kumar SD, Vijaya M, Samy RP, Dheen ST, Ren MQ, et al. (2012) Zinc supplementation prevents cardiomyocyte apoptosis and congenital heart defects in embryos of diabetic mice. Free Radical Biology and Medicine 53: 1595–1606.
11. Babula P, Masarik M, Adam V, Eckschlager T, Stiborova M, et al. (2012) Mammalian metallothioneins: properties and functions. Metallomics 4: 739–750.
12. Tsangaris GT, Tzortzatou-Stathopoulou F (1998) Metallothionein expression prevents apoptosis: A study with antisense phosphorothioate oligodeoxynucleotides in a human T cell line. Anticancer Research 18: 2423–2433.
13. Eckschlager T, Adam V, Hrabeta J, Figova K, Kizek R (2009) Metallothioneins and Cancer. Current Protein and Peptide Science 10: 360–375.
14. Cherian MG, Jayasurya A, Bay BH (2003) Metallothioneins in human tumors and potential roles in carcinogenesis. Mutation Research-Fundamental and Molecular Mechanisms of Mutagenesis 533: 201–209.
15. Ebadi M, Leuschen MP, ElRefaey H, Hamada FM, Rojas P (1996) The antioxidant properties of zinc and metallothionein. Neurochemistry International 29: 159–166.
16. Kang YJ (2006) Metallothionein redox cycle and function. Experimental Biology and Medicine 231: 1459–1467.
17. Sato M, Bremner I (1993) Oxygen free-radicals and metallothionein Free Radical Biology and Medicine 14: 325–337.
18. Iszard MB, Liu J, Klassen CD (1995) Effect of several metallothionein inducers on oxidative stress defense mechanisms in rats. Toxicology 104: 25–33.
19. Aschner M, Conklin DR, Yao CP, Allen JW, Tan KH (1998) Induction of astrocyte metallothioneins (MTs) by zinc confers resistance against the acute cytotoxic effects of methylmercury on cell swelling, Na+ uptake, and K+ release. Brain Research 813: 254–261.
20. Namdarghanbari M, Wobig W, Krezoski S, Tabatabai N, Petering D (2011) Mammalian metallothionein in toxicology, cancer, and cancer chemotherapy. Journal of Biological Inorganic Chemistry 16: 1087–1101.
21. Cai L, Koropatnick J, Cherian MG (1995) Metallothionein protects DNA from copper-induced but not iron-induced cleavage in-vitro. Chemico-Biological Interactions 96: 143–155.
22. Shibuya K, Nishimura N, Suzuki JS, Tohyama C, Naganuma A, et al. (2008) Role of metallothionein as a protective factor against radiation carcinogenesis. Journal of Toxicological Sciences 33: 651–655.
23. Schwarz MA, Lazo JS, Yalowich JC, Allen WP, Whitmore M, et al. (1995) Metallothionein protects against the cytotoxic and DNA-damaging effects of nitric-oxide. Proceedings of the National Academy of Sciences of the United States of America 92: 4452–4456.
24. Kondo Y, Rusnak JM, Hoyt DG, Settineri CE, Pitt BR, et al. (1997) Enhanced apoptosis in metallothionein null cells. Molecular Pharmacology 52: 195–201.
25. Tao X, Zheng JM, Xu AM, Chen XF, Zhang SH (2007) Downregulated expression of metallothionein and its clinicopathological significance in hepatocellular carcinoma. Hepatology Research 37: 820–827.
26. Pedersen MO, Larsen A, Stoltenberg M, Penkowa M (2009) The role of metallothionein in oncogenesis and cancer prognosis. Progress in Histochemistry and Cytochemistry 44: 29–64.
27. Theocharis SE, Margeli AP, Klijanienko JT, Kouraklis GP (2004) Metallothionein expression in human neoplasia. Histopathology 45: 103–118.
28. Takahashi S (2012) Molecular functions of metallothionein and its role in hematological malignancies. Journal of Hematology & Oncology 5.

29. Gumulec J, Masarik M, Krizkova S, Hlavna M, Babula P, et al. (2012) Evaluation of alpha-methylacyl-CoA racemase, metallothionein and prostate specific antigen as prostate cancer prognostic markers. Neoplasma 59: 191–200.
30. Jin RX, Huang JX, Tan PH, Bay BH (2004) Clinicopathological significance of metallothioneins in breast cancer. Pathology & Oncology Research 10: 74–79.
31. Bay BH, Jin RX, Jayasurya A (2001) Analysis of metallothionein expression in human cancers. Acta Histochemica et Cytochemica 34: 171–176.
32. Higgins JPT, Thompson SG (2002) Quantifying heterogeneity in a meta-analysis. Statistics in Medicine 21: 1539–1558.
33. DerSimonian R, Laird N (1986) Meta-analysis in clinical trials. Control Clin Trials 7: 177–188.
34. Borenstein M, Hedges LV, Higgins JPT, Rothstein HR (2010) A basic introduction to fixed-effect and random-effects models for meta-analysis. Research Synthesis Methods 1: 97–111.
35. Weinlich G, Eisendle K, Hassler E, Baltaci M, Fritsch PO, et al. (2006) Metallothionein - overexpression as a highly significant prognostic factor in melanoma: a prospective study on 1270 patients. British Journal of Cancer 94: 835–841.
36. Perez-Gutierrez S, Gonzalez-Campora R, Amerigo-Navarro J, Beato-Moreno A, Sanchez-Leon M, et al. (2007) Expression of P-glycoprotein and metallothionein in gastrointestinal stromal tumor and leiomyosarcomas. Clinical implications. Pathology & Oncology Research 13: 203–208.
37. Sens MA, Somji S, Lamm DL, Garrett SH, Slovinsky F, et al. (2000) Metallothionein isoform 3 as a potential biomarker for human bladder cancer. Environmental Health Perspectives 108: 413–418.
38. Arriaga JM, Levy EM, Bravo AI, Bayo SM, Amat M, et al. (2012) Metallothionein expression in colorectal cancer: relevance of different isoforms for tumor progression and patient survival. Human Pathology 43: 197–208.
39. Ioachim EE, Goussia AC, Agnantis NJ, Machera M, Tsianos EV, et al. (1999) Prognostic evaluation of metallothionein expression in human colorectal neoplasms. Journal of Clinical Pathology 52: 876–879.
40. Ioachim E, Tsanou E, Briasoulis E, Batsis C, Karavasilis V, et al. (2003) Clinicopathological study of the expression of hsp27, pS2, cathepsin D and metallothionein in primary invasive breast cancer. Breast 12: 111–119.
41. Lee SS, Yang SF, Ho YC, Tsai CH, Chang YC (2008) The upregulation of metallothionein-1 expression in areca quid chewing-associated oral squamous cell carcinomas. Oral Oncology 44: 180–186.
42. Theocharis S, Klijanienko J, Giaginis C, Rodriguez J, Jouffroy T, et al. (2011) Metallothionein expression in mobile tongue squamous cell carcinoma: associations with clinicopathological parameters and patient survival. Histopathology 59: 514–525.
43. Tuccari G, Giuffre G, Arena F, Barresi G (2000) Immunohistochemical detection of metallothionein in carcinomatous and normal human gastric mucosa. Histology and Histopathology 15: 1035–1041.
44. Yamasaki Y, Smith C, Weisz D, van Huizen I, Xuan J, et al. (2006) Metallothionein expression as prognostic factor for transitional cell carcinoma of bladder. Urology 67: 530–535.
45. Surowiak P, Materna V, Gyorffy B, Matkowski R, Wojnar A, et al. (2006) Multivariate analysis of oestrogen receptor alpha, pS2, metallothionein and CD24 expression in invasive breast cancers. British Journal of Cancer 95: 339–346.
46. Fresno M, Wu WY, Rodriguez JM, Nadji M (1993) Localization of metallothionein in breast carcinomas - an immunohistochemical study. Virchows Archiv A, Pathological Anatomy and Histopathology 423: 215–219.
47. Oyama T, Takei H, Hikino T, Iino Y, Nakajima T (1996) Immunohistochemical expression of metallothionein in invasive breast cancer in relation to proliferative activity, histology and prognosis. Oncology 53: 112–117.
48. Goulding H, Jasani B, Pereira H, Reid A, Galea M, et al. (1995) Metallothionein expression in human breast-cancer. British Journal of Cancer 72: 968–972.
49. Jin RX, Chow VTK, Tan PH, Dheen ST, Duan W, et al. (2002) Metallothionein 2A expression is associated with cell proliferation in breast cancer. Carcinogenesis 23: 81–86.
50. Hishikawa Y, Kohno H, Ueda S, Kimoto T, Dhar DK, et al. (2001) Expression of metallothionein in colorectal cancers and synchronous liver metastases. Oncology 61: 162–167.
51. Brown JJ, Xu H, Nishitani J, Mohammed H, Osborne R, et al. (2003) Potential biomarkers for head and neck squamous cell carcinoma. Laryngoscope 113: 393–400.
52. Sundelin K, Jadner M, Norberg-Spaak L, Davidsson A, Hellquist HB (1997) Metallothionein and Fas (CD95) are expressed in squamous cell carcinoma of the tongue. European Journal of Cancer 33: 1860–1864.
53. Dutsch-Wicherek M, Lazar A, Tomaszewska R, Kazmierczak W, Wicherek L (2013) Analysis of metallothionein and vimentin immunoreactivity in pharyngeal squamous cell carcinoma and its microenvironment. Cell & Tissue Research.
54. Ioachim E, Assimakopoulos D, Peschos D, Zissi A, Skevas A, et al. (1999) Immunohistochemical expression of metallothionein in benign premalignant and malignant epithelium of the larynx: Correlation with p53 and proliferative cell nuclear antigen. Pathology Research and Practice 195: 809–814.
55. Pastuszewski W, Dziegiel P, Krecicki T, Podhorska-Okolow M, Ciesielska U, et al. (2007) Prognostic significance of metallothionein, p53 protein and Ki-67 antigen expression in laryngeal cancer. Anticancer Research 27: 335–342.
56. Sochor J, Hynek D, Krejcova L, Fabrik I, Krizkova S, et al. (2012) Study of Metallothionein Role in Spinocellular Carcinoma Tissues of Head and Neck Tumours using Brdicka Reaction. International Journal of Electrochemical Science 7: 2136–2152.
57. McCluggage WG, Strand K, Abdulkadir A (2002) Immunohistochemical localization of metallothionein in benign and malignant epithelial ovarian tumors. International Journal of Gynecological Cancer 12: 62–65.
58. Ozer H, Yenicesu G, Arici S, Cetin M, Tuncer E, et al. (2012) Immunohistochemistry with apoptotic-antiapoptotic proteins (p53, p21, bax, bcl-2), c-kit, telomerase, and metallothionein as a diagnostic aid in benign, borderline, and malignant serous and mucinous ovarian tumors. Diagnostic Pathology 7: 124.
59. Tan Y, Sinniah R, Bay BH, Singh G (1999) Metallothionein expression and nuclear size-in benign, borderline, and malignant serous ovarian tumours. Journal of Pathology 189: 60–65.
60. Zagorianakou N, Stefanou D, Makrydimas G, Zagorianakou P, Briasoulis E, et al. (2006) Clinicopathological study of metallothionein immunohistochemical expression, in benign, borderline and malignant ovarian epithelial tumors. Histology and Histopathology 21: 341–347.
61. Murphy D, McGown AT, Crowther D, Mander A, Fox BW (1991) Metallothionein levels in ovarian-tumors before and after chemotherapy. British Journal of Cancer 63: 711–714.
62. Germain I, Tetu B, Brisson J, Mondor M, Cherian MG (1996) Markers of chemoresistance in ovarian carcinomas: An immunohistochemical study of 86 cases. International Journal of Gynecological Pathology 15: 54–62.
63. Schmid KW, Greeff M, Hittmair A, Totsch M, Ofner D, et al. (1994) Metallothionein expression in normal, hyperplastic, and neoplastic thyroid follicular and parafollicular C-cells using monoclonal antimetallothionein antibody-E9. Endocrine Pathology 5: 114–122.
64. Krolicka A, Kobierzycki C, Pula B, Podhorska-Okolow M, Piotrowska A, et al. (2010) Comparison of Metallothionein (MT) and Ki-67 Antigen Expression in Benign and Malignant Thyroid Tumours. Anticancer Research 30: 4945–4949.
65. Nartey N, Cherian MG, Banerjee D (1987) Immunohistochemical localization of metallothionein in human thyroid-tumors. American Journal of Pathology 129: 177–182.
66. Ferrario C, Lavagni P, Gariboldi M, Miranda C, Losa M, et al. (2008) Metallothionein 1G acts as an oncosupressor in papillary thyroid carcinoma. Laboratory Investigation 88: 474–481.
67. Wei H, Desouki MM, Lin S, Xiao D, Franklin RB, et al. (2008) Differential expression of metallothioneins (MTs) 1, 2, and 3 in response to zinc treatment in human prostate normal and malignant cells and tissues. Molecular Cancer 7.
68. Yamasaki M, Nomura T, Sato F, Mimata H (2007) Metallothionein is up-regulated under hypoxia and promotes the survival of human prostate cancer cells. Oncology Reports 18: 1145–1153.
69. Franklin R, Feng P, Milon B, Desouki M, Singh K, et al. (2005) hZIP 1 zinc uptake transporter down regulation and zinc depletion in prostate cancer. Molecular Cancer 4: 32.
70. Suzuki T, Yamanaka H, Tamura Y, Nakajima K, Kanatani K, et al. (1992) Metallothionein of prostatic tissues and fluids in rats and humans. Tohoku Journal of Experimental Medicine 166: 251–257.
71. Gumulec J, Masarik M, Krizkova S, Adam V, Hubalek J, et al. (2011) Insight to Physiology and Pathology of Zinc(II) Ions and Their Actions in Breast and Prostate Carcinoma. Current Medicinal Chemistry 18: 5041–5051.
72. Costello LC, Franklin RB (2012) Cytotoxic/tumor suppressor role of zinc for the treatment of cancer: an enigma and an opportunity. Expert Review of Anticancer Therapy 12: 121–128.
73. Ebara M, Fukuda H, Hatano R, Saisho H, Nagato Y, et al. (2000) Relationship between copper, zinc and metallothionein in hepatocellular carcinoma and its surrounding liver parenchyma. Journal of Hepatology 33: 415–422.
74. Huang GW, Yang LY (2002) Metallothionein expression in hepatocellular carcinoma. World Journal of Gastroenterology 8: 650–653.
75. Lu DD, Chen YC, Zhang XR, Cao XR, Jiang HY, et al. (2003) The relationship between metallothionein-1F (MT1F) gene and hepatocellular carcinoma. Yale Journal of Biology and Medicine 76: 55–62.
76. Kanda M, Nomoto S, Okamura Y, Nishikawa Y, Sugimoto H, et al. (2009) Detection of metallothionein 1G as a methylated tumor suppressor gene in human hepatocellular carcinoma using a novel method of double combination array analysis. International Journal of Oncology 35: 477–483.
77. Chan KYY, Lai PBS, Squire JA, Beheshti B, Wong NLY, et al. (2006) Positional expression profiling indicates candidate genes in deletion hotspots of hepatocellular carcinoma. Modern Pathology 19: 1546–1554.
78. Nakayama A, Fukuda H, Ebara M, Hamasaki H, Nakajima K, et al. (2002) A new diagnostic method for chronic hepatitis, liver cirrhosis, and hepatocellular carcinoma based on serum metallothionein, copper, and zinc levels. Biological & Pharmaceutical Bulletin 25: 426–431.
79. Kubo S, Fukuda H, Ebara M, Ikota N, Saisho H, et al. (2005) Evaluation of distribution patterns for copper and zinc in metallothionein and superoxide dismutase in chronic liver diseases and hepatocellular carcinoma using high-performance liquid chromatography (HPLC). Biological & Pharmaceutical Bulletin 28: 1137–1141.
80. Ebert MPA, Gunther T, Hoffmann J, Yu J, Miehlke S, et al. (2000) Expression of metallothionein II in intestinal metaplasia, dysplasia, and gastric cancer. Cancer Research 60: 1995–2001.

81. Galizia G, Ferraraccio F, Lieto E, Orditura M, Castellano P, et al. (2006) p27 downregulation and metallothionein overexpression in gastric cancer patients are associated with a poor survival rate. Journal of Surgical Oncology 93: 241–252.
82. Janssen AML, van Duijn W, Oostendorp-van de Ruit MM, Kruidenier L, Bosman CB, et al. (2000) Metallothionein in human gastrointestinal cancer. Journal of Pathology 192: 293–300.
83. Saika T, Tsushima T, Nasu Y, Akebi N, Noda M, et al. (1992) Histopathological study of metallothionein in bladder cancer and renal cell carcinoma. Nihon Hinyokika Gakkai Zasshi 83: 636–642.
84. Zhou XD, Sens DA, Sens MA, Namburi V, Singh RK, et al. (2006) Metallothionein-1 and-2 expression in cadmium- or arsenic-derived human malignant urothelial cells and tumor heterotransplants and as a prognostic indicator in human bladder cancer. Toxicological Sciences 91: 467–475.
85. Ishii K, Usui S, Yamamoto H, Sugimura Y, Tatematsu M, et al. (2001) Decreases of metallothionein and aminopeptidase N in renal cancer tissues. Journal of Biochemistry 129: 253–258.
86. Nguyen A, Jing Z, Mahoney PS, Davis R, Sikka SC, et al. (2000) In vivo gene expression profile analysis of metallothionein in renal cell carcinoma. Cancer Letters 160: 133–140.
87. Hoey JG, Garrett SH, Sens MA, Todd JH, Sens DA (1997) Expression of MT-3 mRNA in human kidney, proximal tubule cell cultures, and renal cell carcinoma. Toxicology Letters 92: 149–160.
88. Hellemans G, Soumillion A, Proost P, Van Damme J, Van Poppel H, et al. (1999) Metallothioneins in human kidneys and associated tumors. Nephron 83: 331–340.
89. Sugita K, Yamamoto O, Asahi M (2001) Immunohistochemical analysis of metallothionein expression in malignant melanoma in Japanese patients. American Journal of Dermatopathology 23: 29–35.
90. Zelger B, Hittmair A, Schir M, Ofner C, Ofner D, et al. (1993) Immunohistochemically demonstrated metallothionein expression in malignant-melanoma. Histopathology 23: 257–264.
91. Shukla VK, Aryya NC, Pitale A, Pandey M, Dixit VK, et al. (1998) Metallothionein expression in carcinoma of the gallbladder. Histopathology 33: 154–157.
92. Bruewer M, Schmid KW, Krieglstein CF, Senninger N, Schuermann G (2002) Metallothionein: Early marker in the carcinogenesis of ulcerative colitis-associated colorectal carcinoma. World Journal of Surgery 26: 726–731.
93. McCluggage WG, Maxwell P, Bharucha H (1998) Immunohistochemical detection of metallothionein and MIB1 in uterine cervical squamous lesions. International Journal of Gynecological Pathology 17: 29–35.
94. El Sharkarvy SL, Farrag ARH (2008) Mean nuclear area and metallothionein expression in ductal breast tumors: Correlation with estrogen receptor status. Applied Immunohistochemistry & Molecular Morphology 16: 108–112.
95. Tews DS, Nissen A, Kulgen C, Gaumann AKA (2000) Drug resistance-associated factors in primary and secondary glioblastomas and their precursor tumors. Journal of Neuro-Oncology 50: 227–237.
96. Bier B, Douglasjones A, Totsch M, Dockhorndworniczak B, Bocker W, et al. (1994) Immunohistochemical demonstration of metallothionein in normal human breast-tissue and benign and malignant breast-lesions. Breast Cancer Research and Treatment 30: 213–221.
97. Thirumoorthy N, Kumar KTM, Sundar AS, Panayappan L, Chatterjee M (2007) Metallothionein: An overview. World Journal of Gastroenterology 13: 993–996.
98. Eid H, Geczi L, Bodrogi I, Institoris E, Bak M (1998) Do metallothioneins affect the response to treatment in testis cancers? Journal of Cancer Research and Clinical Oncology 124: 31–36.
99. Meijer C, Timmer A, De Vries EGE, Groten JP, Knol A, et al. (2000) Role of metallothionein in cisplatin sensitivity of germ-cell tumours. International Journal of Cancer 85: 777–781.
100. Huang Y, De La Chapelle A, Pellegata NS (2003) Hypermethylation, but not LOH, is associated with the low expression of MT1G and CRABP1 in papillary thyroid carcinoma. International Journal of Cancer 104: 735–744.
101. Dziegiel P, Jelen M, Muszczynska B, Maciejczyk A, Szulc A, et al. (2004) Role of metallothionein expression in non-small cell lung carcinomas. Roczniki Akademii Medycznej w Bialymstoku 49 Suppl 1: 43–45.
102. Endo T, Yoshikawa M, Ebara M, Kato K, Sunaga M, et al. (2004) Immunohistochemical metallothionein expression in hepatocellular carcinoma: relation to tumor progression and chemoresistance to platinum agents. Journal of Gastroenterology 39: 1196–1201.
103. Johnson LA, Kanak MA, Kajdacsy-Balla A, Pestaner JP, Bagasra O (2010) Differential zinc accumulation and expression of human zinc transporter 1 (hZIP1) in prostate glands. Methods 52: 316–321.
104. Cortesi M, Fridman E, Volkov A, Shilstein SS, Chechik R, et al. (2008) Clinical assessment of the cancer diagnostic value of prostatic Zinc: A comprehensive needle-biopsy study. Prostate 68: 994–1006.
105. Bouzourene H, Chaubert P, Gebhard S, Boman FT, Coucke P (2002) Role of metallothioneins in irradiated human rectal carcinoma. Cancer 95: 1003–1008.
106. Li SY, Yu B, An P, Zuo FY, Cai HY (2005) Expression of metallothionein and FasL in colorectal cancer and its clinical significance. Zhonghua Wai Ke Za Zhi (Chinese Journal of Surgery) 43: 1118–1120.
107. Wulfing C, van Ahlen H, Eltze E, Piechota H, Herde L, et al. (2007) Metallothionein in bladder cancer: correlation of overexpression with poor outcome after chemotherapy. World Journal of Urology 25: 199–205.
108. Ioachim EE, Kitsiou E, Carassavoglou C, Stefanaki S, Agnantis NJ (2000) Immunohistochemical localization of metallothionein in endometrial lesions. Journal of Pathology 191: 269–273.
109. McCluggage WG, Maxwell P, Hamilton PW, Jasani B (1999) High metallothionein expression is associated with features predictive of aggressive behaviour in endometrial carcinoma. Histopathology 34: 51–55.
110. Izawa JI, Moussa M, Cherian MG, Doig G, Chin JL (1998) Metallothionein expression in renal cancer. Urology 52: 767–772.
111. Zhang XH, Takenaka I (1998) Incidence of apoptosis and metallothionein expression in renal cell carcinoma. British Journal of Urology 81: 9–13.
112. Bay BH, Jin RX, Huang JX, Tan PH (2006) Metallothionein as a prognostic biomarker in breast cancer. Experimental Biology and Medicine 231: 1516–1521.
113. Dumanska M, Dziegiel P, Sopel M, Wojnar A, Zabel M (2004) Evaluation of apoptosis, proliferation intensity and metallothionein (MT) expression in comparison with selected clinicopathological variables in primary adenocarcinomas of the large intestine. Folia Morphologica (Poland) 63: 107–110.
114. DouglasJones AG, Navabi H, Morgan JM, Jasani B (1997) Immunoreactive p53 and metallothionein expression in duct carcinoma in situ of the breast - No correlation. Virchows Archiv 430: 373–379.
115. Gallicchio L, Flaws JA, Sexton M, Ioffe OB (2004) Cigarette smoking and metallothionein expression in invasive breast carcinomas. Toxicology Letters 152: 245–253.
116. Gomulkiewicz A, Podhorska-Okolow M, Szulc R, Smorag Z, Wojnar A, et al. (2010) Correlation between metallothionein (MT) expression and selected prognostic factors in ductal breast cancers. Folia Histochemica et Cytobiologica 48: 242–248.
117. Haerslev T, Jacobsen GK, Zedeler K (1995) The prognostic-significance of immunohistochemically detectable metallothionein in primary breast carcinomas. APMIS 103: 279–285.
118. Zhang R, Zhang H, Wei H, Luo X (2000) Expression of metallothionein in invasive ductal breast cancer in relation to prognosis. Journal of Environmental Pathology Toxicology and Oncology 19: 95–97.
119. Jin RX, Bay BH, Chow VTK, Tan PH (2001) Metallothionein 1F mRNA expression correlates with histological grade in breast carcinoma. Breast Cancer Research and Treatment 66: 265–272.
120. Muramatsu Y, Hasegawa Y, Fukano H, Ogawa T, Namuba M, et al. (2000) Metallothionein immunoreactivity in head and neck carcinomas; Special reference to clinical behaviors and chemotherapy responses. Anticancer Research 20: 257–264.
121. Athanassiadou P, Bantis A, Gonidi M, Athanassiades P, Agelonidou E, et al. (2007) The expression of metallothioneins on imprint smears of prostate carcinoma: Correlation with clinicopathologic parameters and tumor proliferative capacity. Tumori 93: 189–194.
122. Moussa M, Kloth D, Peers G, Cherian MG, Frei JV, et al. (1997) Metallothionein expression in prostatic carcinoma: correlation with Gleason grade, pathologic stage, DNA content and serum level of prostate-specific antigen. Clinical and Investigative Medicine-Medecine Clinique Et Experimentale 20: 371–380.
123. El Sharkawy SL, Abbas NF, Badawi MA, El Shaer MA (2006) Metallothionein isoform II expression in hyperplastic, dysplastic and neoplastic prostatic lesions. Journal of Clinical Pathology 59: 1171–1174.
124. Hengstler JG, Pilch H, Schmidt M, Dahlenburg H, Sagemuller J, et al. (2001) Metallothionein expression in ovarian cancer in relation to histopathological parameters and molecular markers of prognosis. International Journal of Cancer 95: 121–127.
125. Surowiak P, Materna V, Kaplenko I, Spaczynski M, Dietel M, et al. (2005) Augmented expression of metallothionein and glutathione S-transferase pi as unfavourable prognostic factors in cisplatin-treated ovarian cancer patients. Virchows Archiv 447: 626–633.
126. Theocharis S, Karkantaris C, Philipides T, Agapitos E, Gika A, et al. (2002) Expression of metallothionein in lung carcinoma: correlation with histological type and. Histopathology 40: 143–151.
127. Hishikawa Y, Koji T, Dhar DK, Kinugasa S, Yamaguchi M, et al. (1999) Metallothionein expression correlates with metastatic and proliferative potential in squamous cell carcinoma of the oesophagus. British Journal of Cancer 81: 712–720.
128. Weinlich G, Topar G, Eisendle K, Fritsch PO, Zelger B (2007) Comparison of metallothionein-overexpression with sentinel lymph node biopsy as prognostic factors in melanoma. Journal of the European Academy of Dermatology and Venereology 21: 669–677.
129. Haerslev T, Jacobsen K, Nedergaard L, Zedeler K (1994) Immunohistochemical detection of metallothionein in primary breast carcinomas and their axillary lymph-node metastases. Pathology Research and Practice 190: 675–681.
130. Schmid KW, Ellis IO, Gee JMW, Darke BM, Lees WE, et al. (1993) Presence and possible significance of immunocytochemically demonstrable metallothionein over-expression in primary invasive ductal carcinoma of the breast. Virchows Archiv A, Pathological Anatomy and Histopathology 422: 153–159.
131. Werynska B, Pula B, Muszczynska-Bernhard B, Gomulkiewicz A, Piotrowska A, et al. (2013) Metallothionein 1F and 2A overexpression predicts poor outcome of non-small cell lung cancer patients. Experimental and Molecular Pathology 94: 301–308.

132. Cardoso SV, Barbosa HM, Candellori IM, Loyola AM, Aguiar MCF (2002) Prognostic impact of metallothionein on oral squamous cell carcinoma. Virchows Archiv 441: 174–178.
133. Ma HQ, Sun HH, Huang FX, Li J, Cao XL, et al. (2009) Expression of ERCC1, Bcl-2, MT and their Clinical Significance in Advanced Non-small-cell Lung Cancer Treated With Cisplatin-based Chemotherapy. Latin American Journal of Pharmacy 28: 827–834.
134. Dziegiel P, Forgacz J, Suder E, Surowiak P, Kornafel J, et al. (2003) Prognostic significance of metallothionein expression in correlation with Ki-67 expression in adenocarcinomas of large intestine. Histology and Histopathology 18: 401–407.
135. Mitropoulos D, Kyroudi-Voulgari A, Theocharis S, Serafetinides E, Moraitis E, et al. (2005) Prognostic significance of metallothionein expression in renal cell carcinoma. World Journal of Surgical Oncology 3.
136. Aloia TA, Harpole DH, Reed CE, Allegra C, Moore MBH, et al. (2001) Tumor marker expression is predictive of survival in patients with esophageal cancer. Annals of Thoracic Surgery 72: 859–866.
137. Joseph MG, Banerjee D, Kocha W, Feld R, Stitt LW, et al. (2001) Metallothionein expression in patients with small cell carcinoma of the lung - Correlation with other molecular markers and clinical outcome. Cancer 92: 836–842.
138. Ryvolova M, Adam V, Kizek R (2012) Analysis of metallothionein by capillary electrophoresis. Journal of Chromatography A 1226: 31–42.

2.2.2 Findings related to the hypothesis 2

***Hypothesis 2*: Increasing zinc concentrations should alter expression of genes and miRNAs involved in CaP carcinogenesis significantly. In the cells derived from the primary prostate tumour, higher cell resistance to apoptosis induced by zinc ions can be expected. This higher resistance should be reflected by changes in expression of pro- and anti-apoptotic genes. This resistance can be diminished in the cells derived from metastases because they do not meet high zinc concentrations in prostate anymore, and therefore adaptation to high zinc concentration in the environment may disappear.**

Rising zinc concentrations affected the expression of the genes involved in the CaP carcinogenesis significantly. The gene for metallothionein MT2A and MT1A, for pro-apoptotic BAX and zinc transporter ZnT1, belong among the genes, expression of which was simulated extensively the by zinc ions within the prostatic lines PNT1A, 22Rv1 and PC-3. In contrast, the gene for KRAS GTPase suppressed its expression due to the short-term elevated zinc ion concentration; the range of tested concentrations was from 0 to 3 x IC50 (50% inhibitory constant) for the given cell line [57]. At lower concentrations (up to 50 μM of ZnSO4), zinc also stimulated expression of the MKI67 proliferation marker and expression of the anti-apoptotic BCL2 [58]. At higher zinc concentrations, expression of BCL2 did not go up any more [57].

Expression of the MKI67 proliferation marker and the anti-apoptotic BCL2 gene was higher in the prostate tumour cells 22Rv1 derived from a primary tumour compared with then non-tumour PNT1A, which shifts the BAX/BCL2 ratio in the tumour cells towards inhibition of apoptosis. Addition of zinc ions stimulated even the gene expression of the p53 tumour suppressor, but only in the non-tumour prostate cells PNT1A; p53 expression in tumour 22Rv1 was not increased and remained very low in general. It has also been observed that the 22Rv1 tumour cells tolerate significantly higher concentrations of the zinc ions than the non-tumour PNT1A [58], this increased tolerance to zinc does not appear in the PC-3 cells derived from a bone metastasis of CaP. The PC-3 cells tolerate zinc much less than the non-tumour prostate epithelial cells PNT1A [57]. Influence of zinc ions on gene expression was assessed in the next study by Sztalmachova et al. (see p. 107) and in the study Holubova et al. that will be reported below (see p. 124).

Effect of increasing concentration of zinc ions on the expression of the selected miRNAs was monitored as well. The aim of the study was also to determine levels of expression of the selected miRNAs in the non-tumour cell line PNT1A compared with the CaP-derived cell lines (22Rv1, PC-3 and LNCaP). Using the bioinformatics approach, miRNAs with binding sites in 3'UTR regions of the metallothioneins 1A and 2A (miR-23a, miR-141, miR-224, miR-296-3p, miR-320, miR-375 and miR-376) were chosen. A significantly increased expression of miR-23a in all tumour lines compared with the non-tumour line PNT1A was observed. The 22Rv1 cell

line derived from the primary CaP had an increased expression of miR-224 compared to other lines. All tumour cell lines expressed significantly higher levels of miR-375 compared to non-tumour PNT1A. The results show that miR-375 and miR-23a could be important in CaP diagnosis. From our other findings, it follows that expression of miR-375 is closely related to resistance against docetaxel. The PC-3 cell line expressing miR-375 most has about 3 times higher resistance to docetaxel than the PNT1A line expressing miR-375 least (IC50 for docetaxel = 200nM for PC-3 and 70nM for PNT1A). This association and the mechanisms leading to it were confirmed later in the study performed by Wang et al [59]. Only the miR-224 expression responded consistently to the addition of the zinc ions, and its expression was in negative correlation with of zinc ion concentrations. Results of the study of the chosen miRNAs are summarized in the attached publication Hlavna et al., available on page 116 [56].

Conclusion: Zinc ions can significantly alter expression of the genes involved in CaP carcinogenesis. The primary prostate tumour derived cells were shown to have a higher cell resistance to the zinc-induced apoptosis. This higher resistance was reflected by changes in gene expression of pro- and anti-apoptotic *BAX* and *BCL2* and in the expression of the *MKI67* proliferation marker. This increased tolerance to zinc did not appear in the PC-3 cells derived from CaP bone metastasis. PC-3 cells tolerate zinc much less than the non-tumour epithelial prostate cells PNT1A. In the next part of the work, zinc was therefore monitored as a possible inhibitor of CaP carcinogenesis and its progression to the castration-resistant prostate cancer (CRPC) phase; (see Hypothesis 3). Furthermore, the significance of miR-375 in CaP and its possible relationship with resistance to docetaxel (which is used as one of few chemotherapeutics to treat metastatic CaP) was revealed.

Author's publications relevant to this chapter

1. Sztalmachova, M., M. Hlavna, et al. (2012). "Effect of zinc(II) ions on the expression of pro- and anti-apoptotic factors in high-grade prostate carcinoma cells." Oncology Reports **28**(3): 806-814.
   Available on page 107
2. Hlavna, M., M. Raudenska, et al. (2012). "MicroRNAs and zinc metabolism-related gene expression in prostate cancer cell lines treated with zinc(II) ions." International Journal of Oncology **41**(6): 2237-2244.
   Available on page 116

ONCOLOGY REPORTS 28: 806-814, 2012

Effect of zinc(II) ions on the expression of pro- and anti-apoptotic factors in high-grade prostate carcinoma cells

MARKETA SZTALMACHOVA[1,2], MARIAN HLAVNA[1,3], JAROMIR GUMULEC[1,2], MONIKA HOLUBOVA[1], PETR BABULA[3,4], JAN BALVAN[1], JIRI SOCHOR[2,4], VERONIKA TANHAUSEROVA[1], MARTINA RAUDENSKA[1], SONA KRIZKOVA[2,4], VOJTECH ADAM[2,4], TOMAS ECKSCHLAGER[5], RENE KIZEK[2,4] and MICHAL MASARIK[1,4]

[1]Department of Pathological Physiology, Faculty of Medicine, Masaryk University/Kamenice 5, CZ-625 00 Brno; [2]Department of Chemistry and Biochemistry, Mendel University in Brno/Zemedelska 1, CZ-613 00 Brno; [3]Department of Natural Drugs, Faculty of Pharmacy, University of Veterinary and Pharmaceutical Sciences, Palackeho 1-3, CZ-612 42 Brno; [4]Central European Institute of Technology, Brno University of Technology, Technicka 3058/10, CZ-616 00 Brno; [5]Department of Paediatric Haematology and Oncology, Second Faculty of Medicine, Charles University and University Hospital Motol/V Uvalu 84, CZ-150 06 Prague 5, Czech Republic

Received February 22, 2012; Accepted May 2, 2012

DOI: 10.3892/or.2012.1897

Abstract. Several typical characteristics of prostate tissue have been identified including the ability to accumulate zinc(II). However, this feature of prostate cells is lost during carcinogenesis and, thus, prostate cells are unable to accumulate zinc(II) ions in high levels. Therefore, we can expect that zinc(II) ions can significantly contribute to the progression of tumour disease and to the ability of prostate cell lines to metastasize. In this study, we aimed our attention on determining the expression of Bcl-2, c-Fos, c-Jun, Ki-67, NF-κB and p53 genes in two prostate cell lines, as the 22Rv1 cell line, a model of aggressive partially androgen-sensitive prostate cancer and the PNT1A cell line, a normal prostate cell line model. Moreover, we were interested in the mechanisms through which exposure of these cell lines to zinc(II) ions could influence expression of the above-mentioned genes. We found that zinc(II) ions caused elevated expression of Ki-67, a marker of proliferation, extremely low expression of p53, high expression of Bcl-2 and no changes in the expression of p53. Our experimental data show different effect of zinc(II) ions on expression of the above-mentioned regulatory genes, which may give us more information on their impact on cancer development and progression with possible using for cancer therapy.

Introduction

Prostate cancer is the second most frequently diagnosed cancer and the sixth leading cause of cancer death in males worldwide (1,2). Due to its high incidence and mortality, early diagnosis, identification of highly aggressive clinically silent forms and understanding of disease pathogenesis with typical metabolic differences in order to develop specifically targeted therapy are needed. To target these issues, biochemistry of normal and tumour prostate cells is investigated. Based on these investigations, several typical characteristics of prostate tissue have been found including the ability to accumulate zinc(II) ions (3-7), which are shown in Fig. 1. The intracellular concentration of zinc(II) ions in prostate tissue exceeds up to ten times the concentrations detected in other cell and tissue types. However, this feature of prostate cell lines is lost during carcinogenesis and, thus, prostate cells are unable to accumulate zinc(II) ions in high levels. Therefore, we can expect that zinc(II) ions can significantly contribute to the progression of tumour disease and to the ability of prostate cell lines to metastasize (8).

As a result of numerous studies on cells as well as on prostate cancer patients, several compounds have been found connected with tumourigenesis in prostate cells including Bcl-2. This intracellular protein belongs to a large group of proteins the Bcl-2 family (9), and acts as an inhibitor of apoptosis. Bcl-2 has been established to block apoptotic death in various cell types such as lymphocytes and motoric neurons. It prevents both apoptosis dependent on caspases and oxidative necrosis. Under normal conditions, Bcl-2 is anchored to the outer mitochondrial membrane and heads out into the cytosol, which gives this protein the opportunity to interact with other proteins. These interactions are important for maintaining mitochondrial membrane integrity and function. By binding to the pro-apoptotic family members, Bcl-2 prevents activation of mitochondrial pathway of apoptosis based on the formation of pores that disrupt the permeability of mitochondrial membrane (10-12). It has been suggested that overexpression of the Bcl-2 oncoprotein in human cancer cells contributes to their resistance to chemotherapy- and radiotherapy-induced apoptosis and is connected with unfavourable prognosis (13). The majority of human prostate tumours overexpress Bcl-2,

Correspondence to: Dr Michal Masarik, Department of Pathological Physiology, Faculty of Medicine, Masaryk University, Kamenice 5, CZ-625 00 Brno, Czech Republic
E-mail: masarik@med.muni.cz

Key words: apoptosis, prostate cancer, prognostic marker, Bcl-2, p53, polymerase chain reaction, thiol group, fluorescence microscopy

which is responsible for tumour resistance to radiotherapy and chemotherapy (14,15). This event is supported by the fact that Bcl-2 knocked down by antisense oligodeoxynucleotides induces radiosensitization in human PC-3 prostate tumour xenografts (13). Moreover, it has been reported that Bcl-2 expression is associated with tumour progression and unfavourable prognosis in prostate cancer patients (13,16,17) and is associated with the development of androgen-independent prostate cancer (18). Possible associations with other proteins connected with tumour processes such as c-Fos, c-Jun, Ki-67, NF-κB and p53 can be expected. Therefore, we aimed our attention at determining of expression of Bcl-2, c-Fos, c-Jun, Ki-67, NF-κB and p53 genes in two prostate cell lines the 22Rv1 cell line, a model of aggressive partially androgen-sensitive prostate cancer and the PNT1A cell line, a model of healthy cell line. Moreover, we were interested in the issue how exposure of these cell lines to zinc(II) ions could influence expression of the above-mentioned genes. The expression levels were correlated with the results obtained with a fluorescence microscopy of treated cells, and zinc and -SH moieties content.

Materials and methods

Chemical and biochemical reagents. RPMI-1640 medium, Ham's F12 medium, fetal bovine serum (FBS) (mycoplasma-free), penicillin/streptomycin and trypsin were purchased from PAA Laboratories GmbH (Pasching, Austria). PBS was purchased from Invitrogen Corp. (Carlsbad, CA, USA). Ethylenediaminetetraacetic acid (EDTA), zinc(II) sulphate (BioReagent grade, suitable for cell cultures), RIPA buffer and all other chemicals of ACS purity were purchased from Sigma-Aldrich Co. (St. Louis, MO, USA), unless noted otherwise.

Cell cultures. Two human prostatic cell lines were used in this study: a) PNT1A human cell line established by immortalisation of normal adult prostatic epithelial cells by transfection with a plasmid containing SV40 genome with a defective replication origin; the primary culture was obtained from the normal prostatic tissue of a 35-year old male at *post mortem*, and b) 22Rv1 human cell line derived from a xenograft that was serially propagated in mice after castration. Both cell lines used in this study were purchased from HPA Culture Collections (Salisbury, UK).

Cell cultivation. PNT1A cells were cultured in RPMI-1640 medium supplemented by 10% FBS. 22Rv1 cells were cultured in RPMI-1640 without phenol red (medium) with 10% FBS. The media were supplemented with penicillin (100 U/ml) and streptomycin (0.1 mg/ml), and the cells were maintained at 37˚C in a humidified (60%) incubator with 5% CO_2 (Sanyo, Japan). The passages of PNT1A and 22Rv1 cell lines ranged from 10 to 35 h.

Zinc(II) treatments of cell cultures. Immediately the cells grew up to 50-60% confluence, the cultivation media were replaced by a fresh medium to synchronize cell growth. Cells were cultivated under these conditions for 24 h, then cells were treated with zinc(II) sulphate (0-100 μM for both cell lines) dissolved in fresh medium for 48 h.

RNA isolation, cDNA preparation. High pure total RNA isolation kit (Roche, Basel, Switzerland) was used for RNA isolation. Briefly, cultivation medium was removed and samples were washed twice with 5 ml of ice-cold PBS. Cells were transferred to clean tubes and centrifuged at 15,000 x g for 5 min at 4˚C. After it, lysis buffer was added and RNA isolation was carried out according to the manufacturer's instructions. Isolated RNA was used for cDNA construction. Total RNA (600 ng) was transcribed using transcriptor first strand cDNA synthesis kit (Roche). Prepared cDNA (20 μl) was diluted with RNase-free water to 100 μl and directly analysed by real-time polymerase chain reaction.

Real-time reverse-transcription polymerase chain reaction (RT-PCR). RT-PCR was performed in triplicates using the TaqMan gene expression assay with 7500 real-time PCR system (Applied Biosystems, Foster City, CA, USA). The amplified DNA was analysed by the comparative Ct method using β-actin as an endogenous control. The primer and probe sets for β-actin (assay ID: Hs00185826_m1), Fos (assay ID: Hs00170630_m1), c-Jun (assay ID: Hs00277190_m1), NF-κB (assay ID: Hs00765730_m1), p53 (assay ID: Hs01034649_m1), Bcl-2 (assay ID: Hs99999018_m1) were selected from TaqMan gene expression assay. Real-time PCR was performed under following amplification conditions: total volume of 20 μl, initial denaturation 95˚C/10 min, then 40 cycles 95˚C/15 sec, 60˚C/1 min.

Cell content quantification. Total cell content was analysed using semi-automated image-based cell analyser (Cedex XS, Innovatis, Roche, Basel, Switzerland) according to the following protocol. Cultivation medium was removed and samples were two times washed with 5 ml of ice-cold PBS to maintain only viable cells. Cells were scraped and transferred to clean tubes. Trypan blue solution (Innovatis) was diluted to 0.2% prior to use and added to samples. Following settings were used in operating software: cell type: standard cells, dilution: none, process type: standard. All samples were measured in duplicates.

Measurements of cell viability - MTT test. MTT assay was used to determine cell viability. The suspension of cells was diluted to the density of 5,000 cells/ml in the cultivation medium. Volume of 200 μl was transferred to 2-11 wells of standard microtiter plates. Medium (200 μl) was added to the first and to the last column (1 and 12, control). Plates were incubated for 2 days at 37˚C to ensure cell growth under the same conditions described in Cell cultivation. Medium was removed from columns 2 to 11. Columns 3-10 were filled with 200 μl of medium containing increasing concentration of zinc(II) (0, 50, 100, 150, 200, 250, 300 and 500 μM). As control, columns 2 and 11 were not filled with medium containing zinc(II) ions. Plates were incubated for 24 h; then, media were removed and replaced by a fresh medium, three times a day. Columns 1 to 11 were filled with 200 μl of medium containing 50 μl of MTT (5 mg/ml in PBS) and incubated in a humidified atmosphere for 4 h at 37˚C, wrapped in aluminium foil. After the incubation, MTT-containing medium was replaced by 200 μl of 99.9% dimethyl sulphoxide (DMSO) to dissolve MTT-formazan crystals. Then, 25 μl of glycine buffer was added to all wells and absorbance was

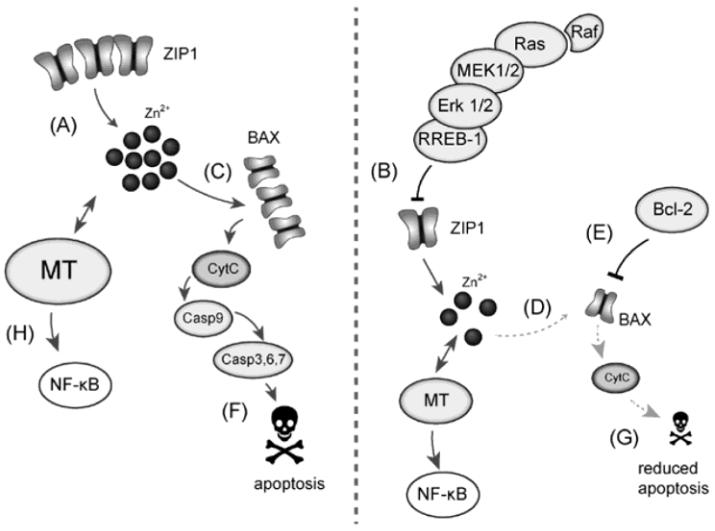

Figure 1. Distinctions in zinc(II) mediated mechanisms in healthy and tumour tissue. (A) In healthy prostate, high level of cellular zinc is present compared to (B) tumour tissue, where zinc-transporter ZIP1 is inhibited by up-regulated Ras-Raf-Mek-Erk cascade. (C) Zinc(II) up-regulates formation of BAX pores on mitochondrial membrane and (F) thus induces cytochrome c (CytC)/caspase(Casp)-mediated apoptosis. On the contrary, in prostate cancer, formation of BAX is inhibited by (E) Bcl-2 and by (D) low intracellular zinc, (G) resulting in lower proapoptic effects. (H) Different zinc(II) levels in healthy and tumour cells interacts with metallotionein (MT), which promotes NF-κB expression differently.

immediately determined at 570 nm (VersaMax microplate reader, Molecular Devices, Sunnyvale, CA, USA).

Cell growth and proliferation assay using impedance measurement with xCELLigence system. The xCELLigence system (Roche Applied Science and ACEA Biosciences, San Diego, CA, USA) consists of four main components: the RTCA analyser, the RTCA DP station, the RTCA computer with integrated software and disposable E-plate 16. Firstly, the optimal seeding concentration for proliferation and cytotoxic assay was determined. After seeding the total number of cells in 200 μl medium to each well in E-plate 16, the attachment, proliferation and spreading of the cells was monitored every 15 min. All experiments were carried out for 250 h. The results are expressed as relative impedance using the manufacturer's software (Roche Applied Science and ACEA Biosciences).

Densitometric and statistical analysis. Software Statistica 10 (StatSoft Inc., Tulsa, OK, USA) was used for statistical analysis. Student's t-test for independent values was used to evaluate differences between two groups. Simple linear correlations were performed to reveal the relationships between variables. Unless noted otherwise, a level of statistical significance was set at $p<0.05$.

Fluorescence microscopy and cell staining. For fluorescence microscopy, cells were cultivated directly on microscope glass slides (75x25 mm, thickness 1 mm, Fischer Scientific, Pardubice, Czech Republic) in Petri dishes in above-described cultivation media (see Cultured cell conditions). Cells were transferred directly onto slides, which were submerged in cultivation media. After treatment, microscope glass slides with monolayer of cells were removed from Petri dishes, rinsed with cultivation medium without zinc(II) supplementation and PBS buffer and directly used for staining and fluorescence microscopy.

For the staining of free thiols, respectively free -SH groups, 5-(bromomethyl)fluorescein (5-BMF, Sigma-Aldrich) was used. This probe reacts more slowly with thiols of peptides, proteins and thiolated nucleic acids in comparison with other fluorescent probes. However, it forms stronger thioether bonds that are expected to remain stable under the conditions required for fluorescence microscopy. Stock solution of 5-BMF (4 mM, anhydrous DMSO) was prepared prior to staining because of 5-BMF stability. Working solution was prepared immediately using stock solution by diluting to final concentration of 20 μM (PBS buffer, pH 7.6). Cells were incubated for 1 h at 37˚C and in dark. Then, cells on microscope glass slide were three times washed by PBS buffer (pH 7.6) and observed using fluorescence microscope (Axioskop 40, Carl Zeiss AG, Oberkochen, Germany) equipped with wideband excitation and set of filters (FITC, DAPI, Carl Zeiss). Photographs were taken using digital camera (Olympus Camedia 750, Olympus, Tokyo, Japan). Program NIS-elements was used for evaluation of intensity of emission, all values were recalculated to control (100%). Ten random fields from each variant and replicate were evaluated.

For free zinc(II) ion staining, fluorescent probe N-(6-methoxy-8-quinolyl)-p-toluene sulphonamide (TSQ, Invitrogen) was used. Working solution (10 μM, phosphate buffer pH 7.6) was prepared by diluting of TSQ stock solution (10 mM, acetone). Cells were carefully rinsed by PBS buffer to remove all cultivation medium containing free zinc(II) ions, subsequently stained by working TSQ solution (30 min, 37˚C, dark), three times washed by PBS buffer (pH 7.6) and observed under a fluorescence microscope (Axioskop 40, Carl Zeiss) equipped by FITC and DAPI filters (Carl Zeiss). Photographs were taken on digital camera (Olympus

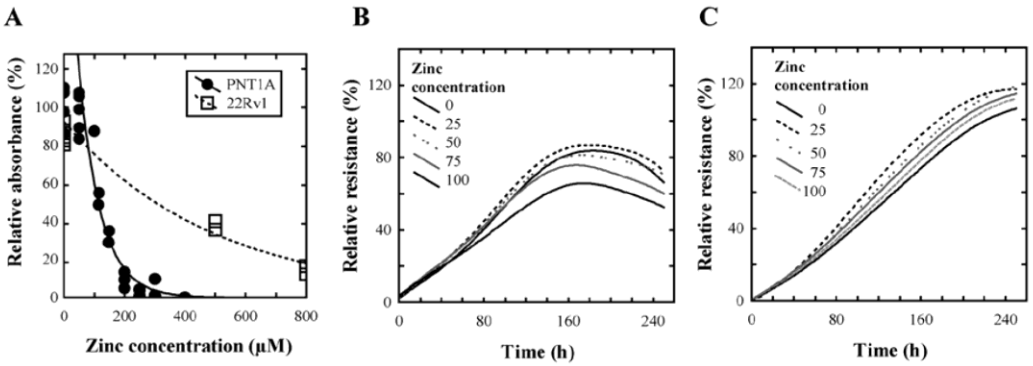

Figure 2. Real-time monitoring of cell adhesion and proliferation using the cytotoxic MTT assay and xCELLigence system. (A) MTT-determined response to zinc(II) treatment. Significantly higher IC_{50} is reached compared to xCELLigence-determined viability in the case of PNT1A and 22Rv1 cells (B vs. C). (B) PNT1A and (C) 22Rv1 cells were seeded at a density of 10,000 cells/well in E-plates 16 (gold working electrodes). After 24 h, the zinc(II) sulphate was added and cell index was monitored (n=2). Other experimental parameters are detailed in Materials and methods.

Camedia 750, Olympus). NIS-element program was used for evaluation of intensity of emission, all values were recalculated to control (=100%). Ten random fields from each variant and replicate were evaluated.

Results

Growth and viability of treated PNT1A and 22Rv1 cells. To select suitable concentration range of zinc(II) ions for treatment of the cell lines, we determined IC_{50} values of zinc(II) for both cell lines using standard MTT cytotoxicity assay with simple linear regression from the descending part of the curve. We obtained IC_{50} corresponding to concentration of 197.9 μM for non-tumour PNT1A and concentration of 369.1 μM for 22Rv1 tumour cells (Fig. 2A). Moreover, we found that PNT1A cells reached stationary phase of growth after 160 h while 22Rv1 cells after 240 h. Thus, we decided to use zinc(II) ion concentrations as follows: 0 (control), 25, 50, 75 and 100 μM for both cell lines for the monitoring of changes in gene expression for 240 h.

Further, we were interested to monitor growth of the cell lines in real time. It is difficult to monitor on-line growth of cell lines during experiment due to the destructive methods for its determination. xCELLigence system offers good possibility to monitor cell growth and proliferation in real time using impedance measurement (19), therefore, we used this system. Primarily, it was necessary to determine optimal cell counts for real time monitoring. We obtained optimal signal with 10,000 cells in each well. This signal corresponded to the cell count. In wells with lower cell count, lower relative impedance signal level was determined and, in some cases, higher relative standard deviation was obtained. Higher cell counts gave also well repeatable results with low relative standard deviation, however, higher count of cells was not optimal from the point of view of 240 h long experiment expecting increasing proliferation and therefore cell count. Therefore, we decided to use 10,000 cells per well to examine the effect of zinc(II) ions on prostatic cells either derived from normal prostate epithelium (PNT1A) or cells derived from primary prostate carcinoma (22Rv1). The IC_{50} values of zinc(II) ions using the xCELLigence system were also determined to evaluate the selected concentration range. These IC_{50} values were as follows: 150.8 μM zinc for PNT1A cells and 445.5 μM zinc for 22Rv1 cells. The changes between these values and values determined using MTT assay can be associated with the fact that both methods are based on measuring of very different physical parameters, which are associated with different physiological phenomena. Based on both measurements of IC_{50} it may be concluded that zinc(II) ions are more toxic to non-tumour cell line at 2.9-fold lower concentration. Based on the obtained results 10,000 cells per well were treated with the above-mentioned concentrations of zinc(II) ions for 240 h. In the beginning of the treatment we observed negligible decrease in relative impedance, i.e. in growth, of PNT1A cells after 15-h long treatment (Fig. 2B) and no changes in cell proliferation of 22Rv1 cells (Fig. 2C). These changes were compared with cell lines treated with 0 μM of zinc(II) ions. Concentrations of 100 μM of zinc(II) ions induced 1.4-and 1.1-fold decrease of relative resistance in PNT1A and 22Rv1 cell lines, respectively, compared to non-treated samples. These results clearly show that the selected concentration range is non-toxic for both cell lines and we can observe the effects of physiological doses of zinc(II) ions on expression of the selected markers as Bcl-2, c-Fos, c-Jun, NF-κB, Ki-67 and p53.

Comparison of the expression of Bcl-2 and other regulatory genes after zinc treatment. Further, we focused on comparison of the base line expression and changes in transcription of Bcl-2, c-Fos, c-Jun, NF-κB, Ki-67 and p53 genes on the RNA level in prostate cell lines treated with zinc(II) ions. Baseline transcription level and zinc(II) ions effect on transcription levels of selected genes was performed by RT-PCR. Fig. 3 shows that 22Rv1 cells demonstrate different expression patterns in monitored genes compared to PNT1A cells. 22Rv1 cell line has 4.5-fold higher level of Bcl-2 anti-apoptotic gene expression (n=5). We found no significant differences ($p>0.05$) in c-Jun gene expression in either cell line. c-Fos gene that together with c-Jun forms important part of AP-1 transcription factor shows 2.5-fold down-regulation in 22Rv1 cells. Ki-67, a nuclear protein that is associated with cellular proliferation, is present in 22Rv1 cell line in 2-fold higher concentration compared to PNT1A.

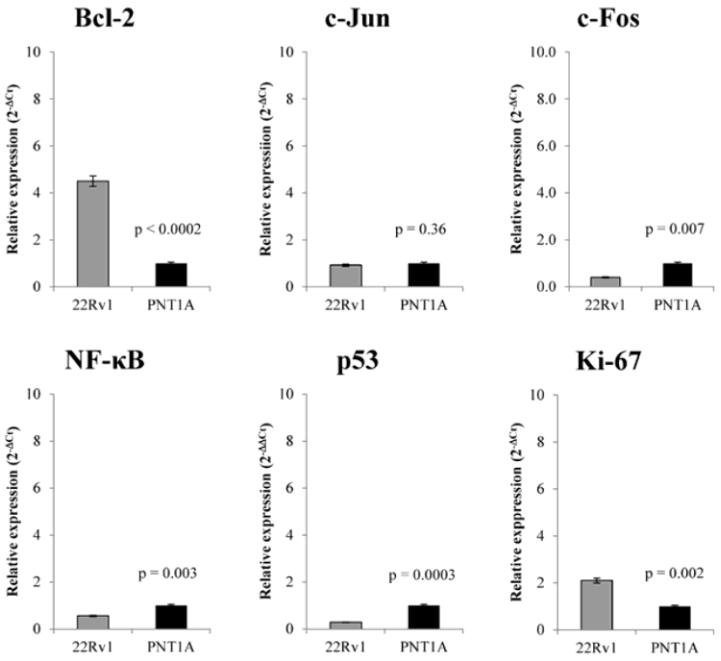

Figure 3. Comparison of the base line expression of c-Fos, c-Jun, NF-κB, Ki-67 and p53 genes on the RNA level. Base line transcription level of selected genes was conducted by RT-PCR. For other experimental parameters see Material and methods.

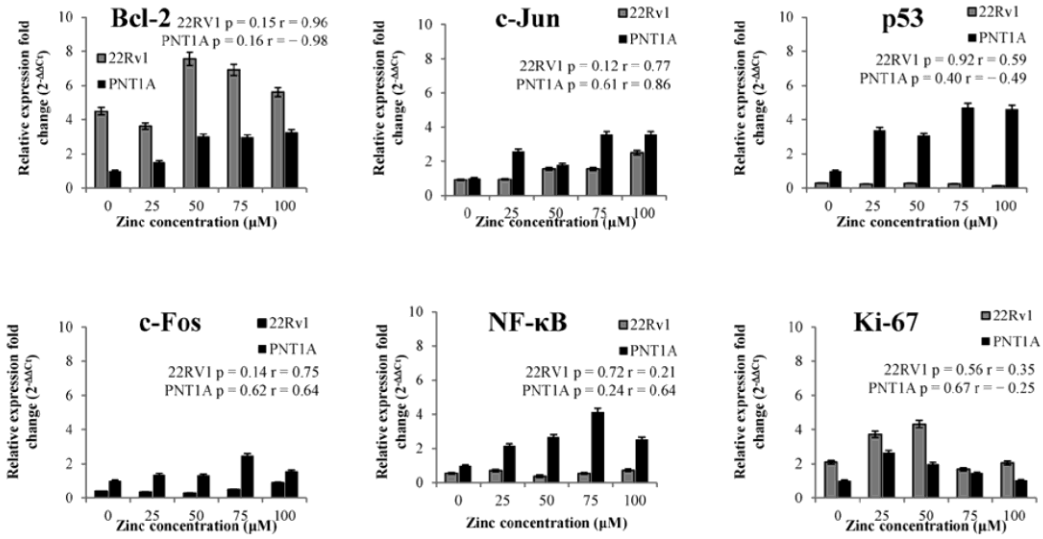

Figure 4. Zinc(II) treatment effect on expression changes of c-Fos, c-Jun, NF-κB, Ki-67 and p53 genes at mRNA level. 22Rv1 cell line shows not only different expression levels of these genes in comparison to healthy PNT1A prostatic cells but also zinc(II) treatment has different effect on their transcriptional levels in both cell lines. For other experimental parameters see Materials and methods and Fig. 2.

Moreover, NF-κB is present in half concentration in 22Rv1cells compared to PNT1A and p53, a key regulator of apoptosis, shows 3.3-fold decreased level compared with PNT1A cell line. After basic characterization of the expression of selected markers in both studied cell lines, we focused on zinc(II) ion treatment effect on the expression changes of these selected regulatory genes (Fig. 4).

We found that zinc(II) ions influence positively expression of Bcl-2 gene in both tested cell lines, however, more in PNT1A cells [≤3.2-fold change in case of 100 μM zinc(II) ions treatment]. In addition, we found no significant difference ($p>0.05$) in p53 expression levels after zinc treatment in 22Rv1 cell line (Fig. 4). On the other hand, zinc(II) ions treatment resulted in the increasing p53 expression from 3- up to 4.7-fold change in

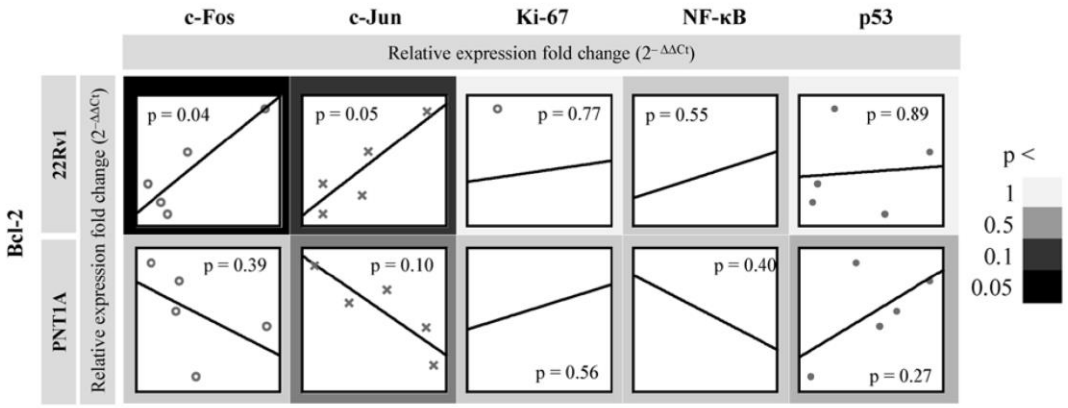

Figure 5. Correlation analysis between Bcl-2 mRNA and other regulatory genes at mRNA level. When exposed to zinc treatment, distinct trends were found between Bcl-2 and c-Fos and c-Jun and no significant correlations between Bcl-2 and Ki-67, NF-κB and p53 in both cell lines. Other experimental parameters are detailed in Materials and methods and in Fig. 2.

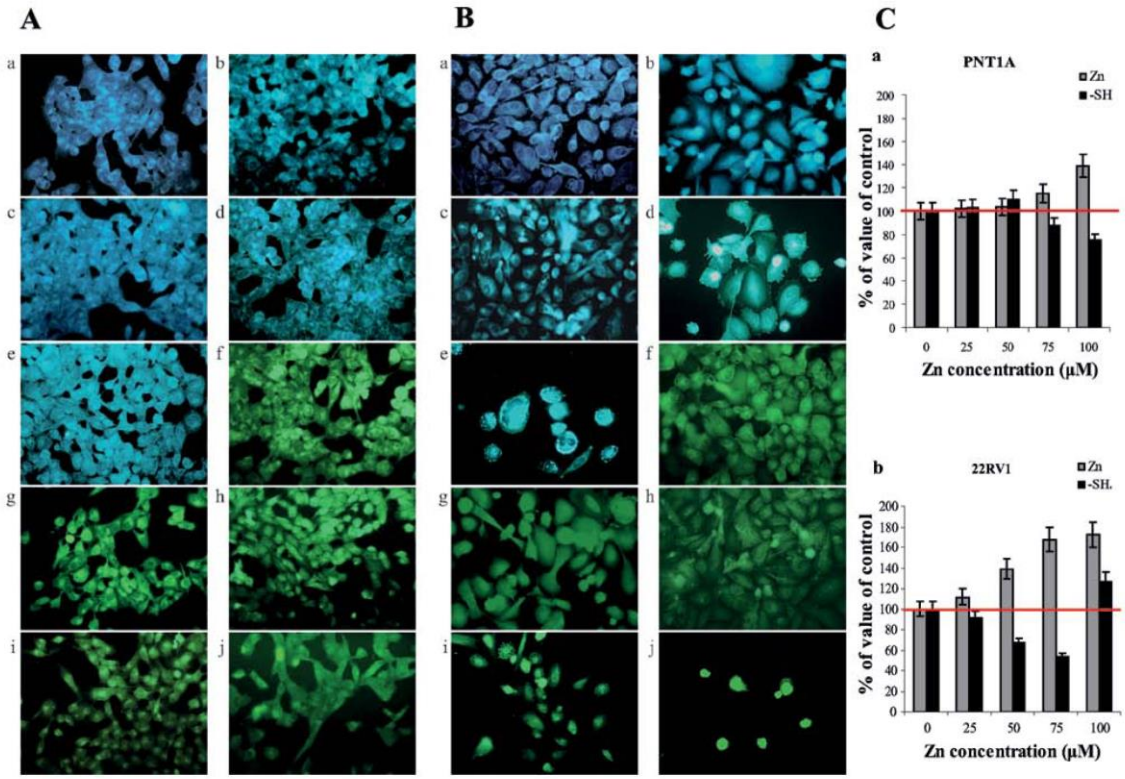

Figure 6. Distribution of free zinc(II) ions and thiols in (A) PNT1A and (B) 22Rv1 cell lines. Cells were treated with 0 (a and f), 25 (b and g), 50 (c and h), 75 (d and i), and 100 μM (e and j) zinc(II) ion concentrations. Distribution of (a-e) free zinc(II) ions and (f-j) free thiol groups. Note presence of bright spots - zincosomes - in 22Rv1 cells treated with the highest zinc(II) ion dose. Evaluation of emission intensity after fluorescence staining using NIE-element program recalculated to control (100%). (C) Content of zinc ions and free thiol moieties in (a) PNT1A and (b) 22Rv1 cell lines. For other experimental parameters see Materials and methods.

PNT1A. Ki-67 gene shows similar pattern in both cell lines after zinc(II) treatment and it is not surprising that 22Rv1 cell line, characterized by higher proliferation rate (Fig. 2A and B), demonstrated higher expression as a gene involved in the proliferation process. Zinc(II) ions had up-regulative effect on c-Jun gene in both cell lines. PNT1A demonstrated higher c-Jun expression in all zinc treatments compared to 22Rv1. In addition, we found no correlation between c-Jun and c-Fos gene expression after zinc treatment, but expression profile of c-Fos showed statistically significant positive correlation (data not shown) with

expression of NF-κB gene after the treatment (compare trends in Fig. 4). Both genes are expressed in higher concentration in PNT1A cell line on the base expression level as well as after zinc treatment.

Correlation analysis of selected genes. Subsequently, we focused on possible dependencies between Bcl-2 mRNA and the mRNA levels of other regulatory genes. After exposure to zinc(II) ions, we observed distinct trends between Bcl-2 and c-Fos and c-Jun and no significant correlations between Bcl-2 and Ki-67, NF-κB and p53 in either cell line (Fig. 5). Bcl-2-p53 showed strong positive correlation at r=0.61. In the case of c-Fos and c-Jun, we found strong positive correlations at r>0.85 in 22Rv1 tumour cell line and strong negative correlations at r<-0.50 in PNT1A non-tumour cell line. In terms of statistical significance, Bcl-2-c-Fos and - c-Jun showed correlations p<0.05 only in 22Rv1 cell line. In contrast, non-tumour cell line PNT1A showed an inverse trend i.e. decrease of Bcl-2 in relation to regulatory genes. In this cell line, negative significant correlation was detected at Bcl-2-c-Jun at p=0.10 with r=-0.79 (Fig. 5).

Determination of free and bound zinc(II) cellular levels after zinc(II) exposure. We characterized cell lines from the point of view of pro- and anti-apoptotic factor expressions, free zinc(II) ions were visualized using fluorescent probe N-(6-methoxy-8-quinolyl)-*p*-toluene sulphonamide, probe specific to these ions. Significant differences in zinc(II) ion localization in both non-tumour PNT1A cells (Fig. 6Aa-e) and tumour 22Rv1 (Fig. 6Ba-e) cells were found. For quantification of changes in free zinc(II) ion levels in cell lines, program NIS-elements for image analysis was used. Detected values (10 fields for each concentration and repetition) were recalculated to control cells (100%) (Fig. 6C). In both PNT1A and 22Rv1 cells, free zinc(II) ions levels were closely connected with zinc(II) ions treatment in concentration-dependent manner. In the case of PNT1A cell line, localization of zinc(II) ions around nuclei and irregularly in nuclei was evident in cells treated with the highest zinc(II) concentration (100 μM). Peripheral parts of cytoplasm demonstrate only weak emission, representing only low free zinc(II) levels in these localizations. In 22Rv1 cells, the intensity of emission of fluorescence product significantly increases with the increased supplementation of cultivation medium by zinc(II) ions (Fig. 6Ba-e). In the lowest Zn(II) supplementation, free zinc(II) ions were localized especially around the nuclei. At the highest Zn(II) supplementation, free zinc(II) ions were localized in nuclei and around the nuclei in the form of spots with high emission. The origin of these spots, which were visible only in the case of 22Rv1 cells in the highest Zn(II) ions supplementation, is probably the zincosomes, compartments of endoplasmic reticulum origin (20).

Determination of free thiols. Compounds rich in -SH moieties including low molecular mass peptides and proteins as reduced glutathione and metallothionein (21-25) are responsible for binging metal ions in intracellular space. Therefore, monitoring of such compounds as well as detection of free zinc(II) ions can answer questions on metabolizing of metal ions in a cell. 5-(bromomethyl)fluorescein, the probe that provides formation of fluorescent product after reaction with -SH groups of thiols, was used for detection and cellular compartmentation of free thiols. In the case of both PNT1A (Fig. 6Af-j) and 22Rv1 cells (Fig. 6Bf-j), amount of free thiols continually decreases with the increasing zinc(II) ions supplementation, however, selection of cells with high content of free thiols was evident. This fact was evident in 22Rv1 cells treated with the highest Zn(II) concentration. In both cell lines, free thiols were localized around the nuclei and in nuclei in cells treated with lower Zn(II) concentrations. On the other hand, highest free thiols levels were detected in the nuclei in the case of tumour 22Rv1 cell line. This fact is evidence on the possible role of free thiols in transcriptional activity, which is regulated not only by free thiols, but also by zinc(II) ions whose concentration was high in nuclei in the same case.

Discussion

Zinc is involved in energetic metabolism (26), proliferation and apoptosis (27-29) in prostate, therefore it is expectable that zinc may play an important role in prostate cancer pathogenesis (4,30,31). Our results revealed that the base line expression of the anti-apoptic gene Bcl-2 is 4.5-fold higher in 22Rv1 than in PNT1A. This result is in accordance with the previously published reports, where elevated Bcl-2 expression in prostate cancer tumours has been reported (14,16). Furthermore, this elevation was associated with the development of androgen-independent prostate cancer (18) and also with radiotherapy and chemotherapy resistance (13,14,32). Interestingly, we observed further increase in Bcl-2 expression in both cell lines after zinc(II) treatment. However, in the case of 22Rv1 this enhancement in expression was higher, up to 7.5-fold, compared to base line expression of Bcl-2 in PNT1A cell line. Although the exact mechanism remains unclear, our findings suggest that higher zinc(II) ion concentrations in prostate may contribute to prostate tumour therapy resistance associated with elevated Bcl-2 expression.

c-Jun forms homodimers and heterodimers with c-Fos and other Jun-related proteins, which together comprise the AP-1 transcription factor that binds TPA response elements (TREs). Therefore, c-Jun mediates transcriptional regulation in response to a variety of stimuli, including cytokines, growth factors and stress (33). Generally, AP-1 controls a number of cellular processes including differentiation, proliferation, and apoptosis (34). Although there is considerable evidence that c-Jun activation can represent a positive step in the events leading towards apoptosis, there are numerous contrary reports. Possible role of c-Jun in inhibition of apoptosis and promoting of proliferation/cell differentiation is reviewed in ref. 35. Growing amount of such evidence implicates c-Jun in the protection of cells from stress-induced apoptosis. It was reported that cells expressing the Ser63Ala, Ser73Ala mutant of c-Jun are not protected against apoptosis triggered by UV irradiation (36). As 22Rv1 cells show higher viability and proliferation (Fig. 2) after zinc treatment, we can conclude that the increasing expression of c-Jun does not have negative impact on 22Rv1 cells.

NF-κB is a transcription factor, which effect cannot be easily evaluated. Its expression strongly correlates with c-Fos transcription in both cell lines used in our experiments. This finding correlates with known fact that NF-κB enhances c-Fos transcription via the direct binding to a response element situ-

ated in the first intron (37). Surprisingly, only PNT1A cells react on zinc(II) treatment by increased expression of NF-κB. In the case of 22Rv1 we observed no significant changes in NF-κB expression. However, this finding is not in accordance with the previously reported studies that show association of progression of prostate cells toward greater tumourigenic potential with the increasing constitutive levels of NF-κB activity (38,39).

NF-κB is generally viewed as anti-apoptotic and oncogenic. However, recent reports suggest that NF-κB may promote apoptosis and is not necessarily an anti-apoptotic factor in some situations (40). For example, Bohuslav *et al* have shown that p53 stimulates the ribosomal S6 kinase, which in turn phosphorylates the p65/RELA subunit (41). This phosphorylation of p65 was found to reduce its affinity to IκBα, thereby preventing IκBα-mediated nuclear export of NF-κB (41). These results indicate a novel non-classical mechanism of NF-κB activation via p53. However, it is worth mentioning at this point that in contrast to these co-operative efforts between p53 and NF-κB, there have been a few reports which indicate an antagonistic relationship. For instance, it was shown that p53 and NF-κB repress each other by competing for a limiting pool of transcriptional co-activator proteins p300 and CREB-binding protein (CBP) (42). In our study, NF-κB expression after zinc(II) treatment correlates with p53 expression in both cell lines, which supports the previous findings. In our experiments, 22Rv1 did not increase expression of p53 after zinc treatment. It has been reported that metals in general are able to induce formation of reactive oxygen species (ROS) and activate p53-dependend apoptotic pathway (43,44). Moreover, it has been published that p53 activation by ROS is in some cases of metal-based drug treatment necessary for induction of apoptosis (45). Based on our results and previously published studies, it can be expected that low expression of p53 and no significant changes in its expression after zinc treatment may prevent cells from undergoing p53-dependent apoptosis e.g., caused by oxidative stress. However, this expectation needs to be experimentally proven.

Ki-67 is a nuclear protein closely associated with ribosomal RNA transcription and may be crucial for cellular proliferation (46). Inactivation of Ki-67 leads to inhibition of ribosomal RNA synthesis (47). Ki-67 has been established as a promising marker of aggressive prostate cancer. There is plenty of evidence on the overexpression of this protein in prostate cancer (48-52). Our results indicate that 22Rv1 cells express at base line two-fold more Ki-67 than PNT1A cells, in accordance with previously published data. Zinc treatment increased Ki-67 significantly in both tumour and non-tumour cell lines.

Collectively, elevated expression of Ki-67, a marker of proliferation, extremely low expression of p53 and also no changes in expression of p53 after zinc treatment, high expression of Bcl-2, especially after zinc treatment and viability and proliferation curves (Fig. 2) indicate that zinc has significant positive effect on 22Rv1 cell line proliferation and viability.

Acknowledgements

Financial support from CYTORES P301/10/0356, CEITEC CZ.1.05/1.1.00/02.0068 and LPR 2011 and project for conceptual development of research organization 00064203 was greatly acknowledged.

References

1. Bray F, Lortet-Tieulent J, Ferlay J, Forman D and Auvinen A: Prostate cancer incidence and mortality trends in 37 European countries: an overview. Eur J Cancer 46: 3040-3052, 2010.
2. Ghoneum M and Gollapudi S: Susceptibility of the human LNCaP prostate cancer cells to the apoptotic effect of marina crystal minerals (MCM) *in vitro*. Oncol Rep 22: 155-159, 2009.
3. Zaichick VY, Sviridova TV and Zaichick SV: Zinc in human prostate gland: normal, hyperplastic and cancerous. J Radioanal Nucl Chem 217: 157-161, 1997.
4. Costello LC and Franklin RB: Zinc is decreased in prostate cancer: an established relationship of prostate cancer! J Biol Inorg Chem 16: 3-8, 2011.
5. Krizkova S, Blahova P, Nakielna J, *et al*: Comparison of metallothionein detection by using of Brdicka reaction and enzyme-linked immunosorbent assay employing chicken yolk antibodies. Electroanalysis 21: 2575-2583, 2009.
6. Krizkova S, Ryvolova M, Gumulec J, *et al*: Electrophoretic fingerprint metallothionein analysis as a potential prostate cancer biomarker. Electrophoresis 32: 1952-1961, 2011.
7. Krizkova S, Masarik M, Eckschlager T, Adam V and Kizek R: Effects of redox conditions and zinc(II) ions on metallothionein aggregation revealed by chip capillary electrophoresis. J Chromatogr A 1217: 7966-7971, 2010.
8. Bataineh ZM, Hani IHB and Al-Alami JR: Zinc in normal and pathological human prostate gland. Saudi Med J 23: 218-220, 2002.
9. Cory S, Huang DCS and Adams JM: The Bcl-2 family: roles in cell survival and oncogenesis. Oncogene 22: 8590-8607, 2003.
10. Bruckheimer EM, Cho S, Brisbay S, *et al*: The impact of bcl-2 expression and bax deficiency on prostate homeostasis in vivo. Oncogene 19: 2404-2412, 2000.
11. Gastman BR: Apoptosis and its clinical impact. Head Neck-J Sci Spec Head Neck 23: 409-425, 2001.
12. Gross A, McDonnell JM and Korsmeyer SJ: Bcl-2 family members and the mitochondria in apoptosis. Genes Dev 13: 1899-1911, 1999.
13. Anai S, Goodison S, Shiverick K, Hirao Y, Brown BD and Rosser CJ: Knock-down of Bcl-2 by antisense oligodeoxynucleotides induces radiosensitization and inhibition of angiogenesis in human PC-3 prostate tumor xenografts. Mol Cancer Ther 6: 101-111, 2007.
14. Xu L, Yang DJ, Wang SM, *et al*: (-)-gossypol enhances response to radiation therapy and results in tumor regression of human prostate cancer. Mol Cancer Ther 4: 197-205, 2005.
15. Nomura T, Yamasaki M, Nomura Y and Mimata H: Expression of the inhibitors of apoptosis proteins in cisplatin-resistant prostate cancer cells. Oncol Rep 14: 993-997, 2005.
16. Concato J, Jain D, Uchio E, Risch H, Li WW and Wells CK: Molecular markers and death from prostate cancer. Ann Intern Med 150: U595-U596, 2009.
17. Dachille G, Cai T, Ludovico GM, *et al*: Prognostic role of cell apoptotic rate in prostate cancer: outcome of a long-time follow-up study. Oncol Rep 19: 541-545, 2008.
18. Catz SD and Johnson JL: Bcl-2 in prostate cancer: a minireview. Apoptosis 8: 29-37, 2003.
19. Masarik M, Gumulec J, Sztalmachova M, *et al*: Isolation of metallothionein from cells derived from aggressive form of high-grade prostate carcinoma using paramagnetic antibody-modified microbeads off-line coupled with electrochemical and electrophoretic analysis. Electrophoresis 32: 3576-3588, 2011.
20. Babula P, Kohoutkova V, Opatrilova R, Dankova I, Masarik M and Kizek R: Pharmaceutical importance of zinc and metallothionein in cell signalling. Chim Oggi-Chem Today 28: 18-21, 2010.
21. Krizkova S, Fabrik I, Adam V, Hrabeta J, Eckschlager T and Kizek R: Metallothionein - a promising tool for cancer diagnostics. Bratisl Med J-Bratisl Lek Listy 110: 93-97, 2009.
22. Eckschlager T, Adam V, Hrabeta J, Figova K and Kizek R: Metallothioneins and cancer. Curr Protein Pept Sci 10: 360-375, 2009.
23. Adam V, Fabrik I, Eckschlager T, Stiborova M, Trnkova L and Kizek R: Vertebrate metallothioneins as target molecules for analytical techniques. TRAC-Trends Anal Chem 29: 409-418, 2010.
24. Ryvolova M, Adam V and Kizek R: Analysis of metallothionein by capillary electrophoresis (review). J Chromatogr A 1226: 31-42, 2012.
25. Ryvolova M, Krizkova S, Adam V, *et al*: Analytical methods for metallothionein detection. Curr Anal Chem 7: 243-261, 2011.

26. Costello LC, Liu YY, Franklin RB and Kennedy MC: Zinc inhibition of mitochondrial aconitase and its importance in citrate metabolism of prostate epithelial cells. J Biol Chem 272: 28875-28881, 1997.
27. Beyersmann D and Haase H: Functions of zinc in signaling, proliferation and differentiation of mammalian cells. Biometals 14: 331-341, 2001.
28. Baranano DE, Ferris CD and Snyder SH: Atypical neural messengers. Trends Neurosci 24: 99-106, 2001.
29. Hogstrand C, Kille P, Nicholson RI and Taylor KM: Zinc transporters and cancer: a potential role for ZIP7 as a hub for tyrosine kinase activation. Trends Mol Med 15: 101-111, 2009.
30. Costello LC and Franklin RB: The intermediary metabolism of the prostate: A key to understanding the pathogenesis and progression of prostate malignancy. Oncology 59: 269-282, 2000.
31. Gumulec J, Masarik M, Krizkova S, *et al*: Insight to physiology and pathology of zinc(II) ions and their actions in breast and prostate carcinoma. Curr Med Chem 18: 5041-5051, 2011.
32. Scott SL, Higdon R, Beckett L, *et al*: Bcl-2 antisense reduces prostate cancer cell survival following irradiation. Cancer Biother Radiopharm 17: 647-656, 2002.
33. Hess J, Angel P and Schorpp-Kistner M: AP-1 subunits: quarrel and harmony among siblings. J Cell Sci 117: 5965-5973, 2004.
34. Ameyar M, Wisniewska M and Weitzman JB: A role for AP-1 in apoptosis: the case for and against. Biochimie 85: 747-752, 2003.
35. Leppa S and Bohmann D: Diverse functions of JNK signaling and c-Jun in stress response and apoptosis. Oncogene 18: 6158-6162, 1999.
36. Wisdom R, Johnson RS and Moore C: c-Jun regulates cell cycle progression and apoptosis by distinct mechanisms. EMBO J 18: 188-197, 1999.
37. Charital YM, van Haasteren G, Massiha A, Schlegel W and Fujita T: A functional NF-kappaB enhancer element in the first intron contributes to the control of c-fos transcription. Gene 430: 116-122, 2009.
38. Huang L, Kirschke CP and Zhang Y: Decreased intracellular zinc in human tumorigenic prostate epithelial cells: a possible role in prostate cancer progression. Cancer Cell Int 6: 1-10, 2006.
39. Golovine K, Uzzo RG, Makhov P, Crispen PL, Kunkle D and Kolenko VM: Depletion of intracellular zinc increases expression of tumorigenic cytokines VEGF, IL-6 and IL-8 in prostate cancer cells via NF-kappa B-dependent pathway. Prostate 68: 1443-1449, 2008.
40. Radhakrishnan SK and Kamalakaran S: Pro-apoptotic role of NF-kappaB: implications for cancer therapy. Biochim Biophys Acta 1766: 53-62, 2006.
41. Bohuslav J, Chen LF, Kwon H, Mu YJ and Greene WC: p53 induces NF-kappa B activation by an I kappa B kinase-independent mechanism involving phosphorylation of p65 by ribosomal S6 kinase 1. J Biol Chem 279: 26115-26125, 2004.
42. Webster GA and Perkins ND: Transcriptional cross talk between NF-kappaB and p53. Mol Cell Biol 19: 3485-3495, 1999.
43. Chowdhury R, Chowdhury S, Roychoudhury P, Mandal C and Chaudhuri K: Arsenic induced apoptosis in malignant melanoma cells is enhanced by menadione through ROS generation, p38 signaling and p53 activation. Apoptosis 14: 108-123, 2009.
44. Li ZS, Shi KJ, Guan LY, *et al*: ROS leads to MnSOD upregulation through ERK2 translocation and p53 activation in selenite-induced apoptosis of NB4 cells. FEBS Lett 584: 2291-2297, 2010.
45. Bragado P, Armesilla A, Silva A and Porras A: Apoptosis by cisplatin requires p53 mediated p38 alpha MAPK activation through ROS generation. Apoptosis 12: 1733-1742, 2007.
46. Bullwinkel J, Baron-Luhr B, Ludemann A, Wohlenberg C, Gerdes J and Scholzen T: Ki-67 protein is associated with ribosomal RNA transcription in quiescent and proliferating cells. J Cell Physiol 206: 624-635, 2006.
47. Rahmanzadeh R, Huttmann G, Gerdes J and Scholzen T: Chromophore-assisted light inactivation of pKi-67 leads to inhibition of ribosomal RNA synthesis. Cell Prolif 40: 422-430, 2007.
48. Nariculam J, Freeman A, Bott S, *et al*: Utility of tissue microarrays for profiling prognostic biomarkers in clinically localized prostate cancer: the expression of Bcl-2, E-cadherin, Ki-67 and p53 as predictors of biochemical failure after radical prostatectomy with nested control for clinical and pathological risk factors. Asian J Androl 11: 109-118, 2009.
49. Mitra AV, Jameson C, Barbachano Y, *et al*: Elevated expression of Ki-67 identifies aggressive prostate cancers but does not distinguish BRCA1 or BRCA2 mutation carriers. Oncol Rep 23: 299-305, 2010.
50. Khatami A, Hugosson J, Wang WZ and Damber JE: Ki-67 in screen-detected, low-grade, low-stage prostate cancer, relation to prostate-specific antigen doubling time, Gleason score and prostate-specific antigen relapse after radical prostatectomy. Scand J Urol Nephrol 43: 12-18, 2009.
51. Jhavar S, Bartlett J, Kovacs G, *et al*: Biopsy tissue microarray study of Ki-67 expression in untreated, localized prostate cancer managed by active surveillance. Prostate Cancer Prostatic Dis 12: 143-147, 2009.
52. Li RL, Heydon K, Hammond ME, *et al*: Ki-67 staining index predicts distant metastasis and survival in locally advanced prostate cancer treated with radiotherapy: an analysis of patients in radiation therapy oncology group protocol 86-10. Clin Cancer Res 10: 4118-4124, 2004.

INTERNATIONAL JOURNAL OF ONCOLOGY 41: 2237-2244, 2012

MicroRNAs and zinc metabolism-related gene expression in prostate cancer cell lines treated with zinc(II) ions

MARIAN HLAVNA[1,4], MARTINA RAUDENSKA[1,2], KRISTYNA HUDCOVA[1], JAROMIR GUMULEC[1,3], MARKETA SZTALMACHOVA[1,2], VERONIKA TANHÄUSEROVA[1], PETR BABULA[4], VOJTECH ADAM[2,3], TOMAS ECKSCHLAGER[5], RENE KIZEK[2,3] and MICHAL MASARIK[1,3]

[1]Department of Pathological Physiology, Faculty of Medicine, Masaryk University, CZ-625 00 Brno; [2]Department of Chemistry and Biochemistry, Mendel University in Brno, CZ-613 00 Brno; [3]Central European Institute of Technology, Brno University of Technology, CZ-616 00 Brno; [4]Department of Natural Drugs, Faculty of Pharmacy, University of Veterinary and Pharmaceutical Sciences, CZ-612 42 Brno; [5]Department of Paediatric Haematology and Oncology, Second Faculty of Medicine, Charles University and University Hospital Motol/V Uvalu 84, CZ-150 06 Prague 5, Czech Republic

Received July 10, 2012; Accepted September 13, 2012

DOI: 10.3892/ijo.2012.1655

Abstract. MicroRNAs (miRNAs) are a large class of single-stranded RNA molecules involved in post-transcriptional gene silencing. miRNAs not only regulate various developmental and physiological processes but also are involved in cancer development. Additionally, they can be considered as biomarkers of some pathological processes. The aim of this study was to determine the expression levels of selected miRNA and zinc(II)-related genes (*ZIP-1*, *BAX*, *MT2A* and *MT1A*) in the non-tumor PNT1A prostate cell line in comparison with the prostate cancer cell lines 22Rv1, PC-3 and LNCaP after zinc(II) treatment. Using bioinformatic approaches we selected miRNAs with putative binding sites in the 3'UTR regions in Metallothionein 1A and 2A as miRNA 23a, 141, 224, 296-3p, 320, 375 and 376. We observed significantly higher expression of miRNA 23a in all tumor lines compared to non-tumor PNT1A (13.6-fold in 22Rv1, 7.3-fold in PC-3, 8.3-fold in LNCaP, $p<0.01$). We also observed that the 22Rv1 cell line has significantly higher expression of miRNA 224 in comparison to other cell lines. In addition, all tumor cell lines expressed significantly higher levels of miRNA 375 in comparison to non-tumor PNT1A (87.1-fold in 22Rv1, nearly 2,000-fold in PC-3, 56.3-fold in LNCaP, $p<0.01$). Nevertheless, miRNA 375 and 23a expression levels strongly suggest their potential to contribute to the diagnosis of prostate cancer and miRNA 224 eventually may be suitable for classification of primary tumors. The expression of miRNA 224 in 22Rv1 cell line was negatively correlated with increasing zinc(II) concentration only. Our experiments revealed significant negative correlation of miRNA 376 and *MT2A* in 22Rv1 and a negative correlation between miRNA 224 and *MT1A* in PC-3 cells which may denote possible direct regulation of *MT* genes by specific miRNAs in prostate cancer.

Correspondence to: Dr Michal Masarik, Department of Pathological Physiology, Faculty of Medicine, Masaryk University, Kamenice 5, CZ-625 00 Brno, Czech Republic
E-mail: masarik@med.muni.cz

Key words: miRNA, prostate cancer, polymerase chain reaction, metallothionein, zinc(II) ions

Introduction

Prostate cancer is the most frequently diagnosed cancer in men in Western countries (1). The therapeutic success of prostate cancer treatment can be enormously improved if the disease is diagnosed soon. Thus, the search for suitable biomarkers used for early detection of the presence and progression of the disease, as well as the prediction after the clinical interventions is ongoing. The current prostate cancer biomarkers do not fulfill all a forementioned requirement as there remains a lack of reliable biomarkers that can specifically distinguish between those patients who should be treated adequately to stop the aggressive form of the disease and those who should avoid overtreatment of the indolent form (2). Specific microRNAs (miRNAs) have been shown to serve key functional roles in prostate cancer (PC) cells, as discovered mainly by overexpression and knockdown experiments in cell cultures (3-5). Key cellular processes such as proliferation, apoptosis, survival, invasion, migration, cell cycle progression and androgen signaling, are regulated by miRNAs in PC cells (6-8). From biochemical point of view, miRNAs are small, phylogenetically conserved, noncoding RNAs that are able to regulate expression of at least 30% of all protein encoding genes (9). Mature miRNAs are involved in post-transcriptional gene silencing. They arise from intergenic or intragenic (both exonic and intronic) genomic regions that are transcribed as long primary transcripts. Recently, miRNAs have received attention as potential cancer diagnostic markers and therapeutic targets (10). miRNA expression profiles have been shown to classify different cancers and identify cancer tissue origins (11). Deregulated miRNA expression was reported in various human cancers including prostate cancer (12). Of particular note is

the polycistronic set of microRNAs consisting of miRNA 17, miRNA 18, miRNA 19a, miRNA 19b and miRNA 92, which are overexpressed in leukemic lines compared with the other cell lines (11). miRNAs expressions can also predict prostate cancer biochemical relapse and are involved in tumor progression (10). miRNA 375 was considered as useful to identify patients with metastatic disease as well as for a positive lymph node status. miRNA 141 was identified as upregulated in the serum of patients with higher grade prostate tumors (13).

The changes of miRNA synthesis profile can be related to changes in prostate cell metabolism. Among metabolic changes, prostate cancer cells have altered ability to uptake and to accumulate zinc(II) ions compared to healthy prostate tissue (14) and one can suggest that miRNAs could be somewhat connected with this phenomenon. Zinc(II) ions themselves play a role in proliferation, differentiation regulation and apoptosis in prostate (15,16). Extracellular zinc(II) ions can increase the formation of insulin-like growth factor (IGF) (17) and stimulate the epidermal growth factor-receptor (EGF-R) (18). At the level of protein phosphorylation uptake of zinc(II) and/or their releasing from zincosomes can modulate the activity of cyclic nucleotide phosphodiesterase (PDE) (19), mitogen-activated protein kinase (MAPK) (20), protein kinase C (PKC), protein tyrosine phosphatases (PTP), Ca(II)-calmodulin activated protein kinase-2 (CaMPK-2) and P70S6 kinase (P70S6K) (21). Altogether with the fact that zinc(II) is involved in apoptosis via translocation of existing resident cytosolic Bax to mitochondria and its increasing total cellular Bax level (22), it is highly likely that zinc(II) plays an important role in prostate cancer pathogenesis (23).

In light of above mentioned facts, it can be assumed that altered zinc(II) metabolism will have a great impact on prostate cancer tumorigenesis. Zinc(II) homeostasis and metabolism in healthy and tumor tissues are maintained mainly by two types of proteins: i) zinc-binding proteins [mostly by metallothioneins, a family of low-molecular-mass (6-10 kDa) proteins characterized by a high cysteine content and a high binding capacity for post-transition metal ions (24)], which act as buffer and donor of zinc(II) for intracellular processes and ii) zinc transporters (ZIP and ZnT protein families), which are responsible for zinc(II) fluxes into/from cells and organelles, because zinc(II) can not freely pass though membranes (25).

In this study we focused on synthesis of miRNAs as miRNA 23a, 141, 224, 296-3p, 320, 375 and 376, which have putative binding sites within 3'UTR of metallothionein genes (*MT2A, MT1A*) in the non-tumor PNT1A prostate cell line and prostate cancer cell lines 22Rv1, PC-3, and LNCaP treated with zinc(II) ions. Our previous studies have provided the evidence of the association between metallothionein (MT) expression and prostate tumor progression (26). Post-transcriptional gene silencing can be involved in metallothionein regulation and different levels of miRNAs in tumor and non-tumor lines can be expected. Therefore, we also determined expression levels of *ZIP-1*, *BAX*, *MT2A* and *MT1A* genes in the treated cell lines.

Materials and methods

Chemical and biochemical reagents. RPMI-1640 medium, Ham's F12 medium, fetal bovine serum (FBS) - mycoplasma free, penicillin/streptomycin and trypsin EDTA were purchased from PAA Laboratories GmbH (Pasching, Austria). PBS was purchased from Invitrogen Corp. (Carlsbad, CA, USA). EDTA, zinc(II) sulfate, RIPA buffer and all other chemicals of ACS purity were purchased from Sigma Aldrich Co. (St. Louis, MO, USA), unless noted otherwise.

miRNA selection. Software Targetscan (http://www.targetscan.org) was used for the selection of suitable miRNAs. miRNAs were selected according to the putative binding sites within 3'UTR of metallothionein genes (*MT2A, MT1A*).

Cell cultures. Four human prostatic cell lines were used in this study: i) PNT1A human cell line established by immortalisation of normal adult prostatic epithelial cells by transfection with a plasmid containing SV40 genome with a defective replication origin. The primary culture was obtained from the prostate of a 35-year-old male at post mortem; ii) cell line 22Rv1 has been derived from a primary human prostatic carcinoma xenograft, CWR22R. iii) LNCaP cells are androgen-sensitive human prostate adenocarcinoma cells derived from the left supraclavicular lymph node metastasis from a 50-year-old Caucasian male; iv) PC-3 human cell line established from a grade 4 androgen independent and unresponsive prostatic adenocarcinoma from 62-year-old Caucasian male and derived from metastatic site in bone. All cell lines used in this study were purchased from Health Protection Agency Culture Collections (Salisbury, UK).

Culture conditions. PNT1A, LNCaP and 22Rv1 cells were cultured in RPMI-1640 medium with 10% FBS. PC-3 cells were cultured in Ham's F12 medium with 7% FBS. All media were supplemented with penicillin (100 U/ml) and streptomycin (0.1 mg/ml), and the cells were maintained at 37˚C in a humidified incubator (Sanyo, Japan) with 5% CO_2. The sub-cultivations of all cell lines were carried out within the range from 10 to 35 h.

Zinc(II) treatment. Cells were treated with five concentrations of $ZnSO_4$ (0-90 μmol/l) at 37˚C for 48 h after cells reached ~50% confluence. Cells were then harvested and washed four times with 1X PBS, pH 7.4.

RNA and miRNA isolation and reverse transcription. High pure total-RNA isolation kit (Roche, Basel, Switzerland) was used for RNA isolation and high pure miRNA isolation kit for miRNA isolation. For both isolations the medium was removed and samples were twice washed with 5 ml of ice-cold PBS. Cells were scraped off, transferred to clean tubes and centrifuged at 20,800 x g for 5 min at 4˚C. After this step, lysis buffer was added and RNA isolation was carried out according to manufacturer's instructions. Isolated RNA and miRNA was used for cDNA synthesis. RNA (600 ng) was transcribed using Transcriptor first strand cDNA synthesis kit (Roche, Switzerland) and 10 ng of miRNA was transcribed using TaqMan® microRNA reverse transcription kit (Applied Biosystems, Carlsbad, CA, USA) according to manufacturer's instructions. Prepared cDNA (20 μl) from total-RNA was diluted with RNase-free water to 100 μl and 5 μl was directly analyzed by 7500 real-time PCR system (Applied Biosystems). In case of miRNA analysis 1.33 μl of transcribed miRNA was used directly in real-time PCR reaction according to manufacturer's instruction.

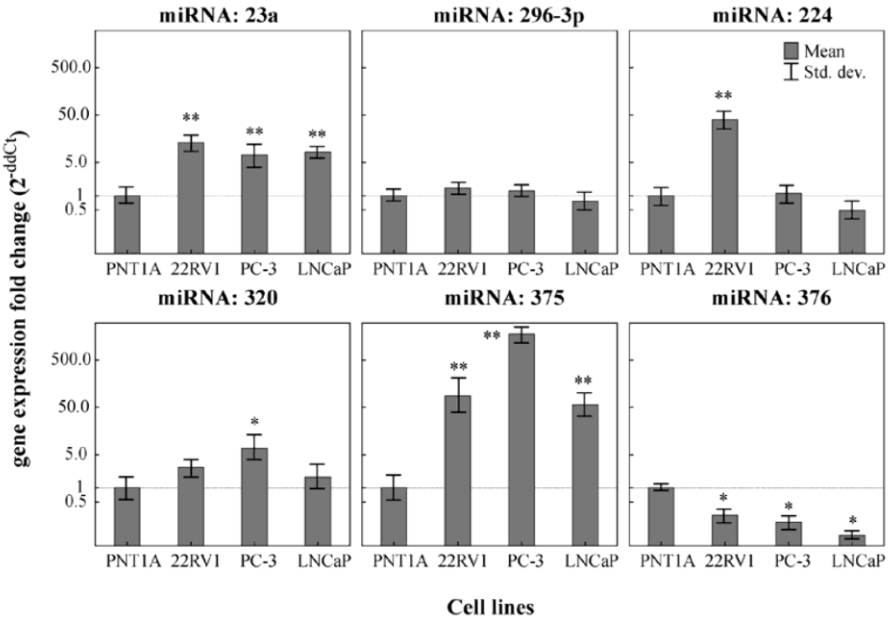

Figure 1. miRNA expression levels without zinc(II) treatment in 22Rv1, PC-3 and LNCaP cell lines relative to non-tumor PNT1A cell line. Base line transcription level of selected miRNAs was conducted by RT-PCR. For other experimental parameters see Materials and methods. *p<0.05; **p<0.01.

Quantitative polymerase chain reaction (q-PCR). Q-PCR was performed in triplicate using the TaqMan gene expression assay system with the 7500 real-time PCR system (Applied Biosystems) and the amplified DNA was analyzed by the comparative Ct method using β-actin as an endogenous control for metallothionein *MT1A* and *MT2A*, *Bax* and *ZIP-1* gene expression quantification. The primer and probe sets for *β-actin* (assay ID: *Hs99999903_m1*), *MT1A* (assay ID: *Hs00831826_s1*), *MT2A* (*Hs02379661_g1*) *ZIP-1* (Hs00205358_m1) and *Bax* (Hs00180269_m1) were selected from TaqMan gene expression assays. Primer probe sets for quantification hsa-miRNA-23a (assay ID: 000399), hsa-miR-141 (assay ID: 000463), hsa-miR-224 (assay ID: 002099), hsa-miR-296 (assay ID: 000527), hsa-miR-320 (assay ID: 002277), hsa-miR-375 (assay ID: 000564), hsa-miR-376 (assay ID: 000565) were selected from TaqMan miRNA expression assays. Q-PCR was performed under the following amplification conditions: total volume of 20 μl, initial incubation 50˚C/2 min followed by denaturation 95˚C/10 min, then 45 cycles 95˚C/15 sec, 60˚C/1 min.

Statistics. The data were analyzed using StatSoft Statistica version 10 (www.statsoft.com). Mann-Whitney U test was used to reveal differences in the gene expression. Associations within variables were determined using the Pearson correlation. $p<0.05$ was considered significant.

Results

miRNA and mRNA baseline expression without zinc(II) treatment. Primarily, we aimed at determination of baseline level of six miRNAs (23a, 296-3p, 224, 320, 375 and 376) selected according to the putative binding sites within 3'UTR of metallothionein genes (*MT2A, MT1A*) and genes *MT1A*, *MT2A*, *ZIP-1* and *BAX* in cell lines used in this study as PNT1A (control) and 22Rv1, LNCaP and PC-3 (cancer cell lines). The relative expression of miRNAs and mRNAs in tumor cell lines was expressed as a relative expression fold change compared to the baseline expression of non-tumor PNT1A cell line.

The differences in expression of particular miRNAs are shown in Fig. 1. We observed significantly higher relative expression of miRNA 23a in all tumor lines compared to non-tumor PNT1A (13.6-fold in 22Rv1, 7.3-fold in PC-3, 8.3-fold in LNCaP, $p<0.01$). Similarly, all tumor lines expressed miRNA 375 in significantly higher levels in comparison with non-tumor PNT1A (87.1-fold in 22Rv1, 1776.7-fold in PC-3, 56.3-fold in LNCaP, $p<0.01$). On the contrary, lower relative expression of miRNA 376 in all tumor lines in comparison with non-tumor PNT1A was observed (3-fold in 22Rv1, 5-fold in PC-3, 10-fold in LNCaP, $p<0.05$). We also found significantly higher ($p<0.05$) relative expression of miRNA 320 in PC-3 line compared to other tumor and non-tumor lines. Significantly higher ($p<0.01$) expression of miRNA 224 in 22Rv1 line compared to other lines has been observed and no differences between cell lines were observed in expression of miRNA 296-3p.

The differences in expression of the selected mRNAs among cell lines are shown in Fig. 2. The expression of Bax mRNA is significantly higher in LNCaP cell line (10.5-fold, $p=0.03$) in comparison with non-tumor PNT1A. Level of MT1A expression in 22Rv1 cell line is higher with marginal significance (1.8-fold, $p=0.055$) in comparison with PNT1A. On the other hand significantly higher MT1A expression is found in LNCaP and PC-3 cell lines (10-fold, $p=0.03$) with comparison to relative expression in PNT1A. The expression of MT2A was higher in all tumor lines in comparison with PNT1A (2.0-fold, $p=0.05$ in

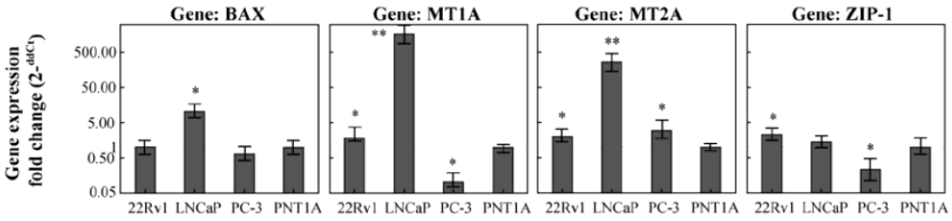

Figure 2. mRNA baseline expression levels of selected genes without zinc(II) treatment in 22Rv1, PC-3 and LNCaP cell lines relative to non-tumor PNT1A cell line. Base line transcription level of selected genes (*BAX*, *MT1A*, *MT2A* and *ZIP-1*) was conducted by RT-PCR. For other experimental parameters see Materials and methods. *p<0.05; **p<0.002.

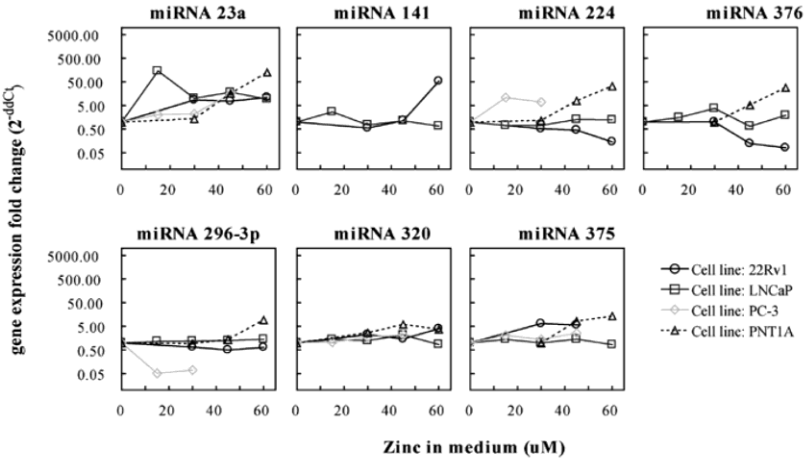

Figure 3. Gene expression fold change of selected miRNAs after zinc(II) treatment. MiRNA 23a shows significant elevating trend after zinc(II) treatment in all cell lines. Other miRNAs demonstrate cell line-specific trends. For other experimental parameters see Materials and methods.

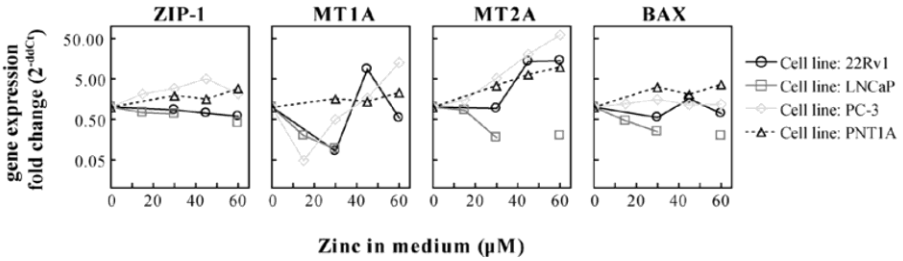

Figure 4. Dependence between mRNA expression levels and zinc(II) concentration in medium. Level of *MT2A* expression in PC3 and 22Rv1 cell lines and *ZIP-1* in PNT1A cell line were significantly increased by the zinc(II) treatment. Expression of *ZIP-1* in LNCaP cell line was significantly decreased by increasing zinc(II) concentration. For other experimental parameters see Materials and methods.

22Rv1, 261.4-fold, p=0.002 in LNCaP, and 2.9-fold, p=0.05 in PC-3 cell line). Moreover, we observed higher relative expression of ZIP-1 in 22Rv1 (2.3-fold, p=0.05) and lower relative expression of ZIP-1 in PC-3 cell line compared to non-tumor PNT1A (5-fold, p=0.05).

miRNA and mRNA expression after zinc(II) treatment. In addition, we determined expression levels of selected miRNA after zinc(II) treatment. Trends in miRNA expressions under zinc(II) treatment are shown in Fig. 3. MiRNA 23a shows significant elevating trend after zinc(II) treatment in all cell lines (11-, 9-, 16- and 128-fold in 22Rv1, LNCaP, PC-3 and PNT1A in the highest zinc(II) concentrations). Other miRNAs demonstrate cell line-specific trends. Expressions of, miRNA 320 in PC3 (up to 2.2-fold, r=0.96 at p=0.038) and miRNA 375 in PNT1A cell line (up to 38-fold, r=0.98 at p=0.014) were significantly elevated after zinc(II) addition. In addition, miRNA 296-3p showed subtle (1.4-fold), but highly significant increase (r=0.98 at p=0.005) in

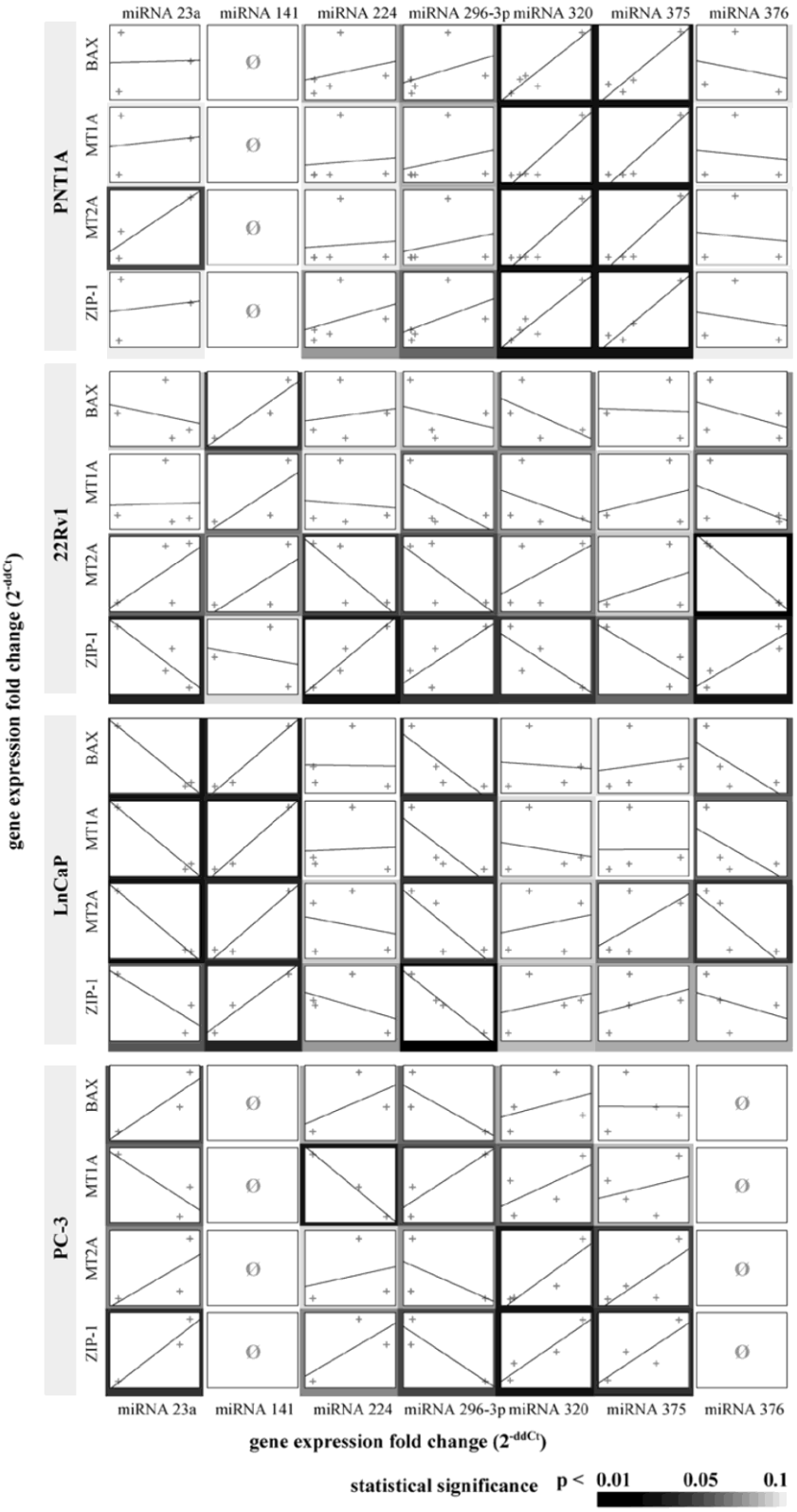

Figure 5. Correlation between miRNA and mRNA expression levels. The shade of the boxes shows the significance of the correlation. The darker the bracket is, the more significant is the correlation. Ø, undetectable.

LNCaP. Expression of miRNA 224 in 22Rv1 cell line was negatively correlated with zinc(II) concentration (7-fold decrease, r=-0.98 at p=0.015). Change in other miRNAs' levels was also observed, however, below the level of statistical significance.

Results of *ZIP-1*, *BAX*, *MT2A* and *MT1A* gene expressions after zinc(II) treatment are shown in Fig. 4. Level of *MT2A* expression in PC3 and 22Rv1 cell lines (r=0.86 at p=0.05 and r=0.93 at p=0.021) and *ZIP-1* in PNT1A (r=0.89 at p=0.04) cell line were significantly increased by the zinc(II) treatment. Expression of *ZIP-1* in LNCaP cell line was significantly decreased by the increasing zinc(II) concentration (r=-0.96 at p=0.01).

To determine the relationship between miRNA 23a, 141, 224, 296-3p, 320, 375 and 376 expression profiles of our cell lines and selected mRNA expressions, correlation analysis was performed (Fig. 5). In general, we expected negative correlations between miRNA and their potential mRNA targets as the miRNAs downregulate post-transcription processes of mRNAs. In the 22Rv1 line a negative correlation between miRNA 376 and *MT2A* was found (r=-1.0, p=0.0001). In the PC-3 line a negative correlation between miRNA 224 and *MT1A* was observed (r=-0.99, p=0.07). In LNCaP cell line, we found negative correlation between miRNA 296-3p and *ZIP-1* (r=-0.99, p=0.01). No significant correlation in the PNT1A line was found. Moreover, significant positive correlation was observed between miRNA 224 and *ZIP-1* in the 22Rv1 cell line (r=0.96, p=0.04).

Discussion

Cancer is characterized by abnormal and uncontrolled cell division, a phenotype that arises from the misregulation of several genes. miRNAs are major regulators of gene expression, with roles in nearly every area of cell biological functions, development and survival. Therefore, it is not surprising that miRNAs are actively altered in all types of cancers (27), acting as oncogenes or tumor suppressor genes. Main criteria for the selection of all miRNAs in our study was putative binding sites in 3'UTR regions in metallothionein 1A and 2A and thus their possible role in the metallothionein regulation.

Porkka *et al* found that miRNA 23a and miRNA 23b are significantly decreased in human prostate cancer in comparison with BPH (benign prostatic hyperplasia) tissue (12). Conversely, our experiments show that level of miRNA 23a in prostate cancer cell lines is increased compared with non-tumor PNT1A cell line. We assume an association between zinc(II) metabolism and miRNAs because BPH is known for its opposite zinc(II) metabolism compared to healthy tissue and prostate cancer cells. While prostate cancer cells have decreased ability to uptake zinc(II) ions, BPH accumulates zinc(II) in higher amounts compared to 'healthy' prostate cells (14,28-30). Besides the miRNA 23a, no other miRNA studied here showed similar trend in the cell lines. On the other hand Gao *et al* reported that the c-Myc oncogenic transcription factor transcriptionally represses miR-23a and miR-23b (31). Nevertheless, the role and function of altered miRNA 23a in prostate cancer cells and BPH remain still unknown.

The miRNA 224 is located in malignancy-associated chromosomal region. It was published that this region shows increased gene expression in some human prostate cancer cells (32). Consistent with this study we observed specific upregulation of miRNA 224 in 22Rv1 line compared to others. The 22Rv1 line was derived from a human prostatic carcinoma xenograft, CWR22R, a primary tumor of prostate cancer. Apart from prostate tumors, elevation of miRNA 224 was described in other tumors. Profiling miRNA expression in hepatocellular carcinoma by Wang *et al* revealed miRNA 224 upregulation (33). Furthermore, consistent with the microarray data, Prueitt *et al* found a significantly higher expression of mature miRNA 224 in PNI (perineural invasion) tumors when compared with non-PNI tumors (34). Collectively, our results suggest that miRNA 224 is a promising biological marker of aggressive metastatic forms of prostate cancer and this miRNA should undergo further investigation also on primary tumors.

All prostate tumor cell lines overexpressed miRNA 375 in our experiments. Szczyrba *et al* previously found that miRNA 375 was upregulated in primary prostate cancer tissue (35), while this miRNA was downregulated in head and neck squamous cell carcinoma (36), esophagus (37), as well as in hepatocellular carcinoma (38). Poor outcome and relapse were associated with elevated levels of miR 375 in gastric carcinoma (39). Likewise, miRNA 375 is overexpressed in breast carcinoma, where it induces cell proliferation via a positive feed-back-loop with the estrogen receptor-α (40). As the expression of the estrogen receptor-α and receptor-β are increased during CaP development (41), it is possible that overexpression of miRNA 375 enhances the progression of this tumor. Moreover, Ladeiro *et al* (38) reported that the reduction of miRNA 375 expression was correlated to the expression of β-catenin. Based on their results, Ladeiro *et al* suggest β-catenin as a positive regulator of miRNA 375 expression. Moreover, β-catenin levels have been found to be increased in prostate cancer. Thus, our results are in concondance with the previously described data as we found increased levels of miRNA 375 in all tumor cell lines.

Key objective of this study was to describe the association of miRNAs and zinc(II)-associated genes. Metallothionein expression was shown to correlate strongly with Gleason score ($p<0.001$) and significantly with pathological staging and Ki-67 immunostaining ($p<0.001$, $p<0.05$, respectively) (42). Our previous study also provided evidence of the association between metallothionein (MT) expression and prostate tumor progression (43). In this study we found significantly increased mRNA levels of *MT2A* isoform in tumor cell lines. Our previous work also suggests *MT2A* is a major isoform of MT in prostate (43,44). Contrary to mRNA, significantly reduced level of MT protein in tumor lines was observed. Due to these facts, post-transcriptional gene silencing can be involved and different levels of miRNAs in tumor and non-tumor lines can be expected. None of the miRNA analyzed here correlated with MT mRNA level after zinc(II) treatment in the prostate cell lines. It can be assumed according to our results that miRNAs act differently in each cell line. In the 22Rv1 tumor line a negative correlation between miRNA 376 and *MT2A* isoform was found. In the PC-3 line a negative correlation between miRNA 224 and *MT1A* was seen. Despite the observed negative correlations between miRNAs and MT after zinc(II) treatment, further exeriments to prove these findings in tissues and patient samples are required.

In terms of other genes involved in zinc(II) metabolism, the baseline expression of Bax mRNA was significantly higher in LNCaP cell line in comparison with non-tumor PNT1A. High

Bax protein expression was shown by Amirghofran *et al* in prostate cancer tissue samples (45). They found a significant correlation between Bax expression and stage of carcinoma, but not with the apoptosis index, suggesting the presence of a non-functional Bax protein or the role of other proapoptotic molecules. Despite of increased level of Bax, we did not observe the enhanced apoptosis in LNCaP cell line compared to other cell lines, which supports the results of Amirghofran *et al* (45).

We observed higher relative expression of *ZIP-1* mRNA in 22Rv1 and lower relative expression of *ZIP-1* in PC-3 cell line compared to non-tumor PNT1A. These findings are not in conflict with the published data. Franklin *et al* (46) and others showed that *ZIP-1* gene expression is downregulated and zinc(II) is depleted in adenocarcinomatous glands since early stages of cancer. Nevertheless, prostate cancer cell lines still retain the ability to express ZIP-1 gene due to its downregulation by RREB zinc finger and not fatal mutations (47,48). These authors did not preclude other regulatory pathways affecting ZIP-1 expression. However, we discovered strong positive correlation between miRNA 224 and ZIP-1 expression in 22Rv1. miRNA 224 expression was significantly elevated in 22Rv1. In light of these findings, we speculate that miRNA 224 serves as another potential regulator of ZIP-1 expression. Nevertheless, no 3'UTR putative binding site of ZIP-1 mRNA for any of miRNAs studied was identified using Targetscan software (http://www.targetscan.org). Thus, this correlation can either be considered as a coincidence or miRNA 224 can affect ZIP-1 expression through other, yet unidentified mediators. These fragmentary results suggest that the area deserves further research.

Nevertheless, miRNA 375 and 23a expression levels strongly suggest their potential to contribute to the diagnosis of prostate cancer and miRNA 224 might be suitable for classification of primary tumors. Since it is also possible to assess miRNA expression patterns in urine (49) or blood serum (50), these miRNAs have the potential of being valuable biomarkers for the diagnosis and prognosis of prostate cancer. An advantage of miRNA analysis is that their molecular features reduce their susceptibility to degradate in archived tissue and samples and allows application of miRNA profiling both on diagnosis and prognosis. Although computer analysis provides data regarding miRNA to metallothionein 3'UTR, the experiment results are ambiguous, pointing to cell line-specific associations between MT and selected miRNAs. Despite the huge progress in miRNA research, we are still far away from a clear genetic demonstration of the involvement of a specific miRNA in the occurrence or progression of a specific tumor.

Acknowledgements

Financial support from NanoBioTECell GA ČR P102/11/1068, doc Ceitec.02/2012 (JG), *CEITEC* CZ.1.05/1.1.00/02.0068 and project for conceptual development of research organization 00064203 is highly acknowledged.

References

1. Haas GP, Delongchamps N, Brawley OW, Wang CY and de La Roza G: The worldwide epidemiology of prostate cancer: perspectives from autopsy studies. Can J Urol 15: 3866-3871, 2008.
2. Madu CO and Lu Y: Novel diagnostic biomarkers for prostate cancer. J Cancer 1: 150-177, 2010.
3. Folini M, Gandellini P, Longoni N, *et al*: miR-21: an oncomir on strike in prostate cancer. Mol Cancer 9: 12, 2010.
4. Kojima K, Fujita Y, Nozawa Y, Deguchi T and Ito M: MiR-34a attenuates paclitaxel-resistance of hormone-refractory prostate cancer PC3 cells through direct and indirect mechanisms. Prostate 70: 1501-1512, 2010.
5. Noonan EJ, Place RF, Basak S, Pookot D and Li LC: miR-449a causes Rb-dependent cell cycle arrest and senescence in prostate cancer cells. Oncotarget 1: 349-358, 2010.
6. Brase JC, Johannes M, Schlomm T, *et al*: Circulating miRNAs are correlated with tumor progression in prostate cancer. Int J Cancer 128: 608-616, 2011.
7. Ozen M, Creighton CJ, Ozdemir M and Ittmann M: Widespread deregulation of microRNA expression in human prostate cancer. Oncogene 27: 1788-1793, 2008.
8. Cronauer MV, Schulz WA, Burchardt T, *et al*: The androgen receptor in hormone-refractory prostate cancer: relevance of different mechanisms of androgen receptor signaling (Review). Int J Oncol 23: 1095-1102, 2003.
9. He L and Hannon GJ: MicroRNAs: small RNAs with a big role in gene regulation. Nat Rev Genet 5: 522-531, 2004.
10. Fendler A, Jung M, Stephan C, *et al*: miRNAs can predict prostate cancer biochemical relapse and are involved in tumor progression. Int J Oncol 39: 1183-1192, 2011.
11. Gaur A, Jewell DA, Liang Y, *et al*: Characterization of microRNA expression levels and their biological correlates in human cancer cell lines. Cancer Res 67: 2456-2468, 2007.
12. Porkka KP, Pfeiffer MJ, Waltering KK, Vessella RL, Tammela TLJ and Visakorpi T: MicroRNA expression profiling in prostate cancer. Cancer Res 67: 6130-6135, 2007.
13. Kelly BD, Miller N, Healy NA, Walsh K and Kerin MJ: A review of expression profiling of circulating microRNAs in men with prostate cancer. BJU Int: May 22, 2012 (Epub ahead of print).
14. Costello LC and Franklin RB: Zinc is decreased in prostate cancer: an established relationship of prostate cancer! J Biol Inorg Chem 16: 3-8, 2011.
15. Gumulec J, Masarik M, Krizkova S, *et al*: Insight to physiology and pathology of zinc(II) ions and their actions in breast and prostate carcinoma. Curr Med Chem 18: 5041-5051, 2011.
16. Beyersmann D and Haase H: Functions of zinc in signaling, proliferation and differentiation of mammalian cells. Biometals 14: 331-341, 2001.
17. Haase I, Evans R, Pofahl R and Watt FM: Regulation of keratinocyte shape, migration and wound epithelialization by IGF-1- and EGF-dependent signalling pathways. J Cell Sci 116: 3227-3238, 2003.
18. Samet JM, Dewar BJ, Wu WD and Graves LM: Mechanisms of Zn(2+)-induced signal initiation through the epidermal growth factor receptor. Toxicol Appl Pharmacol 191: 86-93, 2003.
19. Percival MD, Yeh B and Falgueyret JP: Zinc dependent activation of cAMP-specific phosphodiesterase (PDE4A). Biochem Biophys Res Commun 241: 175-180, 1997.
20. Hogstrand C, Kille P, Nicholson RI and Taylor KM: Zinc transporters and cancer: a potential role for ZIP7 as a hub for tyrosine kinase activation. Trends Mol Med 15: 101-111, 2009.
21. Yamasaki S, Sakata-Sogawa K, Hasegawa A, *et al*: Zinc is a novel intracellular second messenger. J Cell Biol 177: 637-645, 2007.
22. Feng P, Li TL, Guan ZX, Franklin RB and Costello LC: The involvement of Bax in zinc-induced mitochondrial apoptogenesis in malignant prostate cells. Mol Cancer 7: 25, 2008.
23. Huynh H: Induction of apoptosis in rat ventral prostate by finasteride is associated with alteration in MAP kinase pathways and Bcl-2 related family of proteins. Int J Oncol 20: 1297-1303, 2002.
24. Eckschlager T, Adam V, Hrabeta J, Figova K and Kizek R: Metallothioneins and cancer. Curr Protein Pept Sci 10: 360-375, 2009.
25. Eide DJ: Zinc transporters and the cellular trafficking of zinc. Biochim Biophys Acta 1763: 711-722, 2006.
26. Sztalmachova M, Hlavna M, Gumulec J, *et al*: Effect of zinc(II) ions on the expression of pro- and anti-apoptotic factors in high-grade prostate carcinoma cells. Oncol Rep 28: 806-814, 2012.
27. Croce CM: Causes and consequences of microRNA dysregulation in cancer. Cell Oncol 32: 161-162, 2010.
28. Bataineh ZM, Hani IHB and Al-Alami JR: Zinc in normal and pathological human prostate gland. Saudi Med J 23: 218-220,

29. Goel T and Sankhwar SN: Comparative study of zinc levels in benign and malignant lesions of the prostate. Scand J Urol Nephrol 40: 108-112, 2006.
30. Sapota A, Darago A, Taczalski J and Kilanowicz A: Disturbed homeostasis of zinc and other essential elements in the prostate gland dependent on the character of pathological lesions. Biometals 22: 1041-1049, 2009.
31. Gao P, Tchernyshyov I, Chang TC, *et al*: c-Myc suppression of miR-23a/b enhances mitochondrial glutaminase expression and glutamine metabolism. Nature 458: 762-765, 2009.
32. Glinsky GV, Krones-Herzig A and Glinskii AB: Malignancy-associated regions of transcriptional activation: Gene expression profiling identifies common chromosomal regions of a recurrent transcriptional activation in human prostate, breast, ovarian, and colon cancers. Neoplasia 5: 218-228, 2003.
33. Wang Y, Lee ATC, Ma JZI, *et al*: Profiling microRNA expression in hepatocellular carcinoma reveals microRNA-224 up-regulation and apoptosis inhibitor-5 as a microRNA-224-specific target. J Biol Chem 283: 13205-13215, 2008.
34. Prueitt RL, Yi M, Hudson RS, *et al*: Expression of microRNAs and protein-coding genes associated with perineural invasion in prostate cancer. Prostate 68: 1152-1164, 2008.
35. Szczyrba J, Nolte E, Wach S, *et al*: Downregulation of Sec23A protein by miRNA-375 in prostate carcinoma. Mol Cancer Res 9: 791-800, 2011.
36. Tsukamoto Y, Nakada C, Noguchi T, *et al*: MicroRNA-375 is downregulated in gastric carcinomas and regulates cell survival by targeting PDK1 and 14-3-3 zeta. Cancer Res 70: 2339-2349, 2010.
37. Mathe EA, Nguyen GH, Bowman ED, *et al*: microRNA expression in squamous cell carcinoma and adenocarcinoma of the esophagus: associations with survival. Clin Cancer Res 15: 6192-6200, 2009.
38. Ladeiro Y, Couchy G, Balabaud C, *et al*: microRNA profiling in hepatocellular tumors is associated with clinical features and oncogene/tumor suppressor gene mutations. Hepatology 47: 1955-1963, 2008.
39. Zhang X, Yan Z, Zhang J, *et al*: Combination of hsa-miR-375 and hsa-miR-142-5p as a predictor for recurrence risk in gastric cancer patients following surgical resection. Annal Oncol 22: 2257-2266, 2011.
40. Simonini PDR, Breiling A, Gupta N, *et al*: Epigenetically deregulated microRNA-375 is involved in a positive feedback loop with estrogen receptor alpha in breast cancer cells. Cancer Res 70: 9175-9184, 2010.
41. Ito T, Tachibana M, Yamamoto S, Nakashima J and Murai M: Expression of estrogen receptor (ER-alpha and ER-beta) mRNA in human prostate cancer. Eur Urol 40: 557-563, 2001.
42. Athanassiadou P, Bantis A, Gonidi M, *et al*: The expression of metallothioneins on imprint smears of prostate carcinoma: correlation with clinicopathologic parameters and tumor proliferative capacity. Tumori 93: 189-194, 2007.
43. Gumulec J, Masarik M, Krizkova S, *et al*: Evaluation of alpha-methylacyl-CoA racemase, metallothionein and prostate specific antigen as prostate cancer prognostic markers. Neoplasma 59: 191-200, 2012.
44. Masarik M, Gumulec J, Hlavna M, *et al*: Monitoring of the prostate tumour cells redox state and real-time proliferation by novel biophysical techniques and fluorescent staining. Integr Biol 4: 672-684, 2012.
45. Amirghofran Z, Monabati A and Gholijani N: Apoptosis in prostate cancer: bax correlation with stage. Int J Urol 12: 340-345, 2005.
46. Franklin RB, Feng P, Milon B, *et al*: hZIP1 zinc uptake transporter down regulation and zinc depletion in prostate cancer. Mol Cancer 4: 32, 2005.
47. Thiagalingam A, DeBustros A, Borges M, *et al*: RREB-1, a novel zinc finger protein, is involved in the differentiation response to Ras in human medullary thyroid carcinomas. Mol Cell Biol 16: 5335-5345, 1996.
48. Zou J, Milon BC, Desouki MM, Costello LC and Franklin RB: hZIP1 zinc transporter down-regulation in prostate cancer involves the overexpression of Ras responsive element binding protein-1 (RREB-1). Prostate 71: 1518-1524, 2011.
49. Hanke M, Hoefig K, Merz H, *et al*: A robust methodology to study urine microRNA as tumor marker: microRNA-126 and microRNA-182 are related to urinary bladder cancer. Urol Oncol 28: 655-661, 2010.
50. Mitchell PS, Parkin RK, Kroh EM, *et al*: Circulating microRNAs as stable blood-based markers for cancer detection. Proc Natl Acad Sci USA 105: 10513-10518, 2008.

2.2.3 Findings related to the hypothesis 3

***Hypothesis 3*: Prostate carcinoma is characterized by a long-term reduction in zinc ion accumulation. By creating prostate tumour cells capable of accumulating zinc, the tumour phenotype should be adjusted towards the normal state.**

In the next part of the work, zinc was studied as a possible inhibitor of CaP carcinogenesis, and its progression to the castration-resistant prostate cancer (CRPC) phase. The goal was to characterize the behaviour of the prostate tumour cells able to proliferate at the zinc concentrations, which usually cause apoptosis (model of a long-term increase of zinc concentration in tumour microenvironment as the consequence of long-term administration of higher zinc doses to the patients). Some studies suggested that zinc supplementation reduces the risk of CaP [60, 61] or sensitizes the tumour cells to antineoplastic therapy [62]. However, the protective properties of zinc may be controversial [63-66].

Cells grown for a long time period in excess of zinc, are subjected to gradual exhaustion of initial compensatory mechanisms and are forced to accumulate zinc (see Fig. 1 in Kratochvilova *et al.*, p. 146). This should theoretically reverse the tumour phenotype. Nevertheless, during a prolonged exposure to zinc ions, the cells try to compensate the adverse conditions by involving signalling pathways other than in the case of a short-term exposure. In particular, the activation of the KRAS, NF-κB and HIF1α genes is important for the generation of zinc resistance. Activation of these pathways was previously associated with the survival rate and increased aggressiveness of tumour cells [67-69]. Both HIF1α and NF-κB regulate together over a thousand genes that control very important cell processes such as resistance to hypoxia, metabolic changes, inflammatory and reparative responses, degradation of extracellular matrix, migration, and invasive cell potential. In our study Holubová et al. (see p. 125), we also demonstrated that due to the formation of zinc resistance, cells also become more resistant to cisplatin.

Conclusion: Long-term exposure of CaP-derived tumour cells to high zinc concentrations leads to increased accumulation of zinc inside the cells, but on the other side also contributes to activation of the signalling pathways leading to resistance and increased aggressiveness of cells.

Author's publication relevant to this chapter

Holubova, M., M. Axmanova, et al. (2014). "KRAS NF-kappa B is involved in the development of zinc resistance and reduced curability in prostate cancer." Metallomics 6(7): 1240-1253.

Available on page 125

Metallomics

PAPER

KRAS NF-κB is involved in the development of zinc resistance and reduced curability in prostate cancer

Cite this: *Metallomics*, 2014, 6, 1240

Monika Holubova,[a] Martina Axmanova,[a] Jaromir Gumulec,[ab] Martina Raudenska,[ab] Marketa Sztalmachova,[ab] Petr Babula,[c] Vojtech Adam,[bd] Rene Kizek[bd] and Michal Masarik*[ab]

Received 28th February 2014,
Accepted 6th May 2014

DOI: 10.1039/c4mt00065j

www.rsc.org/metallomics

Zinc(II) ions are important components of many proteins and are involved in numerous cellular processes such as apoptosis or drug resistance. Prostate cancer has a unique relationship with zinc(II) ions. However, the relationship was examined only in short-term zinc(II) treatments. Therefore, the aim of this study was to create zinc-resistant prostatic cell lines at various stages of the disease (22Rv1 and PC-3) and a normal prostate epithelium (PNT1A) using a long-term zinc exposure. Consequently, the expression profile of the following genes was analyzed: *BAX, Bcl-2, Beclin-1, CFLAR, HIF1α, KRAS, mTOR, MT1A, MT2A, NF-κB1, p53, survivin, ZIP1, ZnT-1*. The resistance was verified using the MTT test; on average a 1.35-fold lower zinc(II) toxicity (higher IC_{50}) was determined in zinc(II)-resistant cells. The associated resistance to cisplatin was also determined; IC_{50} for cisplatin was 1.52-fold higher. With regard to the gene expression profiles, our results indicate that differential mechanisms participate in the short-term zinc toxicity regulation and long-term resistance; the short-term treatment was associated with *MT2A* ($p < 0.001$), *ZnT-1* ($p < 0.001$), and *MT1A* ($p < 0.03$) and the long-term resistance was associated particularly with *NF-κB1* ($p < 0.001$), *CFLAR* ($p < 0.001$), *KRAS* ($p < 0.001$), p53 ($p < 0.002$), *survivin* ($p = 0.02$), *ZIP1* ($p = 0.002$), *BAX* ($p = 0.005$), and *HIF1α* ($p = 0.05$). Therefore, the *KRAS-PI3K-NF-κB* pathway is expected to play a crucial role in the regulation of zinc resistance. In summary, compared to previous studies, identical mechanisms of resistance were demonstrated on multiple cell lines, both non-tumor and tumorous, derived both from primary and advanced secondary sites.

1 Introduction

Zinc(II) ions represent an essential nutrient and an important constituent of many metalloenzymes, transcription factors, and other key proteins. It is estimated that up to 10% of all human genes encode proteins containing a domain capable of interacting with these ions.[1] Zinc plays a crucial role in cellular processes such as oxidative stress, programmed cell death, cell differentiation and proliferation. It also participates in the regulation of DNA synthesis and mitosis by transmitting cellular signals.[2] Approximately 50% of intracellular zinc is localized in the cytosol and cytosolic organelles, 30–40% in the nucleus, and the rest is associated with the cell membranes.[3] The cellular concentrations of zinc are heavily regulated since disruption of the zinc homeostasis may have serious pathological consequences.

The prostate gland accumulates an unusually high amount of zinc (150 μg of zinc per 1 g of wet tissue compared with 20–50 μg g^{-1} in the other organs).[4] Such a substantial zinc accumulation requires integration of multiple zinc importing and exporting systems. A significant role in maintaining zinc homeostasis is carried out by zinc transporters, as zinc ions are hydrophilic and do not penetrate through the cell membranes by passive diffusion.[5] Three ZIP (Zrt–Irt like protein or zinc iron permease) proteins seem to be important in the prostate as zinc influx transporters involved in the special capability of prostate cells to possess high cellular zinc concentrations.[6] The expression of all three transporters is down-regulated in adenocarcinomatous prostate glands, which have lost the capability to accumulate zinc.[6b] Zinc concentrations found in the malignant prostate tissue tend to be 75% lower than those in the normal prostate.[6a,7]

[a] *Department of Pathological Physiology, Faculty of Medicine, Masaryk University, Kamenice 5, CZ-625 00 Brno, Czech Republic. E-mail: masarik@med.muni.cz; Fax: +420-5-4949-4340; Tel: +420-5-4949-3631*
[b] *Central European Institute of Technology, Brno University of Technology, Technicka 3058/10, CZ-616 00 Brno, Czech Republic*
[c] *Department of Natural Drugs, Faculty of Pharmacy, University of Veterinary and Pharmaceutical Sciences, Palackeho 1-3, CZ-612 42 Brno, Czech Republic*
[d] *Department of Chemistry and Biochemistry, Mendel University in Brno, Zemedelska 1, CZ-613 00 Brno, Czech Republic*

The ZnT transporter proteins (solute-linked carrier 30 (SLC30A)) reduce intracellular zinc levels by ensuring zinc efflux from the cells or zinc uptake into intracellular vesicles or organelles.[8] Most ZnT proteins occur in intracellular compartments (associated with the endoplasmic reticulum, Golgi apparatus, or endosomes). ZnT-1 seems to be the only ZnT transporter occurring within the plasma membrane, which is in concordance with its role of the primary regulator of cellular zinc efflux.[9]

A high zinc concentration in the normal prostate inhibits citrate oxidation through the Krebs cycle and results in the accumulation of citrate in prostatic fluids.[10] Conversely, in the transformed prostate cells, the zinc concentration is very low, citrate oxidation can take place, ATP is generated and provides an unrestricted energy flow for the growth of malignant cells.[11] At the same time, as the intracellular zinc levels diminish, the apoptogenic impact of zinc wanes, hence the proliferation of malignant cells is supported.[11a]

High zinc concentrations have been shown to be cytotoxic for prostate cancer cells,[7,12] which implies that the sustenance of cellular zinc homeostasis is not only the requirement of healthy cells, but it is important for malignant cells as well, especially if the ability to cope with the high zinc concentration present in healthy cells can be impaired in cancer cells. However, the effects of zinc on the prostatic cell lines were examined only by relatively brief exposures in up to date studies (the longest observation period being 7 weeks in the study published by Wong *et al.*[13]).

In order to examine the general role of zinc in cell death regulation and homeostasis maintained in the prostate cell lines, we established PC-3, 22Rv1, and PNT1A cell lines resistant to the long-term (at least 3 months of cultivation), high zinc concentrations in the medium. PC-3 is an androgen-independent and p53 null metastatic prostate cancer cell line. The 22Rv1 cell line represents a model of partially androgen-sensitive p53 expressing prostate cancer, and the PNT1A cell line is a normal prostate cell line model. The use of markedly dissimilar prostate cancer cell lines allowed us to inspect the effect of zinc resistance irrespective of underlying pathways and the grade of transformation. The selection of studied genes was adapted to cover all important pathways that affect cancer cell behavior. We focused on zinc homeostasis (*ZnT-1*, *ZIP1*, *MT1A*, *MT2A*), cell proliferation (*NF-κB1*, *KRAS*), autophagy (*Beclin-1*, *mTOR*), apoptosis (*BAX*, *Bcl-2*, *CFLAR*, *survivin*, *p53*), and redox regulation (*HIF1α*). The aim of our study was to describe the expression profiles of the newly created cell lines and to elucidate changes in their cancerous and malignant potential and curability.

2 Results

2.1 Cell viability analysis

First of all, we prepared prostatic cell lines continuously viable at high zinc(II) concentrations. Half-maximal inhibition concentration (IC_{50}) for zinc(II) of these long-term-treated zinc-resistant cells was determined and compared with the IC_{50} of wild-type (short-term zinc-treated) cells. Prostatic cell lines used for this experiment included non-tumor PNT1A and tumorous 22Rv1 and PC-3. In the previous experiments, the IC_{50} for zinc of these wild-type cell lines was determined as follows: 150.8 μM, 369.1 μM and 55.5 for PNT1A, 22Rv1, and PC-3, respectively.[12c,14] These concentrations for these particular cell lines were further designated as 1-fold baseline IC_{50}. Through a positive selection of zinc resistant cells, we created cell lines continuously viable at concentrations exceeding IC_{50} for zinc(II). The following concentrations of long-term treatments were used: 150 μM, 300 μM and 450 μM for PNT1A, 400 μM, 800 μM and 1200 μM for 22Rv1 and 50 μM, 100 μM and 150 μM for PC-3 (1-, 2- and 3-fold wild-type IC_{50}). The resistant cells were able to divide and grow at zinc concentrations that were even higher than a triple of the standard IC_{50}. A minimum duration of the zinc treatment required for the achievement of a 3-fold IC_{50} resistance was 3 months. The process of selecting the resistant cell lines is illustrated in Fig. 1.

The effect of zinc resistance was verified using MTT analysis. The viability of the "zinc resistant" cell lines after 24 h exposure of up to 2 mM zinc(II) ions was determined (Table 1). The IC_{50} values of zinc resistant cells were on average 1.2- ($p = 0.0002$), 1.4- ($p = 0.18$) and 1.4- ($p < 0.0001$) fold higher in PNT1A, 22Rv1 and PC-3, respectively as compared to the wild type cell lines.

In order to demonstrate that the long-term zinc(II) treatment induces resistance not only to zinc(II) ions, but also to cytostatics and thus that zinc resistance is associated with worse curability, IC_{50} was determined for cisplatin in the zinc-resistant cells and compared with WT cells. For a detailed MTT analysis of WT cells, see Gumulec *et al.*[15] Resistant cells markedly increased their IC_{50} for cisplatin: by 1.4-, 1.6-, and 1.6-fold for PNT1A, 22Rv1, and PC-3, respectively.

2.2 Expression analysis

The expression of all studied genes was related to the expression of the specific gene expression of the PNT1A cell line not exposed to zinc. Expression levels of the other cell lines and zinc(II) concentrations are expressed as a fold change of the PNT1A gene expression. For summary see Fig. 2.

To characterize the expression profile of zinc-resistant cell lines, the effect of zinc concentration, cell line, and zinc resistance was analyzed separately after the adjustment of all other variables using multivariate ANOVA (*i.e.* when analyzing the effect of zinc concentration, the effects of cell line and resistance were adjusted). The following genes were selected: for zinc transporters *ZnT-1* and *ZIP1*, zinc-binding metallothioneins *MT1A* and *MT2A*, regulators *p53*, *mTOR*, *HIF1α*, *KRAS*, and *NF-κB1*, and effectors of programmed cell death and autophagy (*Beclin-1*, *CFLAR*, *survivin*, *Bcl-2*, *BAX*).

There was a significant effect from the zinc concentration, $F(42, 12.63) = 4.15$, $p = 0.004$ and cell line, $F(28, 8) = 37.00$, $p < 0.001$ and no significant effect of zinc resistance on the expression of all genes assessed together. Despite this fact, zinc resistance affected the expression of a particular set of genes. More detailed results will be discussed in the following sections.

2.2.1 Effect of zinc(II) concentration. The effect of zinc concentration as a categorical factor was analyzed after the adjustment of all other variables using multivariate ANOVA.

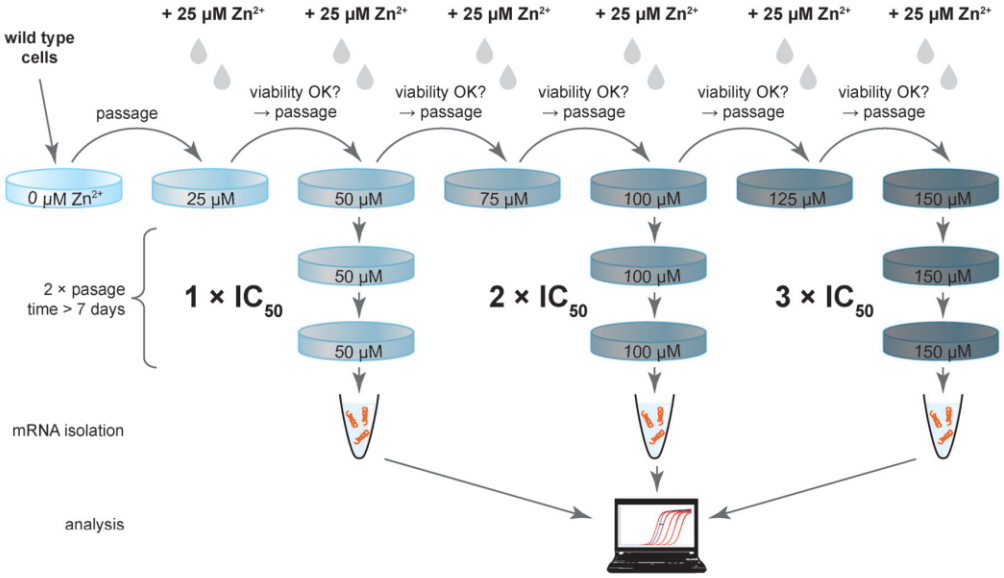

Fig. 1 Preparation of "resistant" cell lines from the wild type common cells. Concentrations mentioned in this figure reflect protocol for the resistant PC-3 cell line. For details regarding the concentrations used for the PNT1A and 22Rv1 preparation see the Experimental section. Viability was controlled before each passage and the time of the cultivation varied depending thereon. The least time required for gaining the resistance was three months.

Table 1 Analysis of half-maximal inhibition concentration (IC_{50}) of zinc

Factor	Cell line	Zinc(II) IC_{50} (μMμ)	Cisplatin IC_{50} (μMμ)
Wild type	PNT1A	150.8	44.0
	22Rv1	369.1	30.8
	PC-3	55.5	74.9
Zinc resistant	PNT1A	177.2 ± 10.9^{a}	60.7 ± 19.4
	22Rv1	514.2 ± 204.0^{c}	50.0 ± 31.0
	PC-3	$83.0 \pm 4.7^{b,c}$	116.7 ± 70.0

Analysis of wild-type cells is based on the previous studies.[12c,14,15] Data is displayed as mean ± standard deviation. [a] Significantly different compared to WT at $p = 0.0002$. [b] Significantly different compared to WT at $p < 0.0001$. [c] Significantly different compared to PNT1A at $p < 0.05$.

There was a significant increase in the expression of *MT1A* and *MT2A* (up to 3.1-fold at $p = 0.03$ and up to 2.5-fold at $p = 0.0001$ for *MT1A* and *MT2A*, respectively) and zinc transporter *ZnT-1* (2.6-fold at $p = 0.0007$) genes. There was also a barely significant decrease of *KRAS* gene expression (0.7-fold at $p = 0.045$). No other significant trend was observed in the expression of the remaining genes (Table 2).

2.2.2 Effect of cell line. The effect of cell line on the gene expression was analyzed after the adjustment of zinc concentration and zinc resistance. Compared to the effect of zinc concentration and zinc resistance, the effect of cell line affected the expression profile most intensively $F(28, 8) = 37.00$, $p < 0.001$. Significantly affected by the cell line were *p53*, *Bcl-2*, *CFLAR*, *ZIP1*, *KRAS*, *survivin*, *mTOR*, *MT1A*, and *HIF1α* gene expressions. As predicted, the expression of non-tumor PNT1A and tumorous 22Rv1 and PC-3 differed mutually. Firstly, the expression was analyzed in the tumorous cell line 22Rv1. Compared to PNT1A, this cell line exhibited rather an up-regulation of the gene expression; there was a significantly up-regulated expression of *Bcl-2* (7.6-fold, $p < 0.001$), *KRAS* (2.6-fold, $p < 0.001$), *mTOR* (2.0-fold, $p < 0.001$), *Beclin-1* (1.5-fold, $p = 0.04$), *MT2A* (1.8-fold, $p < 0.05$), *ZIP1* (1.9-fold, $p < 0.001$), *ZnT-1* (1.9-fold, $p = 0.04$), and *CFLAR* (1.5-fold, $p < 0.001$). Secondly, the expression of cell line derived from metastasis, PC-3, was analyzed. In contrast to 22Rv1, the expression profile of this cell line was rather down-regulated. Compared to PNT1A, there was a significant down-regulation of *p53* (0.2-fold, $p < 0.001$), *MT1A* (0.1-fold, $p < 0.001$), *Bcl-2* (0.4-fold, $p < 0.001$), *ZnT-1* (0.5-fold, $p = 0.04$), and *KRAS* (0.5-fold, $p < 0.001$). The following genes were significantly up-regulated in PC-3: *HIF1a* (2.2-fold, $p < 0.001$), *CFLAR* (2-fold, $p < 0.001$), and *survivin* (1.8-fold, $p < 0.001$) (Table 2).

2.2.3 Effect of long-term treatment (zinc resistance). In this step, the effect of "zinc resistance" (*i.e.* long-term *vs.* short term treatment comparison) was evaluated. Long-term treated cells are further denoted as "zinc-resistant", short-term-treated cells are designated as "wild-type". Despite the fact that there was no significant effect of this factor in the gene expression using a multivariate test, a set of significantly up-regulated genes in zinc-resistant cells was determined using univariate analysis. These include (in the order of significance) *NF-κB1* (1.6-fold increase of expression, $p < 0.001$), *CFLAR* (1.7-fold, $p < 0.001$), *KRAS* (1.7-fold, $p = 0.0005$), *p53* (1.5-fold, $p = 0.001$), *survivin* (1.4-fold, $p = 0.02$), *ZIP1* (1.3-fold, $p = 0.002$), *BAX* (1.4-fold, $p = 0.005$), and *HIF1a* (1.4-fold, $p = 0.05$). The remaining genes did not exhibit a significant trend (Table 2).

2.2.4 *BAX*/*Bcl-2* ratio. In the above sections, the expression of genes was analyzed separately depending on either zinc

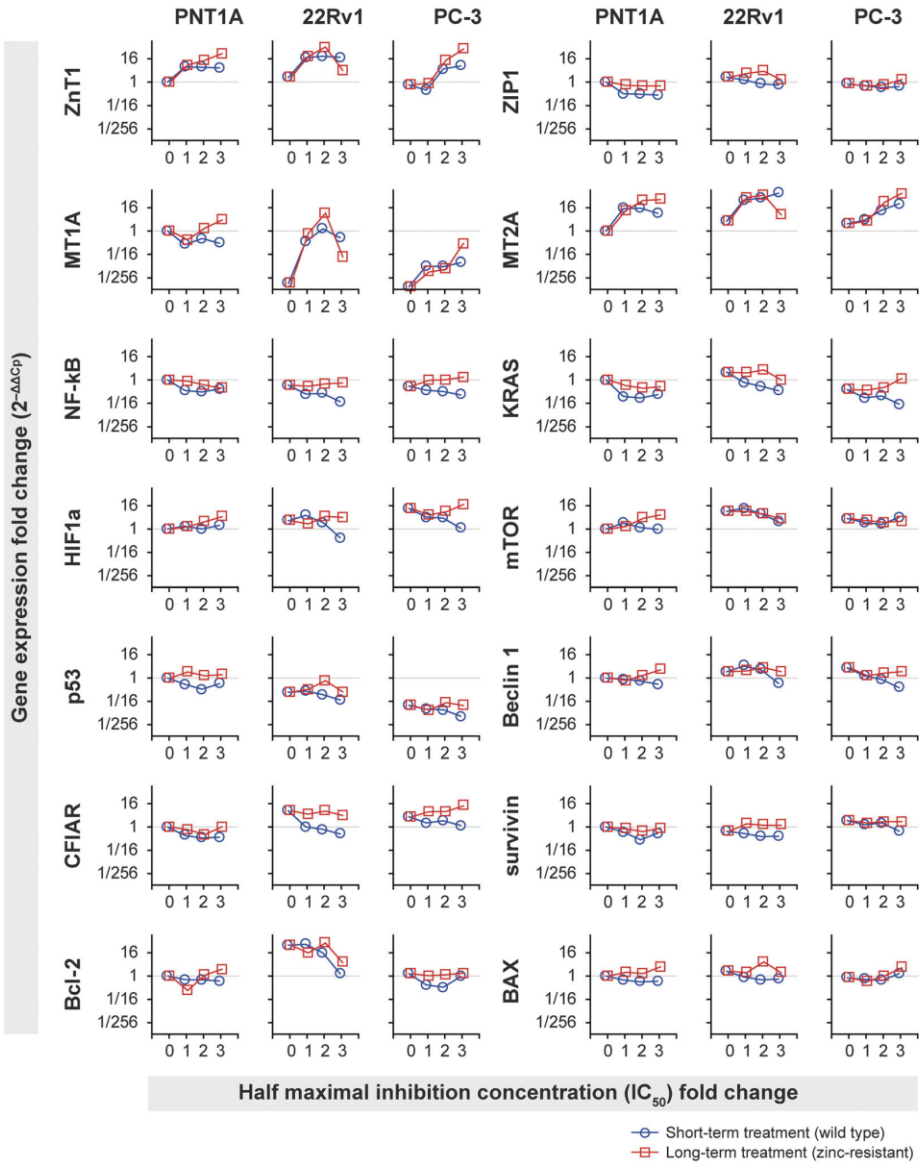

Fig. 2 Expression profile of genes. mRNA expression levels of all analyzed genes in the PNT1A, 22RV1, and PC-3 cell lines in reaction to the long-term ("resistant", red line) and short-term ("wild type", blue line) treatment with zinc(II) ions. The *y*-axis in log scale reflects the relative gene expression fold change of these genes, the *x*-axis reflects the fold change of IC_{50} concentrations.

resistance, zinc(II) treatment, or type of the cell line. Nevertheless, the *BAX*/*Bcl-2* ratio is crucial for the fate of cells. Therefore, a *BAX*/*Bcl-2* ratio was determined (Fig. 3). The most apparent trend was evident with regard to the cell line; while in the non-tumor PNT1A cell line, the *BAX*/*Bcl-2* ratio was above 1.0 (apoptosis triggering), the ratio in the tumorous cell lines 22Rv1 and PC-3 was below 1.0 (anti-apoptotic effect); this trend was significant using Tukey's post-hoc test. With regard to zinc resistance, the ratio was lower in WT cells, but below the level of statistical significance. As to the zinc(II) concentration, an increasing *BAX*/*Bcl-2* ratio was associated with increasing zinc(II) concentration but only up to a value of 0.92 of the *BAX*/*Bcl-2* ratio (no apoptosis triggering), which was achieved by a 2-fold IC_{50} zinc(II) concentration; see Fig. 3B.

2.2.5 Gene co-expression analysis. Previous analyses did not highlight whether there are some common trends in the expression profiles of individual genes. Therefore, correlations between the genes were determined, and the resistant and wild type cells were analyzed separately.

In both resistant and WT cell line forms, a correlation of *ZnT-1* with *MT1A* and *MT2A* was found ($r = 0.58$ at $p = 0.045$

Table 2 Multivariate analysis of the effect of zinc resistance, cell line and IC_{50} fold change

	Level of effect (gene expression fold change)												
Effect	*mTOR*	*Beclin 1*	*HIF1α*	*Bcl-2*	*MT2A*	*BAX*	*p53*	*MT1A*	*ZIP1*	*ZnT1*	*NF-κB*	*Survivin*	*CFLAR*	*KRAS*
Zinc resistance $F(14, 4) = 0.77$, $p = 0.67$														
Resist.	1.10	1.28	1.38[a]	1.24	1.11	1.40[a]	1.46[a]	1.31	1.34[a]	1.30	1.58[a]	1.35[a]	1.72[a]	1.70[a]
Cell line $F(28, 8) = 37.00$, $p < 0.001$														
22Rv1	2.02[a]	1.48[a]	0.85	7.56[a]	1.81[a]	1.29	1.19	1.43	1.87[a]	1.93[a]	0.77	0.77[a]	1.50[a]	2.55[a]
PC-3	0.89	1.00	2.15[a]	0.38[a]	0.77	0.84	0.17[a]	0.11[a]	0.88	0.53[a]	1.14	1.80[a]	2.05[a]	0.52[a]
IC_{50} fold change $F(42, 12.63) = 4.15$, $p = 0.004$														
1-fold	1.12	1.03	0.97	0.80	1.06	0.81	1.04	1.09	0.97	0.80	0.97	1.07	0.89	0.86
2-fold	0.97	1.06	1.06	1.08	2.50[a]	0.97	1.11	3.11[a]	0.91	2.60[a]	0.91	0.85	0.82	0.85[a]
3-fold	0.90	0.69	0.86	0.68	2.32[a]	1.24	0.76	2.12[a]	0.83	2.39[a]	0.78	0.88	0.82	0.71[a]

Displayed as a gene expression fold change after adjustment of all other variables, related to wild type in case of "zinc resistance" effect, PNT1A in case of "cell line" effect, and 0-fold IC_{50} fold change in case of "IC_{50} fold change" effect. [a] Indicates significant at $p < 0.05$. For exact *p*-values see Fig. 4A.

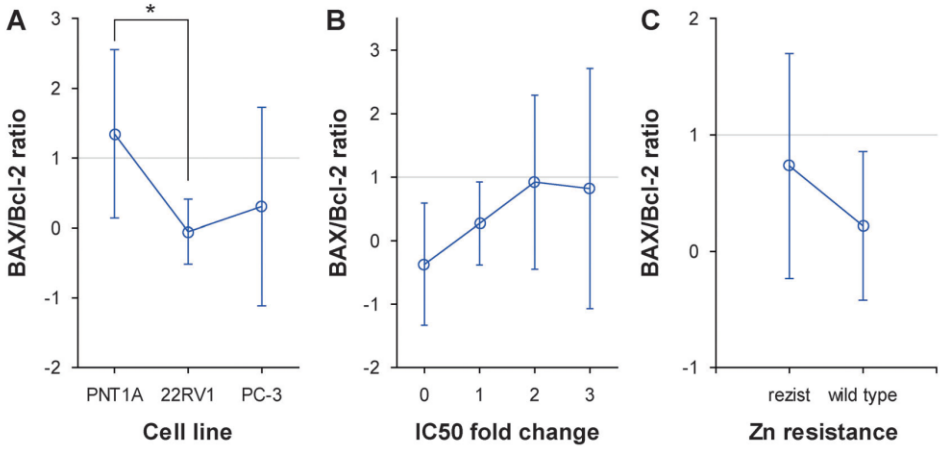

Fig. 3 *BAX/Bcl-2* ratio related to the cell line, zinc treatment, and zinc resistance. *Significantly different using Tukey's post-hoc testing at $p < 0.05$. Displayed as mean ± standard deviation. The *y*-axis reflects the ratio of relative gene expression fold changes of these genes; values > 1 indicate excess of *BAX* gene expression.

and $r = 0.91$ at $p < 0.001$ for WT; and $r = 0.68$ at $p = 0.014$ and $r = 0.97$ at $p < 0.001$ for the resistant cells, respectively). Additionally, there was a positive correlation between *KRAS* and *ZIP1* ($r = 0.75$ at $p = 0.005$ and $r = 0.95$ at $p < 0.001$ for WT and resistant cells). No other similar correlations between WT and resistant cell forms was observed; Wild type cells showed a negative relationship between *MT1A* and *CFLAR* ($r = -0.81$ $p = 0.001$) and a negative correlation between *NF-κB1* and *MT2A* ($r = -0.93$ $p < 0.001$). With regard to the resistant cells, strong positive correlations were determined between *BAX* and *ZnT-1* ($r = 0.80$ at $p = 0.002$), *ZIP1* and *KRAS* ($r = 0.95$ at $p < 0.001$) and between *Bcl-2* and *ZIP1* ($r = 0.85$ at $p < 0.001$), *Bcl-2* and *KRAS* ($r = 0.82$ at $p = 0.001$) and *Bcl-2* and *mTOR* ($r = 0.82$ at $p = 0.001$).

Regardless of zinc resistance, some specific co-expressions typical of particular cell lines were revealed. The results indicated a correlation between the *p53* and *Beclin 1* gene expression in the PC-3 cell line ($r = 0.88$ at $p = 0.004$). Furthermore, in the PC-3 cells, the *p53* expression correlated with *survivin* ($r = 0.89$ at $p = 0.003$), *KRAS* ($r = 0.79$ at $p = 0.02$), and *HIF1α* ($r = 0.88$ at $p = 0.004$) as well. Nevertheless, in the PC-3 cell line, no correlation was found between *p53* and *BAX* in contrast to the other two cell lines (PNT1A and 22Rv1). The 22RV1 cell line expressed *p53* in correlation with *BAX* ($r = 0.88$ at $p = 0.004$) and *ZIP1* ($r = 0.89$ at $p = 0.003$) genes. *CFLAR* and *NF-κB* ($r = 0.98$ at $p < 0.001$ for PC-3; $r = 0.95$ at $p < 0.001$ for 22Rv1) correlated with each other, but only in the cancerous cell lines; in the PNT1A cell line this connection was not found. In the 22Rv1 cell line, a significant correlation between *KRAS* and *BAX* was found ($r = 0.86$ at $p = 0.007$). Furthermore, in PC-3 *KRAS* correlated with *HIF-1α* ($r = 0.92$ at $p = 0.001$). *Survivin* was related to *HIF-1α* in the wild type cell lines ($r = 0.64$ at $p = 0.025$) and in both types of PC-3 cells ($r = 0.90$ at $p = 0.002$). These particular correlations were not found in the other cell lines.

However, a simple correlation does not make it possible for us to reveal the complex co-expression pattern and potential differences between long- and short-term treatments. Therefore, principal component analysis was performed. In addition to the correlation analysis, the component analysis made it possible for us to detect the structure of relationships between

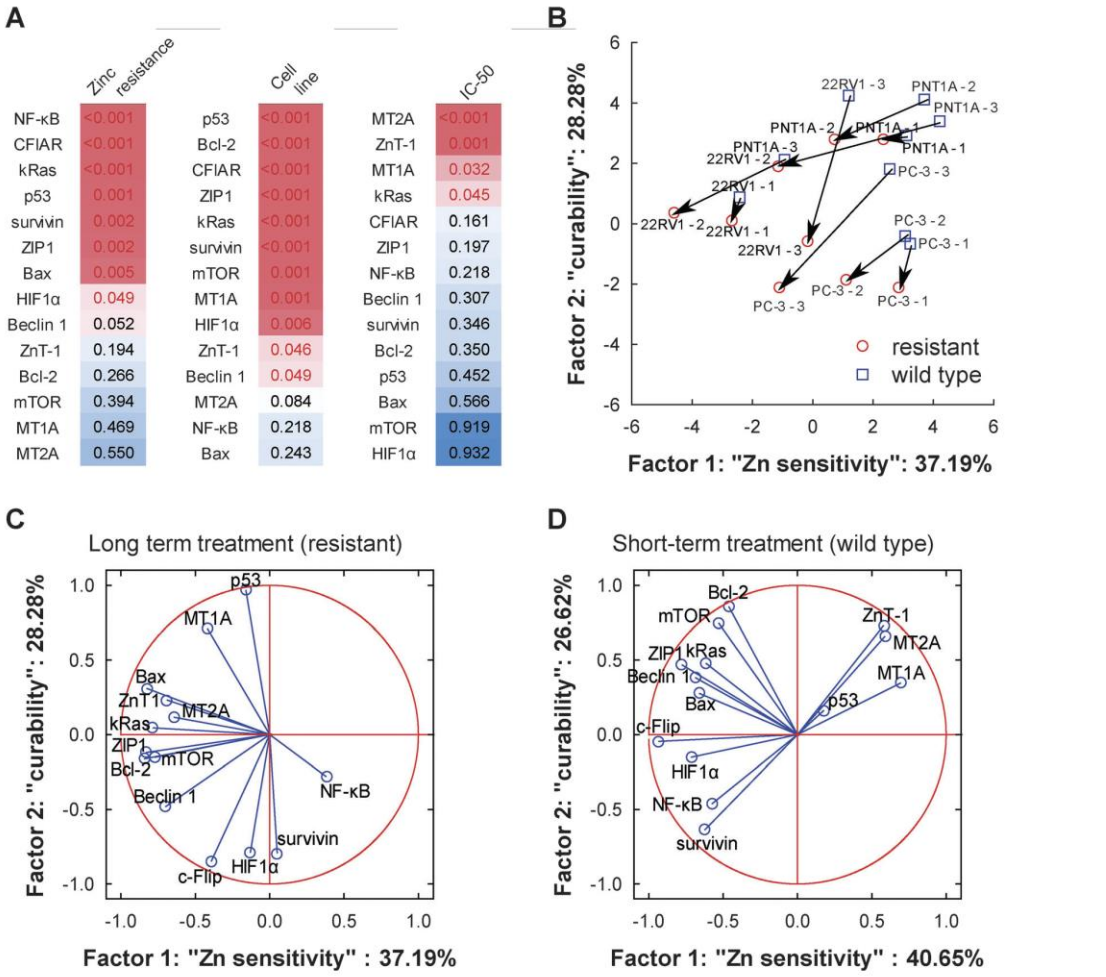

Fig. 4 Analysis of the effect of zinc resistance, cell line and zinc concentration. (A) *p*-values from multivariate ANOVA. Zinc resistance cell line, and IC_{50} fold change used as categorical predictors. Sorted by *p*-value level (genes with the most significant changes in a descending order). Color coding reflects statistical significance. Red-coded genes are significant at $p < 0.05$. (B) Principal component analysis: projection of cases (cell lines) on the two-factor-plane. Arrows indicate "shift" in the phenotype of the cells towards lower zinc(II) sensitivity (factor 1) and worse curability (factor 2). Numbers after the names of the cell lines represent IC_{50}-fold change. (C) and (D) Principal component analysis: projection of variables (genes associated with zinc sensitivity and "curability") on the two-factor plane. Factors in B, C, and D are identical. Distinction between long term (C) and short term (D) corresponds with the shift in Fig. 3B. For details see the Results section.

variables, thus helping us to assess variables in the WT and zinc-resistant groups. Moreover, this analysis allowed us to classify variables (cell lines of particular treatment and of particular zinc resistance condition) based on the expression profile. To illustrate the model of resistance, two-factor analysis was chosen with a total cumulative variance of 65.46% and eigenvalues 5.20 and 3.96 for factor 1 and factor 2, respectively. Firstly, the variables were projected based on resistance (resistant and WT), (Fig. 4C and D). Taking together, the results of multivariate ANOVA and the "direction" of genes in the principal component analysis, we designated the factor 1 of principal component analysis as "sensitivity" and factor 2 as "curability". These conclusions are based on the following findings: (a) *MT*s and *ZnT-1* are genes, which strongly correlate with the zinc concentration (Fig 4A), (b) factors in the "zinc resistance" analysis and "IC_{50} fold-change" refer to the "long-term treatment" and "short-term treatment", respectively; (c) *MT*s and *ZnT-1* are directed to the positive values of factor 1 in the short term treatment and (d) these genes are directed to the negative values in the zinc-resistant cells. Furthermore, the negative factor 1 in the resistant cells is associated with cell survival rather than with cell death. When these factors are used to project cases (*i.e.* cell lines), another apparent trend is evident: (e) cells derived from an advanced tumor, "aggressive" PC-3, are associated with the lower values of factor 2 and cells derived from the primary tumor, 22Rv1 with a lower aggressive potential are associated

with rather higher values of factor 2. However, (f) when the cells become resistant, they move toward the lower values of the two factors 1 and 2, *i.e.* they become less sensitive to zinc (as demonstrated by MTT), and less curable (as determined by the cisplatin treatment, for detail see the section "Cell viability analysis") (Fig. 4B).

2.3 Fluorescent staining

2.3.1 Determination of zinc. Fluorescent staining was performed to confirm that the resistant cell lines are affected by the high amounts of zinc(II) ions. Free zinc(II) ions were visualized by using a fluorescent probe *N*-(6-methoxy-8-quinolyl)-*p*-toluene sulphonamide, *i.e.* a probe specific to these ions. Differences found in the zinc(II) ions localized in all wild type cells and in the resistant (Fig. 5) cells were as follows: in both PNT1A and 22Rv1 cells, levels of intracellular free zinc(II) ions were closely connected with the zinc(II) ion treatment in a concentration-dependent manner. In the PC-3 cells, the difference between the non-treated and zinc(II)-treated cells was less obvious, although it was clear that all cell lines were able to accumulate zinc(II) ions. In the case of the PNT1A cell line, the localization of zinc(II) ions around the nuclei and irregularly within the nuclei was evident. Peripheral parts of the cytoplasm demonstrated only a weak emission, representing only low free zinc(II) levels in these localizations. In the 22Rv1 cells, the intensity of the fluorescence product emission significantly increased with increasing resistance to zinc(II) ions (Fig. 5). In PNT1A and 22RV1 resistant cells, free zinc(II) ions were localized around the nuclei and in the form of high emission spots. These spots are probably zincosomes, compartments of endoplasmic reticulum origin.[16]

2.3.2 Determination of free thiols. Compounds rich in –SH groups (low molecular mass peptides and proteins such as reduced glutathione and metallothionein, *etc.*) are responsible for binding metal ions within the intracellular space. The expression level of metallothionein was verified with 5-(bromomethyl)fluorescein, a probe that provides the formation of a fluorescent product after reaction with the –SH groups of thiols. The detection and cellular compartmentation of free thiols was made. In all cell lines (PNT1A, 22Rv1, and PC-3 see Fig. 5), the amount of free thiols increased within the zinc(II) ion resistant cells and some cells with an extremely high content of free thiols were detected. This fact was more evident in the PC-3 cells. In all cell lines, free thiols were localized around the nuclei and in the cytoplasm.

3 Discussion

In our previous studies, we demonstrated that zinc ions can change the expression levels of metallothionein and other genes connected with oxidative stress and apoptosis.[12c,14] However, the effect of zinc on the prostate cell lines was studied only at relatively short time exposures.[7,17] Through a positive selection of zinc resistant cells, we created cell lines continuously viable at concentrations exceeding the IC_{50} for zinc. Results of the fluorescent staining indicated that all cell lines were able to

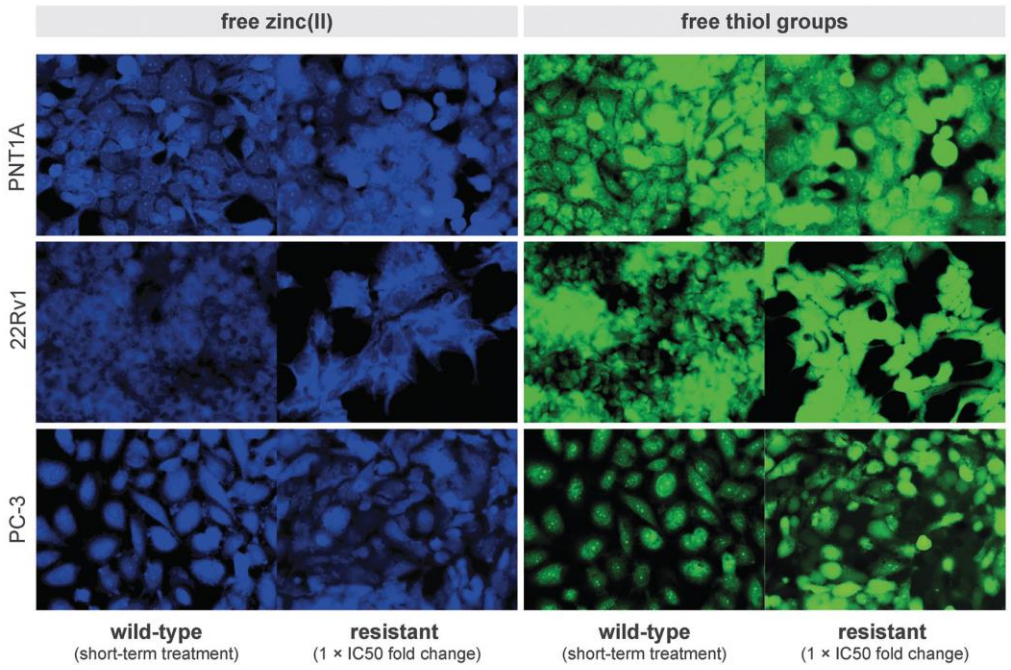

Fig. 5 Distribution of free zinc(II) ions and free thiol groups in the wild type and resistant cell lines. Displayed as pairs of wild-type and one-fold IC_{50} resistant cells. One-fold IC_{50} represents the following concentrations: 150, 400, and 50 μM for PNT1A, 22Rv1, and PC-3, respectively. For details see the Results section.

accumulate zinc(II) ions, which is in compliance with Costelo *et al.*,[11a] and in all cell lines, free thiols were localized around the nuclei and in the cytoplasm. This is considered the evidence for a possible role of free thiols in the transcriptional activity.[14] These results were in accordance with the expression analysis, where the production of *MT* mRNA increased with zinc(II) ions in a concentration-dependent manner. The resistant cells were capable of division at zinc concentrations that were three times higher than the standard IC_{50}. The PC-3 cell line was found to be the least tolerant to zinc (in both wild type and resistant form). In contrast, the most resistant 22Rv1 cells were able to grow at 1200 μM zinc concentrations.

3.1 Buffering of short-term zinc excess

When the intracellular concentration of zinc increases, the cells have a tendency to maintain homeostasis by reducing the impact of potential zinc toxicity. Such homeostasis can be achieved either through lower importing of zinc ions to the cells, by exporting the zinc ions from the cell or through the capability to reduce the amount of free zinc ions by binding it to thiol groups (for instance into metallothioneins). We expected *ZIP1* decreasing expression trends to participate in gaining the resistance, but our results did not turn out to be as good as the results of Wong *et al.*, who studied the LNCaP cell line.[13] Although the expression of *ZIP1* was conversely 1.34 fold higher in the resistant cell lines, this effect was caused mainly by the 22RV1 cell line. In this cell line, the expression of *ZIP1* increased (1.87-fold change). We also expected a negative correlation between *ZIP1* and *KRAS* expression according to previous studies, where a negative regulation was found.[18] Interestingly, however, we found strong positive correlations in all cases. Because significant changes in *ZIP1* expression levels due to increasing zinc concentrations were not found, the importance of the other two mechanisms can be assumed. In correlation with this hypothesis, a statistically significant link was found between *MT2A*, *ZnT-1*, and *MT1A* expression and IC_{50} fold change, which implies the key function of these genes in general zinc resistance regardless of the length of zinc treatment. Accordingly, the lowest *ZnT-1* levels and the slowest enhancement of *ZnT-1*, *MT1A*, and *MT2A* gene expression due to the zinc concentration increase were found in relatively zinc-sensitive PC-3 cells. *MT1A* expression levels in the PC-3 resistant form did not even reach wild-type PNT1A or 22Rv1 levels (see Fig. 2). *ZnT-1* was also identified as a gene liable for causing zinc resistance in baby hamster kidney cells,[9] but was not recognized as a resistance factor in the study published by Wong *et al.*[13] Nevertheless, Wong *et al.* studied *ZnT-1* expression levels at zinc concentrations lower than ours. Moreover, the expression of *ZnT-1* in our experiment highly correlated with the expression of *MT1A* and *MT2A* and with the zinc ion concentrations, which is in accordance with the fact that all these genes are regulated by the MTF-1 transcriptional factor.[19]

3.2 Long-term zinc resistance mechanisms include *PI3K* and *NF-κB* pathways

While the above-mentioned effects are identically exhibited in both WT and resistant cell line types, in the following section we outline mechanisms specific for resistance obtained due to the long-term zinc treatment. In our study, we found that the genes which are important for long-term zinc resistance are *NF-κB1* (p50/p105), *CFLAR*, *KRAS*, *p53*, *survivin*, *ZIP1*, *BAX* and *HIF1α*. On the other hand, these genes had only a small effect in short-term resistance. All these genes are involved in *PI3K* and *NF-κB* signaling pathways[20] (see Fig. 2). Inasmuch as *NF-κB* is a down-stream gene of *KRAS* (through the activity of *PI3K*/*AKT*) and *CFLAR*,[21] *survivin*, and *HIF1α* are the down-stream genes of *NF-κB*, we took the liberty to assume the involvement of the mentioned pathway. All these genes are able to support anti-apoptotic processes and cell survival.[22] Furthermore, a strong negative correlation between *NF-κB* and *MT2A* was found specifically in the wild-type cell lines, which indicates the existence of negative regulation mechanisms between these genes. Accordingly, *MT2A* was previously reported to play a tumor-suppressive role through inhibition of *NF-κB* signaling.[23] This negative correlation between *NF-κB* and *MT2A* expression was not observed in the resistant types of cells. One of the most important ways in which the *NF-κB* activity could influence cell survival at long-term high zinc concentrations is *via* the increased expression of antioxidant proteins such as manganese superoxide dismutase (MnSOD), copper–zinc superoxide dismutase, catalase, thioredoxin-1, and thioredoxin-2, glutathione S-transferase pi, glutathione peroxidase-1, or ferritin heavy chain.[24] Moreover, the activity of *NF-κB* and *PI3K* pathways seems to be enhanced due to the long-term treatment, which can be followed by a higher cell survival rate and by the activation of metastatic mechanisms. It seems presumable that these particular pathways can easily push the healthy cell phenotype toward higher zinc resistance and simultaneously towards lower curability (see Fig. 4B). It was previously demonstrated that extracellular zinc activates *MAPK*s and *PI3K* in different tissues and also in the prostate cancer cells.[25] Collaboration of activated *RAS*/*AKT*/*NF-κB* signaling with other oncogenic signaling pathways could easily change the phosphorylation profile of prostate cancer cells to be more aggressive.[26] Elevated *PI3K*/*AKT* signaling was found in nearly all prostate cancer types, and irregularities in the *RAS* signaling pathways existed in more than 40% of primary prostate tumors and 90% of prostate metastases.[27] Results of some studies indicate that zinc ions inhibit *RAS* and also *NF-κB* mediated signaling.[18,28] These inhibiting effects of zinc ions were observed in our study too, but only in the wild-type (short-term treated) cells, where decreasing trends in the expression of *KRAS*, *CFLAR*, *p53* and *NF-κB1* after zinc administration were found. Some of the other inhibiting effects of zinc related to *RAS*-mediated signaling were specific only for some cell lines (*HIF-1α* inhibition in 22Rv1 and PC-3 cells, *survivin* in 22RV1 cells, *Beclin-1* in PNT1A and PC-3 cells); however, almost all of these mentioned inhibition effects were not present in the resistant forms of cells. Therefore, nearly opposite effects of zinc could be seen due to the different length of the treatment. According to our results, a prolonged zinc treatment could actually induce a more aggressive behavior of the prostate cancer cells. The shift to increased resistance and worse curability status was observed in all the studied long-treated cell lines. These observations were corroborated by results of the MTT test

for cisplatin, which is a potent member of the anticancer drug family. The resistant cell lines were significantly less sensitive to the cisplatin treatment. This is in line with studies declaring that excessive zinc amounts help cells withstand the impact of other toxins.[29]

3.3 Modulation of apoptosis

One of the described effects of zinc on prostate cancer cells is the influence on intrinsic apoptotic pathways through increasing the *BAX* expression,[11b] affecting the *BAX/Bcl-2* proportion,[17a] and helping *BAX* to shift onto the mitochondrial membrane.[17d] In this experiment, both types (wild type and resistant) of the PNT1A cell lines gave a *BAX/Bcl-2* ratio indicating apoptosis triggering. The cell lines derived from cancerous tissues did not show any increase of this ratio. When the long-term and short-term treated cells were analyzed separately, the *BAX/Bcl-2* proportion continuously increased in the resistant cell lines along with the amount of zinc(II) ions. This could be due to the fact, that the cells do not lose the ability to induce mitochondrial apoptotic pathways, but they are also capable of neutralizing these processes with other factors like *survivin* or *CFLAR*. The C-Flip product of the *CFLAR* gene might be important in managing the extrinsic apoptotic pathways after long-term treatments, and obviously in gaining resistance. *CFLAR* is a target gene of *NF-κB* transcription factor[30] and indeed they correlated with each other, but only in the cancerous cell lines; in the PNT1A cell line, this connection was not found. *Survivin* is a potent caspase inhibitor and its expression protected the cells against high zinc concentrations.[22b] It was also shown that the production of *survivin* increases in aggressive prostate carcinoma,[31] which is in agreement with our study.

On the other hand, the wild type (short-treated) cells had an increasing *BAX/Bcl-2* ratio only at lower concentrations of zinc(II) ions. Consequently, zinc amounts exceeding double the IC_{50} concentration apparently do not trigger apoptosis in the WT cells, but rather necrosis. Unlike apoptosis, necrosis does not need functional ATP production.[32] Therefore, the decision between death by apoptosis or by necrosis depends upon the intensity of the cell injury and also upon the availability of intracellular ATP. Accordingly, the resistant cell lines seem to be able to preserve ATP production even at high zinc concentrations.

3.4 Cell lines as a major factor affecting the gene expression profile

Furthermore, we recorded differences in expression trends between the cell lines. The use of markedly dissimilar prostate cancer cell lines allowed us to inspect the effect of zinc resistance irrespective of underlying pathways and grade of transformation. Significantly affected by the cell line influence were almost all examined gene expressions, as we expected, but for instance not *NF-κB* and *MT2A*, which were found to be important in both long-term (*NF-κB*) and short-term (*MT2A*) zinc resistance in spite of the cell line effect. See Fig. 4A (results of multivariate ANOVA, comparing the effect of cell line *vs.* effect of zinc resistance). The greatest effect of the cell line was recorded on the *p53* transcription level. This gene was transcribed less in the metastatic cell line PC-3 as compared to PNT1A. The PC-3 cell line does not produce functional protein p53.[33] Moreover, the results indicated a correlation between *p53* and the pro-autophagic *Beclin1* gene expression in the PC-3 cell line. This suggests that the non-functional protein accumulates and is degraded during the process of autophagy.[34] Furthermore, in the PC-3 cells, the *p53* expression correlated with *survivin*, *KRAS*, and *HIF1α* as well. This implies that the anti-apoptotic mechanisms were triggered. The relationship between *p53* and *HIF1α* could be explained by the hypothesis that both *p53* and *HIF-1α* are degraded by *Mdm2*. This ubiquitin ligase normally prefers to cleave the *HIF-1α* protein, but in this case, the accumulated non-functional *p53* had priority.[35] The expression of *HIF1a* was the highest in the PC-3 cell line, which was in accordance with the previous findings. The malignant prostatic tissue shows a more positive redox status than the healthy tissue and this may explain the connection observed between *HIF-1α* expression and the staging of the tumor.[36] The resistant cell lines showed a higher expression of *HIF-1α* mRNA, which indicates the involvement of *HIF-1α* in the resistance mechanism. According to a study by Feng *et al.*, *HIF-1α* expression inhibits the apoptotic effects of zinc.[17d]

In contrast, in the PC-3 cell line, no correlation was found between *p53* and any pro-apoptotic factor unlike in the other two cell lines (PNT1A and 22Rv1), where *p53* is partially functional. The 22RV1 cell line expressed the wild-type *p53* in correlation with the pro-apoptotic *BAX*. It indicates that the cells were able to induce *p53* dependent apoptosis, but other effectors could oppose the process. The PNT1A cell line is transfected by the Simian Virus 40 vector that affects the *p53* activity;[37] some studies demonstrated, however, that the use of oxidants can negate this inhibition.[15,38] Zinc can also act like an oxidant and our results are in agreement with these findings, because the *p53* expression correlated with *BAX* expression levels in PNT1A. Higher expression of *p53* was found in the resistant forms of cell lines. Nevertheless, it was reported that zinc can cause increases in *p53* expression but interrupts *p53* binding to DNA.[39]

3.5 Overview of complex gene expression changes

In general, our findings indicate the great importance of the zinc treatment duration. Whereas the short-term (24–72 h) zinc treatment induces the apoptotic process in the prostate cancer cell lines,[14,17b,22b] the long term treated (several months) prostate cancer cells change their phenotype into a more aggressive and resistant form (Fig. 6). This shift in phenotype is clearly illustrated in Fig. 4B. The "moving" of zinc treated cell lines along the axis representing zinc sensitivity and tumor curability depicts a thin line between "healthy" phenotype and aggressive cancer characteristics. These findings are in line with those of Wong *et al.*, who revealed that the initial inhibitory effects of Zn(II) on LNCaP cell proliferation were reversed due to the seven week long presence of high intracellular zinc ions.[13]

Some studies claim that dietary zinc supplementation reduces cancer risk,[40] is protective against tumorigenesis[12a] or can sensitize the cells to cytotoxic agents.[28b] These effects of zinc in prostate

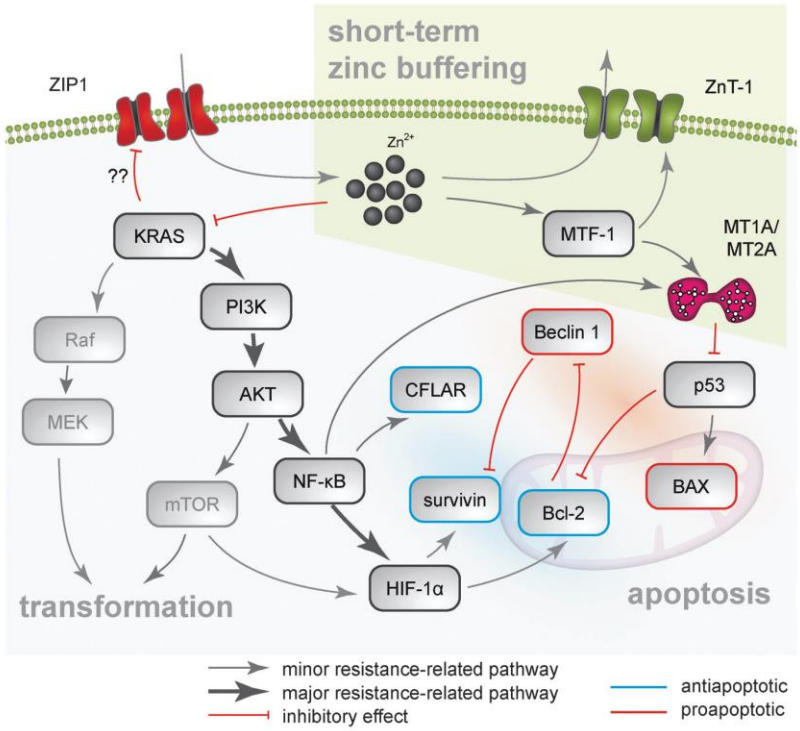

Fig. 6 Mechanisms of zinc resistance (long-term zinc buffering) and short-term zinc buffering. Synthesis of the effect of the zinc(II) ions and major pathways affecting tumor transformation, apoptosis, and short-term zinc buffering based on the results of this study and in accordance with literature (for details see Discussion section). Short-term zinc(II) buffering is indicated by a green background color, long-term zinc buffering displayed in the remaining parts of the scheme. The major *KRAS-PI3K-NF-κB* pathway and its effect on cell survival are accentuated by thick lines. Antiapoptic/proapoptic genes are outlined with blue/red, respectively.

cancer have become popular and many dietary supplements for humans contain zinc. However, according to our results, it can be deduced that zinc protecting abilities on the prostate tissue are not without exception. This suspicion has been also corroborated by several other studies demonstrating that zinc can cause the development of BPH and cancer,[41] or dietary zinc uptake correlates with the increased prostate cancer risk.[42]

4 Experimental

4.1 Chemical and biochemical reagents

RPMI-1640 medium, Ham's F12 medium, fetal bovine serum (FBS) (mycoplasma-free), penicillin/streptomycin and trypsin were purchased from PAA Laboratories GmbH (Pashing, Austria). Phosphate buffered saline PBS was purchased from Invitrogen Corp. (Carlsbad, CA, USA). Ethylenediaminetetraacetic acid (EDTA), zinc(II) sulphate (BioReagent grade, suitable for cell cultures), cisplatin 0.5 mg ml^{-1} solution (Medac, Germany) and all other chemicals of ACS purity were purchased from Sigma Aldrich Co. (St. Louis, MO, USA), unless noted otherwise.

4.2 Cell cultures

Three human prostatic cell lines were used in this study. The PNT1A human cell line derived from normal adult prostatic epithelial cells immortalized by transfection with a plasmid containing SV40 genome with defective replication origin. The primary culture was obtained post mortem from the normal prostatic tissue of a 35 year old male. The 22Rv1 human epithelial cell line derived from a xenograft serially propagated in mice after castration, and the androgen sensitive. PC-3 human epithelial cell line established from a 4 grade prostatic adenocarcinoma, an androgen independent and unresponsive metastatic site in bone. All three cell lines used in this study were purchased from HPA Culture Collections (Salisbury, UK).

4.3 Cell cultivation

The PNT1A and 22RV1 cells were cultivated in RPMI-1640 medium with 10% FBS. The PC-3 cells were cultivated in Ham's F12 medium with 10% FBS. Both mediums were supplemented with antibiotics (penicillin 100 U ml^{-1} and streptomycin 0.1 mg ml^{-1}). The cells were maintained at 37 °C in the humidified (60%) incubator with 5% CO_2 (Sanyo, Japan). Passages of the PNT1A and 22RV1 cell lines ranged from 15 to 35; passages of the PC-3 cell line ranged from 30 to 40.

4.4 Zinc(II) treatment of cell cultures

We used two different treatments in this study. The first one was a short-term treatment. Cells confluent up to 50–60% were

washed with a FBS-free medium and treated in fresh medium with FBS and the required zinc concentration (one-fold to three-fold the value of IC_{50} for the cell line). The cells were cultivated under these conditions for 24 h. The resulting samples are called "wild type" in this study. The second type of treatment was a long-term one. Cells were cultivated at a constant presence of zinc(II) ions. Concentrations of zinc(II) sulfate in the medium were increased gradually by small changes of 25 or 50 μM. The cells were cultivated at each concentration no less than one week before harvesting and their viability was checked before adding more zinc. Zinc resistant cells were selected naturally by this process. These cells with the long-term exposure are denoted as "resistant" in this study. The resulting concentrations in the two types of treatment were 50; 100 and 150 μM for the PC-3 cell line, 150; 300 and 450 μM for the PNT1A cell line, and 400; 800 and 1200 μM for the 22Rv1 cell line. Concentrations of zinc(II) in media and FBS were taken into account.

4.5 RNA isolation, cDNA preparation

We used the high pure total RNA isolation kit (Roche, Basel, Switzerland) to isolate RNA from the treated cells. The cultivation medium was removed; the cells were washed with PBS and trypsinizated. After transporting the cells into the centrifugation tube, the cells were centrifuged at 2700 × *g* for 7 min at 4 °C. The pellet was resuspended in PBS and lysis and binding buffers were added. The whole process was carried out according to the manufacturer's instructions. The obtained RNA was used for cDNA transcription. Total RNA (600 ng) was transcribed using random hexamer primers in a Transcriptor First Strand cDNA synthesis kit (Roche). The prepared cDNA was diluted in water and analyzed using real-time PCR.

4.6 Real-time reverse-transcription polymerase chain reaction (RT-PCR)

We used the TaqMan gene expression assay with 7500 real-time PCR system (Applied Biosystems, Foster City, CA, USA). The reaction was performed in triplicate. The amplified DNA was analyzed using the comparative Ct method using β-actin as an endogenous control. Real-time PCR was carried out under the following amplification conditions: total volume of 20 μl, initial incubation 50 °C/2 min, denaturation 95 °C/10 min, 40 cycles 95 °C/15 s, 60 °C/1 min. The primer and probe sets for β-actin (assay ID: Hs99999903_m1), *BAX* (Hs00180269_m1), *Bcl-2* (Hs00608023_m1), *Beclin-1* (Hs00186838_m1), *CFLAR* (Hs00153439_m1), *HIF1α* (Hs00153153_m1), *KRAS* (Hs00364284_g1), *MT1A* (Hs00831826_s1), *MT2A* (Hs02379661_g1), *mTOR* (Hs00234508_m1), *Nf-kB1* (Hs0076573_m1), *p53* (Hs01034249_m1), *survivin* (Hs04194392_s1), *ZIP1* (Hs00205358_m1) and *ZnT-1* (Hs00253602_m1) were selected from TaqMan gene expression assays (Life Technologies, USA).

4.7 Cell content quantification

We analyzed the total cell content on the Casy model TT system (Roche Applied Science, USA). The following protocol was used: calibration was made from the samples of viable and necrotic cells. 100 μl of necrotic cell suspension was mixed with 800 μl Casy Blue solution and incubated for 5 min at room temperature. The mixture was added 9 ml of Casy Tone. Viable cell standard was prepared from 100 μl of viable cell suspension and 10 ml Casy Tone. Measurements were made on a 100× diluted cell suspension (100 μl). Before each measurement, the background was subtracted and the capillary was cleaned. All samples were measured in duplicate.

4.8 Measurements of cell viability – MTT test

We used the MTT test to determine the cell viability in different conditions. We made 6 different MTT tests; all of them were made 8 times. Each cell line was treated with zinc and with cisplatin. The suspension of cells was diluted in the medium as required. The final density was 5000 cells per 1 well on the plate. The volume of the medium was 200 μl. Two wells for each experiment did not have cells as a control. The plates were incubated at 37 °C for two days. The medium was removed from the wells containing cells, then a new medium with the treatment was added to the cells (concentration ranged between 0 and 2000 μM of the tested substance). Subsequently, the plates were incubated at 37 °C for 24 h. From the wells containing cells and from one control cell, the medium was removed and 200 μl of fresh medium was added to 50 μl of MTT solution (5 mg ml^{-1} in PBS). The plates were subsequently incubated at 37 °C in darkness for 4 h. After this, MTT-formazan crystals were dissolved in 99.9% DMSO (dimethyl sulphoxide). 25 μl of glycine buffer was added to all wells and absorbance at 570 nm was determined (VersaMax microplate reader, Molecular Devices, Sunnyvale, CA, USA).

4.9 Fluorescence microscopy and cell staining

The cells were cultivated directly on microscope glass slides (75 × 25 mm, thickness 1 mm, Fisher Scientific, Pardubice, Czech Republic) laid on the Petri dishes with the conventional medium as described above. After the treatment, the glass slides with a layer of cells were removed from the Petri dishes and washed with a zinc free medium and PBS buffer and directly used for staining and fluorescence microscopy. For staining the free –SH groups, we used 5-(bromomethyl)fluorescein (5-BMF, Sigma-Aldrich). This probe reacts with the thiols of peptides, proteins and thiolated nucleic acids. Its reaction is slow, compared to other probes, but its thioether bonds are stronger, remaining stable under the conditions of fluorescence microscopy. Both stock (4 mM, anhydrous DMSO) and working (diluting stock solution with PBS buffer, pH 7.6) solutions of 5-BMF are unstable. They were prepared immediately before use. The cells were incubated in the dark at 37 °C for 1 h. Then the glass was washed in PBS and observed using a fluorescence microscope (Axioskop 40, Carl Zeiss AG, Oberkochen, Germany) equipped with wideband excitation and a set of filters (FITC, DAPI, Carl Zeiss). Photographs were taken using a digital camera (Olympus Camedia 750, Olympus, Tokyo, Japan). The "NIS-elements" program was used to evaluate the intensity of emission and all values were recalculated to the control (100%). Ten random fields from each variant and replicate were evaluated.

A fluorescent probe *N*-(6-methoxy-8-quinolyl)-*p*-toluene sulphonamide (TSQ, Invitrogen) was used for free zinc(II) ion staining. The stock solution (10 mM, acetone) was diluted to give a working solution (10 μM, phosphate buffer pH 7.6). The cells were carefully washed with PBS buffer and stained in the working solution for 30 min at 37 °C in the dark. After staining, the cells were rinsed three times with PBS and observed under the fluorescence microscope (Axioskop 40, Carl Zeiss) equipped with FITC and DAPI filters (Carl Zeiss). Images were taken using the digital camera (Olympus Camedia 750, Olympus). The intensity of emission was evaluated using the NIS-element. All values were recalculated to the control (100%). Ten random fields from each variant and replicate were evaluated.

4.10 Statistical analysis

The data was checked for normality and log-normal data was transformed. Multivariate ANOVA with Tukey's post-hoc testing were used to reveal differences depending on categorical factors. Pearlson correlation was used to reveal dependencies between the variables. This analysis was completed with the principal component analysis to analyze patterns in the data. Software Statistica 12 (StatSoft Inc., Tulsa, OK, USA) was used for the statistical analysis. Unless noted otherwise, the level of statistical significance was set at $p < 0.05$.

5 Conclusions

A number of studies have demonstrated that zinc(II) levels change during the progression of numerous neoplasms, particularly in prostate cancer. However, the precise mechanisms are still unclear. Therefore, a model where zinc(II) buffering is affected across various stages of tumor progression may shed light on this issue. Through a positive selection of zinc resistant cells, we created cell lines continuously viable at concentrations exceeding their initial IC_{50} for zinc(II). The resistant cells were able to divide at zinc concentrations that were even higher than a triple of the standard IC_{50}. This study clearly illustrates that a mere gene expression analysis makes it possible for us to prove the mechanisms of acquired resistance to zinc ions. This fact is also confirmed and supplemented by fluorescence microscopy. Additionally, principal component analysis as a statistical tool commonly used to reduce data can even visualize changes in the expression of genes, thus enabling us to sort genes according to their involvement in the particular resistance mechanism. Based on these results, it can be confirmed that different "groups" of genes are involved in the regulation of short- and long-term zinc(II) increases. While metallothioneins and zinc transporters play an important role in the regulation of short-term zinc(II) buffering, *KRAS*, *NF-κB*, and *PI3K* are important factors in the modulation of long-term resistance. Furthermore, the results indicate, that the acquisition of zinc resistance is associated with a worse, more aggressive phenotype, less sensitive to cytostatics such as cisplatin. These results may therefore serve as a baseline for further research in to the downstream mechanisms of these genes.

Conflicts of interest

The authors declare they have no competing interests as defined by *Metallomics*, or other interests that might be perceived to influence the results and discussion reported in this paper.

Acknowledgements

Financial support from MUNI/C/0965/2012, MUNI/A/1003/2013, CEITEC CZ.1.05/1.1.00/02.0068 and doc CEITEC 02/2012 (JG) is greatly acknowledged.

References

1 C. Andreini, L. Banci, I. Bertini and A. Rosato, Counting the zinc-proteins encoded in the human genome, *J. Proteome Res.*, 2006, **5**, 196–201, DOI: 10.1021/pr050361j.
2 D. Beyersmann and H. Haase, Functions of zinc in signaling, proliferation and differentiation of mammalian cells, *BioMetals*, 2001, **14**, 331–341, DOI: 10.1023/a:1012905406548.
3 B. L. Vallee and K. H. Falchuk, The biochemical basis of zinc physiology, *Physiol. Rev.*, 1993, **73**, 79–118.
4 L. C. Costello and R. B. Franklin, Novel role of zinc in the regulation of prostate citrate metabolism and its implications in prostate cancer, *Prostate*, 1998, **35**, 285–296, DOI: 10.1002/(sici)1097-0045(19980601)35:4<285::aid-pros8>3.0.co;2-f.
5 R. J. Cousins and R. J. McMahon, Integrative aspects of zinc transporters, *J. Nutr.*, 2000, **130**, 1384S–1387S.
6 (*a*) R. B. Franklin, P. Feng, B. Milon, M. M. Desouki, K. K. Singh, A. Kajdacsy-Balla, O. Bagasra and L. C. Costello, hZIP1 zinc uptake transporter down regulation and zinc depletion in prostate cancer, *Mol. Cancer*, 2005, **4**, DOI: 10.1186/1476-4598-4-32; (*b*) M. M. Desouki, J. Geradts, B. Milon, R. B. Franklin and L. C. Costello, hZip2 and hZip3 zinc transporters are down regulated in human prostate adenocarcinomatous glands, *Mol. Cancer*, 2007, **6**, DOI: 10.1186/1476-4598-6-37; (*c*) R. B. Franklin, J. Ma, J. Zou, Z. Guan, B. I. Kukoyi, P. Feng and L. C. Costello, Human ZIP1 is a major zinc uptake transporter for the accumulation of zinc in prostate cells, *J. Inorg. Biochem.*, 2003, **96**, 435–442, DOI: 10.1016/s0162-0134(03)00249-6.
7 J. Y. Liang, Y. Y. Liu, J. Zou, R. B. Franklin, L. C. Costello and P. Feng, Inhibitory effect of zinc on human prostatic carcinoma cell growth, *Prostate*, 1999, **40**, 200–207, DOI: 10.1002/(sici)1097-0045(19990801)40:3<200::aid-pros8>3.0.co;2-3.
8 (*a*) R. J. Cousins, J. P. Liuzzi and L. A. Lichten, Mammalian zinc transport, trafficking, and signals, *J. Biol. Chem.*, 2006, **281**, 24085–24089, DOI: 10.1074/jbc.R600011200; (*b*) L. A. Gaither and D. J. Eide, Eukaryotic zinc transporters and their regulation, *BioMetals*, 2001, **14**, 251–270.
9 R. D. Palmiter and S. D. Findley, Cloning and functional-characterization of a mammalian zinc transporter that confers resistance to zinc, *EMBO J.*, 1995, **14**, 639–649.
10 L. C. Costello, Y. Y. Liu, R. B. Franklin and M. C. Kennedy, Zinc inhibition of mitochondrial aconitase and its importance in citrate metabolism of prostate epithelial cells,

J. Biol. Chem., 1997, **272**, 28875–28881, DOI: 10.1074/jbc.272.46.28875.

11 (*a*) L. C. Costello, P. Feng, B. Milon, M. Tan and R. B. Franklin, Role of zinc in the pathogenesis and treatment of prostate cancer: critical issues to resolve, *Prostate Cancer Prostatic Dis.*, 2004, **7**, 111–117, DOI: 10.1038/sj.pcan.4500712; (*b*) L. C. Costello and R. B. Franklin, The clinical relevance of the metabolism of prostate cancer; zinc and tumor suppression: connecting the dots, *Mol. Cancer*, 2006, **5**, 17, DOI: 10.1186/1476-4598-5-17.

12 (*a*) R. B. Franklin and L. C. Costello, Zinc as an anti-tumor agent in prostate cancer and in other cancers, *Arch. Biochem. Biophys.*, 2007, **463**, 211–217, DOI: 10.1016/j.abb.2007.02.033; (*b*) M. R. Shah, C. L. Kriedt, N. H. Lents, M. K. Hoyer, N. Jamaluddin, C. Klein and J. Baldassare, Direct intra-tumoral injection of zinc-acetate halts tumor growth in a xenograft model of prostate cancer, *J. Exp. Clin. Cancer Res.*, 2009, **28**, DOI: 10.1186/1756-9966-28-84; (*c*) M. Masarik, J. Gumulec, M. Hlavna, M. Sztalmachova, P. Babula, M. Raudenska, M. Pavkova-Goldbergova, N. Cernei, J. Sochor, O. Zitka, B. Ruttkay-Nedecky, S. Krizkova, V. Adam and R. Kizek, Monitoring of the prostate tumour cells redox state and real-time proliferation by novel biophysical techniques and fluorescent staining, *Integr. Biol.*, 2012, **4**, 672–684, DOI: 10.1039/c2ib00157h.

13 P.-F. Wong and S. Abubakar, Comparative transcriptional study of the effects of high intracellular zinc on prostate carcinoma cells, *Oncol. Rep.*, 2010, **23**, 1501–1516, DOI: 10.3892/or_00000789.

14 M. Sztalmachova, M. Hlavna, J. Gumulec, M. Holubova, P. Babula, J. Balvan, J. Sochor, V. Tanhauserova, M. Raudenska, S. Krizkova, V. Adam, T. Eckschlager, R. Kizek and M. Masarik, Effect of zinc(II) ions on the expression of pro- and anti-apoptotic factors in high-grade prostate carcinoma cells, *Oncol. Rep.*, 2012, **28**, 806–814.

15 J. Gumulec, J. Balvan, M. Sztalmachova, M. Raudenska, V. Dvorakova, L. Knopfova, H. Polanska, K. Hudcova, B. Ruttkay-Nedecky, P. Babula, V. Adam, R. Kizek, M. Stiborova and M. Masarik, Cisplatin-resistant prostate cancer model: Differences in antioxidant system, apoptosis and cell cycle, *Int. J. Oncol.*, 2014, **44**, 923–933, DOI: 10.3892/ijo.2013.2223.

16 P. Babula, V. Kohoutkova, R. Opatrilova, I. Dankova, M. Masarik and R. Kizek, Pharmaceutical importance of zinc and metallothionein in cell signalling, *Chim. Oggi-Chem. Today*, 2010, **28**, 18–21.

17 (*a*) M. Yan, K. Hardin and E. Ho, Differential response to zinc-induced apoptosis in benign prostate hyperplasia and prostate cancer cells, *J. Nutr. Biochem.*, 2010, **21**, 687–694, DOI: 10.1016/j.jnutbio.2009.04.002; (*b*) P. Feng, T. L. Li, Z. X. Guan, R. B. Franklin and L. C. Costello, Direct effect of zinc on mitochondrial apoptogenesis in prostate cells, *Prostate*, 2002, **52**, 311–318, DOI: 10.1002/pros.10128; (*c*) S. Banudevi, K. Senthilkumar, G. Sharmila, R. Arunkumar, M. R. Viiayababu and J. Arunakaran, Effect of zinc on regulation of insulin-like growth factor signaling in human androgen-independent prostate cancer cells, *Clin. Chim. Acta*, 2010, **411**, 172–178, DOI: 10.1016/j.cca.2009.10.023; (*d*) P. Feng, T. L. Li, Z. X. Guan, R. B. Franklin and L. C. Costello, The involvement of bax in zinc-induced mitochondrial apoptogenesis in malignant prostate cells, *Mol. Cancer*, 2008, **7**, 6, DOI: 10.1186/1476-4598-7-25; (*e*) M. Hasumi, K. Suzuki, H. Matsui, H. Koike, K. Ito and H. Yamanaka, Regulation of metallothionein and zinc transporter expression in human prostate cancer cells and tissues, *Cancer Lett.*, 2003, **200**, 187–195, DOI: 10.1016/s0304-3835(03)00441-5; (*f*) J. H. Ku, S. Y. Seo, C. Kwak and H. H. Kim, The role of survivin and Bcl-2 in zinc-induced apoptosis in prostate cancer cells, *Urol. Oncol.: Semin. Orig. Invest.*, 2012, **30**, 562–568, DOI: 10.1016/j.urolonc.2010.06.001.

18 J. Zou, B. C. Milon, M. M. Desouki, L. C. Costello and R. B. Franklin, hZIP1 Zinc Transporter Down-Regulation in Prostate Cancer Involves the Overexpression of Ras Responsive Element Binding Protein-1 (RREB-1), *Prostate*, 2011, **71**, 1518–1524, DOI: 10.1002/pros.21368.

19 S. J. Langmade, R. Ravindra, P. J. Daniels and G. K. Andrews, The transcription factor MTF-1 mediates metal regulation of the mouse ZnT1 gene, *J. Biol. Chem.*, 2000, **275**, 34803–34809, DOI: 10.1074/jbc.M007339200.

20 L. Nardinocchi, V. Pantisano, R. Puca, M. Porru, A. Aiello, A. Grasselli, C. Leonetti, M. Safran, G. Rechavi, D. Givol, A. Farsetti and G. D'Orazi, Zinc Downregulates HIF-1α and Inhibits Its Activity in Tumor Cells In Vitro and In Vivo, *PLoS One*, 2010, **5**, e15048, DOI: 10.1371/journal.pone.0015048.

21 O. Micheau, S. Lens, O. Gaide, K. Alevizopoulos and J. Tschopp, NF-kappa B signals induce the expression of c-FLIP, *Mol. Cell. Biol.*, 2001, **21**, 5299–5305, DOI: 10.1128/mcb.21.16.5299-5305.2001.

22 (*a*) M. Zhang, D. E. Latham, M. A. Delaney and A. Chakravarti, Survivin mediates resistance to antiandrogen therapy in prostate cancer, *Oncogene*, 2005, **24**, 2474–2482, DOI: 10.1038/sj.onc.1208490; (*b*) Y.-J. Yun, S.-H. Li, Y.-S. Cho, J.-W. Park and Y.-S. Chun, Survivin Mediates Prostate Cell Protection by HIF-1 alpha Against Zinc Toxicity, *Prostate*, 2010, **70**, 1179–1188, DOI: 10.1002/pros.21152.

23 (*a*) Y. Pan, J. Huang, R. Xing, X. Yin, J. Cui, W. Li, J. Yu and Y. Lu, Metallothionein 2A inhibits NF-kappa B pathway activation and predicts clinical outcome segregated with TNM stage in gastric cancer patients following radical resection, *J. Transl. Med.*, 2013, **11**, DOI: 10.1186/1479-5876-11-173; (*b*) S. Majumder, S. Roy, T. Kaffenberger, B. Wang, S. Costinean, W. Frankel, A. Bratasz, P. Kuppusamy, T. Hai, K. Ghoshal and S. T. Jacob, Loss of Metallothionein Predisposes Mice to Diethylnitrosamine-Induced Hepatocarcinogenesis by Activating NF-kappa B Target Genes, *Cancer Res.*, 2010, **70**, 10265–10276, DOI: 10.1158/0008-5472.can-10-2839.

24 M. J. Morgan and Z.-g. Liu, Crosstalk of reactive oxygen species and NF-kappa B signaling, *Cell Res.*, 2011, **21**, 103–115, DOI: 10.1038/cr.2010.178.

25 N. Dubi, L. Gheber, D. Fishman, I. Sekler and M. Hershfinkel, Extracellular zinc and zinc-citrate, acting through a putative zinc-sensing receptor, regulate growth and survival of prostate cancer cells, *Carcinogenesis*, 2008, **29**, 1692–1700, DOI: 10.1093/carcin/bgn027.

26 J. M. Drake, N. A. Graham, T. Stoyanova, A. Sedghi, A. S. Goldstein, H. Cai, D. A. Smith, H. Zhang, E. Komisopoulou, J. Huang, T. G. Graeber and O. N. Witte, Oncogene-specific activation of tyrosine kinase networks during prostate cancer progression, *Proc. Natl. Acad. Sci. U. S. A.*, 2012, **109**, 1643–1648, DOI: 10.1073/pnas.1120985109.

27 (*a*) B. S. Taylor, N. Schultz, H. Hieronymus, A. Gopalan, Y. H. Xiao, B. S. Carver, V. K. Arora, P. Kaushik, E. Cerami, B. Reva, Y. Antipin, N. Mitsiades, T. Landers, I. Dolgalev, J. E. Major, M. Wilson, N. D. Socci, A. E. Lash, A. Heguy, J. A. Eastham, H. I. Scher, V. E. Reuter, P. T. Scardino, C. Sander, C. L. Sawyers and W. L. Gerald, Integrative Genomic Profiling of Human Prostate Cancer, *Cancer Cell*, 2010, **18**, 11–22, DOI: 10.1016/j.ccr.2010.05.026; (*b*) H. Cai, S. Memarzadeh, T. Stoyanova, Z. Beharry, A. S. Kraft and O. N. Witte, Collaboration of Kras and Androgen Receptor Signaling Stimulates EZH2 Expression and Tumor-Propagating Cells in Prostate Cancer, *Cancer Res.*, 2012, **72**, 4672–4681, DOI: 10.1158/0008-5472.can-12-0228.

28 (*a*) J. J. Bruinsma, T. Jirakulaporn, A. J. Muslin and K. Kornfeld, Zinc ions and cation diffusion facilitator proteins regulate Ras-mediated signaling, *Dev. Cell*, 2002, **2**, 567–578, DOI: 10.1016/s1534-5807(02)00151-x; (*b*) R. G. Uzzo, P. Leavis, W. Hatch, V. L. Gabai, N. Dulin, N. Zvartau and V. M. Kolenko, Zinc inhibits nuclear factor-kappa B activation and sensitizes prostate cancer cells to cytotoxic agents, *Clin. Cancer Res.*, 2002, **8**, 3579–3583.

29 A. Q. Truong-Tran, L. H. Ho, F. Chai and P. D. Zalewski, Cellular Zinc Fluxes and the Regulation of Apoptosis/Gene-Directed Cell Death, *J. Nutr.*, 2000, **130**, 1459S–1466S.

30 X. Dolcet, D. Llobet, J. Pallares and X. Matias-Guiu, NF-kB in development and progression of human cancer, *Virchows Arch.*, 2005, **446**, 475–482, DOI: 10.1007/s00428-005-1264-9.

31 (*a*) H. Kishi, M. Igawa, N. Kikuno, T. Yoshino, S. Urakami and H. Shiina, Expression of the survivin gene in prostate cancer: Correlation with clinicopathological characteristics, proliferative activity and apoptosis, *J. Urol.*, 2004, **171**, 1855–1860, DOI: 10.1097/01.ju.0000120317.88372.03; (*b*) S. F. Shariat, Y. Lotan, H. Saboorian, S. M. Khoddami, C. G. Roehrborn, K. M. Slawin and R. Ashfaq, Survivin expression is associated with features of biologically aggressive prostate carcinoma, *Cancer*, 2004, **100**, 751–757, DOI: 10.1002/cncr.20039.

32 Y. Eguchi, S. Shimizu and Y. Tsujimoto, Intracellular ATP levels determine cell death fate by apoptosis or necrosis, *Cancer Res.*, 1997, **57**, 1835–1840.

33 S. J. Rubin, D. E. Hallahan, C. R. Ashman, D. G. Brachman, M. A. Beckett, S. Virudachalam, D. W. Yandell and R. R. Weichselbaum, 2 Prostate carcinoma cell-lines demonstrate abnormalities in tumor supressor genes, *J. Surg. Oncol.*, 1991, **46**, 31–36, DOI: 10.1002/jso.2930460108.

34 T. P. Yao, The role of ubiquitin in autophagy-dependent protein aggregate processing, *Genes Cancer*, 2010, **1**, 779–786, DOI: 10.1177/1947601910383277.

35 A. Zagorska and J. Dulak, HIF-1: the knowns and unknowns of hypoxia sensing, *Acta Biochim. Pol.*, 2004, **51**, 563–585.

36 P. W. Hochachka, J. L. Rupert, L. Goldenberg, M. Gleave and P. Kozlowski, Going malignant: the hypoxia-cancer connection in the prostate, *BioEssays*, 2002, **24**, 749–757, DOI: 10.1002/bies.10131.

37 F. I. Schmieg and D. T. Simmons, Characterization of the invitro interaction between SV40 T-antigen and p53 - mapping the p53 binding-site, *Virology*, 1988, **164**, 132–140, DOI: 10.1016/0042-6822(88)90628-9.

38 S. Gonin, C. Diaz-Latoud, M. J. Richard, M. V. Ursini, A. Imbo, F. Manero and A. P. Arrigo, p53/T-antigen complex disruption in T-antigen transformed NIH3T3 fibroblasts exposed to oxidative stress: correlation with the appearance of a Fas/APO-1/CD95 dependent, caspase independent, necrotic pathway, *Oncogene*, 1999, **18**, 8011–8023.

39 M. Yan, Y. Song, C. P. Wong, K. Hardin and E. Ho, Zinc deficiency alters DNA damage response genes in normal human prostate epithelial cells, *J. Nutr.*, 2008, **138**, 667–673.

40 E. Ho, Zinc deficiency, DNA damage and cancer risk, *J. Nutr. Biochem.*, 2004, **15**, 572–578, DOI: 10.1016/j.jnutbio.2004.07.005.

41 (*a*) P. Lagiou, J. Wuu, A. Trichopoulou, C. C. Hsieh, H. O. Adami and D. Trichopoulos, Diet and benign prostatic hyperplasia: A study in Greece, *Urology*, 1999, **54**, 284–290, DOI: 10.1016/s0090-4295(99)00096-5; (*b*) S. P. Weinrich, J. H. Priest, M. A. Moyad and M. C. Weinrich, Intake of selected nutritional supplements by African-American men, *Urology*, 2004, **64**, 1094–1097, DOI: 10.1016/j.urology.2004.08.020.

42 (*a*) S. Gallus, R. Foschi, E. Negri, R. Talamini, S. Franceschi, M. Montella, V. Ramazzotti, A. Tavani, L. Dal Maso and C. La Vecchia, Dietany zinc and prostate cancer risk: A case-control study from Italy, *Eur. Urol.*, 2007, **52**, 1052–1057, DOI: 10.1016/j.eururo.2007.01.094; (*b*) K. A. Lawson, M. E. Wright, A. Subar, T. Mouw, A. Hollenbeck, A. Schatzkin and M. F. Leitzmann, Multivitamin use and risk of prostate cancer in the national institutes of health-AARP diet and health study, *J. Natl. Cancer Inst.*, 2007, **99**, 754–764, DOI: 10.1093/jnci/djk177.

3 PART II: Metabolism of amino acids and prostate carcinoma progression

3.1 Theoretical basis

Metabolites are products of biochemical reactions and largely reflect the cell phenotype. The monitoring of changes in the concentrations of major metabolites, such as amino acids, can provide a promising approach to the study of biomarkers reflecting CaP progression and identification of metabolic pathways suitable for targeted CaP therapy. Amino acids are no longer understood as the building material for cellular structures only but are believed to be of great importance as the signals interconnecting nutrition and key cellular signalling pathways. As the tumour cells and the cells of the immune system have similar nutritional requirements, the competition of these cells for resources is very frequent, which fact can have an essential impact on the progression of the tumour disease [70].

3.1.1 Prostate cancer metabolism

One of the earliest studies focused on prostatic tissue metabolism has identified citrate and spermine as the key metabolites of healthy - i.e. non-tumour - prostatic epithelial tissues. As already mentioned above, elevated zinc levels in the prostatic tissue inhibit mitochondrial aconitase, thus resulting in inhibition of the Krebs cycle, relative energy "inefficiency" of the prostatic epithelial tissue (gain: only 14 ATP per one glucose molecule) and accumulation of citrate used in the seminal fluid [71]. Low levels of citrate and spermine were associated with progression and aggressiveness of CaP [72-74]. Reduced levels of citrate in CaP are caused by its use for the needs of accelerated growth of the tumour cells [75].

Excessive activation of the androgen receptor is able to stimulate glycolysis and anabolic processes leading to the synthesis of lipids, steroid hormones, cholesterol and certain amino acids, for example, sarcosine (N-methylglycine) [76-79]. In conformity with the facts above, several studies reported an increase in sarcosine and cholesterol in CaP [77, 80, 81]. Higher glutamine-dependent lipogenesis was also recorded [82].

Dependence on aspartate import is another characteristic feature of healthy epithelial prostate tissue. Normal prostate epithelial cells accumulate citrate; it requires continuous availability of carbon sources for the mitochondrial production of acetyl coenzyme A (acetyl-CoA) and oxaloacetate (OAA), from which citrate is synthesized. Acetyl-CoA is obtained from pyruvate. Unlike the other cells, where OAA is regenerated by the end of the Krebs cycle, in case of

prostate epithelial cells, OAA is obtained from aspartate, which is imported into the cells by the EAAC1 transporter. Aspartate is thus the essential amino acid for prostate epithelial cells [83]. When CaP occurs, the intracellular concentration of zinc ions drops, m-aconitase begins to work again, and the Krebs cycle is restored. Cellular metabolism will gain about 24 molecules of ATP, and the cells will be transformed from the energy-inefficient healthy cells into the energy-efficient cells of CaP [47, 84]. The Warburg effect can be seen at the metastatic CaP stages only, which excludes the use of FDG-PET (Positron emission tomography utilizing [18F]-fluorodeoxyglucose) as the diagnostic approach at the early stages of the disease (fluorodeoxyglucose behaves like glucose and is caught on the places with high-active glucose metabolism) [85].

3.2 Hypothesis verified under PART II

The following hypotheses were formulated, based on the theoretical starting points shown in the text above:

Hypothesis 1: Changes in cellular functions are reflected in changed metabolism and changed intracellular amino acids concentrations. Long-term reduction in zinc ion accumulation is typical for prostate carcinomas. By creating prostate tumour cells, capable to accumulate zinc, the tumour metabolism should be adjusted to the normal state.

Hypothesis 2: Some of the highly synthesized amino acids may have a supportive effect on the properties of tumour cells, such as invasive potential or ability of migration.

3.2.1 Findings related to the hypothesis 1

***Hypothesis 1*: Changes in cellular functions are reflected in changed metabolism and changed intracellular amino acids concentrations. Long-term reduction in zinc ion accumulation is typical for prostate carcinomas. By creating prostate tumour cells, capable to accumulate zinc, the tumour metabolism should be adjusted to the normal state.**

Though we have managed to increase the zinc accumulation in the prostate tumour cell lines (22Rv1 and PC-3), the amino acid profile of these cells was still unrelated to the benign cells represented by the PNT1A line. On the other hand, changes in the amino acid profile reflecting CaP progression were very similar to those that occurred after the long-term supplementation of the cells with zinc ions. Due to long-term elevated concentrations of zinc in the medium, cells with a higher invasive potential, a higher resistance to cisplatin therapy [57] and a higher gene expression of the SOX2 pluripotency marker were selected positively. The tumour cell lines had a higher SOX2 gene expression, a higher aspartate and sarcosine accumulation and

lower levels of threonine, alanine, methionine, leucine, phenylalanine and lysine compared to benign PNT1A cells. Excessive aspartate accumulation accompanied by depletion of several essential amino acids that can enter the Krebs cycle (threonine, lysine, leucine, phenylalanine and methionine) suggests activation of aspartate biosynthesis through increased MDT2 malate dehydrogenase activity and GOT2 glutamate-oxaloacetate transaminase in CaP cells with the restored Krebs cycle. High levels of MDH2 were associated with a poor prognosis in CaP patients [86]. Results of amino acid profiling in CaP are summarized in Kratochvilova et al. below (see p. 142).

Conclusion: Changes in amino acid levels induced by carcinogenesis and/or resistance to zinc could be relevant for diagnostic purposes and may also potentially lead to new therapeutic options. Ratios of certain logically related amino acids may be a sensitive indicator of the malignant phenotype. Inhibition of aspartate synthesis could also become a promising approach.

Author's publication relevant to this chapter

Kratochvilova, M., M. Raudenska, et al. (2017). "Amino Acid Profiling of Zinc Resistant Prostate Cancer Cell Lines: Associations With Cancer Progression." Prostate **77**(6): 604-616.
Available on page 142

The Prostate 77:604–616 (2017)

Amino Acid Profiling of Zinc Resistant Prostate Cancer Cell Lines: Associations With Cancer Progression

Monika Kratochvilova,[1,2] Martina Raudenska,[1,2] Zbynek Heger,[2,3] Lukas Richtera,[2,3] Natalia Cernei,[2,3] Vojtech Adam,[2,3] Petr Babula,[1] Marie Novakova,[1] Michal Masarik,[1,2,4] and Jaromir Gumulec[1,4]*

[1]*Faculty of Medicine, Department of Physiology, Masaryk University, Brno, Czech Republic*
[2]*Central European Institute of Technology, Brno University of Technology, Brno, Czech Republic*
[3]*Department of Chemistry and Biochemistry, Mendel University in Brno, Brno, Czech Republic*
[4]*Faculty of Medicine, Department of Pathological Physiology, Masaryk University, Brno, Czech Republic*

BACKGROUND. Failure in intracellular zinc accumulation is a key process in prostate carcinogenesis. Nevertheless, epidemiological studies of zinc administration have provided contradicting results. In order to examine the impact of the artificial intracellular increase of zinc(II) ions on prostate cancer metabolism, PNT1A, 22Rv1, and PC-3 prostatic cell lines—depicting different stages of cancer progression—and their zinc-resistant counterparts were used. To determine "benign" and "malignant" metabolic profiles, amino acid patterns, gene expression, and antioxidant capacity of these cell lines were assessed.

METHODS. Amino acid profiles were examined using an ion-exchange liquid chromatography. Intracellular zinc content was measured by atomic absorption spectrometry. Metallothionein was quantified using differential pulse voltammetry. The content of reduced glutathione was determined using high performance liquid chromatography coupled with an electrochemical detector. Cellular antioxidant capacity was determined by the ABTS test and gene expression analysis was performed by qRT-PCR.

RESULTS AND CONCLUSIONS. Long-term zinc treatment was shown to reroute cell metabolism from benign to more malignant type. Long-term application of high concentration of zinc(II) significantly enhanced cisplatin resistance, invasiveness, cellular antioxidant capacity, synthesis of glutathione, and expression of treatment resistance- and stemness-associated genes (*SOX2, POU5F1, BIRC5*). Tumorous cell lines universally displayed high accumulation of aspartate and sarcosine and depletion of essential amino acids. Increased aspartate/threonine, aspartate/methionine, and sarcosine/serine ratios were associated with cancer phenotype with high levels of sensitivity and specificity. *Prostate 77: 604–616, 2017.*

KEY WORDS: **zinc; resistance; amino acid; aspartate; metabolomics**

INTRODUCTION

Metabolism of prostate gland cells is unique and different from metabolism of other cells in human body. Secretory epithelial cells in the prostate are highly specialized in citrate production and are able to secrete high amounts of citrate into the prostatic fluid. This happens due to their capability to accumulate high levels of zinc that inhibit m-aconitase and citrate oxidation in the Krebs cycle. As a consequence, normal prostate glandular epithelial cells exhibit low respiration, unfinished Krebs cycle, low citrate oxidation, and

Grant sponsor: Faculty of Medicine, Masaryk University; Grant number: MUNI/A/1365/2015; Grant sponsor: Czech Science Foundation; Grant number: GACR 16-18917S; Grant sponsor: League Against Cancer Prague.

Conflicts of interest: None.

*Correspondence to: Dr. Jaromir Gumulec, Faculty of Medicine, Department of Physiology, Masaryk University, Kamenice 5, CZ-625 00 Brno, Czech Republic. E-mail: j.gumulec@med.muni.cz
Received 21 October 2016; Accepted 22 December 2016
DOI 10.1002/pros.23304
Published online 19 January 2017 in Wiley Online Library (wileyonlinelibrary.com).

are therefore worse ATP producers as compared to benign epithelial cells in other tissues [1].

In majority of tumors, tumorigenesis is usually associated with a metabolic switch from respiration to glycolysis and reduced catabolic Krebs cycle activity (Warburg effect) which attenuates effectivity of ATP production. Conversely, due to a failure in intracellular zinc accumulation in tumor prostate cells, a metabolic switch from citrate-accumulating, energy-inefficient benign cells to energy-efficient tumor cells occurs [2]. Citrate can be oxidized to carbon dioxide and oxaloacetate for the production of ATP in mitochondria; another possibility is its preferable export to the cytosol, where acetyl coenzyme A (acetyl-CoA) and oxaloacetate is formed due to ATP citrate lyase action. Acetyl-CoA is used for the synthesis of fatty acids and cholesterol, whereas oxaloacetate is an amino acid precursor [3]. Accordingly, prostate cancer cells were shown to contain higher levels of amino acids, fatty acids, and cholesterol [3–6]. Furthermore, N-methyl derivative of glycine (sarcosine) can be accumulated in cells during prostate cancer progression to metastasis [7]. Changes in intracellular concentrations of particular metabolites can influence cancer cell growth and metastatic invasion [8,9]. Many oncogenes—such c-Myc, Ras, or Src—provide cancer cells with alternative metabolic pathways and unconventional use of amino acids [10,11]. Consequently, changes in amino acid profiles may serve as a valuable biomarker for screening, diagnosis, and prognosis, since they are easily measurable in body fluids.

It is obvious that failure in intracellular zinc accumulation is a key process in prostate carcinogenesis. Nevertheless, epidemiological studies of zinc administration have provided rather contradicting results [12]. In order to examine the impact of excessive zinc concentrations on intracellular zinc accumulation and prostate cancer metabolism, PNT1A, 22Rv1, and PC-3 prostatic cell lines—depicting different stages of the cancer disease progression—and their previously created zinc-resistant counterparts have been used in this study [13]. The main focus of this work has been to assess "benign" and "malignant" metabolic profiles. Furthermore, amino acid profiles of each cell line in relation to a degree of zinc accumulation and zinc resistance have been determined.

MATERIALS AND METHODS

Chemical and Biochemical Reagents

RPMI-1640 medium, Ham's F12 medium, fetal bovine serum (FBS) (mycoplasma-free), penicillin/streptomycin, and trypsin were purchased from Sigma Aldrich Co. (St. Louis, MO). Phosphate buffered saline PBS was purchased from Invitrogen Corp. (Carlsbad, CA). Ethylenediaminetetraacetic acid (EDTA), zinc(II) sulphate (BioReagent grade, suitable for cell cultures) and all other chemicals of ACS purity were purchased from Sigma Aldrich Co., unless noted otherwise.

Cell Cultures

Three human prostatic cell lines were used in this study. PNT1A human cell line is derived from normal adult prostatic epithelial cells immortalized by transfection with a plasmid containing SV40 genome with defective replication origin. The primary culture was obtained from the normal prostatic tissue of a 35-year old male post mortem. PNT1A is PTEN positive non-tumorigenic epithelial cell line [14]. 22Rv1 is human prostate carcinoma epithelial cell line derived from a xenograft serially propagated in mice after castration. The cell line expresses prostate specific antigen (PSA). Growth is weakly stimulated by dihydroxytestosterone and lysates are immunoreactive with androgen receptor antibody. 22Rv1 is PTEN positive [15]. PC-3 human epithelial cell line was established from a four grade prostatic adenocarcinoma, androgen independent, and unresponsive metastatic site in bone. PC-3 is PTEN- and p53-negative [15,16]. All cell lines used in this study were purchased from HPA Culture Collections (Salisbury, UK).

Cell Cultivation

PNT1A and 22Rv1 cells were cultured in RPMI-1640 medium with 10% FBS. PC-3 cells were cultured in Ham's F12 medium with 10% FBS. Both media were supplemented with antibiotics (penicillin 100 U/ml and streptomycin 0.1 mg/ml). Cells were maintained at 37°C in a humidified (60%) incubator with 5% CO_2 (Sanyo, Japan). The passages of PNT1A and 22Rv1 cell lines ranged from 25 to 35, the passages of PC-3 cell line ranged from 15 to 25.

Zinc(II) Treatments of Cell Cultures

Two different treatments were used in this study. The first one was short-term treatment. Cells confluent up to 50–60% were washed with FBS-free medium and treated with fresh medium with FBS and required zinc concentration (onefold to threefold the value of IC50 for the cell line). Cells were cultivated under these conditions for 24 hr. The resulting samples are called zinc-treated "wild type" in this study. The second type of treatment was long-term. Cells were cultivated with the constant presence of zinc(II) ions.

The concentrations of zinc(II) sulphate in the medium were increased gradually by small changes of 25 or 50 μM. Cells were cultivated at each concentration no less than 1 week before harvesting and the viability was checked before adding more zinc. This process naturally selected zinc resistant cells. Cells with long-term exposure are called "resistant" in this study. Total time of cultivation of cell lines in zinc(II)-containing media exceeded one year. Resulting concentrations of zinc(II) in media (onefold to threefold the value of IC50 for particular cell line) were 50; 100 and 150 μM for PC-3 cell line, 150; 300 and 450 μM for PNT1A cell line, and 400; 800 and 1200 μM for 22Rv1 cell line. Concentrations of zinc(II) in media and FBS were taken into account.

RNA Isolation, cDNA Preparation

Cultivation medium was removed, cells were washed with PBS and trypsinized. TriPure Isolation Reagent (Roche, Basel, Switzerland) was used for RNA isolation. RNA samples without reverse transcription were used as negative control for qRT-PCR to exclude DNA contamination. The isolated RNA was used for the cDNA synthesis. RNA (1,000 ng) was transcribed using the transcriptor first strand cDNA synthesis kit (Roche, Switzerland) according to manufacturer's instructions. The cDNA (20 μl) prepared from the total RNA was diluted with RNase free water to 100 μl and the amount of 5 μl was directly analyzed.

Quantitative Real-Time Polymerase Chain Reaction (qRT-PCR)

qRT-PCR was performed using the TaqMan gene expression assays with the LightCycler®480 II System (Roche, Basel, Switzerland). The amplified DNA was analyzed by the comparative Ct method using β-actin as a reference. The primer and probe sets for *ACTB* (assay ID: Hs99999903_m1), *MT2A* (Hs02379661_g1), *ZNT1* (Hs00253602_m1), *SOX2* (Hs01053049_s1), *HIF1A* (Hs00153153_m1), *NANOG* (Hs04260366_g1), *BIRC5* (Hs00153353_m1), and *POU5F1* (Hs04260367_gH) were selected from TaqMan gene expression assays (Life Technologies). qRT-PCR was performed under the following amplification conditions: total volume of 20 μl, initial incubation at 50°C/2 min followed by denaturation at 95°C/10 min, then 45 cycles at 95°C/15 sec and at 60°C/1 min.

Preparation of Cells for Determination of Amino Acid Profiles and Zinc Content

Five miligram of cells was digested by Microwave system 3,000 (Anton Paar GmbH, Graz, Austria) using rotor MG-65 in nitric acid (65% v/v) and hydrogen peroxide (30 v/v) in ratio 7:3. Microwave power was set to 100 W (30 min) at a temperature of 140°C.

Amino Acids Profiling

Amino acid profiles were examined using an ion-exchange liquid chromatography (AAA-400, Ingos, Prague, Czech Republic) with post-column derivatization by ninhydrin and absorbance detector in visible light range (IEC-Vis). Measurements were carried out under conditions optimized in our previous study [17].

Zinc Quantitation by Atomic Absorption Spectrometry

Measurements were carried out on 280Z atomic absorption spectrometer (Agilent, Technologies, Santa Clara, CA) with electrothermal atomization and Zeeman background correction. Zinc was measured on primary wavelength: Zn 213.9 nm (spectral bandwidth 0.5 nm, lamp current 10 mA) in the presence of Pd chemical modifier.

Preparation of Cells Prior Sarcosine Analyses

The cells were frozen by liquid nitrogen to disrupt their structure. The frozen samples were further homogenized using ultrasonic homogenizer SONOPLUS mini20 (Bandelin electronic, Berlin, Germany). Then 1 ml of 0.2 M phosphate buffer (pH = 7.0) was added and the sample was homogenized again for 5 min. The cell homogenates were further analyzed using IEC-Vis according to our previous study [17].

Preparation of Cells for Determination of Total Protein, Metallothionein, Glutathione, and Antioxidant Capacity

The cells were frozen by liquid nitrogen and homogenized using ultrasonic homogenizer SONOPLUS mini20 (Bandelin electronic). Subsequently, 1 ml of 0.2 M phosphate buffer (pH 7.0) was added and the sample was homogenized for 5 min. The homogenates were further centrifuged using Microcentrifuge 5417R (Eppendorf, Hamburg, Germany) at 4°C, 15,000*g*, for 15 min. Finally, the supernatant was filtered through a membrane filter (0.45 μm nylon filter disk; Millipore, Billerica, MA) and analyzed.

Determination of Total Protein Content

The total proteins were utilized for results normalization and were performed using SKALAB

CBT 600T kit (Skalab, Svitavy, Czech Republic) according to manufacturer's instructions, using BS-400 automated spectrophotometer (Mindray, Schenzhen, China).

Determination of Amount of Metallothionein

MT was quantified using differential pulse voltammetry (747 VA Stand, connected to the 693 VA processor and 695 Autosampler, Metrohm, Herissau, Switzerland), under the conditions used in our previous study [18].

Determination of Reduced Glutathione

The content of reduced glutathione (GSH) was determined using high performance liquid chromatography coupled with an electrochemical detector (HPLC-ED) system under the conditions used in our previous study [19].

Determination of Antioxidant Capacity by the ABTS Test

Antioxidant capacity was analyzed using the neutralization of a radical-cation arising from one-electron oxidation of the synthetic chromophore 2,2′-azino-bis(3-ethylbenzothiazoline-6-sulfonic acid (ABTS). The reaction was monitored spectrophotometrically by the change of the absorption value at 660 nm using spectrophotometer BS-400 (Mindray).

Real-Time Impedance Based Cell Migration and Invasivity Assay

The impedance-based real-time cell analysis (RTCA) xCELLigence system was used according to the instructions of the supplier (Roche Applied Science and ACEA Biosciences, San Diego, CA). The xCELLigence system consists of four main components: RTCA DP station, RTCA computer with integrated software and disposable CIM-plate 16. Firstly, the optimal seeding concentration for migration and invasivity assay was determined. Optimal response was found in the well containing 20,000 cells. After coating the upper wells with Matrigel and adding FBS as chemoattractant, a total number of cells in 100 μl of medium to each well in CIM-plate 16 was seeded. The cell attachment and growth through the matrigel were monitored every 15 min. Duration of all experiments was 80 hr. Results are expressed as relative impedance using manufacturer's software (Roche Applied Science and ACEA Biosciences) [20].

Statistical Analysis

Data were checked for normality and log-normal data were transformed. Univariate general regression models with all three factors (cell line, resistance, zinc concentration) as categorial predictors were performed in the first step. Consequently, planned comparisons were performed. In the next step, all values were standardized and dependencies were analyzed using principal component analysis on a two-factor plane based on amino-acid levels (oxidative parameters and genes were plotted as supplementary variables), (c) using hierarchical clustering using Ward's method showing linkage distance between cases (cell lines). Finally, receiver-operator statistic using easyROC 1.3 (http://www.biosoft.hacettepe.edu.tr/easyROC/) was performed to assess area under the curve, sensitivity and specificity of selected variables as predictors of tumor presence. Unless noted otherwise, P level <0.05 was considered significant and software Statistica 12 (Dell Inc., Tulsa, OK) was used.

RESULTS

Zinc Accumulation

In previous experiments, IC50 for zinc sulphate of wild-type cell lines was determined as follows: 150.8 μM, 369.1 μM, and 55.5 for PNT1A, 22Rv1, and PC-3, respectively [13].

The levels of accumulated (measured) intracellular zinc in wild-type and resistant cell lines exposed to 0–3-fold of its IC50 concentrations of zinc sulphate were compared (see experimental section for details). Intracellular zinc was accumulated more intensively in resistant cell lines in comparison with wild-type cell lines ($P = 0.01$, see Supplementary Table S1) when exposed to zinc treatment. Nevertheless, cell-line specific differences in zinc accumulation were observed; intracellular zinc(II) content increased extensively and proportionally to added zinc sulphate in all resistant cell lines and also in the wild-type 22Rv1. On the other hand, only a small increase in intracellular levels of zinc due to zinc sulphate treatment was observed in wild-types PC-3 and PNT1A. Maximal increase in intracellular zinc concentration was achieved in zinc-resistant 22Rv1 cultured in threefold IC50 (up to 1,800 μg/g); see Figure 1A.

General Mechanisms of Coping With Increasing Zinc(II) Concentrations

Changes in antioxidant capacity, expression of selected genes, and accumulation of particular amino acids caused by increasing zinc(II) concentration are

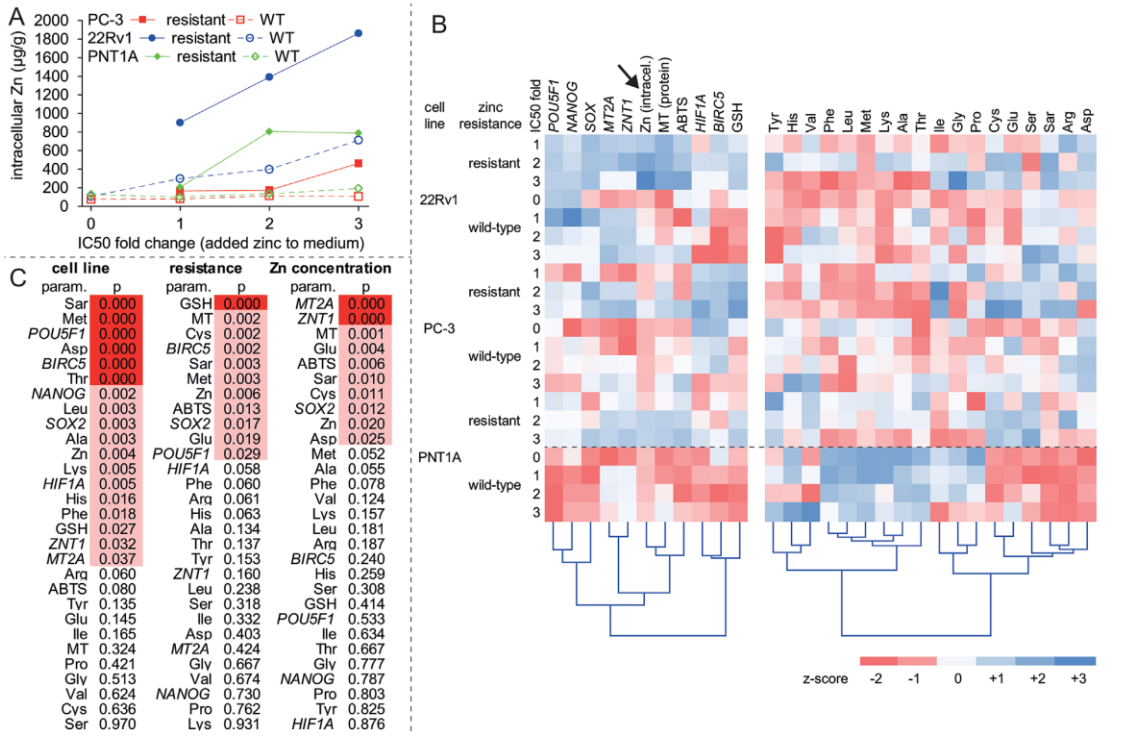

Fig. 1. Concentrations of amino acids, gene expression levels and other parameters in zinc-resistant prostatic cell lines and wild-type counterparts. (**A**) absolute concentration of intracellular (measured) zinc versus concentration of zinc in medium (0, 1, 2, and 3 correspond to IC-50 fold changes). (**B**) Heatmap showing relative amounts of parameters in cells. Displayed as z-scores with mean = 0 and standard deviation = 1. Note the distinctive differences between wild-type PNT1A cells and tumorous counterparts. ``IC50 fold'' indicate fold change of half-maximal concentration of zinc used for treatment, ``Zn'' indicate amount of intracellular zinc (measured). (**C**) results of univariate test, *P*-values for individual variables for three independent predictors—cell line, resistance, and zinc concentration. Sorted based on *P*-level (parameters most significantly affected by cell line/resistance or Zn concentration are dark red, topmost in table).

shown in Figure 1B. According to multivariate ANOVA, MT gene, and protein, *ZnT1,* and *SOX2* genes significantly increased their expression in cells treated with zinc(II)ions ($P \leq 0.001$, $P \leq 0.001$, $P = 0.002$, see supplementary Table S1). Furthermore, zinc(II) treatment significantly enhanced cellular concentrations of sarcosine ($P = 0.03$), aspartate ($P = 0.01$), glutamate ($P = 0.01$), cysteine ($P = 0.005$), valine ($P = 0.03$), and arginine ($P = 0.04$) as well as antioxidant capacity of cells (2,2′-azino-bis(3-ethylbenzothiazoline-6-sulphonic acid, ABTS, $P = 0.05$). On the other hand, cellular concentrations of alanine ($P = 0.04$), methionine ($P = 0.01$), and phenylalanine ($P = 0.04$) significantly decreased due to zinc(II) treatment.

In conclusion, universal mechanisms of coping with increasing zinc concentrations (common to both resistant and wild-type cell lines) were observed. These mechanisms involved chelation of free zinc ions by metallothionein (an increasing trend in MT expression was observed), efflux of zinc(II) ions from the cytoplasm by the ZnT1 transporter and enhancement of the antioxidant capacity (measured by ABTS) followed by the accumulation or depletion of particular amino acids.

Effect of Cell Line

In this step, the effect of the cell line was analyzed after adjustment of zinc concentration and zinc resistance. Using univariate test, there was a significant effect of cell line on the gene expression and amino acid profile $F(30,6) = 16.97$; $P \leq 0.001$ (see Fig. 1C). Among the parameters most distinctly affected by cell line are cellular concentrations of sarcosine, methionine, aspartate, and threonine and gene expression levels of *POU5F1, NANOG,* and *BIRC5.*

Subsequent planned comparisons (multivariate testing) revealed that tumorous 22Rv1 cell line (compared to non-tumor PNT1A) exhibited up-regulation of the gene expression of *SOX2* ($P = 0.001$), *MT2A*

($P = 0.02$), *NANOG* ($P = 0.004$), and *POU5F1* ($P < 0.001$); higher accumulation of zinc ($P = 0.01$), aspartate ($P = 0.002$), and sarcosine ($P < 0.001$) and higher antioxidant capacity ($P = 0.04$). Conversely, intracellular concentrations of threonine ($P = 0.005$), alanine ($P = 0.002$), methionine ($P < 0.001$), leucine ($P = 0.003$), phenylalanine ($P = 0.02$), histidine ($P = 0.005$), and lysine ($P = 0.002$) were lower in 22Rv1 cell line. Secondly, characteristics of the cell line derived from metastasis (PC-3) were analyzed. Compared to PNT1A, there was a significant up-regulation of GSH ($P = 0.01$), *BIRC5* ($P < 0.001$), *SOX2* ($P = 0.03$), and *HIF1A* ($P = 0.002$). Higher accumulation of aspartate ($P < 0.001$), sarcosine ($P < 0.001$), and arginine ($P = 0.03$) was also observed in PC-3. Conversely, intracellular concentrations of threonine ($P < 0.001$), alanine ($P = 0.01$), methionine ($P < 0.001$), leucine ($P = 0.002$), phenylalanine ($P = 0.01$), and lysine ($P = 0.02$) were lower in PC-3 cell line.

In conclusion, tumorous cell lines were characteristic by higher expression of *SOX2,* higher accumulation of aspartate, and sarcosine and lower levels of essential amino acids, in particular: threonine, methionine, leucine, phenylalanine, lysine, and alanine. Primary tumor-derived 22Rv1 was characteristic by depletion of histidine and increased expression of *MT2A*, *NANOG*, and *POU5F*. Bone metastasis-derived PC-3 was typical by increased accumulation of arginine and higher expression of *HIF1A* and *BIRC5*.

Effect of Long-Term Treatment (Zinc Resistance)

In this step, the effect of "zinc resistance" (i.e., long-term vs. short-term treatment) was assessed.

Resistant cells markedly increased their IC50 for cisplatin: by 1.4-, 1.6-, and 1.6-fold for PNT1A, 22Rv1, and PC-3, respectively [21]. Furthermore, morphological changes and increased numbers of polyploid giant cancer cells (PGCCs) in zinc-resistant PC-3 cell line were observed (Fig. 2A). Also, cellular concentrations of metallothionein, cysteine, sarcosine, methionine, glutamine, and GSH were significantly affected by the zinc resistance. Resulting zinc accumulation, antioxidant capacity (ABTS) and higher gene expression of *BIRC5* ($P = 0.002$), *POU5F1* ($P = 0.03$), and *SOX2* ($P = 0.02$) were other consequences of zinc-resistant phenotype (Fig. 1C and supplementary Table SI). Higher accumulation of zinc in resistant cells (see section Zinc Accumulation) could be a direct result of their higher antioxidant capacity (ABTS) ($P = 0.01$) and higher GSH ($P = 0.001$), and metallothionein (MT) production ($P = 0.002$). Resistant cells accumulate also higher levels of sarcosine ($P = 0.003$), cysteine ($P = 0.002$), and glutamate ($P = 0.02$) and relatively lower levels of methionine ($P = 0.003$). The ability of cells to spread in the surrounding tissues was tested by using real-time, label-free monitoring xCELLigence invasivity assay. Higher invasiveness of all tested zinc resistant cell lines (PC-3, PNT1A, 22Rv1) in comparison with their non-resistant counterparts was demonstrated (Fig. 2B).

To reveal the complex connection patterns between long- and short-term treatments and thus to illustrate the involvement of amino acids in zinc resistance, principal component analysis (PCA) was performed. This analysis combines the advantages of correlation analysis with cluster analysis by projecting the variables (amino acids, genes, etc.) on a two-factor plane. The "importance" of the variables increases with their distance from the center of the diagram. A two-factor plane was constructed based on amino acid patterns ("active" variables). This approach explained 66.4% and 59.7% of data heterogeneity in wild-type and resistant cells. In the next step, other parameters (genes, oxidative stress-related parameters) were plotted into this factor plane as supplementary variables. Following associations were evident: (i) The central effect of GSH and its association with amino acid metabolism is typical for zinc-resistant cells (compare the distance of GSH from the PCA center in WT and resistant cells, Fig. 3A); (ii) On the other hand, antioxidant capacity measured by ABTS played a more central role in wild-type cells (compare distances from PCA center accordingly). Because GSH was not in a positive correlation with ABTS, we assume another important role of GSH in resistant metabolism; (iii) Furthermore, "pro-survival and/or antioxidant" markers (such as ABTS, GSH, MT, HIF1A, cysteine, glutamine) are clustered together in wild-type cells (lower left quadrant of PCA), while markers associated with "pluripotency" (*NANOG*, *SOX2*, *POU5F1*) are located in a different (upper left) quadrant in wild-type cells. However, this is not evident in zinc-resistant cells, where all those parameters are clustered together.

Amino Acid Patterns as Predictors of Cancer Phenotype

Previous analyses highlighted amino acids specifically related to zinc resistance, cell lines, or zinc concentration. However, these data do not bring the evidence whether or how the individual amino acids are related to the advancement of the disease. Therefore, hierarchical cluster analysis was performed using amino acid concentrations as variables. Based on interrelationships between amino acids, linkage distance between wild-type untreated PNT1A cell line and others was calculated (Fig. 3B). As expected, remaining wild-type PNT1As (exposed

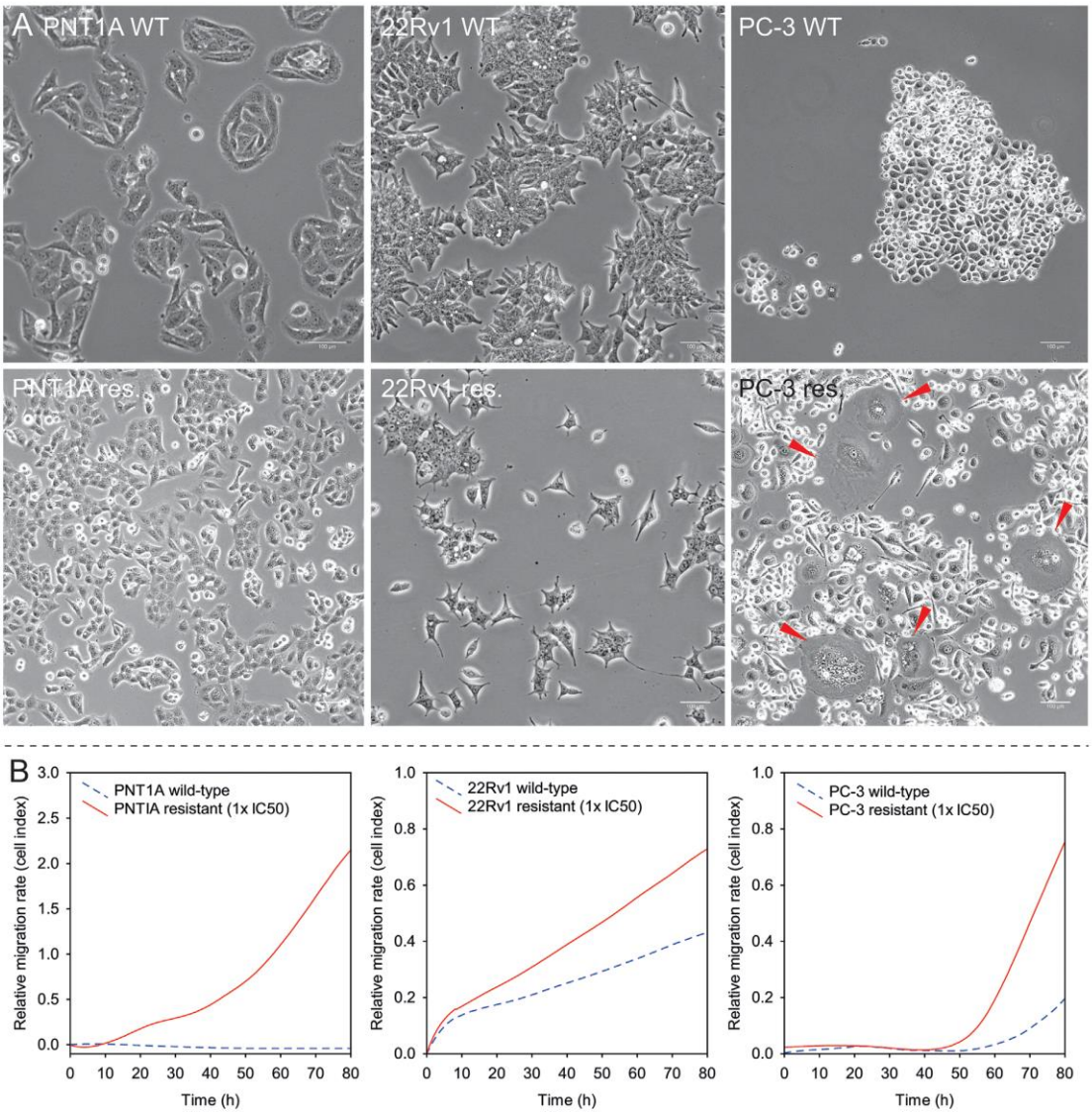

Fig. 2. Cell morphology and invasivity changes due to long-term zinc treatment. (**A**) Morphology of wild-type and zinc-resistant cells. Red arrrow indicate polyploid giant cancer cells. (**B**) real-time label-free monitoring of invasivity. See higher invasiveness of all tested zinc resistant cell lines (PC-3, PNT1A, 22Rv1) in comparison with their non-resistant counterparts.

to zinc) were clustered closely to the untreated one followed by a cluster of tumorous cell lines (see the setting of the plateau on a linkage distance curve in Fig. 3B "tumorous metabolism" characteristic for tumorous cells). Distinct contribution of zinc treatment was also evident: higher concentrations of zinc, as well as resistant variants of particular cell lines, were at greater distance from benign untreated PNT1A. Moreover, another cluster characteristic by the highest linkage distances to PNT1A was observed and designated as "highly resistant metabolism"; this cluster was composed of resistant tumorous cell lines treated by the highest zinc(II) concentrations. This trend was verified using receiver-operator statistics (ROC), showing that linkage distance based on amino acid profiles is highly specific and sensitive indicator of malignant behavior (Fig. 3C). This trend was also in a correlation with pluripotency marker *SOX2* ($r = 0.72$, $P < 0.001$, highlighted as green dots in the chart).

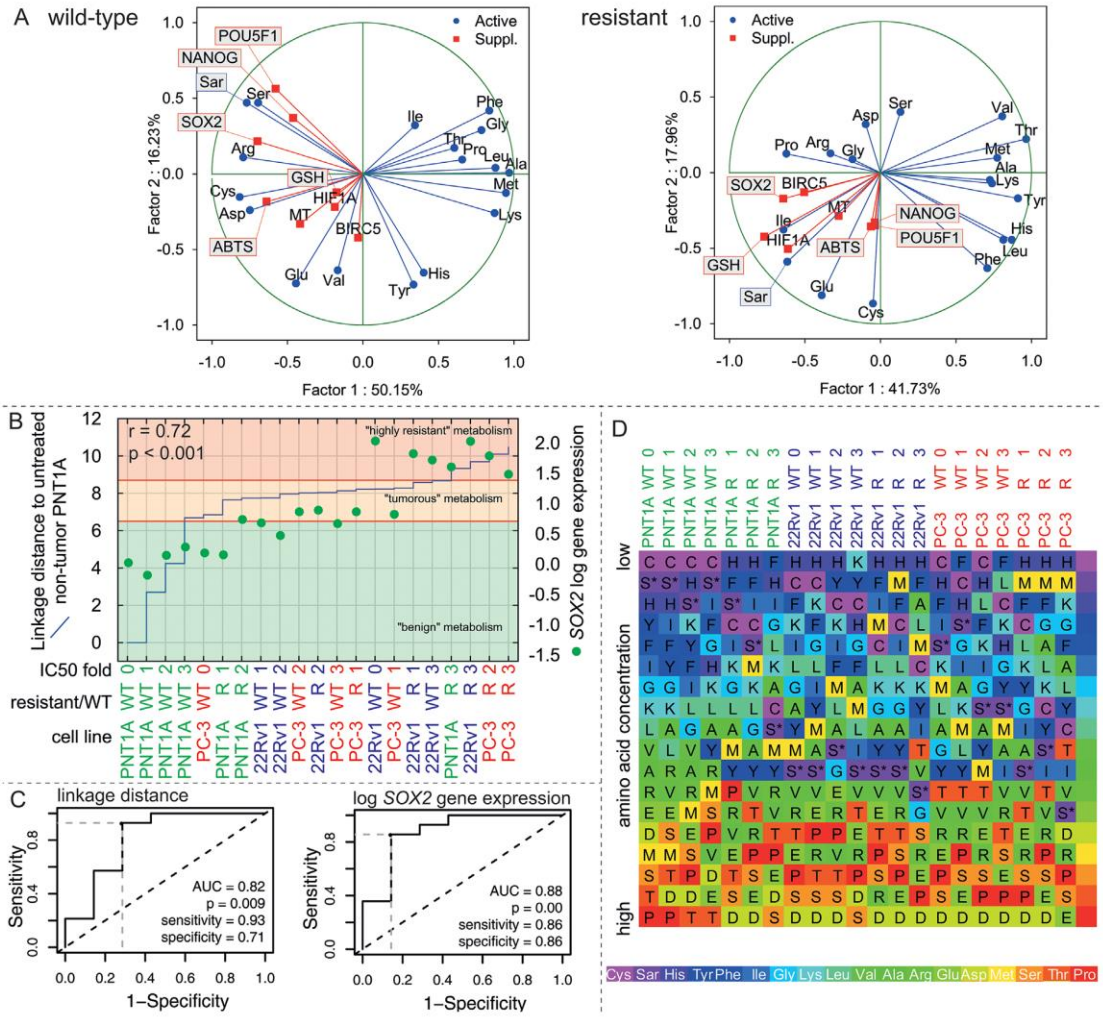

Fig. 3. Amino acid patterns and tumor progression. (**A**) Principal component analysis, projection of variables on two-factor plane based on amino acid concentrations (other parameters plotted on a chart as a supplementary variables). Note that pluripotency-associated genes *NANOG*, *SOX2*, and *POU5F1* are clustered together with pro-survival and oxidative stress parameters in resistant cells (lower left quadrant) and clustered separately in WT cells. (**B**) linkage distance determined by cluster analysis based on amino acid patterns. Linkage distance illustrates level of dissimilarity from non-tumor wild-type untreated PNT1A cells, for whose linkage distance = zero. 0, 1, 2, and 3 correspond to IC-50 fold changes. See that resistance and/or tumorous phenotype enhance linkage distance from PNT1A cells. Based on a linkage distance, benign, tumorous and highly resistant cells were distinguished. Linkage distance correlated with *SOX2* expression in cells (green dots). (**C**) receiver-operator curves and its subsequent statistics for determination of benign/malignant cell lines. (**D**) chart showing relative abundance of particular amino acid in particular cells, sorted from low to high concentrations. 0, 1, 2, and 3 correspond to IC-50 fold changes. Rainbow color order coding based on untreated wild-type PNT1A cells. See the rainbow-colored heatmap distracts by relative increase/decrease of specific amino acids amounts (see online for color). See gradual decrease of Met (high concentrations in non-tumor cells vs. low concentrations in resistant tumorous cells) and increasing concentrations of Sar, Cys, and Asp in relation to the progression of zinc resistance and malignance. S* indicate sarcosine. WT, wild-type; R, resistant.

In order to highlight which of the amino acids contribute to this "model of gradual increase of aggressiveness," a heatmap based on amino acid concentrations was created (Fig. 3D). Several specific phenomena were evident: (i) gradual decrease of methionine (high concentrations in non-tumor cells as compared to low methionine concentrations in resistant tumorous cells) and (ii) increasing concentrations of sarcosine, cysteine, and aspartate in relation to the progression of zinc resistance and malignance. Based

on these data, following product/precursor ratios were calculated: cysteine/methionine and sarcosine/serine. The association of these ratios with malignant phenotype was verified by ROC and multivariate ANOVA (Table I), where both of them demonstrated high levels of sensitivity and specificity. Thus, high cysteine/methionine and sarcosine/serine ratios were shown to be a promising marker of malignant metabolism.

Excessive accumulation of aspartate was accompanied by a depletion of some essential amino acids (threonine, lysine, leucine, phenylalanine, and methionine) in prostate cancer cells. This fact indicated a boosting of aspartate synthesis pathways. Various molecules could serve as a substrate for synthesis of aspartate, including essential amino acids (Fig. 4). In accordance with observed increasing/decreasing trends of amino acids (Fig. 3D), ratios between Asp and other amino acids were calculated and the effect of cell line on the level of these ratios was analyzed using multivariate ANOVA and receiver-operator statistic (Table I). Aspartate/tyrosine, aspartate/methionine, and aspartate/threonine ratios were shown to be promising markers of malignant metabolism. Furthermore, ROC analysis provided evidence that aspartate synthesis pathway is specifically altered in tumorous cell line and thus it is involved in the prostate cancer progression.

DISCUSSION

The key biochemical feature of prostate cancer cells is a steep decrease in intracellular zinc(II) and citrate levels. Metabolic transformation leading to the attenuation of zinc concentration with subsequent triggering of citrate oxidation is fundamental for the manifestation of malignant phenotype [22]. Consequently, it is intriguing to apply this relationship to treatment or prevention of prostate cancer. Our approach in this study was to constitute conditions that would enforce the accumulation of zinc(II) into the malignant cells and to assess consequences of such accumulation for malignant metabolism (Will an artificial intracellular increase of zinc cause a change towards a benign metabolism?). PNT1A, 22Rv1, and PC-3 prostatic cell lines— depicting different stages of the cancer disease progression—and their previously created zinc-resistant counterparts have been used [13]. We have confirmed the higher ability of zinc-accumulation in resistant cell lines (see Fig. 1A). It can be assumed that long-term exposure to excessive zinc(II) is able to exhaust the capacity of cellular zinc(II) exporters and cells are then forced to accumulate this metal and to trigger intrinsic mechanism for coping with it. Universal mechanisms of coping with increasing intracellular zinc(II) concentrations include free zinc ions chelation by metallothionein and an enhancement of the antioxidant capacity. These effects were previously observed in several laboratories, including ours [13,23,24]. The maximal increase in intracellular zinc concentration was achieved in zinc-resistant 22Rv1 derived from primary tumor of prostate (up to 1,800 μg/g). High zinc tolerance in primary tumor cells (especially in comparison with metastatic counterparts) may result from adoption and enhancement of inherited capabilities of benign secretory epithelial cells. These cells are highly specialized and evolved for zinc accumulation [25]; therefore, they can exploit protective mechanisms against the toxic effects of zinc. On the contrary, prostate cancer cells derived from bone metastasis (PC-3 cells) no longer need to cope with high zinc concentrations in prostate gland and hence are more sensitive to zinc(II).

The main focus of this study was to assess "benign" and "malignant" metabolic profiles. Clarifying of metabolic shifts triggered by carcinogenesis is relevant for diagnostic purposes and can also elucidate the molecular basis of malignant processes, which could possibly result in new therapeutic options. In this study, tumorous cell lines displayed higher expression of *SOX2* gene, higher accumulation of aspartate and sarcosine and lower levels of threonine, alanine, methionine, leucine, phenylalanine, and lysine as compared to benign PNT1A. SOX2 is a core transcription factor involved in self-renewal and pluripotency of tumor cells and was reported to be involved in malignant transformation of prostate tissue [26,27] which is in full accordance with our results. *SOX2* expression plays a significant role in cancer phenotype, as it was in a strong correlation with linkage distance depicting the degree of deviation from benign metabolism represented by PNT1A cells (see Fig 3B). With regard to sarcosine and aspartate, we have previously shown that these amino acids affect the progression and migration capacity of prostate cancer cells [9]. Aspartate is usually synthesized in the mitochondrial matrix with the help of malate dehydrogenase (MDH2) and glutamic-oxaloacetic transaminase 2 (GOT2). Nevertheless, the shift in the NAD+/NADH balance after OXPHOS attenuation in healthy prostate secretory cells can inhibit MDH2 and consequently aspartate synthesis in mitochondria [28,29]. Accordingly, aspartate was considered as an essential amino acid for healthy prostate cells [30,31]. Moreover, healthy prostate cells utilize large amounts of aspartate as the carbon source for citrate production [32]. Support of aspartate biosynthesis in proliferating cells was recently revealed as a key activity of respiration [28,33]. Excessive aspartate accumulation accompanied by depletion of

TABLE I. The Effect of Cell Line on Amino Acid Levels and Amino Acid Ratios

	Absolute concentration (estimate and 95%CI)		Aspartate[a]/amino acid ratio				
Amino acid	22Rv1 vs. PNT1A	PC-3 vs. PNT1A	22Rv1 vs. PNT1A (estimate and 95% CI)	PC-3 vs. PNT1A	Benign vs. tumorous (AUC and 95% CI)	Sensitivity	Specificity
Asp	1.62 (−2.36 to 5.60)	8.55* (3.68 to 13.42)	–	–	–	–	–
Thr	−2.46 (−5.78 to 0.86)	−6.29* (−10.35 to −2.22)	2.00* (1.32 to 3.04)	2.95* (1.95 to 4.47)	0.97* (0.9 to 1.04)	99%	100%
Ser	1.83 (−1.92 to 5.57)	0.54 (−4.05 to 5.13)	1.38 (0.97 to 1.96)	1.48* (1.04 to 2.11)	0.85* (0.67 to 1.02)	86%	86%
Glu	4.48* (0.84 to 8.13)	0.20 (−4.27 to 4.67)	1.43* (1.03 to 1.98)	1.22 (0.88 to 1.69)	0.78* (0.56 to 0.99)	93%	57%
Pro	0.84 (−4.92 to 6.6)	−4.44 (−11.49 to 2.62)	1.59 (0.95 to 2.64)	1.54 (0.92 to 2.57)	0.77 (0.49 to 1.04)	86%	71%
Gly	0.41 (−1.56 to 2.37)	−0.46 (−2.87 to 1.94)	1.52 (0.82 to 2.81)	2.22* (1.2 to 4.12)	0.76* (0.52 to 0.99)	71%	86%
Ala	−0.98 (−2.28 to 0.33)	−2.84* (−4.44 to −1.23)	2.47* (1.47 to 4.15)	2.54* (1.51 to 4.27)	0.87* (0.68 to 1.06)	93%	71%
Cys	1.07* (0.46 to 1.67)	0.29 (−0.46 to 1.03)	0.74 (0.35 to 1.59)	0.92 (0.43 to 1.97)	0.51 (0.18 to 0.84)	93%	43%
Val	−0.49 (−2.92 to 1.93)	−1.38 (−4.35 to 1.6)	1.56* (1.15 to 2.1)	1.6* (1.19 to 2.16)	0.92* (0.75 to 1.08)	100%	86%
Met	−2.93* (−4.7 to −1.17)	−6.26* (−8.42 to −4.1)	4.10* (2.86 to 5.88)	5.71* (3.98 to 8.19)	0.92* (0.79 to 1.04)	100%	71%
Ile	0.83 (−0.92 to 2.57)	−0.15 (−2.28 to 1.98)	1.21 (0.5 to 2.93)	0.79 (0.33 to 1.9)	0.49 (0.18 to 0.8)	86%	43%
Leu	−0.77 (−2.09 to 0.56)	−2.68* (−4.29 to −1.06)	2.46* (1.22 to 4.97)	3.63* (1.8 to 7.32)	0.89* (0.72 to 1.06)	86%	86%
Tyr	0.95 (−0.39 to 2.29)	−1.64 (−3.28 to 0.00)	2.65* (1.61 to 4.35)	1.94* (1.18 to 3.18)	0.95* (0.86 to 1.04)	79%	100%
Phe	−0.61 (−1.25 to 0.03)	−0.98* (−1.75 to −0.2)	2.13* (1.09 to 4.17)	2.78* (1.42 to 5.45)	0.82* (0.61 to 1.02)	100%	57%
His	−0.49 (−1.01 to 0.03)	−0.99* (−1.63 to −0.35)	3.19* (1.68 to 6.06)	2.31* (1.22 to 4.39)	0.89* (0.75 to 1.03)	79%	100%
Lys	0.05 (−1.16 to 1.26)	−2.61* (−4.09 to −1.14)	3.21* (1.85 to 5.58)	2.32* (1.33 to 4.03)	0.92* (0.79 to 1.05)	93%	86%
Arg	3.17 (−0.16 to 6.49)	3.85 (−0.22 to 7.92)	0.98 (0.66 to 1.48)	1.02 (0.68 to 1.53)	0.52 (0.24 to 0.80)	93%	29%
Sar[b]	1.70* (0.68 to 2.72)	4.49* (3.24 to 5.73)	0.30* (0.19 to 0.46)	0.49* (0.31 to 0.76)	0.91* (0.78 to 1.03)	71%	100%
Sar/ser	–	–	4.65* (3.77 to 5.74)	3.04* (2.47 to 3.76)	0.99* (0.96 to 1.02)	93%	100%
Cys/met	–	–	5.51* (2.52 to 12.06)	6.2* (2.83 to 13.57)	0.77* (0.52 to 1.01)	100%	57%

CI, confidence interval; AUC, area under curve.
Differences in absolute concentrations between cell lines (first two columns), differences in amino acid ratios ([a]ratios between aspartate and particular amino acid except Sar/Ser and Cys/Met ratios), second two columns. Determined by multivariate ANOVA. Last three columns show results of receiver-operator statistics (difference in ratios between benign and tumorous cell lines). [b]ROC statistics for all amino acids calculated as Asp/amino acid apart from Sarcosine (calculated as Sar/Asp ratio).
Asterisk (*) indicate significant trend at $P < 0.05$.

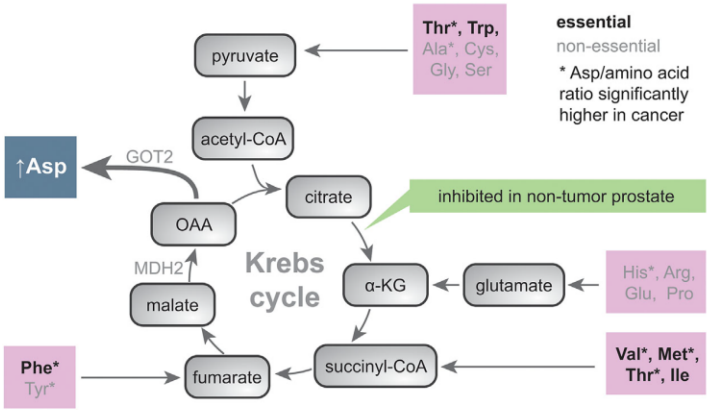

Fig. 4. Crucial role of aspartate in prostate cancer metabolism. Amino acid contributors for Asp synthesis based on amino acid ratios and receiver operator statistics (see Fig. 3 and Table I). Asterisk indicates amino acid whose Asp/amino acid ration differs significantly between non-tumor and tumorous cells. α-KG, α-ketoglutarate; OAA, oxaloacetate; MDH2, malate dehydrogenase; GOT2, glutamic-oxaloacetic transaminase 2.

several essential amino acids (threonine, lysine, leucine, phenylalanine, and methionine) suggests activation of aspartate biosynthesis through enhancement of MDH2/GOT2 activity in prostate cancer cells with renewed Krebs cycle and OXPHOS [28,29]; see Figure 4. In accordance, oncogenic KRAS, a common feature of prostate cancer, plays a role in redirecting of glutamine metabolism toward aspartate production [34,35]. Moreover, high levels of MDH2 were associated with poor prognosis in prostate cancer patients [36]. Based on our previous data, we examined selected product/precursor ratios for associations with a malignant phenotype by multifactorial ANOVA and ROC analysis. Aspartate/threonine, aspartate/methionine, and sarcosine/serine ratios demonstrated high levels of sensitivity and specificity in distinguishing cancer and benign metabolism. Our observation also confirmed the potential for threonine, tyrosine, and methionine restriction as a promising approach in prostate cancer treatment [37–42], especially because methionine is limiting factor for GSH and metallothionein synthesis [43] associated with cisplatin resistance [16].

Last, but not least, short- and long-term zinc treatments were shown to redirect cell metabolism from benign to more malignant type (see Fig. 3B). Zinc has long been associated with prostate health [22], but our findings contradict this statement as well as results of some other studies [44–46]. According to our results, resistant cells markedly increased their IC50 for cisplatin: by 1.4-, 1.6-, and 1.6-fold for PNT1A, 22Rv1, and PC-3, respectively [21] and their ability to invade. Moreover, long-term application of high concentration of zinc significantly enhanced synthesis of glutathione (GSH) (see Fig. 1C), which could result in triggering of molecular mechanisms underlying the stemness and pluripotency [47–49]. Accordingly, we observed increasing number of polyploid giant cancer cells (PGCCs) in our zinc-resistant PC-3 cell line. Due to their possible stem cell-like properties, these PGCCs cells could represent an escape route to survive a genotoxic stress and to enhance aggressiveness of cancer cells [50–52]. Increased cellular antioxidant capacity and higher gene expression of treatment resistance-, pluripotency-, and stemness-associated genes *BIRC5*, *POU5F1*, and *SOX2* were other consequences of zinc-resistant phenotype showing potential danger of long-term zinc supplementation.

CONCLUSIONS

In this study, we demonstrated that an intriguing idea to reestablish intracellular zinc concentrations in prostatic tumors does not restore benign phenotype in malignant prostate cells. Conversely, this approach drives tumor cells toward a higher level of aggressiveness and resistance through the activation of pluripotency- and stemness-associated regulatory molecules. Furthermore, changes of amino acid levels triggered by carcinogenesis and/or resistance are relevant for diagnostic purposes and may elucidate the molecular basis of malignant processes, which could possibly result in new therapeutic options. Ratios of certain logically-related amino acids may then be a sensitive indicator of the malignant phenotype. Moreover, the restriction of essential amino acids, such as threonine or methionine, or the inhibition of aspartate synthesis may be a promising

approach for the prostate cancer therapy with minimal toxic side effects.

ACKNOWLEDGMENT

This work was supported by funds from the Faculty of Medicine, Masaryk University to junior researcher (Jaromir Gumulec), by the project MUNI/A/1365/2015 with the support of the Specific University Research Grant, as provided by the Ministry of Education, Youth and Sports of the Czech Republic in the year 2016, by the Czech Science Foundation GACR 16-18917S, and League Against Cancer Prague.

REFERENCES

1. Costello LC, Franklin RB, Feng P. Mitochondrial function, zinc, and intermediary metabolism relationships in normal prostate and prostate cancer. Mitochondrion 2005;5(3):143–153.
2. Massie CE, Lynch A, Ramos-Montoya A, Boren J, Stark R, Fazli L, Warren A, Scott H, Madhu B, Sharma N, Bon H, Zecchini V, Smith D-M, DeNicola GM, Mathews N, Osborne M, Hadfield J, MacArthur S, Adryan B, Lyons SK, Brindle KM, Griffiths J, Gleave ME, Rennie PS, Neal DE, Mills IG. The androgen receptor fuels prostate cancer by regulating central metabolism and biosynthesis. EMBO J 2011;30(13):2719–2733.
3. Lloyd SM, Arnold J, Sreekumar A. Metabolomic profiling of hormone-dependent cancers: a bird's eye view. Trends Endocrinol Metab 2015;26(9):477–485.
4. Putluri N, Shojaie A, Vasu VT, Nalluri S, Vareed SK, Putluri V, Vivekanandan-Giri A, Byun J, Pennathur S, Sana TR, Fischer SM, Palapattu GS, Creighton CJ, Michailidis G, Sreekumar A. Metabolomic profiling reveals a role for androgen in activating amino acid metabolism and methylation in prostate cancer cells. PLoS ONE 2011;6(7):e21417.
5. Kaushik AK, Vareed SK, Basu S, Putluri V, Putluri N, Panzitt K, Brennan CA, Chinnaiyan AM, Vergara IA, Erho N, Weigel NL, Mitsiades N, Shojaie A, Palapattu G, Michailidis G, Sreekumar A. Metabolomic profiling identifies biochemical pathways associated with castration-Resistant prostate cancer. J Proteome Res 2014;13(2):1088–1100.
6. Dasgupta S, Putluri N, Long WW, Zhang B, Wang JH, Kaushik AK, Arnold JM, Bhowmik SK, Stashi E, Brennan CA, Rajapakshe K, Coarfa C, Mitsiades N, Ittmann MM, Chinnaiyan AM, Sreekumar A, O'Malley BW. Coactivator SRC-2-dependent metabolic reprogramming mediates prostate cancer survival and metastasis. J Clin Invest 2015;125(3):1174–1188.
7. Sreekumar A, Poisson LM, Rajendiran TM, Khan AP, Cao Q, Yu JD, Laxman B, Mehra R, Lonigro RJ, Li Y, Nyati MK, Ahsan A, Kalyana-Sundaram S, Han B, Cao XH, Byun J, Omenn GS, Ghosh D, Pennathur S, Alexander DC, Berger A, Shuster JR, Wei JT, Varambally S, Beecher C, Chinnaiyan AM. Metabolomic profiles delineate potential role for sarcosine in prostate cancer progression. Nature 2009;457(7231):910–914.
8. Arakaki AK, Mezencev R, Bowen NJ, Huang Y, McDonald JF, Skolnick J. Identification of metabolites with anticancer properties by computational metabolomics. Mol Cancer 2008;7.
9. Heger Z, Gumulec J, Cernei N, Polanska H, Raudenska M, Masarik M, Eckschlager T, Stiborova M, Adam V, Kizek R. Relation of exposure to amino acids involved in sarcosine metabolic pathway on behavior of non-tumor and malignant prostatic cell lines. Prostate 2016;76(7):679–690.
10. Pavlova NN, Thompson CB. The emerging hallmarks of cancer metabolism. Cell Metab 2016;23(1):27–47.
11. Wang JB, Erickson JW, Fuji R, Ramachandran S, Gao P, Dinavahi R, Wilson KF, Ambrosio AL, Dias SM, Dang CV, Cerione RA. Targeting mitochondrial glutaminase activity inhibits oncogenic transformation. Cancer Cell 2010;18(3):207–219.
12. Kolenko V, Teper E, Kutikov A, Uzzo R. Zinc and zinc transporters in prostate carcinogenesis. Nat Rev Urol 2013;10 (4):219–226.
13. Holubova M, Axmanova M, Gumulec J, Raudenska M, Sztalmachova M, Babula P, Adam V, Kizek R, Masarik M. KRAS NF-kappaB is involved in the development of zinc resistance and reduced curability in prostate cancer. Metallomics 2014;6(7):1240–1253.
14. Sharrard RM, Maitland NJ. Regulation of protein kinase B activity by PTEN and SHIP2 in human prostate-derived cell lines. Cell Signal 2007;19(1):129–138.
15. Fraser M, Zhao H, Luoto KR, Lundin C, Coackley C, Chan N, Joshua AM, Bismar TA, Evans A, Helleday T, Bristow RG. PTEN deletion in prostate cancer cells does not associate with loss of RAD51 function: Implications for radiotherapy and chemotherapy. Clin Cancer Res 2012;18(4):1015–1027.
16. Gumulec J, Balvan J, Sztalmachova M, Raudenska M, Dvorakova V, Knopfova L, Polanska H, Hudcova K, Ruttkay-Nedecky B, Babula P, Adam V, Kizek R, Stiborova M, Masarik M. Cisplatin-resistant prostate cancer model: Differences in antioxidant system, apoptosis and cell cycle. Int J Oncol 2014;44(3):923–933.
17. Heger Z, Cernei N, Gumulec J, Masarik M, Eckschlager T, Hrabec R, Zitka O, Adam V, Kizek R. Determination of common urine substances as an assay for improving prostate carcinoma diagnostics. Oncol Rep 2014;31(4):1846–1854.
18. Tmejova K, Hynek D, Kopel P, Gumulec J, Krizkova S, Guran R, Heger Z, Kalina M, Vaculovicova M, Adam V, Kizek R. Structural effects and nanoparticle size are essential for quantum dots-metallothionein complex formation. Colloids Surf B Biointerfaces 2015;134:262–272.
19. Kominkova M, Michalek P, Cihalova K, Guran R, Cernei N, Nejdl L, Smerkova K, Dostalova S, Chudobova D, Heger Z, Vesely R, Gumulec J, Kynicky J, Xhaxhiu K, Zitka O, Adam V, Kizek R. Study of linkage between glutathione pathway and the antibiotic resistance of escherichia coli from patients' swabs. Int J Mol Sci 2015;16(4):7210–7229.
20. Masarik M, Gumulec J, Hlavna M, Sztalmachova M, Babula P, Raudenska M, Pavkova-Goldbergova M, Cernei N, Sochor J, Zitka O, Ruttkay-Nedecky B, Krizkova S, Adam V, Kizek R. Monitoring of the prostate tumour cells redox state and real-time proliferation by novel biophysical techniques and fluorescent staining. Integr Biol 2012;4(6):672–684.
21. Holubova M, Axmanova M, Gumulec J, Raudenska M, Sztalmachova M, Babula P, Adam V, Kizek R, Masarik M. KRAS NF-kappa B is involved in the development of zinc resistance and reduced curability in prostate cancer. Metallomics 2014;6(7):1240–1253.
22. Costello LC, Feng P, Milon B, Tan M, Franklin RB. Role of zinc in the pathogenesis and treatment of prostate cancer: Critical issues to resolve. Prostate Cancer Prostatic Dis 2004;7(2):111–117.
23. Hardyman JE, Tyson J, Jackson KA, Aldridge C, Cockell SJ, Wakeling LA, Valentine RA, Ford D. Zinc sensing by metal-responsive transcription factor 1 (MTF1) controls metallothionein and ZnT1 expression to buffer the sensitivity of the transcriptome response to zinc. Metallomics 2016;8(3):337–343.

24. Raudenska M, Gumulec J, Podlaha O, Sztalmachova M, Babula P, Eckschlager T, Adam V, Kizekb R, Masarik M. Metallothionein polymorphisms in pathological processes. Metallomics 2014;6(1):55–68.
25. Costello LC, Franklin RB. Novel role of zinc in the regulation of prostate citrate metabolism and its implications in prostate cancer. Prostate 1998;35(4):285–296.
26. Bae KM, Dai Y, Vieweg J, Siemann DW. Hypoxia regulates SOX2 expression to promote prostate cancer cell invasion and sphere formation. Am J Cancer Res 2016;6(5):1078–1088.
27. Russo MV, Esposito S, Tupone MG, Manzoli L, Airoldi I, Pompa P, Cindolo L, Schips L, Sorrentino C, Di Carlo E. SOX2 boosts major tumor progression genes in prostate cancer and is a functional biomarker of lymph node metastasis. Oncotarget 2016;7(11):12372–12385.
28. Birsoy K, Wang T, Chen WW, Freinkman E, Abu-Remaileh M, Sabatini DM. An essential role of the mitochondrial electron transport chain in cell proliferation is to enable aspartate synthesis. Cell 2015;162(3):540–551.
29. Yang H, Zhou LS, Shi Q, Zhao YZ, Lin HP, Zhang ML, Zhao SM, Yang Y, Ling ZQ, Guan KL, Xiong Y, Ye D. SIRT3-dependent GOT2 acetylation status affects the malate-aspartate NADH shuttle activity and pancreatic tumor growth. EMBO J 2015;34(8):1110–1125.
30. Franklin RB, Zou J, Yu Z, Costello LC. EAAC1 is expressed in rat and human prostate epithelial cells; functions as a high-affinity L-aspartate transporter; and is regulated by prolactin and testosterone. BMC Biochem 2006;7:10.
31. Costello LC, Franklin RB. The clinical relevance of the metabolism of prostate cancer; zinc and tumor suppression: Connecting the dots. Mol Cancer 2006;5.
32. Costello LC, Franklin RB. Prostate epithelial-cells utilize glucose and aspartate as the carbon-sources for net citrate production. Prostate 1989;15(4):335–342.
33. Sullivan LB, Gui DY, Hosios AM, Bush LN, Freinkman E, Vander Heiden MG. Supporting aspartate biosynthesis is an essential function of respiration in proliferating cells. Cell 2015;162(3):552–563.
34. Ahn CS, Metallo CM. Mitochondria as biosynthetic factories for cancer proliferation. Cancer Metab 2015;3:1.
35. Ngalame NNO, Tokar EJ, Person RJ, Waalkes MP. Silencing KRAS overexpression in arsenic-Transformed prostate epithelial and stem cells partially mitigates malignant phenotype. Toxicol Sci 2014;142(2):489–496.
36. Liu Q, Harvey CT, Geng H, Xue CH, Chen V, Beer TM, Qian DZ. Malate dehydrogenase 2 confers docetaxel resistance via regulations of JNK signaling and oxidative metabolism. Prostate 2013;73(10):1028–1037.
37. Fu YM, Yu ZX, Li YQ, Ge XK, Sanchez PJ, Fu X, Meadows GG. Specific amino acid dependency regulates invasiveness and viability of androgen-independent prostate cancer cells. Nutr Cancer 2003;45(1):60–73.
38. Lu S, Hoestje SM, Choo EM, Epner DE. Methionine restriction induces apoptosis of prostate cancer cells via the c-Jun N-terminal kinase-mediated signaling pathway. Cancer Lett 2002;179(1):51–58.
39. Shiraki N, Shiraki Y, Tsuyama T, Obata F, Miura M, Nagae G, Aburatani H, Kume K, Endo F, Kume S. Methionine metabolism regulates maintenance and differentiation of human pluripotent stem cells. Cell Metab 2014;19(5):780–794.
40. Fu YM, Yu ZX, Ferrans VJ, Meadows GG. Tyrosine and phenylalanine restriction induces G0/G1 cell cycle arrest in murine melanoma in vitro and in vivo. Nutr Cancer 1997; 29(2):104–113.
41. Abdallah RM, Starkey JR, Meadows GG. Dietary restriction of tyrosine and phenylalanine: Inhibition of metastasis of three rodent tumors. J Natl Cancer Inst 1987;78(4):759–769.
42. Zhang J, Nuebel E, Daley GQ, Koehler CM, Teitell MA. Metabolic regulation in pluripotent stem cells during reprogramming and self-Renewal. Cell Stem Cell 2012;11(5):589–595.
43. Stein AF, Bracken WM, Klaassen CD. Utilization of methionine as a sulfhydryl source for metallothionein synthesis in rat primary hepatocyte cultures. Toxicol Appl Pharmacol 1987;87(2):276–283.
44. Leitzmann MF, Stampfer MJ, Wu KN, Colditz GA, Willett WC, Giovannucci EL. Zinc supplement use and risk of prostate cancer. J Natl Cancer Inst 2003;95(13):1004–1007.
45. Ko YH, Woo YJ, Kim JW, Choi H, Kang SH, Lee JG, Kim JJ, Park HS, Cheon J. High-dose dietary zinc promotes prostate intraepithelial neoplasia in a murine tumor induction model. Asian J Androl 2010;12(2):164–170.
46. Makhov P, Golovine K, Uzzo RG, Rothman J, Crispen PL, Shaw T, Scoll BJ, Kolenko VM. Zinc chelation induces rapid depletion of the X-linked inhibitor of apoptosis and sensitizes prostate cancer cells to TRAIL-mediated apoptosis. Cell Death Differ 2008;15(11):1745–1751.
47. Marsboom G, Zhang GF, Pohl-Avila N, Zhang YM, Yuan Y, Kang HJ, Hao B, Brunengraber H, Malik AB, Rehman J. Glutamine metabolism regulates the pluripotency transcription factor OCT4. Cell Rep 2016;16(2):323–332.
48. Lu HQ, Samanta D, Xiang LS, Zhang HM, Hu HX, Chen I, Bullen JW, Semenza GL. Chemotherapy triggers HIF-1-dependent glutathione synthesis and copper chelation that induces the breast cancer stem cell phenotype. Proc Natl Acad Sci USA 2015;112(33):E4600–E4609.
49. Hu J, Yang ZY, Wang JB, Yu J, Guo J, Liu SY, Qian CM, Song LW, Wu Y, Cheng JJ. Zinc chloride transiently maintains mouse embryonic stem cell pluripotency by activating stat3 signaling. PLoS ONE 2016;11(2):e0148994.
50. Ivanov A, Cragg MS, Erenpreisa J, Emzinsh D, Lukman H, Illidge TM. Endopolyploid cells produced after severe genotoxic damage have the potential to repair DNA double strand breaks. J Cell Sci 2003;116(20):4095–4106.
51. Zhang D, Wang YJ, Zhang SW. Asymmetric cell division in polyploid giant cancer cells and low eukaryotic cells. Biomed Res Int 2014;2014:432652.
52. Zhang S, Mercado-Uribe I, Xing Z, Sun B, Kuang J, Liu J. Generation of cancer stem-like cells through the formation of polyploid giant cancer cells. Oncogene 2014;33(1):116–128.

SUPPORTING INFORMATION

Additional supporting information may be found in the online version of this article at the publisher's web-site.

3.2.2 Findings related to the hypothesis 2

***Hypothesis 2*: Some of the highly synthesized amino acids may have a supportive effect on the properties of tumour cells, such as invasive potential or ability of migration.**

Sarcosine (N-methylglycine) was indicated as an important CaP oncometabolite in several studies [79, 87]. Based on our results, sarcosine metabolism is involved significantly in the development and behaviour of CaP [88]. Amino acids of the sarcosine pathway (glycine, dimethylglycine and sarcosine) affected significantly the ability of cells derived from CaP (22Rv1, PC-3) to migrate, as well as their ability to divide. These findings are consistent with other studies [79, 80, 89]. We also proved that the gene expression of glycine N-methyltransferase (GNMT) is low in benign prostatic cells PNT1A and rises explicitly in the 22Rv1 cells derived from a primary tumour. With the progression to the metastatic form, GNMT expression is somewhat reduced, but still remains elevated as compared to PNT1A expression. Expression of GNMT mRNA reflects sarcosine levels in the lines studied by us. Thus, our results support the hypothesis that sarcosine (generated from glycine using GNMT) could be used as an early CaP biomarker. Our data further show that the cell supplementation with glycine, dimethylglycine or sarcosine affects significantly the metabolism of amino acids in prostatic cells. We further confirmed that amino acid profiles are highly specific for individual cell lines (can be seen from an analysis of the main components, see Fig. 5 on page 165 [88]).

In the study below [90] Heger *et al.*, see p. 170, the effect of sarcosine on CaP-derived metastatic cells (androgen-dependent LNCaP and androgen-independent PC-3) was studied. We proved that sarcosine stimulates proliferation of these cells *in vitro* and also *in vivo*. In mice with induced CaP, the repeated administration of sarcosine promotes the growth of tumours and significantly reduces weight and welfare in treated mice. In addition, we observed a sarcosine-induced increase in glycine and serine concentrations in the tumour mass in both types of tumours (LNCaP-induced and PC-3-induced tumours), and this increase was accompanied by the increased levels of sarcosine dehydrogenase (SARDH). The impact of the repeated sarcosine administration was also evident at the level of gene expression. Bioinformatic methods revealed a strong link between sarcosine administration and induction of the genes involved in cell cycle progression. In both types of CaP xenografts, the administration of sarcosine stimulated the expression of the gene for the androgen receptor (*AR*) and the gene for the prostate-specific antigen (*KLK3*). In a tumour induced by the PC-3 cells derived from bone metastases, the sarcosine administration resulted in increased expression of the gene for the Aurora kinase A (*AURKA*). Amplification of the *AURKA* gene was observed in 67% of CaP, which progressed

to a highly aggressive form [91]. *AURKA* is one of the genes that can contribute to the generation of giant polyploid tumour cells (PGCC) [92] playing a role in developing resistance to therapy; see Part III of this work.

As our previous studies proved that sarcosine is an important oncometabolite, we prepared two types of liposomes which – when targeted towards the tumour tissue – affected the function and the metabolism of sarcosine, see Heger *et al.* on page 190. To increase the absorption of liposomes into the CaP target tissue, the liposome surface was modified by the folic acid (FA); (tumour cells often express large amounts of the folate receptor [93-95]). The first type of antisarAbs@LIP liposome contained anti-sarcosine antibodies, the second type of sar@LIP liposome contained sarcosine. The affinity of liposomes to the folate receptor also facilitated the entry of liposomes into the cells through clathrin-mediated endocytosis [96]. We examined effects of repeated administration of these liposomes on the growth of tumours induced by human PC-3 cells that had been implanted to immunodeficient nu/nu mice. Administration of Sar@LIP liposome significantly increased the tumour volume and weight as compared with the controls treated with empty liposomes. On the contrary, the administration of antisarAbs@LIP showed a mild antitumor effect. Gene expression was altered significantly as a result of treatment, expression patterns differed significantly due to the administration of different liposomes. It is interesting that both types of therapy (Sar@LIP and antisarAbs@LIP) resulted in higher expression of *KLK3*, the gene for the prostate-specific antigen (PSA), which is understood the clinically utilized CaP biomarker. We assume that this phenomenon was due to using FA for the modification of liposome surfaces. The FA supplementation in the CaP patients was associated with increased PSA levels, whereas its elimination from the diet resulted in a significant PSA reduction [97]. Glutaminase (*GLS*) expression was also increased due to the administration of Sar@LIP, but not antisarAbs@LIP. Glutaminase is the key enzyme involved in glutaminolysis and its task is to hydrolyse glutamine, the amino acid necessary for tumour growth, into glutamic acid [98, 99].

Significant reduction in the concentration of zinc ions and total metallothionein in the tumour tissue is another important effect of the sarcosine-containing liposome (Sar@LIP). It is therefore probable that the accumulation of sarcosine is closely related to the depletion of zinc ions, which plays a significant role in the progression of CaP. We also proved that FA-modified liposomes are suitable for targeting the CaP tissues. These findings are further extended in the following study.

Conclusion: Amino acids accumulated in tumour cells or tissues are able to affect substantially the events associated with CaP carcinogenesis. Amino acids of the sarcosine pathway (glycine,

dimethylglycine and sarcosine) affect the ability of cells derived from CaP (22Rv1, PC-3) to migrate, as well as their ability to divide. The tumour-supporting effect of sarcosine could be observed on the rate of tumour growth in mice. Sarcosine is thus probably a key metabolite affecting the progression of CaP and is a suitable target for diagnostic approaches as well as for possible targeted therapy. Though our antisarAbs@LIP liposomes showed only moderate anti-tumour effects, they should be further tested when co-administered with other antineoplastic drugs.

Author's publications relevant to this chapter

1. Heger, Z., J. Gumulec, et al. (2016). "Relation of exposure to amino acids involved in sarcosine metabolic pathway on behavior of non-tumor and malignant prostatic cell lines." Prostate **76**(7): 679-690.
   Available on page 158

2. Heger, Z., M. A. M. Rodrigo, et al. (2016). "Sarcosine Up-Regulates Expression of Genes Involved in Cell Cycle Progression of Metastatic Models of Prostate Cancer." Plos One **11**(11).
   Available on page 170

3. Heger, Z., H. Polanska, et al. (2016). "Prostate tumor attenuation in the nu/nu murine model due to anti-sarcosine antibodies in folate-targeted liposomes." Sci Rep **6**: 33379.
   Available on page 190

The Prostate

Relation of Exposure to Amino Acids Involved in Sarcosine Metabolic Pathway on Behavior of Non-Tumor and Malignant Prostatic Cell Lines

Zbynek Heger,[1,2] Jaromir Gumulec,[2,3] Natalia Cernei,[1,2] Hana Polanska,[2,3] Martina Raudenska,[2,3] Michal Masarik,[2,3] Tomas Eckschlager,[4] Marie Stiborova,[5] Vojtech Adam,[1,2] and Rene Kizek[1,2]*

[1]*Department of Chemistry and Biochemistry, Mendel University in Brno, Brno, Czech Republic, European Union*

[2]*Central European Institute of Technology, Brno University of Technology, Brno, Czech Republic, European Union*

[3]*Faculty of Medicine, Department of Physiology, Masaryk University, Brno, Czech Republic, European Union*

[4]*2nd Faculty of Medicine, Department of Paediatric Haematology and Oncology, Charles University and University Hospital Motol, Czech Republic, European Union*

[5]*Faculty of Science, Department of Biochemistry, Charles University, Czech Republic, European Union*

BACKGROUND. Sarcosine (*N*-methylglycine) was previously delineated as a substantial oncometabolite of prostate cancer (PCa) and its metabolism seems to be significantly involved in PCa development and behavior.

METHODS. We focused on investigation whether the exposure of prostate cells (PNT1A, 22Rv1, and PC-3) to sarcosine-related amino acids (glycine, dimethylglycine, and sarcosine) affects their aggressiveness (cell mobility and division rates, using real-time cell based assay). The effect of supplementation on expression of glycine-*N*-methyltransferase (GNMT) mRNA was examined using qRT-PCR. Finally, post-treatment amino acids patterns were determined with consequent statistical processing using the Ward's method, factorial ANOVA and principal component analysis ($P < 0.05$).

RESULTS. The highest migration induced sarcosine and glycine in metastatic PC-3 cells (a decrease in relative free area about 53% and 73%). The highest cell division was achieved after treatment of 22Rv1 and PC-3 cells with sarcosine (time required for division decreased by 65% or 45%, when compared to untreated cells). qRT-PCR revealed also significant effects on expression of GNMT. Finally, amino acid profiling shown specific amino acid patterns for each cell line. In both, treated and untreated PC-3 cells significantly higher levels of serine, glutamic acid, and aspartate, linked with prostate cancer progression were found.

Grant sponsor: Czech Science Foundation; Grant number: GA CR 16-18917S; Grant sponsor: The Ministry of Health of the Czech Republic for conceptual development of research organization 00064203 (University Hospital Motol, Prague, Czech Republic).

Conflicts of interest: The authors declare no conflict of interest.

*Correspondence to: Prof. Rene Kizek, Department of Chemistry and Biochemistry, Mendel University in Brno, Zemedelska 1, CZ-613 00 Brno, Czech Republic. E-mail: kizek@sci.muni.cz

Received 15 December 2015; Accepted 12 January 2016
DOI 10.1002/pros.23159
Published online in Wiley Online Library
(wileyonlinelibrary.com).

CONCLUSIONS. Sarcosine-related amino acids can exceptionally affect the behavior of benign and malignant prostate cells. *Prostate* © 2016 Wiley Periodicals, Inc.

KEY WORDS: **cancer metabolism; dimethylglycine; folate; glycine; sarcosine pathway; prostate cancer**

INTRODUCTION

The amino acid sarcosine is currently studied as a potential biomarker for the early stages of prostate carcinoma (PCa). Even though the linkage of sarcosine with PCa development and its potential in a diagnosis of early stages of tumors was described [1,2], its usage as a marker remains still unclear [3,4]. Hence, it is necessary to study the fate of sarcosine and other amino acids, which act as the intermediate products of tumor metabolism in PCa. Formation and oxidation of sarcosine occurs in mitochondria and are provided by two basic pathways (schematically depicted in Fig. 1), where sarcosine can be simultaneously produced from dimethylglycine (Dmg) or glycine. The first pathway involves repeated methylation of phosfatidylethanolamine (PE) by S-adenosylmethionine (SAM) to form phosphatidylcholine (PC) with the resulting intermediate product betaine. This reaction forms Dmg and regenerates methionine from homocysteine. The Dmg is subsequently converted to sarcosine via dimethylglycine dehydrogenase (DMGDH) [5]. The second metabolic pathway creates sarcosine during the transformation of the methyl group of S-adenosylmethionine catalyzed by the enzyme glycine *N*-methyltransferase (GNMT) [6,7]. These two reactions ultimately produce 5,10-methylenetetrahydrofolate and are dependent on oxidized flavine cofactors (e.g., flavine adenine dinucleotide) [5].

GNMT acts as an essential enzyme that influences synthesis of sarcosine [8]. Due to properties of GNMT, its excessive production causes conversion of glycine

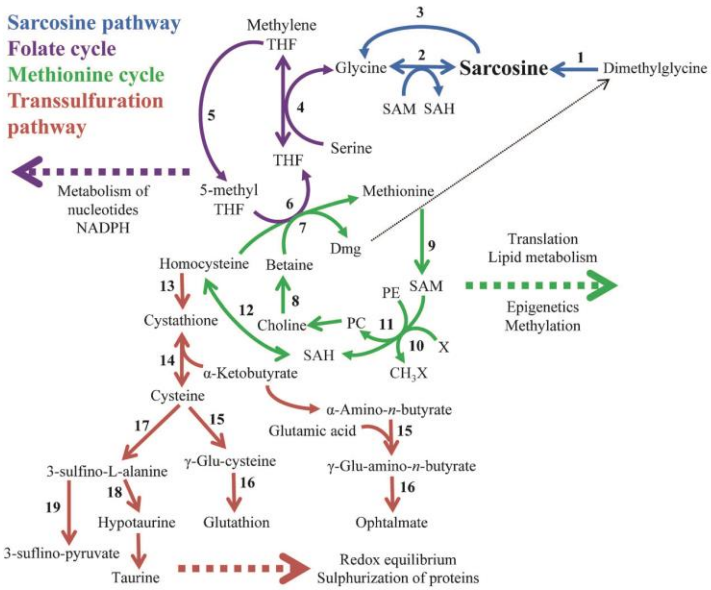

Fig. 1. Scheme of metabolical pathway of sarcosine biosynthesis and degradation to its non-methylated precursor—glycine and its connection to other important metabolical pathways. Enzymes in scheme are numbered and depicted as follows: 1, DMGDH, dimethylglycine dehydrogenase; 2, GNMT, glycine-*N*-methyltransferase; 3, SARDH, sarcosine dehydrogenase; 4, SHMT1/2, serine hydroxymethyltransferase; 5, 11, MTHFR, 5,10-methylenetetrahydrofolate reductase; 6, MTR, methionine synthase; 7, BHMT, betaine-homocysteine methyltransferase; 8, CHDH, choline oxidase; 9, MAT, methionine adenosyltransferase; 10, SAM-dependent methyltransferase; 11, PEMT, phosphatidylethanolamine methyltransferase; 12, AHCY, S-adenosylhomocysteine hydrolase; 13, CBS, cystathionine β-synthase; 14, CTH, cystathionase; 15, GCL, glutamate-cysteine ligase; 16, GSS, glutathione synthetase; 17, CDO1, cysteine dioxygenase 1; 18, CSAD, cysteine sulfinic acid decarboxylase; 19, GOT1, glutamate oxaloacetate transaminase 1. Dmg stays for dimethylglycine, SAM for S-adenosyl-methionine, SAH for S-adenosyl-homocysteine, PE for phosphatidylethanolamine, PC for phosphatidylcholine, and THF for tetrahydrofolate.

to sarcosine and elevates the sarcosine levels in urine. This makes sarcosine interesting in the field of non-invasive cancer biomarkers. Thus, sarcosine appears to be not only a non-proteogenic amino acid but also an important metabolite in oncogenesis. According to Sreekumar et al., the elevated levels of sarcosine correlated with progression of prostate cancer and metastatic process [9] and accordingly, it has been revealed that supplementation of sarcosine to prostate cancer cell lines induced a selection of invasive phenotype in culture [10]. Nevertheless, the explanation for these phenomena remains unclear. Moreover, the metabolic fate of sarcosine in prostate cancer cells has not been fully resolved yet.

Therefore, the insight into the metabolic pathways of sarcosine and the mechanisms of its regulation are required to be investigated. This study is aimed to evaluate the effects of treatment of three prostatic cell lines (a "non-tumor" PNT1A, a primary tumor-derived 22Rv1 and metastasis-derived PC-3) with three sarcosine-pathway-related amino acids (glycine, dimethylglycine, and sarcosine) on the cell cancergeneous status. The evaluation was carried out using as a combination of assays determining the effects of these amino acids on the expression of GNMT mRNA, cell migration, invasiveness, their division and growth capabilities.

EXPERIMENTAL SECTION

Chemical Compounds

All standards and other chemicals were purchased from Sigma–Aldrich (St. Louis, MO) in ACS purity, unless noted otherwise.

Prostatic Cell Lines

Three human prostatic cell lines were used in this study: (i) the PNT1A human cell line established by immortalization of normal adult prostatic epithelial cells by transfection with a plasmid containing SV40 genome with a defective replication origin. The primary culture was obtained from the prostate of a 35-year-old male post mortem; (ii) 22Rv1 which is a human prostate carcinoma epithelial cell line derived from a xenograft that was serially propagated in mice after castration-induced regression and relapse of the parental, androgen-dependent CWR22 xenograft. (iii) The PC-3 human cell line established from a grade 4 androgen independent and unresponsive prostatic adenocarcinoma from 62-year-old Caucasian male and derived from metastatic site in bone. All cell lines used in this study were purchased from Health Protection Agency Culture Collections (Salisbury, UK).

Culture Conditions

PNT1A and 22Rv1 cells were cultured in RPMI-1640 medium with 10% fetal bovine serum (FBS). PC-3 cells were cultured in Ham's F12 medium with 7% fotel bovine serum (FBS). All media were supplemented with penicillin (100 U/ml) and streptomycin (0.1 mg/ml), and the cells were maintained at 37°C in a humidified incubator (Sanyo, Moriguchi, Japan) with 5% CO_2. The treatment with amino acids was initiated after cells reached ~60–80% confluence. Cells were then harvested and washed four times with PBS, pH 7.4.

Cell Content Quantification

Total cell content was analyzed using Casy model TT system (Roche Applied Science, Penzberg, Germany). To prepare a viable cell standard, 100 μl cell suspension was mixed with 10 ml Casy Tone. All subsequent measurements were performed on 100× diluted 100 μl cell suspension. Prior each measurement, background was subtracted.

Measurements of Cell Viability—MTT Assay

The suspension of 10,000 cells was added to each well of standard microtiter plates (E-plates 16). After addition of medium (200 μl), plates were incubated for 2 days at 37°C to ensure cell growth. To determine the effects on cell viability, the amino acids (sarcosine, glycine, and dimethylglycine) in concentration 0–3 mmol/l were used. Plates were incubated for 24 hr; then, media were removed and replaced by a fresh medium, three times a day. Further, a medium was replaced by 200 μl of fresh medium containing 50 μl of MTT (5 mg/ml in PBS) and incubated in a humidified atmosphere for 4 hr at 37°C, wrapped in aluminum foil. After the incubation, MTT-containing medium was replaced by 200 μl of 99.9% dimethyl sulphoxide to dissolve MTT-formazan crystals. Then, 25 μl of glycine buffer (pH 10.5) was added to all wells and absorbance at 570 nm was immediately determined (VersaMax microplate reader, Molecular Devices, Sunnyvale, CA).

In Vitro Wound-Healing Assay

The cells were pipetted into 16-well plate to reach the confluence ~80%. After seeding of cells on the bottom of a plate, a pin was used to scratch and remove cells from a discrete area of the confluent monolayer to form a cell-free zone. After that, cells were re-suspended in a fresh medium enriched with sarcosine, glycine, and dimethylglycine (1.5 mmol/l). After 24 hr, the pictures of cells were taken and compared with pictures obtained in 0 hr, using TScratch software (CSElab, Zurich, Switzerland).

Growth and Proliferation Assay Using Real-Time Cell-Based Assay

The real-time cell-based assay (RTCA) was carried out using the xCELLigence system (Roche Applied Science and ACEA Biosciences, San Diego, CA). After seeding the total number of cells (10,000) in 100 µl medium to each well in E-plate, the attachment, proliferation and spreading of the cells was monitored every 15 min. After 24 hr, amino acids (1.5 mmol/l) or MiliQ water (control measurements) were added and cell impedance was monitored for 250 h. For evaluation of exposure, a "doubling time" function, describing the cell division rate, was employed.

Isolation of RNA and Reverse Transcription

High pure total-RNA isolation kit (Roche, Basel, Switzerland) was used for isolation of cellular RNA. The medium was removed and samples were twice washed with 5 ml of ice-cold PBS. Cells were scraped off, transferred to clean tubes and centrifuged at 20,800*g* for 5 min at 4°C. After this step, lysis buffer was added and RNA isolation was carried out from 22Rv1, PNT1A, and PC-3 according to manufacturer's instructions. Isolated RNA was used for cDNA synthesis. RNA (500 ng) was transcribed using transcriptor first strand cDNA synthesis kit (Roche) according to manufacturer's instructions. Prepared cDNA (20 µl) from total-RNA was diluted with RNase-free water to a total volume of 100 µl and 5 µl of this solution was directly analyzed by q-PCR.

Quantitative Polymerase Chain Reaction (q-PCR)

q-PCR was performed using the TaqMan gene expression assay system with the Lightcycler 480 II RT-PCR system (Roche, Basel, Switzerland) and the amplified DNA was analyzed by the comparative Ct method using *β-actin* as a housekeeping gene. The primer and probe sets for *β-actin* (assay ID: Hs99999903_ m1) and *GNMT* (Hs00219089-m1) were selected from TaqMan gene expression assays (Life Technologies, Carlsbad, CA). q-PCR was performed under the following amplification conditions: total volume of 20 µl, initial incubation 50°C/2 min followed by denaturation 94°C/10 min, then 40 cycles 94°C/10 sec, 60°C/1 min.

Preparation of Cell Lines for Determination of Patterns of Cellular Amino Acids

The harvested cells were frozen in liquid nitrogen to disrupt their structure. The frozen sample was homogenized using ultrasonic homogenizer SONOPLUS mini20 (Bandelin Electronic, Berlin, Germany). Subsequently, 1 ml of 0.2 M phosphate buffer (pH, 7.0) was added and the sample was homogenized for 5 min. The homogenate was further centrifuged using Microcentrifuge 5417R under the following conditions at 4°C for 15 min. Finally, the supernatant was filtered through a membrane filter (0.45-µm nylon filter disk; Millipore, Billerica, MA) and analyzed.

Ion-Exchange Chromatography

Amino acids including sarcosine were determined using ion-exchange chromatography with Vis detection after post-column derivatization with ninhydrin (AAA-400, Ingos, Prague, Czech Republic), following conditions employed in our previous study [3].

Quantification of Total Protein in Cell Lines

Total protein was determined using the SKALAB CBT 600T kit (Skalab, Svitavy, Czech Republic), on automatic spectrophotometer BS-400 (Mindray, Shenzhen, China), following the manufacturer's instructions.

Statistical Analysis

Prior all analyses, data were standardized. Correlation analysis followed by hierarchical clustering using the Ward's method was exploited to reveal dependencies between variables. To analyze the effects of cell line, amino acid used for treatment and the concentration of amino acid used for treatment, factorial ANOVA was used. To reveal dependences in complex data, principal component analysis was employed. Unless noted otherwise, the threshold for significance was $P < 0.05$. For analyses Software Statistica 12 (StatSoft, Tulsa, OK) was employed.

RESULTS

Cytotoxicity of Sarcosine, Glycine, and Dimethylglycine on Prostate Cells

In the first step, prostatic cell lines were tested for their susceptibility to applied amino acids using MTT assay. Figure 2A–C illustrates that treatment with glycine (Gly), sarcosine (Sar), and dimethylglycine (Dmg), respectively, resulted in low or no inhibition of cell lines growth, observed particularly by the highest applied concentration or above the used concentration range (2.0–3.5 mmol/l). The found data were further employed to design the experimental workflow. Because the undesired cytotoxicity can affect performance of further analyses, concentrations not exceeding 1.5 mmol/l were utilized for subsequent treatments only.

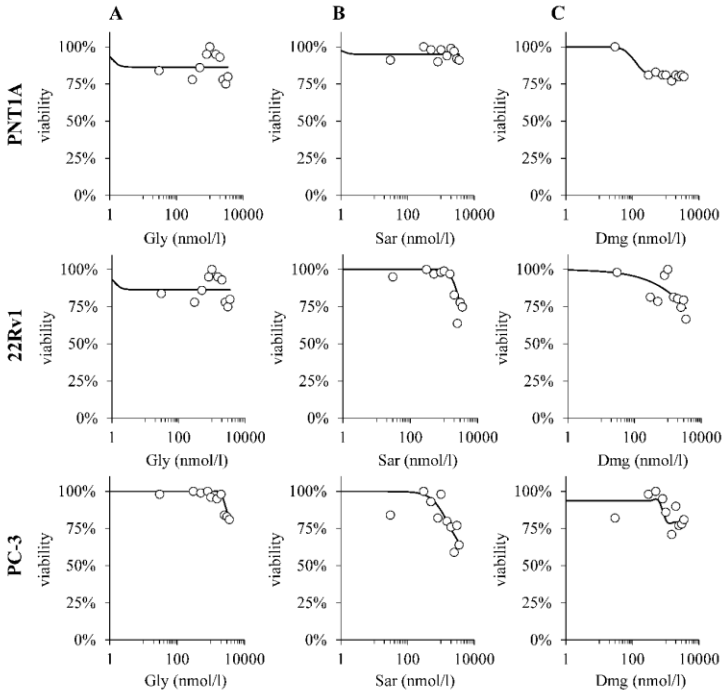

Fig. 2. Viability assay data of (**A**) PNT1A, (**B**) 22Rv1, and (**C**) PC-3 cells after application of glycine, sarcosine, and dimethylglycine (0.0–3.5 mmol/l). Growth inhibition in each treatment is expressed as a percentage of the control (untreated) cells. The data shown were obtained by the MTT assay. Values are means of three independent replicates (n = 3).

An Effect of Sarcosine, Glycine, and Dimethylglycine on Growth Properties of Prostate Cells

The growth of the cells were tested using wound-healing assay (Fig. 3A), which is an easy, low-cost and well-developed method to measure cell migration in vitro [11]. After formation of a new artificial gap on a confluent cell monolayer and subsequent supplementation with 1.5 mmol/l of sarcosine, glycine, or dimethylglycine, it was found that the cell migration was induced distinctly by sarcosine and glycine in PC-3 (relative free area of 53% and 73%, respectively) and 22Rv1 cells (57% and 87%), which is shown in Figure 3B. Contrary to that, dimethylglycine treatment suppressed migration in 22Rv1 and PC-3 (150% in 22Rv1 and 202% in PC-3), whereas the treatment of PNT1A led to increase in cell migration (80%). Using the real-time cell-based assay, we also focused on investigation of the effects of sarcosine, glycine, and dimethylglycine on the division rates of the tested prostate cells. As shown in Figure 3C, the most significant effects were achieved after cultivation with exogenously added sarcosine, which resulted in elevation of a division rate of 22Rv1 and PC-3 cell lines (time required for their division was 65% and 45%, respectively). Furthermore, the 22Rv1 cells were also boosted by treatment with glycine and dimethylglycine.

An Effect of Treatment of Prostate Cells With Sarcosine, Glycine, and Dimethylglycine on Expression of mRNA of Cellular GNMT

The results shown in Figure 4A demonstrate that relative expression of GNMT mRNA differs among the tested cell lines. The lowest GNMT mRNA expression was identified in non-malignant PNT1A cells, followed by metastatic PC-3 and primary tumor 22Rv1 cells, which corresponds to the known fact that GNMT over-expression is associated with the cancer cells more than with the non-tumor ones [12]. In the case of PC-3 cells, glycine treatment induced significant down-regulation of GNMT mRNA. Similar effect was observed in 22Rv1 cells, where 0.1 and 0.5 mmol/l of glycine stimulated expression of GNMT, however, higher applied concentrations resulted in down-regulation as in PC-3 cells. The highest increase in GNMT mRNA expression by glycine was found in PNT1A cells; nevertheless, the higher concentration (1.0 and 1.5 mmol/l) led to a decrease in GNMT mRNA expression (Fig. 4B). Contrary to relatively low effects of glycine, sarcosine

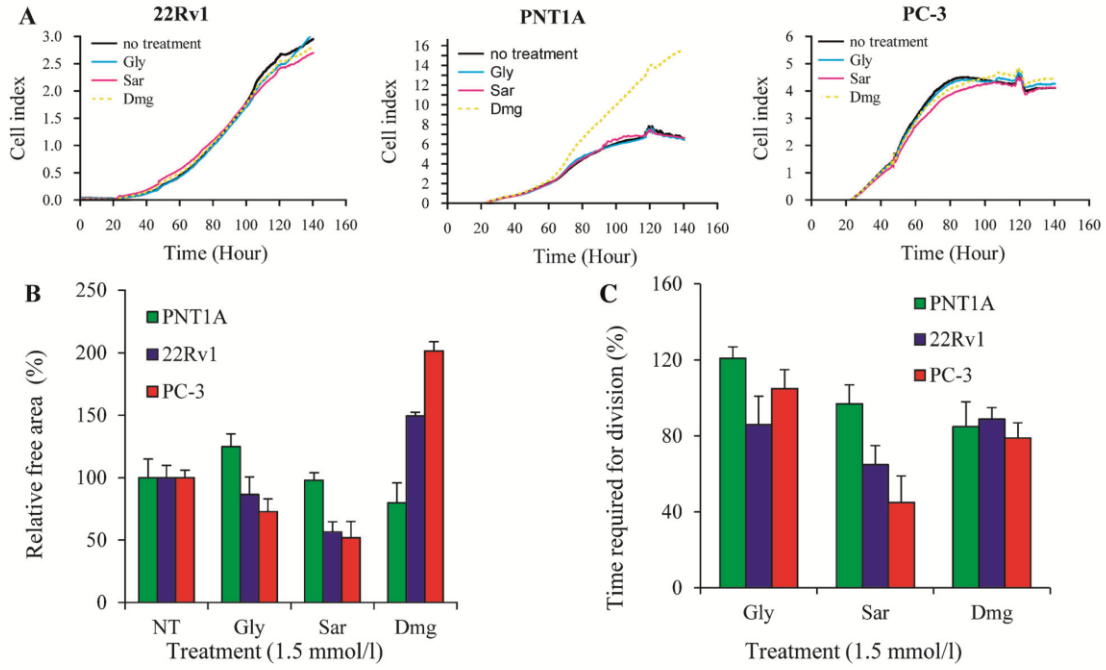

Fig. 3. Cell growth and invasiveness. (**A**) Growth of cell lines after treatment of amino acids compared to untreated cells. Displayed as a relative impedance (cell index). The effect of amino acids on (**B**) cell mobility, assessed by wound-healing assay, NT stands for no amino acid treatment (as reference free areas in NT cell lines were employed) and (**C**) the cell division rate (related to cell division rate of cells without treatment. Cells were seeded at a density of 10,000 cells per well in microtiter E-Plates 16. The cell index was monitored after application of 1.5 mmol/l of each amino acid. Values are means of three independent replicates (n = 3). Vertical bars indicate standard error.

supplementation mostly induced down-regulation of *GNMT* gene among all tested cell lines (PNT1A > PC-3 > 22Rv1) (Fig. 4C). Dimethylglycine treatment stimulated expression of GNMT mRNA in PNT1A cells, whereas this amino acid inhibited expression of mRNA of this enzyme in primary tumor (22Rv1) and metastatic cell lines (PC-3) (Fig. 4D). Taken together, the results demonstrate that supplementation of cells with even low concentrations of sarcosine and its pathway-related amino acids is able to trigger overexpression of GNMT (particularly in the case of dimethylglycine in PNT1A cells) or its down-regulation during treatment of PC-3 cells with glycine, sarcosine and dimethylglycine or, 22Rv1 cells supplemented with sarcosine and dimethylglycine.

Analysis of the Effect of Treatment of Prostate Cells With Sarcosine, Glycine, and Dimethylglycine on Patterns of Cellular Amino Acids

In the next step, the effect of treatment with glycine, dimethylglycine and sarcosine on the spectrum of amino acids in the tested prostate cell lines was analyzed. The correlation heatmap showing the response of cellular amino acid spectra to exposure of cells with sarcosine, glycine, and dimethylglycine is shown in Figure 5A. There was a significant positive correlation of all supplemented amino acids with intracellularly measured ones; $r = 0.62$, 0.38, and 0.48 at $P < 0.05$ for glycine, dimethylglycine, and sarcosine, respectively. Based on factorial ANOVA, a significant effect of all prediction factors on the amino acid pattern was found as follows: cell line $F(28, 144) = 136.6$, $P < 0.001$ (Fig. 5C), amino acid used for treatment $F(38, 144) = 28.66$, $P < 0.001$ (Fig. 5D) and the concentration of treatment $F(76, 286) = 7.2$, $P < 0.001$ (Fig. 5E). The combined effect of all three variables was significant, $F(304, 930) = 2.7$, $P < 0.001$, too. Noteworthy, the highest sarcosine levels were found in 22Rv1 (mean in untreated cells 3.12 μmol/mg of total protein), followed by PC-3 (1.78 μmol/mg of total protein) and PNT1A (0.84 μmol/mg of total protein), which corresponds to the expression of the *GNMT* gene. Inasmuch, glycine, sarcosine, and dimethylglycine treatment led to large

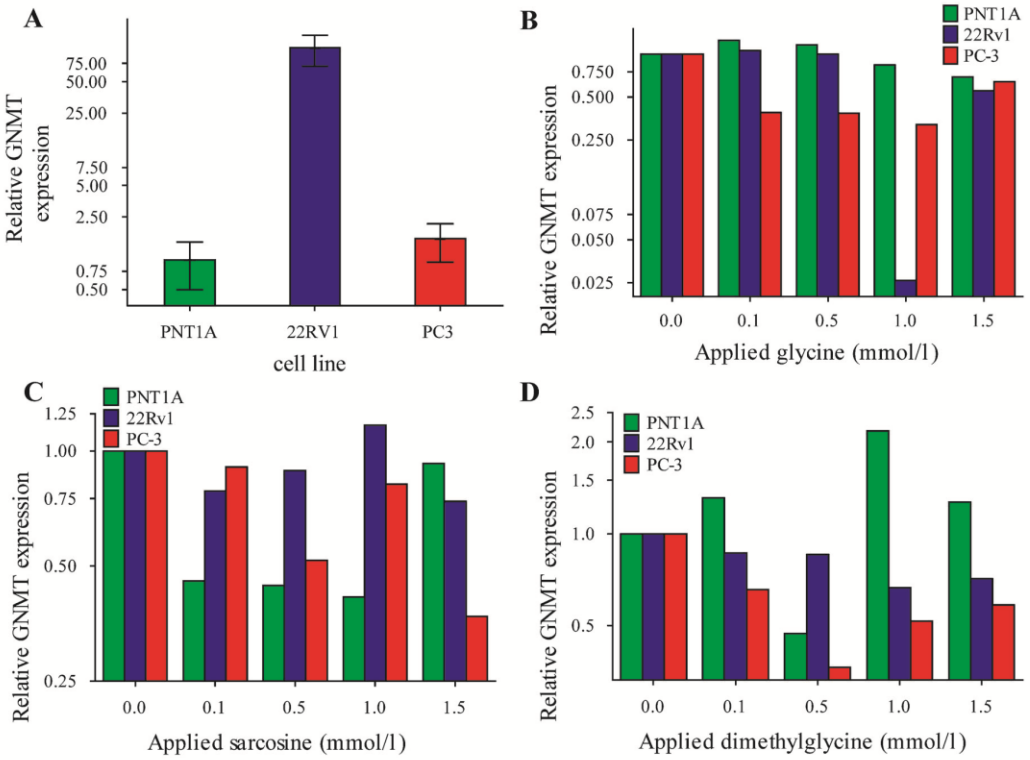

Fig. 4. Glycine-*N*-methyltransferase (GNMT) mRNA expression determined in (**A**) untreated cell lines (PNT1A, 22Rv1, and PC-3), related to *β-actin* as housekeeping and the same cell lines after application of 0.1–1.5 mmol/l (**B**) glycine, (**C**) sarcosine, and (**D**) dimethylglycine, assessed by qRT-PCR. Values are expressed using the delta-delta Ct method to derive relative fold change compared to untreated cell lines GNMT expression. Values are means of three independent replicates (n = 3).

changes in amino acid patterns in the cells (for details, see Table S1 in supplementary data). The obtained data indicate that the cell line type is highly specific for its amino acid pattern and this pattern is significantly influenced by amino acid supplementation.

Characterization of Patterns of Cellular Amino Acids

The previous analyses did not sufficiently highlight trends and relationships in the complex amino acid profile of the cell lines. Therefore, correlations among the individual amino acids detected in the cells were performed (Fig. 5B). Based on the results found by correlation analyses, amino acids can be divided into three clusters: cluster Lys, His, Dmg, Sar, Cys (cluster 1 in Fig. 5B), which is characterized by minimal correlations between these amino acids. The other two clusters, Phe, Ile, Ala, Arg, Thr (cluster 2 in Fig. 5B) and Tyr, Leu, Gly, Val, Met, Pro, Glu, Ser, Asp (cluster 3 in Fig. 5B) are characterized by strong correlation between those amino acids. A specific correlation pattern is apparent for sarcosine and cysteine, which demonstrate a negative correlation with all other amino acids except themselves.

Nevertheless, the correlation analysis did not allow to interpret complex multidimensional relationships between the amino acids' levels after the treatment of cells with sarcosine, glycine, and dimethylglycine—so called "amino acid patterns" of cell lines. Therefore, the principal component analysis was used. The component analysis allowed us to detect the structure in relationships between amino acid levels, and thus helped us to reveal characteristic patterns for the respective cell lines—non-tumor, primary tumor, and secondary/metastatic tumor cells. A two-factor model was employed with the eigenvalue 3.61, thus 49.4% of total variability of data (30.4 and 19.0 for factors 1 and 2, respectively) is explained. First, cases (cell lines, and amino acids used for supplementation) were projected into a factor plane (Fig. 6A). A color-coding by the cell line revealed a significant clustering of cell lines by a factor 2, whereas non-tumor PNT1A cells are clustered rather by positive values of factor 2, metastatic PC-3

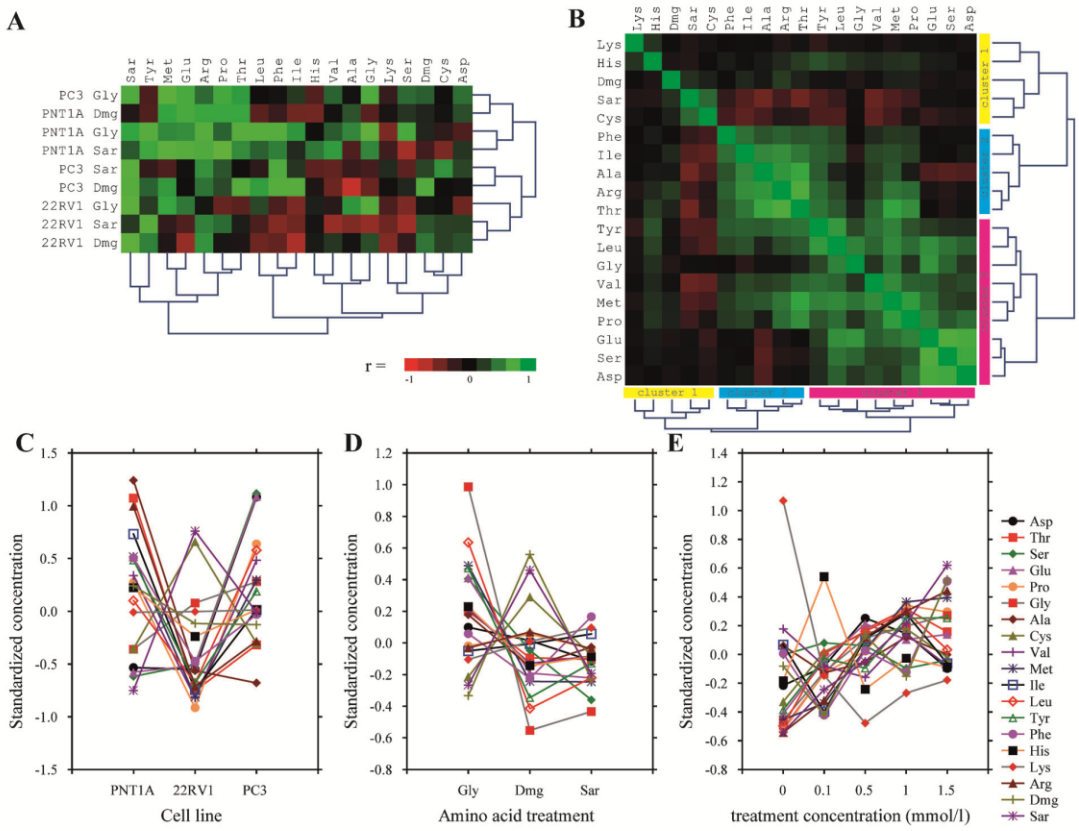

Fig. 5. Effect of treatment with glycine, dimethylglycine, and sarcosine on the cellular amino acid profile. (**A**) Heatmap showing clustered correlation analysis of amino acids used for treatment and amino acids profile measured in cells. Note the differential response of individual cell lines. (**B**) Heatmap showing correlation of amino acid profile measured in all three cell lines. Notice the differential negative correlation of sarcosine and cysteine with the majority of other amino acids. (**C**) Effect of the cell line on the level of amino acids, factorial ANOVA. Notice the differential response of cysteine, sarcosine, dimethylglycine, glycine, lysine, and alanine compared to the remaining amino acids. (**D**) Effect of amino acid used for treatment, factorial ANOVA. (**E**) Effect of concentration of the amino acids used for treatment, factorial ANOVA. Error bars not displayed for purposes of clarity.

are associated rather with negative values of this factor. Primary tumor 22Rv1 cluster is located between PNT1A and PC-3. Thus, the second factor is considered as "non-malignant—aggressive tumor cluster." In the next step, cases were color-coded by the amino acid used for treatment of prostate cell lines. This correlated with factor 1 on a factor plane; for each cell line the precursors—notably glycine was associated with more negative values than sarcosine. Thus, this factor was further designated as "precursor-product" (Fig. 6B). When variables (i.e., determined amino acids) were plotted to this factor plane, a similar shift is apparent (Fig. 6C). Whereas an amino acid pattern of the non-tumor PNT1A cell line is associated rather with negative values of factor 1, a metastatic-derived PC-3 amino acid pattern is associated with positive values of this factor, which corresponds also to "precursor" factor in Fig. 6B demonstrating sarcosine connection to prostate cancer.

DISCUSSION

The metabolic abnormalities of prostate cancer cells have not yet been fully elucidated [13]. Amino acids play an important role in cellular physiology, since they are involved in a number of fundamental metabolic processes [14,15]. Thus, we have focused on determination of response of the prostate cell biomolecules involved in a sarcosine metabolic pathway to supplementation of these cells with amino acids with emphasis on sarcosine, a widely discussed biomarker of PCa.

Only the high concentrations of sarcosine, glycine, and dimethylglycine are toxic to the tested prostate

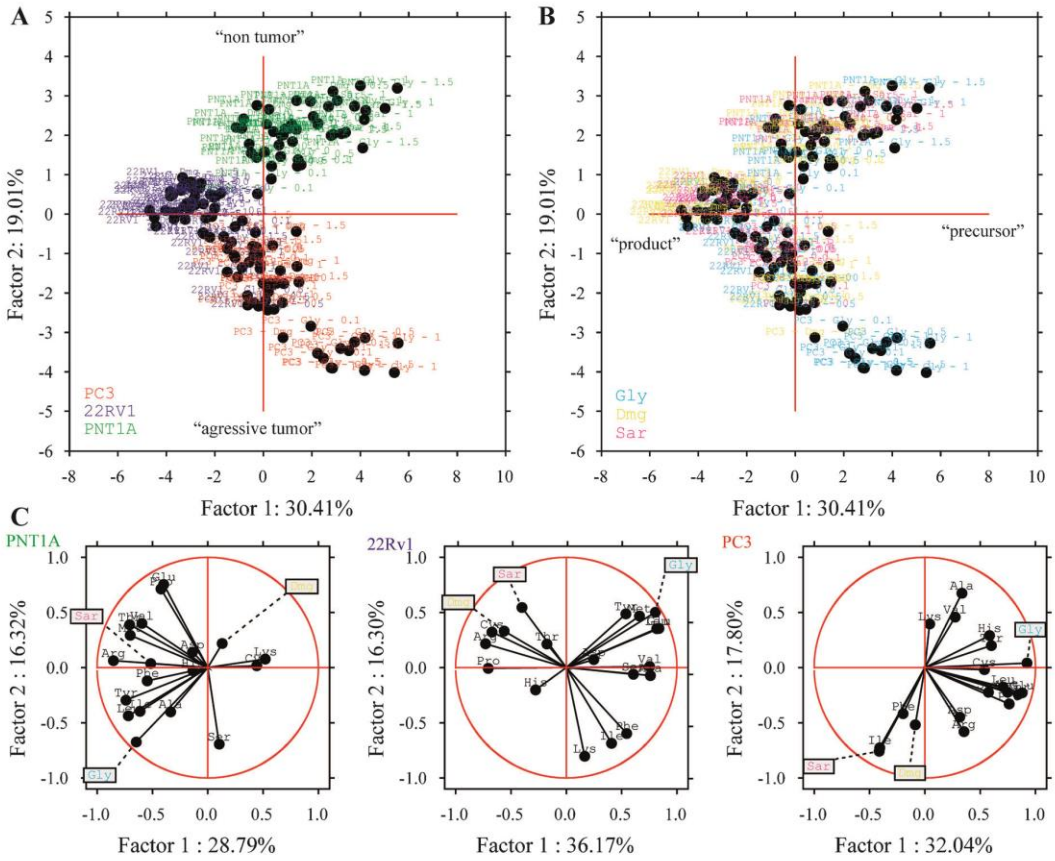

Fig. 6. Fingerprinting of prostate cells according to amino acid patterns, principal component analysis. (**A**) Projection of cases on a two-factor plane, color coded according to the cell line. Notice apparent clustering of cell lines by factor 2, thus this factor is considered "non-tumor–tumor." (**B**) Identical projection as (**A**), color coded by amino acid used for treatment. Notice the clustering for each cell line by Factor 1 so Sar precursors are more to the right from Sar for each cell line, so this factor is considered as "precursor–product." (**C**) Projection of variables (cellular amino acids) on two-factor plane identical as (**A**) and (**B**). See differential distribution of amino acids between cell lines (PNT1A, 22Rv1, and PC-3)—"left-to-right" shift on factor 1.

cells. Their cytotoxic concentrations are in conformity with those described by Stachlewitz et al., who have found that only the high concentrations of glycine (units of mM) are able to prevent increases in Ca^{2+} in cells, thereby inhibiting cell proliferation [16]. Likewise, we have found in our previous study, focused on possible effects of sarcosine on PC-3 cells, that only the high concentrations of sarcosine are able to inhibit cell growth, as a result of disruption of redox equilibrium [14]. Importantly, throughout our study, supplementation of prostate cells with tested amino acids did not exceed the concentrations of 1.5 mmol/l.

Sarcosine metabolism is suspicious to be an important part of malignant transformation of prostate cells. According to the changes in the cell mobility and division rates, sarcosine and glycine, but not dimethylglycine, can stimulate the migration of malignant cell lines (22Rv1 and PC-3). These findings are in agreement with a study carried out by Sreekumar et al., who have found that direct addition of sarcosine imparted an invasive phenotype to benign prostate cells and the number of motile prostate cells was significantly higher upon sarcosine treatment ($P = 6.997^{-6}$, n = 10) [9]. Similar, to that, Khan et al. demonstrated that addition of sarcosine to prostatic GNMT knockdown cells partially rescued their invasive properties, while addition of a sarcosine isomer, alanine, failed to rescue the invasive phenotype [17]. Notably, both studies highlighted the role of glycine, inducing invasion in the cells, however, to a lesser degree than sarcosine. It is plausible that this phenomenon is linked with the conversion of glycine to sarcosine catalyzed by GNMT.

Song et al. have reported that GNMT activity is connected with the progression of prostate cancer [12]. In agreement with their data, we have shown that GNMT mRNA expression is low predominantly in benign prostate cells, whereas high in the malignant cells. Hence, our results support the finding that sarcosine, generated from glycine by GNMT could be exploited as a PCa biomarker [3,9]. The GNMT enzyme is expected to play a substantial role in modulating prostate cancer cells invasion [18], and thus can be involved in promotion of the oncogenic potential of prostate cells with subsequent facilitating conversion of glycine to sarcosine. We demonstrated that dimethylglycine causes inhibition of GNMT mRNA expression in malignant cells, however, benign PNT1A were affected in a different manner. Increased amount of endogenously added dimethylglycine can stimulate sarcosine formation through action of dimethylglycine dehydrogenase (DMGDH), utilizing dimethylglycine as a substrate, instead of GNMT; nevertheless, whether the activity of DMGDH is disturbed in prostate cancer cells is unknown. The data found in the present work further illustrate that applied sarcosine significantly inhibited expression of GNMT in PNT1A cells, and to a lower extent in malignant PC-3 and 22Rv1. Thus, it can be hypothesized that by this kind of blocking, GNMT is not able to catalyze transformation of sarcosine to glycine and sarcosine can be thus accumulated in cancerous cells, as was shown in many studies [2,9,19]. However, plausible mechanism of this phenomenon is still not defined. Treatment of cells with glycine triggered only slight expression differences in GNMT, thus it can be stated that its expression is not glycine inducible. Our results illustrate the divergent significance of GNMT among the prostate cell lines and confirm the role of free amino acid pool as important metabolic factor, influencing PCa cells as was suggested by Fu et al. [15].

It has been shown that amino acids are substantial for cellular physiology [20–22] and our results demonstrate that free glycine and sarcosine can influence the GNMT expression in PCa cells. Jain et al. have revealed increased reliance of cancer cells on glycine mitochondrial metabolic pathway, which involves sarcosine and dimethylglycine [23]. Importantly, recent works have identified that sarcosine and related metabolites or their associated metabolic pathways, are central to cancer metastasis [9], cellular transformation [24,25], or murine embryonic stem cell proliferation [26]. Hence, we focused on patterns of amino acids in prostate cell lines and on the effect of exogenous supplementation with sarcosine-related amino acids on amino acid patterns in these cells. Our profiling revealed unique amino acid patterns, exhibiting exceptional specificity toward prostate cell types. This phenomenon is likely connected with disturbances in carbohydrate, lipid, and protein metabolism during oncogenesis. Considering the Warburg effect [27], metabolic shifts in tumor cells from respiration to fermentation should result in an increased demand for consumption of amino acids and complex metabolic derangements reflected by alteration in amino acid patterns. Noteworthy, statistical processing of amino acid patterns revealed that malignant cell lines (22Rv1 and PC-3) exhibit common features in increased (Glu, Sar, Gly, Asp, Ser) and decreased (Ala, Thr, Arg, Ile, Phe, Dmg) amino acids, when compared to benign PNT1A cells (Fig. 5C).

First, our interest was caught by differences in glutamic acid. This amino acid is a precursor for glutamine in its interconvertible biosynthesis. In cancer cells, glutamine is the primary mitochondrial substrate, maintaining mitochondrial membrane potential and integrity [28]. Moreover, it provides support for the NADPH production required for redox control and macromolecular synthesis [29]. Our results show that oncogenesis results in elevated level of intracellular glutamic acid. This phenomenon is likely connected with the fact that many of the signaling pathways promoting oncogenesis also reprogramms the glutamine metabolism. For instance, Myc coordinates the reprogramming of metabolism to depend on glutamine and to sustain cellular viability and the citric acid cycle (TCA) anaplerosis through carbon donation [30,31]. Interestingly, glycine supplementation led to a significant elevation of glutamic acid levels within the cell lines; however, the reason explaining this phenomenon is not yet clear. Taken together, divergence in glutamic acid metabolism supports the idea that interventions into metabolism could be a potential therapeutic approach in PCa management, as was shown by Wang et al. [32].

Figure 6C illustrates that contrary to benign prostate cells, in malignant cells, glutamic acid essentially shares similar distribution with glycine and serine. Serine and glycine are linked biosynthetically. They provide the precursors for the synthesis of proteins, nucleic acids, and lipids [33]. Our results show that cancer cells benefit from higher levels of these amino acids. Serine biosynthesis is a component of glycolysis-diverting pathways, resulting in expression of phosphoglycerate dehydrogenase (PHGDH), which is necessary to sustain cancer growth and oncogenic transformation through production of anaplerotic intermediate of TCA α-ketoglutarate [34]. Serine also supports aerobic glycolysis and lactate production by affecting the activity of pyruvate kinase M2 (PKM2), converting phosphoenolpyruvate to pyruvate and one molecule

of ATP [35]. Glycine promotes tumorigenesis and its upregulation correlates with cell proliferation and poor prognosis. Its conversion significantly contributes to the biosynthetic requirements of purines, ATP and NADPH in cancer cells [23].

Elevated levels of aspartate in both types of malignant prostate cells are likely related to glutaminolysis, which lyses glutamine to citrate [36]. Such process takes place in all proliferating cells and especially in tumor cells, where the TCA is truncated due to an inhibition of aconitase [37]. Aspartic acid, produced from oxaloacetate during conversion of glutamate to α-ketoglutarate is utilized as a precursor for synthesis of nucleic acids and serine [38]. Taken together, both malignant prostate cell lines exhibited high dependency on glutamine metabolism, when compared to benign ones.

Our data further indicate that glycine supplementation influences all prostate cell amino acid patterns most effectively, which is likely due to a linkage with serine biosynthesis. Glycine treatment also resulted in elevation of amounts of amino acids connected to glutamine metabolism. Hence, we put evidence that glycine plays substantial role in prostate cells and glycine deprivation (dietetic or enzymatic depletion) may be a new strategy for human cancer therapy as was described earlier [23,33,39]. On the contrary, the highest increase in sarcosine concentrations was found after supplementation with exogenous dimethylglycine, whose role in prostate cancer development is not yet well elucidated. Elevated sarcosine levels during prostate cancer progression [3,9,17,19] are thus likely associated with action of both substrates—glycine and dimethylglycine and catalytic actions of corresponding enzymes—GNMT and DMGDH. One may speculate that inhibition of those enzymes may be used in prevention of prostate cancer.

CONCLUSION

The present study illustrates that exogenous supplementation of prostate cells with amino acids, closely related to sarcosine metabolism, can significantly affect the expression of GNMT mRNA in tested cells as well as their growth attributes. The results found indicate that sarcosine production is triggered by dimethylglycine treatment more than by glycine; however, glycine, a well-known cancer-related metabolite, significantly influences the prostate cell amino acid patterns. Above-mentioned data support the studies, which demonstrate that the deprivation of some amino acids can be helpful in management of cancer and furthermore proves the elevated levels of sarcosine in primary and secondary tumor cell lines when compared with non-tumor ones, which corresponds to their GNMT expression levels. We anticipate that sarcosine metabolic pathway is highly important in prostate cancer behavior, and thus further studies, dealing with involved amino acids and their enzymes and also with inhibition of their activity in relation to physical and molecular parameters of prostate cells are strongly required to elucidate this phenomenon. Moreover, it was shown that amino acid patterns unequivocally describe if the prostate cells demonstrate malignant or non-tumor parameters.

ACKNOWLEDGMENTS

The authors wish to express their thanks to Andrea Tomeckova and Martina Stankova for technical assistance.

REFERENCES

1. Armstrong AJ, Eisenberger MA, Halabi S, Oudard S, Nanus DM, Petrylak DP, Sartor AO, Scher HI. Biomarkers in the management and treatment of men with metastatic castration-resistant prostate cancer. Eur Urol 2012;61(3):549–559.
2. Lucarelli G, Fanelli M, Larocca AMV, Germinario CA, Rutigliano M, Vavallo A, Selvaggi FP, Bettocchi C, Battaglia M, Ditonno P. Serum sarcosine increases the accuracy of prostate cancer detection in patients with total serum PSA less than 4.0ng/ml. Prostate 2012;72(15):1611–1621.
3. Zitka O, Heger Z, Kominkova M, Skalickova S, Krizkova S, Adam V, Kizek R. Preconcentration based on paramagnetic microparticles for the separation of sarcosine using hydrophilic interaction liquid chromatography coupled with coulometric detection. J Sep Sci 2014;37(5):465–475.
4. Cernei N, Heger Z, Gumulec J, Zitka O, Masarik M, Babula P, Eckschlager T, Stiborova M, Kizek R, Adam V. Sarcosine as a potential prostate cancer biomarker—A review. Int J Mol Sci 2013;14(7):13893–13908.
5. Metallo CM. Expanding the reach of cancer metabolomics. Cancer Prev Res 2012;5(12):1337–1340.
6. Luka Z, Pakhomova S, Loukachevitch LV, Newcomer ME, Wagner C. Differences in folate-protein interactions result in differing inhibition of native rat liver and recombinant glycine N-methyltransferase by 5-methyltetrahydrofolate. Biochim Biophys Acta 2012;1824(2):286–291.
7. Mitchell AD, Benevenga NJ. Importance of sarcosine formation in methionine methyl carbon oxidation in rat. J Nutr 1976;106-(12):1702–1713.
8. Soriano A, Castillo R, Christov C, Andres J, Moliner V, Tunon I. Catalysis in glycine N-methyltransferase: Testing the electrostatic stabilization and compression hypothesis. Biochemistry 2006;45(50):14917–14925.
9. Sreekumar A, Poisson LM, Rajendiran TM, Khan AP, Cao Q, Yu JD, Laxman B, Mehra R, Lonigro RJ, Li Y, Nyati MK, Ahsan A, Kalyana-Sundaram S, Han B, Cao XH, Byun J, Omenn GS, Ghosh D, Pennathur S, Alexander DC, Berger A, Shuster JR, Wei JT, Varambally S, Beecher C, Chinnaiyan AM. Metabolomic profiles delineate potential role for sarcosine in prostate cancer progression. Nature 2009;457(7231):910–914.
10. Cao DL, Ye DW, Zhang HL, Zhu Y, Wang YX, Yao XD. A multiplex model of combining gene-based, protein-based,

and metabolite-based with positive and negative markers in urine for the early diagnosis of prostate cancer. Prostate 2011;71(7):700–710.

11. Liang CC, Park AY, Guan JL. In vitro scratch assay: A convenient and inexpensive method for analysis of cell migration in vitro. Nat Protoc 2007;2(2):329–333.
12. Song YH, Shiota M, Kuroiwa K, Naito S, Oda Y. The important role of glycine N-methyltransferase in the carcinogenesis and progression of prostate cancer. Mod Pathol 2011;24(9):1272–1280.
13. Fu YM, Lin HM, Fang WG, Meadows GG. Cell death of prostate cancer cells by specific amino acid restriction depends on alterations of glucose metabolism. J Cell Physiol 2010;224-(2):491–500.
14. Heger Z, Cernei N, Kudr J, Gumulec J, Blazkova I, Zitka O, Eckschlager T, Stiborova M, Adam V, Kizek R. A novel insight into the cardiotoxicity of antineoplastic drug doxorubicin. Int J Mol Sci 2013;14(11):21629–21646.
15. Fu YM, Yu ZX, Li YQ, Ge XK, Sanchez PJ, Fu X, Meadows GG. Specific amino acid dependency regulates invasiveness and viability of androgen-independent prostate cancer cells. Nutr Cancer 2003;45(1):60–73.
16. Stachlewitz RF, Li XL, Smith S, Bunzendahl H, Graves LM, Thurman RG. Glycine inhibits growth of T lymphocytes by an IL-2-independent mechanism. J Immunol 2000;164(1):176–182.
17. Khan AP, Rajendiran TM, Ateeq B, Asangani IA, Athanikar JN, Yocum AK, Mehra R, Siddiqui J, Palapattu G, Wei JT, Michailidis G, Sreekumar A, Chinnaiyan AM. The role of sarcosine metabolism in prostate cancer progression. Neoplasia 2013;15-(5):491–501.
18. Huang YC, Lee CM, Chen M, Chung MY, Chang YH, Huang WJS, Ho DMT, Pan CC, Wu TT, Yang S, Lin MW, Hsieh JT, Chen YMA. Haplotypes, loss of heterozygosity, and expression levels of glycine N-methyltransferase in prostate cancer. Clin Cancer Res 2007;13(5):1412–1420.
19. Heger Z, Cernei N, Krizkova S, Masarik M, Kopel P, Hodek P, Zitka O, Adam V, Kizek R. Paramagnetic nanoparticles as a platform for FRET-based sarcosine picomolar detection. Sci Rep 2015;5:1–7.
20. Bar-Peled L, Sabatini DM. Regulation of mTORC1 by amino acids. Trends Cell Biol 2014;24(7):400–406.
21. Torrente M, Guetg A, Sass JO, Arps L, Ruckstuhl L, Camargo SMR, Verrey F. Amino acids regulate transgene expression in MDCK cells. PLoS ONE 2014;9(5):1–13.
22. Mann GE, Yudilevich DL, Sobrevia L. Regulation of amino acid and glucose transporters in endothelial and smooth muscle cells. Physiol Rev 2003;83(1):183–252.
23. Jain M, Nilsson R, Sharma S, Madhusudhan N, Kitami T, Souza AL, Kafri R, Kirschner MW, Clish CB, Mootha VK. Metabolite profiling identifies a key role for glycine in rapid cancer cell proliferation. Science 2012;336(6084):1040–1044.
24. Zhang WC, Shyh-Chang N, Yang H, Rai A, Umashankar S, Ma SM, Soh BS, Sun LL, Tai BC, Nga ME, Bhakoo KK, Jayapal SR, Nichane M, Yu Q, Ahmed DA, Tan C, Sing WP, Tam J, Thirugananam A, Noghabi MS, Pang YH, Ang HS, Robson P, Kaldis P, Soo RA, Swarup S, Lim EH, Lim B. Glycine decarboxylase activity drives non-small cell lung cancer tumor-initiating cells and tumorigenesis. Cell 2012;148(1–2):259–272.
25. Locasale JW, Grassian AR, Melman T, Lyssiotis CA, Mattaini KR, Bass AJ, Heffron G, Metallo CM, Muranen T, Sharfi H, Sasaki AT, Anastasiou D, Mullarky E, Vokes NI, Sasaki M, Beroukhim R, Stephanopoulos G, Ligon AH, Meyerson M, Richardson AL, Chin L, Wagner G, Asara JM, Brugge JS, Cantley LC, Vander MG, Heiden. Phosphoglycerate dehydrogenase diverts glycolytic flux and contributes to oncogenesis. Nat Genet 2011;43(9):869–874.
26. Wang J, Alexander P, Wu LJ, Hammer R, Cleaver O, McKnight SL. Dependence of mouse embryonic stem cells on threonine catabolism. Science 2009;325(5939):435–439.
27. Warburg O, Wind F, Negelein E. The metabolism of tumors in the body. J Gen Physiol 1927;8(6):519–530.
28. Barger JF, Plas DR. Balancing biosynthesis and bioenergetics: Metabolic programs in oncogenesis. Endocr Relat Cancer 2010;17(4):287–304.
29. Wise DR, Thompson CB. Glutamine addiction: A new therapeutic target in cancer. Trends Biochem Sci 2010;35(8):427–433.
30. Wise DR, DeBerardinis RJ, Mancuso A, Sayed N, Zhang XY, Pfeiffer HK, Nissim I, Daikhin E, Yudkoff M, McMahon SB, Thompson CB. Myc regulates a transcriptional program that stimulates mitochondrial glutaminolysis and leads to glutamine addiction. Proc Natl Acad Sci USA 2008;105(48):18782–18787.
31. Dang CV. Rethinking the Warburg effect with Myc micromanaging glutamine metabolism. Cancer Res 2010;70(3):859–862.
32. Wang Q, Hardie RA, Hoy AJ, van Geldermalsen M, Gao D, Fazli L, Sadowski MC, Balaban S, Schreuder M, Nagarajah R, Wong JJL, Metierre C, Pinello N, Otte NJ, Lehman ML, Gleave M, Nelson CC, Bailey CG, Ritchie W, Rasko JE, Holst J. Targeting ASCT2-mediated glutamine uptake blocks prostate cancer growth and tumour development. J Pathol 2015;236(3): 278–289.
33. Amelio I, Cutruzzola F, Antonov A, Agostini M, Melino G. Serine and glycine metabolism in cancer. Trends Biochem Sci 2014;39(4):191–198.
34. DeBerardinis RJ. Serine metabolism: Some tumors take the road less traveled. Cell Metab 2011;14(3):285–286.
35. Chaneton B, Hillmann P, Zheng L, Martin ACL, Maddocks ODK, Chokkathukalam A, Coyle JE, Jankevics A, Holding FP, Vousden KH, Frezza C, O'Reilly M, Gottlieb E. Serine is a natural ligand and allosteric activator of pyruvate kinase M2. Nature 2012;491(7424):458–462.
36. Moreadith RW, Lehninger AL. The pathways of glutamate and glutamine oxidation by tumor-cell mitochondria—Role of mitochondrial NADP(P)+-dependent malic enzyme. J Biol Chem 1984;259(10):6215–6221.
37. Kim KH, Rodriguez AM, Carrico PM, Melendez JA. Potential mechanisms for the inhibition of tumor cell growth by manganese superoxide dismutase. Antioxid Redox Signal 2001;3-(3):361–373.
38. Newsholme P, Lima MMR, Porcopio J, Pithon-Curi TC, Doi SQ, Bazotte RB, Curi R. Glutamine and glutamate as vital metabolites. Braz J Med Biol Res 2003;36(2):153–163.
39. Maddocks ODK, Berkers CR, Mason SM, Zheng L, Blyth K, Gottlieb E, Vousden KH. Serine starvation induces stress and p53-dependent metabolic remodelling in cancer cells. Nature 2013;493(7433):542–546.

SUPPORTING INFORMATION

Additional supporting information may be found in the online version of this article at the publisher's web-site.

PLOS | ONE

RESEARCH ARTICLE

Sarcosine Up-Regulates Expression of Genes Involved in Cell Cycle Progression of Metastatic Models of Prostate Cancer

Zbynek Heger[1,2], Miguel Angel Merlos Rodrigo[1,2], Petr Michalek[1,2], Hana Polanska[3], Michal Masarik[2,3], Vitezslav Vit[4], Mariana Plevova[4], Dalibor Pacik[4], Tomas Eckschlager[5], Marie Stiborova[6], Vojtech Adam[1,2]*

1 Department of Chemistry and Biochemistry, Mendel University in Brno, Zemedelska 1, CZ-613 00, Brno, Czech Republic, **2** Central European Institute of Technology, Brno University of Technology, Purkynova 123, Brno, CZ-612 00, Czech Republic, **3** Department of Physiology, Faculty of Medicine, Masaryk University, Kamenice 5, Brno, CZ-625 00, Czech Republic, **4** Department of Urology, University Hospital Brno, Jihlavska 20, Brno, CZ-625 00, Czech Republic, **5** Department of Paediatric Haematology and Oncology, 2nd Faculty of Medicine, Charles University, and University Hospital Motol, V Uvalu 84, CZ-150 06, Prague 5, Czech Republic, **6** Department of Biochemistry, Faculty of Science, Charles University, Albertov 2030, CZ-128 40, Prague 2, Czech Republic

* vojtech.adam@mendelu.cz

OPEN ACCESS

Citation: Heger Z, Merlos Rodrigo MA, Michalek P, Polanska H, Masarik M, Vit V, et al. (2016) Sarcosine Up-Regulates Expression of Genes Involved in Cell Cycle Progression of Metastatic Models of Prostate Cancer. PLoS ONE 11(11): e0165830. doi:10.1371/journal.pone.0165830

Editor: Natasha Kyprianou, University of Kentucky College of Medicine, UNITED STATES

Received: June 29, 2016

Accepted: October 18, 2016

Published: November 8, 2016

Data Availability Statement: All relevant data are within the paper and its Supporting Information files.

Funding: Financial support from The Czech Science Foundation (GA CR 16-18917S) and Central European Institute of Technology (CEITEC 2020 LQ1601) is highly acknowledged.

Competing Interests: The authors have declared that no competing interests exist.

Abstract

The effects of sarcosine on the processes driving prostate cancer (PCa) development remain still unclear. Herein, we show that a supplementation of metastatic PCa cells (androgen independent PC-3 and androgen dependent LNCaP) with sarcosine stimulates cells proliferation *in vitro*. Similar stimulatory effects were observed also in PCa murine xenografts, in which sarcosine treatment induced a tumor growth and significantly reduced weight of treated mice ($p < 0.05$). Determination of sarcosine metabolism-related amino acids and enzymes within tumor mass revealed significantly increased glycine, serine and sarcosine concentrations after treatment accompanied with the increased amount of sarcosine dehydrogenase. In both tumor types, dimethylglycine and glycine-*N*-methyltransferase were affected slightly, only. To identify the effects of sarcosine treatment on the expression of genes involved in any aspect of cancer development, we further investigated expression profiles of excised tumors using cDNA electrochemical microarray followed by validation using the semi-quantitative PCR. We found 25 differentially expressed genes in PC-3, 32 in LNCaP tumors and 18 overlapping genes. Bioinformatical processing revealed strong sarcosine-related induction of genes involved particularly in a cell cycle progression. Our exploratory study demonstrates that sarcosine stimulates PCa metastatic cells irrespectively of androgen dependence. Overall, the obtained data provides valuable information towards understanding the role of sarcosine in PCa progression and adds another piece of puzzle into a picture of sarcosine oncometabolic potential.

Introduction

Sarcosine, also known as *N*-methylglycine, is a non-proteinogenic imino acid occurring as an intermediate and byproduct in glycine synthesis and degradation [1]. In 2009, Sreekumar *et al.* delineated its potential role as urinary, non-invasive biomarker exploitable for early diagnosis of prostate cancer (PCa) [2]. This publication triggered sarcosine research, which resulted in a number of reports studying the connection between this low molecular mass metabolite and PCa diagnostics. Anyway, it has to be noted that the presented results have been somehow contradictory, whereas some of them have demonstrated a positive linkage only [3–5], while some of them have been negative [6, 7]. Thus, the further research is necessary to elucidate the role of sarcosine and its impact on properties of PCa cells.

In our initial study, we revealed that sarcosine supplementation increases the cell migration and decreases the doubling time of malignant prostatic cells *in vitro* [8]. Similar efforts were put by Sudhakaran and colleagues, who described that sarcosine modulates angiogenesis in endothelial cells *in vitro* through PI3K/Akt/mTOR pathway [9]. Moreover, Khan *et al.* demonstrated that sarcosine induces invasion and intravasation in *in vivo* PCa model [10]. Taken together, above mentioned studies showed sarcosine as an oncometabolite and substantiated its role in PCa progression. Although a relatively complex pool of data has been provided, to the best of our knowledge, there still exists a lack of reports on the sarcosine regulatory effects on expression of pivotal genes involved in a cell cycle and apoptosis, which lie beneath the complexity and idiopathy of each cancer [11].

To unravel the putative mechanisms involved in abnormal growth of cancer cells is a complex and vast task requiring powerful tools. One of them is a microarray technology, which accelerated the completion of the human genome project and eliminated numerous previous boundaries [12]. DNA microarrays, also called "gene chips" enable studying of differential gene expression using complex population of RNA [13]. As a result, microarrays provide large gene expression data sets for consequent data mining, which can be carried out using a number of available software applications.

Hence, in our study, we have employed a special type of DNA microarray, based on redox enzyme mediated analysis of cDNA hybridization, to give another piece to the puzzle of sarcosine oncometabolic potential. Using preclinical *in vivo* murine models (PC-3 and LNCaP xenografts); we focused on an investigation of effects of sarcosine treatment on expression of genes involved particularly in a cell cycle and apoptosis. Overall, this study reveals that sarcosine significantly up-regulates the expression of some of those genes, irrespective of androgen dependence status.

Material and Methods

Chemicals

Sarcosine standard and other chemicals were purchased from Sigma-Aldrich (St. Louis, MO, USA) in ACS purity, unless noted otherwise.

Cells

The PC-3 cell line, established from a grade IV androgen-independent prostatic adenocarcinoma and the LNCaP cell line, derived from the left supraclavicular androgen-dependent lymph node PCa metastasis were purchased from the Health Protection Agency Culture Collection (Salisbury, UK). The PC-3 cells were grown in Ham's F12 medium with 7% foetal bovine serum. The LNCaP cells were grown in RPMI-1640 with 10% fetal bovine serum. Media were supplemented with penicillin (100 U/mL) and streptomycin (0.1 mg/mL). The

cells were maintained at 37°C in a humidified incubator with 5% CO_2. The treatments with sarcosine were initiated after cells reached ~70–80% confluency. Cells were then harvested and washed four times with phosphate-buffered saline (PBS, pH 7.4).

Viability (MTT) assay

The suspension of 10 000 cells was added to each well of standard microtiter plates. After addition of medium (200 μL), plates were incubated for 2 days at 37°C to ensure cell growth. To determine the effects on cell viability sarcosine in concentrations 0–10 μM was applied. Plates were incubated for 24 h; then, media were removed and replaced by fresh ones, three times a day. Further, for each plate, a medium was replaced by 200 μL of fresh medium containing 50 μL of MTT (5 mg/mL in PBS) and incubated in a humidified atmosphere for 4 h at 37°C, wrapped in aluminum foil. After the incubation, MTT-containing medium was replaced by 200 μL of 99.9% dimethyl sulphoxide (*v/v*) to dissolve MTT-formazan crystals. Then, 25 μL of glycine buffer (pH 10.5) was added to all wells and absorbance at 570 nm was immediately determined using the Infinite 200PRO reader (Tecan, Männedorf, Switzerland).

Light microscopy

For light microscopy, the cells (1×10^5 at time point 0 h) were cultivated directly on glass microscopy slides (75×25 mm, thickness 1 mm) in medium without and with 1 μM sarcosine. Prior microscopic examination, slides with a monolayer of cells were removed from Petri dishes, rinsed with a medium and PBS and directly used for investigation of their density under an inverted microscope (Olympus IX 71S8F-3, Olympus, Tokyo, Japan).

Prostate tumor xenograft models and the treatment protocol

Twelve five-week-old male nude athymic BALB/c nu/nu mice were used for xenograft studies. PC-3 or LNCaP cells (5×10^6) were resuspended in 100 μL of PBS with 20% Matrigel (*v/v*, BD Biosciences, Franklin Lakes, NJ, USA) and were then implanted subcutaneously (*s.c.*) into the left flank regions of the mice (six mice for PC-3 tumors and six mice for LNCaP tumors) under general anesthesia (1% Narkamon + 2% Rometar, 0.5 mL/100 g of weight). Six mice were utilized as the non-treated controls. All animals were housed in individually ventilated cages at a 12/12 h light/dark cycle and were provided *ad libitum* with standard diet and water. A tumor volume was measured twice per week following the equation (length × width^2 × 0.5) as well as well-being of the mice. The treatment of mice was carried out *i.p.* two times a week for 21 days (total 6 applications) using 100 μL of 5 μM sarcosine solution. After termination by isoflurane inhalation, tumors were excised immediately and stored in RNA*later* (Thermo Fisher, Waltham, MA, USA) prior to further experiments. The use of the animals followed the European Community Guidelines as accepted principles for the use of experimental animals. The experiments were performed with the approval of the Ethics Commission at the Faculty of Medicine, Masaryk University, Brno, Czech Republic.

Histological procedures

The samples were fixed in formaldehyde (10% *v/v*) overnight, subsequently dehydrated in serial ethanol concentrations and embedded in paraffin. Sections were cut at 5 μm, mounted on glass slides, deparaffinized and stained with hematoxylin-eosin (H&E). The microscopic observations were conducted using an Olympus IX 71S8F-3 (Olympus, Tokyo, Japan).

Ion-exchange chromatography (IEC)

Amino acids (glycine, serine and dimethylglycine) and sarcosine in tumor tissue were determined using IEC with Vis detection after post-column derivatization with ninhydrin (AAA-400, Ingos, Prague, Czech Republic), following conditions employed in our previous study [14].

Quantitation of glycine-*N*-methyltransferase (GNMT) and sarcosine dehydrogenase (SARDH)

Amounts of GNMT and SARDH in sarcosine treated and non-treated tumors were quantified by human sandwich ELISA kits with HRP-conjugated secondary antibody and 3,3',5,5'-tetramethylbenzidine (TMB) as a substrate (LSBio, Seattle, WA, USA). Color intensity at 495 nm was read in a VersaMax microplate reader (Molecular Devices, Sunnyvale, CA, USA).

Isolation of RNA and reverse transcription (RT)

High pure total-RNA isolation kit (Roche, Basel, Switzerland) was used for an isolation of tissue RNA. The medium was removed and samples were twice washed with 5 mL of ice-cold PBS. Cells were scraped off, transferred to clean tubes and centrifuged at 20 800×*g* for 5 min at 4°C. After that, lysis buffer was added and RNA isolation was carried out according to manufacturer's instructions. Isolated RNA was used for cDNA synthesis. RNA (500 ng) was transcribed using transcriptor first strand cDNA synthesis kit (Roche) according to manufacturer's instructions. Prepared cDNA (20 μL) was diluted with RNase-free water to a total volume of 100 μL and 5 μL of this solution was employed for microarray analyses.

Electrochemical microarray

cDNA was biotinylated on its 3' end using the Biotin 3' End DNA Labeling Kit (Thermo Scientific, Waltham, MA, USA) following the manufacturer's instructions. The microarray was performed as previously described by Roth *et al.* [15]. For hybridization, Human Cancer 3711 ElectraSense medium density 4×2k array slides with 1,609 DNA probes (Custom Array, Bothell, WA, USA), were firstly pre-hybridized for 30 min at 50°C using 6× SSPE (0.9 M NaCl, 60 mM sodium phosphate, 6 mM EDTA), 5× Denhardt´s solution and sonicated salmon sperm DNA (100 μg/mL). Then, hybridization of biotin-labeled cDNA was performed at 50°C for 18 h in 6× SSPE and salmon sperm DNA (100 μg/mL). Array chips were rinsed with low ionic strength 3× SSPET (3× SSPE, 0.05% Tween-20) and PBST (2× phosphate-buffered saline, pH 7.4, 0.1% Tween-20) to remove weakly bound DNA. Subsequently, array chips were blocked with biotin blocking solution for 15 min. Chips were then incubated for 30 min with poly-horseradish peroxidase-streptavidin (1:1,000 in PBS containing 1% bovine serum albumin and 0.05% Tween-20). Next, chips were rinsed three times with biotin wash solution and TMB rinse solution, followed by incubation with TMB substrate. Measurements were performed using the ElectraSense detection kit (Custom Array). All post-hybridization processing steps were performed at 25°C.

Semi-quantitative RT-PCR for validation of selected genes

To confirm selected microarray results we separately performed semi-quantitative RT-PCR (SQ-RT-PCR) of genes with the expression 2.5-fold stronger than non-treated individuals. To adjust the amount of transcribed cDNA, *β-actin* was selected as an internal control. The primer sequences were as follows: 5´-TCCATCGTCCACAGAAAG-3´ (forward) and 5´-AAATGTCC TCCGCAAGCT-3´ (reverse). For designing the primers of tested genes, the sequence information was collected from the NCBI GenBank (www.ncbi.nih.gov). Information about the PCR

primers is available upon request to the corresponding author. SQ-RT-PCR experiments were performed in conditions described in our previous study [16]. For evaluation of differences in gene expression between sarcosine treatment and non-treated controls, 10 μL of each SQ-RT-PCR product was electrophoresed on a 2.0% agarose gel and stained with ethidium bromide.

Descriptive statistics and exploited bioinformatical tools

For the statistical evaluation of the results, the mean was taken as the measurement of the main tendency, while standard deviation was taken as the dispersion measurement. Differences between groups were analyzed using paired *t*-test and ANOVA. Unless noted otherwise, the threshold for significance was $p < 0.05$. For analyses Software Statistica 12 (StatSoft, Tulsa, OK, USA) was employed. The annotation analyses were performed using the GoMiner (http://discover.nci.nih.gov/gominer/index.jsp), interactome network was constructed using the STRING software (http://string-db.org/) and the PCa metabolic pathway was visualized using Kyoto Encyclopedia of Genes and Genomes (KEGG) pathway database (http://www.genome.jp/kegg/), which provides gold standard sets of molecular pathways. The involvement of genes involved in a cell cycle was carried out using the Reactome (www.reactome.org).

Results

Effect of sarcosine on PC-3 cells viability and proliferation *in vitro*

In the first step, we considered pivotal to determine the sarcosine effects on the PC-3 and LNCaP cells viability *in vitro*. Fig 1Aa illustrates that even the lowest applied sarcosine supplementation stimulated the growth of PC-3 cells after 24 h. Noteworthy, the plateau of the stimulation effects was reached using approx. 0.2 μM sarcosine and higher concentrations resulted in slow decreasing viability trends. Similarly, sarcosine treatment stimulated the proliferation of LNCaP cells, but the stimulatory effects were significantly lower than those found in PC-3 cells (Fig 1Ab). As there were obvious impacts on a growth rate of cells, we further analyzed sarcosine influence on their confluency. Light microscopy photographs in Fig 1Ba and 1Bb show that sarcosine supplementation stimulates the proliferation of both PC-3 and LNCaP cells, which can be observed as the increased density of these cells after 72 h cultivation. The found *in vitro* data led us to further proceed to *in vivo* experiments utilizing murine PC-3 and LNCaP xenografts focusing on the effects of sarcosine treatment on a tumor growth and gene expression profiles related to repeated sarcosine supplementation.

Sarcosine treatment effects on growth of tumors *in vivo*

Murine xenografts were induced by using *s.c.* inoculation of PCa cells. The experimental workflow of the *in vivo* experiment, showing the treatment course, termination and subsequent analyses is depicted in **Fig 2A**. The results obtained by weighing the treated and non-treated mice demonstrate that in both cases, sarcosine induced significant losses of weight when compared to non-treated individuals [$p < 0.05$, (Fig 2B)]. No mice died or had to be euthanized before the endpoint of the experiment. After the termination, considerable differences between the sizes of excised ectopic prostate tumors were found (Fig 2C), as well as the significant differences in the tumor weights [175 mg *vs*. 94 mg for PC-3 and 137 mg *vs*. 90 mg for LNCaP, $p < 0.05$ (Fig 2D)]. The histological examination of tumor sections however did not reveal any changes within them (Fig 2E).

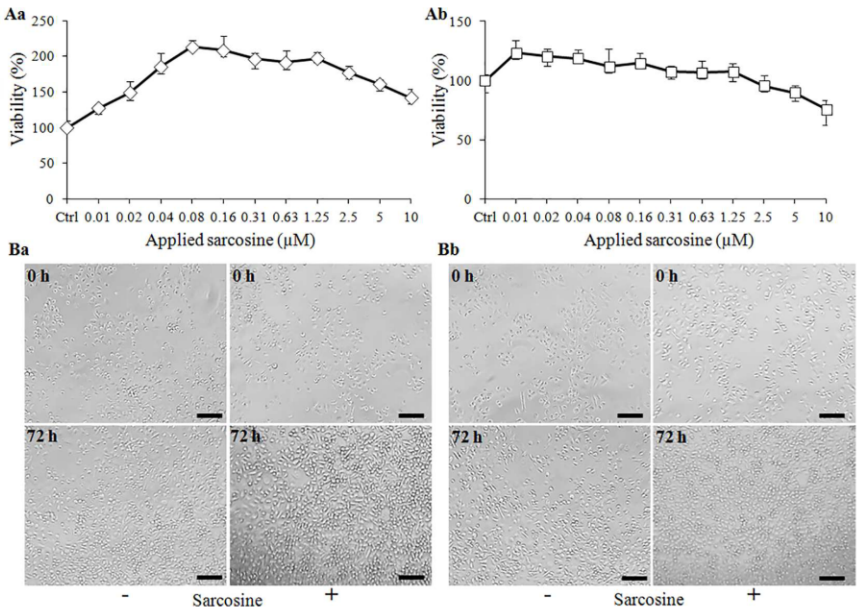

Fig 1. *In vitro* supplementation of PCa cells with sarcosine. (**A**) Viability (MTT) assay showing the trend in (**Aa**) PC-3 and (**Ab**) LNCaP cells growth under 24 h supplementation with sarcosine (0–10 μM). Values are expressed as the means ± standard deviations of six independent replicates ($n = 6$). (**B**) Micrographs of densities of (**Ba**) PC-3 cultivated in standard Ham's F12 medium (*left*) and in Ham's F12 medium enriched for 1 μM sarcosine (*right*) and (**Bb**) LNCaP cultivated in RPMI-1640 medium (*left*) and in RPMI-1640 medium enriched for 1 μM sarcosine (*right*). The length of scale bar is 500 μm.

doi:10.1371/journal.pone.0165830.g001

Sarcosine treatment effect on concentration of sarcosine pathway-related amino acids in tumors

As sarcosine pathway involves amino acids providing the essential precursors for the synthesis of proteins, lipids and nucleic acids (particularly serine and glycine), we tested the influence of sarcosine treatment on their tumor tissue concentrations. We also included dimethylglycine (Dmg), the amino acid that can be demethylated by dimethylglycine dehydrogenase to form sarcosine (schematic depiction is shown in Fig 3A). The results found indicate that in PC-3 xenografts, sarcosine treatment resulted in significant ($p < 0.05$) increase in glycine and serine levels (Fig 3B). Moreover, we also detected increased concentrations of sarcosine (0.65 nmol of sarcosine per mg of treated tumor tissue *vs.* 0.43 nmol of sarcosine per mg of non-treated tumor) there. On the other hand, the amount of Dmg was not significantly affected by the sarcosine treatment.

Moreover, Fig 3C demonstrates that LNCaP tumors exhibited very similar response to the sarcosine treatment, having lower initial and induced concentration of sarcosine (0.33 nmol of sarcosine per mg of treated tumor tissue *vs.* 0.19 nmol of sarcosine per mg of non-treated tumor). As GNMT and SARDH are the major enzymes involved in sarcosine metabolism, we further analyzed their amounts within the tumor tissue. Fig 3C and 3D show that sarcosine treatment resulted in significant ($p < 0.05$) increase in concentration of SARDH, which catalyzes sarcosine-to-glycine conversion. In case of GNMT we identified only negligible effects on its amount after sarcosine treatment in both tumor tissues.

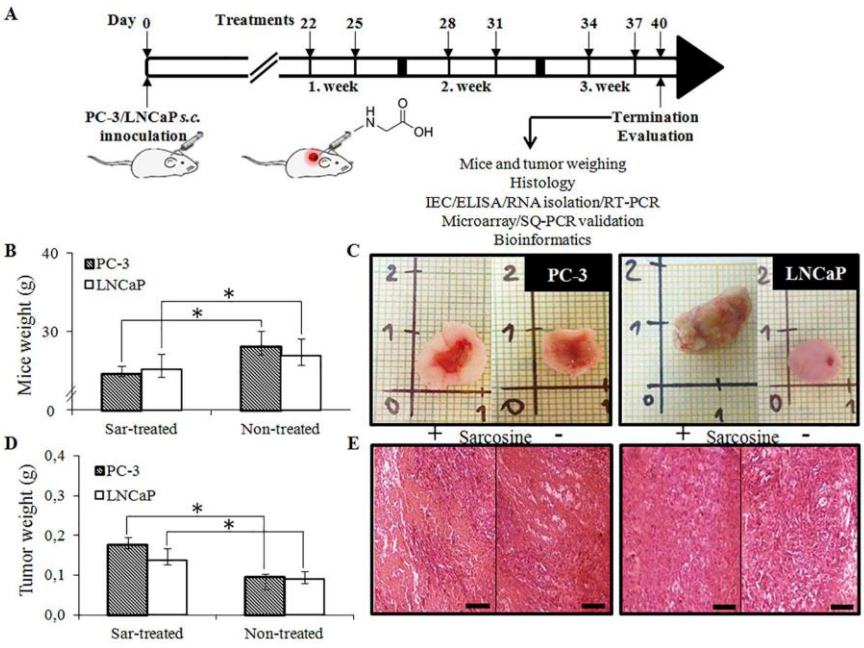

Fig 2. The murine PC-3 and LNCaP xenografts were treated with sarcosine *i.p.* (**A**) Schematic depiction of experimental workflow beginning with the PCa cells (5×10^6) *s.c.* inoculation. (**B**) Average weight of mice determined after the termination of experiment. (**C**) Selected photographs of excised ectopic prostate tumors treated with sarcosine (*left*) and non-treated after termination of the experiment (*right*). (**D**) Average tumor weight at the endpoint of the experiment. Values are expressed as the means ± standard deviations of three independent replicates ($n = 3$). Vertical bars indicate standard error. Asterisks indicate significant differences ($p < 0.05$) compared to the untreated group. (**E**) H&E-stained tissue sections of ectopic prostate tumors after treatment with sarcosine (*left*) and non-treated (*right*). The length of scale bar is 100 μm.

doi:10.1371/journal.pone.0165830.g002

Sarcosine effects on gene expression profiling in tumors

The tumors were further used for isolation of RNA, subsequent reverse transcription and electrochemical microarray profiling (representative microarray heatmaps for the treated and non-treated PC-3 and LNCaP tumors are shown in S1 Fig. Table 1 and Table 2 show the lists of genes ($n = 43$ for PC-3 and $n = 50$ for LNCaP), along with their accession numbers, which were found up-regulated in six independent analyses ($n = 6$). As a threshold for up-regulation, medians, whose fold ratio was ≥ 1.5 compared to non-treated xenografts were exploited. Microarray analyses revealed also seven genes in PC-3 and four genes in LNCaP tumors, which could be classified as down-regulated; however, in both types of cells, none of them reached threshold expression ≤ 1.5 (S1 Table). Thus, they were not considered for further analyses. The complete list of up-regulated genes served as input for further bioinformatical analyses.

SQ-RT-PCR validation of microarray data

Overall, our microarray analyses revealed 18 overlapping genes, which were up-regulated in both tested PCa cell lines as the response to sarcosine treatment (Fig 4A). To validate the microarray results, we performed SQ-RT-PCR analyses using the sarcosine treated and non-treated tumors and evaluated gene expression after normalization according to the expression

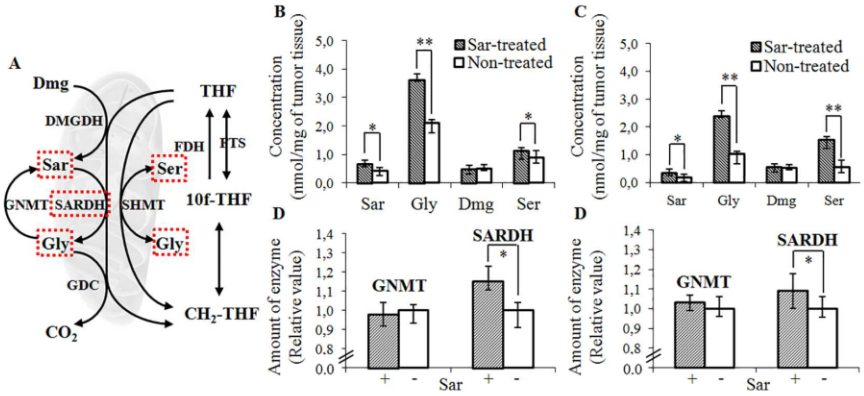

Fig 3. Effect of sarcosine treatment on the tumor tissue concentrations of sarcosine pathway-related amino acids. (**A**) Schematic depiction showing the sarcosine pathway ongoing in mitochondrion. Red rectangles highlight the amino acids, whose tissue levels were increased due to sarcosine treatment. Dmg-Dimethylglycine, Gly-Glycine, Ser-Serine, DMGHD-Dimethylglycine dehydrogenase, SARDH-Sarcosine dehydrogenase, GNMT-Glycine-*N*-methyltransferase, GDC-Glycine decarboxylase, SHMT-Serine hydroxymethyltransferase, THF-Tetrahydrofolate, 10f-THF-10-Formyltetrahydrofolate, CH_2-THF-Methylenetetrahydro-folate, FDH-Formyltetrahydrofolate dehydrogenase, FTS-Formyltetrahydrofolate synthase. Bar graphs showing the differences in tumor tissue Sar, Gly, Dmg and Ser levels in sarcosine treated and non-treated (**B**) PC-3 and (**C**) LNCaP mice. The levels of GNMT and SARDH were estimated in (**D**) PC-3 and (**E**) LNCaP mice by ELISA. Values are means ± standard deviations of three independent replicates ($n = 3$). Asterisks indicate significant differences (*, $p < 0.05$) or (**, $p < 0.01$) compared to the untreated group.

doi:10.1371/journal.pone.0165830.g003

of *β-actin*. Fig 4B shows the SQ-RT-PCR results for the most up-regulated genes, which were selected for validation (up-regulation fold ratio ≥ 2.5). Noteworthy, all of the results corroborated our microarray analyses and confirmed the considerable influence on genes expression caused by sarcosine administration.

Classification of biological roles of genes influenced by sarcosine treatment

To evaluate biological relevance of the differentially expressed genes in sarcosine treated and non-treated prostate tumors, we carried out an annotation analysis, which identifies the involvement of particular genes within biological processes. For both types of PCa cells xenografts, the up-regulated gene set was found to mostly include the genes belonging to "metabolic process", "cellular process", "biological regulation", "response to stimulus", "developmental process", "apoptotic process" and others (Table 3). Taken together this analysis provided a preliminary insight into the function of genes that are up-regulated as a response to sarcosine treatment.

Further, to prioritize the differentially expressed genes involved in the apoptosis and cell cycle, which are the major hallmarks of each type of cancer, we utilized STRING database of known and predicted interactions. Fig 5 illustrates the interactome network, where the red nodes highlight the genes from our up-regulated set, whose expression is stimulated by sarcosine treatment and which may be involved in a cell death of PC-3 cells (namely *FOXP1*, *LTF1*, *TCF7*, *DNAJB6*, *JUN*, *MAPK8*, *ERBB3*, *BTG2*, *AURKA*, *PA2G4*, *PML*, *PRDX5*, *PRAME* and *IVNS1ABP*) and LNCaP cells (namely *ITGA6*, *BRCA1*, *CBL*, *ERBB3*, *PA2G4*, *KLF4*, *MAPK7*, *ASNS*, *SOX4*, *TCF7*, *NR4A3*, *TGFB3*, *GAS6*, *TIMP1*, *BAX*, *BCL2A1*, *NFKBIA*, *HSP9OB1*, *DNAJB6*, *XBP1*, *BCL6* and *PRAME*). Noteworthy, *TCF7*, *DNAJB6*, *ERBB3* and *PRAME* were

Table 1. List of genes up-regulated in PC-3 xenografts in a response to sarcosine treatment (genes with the median fold ratio ≥ 1.5 are shown).

Accession No.	Gene name	Symbol	Fold ratio	*p*-value
NM_001071	Thymidylate synthetase	*TYMS*	4.2	0.0016
NM_001323304	Aurora kinase A	*AURKA*	3.7	0.0041
NM_006101	Kinetochore associated 2	*KNTC2*	3.5	0.0012
NM_053056	Cyclin D1	*CCND1*	3.4	0.0004
NM_006469	Influenza virus NS1A binding protein	*IVNS1ABP*	3.1	0.0023
NM_001278547	Mitogen-activated protein kinase 8	*MAPK8*	3.0	0.0067
NM_001302961	Kallikrein 4	*KLK4*	3.0	0.0066
NM_001315	Mitogen-activated protein kinase 14	*MAPK14*	2.6	0.0011
NM_000044	Androgen receptor	*AR*	2.6	0.0024
NM_001030047	Prostate-specific antigen	*KLK3*	2.5	0.0090
NM_001256339	Homeobox protein NK-3 homology A	*NKX3-1*	2.2	0.0016
NM_001281741	Ubiquitin-conjugating enzyme E2C	*UBE2C*	2.2	0.0000
NM_012094	Peroxiredoxin 5	*PRDX5*	2.2	0.0015
NM_001276464	Nuclear receptor subfamily 5, group A	*NR5A2*	2.0	0.0068
NM_001179425	Ribophorin II	*RPN2*	2.0	0.0097
NM_003681	Pyridoxal kinase	*PDXK*	1.9	0.0087
NM_001005915	V-erb-b2 viral oncogene	*ERBB3*	1.9	0.0020
NM_015286	Synemin	*SYNM*	1.9	0.0009
NM_002228	Jun proto-oncogene	*JUN*	1.9	0.0082
NM_001012505	Forkhead box P1	*FOXP1*	1.8	0.0036
NM_001137559	Anaphase promoting complex subunit 5	*ANAPC5*	1.8	0.0030
NM_001291715	Preferentially expressed antigen in melanoma	*PRAME*	1.8	0.0005
NM_006571	Cyclin-dependent kinase inhibitor 1B	*p27*	1.8	0.0012
NM_175620	Metallothionein M	*MTM*	1.7	0.0003
NM_001199149	Lactotransferrin	*LTF*	1.7	0.0012
NM_005494	DnaJ homology, subfamily B, member 6	*DNAJB6*	1.7	0.0082
NM_001077500	Kallikrein 10	*KLK10*	1.7	0.0085
NM_000918	Procollagen-proline, 2-oxoglutarate 4-dioxygenase	*P4HB*	1.7	0.0075
NM_001007226	Speckle-type POZ protein	*SPOP*	1.7	0.0003
NM_001098209	T-cell factor/lymphoid enhancer factor	*TCF/LEF*	1.7	0.0062
NM_000314	Phosphatase and tensin homolog	*PTEN*	1.7	0.0027
NM_002675	Promyelocytic leukemia	*PML*	1.7	0.0023
NM_001291309	Proprotein convertase subtilisin/kexin type 6	*PCSK6*	1.7	0.0033
NM_003183	ADAM metallopeptidase domain 17	*ADAM17*	1.7	0.0003
NM_006191	Proliferation-associated 2G4	*PA2G4*	1.7	0.0005
NM_005066	Splicing factor proline/glutamine-rich	*SFPQ*	1.6	0.0048
NM_001291428	Bcl2-associated X protein	*BAX*	1.6	0.0081
NM_002965	S100 calcium-binding protein A9	*S100A9*	1.6	0.0009
NM_001300960	Cyclin-dependent kinase 19	*CDK19*	1.6	0.0044
NM_006763	BTG family member 2	*BTG2*	1.5	0.0066
NM_006275	Serine/arginine-rich splicing factor 6	*SRSF6*	1.5	0.0023
NM_007203	Paralemmin 2	*PALM2*	1.5	0.0041
NM_001134851	Transcription factor 7	*TCF7*	1.5	0.0025

doi:10.1371/journal.pone.0165830.t001

up-regulated in both types of cells pointing out their importance for cell cycle and apoptosis of metastatic PCa cells.

Table 2. List of genes up-regulated in LNCaP xenografts in a response to sarcosine treatment (genes with the median fold ratio ≥ 1.5 are shown).

Accession No.	Gene name	Symbol	Fold ratio	*p*-value
NM_003981	Reticulocalbin 1	*RCN1*	10.0	0.0071
NM_002901	Nuclear receptor subfamily 4, group A, member 3	*NR4A3*	6.6	0.0005
NM_000044	Androgen receptor	*AR*	6.1	0.0001
NM_022002	Breast cancer 1, early onset	*BRCA1*	5.5	0.0069
NM_006191	Proliferation-associated 2G4	*PA2G4*	4.7	0.0042
NM_006571	Cyclin-dependent kinase inhibitor 1B	*p27*	4.1	0.0060
NM_003724	Programmed cell death 2	*PDCD2*	3.9	0.0003
NM_000295	SRY (sex determining region Y)-box 2	*SOX2*	3.7	0.0001
NM_001291715	Preferentially expressed antigen in melanoma	*PRAME*	3.7	0.0087
NM_005033	Procollagen-proline, 2-oxoglutarate 4-dioxygenase	*P4HB*	3.3	0.0036
NM_001302961	Kallikrein 4	*KLK4*	3.1	0.0001
NM_001005915	V-erb-b2 viral oncogene	*ERBB3*	3.1	0.0095
NM_012142	X-box binding protein 1	*XBP1*	2.5	0.0037
NM_005494	DnaJ homology, subfamily B, member 6	*DNAJB6*	2.4	0.0005
NM_004911	Proliferating cell nuclear antigen	*PCNA*	2.4	0.0025
NM_006516	Nuclear factor of kappa light gene inhibitor	*NFKBIA*	2.4	0.0004
NM_001256339	Homeobox protein NK-3 homology A	*NKX3-1*	2.4	0.0063
NM_001005909	B-cell lymphoma 6	*BCL6*	2.3	0.0011
NM_001071	Thymidylate synthetase	*TYMS*	2.3	0.0007
NM_002598	SRY (sex determining region Y)-box 4	*SOX4*	2.3	0.0040
NM_016221	Interleukin 6 (interferon, beta 2)	*IL6*	2.3	0.0000
NM_015927	Nuclear receptor subfamily 4, group A, member 3	*NR4A3*	2.3	0.0033
NM_000314	Phosphatase and tensin homolog	*PTEN*	2.3	0.0014
NM_173158	E2F transcription factor 4	*E2F4*	2.2	0.0040
NM_138320	Asparagine synthetase	*ASNS*	2.2	0.0010
NM_001098209	T-cell factor/lymphoid enhancer factor	*TCF/LEF*	2.1	0.0030
NM_006852	Ubiquitin-conjugating enzyme E2C	*UBE2C*	2.0	0.0036
NM_001137559	Anaphase promoting complex subunit 5	*ANAPC5*	2.0	0.0027
NM_182790	BCL2-associated X protein	*BAX*	2.0	0.0044
NM_000434	Primase, polypeptide 2A	*PRIM2A*	2.0	0.0009
NM_002916	Cathepsin C	*CTSC*	1.9	0.0090
NM_000158	Mitogen-activated protein kinase 7	*MAPK7*	1.9	0.0082
NM_012296	Transforming growth factor, beta 3	*TGFB3*	1.9	0.0010
NM_001030047	Prostate-specific antigen	*KLK3*	1.8	0.0022
NM_015286	Synemin	*SYNM*	1.8	0.0011
NM_015286	Kallikrein 10	*KLK10*	1.8	0.0024
NM_001122	Mitogen-activated protein kinase 10	*MAPK10*	1.8	0.0081
NM_006681	Growth arrest-specific 6	*GAS6*	1.8	0.0006
NM_001001567	ADAM metallopeptidase domain 17	*ADAM17*	1.8	0.0009
NM_007106	Cyclin D2	*CCND2*	1.7	0.0020
NM_004528	BCL2-related protein A1	*BCL2A1*	1.7	0.0071
NM_001470	Splicing factor proline/glutamine-rich	*SFPQ*	1.7	0.0087
NM_138609	Cas-Br-M ecotropic retroviral sequence	*CBL*	1.6	0.0097
NM_004290	Protein kinase, cAMP dependent	*PRKACB*	1.6	0.0067
NM_022805	TIMP metallopeptidase inhibitor 1	*TIMP1*	1.6	0.0015
NM_016237	Replication factor C	*RFC4*	1.6	0.0087
NM_020738	Protein kinase C, beta 1	*PRKCB1*	1.5	0.0068

(*Continued*)

Table 2. (*Continued*)

Accession No.	Gene name	Symbol	Fold ratio	*p*-value
NM_000593	Transcription factor 7 (T-cell specific, HMG-box)	*TCF7*	1.5	0.0011
NM_003290	Integrin, beta 5	*ITGB5*	1.5	0.0039
NM_014573	Proteasome (prosome, macropain) subunit	*PSMD2*	1.5	0.0098

doi:10.1371/journal.pone.0165830.t002

Sarcosine and induction of genes involved in PCa-specific metabolic pathway and cell cycle

Further, we analyzed the expression changes associated with the PCa biochemical pathway defined in the KEGG database [17]. It is worth noting that KEGG pathway maps are an abbreviated representation of known interactions, focusing on those considered being the best supported by the evidence and relevance. Fig 6 and Fig 7 show the PCa metabolic pathway-specific KEGG diagrams, where the up-regulated genes are highlighted in red. Noteworthy, these genes are involved in the most fundamental processes, such as the cell proliferation and survival [*TCF/LEF*, *KLK3* (or *PSA*)], cell cycle and its progression (*p27*), PI3K/Akt signaling pathway (*NKX3.1* and *PTEN*) and hormone signaling (*AR*). The diagrams underscore that in both

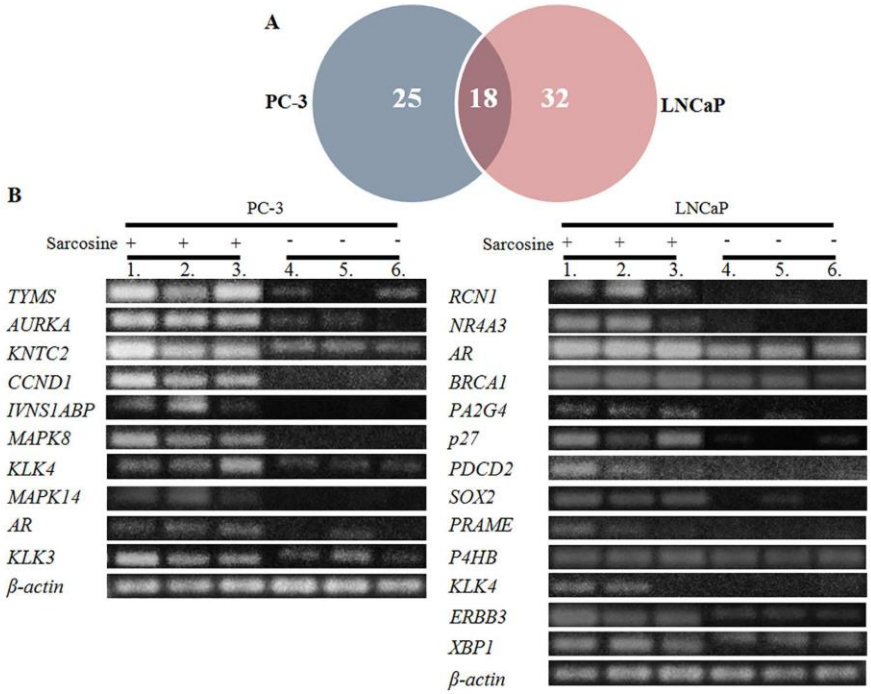

Fig 4. Comparison of gene expression in PC-3 and LNCaP xenografts. (**A**) Venn diagram showing the number of overlapping genes up-regulated after treatment of PC-3 and LNCaP cells with sarcosine. (**B**) SQ-RT-PCR validation of 10 selected genes up-regulated in murine PC-3 and LNCaP xenografts after sarcosine treatment (up-regulation $\geq$ 2.5). Expression of *β-actin* constituted as loading control. Lanes **1**–**3**—RNA isolated from sarcosine treated mice, lane **4**–**6**—RNA isolated from non-treated mice.

doi:10.1371/journal.pone.0165830.g004

Table 3. Percentage of genes up-regulated in ectopic prostate xenografts treated with sarcosine classified with respect to their biological functions.

	PC-3	LNCaP
Gene biological process	**% of total genes**	**% of total genes**
Metabolic process	55.8	52.0
Cellular process	44.2	51.5
Biological regulation	26.7	36.5
Response to stimulus	20.0	15.5
Developmental process	20.0	14.8
Apoptotic process	15.8	23.2
Multicellular organism process	10.8	26.1
Cellular component organization or biogenesis	5.8	10.1
Reproduction	5.8	3.1
Immune system process	5.0	4.2
Locomotion	2.5	1.1
Biological adhesion	2.5	2.0

doi:10.1371/journal.pone.0165830.t003

metastatic PCa cells, sarcosine affects nearly the same targets involved in fundamental metabolic processes. Fig 8 demonstrates a general cell cycle and the phases of mitosis. This detailed insight into the specific effects of sarcosine treatment revealed that in PC-3 tumors, sarcosine up-regulates genes, which are vital for a cell cycle, such as *RPN2* involved in all cell cycle phases, *UBE2C* involved in S phase and M phase (specifically prometaphase and anaphase), *KNTC2* and *ANAPC5* involved in S and M phases, *TYMS* and *CCND1* involved in G_1-G_1/S phases and *SYNM* involved in G_2-G_2/M phases. Fig 8 illustrates that similarly, in LNCaP tumors, sarcosine affects a cell cycle. Remarkably, up-regulation of *ANAPC5*, *SYNM* and *UBEC2C* and *TYMS* was identified within both tumor tissues exposed to sarcosine, irrespective of androgen dependence. Overall, the sarcosine-induced up-regulation of cell cycle controlling genes is likely one of the factor standing behind the sarcosine treatment-stimulated PCa cells proliferation and tumor growth.

Discussion

PCa remains a leading cause of illness and death among men in the US and Western Europe. The optimal course of treatment for a given individual is often uncertain. Recent metabolomic studies have identified various oncometabolites of PCa that could be likely associated with aggressive disease [2, 18, 19]. However, an understanding the biological actions of these molecules is anticipated to provide valuable information that can be helpful not only for enhancement of diagnostic and prognostic possibilities, but also for the development of novel biological treatment agents.

Numerous studies highlighted the significance of sarcosine as oncometabolite in PCa progression [2–4, 10]. Previously, we showed that sarcosine supplementation stimulates the cell proliferation and decreased the time required for cell division in malignant (22Rv1) and metastatic (PC-3) PCa cells [8]. In the present work we show that sarcosine exhibits considerable stimulatory effects on growth of PC-3 and LNCaP cells, even at very low concentrations, which are comparable to those found in urinary specimens of subjects suffering from aggressive PCa [3]. Similar efforts were put by Khan and coworkers using benign DU145 prostate cells as it was found that sarcosine did not affect their ability to progress through the cell cycle or impair cell proliferation [10]. Thus, these findings, which are in good agreement with ours, highlight the particular importance of sarcosine in malignant/metastatic prostate cells.

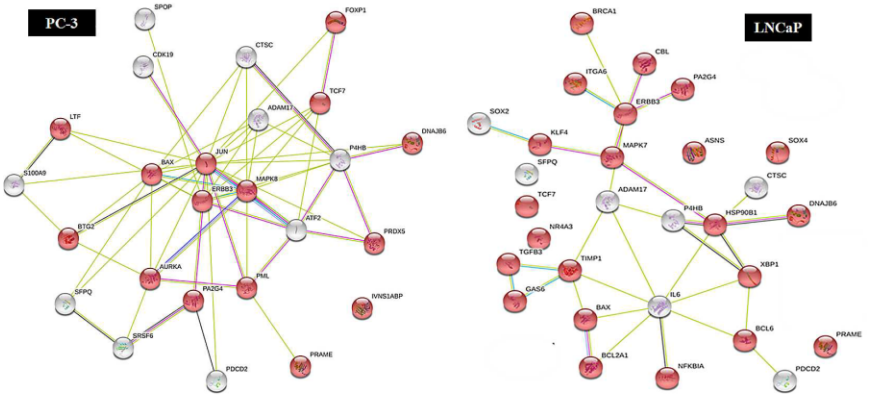

Fig 5. Interactome network showing the genes, which were up-regulated after sarcosine treatment and which are fundamental for apoptosis and cell cycle (PC-3 on the left, LNCaP on the right). The red nodes highlight the genes, which were up-regulated and are involved in negative regulation of a cell death. The interior of the circle represents the structure of proteins. The color of the line provides evidence of the different interactions among proteins. A red line indicates the presence of fusion evidence; a green line, neighborhood evidence; a blue line, concurrence evidence; a purple line, experimental evidence; a light blue line, database evidence; a black line, coexpression evidence. The genes were analyzed using STRING software (version 10.0).

doi:10.1371/journal.pone.0165830.g005

Despite that an utilization of *in vivo* preclinical model is critical for complex understanding of the actions triggered by sarcosine treatment, we established a system that mimics the tumor biology and its microenvironment by using xenografts. Sarcosine treatment of PC-3 and

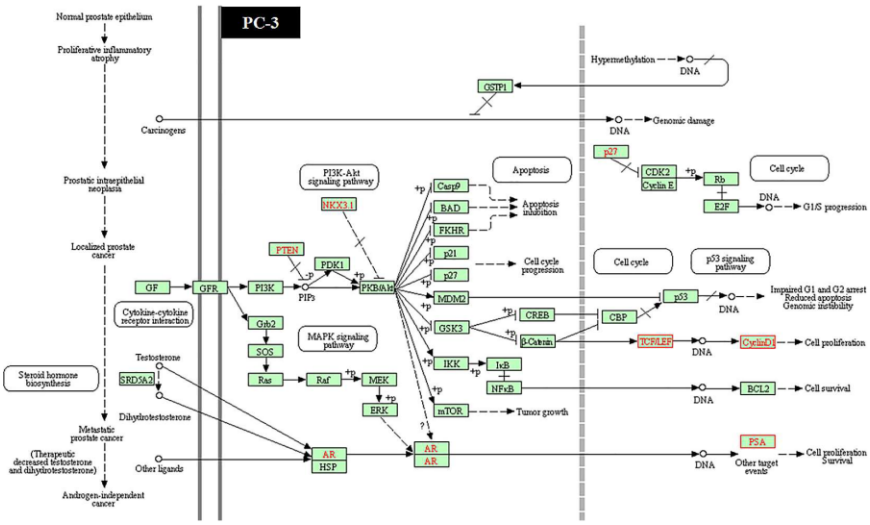

Fig 6. KEGG PCa-specific metabolism diagram for PC-3 cells. Gene expression shifts are projected as comparison of sarcosine treated and non-treated prostate tumors. The genes highlighted in red were found up-regulated after the sarcosine treatment in both PCa xenografts. The pathway map is species-specific (*Homo sapiens*).

doi:10.1371/journal.pone.0165830.g006

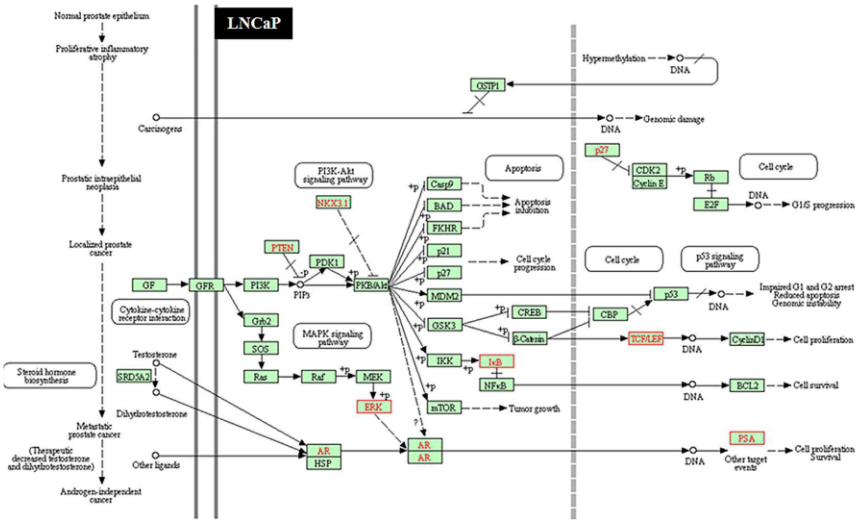

Fig 7. KEGG PCa-specific metabolism diagram for LNCaP cells. Gene expression shifts are projected as comparison of sarcosine treated and non-treated prostate tumors. The genes highlighted in red were found up-regulated after the sarcosine treatment in both PCa xenografts. The pathway map is species-specific (*Homo sapiens*).

doi:10.1371/journal.pone.0165830.g007

LNCaP xenografts resulted in a significant decrease ($p < 0.05$) in weight of treated mice, concomitantly with the increased size of their tumors. This indicates the stimulation of cancer progression with simultaneous deterioration of the conditions of treated animals. Previously, it has been demonstrated that stable overexpression of the SARDH enzyme or knock-down of the GNMT enzyme led to inhibition of the growth of PCa xenografts [10]. Nevertheless, the effect of direct sarcosine supplementation was not investigated. Hence, in this work, we provide further evidence of the stimulatory effects of sarcosine on a model of androgen dependent (LNCaP) and androgen independent (PC-3) metastatic PCa, which was firstly studied on a level of the impact on free amino acids and enzymes, which are involved in sarcosine biosynthesis and/or conversion schematized in Fig 3A.

Moreover, our results revealed sarcosine-induced increase of glycine and serine within the tumor mass formed by both types of PCa cells. In general, cancer cells undergo specific metabolic reprogramming to sustain cell growth and proliferation [20]. In addition to a large energy requirement, they tend to accumulate building blocks for the construction of new cellular components including nucleic acids, proteins, and lipids, as well as important cofactors for the maintenance of the cellular redox status [21]. The importance of serine and glycine as precursors in those processes is comprehensively summarized in the review by Amelio and coworkers [22]. Briefly, both serine and glycine contribute to cellular metabolism through the glycine cleavage system, which refuels one-carbon metabolism based on chemical reactions of folate compounds [23]. The importance of folate metabolism is underlined by the fact that antifolate chemotherapy is currently widely used in cancer treatment [24]. Similarly to serine and glycine, we also identified significantly higher amount of sarcosine, but not its precursor—dimethylglycine. Sarcosine likely accumulates within the tumor mass with the consequent increase in serine and glycine, which act as the tumor growth promoters. As it was evidenced, sarcosine increased amount also stimulates the SARDH expression. Although there is a lack of direct

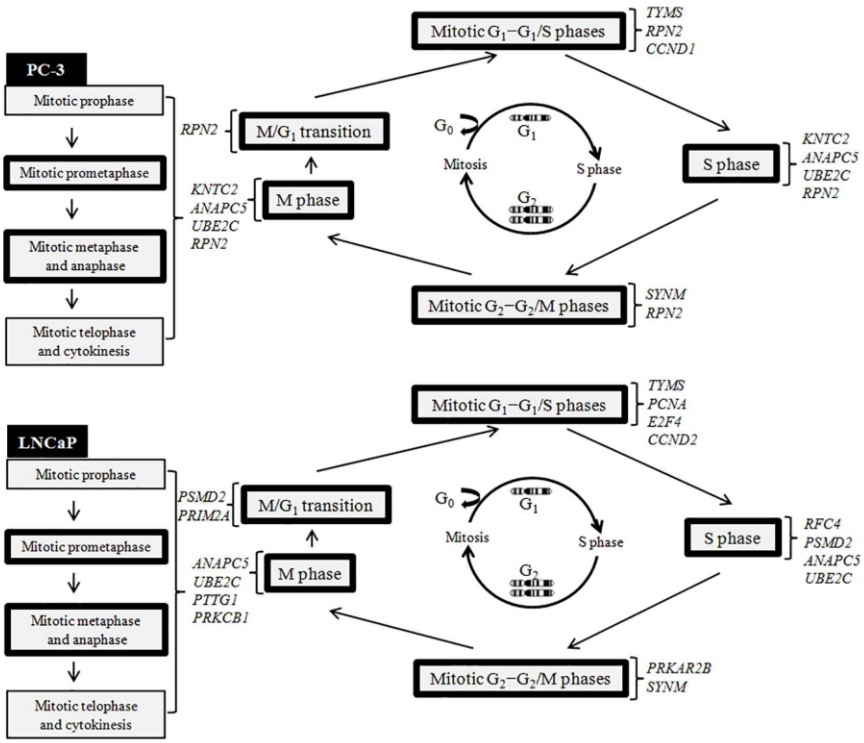

Fig 8. Schematic depiction of cell cycle and illustration of genes, which induce progression of cell cycle, performed using the Reactome software. Black frames indicate the genes, which were up-regulated after sarcosine treatment.

doi:10.1371/journal.pone.0165830.g008

evidence of linkage between SARDH and PCa aggressiveness, Yoon and coworkers demonstrated that the expression of SARDH is associated with shorter overall survival of subjects suffering from luminal A type breast cancer [25]. Although here we report obvious effects of sarcosine treatment on its pathway *in vivo*, further analysis of metabolic activities of sarcosine associated enzymes might be done to shed more light into this phenomenon.

As another level of regulation, we further investigated the differential gene expression sets related to sarcosine treatment. Particularly, we exploited electrochemical DNA microarrays, which are designated to analyze 2000 genes, involved in any aspect of cancer disease. Such approach provides a complex insight into the expression of genes that are involved in regulation of cell cycle and apoptosis, which are the major hallmarks of cancer [11]. Within the set of the identified differentially expressed genes, we found significant up-regulation of genes involved in a regulation of cell cycle and genes stimulating cell proliferation. Interestingly, in both types of PCa cells, we also identified sarcosine-related up-regulation of gene encoding androgen receptor (AR), which is a transcription factor mediating the transcription of both SARDH and GNMT [26].

TYMS enzyme (encoded by *TYMS*) plays a role in DNA synthesis and G_1-S transition. Its expression is higher in neoplastic than in normal prostate epithelium and was shown to be tightly linked to high GS, pathological tumor stage and early PSA recurrence ($p < 0.0001$) [27].

Noteworthy, TYMS protein is important target for 5-fluorouracil (5-FU) treatment, however this drug has only limited response rates in PCa [28]. Our findings encourage further studies to compare the expression of TYMS and amounts of urinary sarcosine, which can be exploited as non-invasive predictor of success of 5-FU chemotherapy.

Similarly, *AURKA* gene amplification has been documented in 67% of neuroendocrine PCa, which progress to highly aggressive variants [29]. *CCND1* overexpression accounts for cisplatin resistance through cell cycle control and inhibits cellular apoptosis pathway in the most of tumors [30]. Overexpression of *KLK4* was observed in patients with high T stage and GS [31] and *KLK3* encodes PSA, a widely used biomarker for PCa detection and disease monitoring [32]. *KNTC2* encodes the Hec1 protein, which plays an essential role in chromosome segregation by interacting through its coiled-coil domains with several proteins modulating the G_2/M transition [33]. Hec1 is a critical modulator of mitosis, highly expressed in most cancer cells, including PCa [34], however in this case the comparison of their expression with sarcosine amounts was not carried out, too.

In LNCaP tumors, we found that the most up-regulated gene was *RCN1*; encoding the homonymous protein RCN1, which has been identified as surface adhesion molecule that might participate in metastasis of PCa [35]. *NR4A3* is a member of the orphan nuclear receptor family referred to as NR4A. These receptors have been implicated in cell cycle regulation, apoptosis and carcinogenesis [36]. As it has been found that *NR4A3* controls both, survival and cell death of cancer cells, it is worth noting that sarcosine significantly stimulates its up-regulation, which can be one of the mechanisms of PCa proliferation.

In both types of PCa xenografts, we have revealed that sarcosine treatment stimulated the expression of AR, whose activity was intimately linked to PCa. Kim *et al*. show that AR and sarcosine metabolism-related enzymes have significant relationships with each other [37] and androgens can increase GNMT expression through AR binding the androgen response element existing on the first exon coding region of *GNMT*. Similarly, Sreekumar and coworkers indicated that AR appears to directly regulate sarcosine levels *via* transcriptional control of its regulatory enzymes [2]. Nevertheless, the principle of the *vice versa* mechanism (sarcosine stimulation of AR expression) needs to be clarified. Recently, it was demonstrated that exogenous addition of sarcosine to LNCaP cells *in vitro* caused negligible stimulation of AR expression only [38]. Discrepancy in our results is likely due to the experimental level (*in vitro vs. in vivo*), where the induced tumors can be influenced by hormones floating in the bloodstream of the host organism. Overall, we anticipate that the linkage between androgen signaling and sarcosine metabolism may be vital for a development and progression of PCa and further research on this phenomenon may provide valuable information into the biology of these malicious diseases.

On the other hand, in PC-3 tumors, we have identified sarcosine-related up-regulation of *MAPK8* and *MAPK14*, which act as integration points for multiple biochemical signals and affect cellular processes, including proliferation [39]. Both *MAPK8* (encoding JNK1) and MAPK14 (encoding p38) signaling pathways are activated by pro- or anti-inflammatory cytokines, but also in response to cellular stress (genotoxic, osmotic, hypoxic or oxidative) to cause growth inhibition and apoptosis [40]. Contrary to that, it was also demonstrated that both JNK1 and p38 can act as PCa promoters. This depends on the cell type and specific stimuli inducing the ability to regulate cell adhesion, invasion and migration [41]. Considering all found results, it is obvious that sarcosine treatment did not exert significant antitumor action through up-regulation of *MAPK8* and *MAPK14*. Similar phenomenon has been identified in case of *p27* as the cyclin-dependent kinase inhibitor regulating cell proliferation, motility and apoptosis. Interestingly, it can exert both a positive and a negative action on these processes in dependence on diverse post-translation modifications [42]. We did not find any expression in

non-treated LNCaP tumors; however sarcosine exposure resulted in a significant up-regulation of *p27*. Further studies on a protein level might be performed to investigate, whether the gene expression correlates with the protein amount and to elucidate, whether the protein translated in response to sarcosine presence, behaves as the good or the bad one. Overall, we show that sarcosine plays a pivotal role in influencing metastatic PCa cells, irrespective of androgen dependence status.

Conclusion

The present study demonstrates that sarcosine treatment stimulates the PCa cells, both *in vitro* and *in vivo*. Our results indicate that direct, repeated administration to sarcosine has significant stimulatory effects on the growth of ectopic prostate tumors. Further biochemical and molecular-biology analyses revealed considerable impact of treatment on sarcosine metabolic pathway and the expression of genes involved in cell proliferation, cell cycle and apoptosis, which are the major hallmarks of each cancer. To the best of our knowledge, this is the first study showing the direct effects of repeated sarcosine treatment on an organism bearing prostate tumor. Despite the complexity of obtained data, there are still questions arising, including the impact of enzymatic activities of sarcosine metabolism enzymes on PCa development. Moreover, our results might be verified by a detailed proteomic screening. Despite those facts, the present study confirmed sarcosine as important PCa oncometabolite in both androgen dependent and androgen independent metastatic PCa cells, and provided pivotal information, which could be further investigated and developed.

Supporting Information

S1 Fig. ElectraSense microarray heatmaps, where each spot represents expression of one gene (gray scale intensity describes the rate of individual mRNA expression).
(DOCX)

S1 Table. List of genes down-regulated in PC-3 and LNCaP xenografts in a response to sarcosine treatment.
(DOCX)

Acknowledgments

We express our thanks to Zuzana Lackova for perfect technical support.

Author Contributions

Conceptualization: VA ZH.

Data curation: ZH MAMR.

Funding acquisition: VA.

Investigation: MAMR PM HP.

Methodology: ZH.

Project administration: ZH MM.

Resources: VV MP DP.

Supervision: TE MS VA.

Validation: PM MAMR.

Visualization: ZH PM.

Writing – original draft: ZH.

Writing – review & editing: MS TE MM DP.

References

1. Cernei N, Heger Z, Gumulec J, Zitka O, Masarik M, Babula P, et al. Sarcosine as a Potential Prostate Cancer Biomarker-A Review. Int J Mol Sci. 2013; 14(7):13893–908. doi: 10.3390/ijms140713893 PMID: WOS:000322171700060.
2. Sreekumar A, Poisson LM, Rajendiran TM, Khan AP, Cao Q, Yu JD, et al. Metabolomic profiles delineate potential role for sarcosine in prostate cancer progression. Nature. 2009; 457(7231):910–4. doi: 10.1038/nature07762 PMID: WOS:000263266700051.
3. Heger Z, Cernei N, Gumulec J, Masarik M, Eckschlager T, Hrabec R, et al. Determination of common urine substances as an assay for improving prostate carcinoma diagnostics. Oncol Rep. 2014; 31 (4):1846–54. doi: 10.3892/or.2014.3054 PMID: WOS:000334345600046.
4. Kumar D, Gupta A, Mandhani A, Sankhwar SN. Metabolomics-Derived Prostate Cancer Biomarkers: Fact or Fiction? J Proteome Res. 2015; 14(3):1455–64. doi: 10.1021/pr5011108 PMID: WOS:000350840900011.
5. Heger Z, Cernei N, Krizkova S, Masarik M, Kopel P, Hodek P, et al. Paramagnetic Nanoparticles as a Platform for FRET-Based Sarcosine Picomolar Detection. Sci Rep. 2015; 5:1–7. 8868 doi: 10.1038/srep08868 PMID: WOS:000350549200018.
6. Ankerst DP, Liss M, Zapata D, Hoefler J, Thompson IM, Leach RJ. A case control study of sarcosine as an early prostate cancer detection biomarker. BMC Urol. 2015; 15:1–4. 99 doi: 10.1186/s12894-015-0095-5 PMID: WOS:000362161700001.
7. Jentzmik F, Stephan C, Miller K, Schrader M, Erbersdobler A, Kristiansen G, et al. Sarcosine in Urine after Digital Rectal Examination Fails as a Marker in Prostate Cancer Detection and Identification of Aggressive Tumours. Eur Urol. 2010; 58(1):12–8. doi: 10.1016/j.eururo.2010.01.035 PMID: WOS:000278414100003.
8. Heger Z, Gumulec J, Cernei N, Polanska H, Raudenska M, Masarik M, et al. Relation of exposure to amino acids involved in sarcosine metabolic pathway on behavior of non-tumor and malignant prostatic cell lines. Prostate. 2016; 76(7):679–90. doi: 10.1002/pros.23159 PMID: WOS:000373932700007.
9. Sudhakaran PR, Binu S, Soumya SJ. Effect of sarcosine on endothelial function relevant to angiogenesis. J Canc Res Ther. 2014; 10(3):603–10. doi: 10.4103/0973-1482.137945 PMID: WOS:000346890600028.
10. Khan AP, Rajendiran TM, Ateeq B, Asangani IA, Athanikar JN, Yocum AK, et al. The Role of Sarcosine Metabolism in Prostate Cancer Progression. Neoplasia. 2013; 15(5):491–501. doi: 10.1593/neo.13314 PMID: WOS:000324486500004.
11. Evan GI, Vousden KH. Proliferation, cell cycle and apoptosis in cancer. Nature. 2001; 411(6835):342–8. doi: 10.1038/35077213 PMID: WOS:000168710000056.
12. Geschwind DH. DNA microarrays: translation of the genome from laboratory to clinic. Lancet Neurol. 2003; 2(5):275–82. doi: 10.1016/s1474-4422(03)00379-x PMID: WOS:000182363400015.
13. Lipshutz RJ, Fodor SPA, Gingeras TR, Lockhart DJ. High density synthetic oligonucleotide arrays. Nature Genet. 1999; 21:20–4. doi: 10.1038/4447 PMID: WOS:000078008200007.
14. Heger Z, Cernei N, Kudr J, Gumulec J, Blazkova I, Zitka O, et al. A Novel Insight into the Cardiotoxicity of Antineoplastic Drug Doxorubicin. Int J Mol Sci. 2013; 14(11):21629–46. doi: 10.3390/ijms141121629 PMID: WOS:000328624400027.
15. Roth KM, Peyvan K, Schwarzkopf KR, Ghindilis A. Electrochemical detection of short DNA oligomer hybridization using the CombiMatrix ElectraSense Microarray reader. Electroanalysis. 2006; 18(19–20):1982–8. doi: 10.1002/elan.200603603 PMID: WOS:000241621300017.
16. Heger Z, Michalek P, Guran R, Havelkova B, Kominkova M, Cernei N, et al. Exposure to 17 beta-Oestradiol Induces Oxidative Stress in the Non-Oestrogen Receptor Invertebrate Species Eisenia fetida. PLoS One. 2015; 10(12). e0145426 doi: 10.1371/journal.pone.0145426 PMID: WOS:000367092500046.
17. Kanehisa M, Goto S, Furumichi M, Tanabe M, Hirakawa M. KEGG for representation and analysis of molecular networks involving diseases and drugs. Nucleic Acids Res. 2010; 38:D355–D60. doi: 10.1093/nar/gkp896 PMID: WOS:000276399100055.

18. Ding ZH, Wu CJ, Chu GC, Xiao YH, Ho D, Zhang JF, et al. SMAD4-dependent barrier constrains prostate cancer growth and metastatic progression. Nature. 2011; 470(7333):269–73. doi: 10.1038/nature09677 PMID: WOS:000287144200046.

19. Tomlins SA, Aubin SMJ, Siddiqui J, Lonigro RJ, Sefton-Miller L, Miick S, et al. Urine TMPRSS2:ERG Fusion Transcript Stratifies Prostate Cancer Risk in Men with Elevated Serum PSA. Sci Transl Med. 2011; 3(94). 94ra72 doi: 10.1126/scitranslmed.3001970 PMID: WOS:000293459700006.

20. Heiden MGV, Cantley LC, Thompson CB. Understanding the Warburg Effect: The Metabolic Requirements of Cell Proliferation. Science. 2009; 324(5930):1029–33. doi: 10.1126/science.1160809 PMID: WOS:000266246700031.

21. Locasale JW. Serine, glycine and one-carbon units: cancer metabolism in full circle. Nat Rev Cancer. 2013; 13(8):572–83. doi: 10.1038/nrc3557 PMID: WOS:000322158200011.

22. Amelio I, Cutruzzola F, Antonov A, Agostini M, Melino G. Serine and glycine metabolism in cancer. Trends BiochemSci. 2014; 39(4):191–8. doi: 10.1016/j.tibs.2014.02.004 PMID: WOS:000335426200007.

23. Brosnan ME, MacMillan L, Stevens JR, Brosnan JT. Division of labour: how does folate metabolism partition between one-carbon metabolism and amino acid oxidation? Biochem J. 2015; 472:135–46. doi: 10.1042/bj20150837 PMID: WOS:000369171700002.

24. Marchetti C, Palaia I, Giorgini M, De Medici C, Iadarola R, Vertechy L, et al. Targeted drug delivery via folate receptors in recurrent ovarian cancer: a review. OncoTargets Ther. 2014; 7:1223–36. doi: 10.2147/ott.s40947 PMID: WOS:000338714100001.

25. Yoon JK, Kim DH, Koo JS. Implications of differences in expression of sarcosine metabolism-related proteins according to the molecular subtype of breast cancer. J Transl Med. 2014; 12. 149 doi: 10.1186/1479-5876-12-149 PMID: WOS:000338471000001.

26. Green T, Chen XF, Ryan S, Asch AS, Ruiz-Echevarria MJ. TMEFF2 and SARDH cooperate to modulate one-carbon metabolism and invasion of prostate cancer cells. Prostate. 2013; 73(14):1561–75. doi: 10.1002/pros.22706 PMID: WOS:000323450800008.

27. Burdelski C, Strauss C, Tsourlakis MC, Kluth M, Hube-Magg C, Melling N, et al. Overexpression of thymidylate synthase (TYMS) is associated with aggressive tumor features and early PSA recurrence in prostate cancer. Oncotarget. 2015; 6(10):8377–87. PMID: WOS:000354885300075. doi: 10.18632/oncotarget.3107

28. Brody JR, Hucl T, Costantino CL, Eshleman JR, Gallmeier E, Zhu H, et al. Limits to Thymidylate Synthase and TP53 Genes as Predictive Determinants for Fluoropyrimidine Sensitivity and Further Evidence for RNA-Based Toxicity as a Major Influence. Cancer Res. 2009; 69(3):984–91. doi: 10.1158/0008-5472.can-08-3610 PMID: WOS:000263048700034.

29. Park K, Chen ZM, MacDonald TY, Siddiqui J, Ye HH, Erbersdobler A, et al. Prostate cancer with Paneth cell-like neuroendocrine differentiation has recognizable histomorphology and harbors AURKA gene amplification. Hum Pathol. 2014; 45(10):2136–43. doi: 10.1016/j.humpath.2014.06.008 PMID: WOS:000343528200020.

30. Zhou XJ, Zhang ZY, Yang X, Chen WT, Zhang P. Inhibition of cyclin D1 expression by cyclin D1 shRNAs in human oral squamous cell carcinoma cells is associated with increased cisplatin chemosensitivity. Int J Cancer. 2009; 124(2):483–9. doi: 10.1002/ijc.23964 PMID: WOS:000262010600032.

31. Mukai S, Yorita K, Yamasaki K, Nagai T, Kamibeppu T, Sugie S, et al. Expression of human kallikrein 1-related peptidase 4 (KLK4) and MET phosphorylation in prostate cancer tissue: immunohistochemical analysis. Hum Cell. 2015; 28(3):133–42. doi: 10.1007/s13577-015-0114-6 PMID: WOS:000358902800004.

32. Kote-Jarai Z, Al Olama AA, Leongamornlert D, Tymrakiewicz M, Saunders E, Guy M, et al. Identification of a novel prostate cancer susceptibility variant in the KLK3 gene transcript. Hum Genet. 2011; 129(6):687–94. doi: 10.1007/s00439-011-0981-1 PMID: WOS:000290540900010.

33. Wang HF, Gao X, Lu X, Wang Y, Ma CF, Shi ZK, et al. The mitotic regulator Hec1 is a critical modulator of prostate cancer through the long non-coding RNA BX647187 in vitro. Biosci Rep. 2015; 35. e00273 doi: 10.1042/bsr20150003 PMID: WOS:000368296800009.

34. Chen YM, Riley DJ, Zheng L, Chen PL, Lee WH. Phosphorylation of the mitotic regulator protein Hec1 by Nek2 kinase is essential for faithful chromosome segregation. J Biol Chem. 2002; 277(51):49408–16. doi: 10.1074/jbc.M207069200 PMID: WOS:000180028900040.

35. Cooper CR, Graves B, Pruitt F, Chaib H, Lynch JE, Cox AK, et al. Novel surface expression of reticulocalbin 1 on bone endothelial cells and human prostate cancer cells is regulated by TNF-alpha. J Cell Biochem. 2008; 104(6):2298–309. doi: 10.1002/jcb.21785 PMID: WOS:000258387200031.

36. Deutsch AJA, Angerer H, Fuchs TE, Neumeister P. The Nuclear Orphan Receptors NR4A as Therapeutic Target in Cancer Therapy. Anti-Cancer Agents Med Chem. 2012; 12(9):1001–14. PMID: WOS:000310055000001.

37. Kim MJ, Jung WH, Koo JS. Expression of sarcosine metabolism-related proteins in estrogen receptor negative breast cancer according to the androgen receptor and HER-2 status. Int J Clin Exp Pathol. 2015; 8(7):7967–77. PMID: WOS:000361538900032.

38. Dahl M, Bouchelouche P, Kramer-Marek G, Capala J, Nordling J, Bouchelouche K. Sarcosine induces increase in HER2/neu expression in androgen-dependent prostate cancer cells. Mol Biol Rep. 2011; 38(7):4237–43. doi: 10.1007/s11033-010-0442-2 PMID: WOS:000294362500001.

39. Tiwari N, Meyer-Schaller N, Arnold P, Antoniadis H, Pachkov M, van Nimwegen E, et al. Klf4 Is a Transcriptional Regulator of Genes Critical for EMT, Including Jnk1 (Mapk8). PLoS One. 2013; 8(2). e57329 doi: 10.1371/journal.pone.0057329 PMID: WOS:000316849500090.

40. Junttila MR, Li SP, Westermarck J. Phosphatase-mediated crosstalk between MAPK signalling pathways in the regulation of cell survival. Faseb J. 2008; 22(4):954–65. doi: 10.1096/fj.06-7859rev PMID: WOS:000254581000003.

41. Chien CS, Shen KH, Huang JS, Ko SC, Shih YW. Antimetastatic potential of fisetin involves inactivation of the PI3K/Akt and JNK signaling pathways with downregulation of MMP-2/9 expressions in prostate cancer PC-3 cells. Mol Cell Biochem. 2010; 333(1–2):169–80. doi: 10.1007/s11010-009-0217-z PMID: WOS:000272869200020.

42. Chu IM, Hengst L, Slingerland JM. The Cdk inhibitor p27 in human cancer: prognostic potential and relevance to anticancer therapy. Nat Rev Cancer. 2008; 8(4):253–67. doi: 10.1038/nrc2347 PMID: WOS:000254133500014.

www.nature.com/scientificreports

OPEN

Received: 11 April 2016
Accepted: 25 August 2016
Published: 20 September 2016

Prostate tumor attenuation in the nu/nu murine model due to anti-sarcosine antibodies in folate-targeted liposomes

Zbynek Heger[1,2], Hana Polanska[1,3], Miguel Angel Merlos Rodrigo[1,2], Roman Guran[1,2], Pavel Kulich[4], Pavel Kopel[1,2], Michal Masarik[1,3], Tomas Eckschlager[5], Marie Stiborova[6], Rene Kizek[1,2] & Vojtech Adam[1,2]

Herein, we describe the preparation of liposomes with folate-targeting properties for the encapsulation of anti-sarcosine antibodies (antisarAbs@LIP) and sarcosine (sar@LIP). The competitive inhibitory effects of exogenously added folic acid supported the role of folate targeting in liposome internalization. We examined the effects of repeated administration on mice PC-3 xenografts. Sar@LIP treatment significantly increased tumor volume and weight compared to controls treated with empty liposomes. Moreover, antisarAbs@LIP administration exhibited a mild antitumor effect. We also identified differences in gene expression patterns post-treatment. Furthermore, Sar@LIP treatment resulted in decreased amounts of tumor zinc ions and total metallothioneins. Examination of the spatial distribution across the tumor sections revealed a sarcosine-related decline of the MT1X isoform within the marginal regions but an elevation after antisarAbs@LIP administration. Our exploratory results demonstrate the importance of sarcosine as an oncometabolite in PCa. Moreover, we have shown that sarcosine can be a potential target for anticancer strategies in management of PCa.

Prostate cancer (PCa) was the most common cause of cancer in men in the USA in 2013, afflicting one in nine men over the age of 65[1]. Distinct sets of genes, proteins, and metabolites orchestrate cancer progression from a precursor lesion to localized disease and finally to metastatic cancer[2]. However, despite a broad knowledge of gene/protein expression profiles in PCa, complex metabolomic alterations are still not yet understood. PCa-specific metabolites can be effective targets that are exploitable in not only early diagnostics but also in the enhancement of therapeutic possibilities.

In 2009, Sreekumar and coworkers discovered that the urinary level of sarcosine (*N*-methylglycine), an intermediate by-product of glycine synthesis and degradation, increased within the localized PCa and metastatic PCa cohorts[3]. Although the linkage of sarcosine with PCa development[4–6] and its potential in the diagnosis of early-stage tumors have been reported[7], its use as a biomarker is still unclear[8]. Khan *et al.* demonstrated that addition of sarcosine induced invasion and intravasation in an *in vivo* PCa model[9]. Their comprehensive study of sarcosine-related enzymes shed light on sarcosine as a substantial PCa oncometabolite that can impact the oncogenic potential of prostate cells. Similarly, our *in vitro* pilot study revealed that sarcosine supplementation affects the redox status of PC-3 cells[10]. Hence, we used our anti-sarcosine antibodies (antisarAbs), whose immunoperformance was tested in ref. 11, as cargo for liposomal nanotransporters (antisarAbs@LIP) to promote the internalization of these antibodies into intracellular regions and the subsequent neutralization of sarcosine. To increase the liposomal shuttling efficiency, the outer surface was modified with folic acid (FA)[12]. This Trojan horse

[1]Central European Institute of Technology, Brno University of Technology, Purkynova 123, CZ-612 00 Brno, Czech Republic. [2]Department of Chemistry and Biochemistry, Mendel University in Brno, Zemedelska 1, CZ 613 00 Brno, Czech Republic. [3]Department of Pathological Physiology, Faculty of Medicine, Masaryk University, Kamenice 5, Brno CZ-625 00, Czech Republic. [4]Department of Chemistry and Toxicology, Veterinary Research Institute, Hudcova 296/70, CZ 621 00 Brno, Czech Republic. [5]Department of Pediatric Hematology and Oncology, 2nd Faculty of Medicine, Charles University, and University Hospital Motol, V Uvalu 84, CZ-150 06 Prague 5, Czech Republic. [6]Department of Biochemistry, Faculty of Science, Charles University, Albertov 2030, CZ-128 40 Prague 2, Czech Republic. Correspondence and requests for materials should be addressed to V.A. (email: vojtech.adam@mendelu.cz)

Carrier	Cargo	LE%	SD
FA- Liposomes	Sarcosine	78.9	6.21
	antisarAbs	56.2	5.16

Table 1. Loading efficiencies (LE%) of sarcosine and antisarAbs in folate-targeted liposomes. Values are expressed as the mean of three independent replicates ($n = 3$).

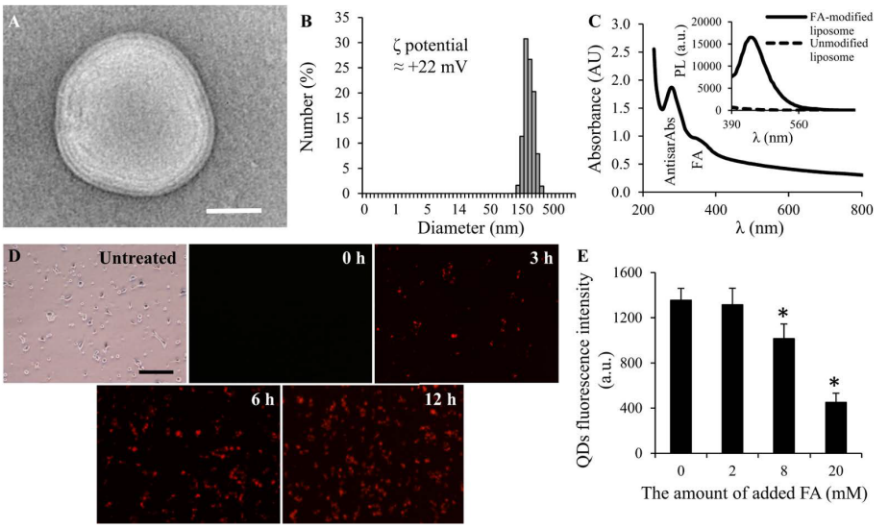

Figure 1. Characterization of FA-modified liposomal formulations of sarcosine and antisarAbs. (**A**) TEM micrograph (length of scale bar is 50 nm) and (**B**) dynamic light scattering analyzed in PBS, pH 7.4, with corresponding ζ potential inserted. (**C**) UV-Vis absorption spectrum of antisarAbs-bearing liposomes ($\lambda = 270$ nm corresponds to encapsulated antisarAbs, and $\lambda = 365$ nm corresponds to surface modification with FA) with the inserted photoluminescence spectra of liposomes before and after modification with FA ($\lambda_{exc} = 360$ nm). (**D**) Time dependence of the cellular uptake of QD-labeled antisarAbs@LIP into PC-3 cells obtained via inverted fluorescence microscopy (length of scale bar is 200 μm). Cells were incubated with 10 μM QD-labeled antisarAbs@LIP. (**E**) Competitive inhibitory effects in PC-3 cells. Values represent the mean ± SD of three experiments. Asterisks indicate significant differences ($p < 0.05$).

process performed through FA-folate receptor affinity promotes cellular uptake *via* clathrin-mediated endocytosis, which enables the passage of larger objects (including liposomes) across cellular membranes[13].

The main objective of our study was to determine whether the administration of antisarAbs and sarcosine liposomal formulations affected PC-3 xenografts in terms of tumor growth and gene expression patterns to obtain insight into the uncertain role of sarcosine in PCa development. To enhance the uptake into prostate tumor tissue, we utilized FA-targeted liposomes, which enabled us to investigate sarcosine-related cellular issues in highly specific way. A special emphasis was placed on the administration effects on a key regulatory factor in the intermediary metabolism of prostate cells (zinc) and a substantial transporter protein involved in zinc homeostasis (metallothioneins, MTs).

Results

Characterization and *in vitro* intracellular uptake of 1,2-dioleoyl-sn-glycero-3-phosphoethanolamine (DOPE) liposomes. Liposomal sarcosine and antisarAbs were produced using the lipidic thin-film hydration method[14] as well as control liposomes without cargo (hereinafter denoted as No cargo). Subsequent surface modification with FA was achieved through an esterification reaction using the zero-length linker 1,1′-carbonyldiimidazole (CDI). Table 1 demonstrates the relatively high yields of encapsulation for both types of cargos [loading efficiency (LE) 78.9% for sarcosine, LE 56.2% for antisarAbs].

Transmission electron microscopy (TEM) observations revealed spherical multilamellar vesicles (Fig. 1A) averaging 172 nm in diameter (Fig. 1B). FA-modified liposomes exhibited ζ potential ≈ +22 mV. Successful surface modification was confirmed using optical methods (Fig. 1C). The absorption spectra of antisarAbs@LIP revealed two absorption maxima, one due to the presence of encapsulated antibodies ($\lambda = 280$ nm) and one due to FA ($\lambda = 365$ nm). Liposome suspensions exhibited the characteristic fluorescence emission peaks of FA (insert in Fig. 1C), suggesting successful coating of FA molecules onto the liposome surfaces.

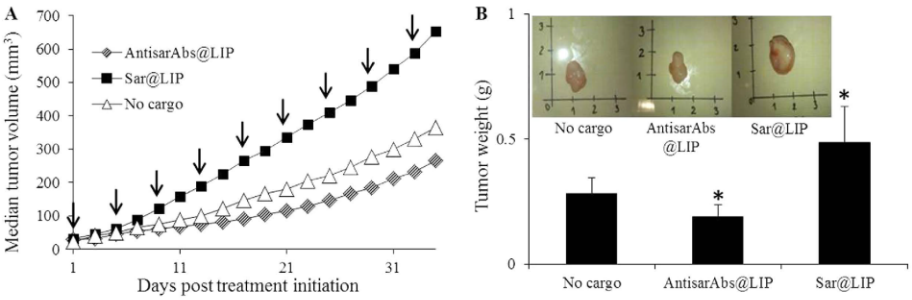

Figure 2. ***In vivo*** **antitumor efficacy of liposomal formulations in PC-3 tumor xenografts.** (**A**) Average tumor volume in nude mice bearing subcutaneous PC-3 tumors. Arrows indicate the time of therapeutic injections (*i.p.*). (**B**) Average tumor weight at the endpoint of the experiment. Inserted are chosen photographs of PC-3 tumors after termination. Values are expressed as the mean of five independent replicates ($n = 5$). Vertical bars indicate standard error. Asterisks indicate significant differences ($p < 0.05$) compared to the group treated with empty liposomes.

In vitro cellular uptake experiments were performed using human prostate cancer PC-3 cells, which overexpress folate receptors[15,16]. The uptake of quantum dots (QD)-labeled antisarAbs@LIP was evaluated over time (0–12 h) and is shown in Fig. 1D. After 6 h of incubation, the fluorescence considerably increased, and high uptake was also measured after 12 h of incubation, demonstrating that liposomes interacted with PC-3 cells. The uptake of substances into cells *via* folate receptors is reduced in the presence of excess amounts of FA due to competitive inhibitory effects. Hence, to ascertain that liposomes were indeed internalized through folate targeting, we assessed the cellular uptake of QD-labeled antisarAbs@LIP in the presence of FA, and the results from this assay are illustrated in Fig. 1E. The cellular uptake of QD-labeled antisarAbs@LIP was significantly reduced in PC-3 cells as the FA concentration increased. Thus, our results indicate the important role of folate receptors in the cellular uptake of our liposomal formulations in PC-3 cancer cells.

In vivo **effects of antisarAbs@LIP and sar@LIP on PC-3 xenografts.** Treatment of mice PC-3 xenografts with various formulations of liposomes began when the tumor volume reached approximately 30 mm^3 and was considered the first treatment day. The mice in all experimental groups were administered treatments nine times by intraperitoneal injection for 35 days. The tumor growth time profile obtained by measuring the tumor diameter in the test animals twice per week is presented in Fig. 2A. Treatment with sar@LIP remarkably enhanced tumor growth from approximately the 7th day of administration. In contrast, antisarAbs@LIP administration showed moderate antitumor activity. Tumor weight was calculated to evaluate the impact on tumors and is shown in Fig. 2B. Administration of antisarAbs@LIP led to the inhibition of tumor weight by 32.5%. Notably, the mean weight of the excised tumors was approximately 71.4% higher in mice treated with sar@LIP than in mice treated with empty liposomes (No cargo). No mice died or had to be euthanized before the endpoint of the experiment, and administration did not cause significant differences in mouse weight.

Gene expression patterns and apoptosis in excised tumors. To understand the gene expression patterns, we performed electrochemical microarray analyses of RNA isolated from tumor tissues. We compared the effects of both administration types with the expression patterns of PC-3 xenografts treated with empty liposomes (complete array heatmaps are depicted in Supplementary Figure 1, together with a control expression heatmap of benign prostate PNT1A cells). The Venn diagram in Fig. 3A illustrates that the administration of sar@LIP and antisarAbs@LIP resulted in significant differential expression patterns, with only 17 overlapping genes up-regulated as a result of treatment with either sar@LIP or antisarAbs@LIP. The other ($n = 121$ and $n = 118$, respectively) up-regulated genes were uniquely connected to individual treatments. The complete lists of up- and down-regulated genes and their relative expression levels are shown in Supplementary Tables 2 and 3. Furthermore, we highlighted 12 genes that were specific to any aspect of PCa (Fig. 3B). Most ($n = 10$) were significantly up-regulated by the presence of exogenously added liposomal sarcosine ($p < 0.05$). In contrast, antisarAbs@LIP administration led to the up-regulation of only two of these genes (*KLK3* [*kallikrein 3*] and pro-apoptotic *BAX* [*Bcl2-associated X protein*) and, moreover, caused significant down-regulation of *GAB2* (*growth factor receptor-bound protein 2* (*GRB2*)*-associated binding protein 2*). The annotation analysis from GoMiner indicated that some of those genes, including *CCND1* (*cyclin D1, alpha polypeptide*), *BAX*, *TEGT* (*transmembrane BAX inhibitor motif containing 6*), *E2F3* (*E2F transcription factor 3*) or *PDGFRB* (*platelet-derived growth factor receptor, beta polypeptide*), were related to the positive regulation of cell proliferation and apoptosis. Noteworthy, sar@LIP induced the up-regulation of *SLC43A1* (*solute carrier family 43, member 1*), whose major role is amino acid transport and the supply of nutrients into cancer cells. We further detected the apoptosis-related proteins in excised xenografts. Figure 3C demonstrates that antisarAbs@LIP treatment slightly increased the amount of cleaved caspase-3 when compared to sar@LIP administration, which is in agreement with the expression of pro-apoptotic *BAX*.

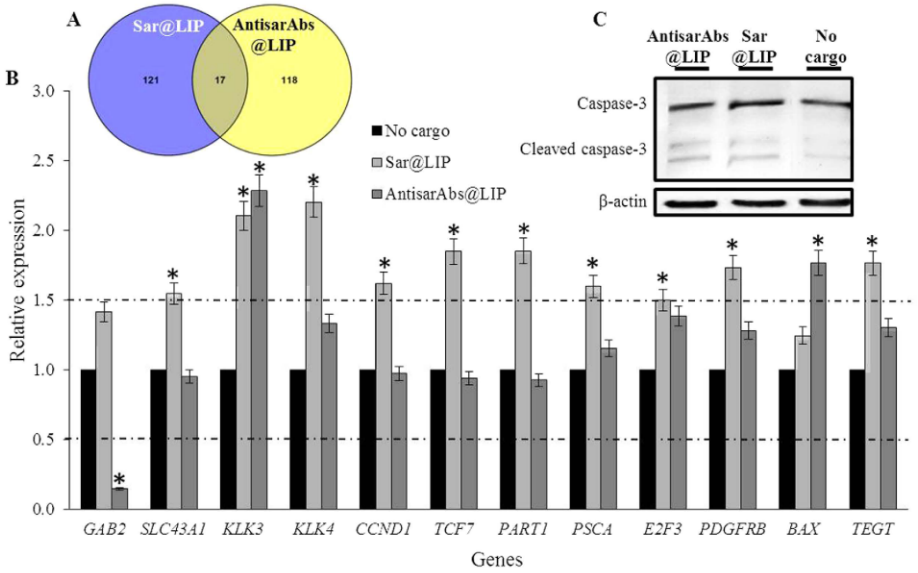

Figure 3. Effects of administration on the gene expression patterns. (**A**) Venn diagram showing the overlapping genes that were up-regulated after both types of administration. (**B**) Representation of the relative expression levels of genes specific to any aspect of PC, which were significantly up- or down-regulated in post-treatment tumor tissues. *GAB2 – Growth factor receptor-bound protein 2 (GRB2)-associated binding protein 2*; *SLC43A1 – Solute carrier family 43, member 1*; *KLK3 – Kallikrein 3 (prostate-specific antigen) PSA*; *KLK4 – Kallikrein 4 (prostase, enamel matrix, prostate)*; *CCND1 – Cyclin D1, alpha polypeptide*; *TCF7 – Transcription factor 7 (T-cell specific, HMG-box)*; *PART1 – Prostate androgen regulated transcript 1*; *PSCA – Prostate stem cell antigen*; *E2F3 – E2F transcription factor 3*; *PDGFRB – Platelet-derived growth factor receptor, beta polypeptide*; *BAX – Bcl2-associated X protein*, *TEGT – Transmembrane BAX inhibitor motif containing 6*. Values are expressed as the mean of three independent replicates ($n = 3$). Vertical bars indicate standard error. Asterisks indicate significant differences ($p < 0.05$) compared to the group treated with empty liposomes. (**C**) Western blot analysis for the xenografts expression of caspase-3 and cleaved caspase-3.

Zinc and MT content in tumor tissue. Zinc homeostasis maintains physiological conditions in PCa, and zinc levels are significantly diminished in cancerous tissue (Fig. 4A). Thus, we determined the zinc levels in excised tumors. Figure 4B illustrates that sar@LIP administration significantly decreased the amount of zinc in tumor tissue (mean of 14.3 μg/g compared to 23.2 μg/g in mice treated with empty liposomes). In contrast, treatment with antisarAbs@LIP did not alter zinc levels in tumor tissue. Zn regulation is partially performed through MT proteins. Thus, we focused on the expression profiles of mRNAs encoding three isoforms of MT (1B, 1X and M). Figure 4C indicates that only antisarAbs@LIP administration significantly up-regulated MT1X and MTM mRNA expression levels ($p < 0.05$). To further elucidate the disparities in MT levels in tumor tissue after the treatments, we performed electrochemical examination by differential pulse voltammetry utilizing Brdicka's solution as an electrolyte. Because the MTs exhibit exceptional thermal stability, tumor homogenates were denatured and filtered to remove undesired interfering particles. Figure 4D demonstrates that voltammetry partially supported the results obtained using microarray and that antisarAbs@LIP administration elevated the MT content to 35.3 μg/g compared to mice treated with empty liposomes (mean 30.3 μg/g). In contrast, sar@LIP treatment significantly decreased MT content in xenograft tumors (mean 13.6 μg/g). Overall, our results indicate a plausible linkage between sarcosine metabolism and metal homeostasis in PCa.

Examination of tumor cross-sections. We further visualized molecules using imaging mass spectrometry (IMS). Figure 5 shows the images that were first obtained by performing matrix-assisted laser/desorption ionization (MALDI)-IMS and a hematoxylin and eosin (H&E) staining of the tumor section. The tumor specimens stained by H&E were ascertained by microscopic examination, which revealed no observable histological changes in the control and post-treatment excised tumor xenografts (Fig. 5A–C). Figure 5Aa–Cd depicts typical images that were obtained from MALDI-IMS and were used to visualize the distribution of predominant peaks (*m/z* 4484 Da, *m/z* 7207 Da and *m/z* 14739 Da) determined in the mean mass spectra represented in Fig. 5Ae–Ce. Generally, our treatment protocol did not result in expression pattern changes. However, our treatment protocol did affect the intensities of chosen peaks. The highest differences were found in the case of *m/z* 7207 Da after sar@LIP administration, with a substantially reduced ion signal compared to empty liposomes and antisarAbs@LIP. The spatial distribution was relatively homogenous, except for the margins of tumors treated with sar@LIP, where the ion signal was nearly lost. AntisarAbs@LIP treatment resulted in elevated signal at the margins. Subsequent on-tissue digestion resulted in the successful identification of three predominant peaks as follows: *m/z* 4 484 Da corresponded

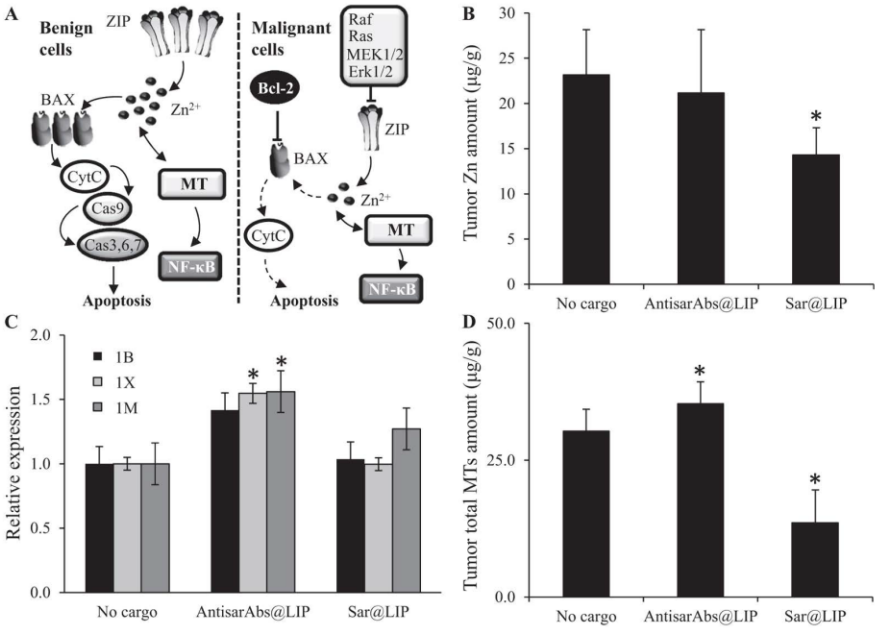

Figure 4. Effect on treatment on tumor zinc and metallothionein content. (**A**) Schematic depiction of zinc and metallothioneins and their importance in benign and malignant prostate cells. In malignant cells, ZIP transporters are inhibited through the Ras-Raf-Mek-Erk cascade, resulting in a decrease of Zn^{2+} ions in the cytosol. This phenomenon, together with Bcl-2 activity, inhibits the pro-apoptotic activity of cytochrome 1 *c* (CytC) in these cells. MT expression is closely linked to the Zn amount in the intracellular space. (**B**) Zinc levels in PC- 3 tumors after administration of liposomal sarcosine and antisarAbs. (**C**) Relative expression levels of mRNAs encoding different human metallothionein isoforms (1B, 1X and 1M) in tumor tissue after administration of liposomal sarcosine and antisarAbs, analyzed using electrochemical microarray. (**D**) Determination of total MTs using the Brdicka reaction after sample denaturation. Values are expressed as the mean of three independent replicates ($n = 3$). Vertical bars indicate standard error. Asterisks indicate significant differences ($p < 0.05$) compared to the group treated with empty liposomes.

to beta-defensin 1 (DEFB1, approx. MASCOT score 65.2), *m/z* 7 207 Da corresponded to MT isoform 1X (MT1X approx. score 55.0), and *m/z* 14 739 Da corresponded to cytochrome b5 (CYB5, approx. score 78.1).

Discussion

In this study, we demonstrated that FA-modified liposomes are suitable to target cancer cells, as folate receptors are overexpressed in a wide variety of tumors, including PCa[17]. We provide evidence that sarcosine plays a substantial role in PCa progression and can be a potential target for the development of novel treatment modalities.

PCa remains a leading cause of illness and death among men in the US and Western Europe. Autopsy series have revealed small prostatic carcinomas in up to 29% of men age 30 to 40 years and 64% of men age 60 to 70 years. Moreover, the risk of PCa is 1 in 6, and the risk of death due to metastatic PCa is 1 in 30[18]. Despite these astounding statistics, the mechanism of prostate tumorigenesis is still not well understood, although it appears to be multifactorial.

Thus, the rationale of encapsulating sarcosine and antisarAbs is primarily to further understand the role of sarcosine as a suspicious oncometabolite important in PCa development. We used a liposomal transporter due to the inability of antibodies to enter the intracellular space, which can occur through the well-described FA-folate receptor interaction[19–21], leading to folate receptor-mediated endocytosis. The encapsulation into the FA-modified liposomes produced stable delivery systems, which enabled highly specific investigation of sarcosine-induced cellular events. We anticipate that exploitation of advanced nanomaterials for research on cancer metabolism can benefit from their exceptional properties, including specificity, prolonged circulation and wide payload spectrum of studied substance. Indeed, our results confirmed interactions between PC-3 cells and our designated nanotransporter *in vitro*. These were first provided by electrostatics between the negatively charged proteoglycans contained on cellular surfaces and the positively charged liposome surface. Second, folate targeting facilitated the endocytosis of liposomes, as was proved by our competitive inhibitory assay (Fig. 1E). Considering the *in vivo* tumor microenvironment, the enhanced permeability and retention effects should be taken into account as important mediators of the increased liposome accumulation in the tumor mass[22].

As approximations of human disease, animal models of cancer are critical for the understanding of the pivotal mechanisms of cellular transformation and the development of novel antitumor therapies. Therefore, it is

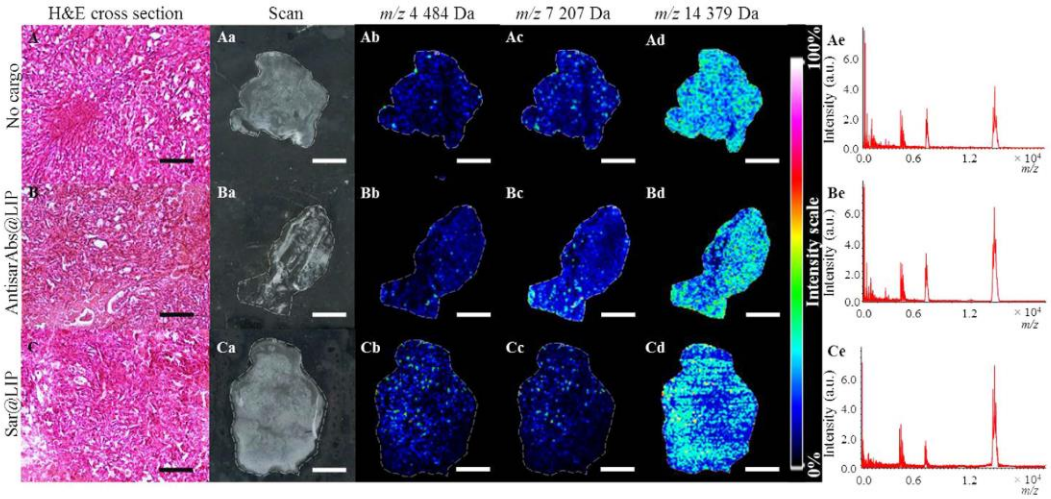

Figure 5. Administration results in disparities in a spatial distribution of proteins. H&E-stained cross sections of PC-3 xenografts (**A**) without treatment and after treatment with (**B**) liposomal antisarAbs and (**C**) liposomal sarcosine. Tumor sections (scale bar = 100 μm) were (a) scanned and utilized for MALDI-IMS profiling. Normalized pseudo-colored images of the spatial distribution of proteins with *m/z* values of: (b) 4484 ± 0.25% Da, (c) 7207 ± 0.25% Da and (d) 14379 ± 0.25% Da. (e) Mean mass spectrum of spectra obtained from MALDI IMS of PC-3 tumors. DHB was used as a matrix. The conditions used to acquire the MALDI spectra were as follows: 1,600 shots per raster spot, 65% laser energy and spatial resolution of 100 μm. All treated animals were euthanized 35 days after dosing. The scale bar length for the MALDI-IMS scans is 2 mm.

important to have systems that can mimic the tumor biology observed in patients, providing accurate information on the signaling networks and biochemical pathways in the tumor microenvironment[23]. The direct addition of sarcosine imparted an invasive phenotype to benign prostate cells, and the number of motile prostate cells was significantly higher upon sarcosine treatment[3]. Therefore, in this work, PC-3 cells were grown as xenografts in nude mice as a model for sar@LIP and antisarAbs@LIP administration. We found that sar@LIP exerted a dramatic tumor growth-supporting activity, leading to increases in tumor volume and weight. In contrast, antisarAbs@LIP exerted mild antitumor activity, as shown in Fig. 2A,B.

We acknowledge that these findings are in agreement with results published by Khan and coworkers, who reported the substantial role of sarcosine in invasion and intravasation in an *in vivo* PCa model[9]. We believe that these findings portray the importance of sarcosine in PCa progression. Furthermore, we expanded this knowledge to include the possible exploitation of anti-sarcosine antibodies, which caused mild antitumor effects. However, further examination must be performed to distinguish and overcome possible drawbacks, such as their low tissue penetration[24].

Sarcosine is produced from glycine by the enzymatic action of glycine-*N*-methyltransferase (GNMT), which is frequently elevated in localized and metastatic PCa relative to benign tissue[25]. However, how the elevated sarcosine levels affect the cellular microenvironment is uncertain. As a first level of organization, we examined the administration-related gene expression patterns of tumors using microarrays, which provided a snapshot of the cell functions and processes of thousands of genes and should yield insights concerning changes in gene expression associated with tumor cellular dysfunction and any concomitant regulatory pathways. Gene microarrays revealed the interesting differential expression profiles of a number of cancer-related genes in post-administration analyses. In particular, the *c-JUN* and *c-FOS* proto-oncogenes, *MMP2*, an independent predictor of decreased PCa survival rates, and *CCDN1*, a cell cycle progression regulator[26–28], were up-regulated only after sar@LIP treatment, illustrating that sarcosine can markedly affect the cellular microenvironment of PCa cells. Within the significantly regulated genes, we further selected those that are associated with any aspect of PCa (Fig. 3B). Noteworthy, *GAB2*, which encodes the GAB2 scaffolding protein, which serves as a platform for the assembly of signaling systems fundamental for PCa development[29], was significantly down-regulated by antisarAbs@LIP ($p < 0.05$). This prevents PCa cells from interactions with signaling molecules, which are vital for tumorigenesis[30]. On the contrary, sar@LIP treatment induced slight up-regulation of *GAB2*, which supports its tumor stimulatory role. These findings describe a plausible mechanism for the moderate antitumor activity of antisarAbs@LIP, together with the capability to up-regulate *BAX*, encoding Bcl-2-like protein 4, which accelerates programmed cell death through increase of the opening of the mitochondrial voltage-dependent anion channels, which leads to the loss in membrane potential and the release of cytochrome c (Fig. 4A)[31]. In contrast, sar@LIP induced the up-regulation of a broad spectrum of genes related to the positive induction of cell proliferation (*CCND1*, *E2F3*, *PDGFRB* and *TEGT*, a described *BAX* inhibitor), which corresponds to the tumor growth enhancement observed *in vivo* after sar@LIP administration. Interestingly, both types of treatments triggered up-regulation of *KLK3*,

which encodes prostate-specific antigen (PSA) - a serine protease produced by epithelial cells in prostate, which represents the gold standard biomarker of PCa[32]. We hypothesize that this phenomenon is due to utilization of FA for liposomes surface modification. Tisman and Garcia have demonstrated that FA supplementation is associated with a serum PSA acceleration, while its withdrawal from diet resulted in a significant PSA decline[33]. Despite that there is a lack of information describing a stimulation of PSA through FA exploited for folate targeting. Hence, further research is needed to rule out this phenomenon. Proliferative stimuli are highly dependent on metabolic responses. A critical aspect of the re-programming of cancer cell metabolism involves changes in the glycolytic pathway, referred to as the Warburg effect. Glutaminase is a key enzyme involved in the Warburg effect, and its role is to convert glutamine, an amino acid essential for tumor growth, to glutamate[34]. In sar@LIP, but not in antisarAbs@LIP-administered tumors, we found significantly up-regulated expression of *GLS*, which encodes glutaminase. Furthermore, PCa cells overexpress L-type amino acid transporters (LATs) to enhance their nutrient status and to stimulate cell growth[35]. Our results also illustrate that sar@LIP administration results in significant up-regulation of *SLC43A1*, which encodes LAT3 proteins. LAT3 can contribute to various signaling pathways, including mammalian target of rapamycin complex 1, implicated in tumorigenesis[36]. Our pioneering data highlight the important role of sarcosine in PCa cells. However, the mechanism of action by which sarcosine affects these genes needs to be further investigated.

In normal prostate tissue, Zn^{2+} ions enter cells *via* ZIP (Zrt- and Irt-like protein) transporters. Crossing the membranes, zinc induces BAX to form pores in the outer mitochondrial membrane, through which cytochrome c (CytC) is released into the cytosol. CytC then interacts with caspases to cause apoptosis (Fig. 4A). The growth effect of low intracellular zinc levels results from the elimination of the pro-apoptotic effects of zinc. Together with increased energy production, the growth effect promotes transformation into energy-efficient, proliferative, malignant cells. Our data suggest that sar@LIP administration is significantly associated with decreased amounts of zinc in tumor tissue ($p < 0.05$). We anticipate that the disruption of the tight homeostatic control of the cellular zinc level serves as an indicator of the stimulant effects of sarcosine on PCa cells. AntisarAbs@LIP treatment resulted in the partial regression of zinc homeostasis. Thus, sarcosine accumulation and zinc depletion appear to play important roles in PCa development.

MTs are intracellular proteins that bind transition metals, including zinc. Hasumi *et al.* demonstrated that similarly to zinc, decreased levels of MT are associated with PCa[37]. Furthermore, zinc treatment up-regulates MT expression. Notably, after antisarAbs@LIP administration, similar effects were achieved on both the mRNA (isoforms 1B; 1X and 1M) and protein levels (total MTs). In contrast, sar@LIP significantly decreased the amount of total MT protein but not the transcribed mRNA. These results correspond to our preliminary *in vitro* study with PC-3 cells administered sarcosine[10]. The amount of MT was reduced in sarcosine-supplemented cells in a time-dependent manner. Alterations in zinc-metallothionein metabolism are described as the early signs of PCa progression[38], and our data reveal that sarcosine decreases their amounts in tumor tissue. MT expression is tightly regulated by the intracellular zinc pool through metal-regulatory transcription factor 1. Thus, MT down-regulation is likely linked to decreased zinc, which reflects the proliferative and malignant transformation of the prostate cells. Such a phenomenon should also be reflected in a significant down-regulation of MT-encoding mRNA. Nevertheless, it is important to note that we examined only the three basic isoforms of MT1, and many other distinct isoforms have been identified[39]. Moreover, the correlation between transcription and translation is affected by a number of factors, including expression rates and protein stability[40]. Thus, single-cell analysis with RNA probes and antibodies should be performed to provide detailed insight.

Previously, it was shown that zinc biodistribution is not uniform, even in the same anatomical region of the prostate. Leitao and coworkers identified significant differences among transitional and peripheral zones[41]. However, to the best of our knowledge, the zinc-MT biodistribution in PCa is not known. Hence, we performed IMS visualization of proteins in the m/z range of 0–20 kDa, where MTs are expected. Instead of a number of low-intensity peaks, the three major peaks were detected, where MT isoform 1X was identified. Disparities in MT1X expression reflected the administration type, and the lowest overall intensities were achieved in sar@LIP-administered tumors, consistent with our previous electrochemical analyses. Furthermore, the administration-related changes were found mostly in the marginal regions of tumors. One plausible explanation is the enhanced angiogenesis of the margins, causing the accumulation of our designated nanotransporters. Hence, the liposomal formulations act mostly in these regions, significantly affecting prostate tumor progression. Although additional work is necessary to understand the mechanistic basis of sarcosine-induced MT down-regulation, it is apparent that pathological changes in sarcosine metabolism leading to its accumulation in cells can be an important player in prostate tumorigenesis.

In conclusion, our exploratory study revealed that sarcosine plays an important role in PCa progression. Sarcosine administration significantly affected genes linked with proliferation and apoptosis, and thus, significantly stimulated *in vivo* tumor xenograft growth. Treatment with sar@LIP decreased the amounts of tumor zinc and MT. However, the mechanistic basis of the sarcosine influence on MT regulation needs to be further investigated. In contrast, using a liposomal formulation of our developed antisarAbs, we achieved mild antitumor activity, together with positive regulation of selected pro-apoptotic genes and elevations of tumor zinc and MT. Overall, sarcosine is an important oncometabolite affecting PCa progression. We have shown that sarcosine molecules are suitable targets for the development of biological treatment modalities. Although our antibodies exhibited only moderate antitumor effects, further co-administration with various anticancer drugs should be tested to enhance the treatment efficiency. One option could be exploitation of specific inhibitors of enzymes involved in sarcosine biosynthesis, such as siRNA or aptamers. Song and coworkers have shown that siRNA knock-down of GNMT in PC-3 and LNCaP cells resulted in apparent decrease in proliferation with simultaneous increase of apoptotic cell counts[42], however the knock-down effect on sarcosine amount was not investigated. Hence a question, whether the antiproliferative effects were due to a decrease in concentrations of intracellular sarcosine remains unanswered and further research is required to shed light into this phenomenon.

Materials and Methods

Chemicals. All reagents for syntheses, standards, and other chemicals were purchased from Sigma-Aldrich (St. Louis, MO, USA) in ACS purity, unless otherwise noted.

Liposome synthesis and sarcosine and antisarAbs encapsulation. Liposomes were prepared following the lipidic thin-film hydration method. Briefly, 100 mg of cholesterol, 100 mg of 1,2-dioleoyl-sn-glycero-3-phosphoethanolamine (DOPE) and 100 mg of phosphatidylcholine were dissolved in chloroform (4.5 mL). A lipidic film was obtained by rotary evaporation of solvent. The residual chloroform was blown out with nitrogen until a thin film was formed. For encapsulation, 500 μL of sarcosine (200 μg/mL) and antisarAbs (500 μg/mL), produced in leghorn hens as described in our previous study[11], was utilized. After addition to the lipidic film (10 mg), the samples were sonicated in an ultrasonic bath (15 min). The sample was then heated on a Biosan Thermo Shaker TS-100C (Biosan, Riga, Latvia) for 15 min at 60 °C. After cooling, FA was poured, followed by the addition of 1,1′-carbonyldiimidazole (CDI) (the molar ratio of CDI to FA was 1:1). The samples were shaken on a thermoshaker for 2 h. Finally, the liposomes were filtered using Amicon® Ultra 0.5 mL centrifugal filters (Merck Millipore, Billerica, MA, USA) to remove unbound residual impurities.

Transmission electron microscopy (TEM). Liposomes were suspended within a drop of MilliQ purified H_2O. The resulting suspension was covered with a grid-coated formvar film (Sigma-Aldrich) and carbon (Agar Scientific, Essex, UK). After drying, 2% ammonium molybdate was placed onto the grid, and the excess was dried. Liposomes were examined using a Philips 208 S Morgagni transmission electron microscope (FEI, Brno, Czech Republic) at 18,000× magnification and an accelerating voltage of 80 kV.

Determination of the mean hydrodynamic diameter of the liposomal transporter. The liposome hydrodynamic diameters were examined using a Particle Size Analyzer (Zetasizer Nano ZS90, Malvern Instruments, Malvern, UK). Particles were dispersed in phosphate-buffered saline (PBS, 137 mM NaCl, 2.7 mM KCl, 1.4 mM NaH_2PO_4, and 4.3 mM Na_2HPO_4, pH 7.4) and were incubated at 25 °C for 15 min before the measurement.

Optical characterization of liposomes. Absorbance and photoluminescence were examined using a Tecan Infinite 200 PRO multifunctional microplate reader (Tecan, Männedorf, Switzerland) in Costar® UV-transparent 96-well microplates with flat bottoms (Corning Inc., Corning, NY, USA). To determine the surface modification, $\lambda_{exc} = 360$ nm of FA was used.

Determination of loading efficiency in the liposomes. Loading efficiency (LE%) was determined by measuring the concentration of unencapsulated free sarcosine and antisarAbs in aqueous medium. For this purpose, 400 μL of liposomes was centrifuged (10,000 rpm, 15 min, 4 °C) in Amicon® Ultra 0.5 mL centrifugal filters (Merck Millipore), and the concentration of free sarcosine was quantified using ion-exchange chromatography according to Heger *et al.*[6]. The concentration of free antisarAbs was examined using the Bradford assay[43]. LE% was estimated with the following formula: $(Cargo_{total} - Cargo_{supernatant})/Cargo_{total} \times 100$.

Cells. The PC-3 human cell line, established from a grade 4 androgen-independent prostatic adenocarcinoma, was purchased from the Health Protection Agency Culture Collection (Salisbury, UK). The cells were grown in Ham's 12 medium with 7% fetal bovine serum (FBS) supplemented with penicillin (100 U/mL) and streptomycin (0.1 mg/mL). The PNT1A human cell line established by the immortalization of normal adult prostatic epithelial cells by transfection with a plasmid containing the SV40 genome with a defective replication origin was employed as a control model for microarray analyses (S1). The cells were cultured in RPMI-1640 medium with 10% FBS. The cells were maintained at 37 °C in a humidified incubator (Sanyo, Moriguchi, Japan) with 5% CO_2.

Determination of intracellular uptake of antisarAbs@LIP. To determine the intracellular uptake, antisarAbs were fluorescently labeled with CdTe quantum dots (QDs) through a synthetic heptapeptide HWR linker prior to encapsulation, as described in our previously published studies[11,44]. PC-3 cells were seeded onto a plate at a density of 2.0×10^5 cells/well and were incubated for 24 h. Microscopy studies were performed using an Olympus IX 71S8F-3 inverted fluorescence microscope (Olympus, Tokyo, Japan) equipped with an HBO 50 W mercury arc lamp (Osram GmbH, Munich, Germany). The 545 and 580 nm excitation filters and the 610 nm emission filter were utilized. Images were acquired with an Olympus DP73 camera and processed using Stream Basic 1.7 software (Olympus) at a resolution of 1,600 × 1,200 pixels. To evaluate the competitive inhibitory effects of FA, various FA concentrations (final FA concentrations 2; 8 and 20 mM) were utilized for pre-treatment, followed by subsequent treatment with 10 μM QD-labeled antisarAbs@LIP and incubation for 4 h. The cells were then washed with medium, trypsinized and harvested. The median QD fluorescence values were analyzed using a Tecan Infinite 200 PRO multifunctional microplate reader (Tecan, Maennedorf, Switzerland) using $\lambda_{ex} = 500$ nm and $\lambda_{em} = 610$ nm.

Prostate tumor xenograft models. Five-week-old male nude athymic BALB/c nu/nu mice were used for xenograft studies. PC-3 cells (5×10^6) were resuspended in 100 μL of PBS with 20% Matrigel (BD Biosciences, Franklin Lakes, NJ, USA) and were then implanted subcutaneously into the left flank regions of the mice under general anesthesia (1% Narkamon + 2% Rometar, 0.5 mL/100 g of weight). Growth in tumor volume was recorded using digital calipers, and tumor volumes were calculated using the formula: $(\pi/6) \times (L \times W^2)$, where L is the length of tumor and W is the width. The use of the animals followed the European Community Guidelines as

accepted principles for the use of experimental animals. The experiments were performed with the approval of the Ethics Commission at the Faculty of Medicine, Masaryk University, Brno, Czech Republic.

RNA isolation and reverse transcription. Tumors were crushed using a mortar and pestle under liquid nitrogen and were then mixed with 350 μL of Tissue Lysis Buffer (Roche, Basel, Switzerland) in an Eppendorf tube. After 30 min incubation at 25 °C, samples were centrifuged (13,000 × g at 20 °C for 2 min) using an Eppendorf 5402 microcentrifuge (Eppendorf, Hamburg, Germany). Next, 350 μL of the lysate supernatant was pipetted into the sample tube, a component of the MagNA Pure Compact RNA Isolation Kit (Roche, Basel, Switzerland). The isolation steps were performed according to the manufacturer's instructions. The concentration of the RNA was quantified using an Infinite M200 PRO (Tecan). The RNA was converted to cDNA using a PrimeScript One Step RT-PCR Kit (TaKaRa, Mountain View, CA, USA) with the following reaction profile: 25 °C for 10 min, 37 °C for 120 min and 85 °C for 5 min. The cDNA integrity was tested by PCR of *β-actin* with the following primers: forward 5′-CCTGAACCCTAAGGCCAACC-3′ and reverse 5′-GCAATGCCTGGGTACATGGT-3′. The resulting DNA fragment (600 bp) was visualized using agarose gel electrophoresis with ethidium bromide staining as previously described by Nejdl *et al.*[45].

Electrochemical microarray analyses. Obtained cDNA was biotinylated on its 3′ end using the Biotin 3′ End DNA Labeling Kit (Thermo Scientific, Waltham, MA, USA) following the manufacturer's instructions. The microarray was performed as previously described by Roth *et al.*[46]. For hybridization, Human Cancer 3711 ElectraSense 4 × 2k array slides with 1,609 DNA probes (Custom Array, Bothell, WA, USA) were first pre-hybridized for 30 min at 50 °C using 6× SSPE (0.9 M NaCl, 60 mM sodium phosphate, 6 mM EDTA), 5× Denhardt's solution and sonicated salmon sperm DNA (100 μg/mL). Then, hybridization of biotin-labeled cDNA was performed at 50 °C for 18 h in 6× SSPE and salmon sperm DNA (100 μg/mL). Array chips were rinsed with low ionic strength 3× SSPET (3× SSPE, 0.05% Tween-20) and PBST (2× phosphate-buffered saline, pH 7.4, 0.1% Tween-20) to remove weakly bound DNA. Subsequently, array chips were blocked with biotin blocking solution for 15 min. Chips were then incubated for 30 min with poly-horseradish peroxidase-streptavidin (1:1,000 in PBS containing 1% BSA and 0.05% Tween-20). Next, chips were rinsed three times with biotin wash solution and 3,3′, 5,5′-tetramethylbenzidine (TMB) rinse solution, followed by incubation with TMB substrate. Measurements were performed using the ElectraSense detection kit (Custom Array). All post-hybridization processing steps were performed at 25 °C. The expression levels of selected genes were validated through qRT-PCR using SYBR® Green I Nucleic Acid Gel Stain (Invitrogen, Waltham, MA, USA) and the primers shown in Supplementary Table 1.

Western blot analysis. Tumor tissue for detection of caspase-3, cleaved caspase-3 and β-actin was processed and analyzed according to previously published protocol[47]. In brief, after the lysis, 50 μg of proteins were separated by 12% (*w/v*) sodium dodecyl sulfate-polyacrylamide gel electrophoresis. After transfer onto polyvinylidene fluoride (PVDF) membranes and blocking with 5% (*w/v*) skim milk, the primary antibodies (Cell Signaling Technology, Danvers, MA, USA) were added overnight on the shaker at 4 °C. Then PVDF membranes were incubated with horseradish peroxidase-conjugated secondary antibodies for 1 h at 25 °C. The detection was carried out using 3-aminoethyl-9-carbazole in 0.5 M acetate buffer as substrate.

Histological procedures. The samples were fixed in formaldehyde (10%) overnight, subsequently dehydrated in serial ethanol concentrations and embedded in paraffin wax. Sections were cut at 5 μm, mounted on glass slides, deparaffinized and stained with hematoxylin-eosin. The microscopic observations were conducted using an Olympus IX 71S8F-3 (Olympus, Tokyo, Japan).

Matrix-assisted laser desorption/ionization time-of-flight (MALDI-TOF) imaging mass spectrometry (IMS) and peptide mass fingerprinting (PMF). Sections of excised tumors (thickness 10 μm) were mounted onto ITO glass slides (Bruker Daltonik, GmbH). Deparaffinization and antigen retrieval were performed according to Casadonte and Caprioli[48]. The glass slides were scanned with an Epson Perfection V500 (Epson Europe, Amsterdam, Netherland) with a resolution of 2,400 DPI. Subsequently, 2,5-dihydroxybenzoic acid (DHB) (30 mg/mL in 50% methanol and 0.2% trifluoroacetic acid) was sprayed using an ImagePrep vibrational sprayer system (Bruker Daltonik, GmbH). The experiments were performed on a MALDI-TOF/TOF Bruker ultrafleXtreme (Bruker Daltonik, GmbH). The scanning raster was set to 100 μm. Analyses were performed in reflectron positive mode with a laser power of 65%. The mass spectra were typically acquired in the *m/z* range 0.5–20 kDa by averaging 1,600 sub spectra from a total of 1,600 laser shots per raster spot. After analyses, the mass spectra were automatically loaded into flexAnalysis and processed (baseline subtraction). Pseudo-colored images of spatial distribution were generated using GIMP 2.8 (http://www.gimp.org/). Identification of proteins was performed using PMF with *in situ* trypsin digestion. First, trypsin (0.05 μg/μL in water) was deposited to cover the entire tissue surface. Subsequently, DHB (30 mg/mL in 50% methanol and 0.2% trifluoroacetic acid) was deposited using a vibrational sprayer system (Bruker Daltonik, GmbH). Identification of trypsinized proteins was achieved with conventional algorithms using the MASCOT server (Matrix Science, Boston, MA, USA). The following parameters were used for database searches: trypsin was used as the enzyme, zero or one missed cleavage was allowed, taxonomy was set to *Homo sapiens*, oxidation of methionine or/and *N*-term acetylation were added as variable modifications, peptide tolerance was set to ±0.5 Da, and mass values were set as MH^+.

Preparation of tumor tissue to determine zinc content. Ten milligrams of tumor was digested in nitric acid (65% *v/v*) and hydrogen peroxide (30 *v/v*) at a ratio of 7:3 in a Microwave System 3000 (Anton Paar GmbH, Graz, Austria) using a MG-65 rotor. Microwave power was set to 100 W (30 min) at 140 °C.

Atomic absorption spectrometry of zinc. Measurements were performed on a 280Z atomic absorption spectrometer (Agilent, Technologies, Santa Clara, CA, USA) with electrothermal atomization and Zeeman background correction. Zinc was measured on the primary wavelength Zn 213.9 nm (spectral bandwidth 0.5 nm, lamp current 10 mA) in the presence of a Pd chemical modifier.

Preparation of tumor tissue to determine total protein and MT amounts. Tumors were frozen with liquid nitrogen and homogenized using a SONOPLUS mini20 ultrasonic homogenizer (Bandelin Electronic, Berlin, Germany). Subsequently, 1 mL of 0.2 M phosphate buffer (pH, 7.0) was added, and the sample was homogenized for 5 min. The homogenates were further centrifuged using a Microcentrifuge 5417R (Eppendorf, Hamburg, Germany) at 15,000 $\times g$, 4 °C for 15 min. Finally, the supernatant was filtered through a membrane filter (0.45 μm nylon filter disk; Millipore, Billerica, MA, USA) and analyzed.

Determination of total protein content. The total protein concentrations were utilized for results normalization and were quantified using a SKALAB CBT 600T kit (Skalab, Svitavy, Czech Republic) according to manufacturer instructions with a BS-400 automated spectrophotometer (Mindray, Schenzhen, China).

Determination of amount of total MTs. MT was quantified using differential pulse voltammetry (747 VA Stand, connected to a 693 VA processor and 695 Autosampler, Metrohm, Herissau, Switzerland) with the conditions used in our previous study[49].

Descriptive statistics. Results are expressed as the mean ± standard deviation unless noted otherwise. Differences between groups were analyzed using the paired *t*-test and analysis of variance (ANOVA). Unless noted otherwise, the threshold for significance was $p < 0.05$. Statistica 12 software (StatSoft, Tulsa, OK, USA) was employed for analyses.

References

1. Siegel, R. L., Miller, K. D. & Jemal, A. Cancer Statistics, 2015. *CA-Cancer J. Clin.* **65,** 5–29 (2015).
2. Abate-Shen, C. & Shen, M. M. Molecular genetics of prostate cancer. *Genes Dev.* **14,** 2410–2434 (2000).
3. Sreekumar, A. *et al.* Metabolomic profiles delineate potential role for sarcosine in prostate cancer progression. *Nature* **457,** 910–914 (2009).
4. Cao, D. L. *et al.* Efforts to resolve the contradictions in early diagnosis of prostate cancer: a comparison of different algorithms of sarcosine in urine. *Prostate Cancer Prostatic Dis.* **14,** 166–172 (2011).
5. Cao, D. L. *et al.* A Multiplex Model of Combining Gene-Based, Protein-Based, and Metabolite-Based With Positive and Negative Markers in Urine for the Early Diagnosis of Prostate Cancer. *Prostate* **71,** 700–710 (2011).
6. Heger, Z. *et al.* Determination of common urine substances as an assay for improving prostate carcinoma diagnostics. *Oncol. Rep.* **31,** 1846–1854 (2014).
7. Lucarelli, G. *et al.* Serum sarcosine increases the accuracy of prostate cancer detection in patients with total serum PSA less than 4.0?ng/ml. *Prostate* **72,** 1611–1621 (2012).
8. Jentzmik, F. *et al.* Sarcosine in Urine after Digital Rectal Examination Fails as a Marker in Prostate Cancer Detection and Identification of Aggressive Tumours. *Eur. Urol.* **58,** 12–18 (2010).
9. Khan, A. P. *et al.* The Role of Sarcosine Metabolism in Prostate Cancer Progression. *Neoplasia* **15,** 491–501 (2013).
10. Cernei, N. *et al.* Effect of sarcosine on antioxidant parameters and metallothionein content in the PC-3 prostate cancer cell line. *Oncol. Rep.* **29,** 2459–2466 (2013).
11. Heger, Z. *et al.* Paramagnetic Nanoparticles as a Platform for FRET-Based Sarcosine Picomolar Detection. *Sci Rep* **5,** 1–7 (2015).
12. Leamon, C. P. Folate-targeted drug strategies for the treatment of cancer. *Curr. Opin. Investig. Drugs* **9,** 1277–1286 (2008).
13. Pollock, S. *et al.* Uptake and trafficking of liposomes to the endoplasmic reticulum. *Faseb J.* **24,** 1866–1878 (2010).
14. Heger, Z. *et al.* 17 beta-estradiol-containing liposomes as a novel delivery system for the antisense therapy of ER-positive breast cancer: An *in vitro* study on the MCF-7 cell line. *Oncol. Rep.* **33,** 921–929 (2015).
15. Hattori, Y. & Maitani, Y. Folate-linked nanoparticle-mediated suicide gene therapy in human prostate cancer and nasopharyngeal cancer with herpes simplex virus thymidine kinase. *Cancer Gene Ther.* **12,** 796–809 (2005).
16. Zhao, D. M. *et al.* Preparation, characterization, and *in vitro* targeted delivery of folate-decorated paclitaxel-loaded bovine serum albumin nanoparticles. *Int. J. Nanomed.* **5,** 669–677 (2010).
17. Bahrami, B. *et al.* Folate-conjugated nanoparticles as a potent therapeutic approach in targeted cancer therapy. *Tumor Biol.* **36,** 5727–5742 (2015).
18. Nelson, W. G., De Marzo, A. M. & Isaacs, W. B. Mechanisms of disease: Prostate cancer. *N. Engl. J. Med.* **349,** 366–381 (2003).
19. Chen, C. *et al.* Structural basis for molecular recognition of folic acid by folate receptors. *Nature* **500,** 486–489 (2013).
20. Chaudhury, A. & Das, S. Folate Receptor Targeted Liposomes Encapsulating Anti-Cancer Drugs. *Curr. Pharm. Biotechnol.* **16,** 333–343 (2015).
21. Sabharanjak, S. & Mayor, S. Folate receptor endocytosis and trafficking. *Adv. Drug Deliv. Rev.* **56,** 1099–1109 (2004).
22. Maeda, H. Macromolecular therapeutics in cancer treatment: The EPR effect and beyond. *J. Control. Release* **164,** 138–144 (2012).
23. Talmadge, J. E., Singh, R. K., Fidler, I. J. & Raz, A. Murine models to evaluate novel and conventional therapeutic strategies for cancer. *Am. J. Pathol.* **170,** 793–804 (2007).
24. Chames, P., Van Regenmortel, M., Weiss, E. & Baty, D. Therapeutic antibodies: successes, limitations and hopes for the future. *Br. J. Pharmacol.* **157,** 220–233 (2009).
25. Cernei, N. *et al.* Sarcosine as a Potential Prostate Cancer Biomarker-A Review. *Int. J. Mol. Sci.* **14,** 13893–13908 (2013).
26. Trudel, D., Fradet, Y., Meyer, F., Harel, F. & Tetu, B. Significance of MMP-2 expression in prostate cancer: An immunohistochemical study. *Cancer Res.* **63,** 8511–8515 (2003).
27. Peng, B. *et al.* AP-1 Transcription Factors c-FOS and c-JUN Mediate GnRH-Induced Cadherin-11 Expression and Trophoblast Cell Invasion. *Endocrinology* **156,** 2269–2277 (2015).
28. Kaukoniemi, K. M. *et al.* Epigenetically altered miR-193b targets cyclin D1 in prostate cancer. *Cancer Med.* **4,** 1417–1425 (2015).
29. Adams, S. J., Aydin, I. T. & Celebi, J. T. GAB2-a Scaffolding Protein in Cancer. *Mol. Cancer Res.* **10,** 1265–1270 (2012).
30. Ding, C. B., Yu, W. N., Feng, J. H. & Luo, J. M. Structure and function of Gab2 and its role in cancer (Review). *Mol. Med. Rep.* **12,** 4007–4014 (2015).
31. Mignard, V., Lalier, L., Paris, F. & Vallette, F. M. Bioactive lipids and the control of Bax pro-apoptotic activity. *Cell Death Dis.* **5,** 1–8 (2014).
32. Schmid, M. *et al.* The role of biomarkers in the assessment of prostate cancer risk prior to prostate biopsy: Which markers matter and how should they be used? *World J. Urol.* **32,** 871–880 (2014).

33. Tisman, G. & Garcia, A. Control of prostate cancer associated with withdrawal of a supplement containing folic acid, L-methyltetrahydrofolate and vitamin B12: a case report. *J Med. Case Rep.* **5,** 413–418 (2011).
34. Pan, T. J. *et al.* Elevated expression of glutaminase confers glucose utilization via glutaminolysis in prostate cancer. *Biochem. Biophys. Res. Commun.* **456,** 452–458 (2015).
35. Wang, Q. *et al.* Targeting Amino Acid Transport in Metastatic Castration-Resistant Prostate Cancer: Effects on Cell Cycle, Cell Growth, and Tumor Development. *JNCI-. Natl. Cancer Inst.* **105,** 1463–1473 (2013).
36. Beauchamp, E. M. & Platanias, L. C. The evolution of the TOR pathway and its role in cancer. *Oncogene* **32,** 3923–3932 (2013).
37. Hasumi, M. *et al.* Regulation of metallothionein and zinc transporter expression in human prostate cancer cells and tissues. *Cancer Lett.* **200,** 187–195 (2003).
38. Franklin, R. B. *et al.* hZIP1 zinc uptake transporter down regulation and zinc depletion in prostate cancer. *Mol. Cancer* **4,** 1–13 (2005).
39. Heger, Z. *et al.* Metallothionein as a Scavenger of Free Radicals - New Cardioprotective Therapeutic Agent or Initiator of Tumor Chemoresistance? *Current Drug Targets* In press (2015).
40. Vogel, C. & Marcotte, E. M. Insights into the regulation of protein abundance from proteomic and transcriptomic analyses. *Nat. Rev. Genet.* **13,** 227–232 (2012).
41. Leitao, R. G. *et al.* Study of human prostate spheroids treated with zinc using X ray microfluorescence. *2014 Ieee International Symposium on Medical Measurements and Applications (Memea)* 599–603 (2014).
42. Song, Y. H., Shiota, M., Kuroiwa, K., Naito, S. & Oda, Y. The important role of glycine N-methyltransferase in the carcinogenesis and progression of prostate cancer. *Mod. Pathol.* **24,** 1272–1280 (2011).
43. Bradford, M. M. Rapid and sensitive method for quantification of microgram quantities of protein utilizing principle of protein-dye binding. *Anal. Biochem.* **72,** 248–254 (1976).
44. Heger, Z. *et al.* 3D-printed biosensor with poly(dimethylsiloxane) reservoir for magnetic separation and quantum dots-based immunolabeling of metallothionein. *Electrophoresis* **36,** 1256–1264 (2015).
45. Nejdl, L. *et al.* Interaction study of arsenic (III and V) ions with metallothionein gene (MT2A) fragment. *Int. J. Biol. Macromol.* **72,** 599–605 (2015).
46. Roth, K. M., Peyvan, K., Schwarzkopf, K. R. & Ghindilis, A. Electrochemical detection of short DNA oligomer hybridization using the CombiMatrix ElectraSense Microarray reader. *Electroanalysis* **18,** 1982–1988 (2006).
47. Kaushal, V., Herzog, C., Haun, R. S. & Kaushal, G. P. In *Caspases, Paracaspases, and Metacaspases: Methods and Protocols* Vol. 1133 *Methods in Molecular Biology* (eds Bozhkov, P. V. & Salvesen, G.) 141–154 (Humana Press Inc, 2014).
48. Casadonte, R. & Caprioli, R. M. Proteomic analysis of formalin-fixed paraffin-embedded tissue by MALDI imaging mass spectrometry. *Nat. Protoc.* **6,** 1695–1709 (2011).
49. Tmejova, K. *et al.* Structural effects and nanoparticle size are essential for quantum dots-metallothionein complex formation. *Colloid Surf. B-Biointerfaces* **134,** 262–272 (2015).

Acknowledgements

This research was carried out under the project CEITEC 2020 (LQ1601) with financial support from the Ministry of Education, Youth and Sports of the Czech Republic under the National Sustainability Programme II, and The financial support from GACR 16-18917S is highly acknowledged. The authors wish to thank Renata Kensova, Lukas Richtera and Marketa Kominkova for their excellent technical assistance.

Author Contributions

Z.H. wrote the manuscript and performed the basic characterization of synthesized liposomes and folate targeting. H.P. treated and euthanized the animals and carried out the tumor excisions and measurements. M.A.M.R. performed electrochemical microarrays and PCR analyses. R.G. carried out MALDI-TOF analyses. P.Ku. performed TEM analyses. P.Ko. carried out whole synthesis of liposomes and quantum dots. M.M. participated on design of study and metallothionein and zinc measurements. T.E., M.S. and R.K. participated on design of study and helped with the results and discussion. V.A. designed experiments, discussed the results and submitted the manuscript.

Additional Information

Supplementary information accompanies this paper at http://www.nature.com/srep

Competing financial interests: The authors declare no competing financial interests.

How to cite this article: Heger, Z. *et al.* Prostate tumor attenuation in the nu/nu murine model due to anti-sarcosine antibodies in folate-targeted liposomes. *Sci. Rep.* **6**, 33379; doi: 10.1038/srep33379 (2016).

4 PART III: Redox status and oxidative stress of prostatic cells

4.1 Theoretical basis

Reactive forms of oxygen (ROS – reactive oxygen species) are produced by living organisms due to normal cellular metabolism. At low to moderate concentrations, they work in physiological cell processes, but at high concentrations, they cause undesirable modifications of significant bio-macromolecules such as lipids, proteins and DNA [100]. ROS are often called oxidants. Aerobic organisms have integrated antioxidant systems incorporating enzymatic and non-enzymatic antioxidants that are usually efficient in blocking the harmful ROS effects. A significant deflection of the balance between oxidizing and anti-oxidizing agents in favour of oxidants is called the oxidative stress status. Oxidative stress contributes to many pathological conditions including tumour diseases, atherosclerosis, hypertension, and diabetes [101].

Although the term ROS often refers to individual entities only, it is a very complex system and includes a number of oxidants. The major ROS of physiological importance are as follows: superoxide anion (O^{2-}), hydroxyl radical ($\bullet$ OH) and hydrogen peroxide (H_2O_2). The intracellular ROS producers include mitochondria (I and III respiratory chain complexes being the main producer) and the endoplasmic reticulum. Within the whole organism, ROS produce leukocytes, macrophages and erythrocytes. Exogenous effects, contributing to the onset of the oxidative stress state, include smoking, heavy metals, ionizing radiation and hyperoxia [101]. Induction of oxidative stress is also associated with chemotherapy and radiotherapy. Oxidative stress can significantly affect tumour cell signalling pathways and slow progression through the cell cycle, which may affect the efficacy of the applied therapy [102, 103].

Prostate carcinoma cells, unlike healthy cells, are characterized by the so-called innate oxidative stress, a characteristic feature for the aggressive phenotype of this disease. In prostate carcinoma, the increased ROS production is caused by various processes including internal factors such as metabolic alterations, AR activation, and mutations causing mitochondrial dysfunctions. External factors include inflammation, metabolism of xenobiotics and hypoxia [104]. In addition to the activation of the androgen receptor, the (NF-E2)-related factor 2 (Nrf2) also plays a role in the redox status of CaP, i.e. it mediates expression of key protective enzymes through the antioxidant response element (ARE) [105, 106]. Some studies suggest that expression of Nrf2 and some of its target genes is reduced significantly in CaP [107]. The glutathione-containing enzymes are another important component involved in maintaining redox balance in the

cell. The somatic mutation causing inactivation of the glutathione-S-transferase gene (*GSTP1*) was identified in almost all CaP-derived tissues examined by Nelson et al. [108]. The sensitive balance between oxidative and antioxidative cell components and their regulatory mechanisms plays probably a crucial role in the development of malignant status in the prostate tissue. Resistance to oxidative stress also seems to be one of the main mechanisms of chemo- and radioresistance. In addition to the direct impact on mutagenesis and genomic instability, ROS also contribute to development and progression of the tumour disease by acting as signalling molecules for mitogenic processes and as inductors of the genetic programs leading to invasion and malignity [109]. The signalling effect of ROS does not have to be limited to the tumour cells themselves, but can also have a paracrine effect on the cells of the tumour microenvironment. Some studies suggest that the activation of tumour associated fibroblasts (CAFs), influencing cancerogenesis and resistance of tumour cell, is affected by ROS [110]. ROS promote conversion of fibroblasts into highly migrating myofibroblasts by activating the hypoxia-induced factor (HIF-1α) and chemokine CXCL12 [111].

4.2 Hypothesis verified under PART III

The following hypotheses were formulated, based on the theoretical starting points shown in the text above.

Hypothesis 1: Differences in the zinc levels of prostate non-tumour and tumour cells correspond with differences in the systems of major antioxidant mechanisms; oxidative stress also calls up defence mechanisms leading to further disease progression (polyploidization, mitophagy, development of drug resistance).

Hypothesis 2: The previously studied molecule, sarcosine, is associated with changes in antioxidant mechanisms.

4.2.1 Findings related to the hypothesis 1

***Hypothesis 1*: Differences in the zinc levels of prostate non-tumour and tumour cells correspond with differences in the systems of major antioxidant mechanisms; oxidative stress also calls up defence mechanisms leading to further disease progression (polyploidization, mitophagy, devel-opment of drug resistance).**

Disability to catch and accumulate zinc ions is one of the features of prostate tumour cells. This was demonstrated in our earlier studies (see sec. 2.2.2.) and corresponds to literature sources [26]. A study by Masarik *et al.* [53] (p. 206 of this work) confirms these findings and demonstrates

further that PC-3 cells respond most sensitively to intracellular zinc increase - their 50% zinc inhibition concentration is one-third compared to the non-tumour PNT1A.

A number of studies in the past confirmed that the increased intracellular concentration of zinc ions leads to a higher oxidative stress [112] while metallothionein, the major intracellular zinc-binding protein, at the same time works as a significant antioxidant [113]. The work by Masarik *et al.* was further focused on the following mechanisms: A correlation between the rising intracellular zinc and the metallothionein-binding zinc was demonstrated in both cell lines. A significant difference was found in this inducibility: PC-3 cells showed up to a tenfold increase in metallothionein concentration after exposure to 10 μM zinc concentration, whilst in PNT1A this inducibility was only half as high. This finding is relatively inconsistent with the results of 50% inhibitory concentrations (IC50) - the metastatic line may induce higher amounts of metallothionein than the non-tumour line, but at the same time this quantity of metallothionein is not sufficient to buffer the increased zinc charge and the metastatic line is inhibited at lower zinc concentrations. Therefore, other antioxidant systems of these cells were investigated. The difference between PNT1A and PC-3 was also demonstrated in the reduced/oxidized glutathione (GSH/GSSG) system: While the reduced glutathione form prevails in the non-tumour cells (a higher GSH/GSSG ratio), the situation is opposite in the PC-3 cells where the oxidized form of GSSG prevails significantly.

The next step was to describe whether or not this fact is related to the development of resistance against cytotoxic agents; the mechanism of the action of most cytostatics is mediated just through the oxidative damage of cell structures. Cisplatin was chosen as a model cytostatic drug. It is bound to DNA and to other important molecules thus resulting in cell death [114]. The panel of PNT1A-22Rv1-PC-3 cell lines has been chosen intentionally for testing resistance against this cytostatic drug: PC-3 cells represent a model of aggressive carcinoma inter alia due to dysfunctional p53. Because this tumour suppressor plays a central role in regulating the cell cycle arrest, DNA repair and the start of apoptosis, it is expected that PC-3 will exhibit a resistant phenotype.

The experiment revealed that cells with non-functioning p53 are characterized by the following features supporting the tumour growth: the increased capacity of antioxidant mechanisms, low expression of the pro-apoptotic protein BAX and absence of cell cycle arrest. The rate of cell sensitivity to cisplatin was analyzed by two techniques – the MTT metabolic assay and the real-time cell growth analysis based on impedance measurements were used. IC50 values determined by MTT were significantly lower than the values established by the real-time growth

assay; this was due to the fact that cells, when stressed, are switched to the autophagy status where they can be falsely identified as "dead" by some tests (see page 219).

Oxidative stress effects on metastatic cells were further studied in Balvan *et al*. [115], see p. 230, where the impact of oxidative stress on cell death, autophagy, polyploidization and other mechanisms associated with the development of resistance against cytostatic drugs was investigated. It was found that the long-term exposure of cells to oxidative stress acts as a selection pressure for the development of various resistance processes. Due to the activation of autophagy cascades, the metabolism of cells slows down and hence we can see a proportional difference between the determination of cell viability by MTT test and the impedance-based methods (see previous experimental works on the effect of cisplatin, p. 219). Mitochondria, the major ROS producers in cells, were enveloped by an autophagic membrane and degraded by mitophagy. Furthermore, a substantial part of cell population changed the cell size which was caused by polyploidization. In agreement with Erenpreisa et al., this strategy is understood as an escape from the destruction of cells by senescence and apoptosis and also as the possible way how to do reprogramming into a "cancer stem cell" phenotype by conferring significant genetic plasticity [116].

Consequently, the elevated expression of typical pluripotency markers - *NANOG*, *SOX2*, *POU5F1* was observed. Our experiments also clearly demonstrated that the cells that have undergone cell fusion leading to polyploidization through the entotic process and cells utilizing opportunistic ways to obtain nutrients (such as cannibalism) have a clear advantage - they can survive significantly much longer under oxidative stress conditions than the surrounding cells.

Conclusion: In our experimental work, we have devoted ourselves mainly to the effect of external factors on the change of the cellular redox status and thus on the potential development of oxidative stress state in the prostate tumour cells. The importance of zinc ions associated with the development and progression of prostate carcinoma was clarified sufficiently in PART I (see PART I: Zinc, metallothionein and progression of prostate carcinoma). However, the zinc ions play a role of exogenous stimulators of ROS production and increase the level of oxidative stress in cells. We demonstrated that the sensitivity of individual prostate cell lines to the increasing concentrations of zinc ions differs considerably. After the application of zinc ions, different behaviour of the tumour and non-tumour cells and their antioxidant systems was demonstrated. Based on the integrative approaches we were able monitoring of the redox status in the individual cell lines. These methods were then used for the evaluation of cisplatin effects. Cisplatin belongs to commonly used cytostatic drugs. We focused on the analysis of oxidative stress, cell cycle, apoptosis and selected cytotoxic analyses. Our attention was directed to the

PC3 line, representing a model of the aggressive prostate carcinoma. After the application of cisplatin, we could not see in this line a typical cell cycle arrest in the G1/G0 phase, and at the same time, we observed a decreased tendency for apoptosis. Moreover, we demonstrated that this cell line exhibits a higher antioxidant activity and higher metallothionein content after the administration of cisplatin and thus can be used as a model of cisplatin resistance.

Author's publications relevant to this chapter

1. Masarik M, Gumulec J, Hlavna M, et al. Monitoring of the prostate tumour cells redox state and real-time proliferation by novel biophysical techniques and fluorescent staining. Integrative Biology. 2012;4(6):672-684.
   Available on page 206
2. Gumulec J, Balvan J, Sztalmachova M, et al. Cisplatin-resistant prostate cancer model: Differences in antioxidant system, apoptosis and cell cycle. International Journal of Oncology. 2014;44(3):923-933.
   Available on page 219
3. Balvan J, Gumulec J, Raudenska M, et al. Oxidative Stress Resistance in Metastatic Prostate Cancer: Renewal by Self-Eating. Plos One. 2015;10(12).
   Available on page 230

Integrative Biology

Dynamic Article Links

Cite this: *Integr. Biol.*, 2012, **4**, 672–684

www.rsc.org/ibiology

PAPER

Monitoring of the prostate tumour cells redox state and real-time proliferation by novel biophysical techniques and fluorescent staining

Michal Masarik,*[a] Jaromir Gumulec,[a] Marian Hlavna,[ac] Marketa Sztalmachova,[ab] Petr Babula,[c] Martina Raudenska,[a] Monika Pavkova-Goldbergova,[a] Natalia Cernei,[bd] Jiri Sochor,[bd] Ondrej Zitka,[bd] Branislav Ruttkay-Nedecky,[b] Sona Krizkova,[b] Vojtech Adam[bd] and Rene Kizek[bd]

Received 5th November 2011, Accepted 6th April 2012
DOI: 10.1039/c2ib00157h

The present paper is focused on zinc(II) treatment effects on prostatic cell lines PC-3 (tumour) and PNT1A (non-tumour). Oxidative status of cells was monitored by evaluation of expression of metallothionein (MT) isoforms 1A and 2A at the mRNA and protein level, glutathione (oxidised and reduced), and intracellular zinc(II) after exposition to zinc(II) treatment at concentrations of 0–150 μM using electrochemical methods, western blotting and fluorescent microscopy. A novel real-time impedance-based growth monitoring system was compared with widely used end-point MTT assay. Impedance-based IC_{50} for zinc(II) is 55.5 and 150.8 μM for PC-3 and PNT1A, respectively. MTT-determined IC_{50} are >1.3-fold higher. Impedance-based viability correlates with viable count ($r > 0.92$; $p < 0.03$), not with MTT. Two-fold lower intracellular zinc(II) in the tumour PC-3 cell line was found. After zinc(II) treatment >2.6-fold increase of intracellular zinc(II) was observed in non-tumour PNT1A and in tumour PC-3 cells. In PC-3 cells, free and bound zinc(II) levels were enhanced more markedly as compared to PNT1A. PNT1A produced 4.2-fold less MT compared to PC3. PNT1A cells showed a 4.8-fold increase trend ($r = 0.94$; $p = 0.005$); PC-3 did show a significant trend at MT1 and MT2 protein levels ($r = 0.93$; $p = 0.02$) with nearly ten-fold increase after 100 μM zinc(II) treatment. In terms of redox state, PNT1A had a predominance of reduced GSH forms (GSH : GSSG ratio > 1), when exposed to zinc(II) compared to PC3, where predominance of oxidised forms remains at all concentrations. IC_{50} differs significantly when determined by MTT and real-time impedance-based assays due to dependence of impedance on cell morphology and adhesion. When real-time growth monitoring, precise electrochemical methods and fluorescent microscopy are performed together, accurate information for metal fluxes, their buffering by thiol compounds and monitoring of the redox state become a powerful tool for understanding the role of oxidative stress in carcinogenesis.

[a] *Department of Pathological Physiology, Faculty of Medicine, Masaryk University, Kamenice 5, CZ-625 00 Brno, Czech Republic. E-mail: masarik@med.muni.cz; Fax: +420-5-4949-4340; Tel: +420-5-4949-3631*
[b] *Department of Chemistry and Biochemistry, Faculty of Agronomy, Mendel University in Brno, Zemedelska 1, CZ-613 00 Brno, Czech Republic*
[c] *Department of Natural Drugs, Faculty of Pharmacy, University of Veterinary and Pharmaceutical Sciences, Palackeho 1-3, CZ-612 42 Brno, Czech Republic*
[d] *Central European Institute of Technology, Brno University of Technology, Technicka 3058/10, CZ-616 00 Brno, Czech Republic*

Insight, innovation, integration

Prostate cancer cells have altered the ability to uptake and accumulate zinc(II) ions compared to healthy prostate tissue, however, the mechanism is not clear, but it is obvious that some thiols such as metallothionein and glutathione can be involved. This study was focused on zinc(II) treatment effects on the PC-3 prostate cancer cell line and the PNT1A cell line representing non-tumorous prostate epithelial cells. We suggested, optimized and applied various methods and protocols to monitor redox status, gene expression of metallothionein isoforms 1A and 2A at the RNA and protein level, reduced and oxidized glutathione content. In addition, this study describes application of a new label-free and non-invasive method based on impedance determination for real-time analysis of cell proliferation, adhesion and spreading.

Introduction

It has been repeatedly reported that prostate cancer cells are characterised by altered ability to uptake and accumulate zinc(II) ions as compared to healthy prostate tissue.[1] In fact, there is no evidence or records on prostate tumours with unchanged ability to accumulate zinc. In healthy tissue, zinc(II) plays an important role in proliferation, differentiation regulation and apoptosis in prostate (Fig. 1).[2] In healthy and tumour prostate, intracellular zinc(II) is buffered by numerous proteins (metalloenzymes, nucleoproteins and metalloproteins, in particular metallothioneins).[3] Metallothioneins (MTs) are ubiquitous low-molecular mass cysteine-rich proteins, playing a key role in maintaining zinc(II) homeostasis. They are also involved in the protection of cells against oxidative stress in association with reduced glutathione (GSH).[4] Due to these functions, it is natural that MTs are overexpressed under conditions with the increased risk of reactive oxygen species formation, such as cell proliferation, embryonic development or carcinogenesis.[4b,5] Due to MTs' low molecular mass and unique primary structure, commonly used methods for detection of proteins suffer from many deficiencies including insufficient specificity and sensitivity. The most frequent methods used for the detection of these proteins are immunological and/or electrochemical ones with the lowest detection limits at aM concentrations.[6]

This study was focused on zinc(II) treatment effects on the PC-3 prostate cancer cell line and the PNT1A cell line representing non-tumorous prostate epithelial cells. Particularly, monitoring of redox status influenced by zinc(II) ions was performed, in particular gene expression of metallothionein isoforms 1A and 2A at the RNA and protein level. In addition to redox status, reduced and oxidized glutathione was also determined. Moreover, cell viability and proliferation after zinc(II) ions treatment were studied since cell viability, adhesion and spreading can be affected by the cell redox state.[7] In addition, this study describes application of a new label-free and non-invasive method based on impedance determination for real-time analysis of cell proliferation, adhesion and spreading. Together with utilization of electrochemical methods for determination of some biochemical markers, such comprehensive results have not been obtained yet on tumour and non-tumour prostate cell lines.

Experimental

Chemical and biochemical reagents

Commercial materials were obtained as follows: RPMI-1640 medium, Ham's F12 medium, foetal bovine serum (FBS) – mycoplasma free, penicillin/streptomycin and trypsin EDTA were purchased from PAA Laboratories GmbH (Austria). PBS was purchased from Invitrogen Corp. (USA). EDTA, zinc(II) sulphate, RIPA buffer and all other chemicals of ACS purity were purchased from Sigma Aldrich Co. (USA), unless noted otherwise. Primary mouse metallothionein antibody and secondary anti-mouse HRP conjugated antibody were purchased from Abcam (USA), primary PSA antibody was purchased from Santa Cruz Biotechnology Inc (USA). For chemiluminescent detection of western blot membranes an ECL WB detection reagents system from Amersham Pharm. biotech was used (USA).

Cell cultures

Two human prostatic cell lines were used in this study: (a) PNT1A human cell line established by immortalisation of normal adult prostatic epithelial cells by transfection with a plasmid containing SV40 genome with a defective replication origin. The primary culture was obtained from the normal prostatic tissue of a 35 years old male at post-mortem; (b) PC-3 human cell line established from a grade 4 prostatic adenocarcinoma from

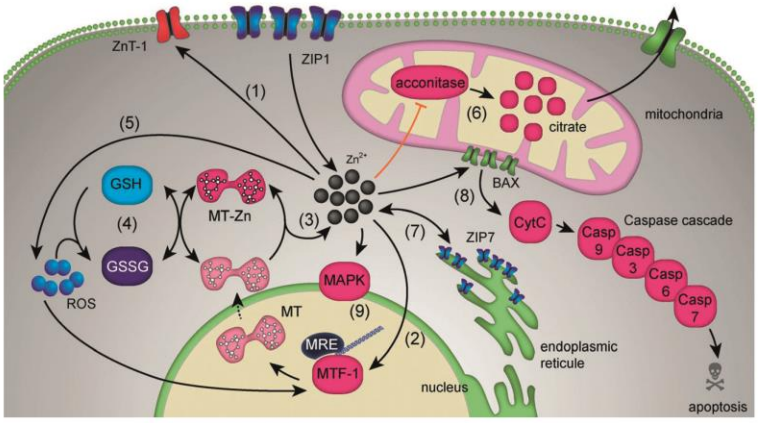

Fig. 1 Effect of zinc(II) in prostatic tissue. ZIP and ZnT maintain intracellular zinc transport (1); ZIP1 is a major zinc(II) importer, ZnT-1 is the only export transporter. Intracellular free zinc(II) induces metallothionein (MT) expression through MTF-1 and MRE (2) and is buffered by MT (3) (white MT represents reduced/metal-free form, grey MT represents oxidized/metal-bound form). High zinc(II) load induces oxidative stress (ROS) (5), which is reduced by the glutathione system in cooperation with MT (4); MT converts glutathione to its reduced form while being oxidized. Endoplasmic reticulum regulates the cytoplasmic free zinc level by ZIP7 transporter (7). Free zinc(II) affects gene expression through a mitogen-activated protein kinase cascade (MAPKs, 9). In prostate, a high zinc(II) level inhibits mitochondrial aconitase (mAC), thus citrate is accumulated (6) and released in high levels. Zinc induces a prostate-specific BAX pore formation (8) causing cytochrome C (CytC) release from mitochondria and subsequent caspase-mediated apoptosis. Adapted according to Franklin and Costello[30] and Eckschlager *et al.*[4b]

a 62 years old Caucasian male and derived from the metastatic site in bone. Both cell lines used in this study were purchased from HPA Culture Collections (Salisbury, UK).

Cultured cell conditions

PNT1A cells were cultured in RPMI-1640 medium with 10% FBS. PC-3 were cultured in Ham's F12 medium with 7% FBS. All media were supplemented with penicillin (100 U ml^{-1}) and streptomycin (0.1 mg ml^{-1}), and the cells were maintained at 37 °C in a humidified incubator with 5% CO_2. The passages of PNT1A and PC-3 cell lines ranged from 10 to 35.

Zinc(II) treatments of cell culture

Once the cells grew up to 50–60% confluence of the culture, the growth media were replaced by fresh medium for 24 h to synchronize cell growth. The cells were then treated with or without zinc(II) sulphate (0–100 μM for both cell lines) in fresh medium for 48 h. In the case of viability and proliferative assays (MTT and xCELLigence measurements) cells were treated with a concentration of 300 μM.

Sample preparation

RIPA buffer lysate. Cell line's medium was removed and samples were quickly rinsed with 5 ml of ice-cold PBS twice. Cells were scraped, transferred to clean tubes and were centrifuged at 800 × *g* for 5 minutes (Eppendorf 5402, Germany) at room temperature. Then the cell pellet was transferred to 1.5 ml tubes and washed with PBS twice and centrifuged at 800 × *g* for 5 minutes again. RIPA buffer was added and tubes were intermittently mixed for 15 minutes on ice by vortexing. Then, samples were centrifuged at 20 800 × *g* for 15 min at 4 °C and the supernatant was used for further analysis.

Thermo-lysate. Approximately 0.01 g of the cells in 500 μl of PBS was mechanically disintegrated using an Ultra-Turrax T8 homogenizer (Ika, Germany) placed in an ice bath for 3 min at 25 000 rpm. The cell homogenates were kept at 99 °C in a thermomixer (Eppendorf 5430, Germany) for 15 min with shaking. The denatured homogenates were centrifuged at 4 °C, 15 000 × *g* for 30 min (Eppendorf 5402, Germany). Heat treatment effectively denatures and removes thermolabile and high molecular mass proteins out from the samples.[8] The prepared samples were used for metallothionein and GSH/GSSG analyses.

RNA isolation, cDNA preparation

For RNA isolation a High pure total RNA isolation kit (Roche, Switzerland) was used. Cell line's medium was removed and samples were quickly rinsed with 5 ml of ice-cold PBS twice. Cells were scraped, transferred to clean tubes and centrifuged at 20 800 × *g* for 5 min at 4 °C. After this step, lysis buffer was added and RNA isolation was carried out according to manufacturer's instructions. Isolated RNA was used for cDNA synthesis. 600 ng of total RNA was transcribed using a Transcriptor first strand cDNA synthesis kit (Roche, Switzerland) according to manufacturer's instructions. 20 μl of prepared cDNA was diluted with RNase free water to 100 μl and directly analysed by real-time PCR.

Real-time reverse-transcription polymerase chain reaction (RT-PCR)

RT-PCR was performed in triplicate using the TaqMan gene expression assay system with the 7500 real-time PCR system (Applied Biosystems, USA). The amplified DNA was analysed by the comparative Ct method using β-actin as an endogenous control. The primer and probe sets for β-actin (Assay ID: Hs00185826_m1), MT1 Assay ID: Hs00185826_m1) and MT2 (Hs00794796_m1) were selected from TaqMan gene expression assay. Real-time PCR was performed under the following amplification conditions: total volume of 20 μl, initial denaturation 95 °C per 10 min, than 45 cycles 95 °C per 15 s, 60 °C per 1 min.

Cell content quantification

Total cell content was analysed using a Cedex XS (Innovatis) semi-automated image-based cell analyser according to manufacturer's instructions. Cell line's medium was removed and samples were washed with 5 ml of ice-cold PBS twice to maintain only viable cells. Cells were scraped and transferred to clean tubes. Trypan blue solution (Innovatis) was diluted to 0.2% before use and was added to samples according to manufacturer's manual. Following settings were used in operating software: cell type: standard cells, dilution: none, process type: standard. All samples were measured in duplicates.

Measurements of cell viability – MTT test

The MTT assay was used to determine cell viability. The suspension of cells in growth medium was diluted to a density of 5×10^3 cells per ml and 200 μl were transferred to 2–11 wells of standard microtiter plates. Medium (200 μl) was added to the first and to the last column (1 and 12). Plates were incubated for 2 days at 37 °C to ensure cell growth. Medium was removed from columns 2 to 11. Columns 3 to 10 were filled with 200 μl of medium containing different concentrations of zinc (0, 25, 50, 75 and 100 μM). As control, columns 2 and 11 were fed with medium without drug. Plates were incubated for 24 hours; then, all media were removed and exchanged with a fresh medium, daily three times. After that, columns 1 to 11 were fed with 200 μl of medium with 50 μl of MTT (5 mg ml^{-1} in PBS) and incubated for 4 h in a humidified atmosphere at 37 °C, wrapped in aluminium foil. After that, medium-MTT was exchanged with 200 μl of 99.9% DMSO to dissolve MTT-formazan crystals. Then, 25 μl of glycine buffer was added to all wells with DMSO and the absorbance was recorded at 570 nm (VersaMax microplate reader, Molecular devices).

Cell growth and proliferation assay using impedance measurement with the xCELLigence system

The xCELLigence system was used according to the instructions of the supplier (Roche Applied Science and ACEA Biosciences). The xCELLigence system consists of four main components: the RTCA analyser, the RTCA DP station, the RTCA computer with integrated software and disposable E-plate 16. Firstly, the optimal seeding concentration for proliferation and cytotoxic assay was determined. After seeding the total number of cells in 200 μl medium to each well in E-plate 16, the attachment, proliferation and spreading of the cells were monitored every 15 min. All experiments were carried out for 200 h.

Total proteins quantification – Bradford and Biuret methods

Protein amount in cell lysates was measured spectrometrically by the Bradford method and verified by the Biuret method on an automated analyser. The Bradford method was performed on an MBA 2000 analyser (Perkin Elmer, USA) at a wavelength of 595 nm. Total protein amount was determined using the automated biochemical analyzer BS-200 (Mindray, China). Reagents and samples handling were controlled by BS-200 software (Mindray). The absorbance was measured at 510 nm.

Differential pulse voltammetry – Brdicka reaction

Differential pulse voltammetric measurements were performed with a 747 VA Stand instrument connected to a 746 VA Trace Analyzer and a 695 Autosampler (Metrohm, Switzerland), using a standard cell with three electrodes and a cooled sample holder (4 °C). A hanging mercury drop electrode (HMDE) with a drop area of 0.4 mm^2 was the working electrode. An Ag/AgCl/3 M KCl electrode was the reference and a glassy carbon electrode was auxiliary. For data processing GPES 4.9 supplied by EcoChemie was employed. The analysed samples were deoxygenated prior to measurements by purging with argon (99.999%) and saturated with water for 120 s. The Brdicka supporting electrolyte containing 1 mM $Co(NH_3)_6Cl_3$ and 1 M ammonia buffer (NH_3(aq.) + NH_4Cl, pH = 9.6) was used. The supporting electrolyte was exchanged after each analysis. The parameters of the measurement were as follows: an initial potential of −0.7 V, an end potential of −1.75 V, a modulation time of 0.057 s, a time interval of 0.2 s, a step potential of 2 mV, a modulation amplitude of −250 mV, E_{ads} = 0 V, volume of the injected sample: 20 μl (100 × diluted sample with 0.1 M phosphate buffer, pH 7.0). All experiments were carried out at a temperature of 4 °C employing thermostat Julabo F25 (Labortechnik GmbH, Germany).

Electrochemical determination of zinc(II) ions

An electrochemical analyser (Metrohm AG, Switzerland) was used for determination of Zn(II). The analyser (757 VA Computrace from Metrohm, Herisau, Switzerland) employs a conventional three-electrode configuration with a hanging mercury drop electrode (HMDE) as the working electrode: 0.4 mm^2, Ag/AgCl/3M KCl as the reference electrode, and a platinum auxiliary electrode. The following setup assembled for automated voltammetric analysis is supplied by Metrohm. A sample changer (Metrohm 813 Compact Autosampler) performs the sequential analysis of up to 18 samples in plastic test tubes. For the addition of standard solutions and reagents, two automatic dispensers (Metrohm 765 Dosimat) are used, while two peristaltic pumps (Metrohm 772 Pump Unit, controlled by an Metrohm 731 Relay Box) are employed for transferring the rinsing solution into the voltammetric cell and for removing solutions from it. Differential pulse voltammetric measurements were carried out under the following conditions: deoxygenating with argon for 60 s; deposition potential: −1.3 V; time of deposition: 240 s; start potential: −1.3 V; end potential: 0.15 V; pulse amplitude: 0.025 V; pulse time: 0.04 s; step potential: 5.035 mV; time of step potential: 0.3 s.

Determination of low-molecular-mass thiols

A high performance liquid chromatograph with an electrochemical detection (HPLC-ED) system consisted of two solvent delivery pumps operating in the range of 0.001–9.999 ml min^{-1} (Model 582 ESA Inc., Chelmsford, MA), a Zorbax Eclipse AAA Column (4.6 × 150 mm 3.5 micron particle size; Varian Inc., CA, USA), and a CoulArray electrochemical detector (Model 5600A, ESA, USA). The sample (30 μl) was injected using an autosampler (Model 540 Microtiter HPLC, ESA, USA). HPLC-ED experimental conditions were as follows – mobile phase compositions: A: 80 mM trifluoroacetic acid and B: methanol. They were mixed in gradient from 3% B in the 1st min, 10% B in the 2nd to the 6th min and 98% B from the 7th min of separation; flow of the mobile phase was 0.8 ml min^{-1}, temperature of the separation was 40 °C; working electrodes potential was 900 mV; detector temperature was 30 °C; each measurement was repeated three-times. Retention time of the reduced glutathione (GSH) was 5 min. GSH concentration was calculated from a calibration curve (0.5–100 μM). The signal was quantified as a sum of current responses from all working electrodes.[9] In the case of real sample measurements, the shift of the retention time was about ±2%.

Western blotting analysis

Samples were prepared (4 μl of DTT and 8 μl of LDS buffer, 4 μl of sample per well) and incubated for 5 minutes at 37 °C. Electrophoresis was done on 10% and 12% 0.75 mm SDS-PAGE gels at 100 V for 90 minutes. After the electrophoretic separation, the proteins were transferred onto a nitrocellulose membrane (Bio-Rad, USA) in a Bio-rad apparatus (Bio-Rad, USA). The blotting was carried out for 1 h at a constant current of 0.9 mA for 1 cm^2 of the membrane. After the transfer, the membrane was blocked with 5% non-fat milk in PBS (137 mM NaCl, 2.7 mM KCl, 1.4 mM NaH_2PO_4, and 4.3 mM Na_2HPO_4; pH 7.4) for 2 hours. The incubation with the mouse primary antibody in dilution of 1 : 750 in PBS with 5% non-fat milk was carried out for 12 h at 4 °C. After washing three times with PBS containing 0.05% (v/v) Tween-20 (PBS-T) for 5 min the membrane was incubated with a secondary antibody (anti-mouse labelled with horseradish peroxidase, Sigma Aldrich Co., diluted 1 : 5000) for 1 h at room temperature. Then, the membrane was washed three times with PBS-T for 5 min and incubated with a chromogenic substrate (0.4 mg ml^{-1} AEC – 3-aminoethyl-9-carbazole in 0.5 M acetate buffer with 0.1% H_2O_2, pH 5.5).

Fluorescence microscopy and cell staining

For fluorescence microscopy, cells were cultivated directly on microscope glass slides (75 × 25 mm, thickness 1 mm, Fischer Scientific, Czech Republic) in Petri dishes in the above-described cultivation media (see Cultured cell conditions). Cells were transferred directly onto slides, which were submerged in cultivation media. After treatment, microscope glass slides with a monolayer of cells were removed from Petri dishes, rinsed with cultivation medium without zinc(II) supplementation and PBS buffer and directly used for staining and fluorescence microscopy.

For the staining of free thiols, respectively, free –SH groups, 5-(bromomethyl)fluorescein (5-BMF, Sigma-Aldrich, USA) was used. This probe reacts more slowly with thiols of peptides, proteins and thiolated nucleic acids in comparison with other fluorescent probes. However, it forms stronger thioether bonds that are expected to remain stable under the conditions required for fluorescence microscopy. Stock solution of 5-BMF (4 mM, anhydrous dimethyl sulfoxide) was prepared prior to staining because of 5-BMF stability. Working solution was prepared immediately using stock solution by diluting to a final concentration of 20 μM (PBS buffer, pH = 7.6). Cells were incubated for one hour at 37 °C and in the dark. Then, cells on the microscope glass slide were washed with PBS buffer (pH = 7.6) and observed using a fluorescence microscope (Axioskop 40, Carl Zeiss, Germany) equipped with wideband excitation and set of filters (FITC-DAPI, Carl Zeiss, Germany). Photographs were taken using a digital camera (Olympus Camedia 750, Olympus, Japan).

For free zinc(II) ions staining, fluorescent probe *N*-(6-methoxy-8-quinolyl)-*p*-toluene sulphonamide (TSQ, Invitrogen, USA) was used. Working solution (10 μM, phosphate buffer, pH = 7.6) was prepared by diluting TSQ stock solution (10 mM, acetone). Cells were carefully rinsed by PBS buffer to remove all cultivation media containing free zinc(II) ions, subsequently stained by working TSQ solution (30 min, 37 °C, dark), washed with PBS buffer (pH = 7.6) and observed under a fluorescence microscope (Axioskop 40, Carl Zeiss, Germany) equipped with FITC and DAPI filters (Carl Zeiss, Germany). Photographs were taken on a digital camera (Olympus Camedia 750, Olympus, Japan).

Statistical data analysis

Software Excel 2007 (Microsoft, USA) was used to arrange the data set. Software Statistica 10 (StatSoft, USA) was used to perform statistical analysis and chart construction. Signal intensity of western blotting was determined using ImageJ 1.45 software (NIH, USA) as an area under the curve. Viability was determined by quadratic regression of MTT ("MTT viability") and by fitting a real-time impedance chart at t = 72 h, data transposition and regression from the linear part of the curve. t-tests were used to reveal significant differences between groups. Simple linear correlations were performed to reveal the relationship between variables. Unless noted otherwise, a level of statistical significance was designated to $p = 0.05$. Scatterplots were fitted with the negative exponentially-weighted fitting algorithm.

Results

Real-time monitoring of cell adhesion and proliferation using the xCELLigence system

The question addressed in this study was whether zinc(II) ions would affect the prostatic cells proliferation and morphology. Zinc(II) metabolism in prostate (cancer) cells has been not entirely clear to date.[10] Primarily, the optimal cell concentration for real-time proliferation and viability assays was determined. Cells in count 5000, 10 000, 15 000, 20 000, 30 000, and 40 000 per well were seeded in E-plate 16 and the measurement was carried out (data not shown). Optimal response was found for the well containing 10 000 cells. For wells with lower cell count, a lower relative impedance signal level was yielded (represented as "cell index" in manufacturer's software) and it was associated with higher standard deviation (coefficient of variation: 3.1% and 0.8% in 5000 cells and 10 000 cells, respectively). In contrast, for wells with higher cell count overgrowing of cells on one another was observed when the E-plate was viewed under a microscope. Thus high cell density had inhibitory effects resulting in end of linear increase of relative impedance depending on the cell count (data not shown). Therefore, 10 000 cells per well were used to examine the effect of zinc(II) ions on prostatic cell lines.

Consequently, IC_{50} of zinc(II) on cell lines obtained by MTT cytotoxicity assay were determined. IC_{50} values of zinc(II) treatments were 194.3 μM for non-tumour cells PNT1A and 93.9 μM for PC3 tumour cells (Fig. 3A, Table 1). However, during the first measurements with xCELLigence proliferation and viability assay it was observed that chosen zinc(II) concentrations around and above MTT assay determined IC_{50} values exhibit more cytotoxic effects than was expected (compare Fig. 3A and B). Thus, for the proliferation and viability assay lower zinc(II) ions treatment concentrations were optimized as follows: 0 (control), 25 μM, 50 μM, 75 μM and 100 μM for both cell lines. Both cell lines reach a stationary phase of growth in 160 h. However, apparent difference in relative impedance values

Table 1 Comparison of viability determination, protein content and cell size in cell lines. xCelligence relative impedance, MTT absorbance, cell concentrations, protein content and cell size are displayed as a relative ratio of not treated/treated samples for more obvious comparison. IC_{50} is calculated from these methods. Apparent differences in MTT-determined and xCELLigence-determined IC_{50} are due to different cell size and cell count in PC-3 and PNT1A

		xCelligence		MTT		Cell count		Protein	Cell size
Cell line	Zinc(II) in medium/ μM	Relative impedance (%)	IC_{50}/ μM	Relative viability MTT (%)	IC_{50}/ μM	Relative cell count (%)	IC_{50}/ μM	Relative concentration (%)	Relative cell (%)
PC-3	0	100.0	55.5	100.0	93.9	100.0	60.7	100.0	100.0
	25	89.5		101.4		84.6		72.6	112.2
	50	33.1		101.4		102.0		94.4	88.2
	75	9.7		92.0		2.0		71.8	81.1
	100	3.0		7.8		0.4		14.5	74.1
PNT1A	0	100.0	150.8	100.0	194.3	100.0	131.3	100.0	100.0
	25	98.1		99.3		112.5		102.3	105.3
	50	99.9		98.9		139.2		106.4	111.5
	75	97.9		95.9		140.5		106.4	92.6
	100	87.7		97.0		133.6		98.4	91.6

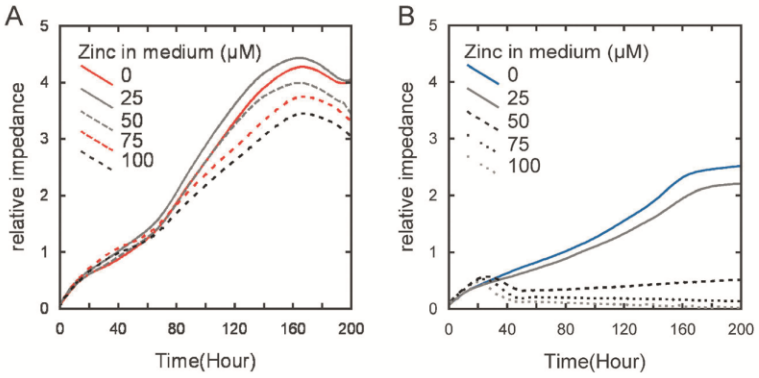

Fig. 2 Real-time monitoring of cell adhesion and proliferation using the xCELLigence system. PNT1A (A) and PC-3 (B) cells were seeded at a density of 10 000 cells per well in E-Plates 16. After 24 hours, zinc(II) sulphate was added and the cell index was monitored. The measurements were done in duplicates.

between cell lines was observed. Tumour cell line PC-3 reached 1.7-fold lower relative impedance in stationary phase of growth as compared to non-tumour cell line PNT1A (compare Fig. 2A and B at 0 μM zinc(II) concentration).

After adding zinc(II) ions (24 h after initiation of the experiment, see Fig. 2A and B), a rapid decrease in relative impedance in less than 2 h after the treatment was observed; it stabilized after 10 h, notably at high zinc(II) concentrations. After the stabilization, a less steep decrease of relative impedance in a concentration-dependent manner was observed. Concentrations of 150 μM in the case of PNT1A and 50 μM and more in the case of PC-3 induced a 2.6-fold and >24.8-fold decrease of relative impedance in PNT1A and PC-3 cell lines, respectively, compared to non-treated samples. On the other hand, zinc(II) concentration of 25 μM induced a 5% increase of the relative impedance value in PNT1A cells. In contrast, no such elevation of cell concentration after zinc(II) treatment is evident in PC-3 cells.

The IC_{50} values of zinc(II) ions using the xCELLigence system were also determined for the same period of time as MTT assay (72 h from the beginning of the experiment). These IC_{50} values were 150.8 μM zinc for PNT1A cells and 55.5 μM zinc for PC-3 cells. Thus, it may be concluded that zinc(II) is toxic to a tumour cell line in 2.7-fold lower concentration (see Table 1). However, IC_{50} values obtained from the xCELLigence system are 1.3-fold and 1.7-fold lower in PNT1A and PC-3 cell line, respectively, than IC_{50} values determined by MTT cytotoxicity assay. Due to this discrepancy MTT and xCELLigence system assays combined with other methods were further compared. It was shown that the relative impedance is influenced mostly by cell count, its adherence and morphology.[11] Hence the area of cells and the total viable cell count were determined in order to assess how these variables affect relative impedance. In terms of average cell area, it was found that PC-3 cells are 2-fold larger compared to PNT1A cells (135.1 ± 14.6 μm^2 and 67.7 ± 5.4 μm^2) (Fig. 3D). When treated with zinc(II), PNT1A cells do not show differences in cell size, whereas PC-3 cells area decrease with increasing zinc(II) treatment concentration (Fig. 3D). Then the cell content was determined and it was found that PC-3 cell lines achieved 1.6-fold smaller cell count at the same time interval (48 h) as compared to PNT1A (686.4 ± 46.1 cells per μl and 1083.8 ± 33.7 cells per μl in PC-3 and PNT1A cell line, respectively) (Fig. 3C). Significant statistical correlation ($r > 0.92$; $p < 0.03$) between results from the xCELLigence system and viable cell count during zinc(II) treatments was found. On the other hand, no significant correlation between xCELLigence system monitoring and MTT assay ($r > 0.80$; $p < 0.10$) was observed.

Cytology and gene expression

Primarily, this study focused on general cytology of both PC-3 and PNT1A cell lines. For these purposes, acridine orange (AO) was used. Acridine orange can serve as a marker of the lysosomal proton pump, an important marker of lysosomal function.[12] Treatment of PC-3 and PNT1A cell cultures with zinc(II) ions led to significant changes in cell morphology and especially in the formation of a monolayer. In control cells and cells treated at zinc(II) concentrations of 50 and 75 μM, lysosomes are well evident and their visualisation is connected with functioning of the lysosomal proton pump. Under higher zinc(II) concentrations (100 μM), lysosomes are not visible, but cytoplasm diffusely emits in the red area.

On the other hand, AO can be used for monitoring the RNA biosynthesis.[13] The incorporation of AO into nucleic acids depends on their structure. Double-helical DNA forms enable emission of AO at an emission maximum of 530 nm (green fluorescence), simpler non-helical RNA organization leads to the shift of AO emission at 660 nm (not shown). There are distinctive differences between cell lines in terms of RNA synthesis. RNA localisation is possible in nucleoli and cytoplasm. Whereas increased RNA synthesis in "healthy", non-tumour cell line PNT1A is evident only at higher zinc(II) ion concentrations (100 μM), increased RNA synthesis in tumour cell line PC-3 is apparent in all variants – in control (untreated cells) as well as cells treated at all zinc(II) ion concentrations (not shown). Similarly, the nucleoli, *i.e.* sites of RNA localization, are clearly visible in the control and in all treated cells of tumour cell line PC-3. On the other hand, in "healthy" non-tumour PNT1A cells the nucleoli are visible only in the cells treated with the two highest zinc(II) concentrations. This also corresponds to increased RNA biosynthesis at these two concentrations.

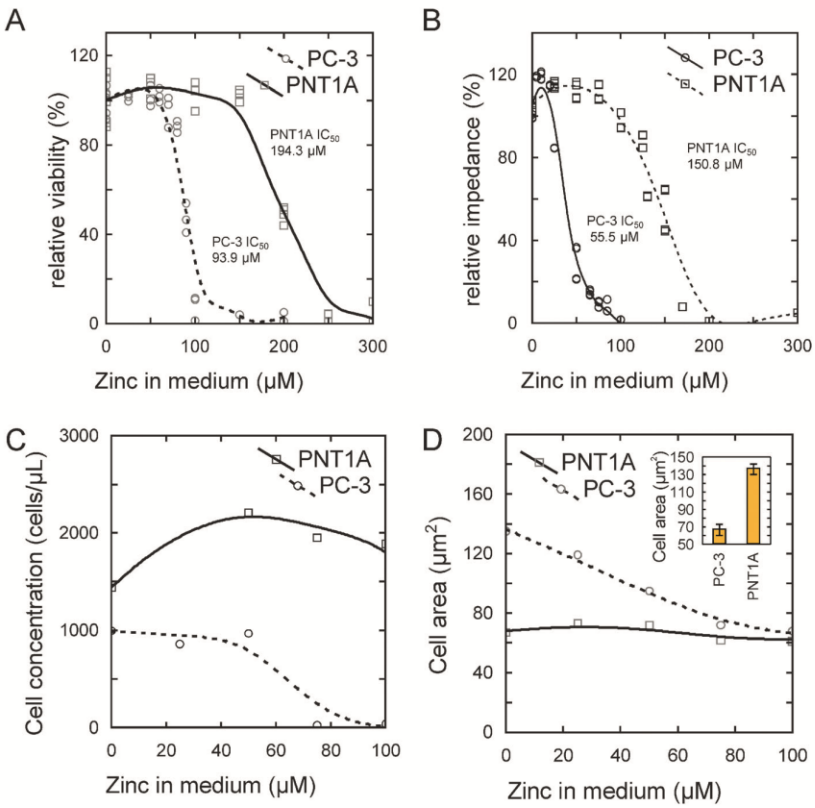

Fig. 3 Comparison of MTT, xCELLigence and cell concentration viability and cell size. (A) MTT-determined response to zinc(II) treatment, (B) xCELLigence determined response to zinc(II) treatment. Significantly higher IC_{50} are reached compared to xCELLigence-determined viability (A *vs.* B). (C) Dependency of cell count on zinc(II) treatment. Cell concentration in relation to zinc(II) treatment is elevated at concentrations of 50–100 µM in PNT1A compared to PC-3 cell lines. (D) Cell size in response to zinc(II) treatment. The PC-3 cell area is reduced during zinc(II) treatment, PNT1A maintains the same cell size. Whereas xCELLigence impedance monitoring is influenced by cell count and cell size, due to (D) is more pronounced decrease of viability in (B) in the PC-3 cell line compared to MTT (A). (D, inset): cell area in cell lines not exposed to zinc treatment (mean ± SD).

Determination of free and bound zinc(II) cellular levels after zinc(II) exposure

To investigate the relationship between zinc(II) metabolism, MT1 and MT2 gene expression and the cell redox state, the levels of intracellular free and protein bound zinc(II) ions were determined. To allow comparison of zinc(II) levels between various samples, the determined zinc(II) content was related to the viable cell count (relative impedance determined by xCELLigence assay (zinc concentration µM/relative impedance)). When the untreated cell lines were compared, significantly higher cellular bound (2.1-fold) and significantly lower free zinc(II) levels (2.3-fold) were found in non-tumour PNT1A cells as compared to PC-3 cells (compare insets in Fig. 4A and B).

After the zinc(II) treatment, a significant enhancement of the bound and free intracellular zinc(II) forms was observed in both cell lines. This increase correlated with zinc(II) concentration in growth medium at $r = 0.91$ ($p = 0.03$) and 0.98 ($p = 0.003$) for free and bound zinc(II) in the PC-3 cell line and at $r = 0.86$ ($p = 0.02$) and 0.98 ($p = 0.001$) for free and bound zinc(II) in the PNT1A cell line, respectively. When 100 µM zinc(II) treatment is compared to non-treated samples, 4.1-fold increase of bound zinc(II) and 3.5-fold increase of free zinc(II) were observed in PNT1A cells. In contrast, a more pronounced increase was detected in bound (5.7-fold) and free (30-fold) zinc(II) fractions in PC-3 cells.

Consequently, the zinc(II) content was determined by the use of fluorescent microscopy. Localisation of free zinc(II) ions with the use of fluorescent probe *N*-(6-methoxy-8-quinolyl)-*p*-toluene sulphonamide, which is specific for these ions, led to detection of differences between free zinc(II) ions localisation in non-tumour PNT1A cells and tumour PC-3 cells. In PC-3 cells, the amount of free zinc(II) ions is connected with treatment (not shown). At the lowest zinc(II) concentration, decrease of emission intensity is well evident. At other zinc(II) concentrations in this cell line intensity of emission increases. At the highest zinc(II) concentration (100 µM), localisation of these ions around nuclei, in nuclei and in the inner part of cytoplasm in the form of spots is well visible. Peripheral parts of cytoplasm demonstrate only weak emission, representing only low free zinc(II) levels in these localizations. In PNT1A cells, intensity of emission of the fluorescence product between the above-mentioned fluorescent probe and free zinc(II) significantly increases with increased supplementation of cultivation medium

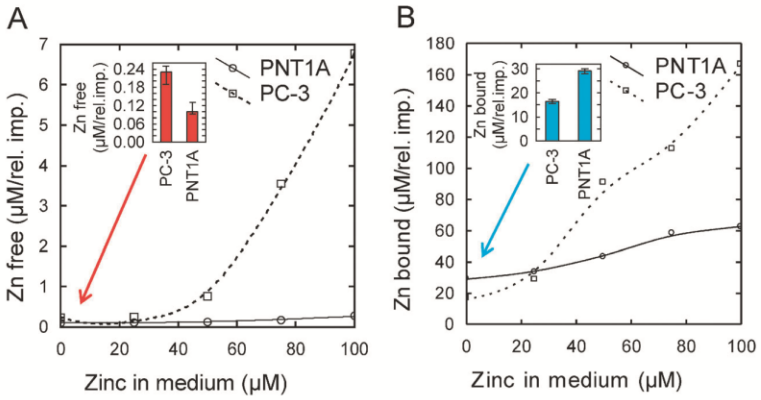

Fig. 4 Intracellular zinc in cell lines. (A) Intracellular free zinc(II) content in human prostate cells human prostatic tumour (PC-3) and normal prostatic (PNT1A) cells treated with 0–100 μM of zinc(II) sulphate. Both cell lines elevate intracellular free(II) zinc. Intracellular free zinc(II) content in untreated samples (A, inset, mean ± SD), significantly higher free zinc in PC-3 cell line. (B) Response to zinc, intracellular bound zinc fraction; bound zinc(II) in untreated samples (B, inset, mean ± SD). Untreated PC-3 cell lines show lower bound zinc, but demonstrate more distinct increase when treated.

by zinc(II) (not shown). Localisation of free zinc(II) is also well visible – at the lowest concentration (25 μM) around nuclei (Golgi, endoplasmic reticulum) and in nuclei. With increasing zinc(II) concentration, increase in the level of free zinc(II) around nuclei is visible. In comparison with tumour cell line PC-3, PNT1A cells did not demonstrate localisation of free zinc(II) in the form of spots.

Effect of zinc(II) on the expression of MT1 and MT2 mRNA and protein levels in prostate cells

Further, this study was focused on two MT isoforms (MT1A and MT2A) at the RNA level and at the level of translated proteins. It is shown in Fig. 5 that zinc(II) treatment has different effects on transcriptional and translational levels of MT1 and MT2 in prostate cells. The zinc(II) effect on the transcription level of MT1 and MT2 was studied by RT-PCR. We found no significant difference ($p > 0.05$) in MT1A and MT2A mRNA levels between cell lines (Fig. 5C). When the level of MT isoforms is compared, significantly ($p < 0.001$) a higher MT2A mRNA level (12-fold) is found in both cell lines. No distinct level change of MT1A mRNA isoform was observed when exposed to zinc(II) treatment (Fig. 5A). In contrast, significant up-regulation of MT2A isoform was observed in PC-3 ($r = 0.99$; $p = 0.001$) and PNT1A ($r = 0.89$; $p = 0.039$) cell lines (Fig. 5B). More distinct elevation in MT2A class mRNA was observed in the PC-3 cell line (80-fold).

Then the MT1 and MT2 at a protein level using western blot assay were determined (Fig. 5F). When treated with zinc(II), the PC-3 cell line showed >4-fold increase in the MT level. In the PNT1A cell line, no such trend was observed. To refine the detection of MT by a sensitive method, the level of endogenous MT1 and MT2 proteins using differential pulse voltammetry Brdicka reaction was determined.[14] To normalise the protein content, values were related to viable cell count (relative impedance determined by xCELLigence assay (MT concentration nM/relative impedance)). Untreated PC3 cells produced 3.6-fold more MT protein as compared to PNT1A cells (Fig. 5E, inset), 15.6 ± 1.1 ng per rel. imp. and 4.2 ± 0.2 ng per rel. imp., respectively. After zinc(II) treatment apparent differences in MT protein in cell lines were observed. Whilst the PNT1A cell line showed mild 4.2-fold increase after zinc(II) treatment (17.7 ± 0.9 ng per rel. imp. MT at 100 μM zinc(II) concentration, positive correlation at $r = 0.94$ and $p = 0.005$), the PC-3 cell line showed more distinct increase in the MT protein level after the treatment. When PC-3 cells were treated with 100 μM zinc(II), 147.2 ± 3.2 ng per rel. imp. MT1 and MT2, *i.e.* tenfold increase was observed. Thus, these results were in good accordance with western blot analysis. Our results show that MT2 RNA and MT protein maintain the same increasing trend in both cell lines (Fig. 5B and E) and thus significant correlation ($r = 0.94$ at $p = 0.017$) was observed. However, although a similar increasing trend was observed in the PNT1A cell line, it was below the level of statistical significance ($r = 0.72$; $p = 0.102$).

Cell redox state

Microscopic detection of proteins with free –SH groups is enabled by the use of the specific probe 5-(bromomethyl)fluorescein, which includes formation of the fluorescent product after reaction with –SH groups of thiols. In the PNT1A non-tumour cells, the amount of proteins with free –SH groups continually decreases with increasing zinc(II) ions supplementation. At the highest concentration, proteins with free –SH groups are visible practically only in newly originated cells, whereas in older cells their amount is only omissible. In this cell line, distribution of thiols takes place especially around nuclei and in nuclei, and is limited in peripheral parts of cells. Compared to PNT1A, contradictory results were obtained for the tumour PC-3 cell line: increasing supplementation of cultivation medium by zinc(II) ions led to increased synthesis of proteins with free thiol group/groups localised in nuclei and especially around nuclei in endoplasmic reticulum and Golgi apparatus (not shown).

Discussion

Real-time monitoring of cell adhesion and proliferation using the xCELLigence system

Standard methods for cell viability or proliferation determination include time-consuming end-point analysis assays of

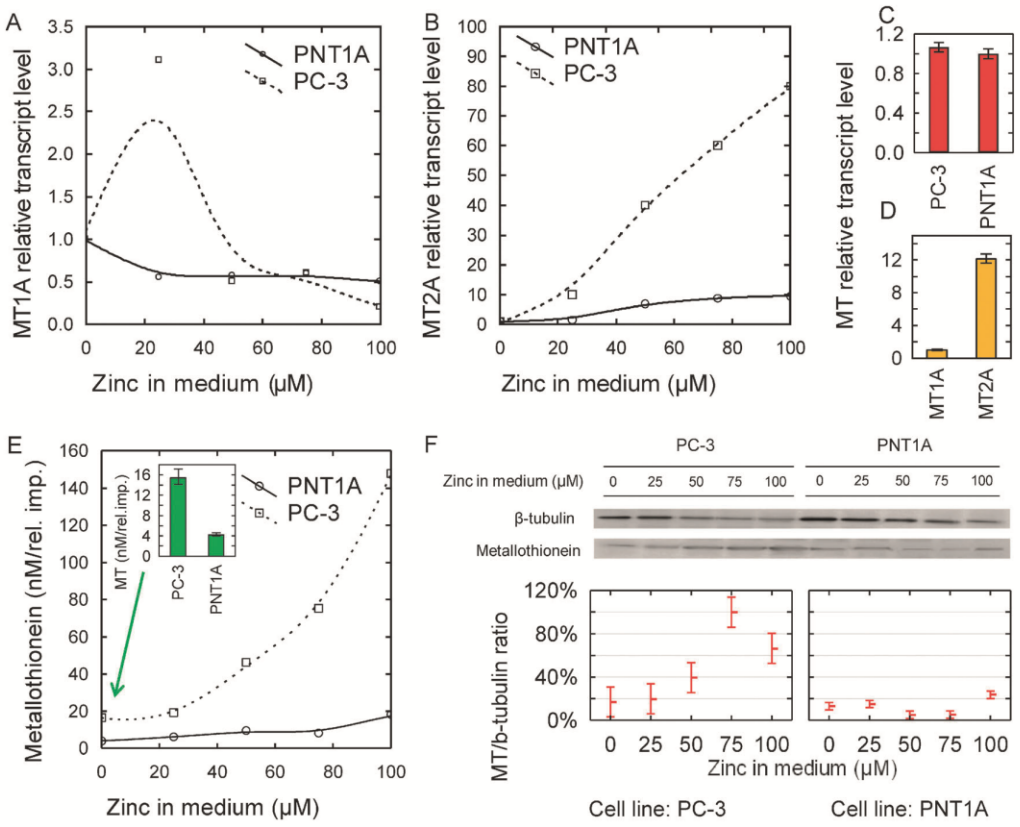

Fig. 5 Determination of MT1A and MT2A expression in PNT1A and PC-3 cells by qRT-PCR and MT1/2 by Western blot analysis and electrochemistry. Metallothionein MT1A (A) and MT2A (B) isoform mRNA levels in cell lines exposed to zinc(II) treatment, (C) total relative MT mRNA levels in untreated samples, (D) relative levels of MT1A and MT2A in untreated samples, (E) metallothionein protein levels exposed to zinc and in untreated samples (inset, displayed as mean ± SD), (F) Western-blot MT detection. Level of MT displayed as a ratio to β-tubulin from the same samples.

whole cell populations (MTT or XTT assays) and advanced techniques of analysis of individual cells (flow cytometry or digital microscopic techniques and image analysis). However, these techniques are not capable of registering very small and rapid changes in cellular morphology.[15] Most of the studied compounds used for various cell treatments in experiments have different effects not only on cell viability but also on cell proliferation, cell adhesion and spreading. These effects are highly dynamic and may also show differences in various cell types. This is evident from different values of IC_{50} obtained by MTT and xCELLigence assays (1.3- and 1.7-fold higher in PNT1A and in PC-3 when using MTT assay). More pronounced difference in PC-3 may be explained by decrease of its cell size in relation to zinc(II) treatment compared to PNT1A, where no size change is observed (Fig. 3D). In the case of the PNT1A cell line, under 25 μM zinc(II) treatment the relative impedance is approx. 5% increased as it is evident from proliferation assay. It is evident from Fig. 3C and D that average cell area of PNT1A cells is relatively stable but number of cells increased. Such 5% increase of impedance therefore represents a higher cell proliferation rate in PNT1A cells (higher cell concentration *vs.* stable cell size).

It may be concluded from the present findings that the xCELLigence assay reflects more the cell concentration than its MTT-based metabolic activity. This conclusion is supported by the fact that xCelligence correlates significantly with the cell count and not with MTT results. We believe that determination of cell viability/cytotoxicity of compounds used in experiments by conventional methods like MTT or XTT is not sufficient. It brings out only end-point analysis of the state of whole cell populations which cannot capture important effects of treatments on proliferation dynamics. Here we demonstrated that the xCELLigence system represents an ideal tool for identification of the onset and the rate of cytotoxicity and for determination of the optimal time point for further molecular and biochemical analyses of cellular events. Moreover, the real-time data stream of the xCELLigence system provides a continuous, label-free measure of cell culture quality.

Zinc, metallothionein and redox state

It has been demonstrated in numerous studies that healthy prostate tissue accumulates a distinctly higher zinc(II) content compared to other cells and this accumulation is altered in prostate cancer tissue.[1a,c] These findings are summarised in the work by Costello and Franklin.[10] They reported that the mean decrease of tissue zinc(II) in cancer tissue compared to healthy tissue is −62% ± 5%. In healthy tissue, a high zinc(II) level is

crucial for the proper functioning and proliferation of the gland.[16] The high level induces apoptosis and inhibits cell growth, whereas the lower level may create an environment more suitable for tumour progression.[17] Zinc transporters, notably ZIP1, play a key role in zinc(II) accumulation and some of them (to date described in ZIP1–3) are down-regulated in prostate cancer. They can therefore be considered as tumour suppressors.[18]

To date, there has been only limited evidence studying zinc(II) levels and effects of zinc(II) treatment on prostate cancer cell line PC-3 and no evidence studying zinc(II) levels in healthy prostate cell line PNT1A. We have demonstrated approx. −48% decrease of (bound) zinc(II) content in prostate cancer cell line PC-3 in comparison to non-tumour PNT1A. According to the study by Feng *et al.*, the intracellular zinc(II) level in the PC-3 cell line is decreased −53% compared to non-tumour HPR-1 cell lines.[17a] Although different non-tumorous cell lines were used in this study, the authors obtained similar results. Our results are also in good agreement with results obtained from *in vivo* biopsies in 16 studies summarised by Costello and Franklin[10] (see the previous paragraph) suggesting that PC-3 and PNT1A cell lines may represent zinc(II) buffering conditions *in vivo*.

When exposed to zinc treatment, we observed elevation of both bound and free zinc(II) fractions in both cell lines suggesting that even tumour PC-3 cell line has retained zinc-transport mechanisms. Interestingly, tumour cell line PC-3 shows much more distinct increase in free and bound zinc fractions compared to PNT1A. When treated with 100 μM zinc(II), elevation of intracellular bound zinc levels up to the two-fold concentrations of non-tumour cell line PNT1A was observed in PC-3 (compare Fig. 4A and B). This trend was not only occurring in the bound zinc(II) fraction, but also free zinc(II) demonstrated a similar trend. However, under these conditions (100 μM zinc(II) treatment) the PC-3 cell line retains only approx. 3% viability compared to the untreated sample (Fig. 3A, Table 1). In contrast, the PNT1A cell line still retains high viability when treated with 100 μM zinc(II) (88%). According to these results, it is possible to argue that the increased rate of apoptosis/necrosis is associated rather with an increased relative ratio of intracellular zinc(II) (ratio of zinc after treatment/zinc before treatment) than only with the absolute amount of zinc(II) treatment concentration in the medium. This may be evidenced from the fact that there is an elevation of bound zinc (2.7-fold and 5-fold for PNT1A and PC-3, respectively) after exposure to concentrations equal to IC_{50} of these lines (150 μM and 56 μM for PNT1A and PC3, respectively). This is in agreement with the study by Feng *et al.*, which has previously demonstrated a similar difference between tumour and non-tumour cell lines – exposure to zinc induced apoptosis in PC-3 and BPH cells, which accumulate high intracellular levels of zinc(II), but not in HPR-1 cells, which do not accumulate high levels of zinc(II).[17a]

For visualization of general cytology and distribution of free zinc(II) and thiols with free –SH groups, a modified method of cell cultivation directly on microscopic slides was used. This technique enables easy manipulation of cells growing in monolayers including staining and washing steps as well as excellent visualization of cell structures without the necessity of usage of confocal microscopy.[19] Microscopic observations in our study fully confirmed precise analytical data and enabled localisation (not shown) of structures and compounds of interest directly in studied cells. Regarding the results of electrochemistry and microscopy, similar increasing trends in free zinc(II) levels were observed in both cell lines after zinc(II) treatment. Also more intense fluorescence in the PNT1A cell line was observed where higher free zinc(II) content was determined using electrochemistry. In PC-3 cells, decrease of emission is probably caused by their linkage to competent proteins. At other zinc(II) concentrations intensity of emission increases. Generally, distribution of free zinc(II) ions in PC-3 cells is well evident in cytoplasm surrounding nuclei and in nuclei, where zinc(II) ions play a crucial role in activation and/or regulation of transcription due to formation of zinc(II) fingers. In comparison to tumour cell line PC-3, PNT1A cells did not demonstrate localisation of free zinc(II) in the form of spots. These results are partly in agreement with the studies by Feng *et al.*[17a,20] and Wei *et al.*,[21] which demonstrated 4.3-fold elevation of zinc(II) levels in PC-3 after 15 μM (exactly 1 μg ml^{-1}) zinc(II) treatment. Intracellular zinc(II) elevation was determined as 1.5-fold increase (under 25 μM zinc(II) treatment). According to our knowledge, no previous study did show effects of zinc(II) treatment on PNT1A cell lines and therefore our findings cannot be compared to any other results. The above-mentioned work by Feng *et al.* used the HPR-1 cell line as a model of non-tumorous tissue. To date, prostate-specific direct effects of zinc(II) on apoptosis have been well-identified and are discussed in the following reviews.[20,22]

When fluorescent microscopy was utilised in the determination of RNA biosynthesis, notable differences, probably connected with zinc(II) ions treatment, were evident. Whereas increased RNA synthesis in PNT1A is evident under higher zinc(II) ion concentrations, increased RNA synthesis in tumour cell line PC-3 is well evident at all concentrations (not shown). In comparison to nucleoli of both cell lines, sites of RNA localization are well evident in control and all treated cells of tumour cell line PC-3. In non-tumour PNT1A cells, nucleoli are visible only at the two highest zinc(II) concentrations, which also correspond to increased RNA biosynthesis at these two concentrations. This fact may be connected with the response of non-tumour PNT1A cells to zinc(II) treatment and resistance of tumour PC-3 cells to zinc(II) ions. This response does not necessarily result in enhanced biosynthesis of thiol compounds (including MTs), but it may also result in synthesis of non-thiol proteins connected with stress (triggered by zinc(II) ions and proteins connected to cellular responses to stress factors, such as proteins of the apoptosis pathway).

Significantly higher MT protein content in the PC-3 cell line was observed compared to the PNT1A cell line in untreated, *e.g.* control samples. Interestingly, no significant difference between cell lines was determined at the mRNA level (compare Fig. 5C and the inset in Fig. 5E). This fact implies that another regulating mechanism in post-translation exists in PC-3 and PNT1A cell lines. Such a regulation mechanism can be based on small RNAs.[23] Inasmuch as MT binds zinc(II) and bound zinc(II) levels are higher in the PC-3 cell line, it is obvious that

MT levels should be higher in this cell line. Binding of "free" zinc(II) ions by MTs diminishes the amount of this metal available to generate free radicals, especially reactive oxygen and nitrogen species.[24] This is in contradiction with the study by Wei *et al.* which also showed a significantly lower MT1/2 protein level in the PC-3 cell line. However, this study used the non-tumour HPR-1 cell line as a control.[21] To date, no study determined the metallothionein content in PNT1A cell lines; comparison with other cell lines gives therefore only approximate results.

When cell lines are treated with zinc(II), increased MT2A mRNA and protein levels in both cell lines and no changes in MT1A mRNA are observed. In our recent studies we found out that MT2A is a major MT isoform in healthy and tumour prostate cell lines PNT1A and 22Rv1.[25] This study show similar results – MT2A is a dominant isoform also in the PC-3 cell line (Fig. 5D). Thus, this explains the fact that a correlation between mRNA and protein is only in MT2A isoform. Interestingly, PC-3 cells exhibit enhanced increase in MT mRNA and protein compared to PNT1A cells. This increase apparently corresponds to the enhanced elevation of endogenous zinc(II) levels after zinc(II) treatment in this cell line, however, it is caused by different expression of zinc(II) transport proteins, the MT-regulating miRNAs, or other mechanisms that have been unknown to date. Using fluorescent microscopy, we observed an increase of –SH fluorescence in the zinc(II)-treated PC-3 cell line and no such distinct changes in fluorescence were observed in the PNT1A cell line, which is in accordance with increasing trend of MT. These findings are in good agreement with works by Wei *et al.*, Hasumi *et al.*, Lin *et al.*, Iguchi *et al.* and Yamasaki *et al.*, who in general demonstrated up-regulation of MT expression when exposed to zinc(II) treatment or other stress stimuli.[16b,21,26] Wei *et al.* reported up-regulation of MT gene expression in PC-3 when exposed to zinc(II) treatment. Similarly, Hasumi *et al.* and Iguchi *et al.* found that MT gene expression is zinc-inducible.[16b,26a] Our results are also in agreement with the work by Yamasaki *et al.*, who found up-regulated MT-2A expression in the PC-3 cell line under stress conditions such as hypoxia.[27] A study by Lin *et al.* determined expression of various MT1 isoforms after loading 20 μM zinc(II) in the PC-3 cell line.[26b] Interestingly, this study showed only up-regulation of MT-1J and MT-1M gene expression when exposed to zinc(II) and no significant change in MT-1A gene expression when exposed to zinc(II). These data suggest that zinc(II) may act as an isoform-specific MT inductor.

The GSH–GSSG redox pair can be efficiently coupled with MTs and thus can protect cells against oxidative stress (ROS).[4b] Therefore monitoring of the GSH–GSSG ratio with determination of MTs may represent an effective tool for studying zinc(II) effects on cell redox potential. Biological disulphides such as oxidized glutathione (GSSG) oxidize MTs with a concomitant release of zinc, while reduced glutathione (GSH) reduces the oxidized protein to thionein, which then binds the free zinc(II) ions.[28] Conversely, thiol depletion is associated with activating caspase-3 and thus apoptosis.[29] In our experiments, we found some changes in the thiol-containing peptides and proteins and their further study will be needed.

Conclusions

In this study, characteristics of prostatic cell lines PC-3 and PNT1A exposed to zinc(II) treatment determined by novel real-time monitoring system xCELLigence are provided. This system allows description of the cell lines response to metal toxicity more precisely as compared to commonly used end-point assays. Significant differences in IC_{50} determination were found using both methods due to dependence of impedance assay on cell morphology, cell adhesion and cell count and due to changes of those variables when treated with zinc(II). To date, there has been no evidence of the PNT1A cell line in response to zinc(II). Furthermore, elevation of intracellular bound and free zinc(II) in these cell lines after zinc(II) treatment was observed. These results are in good agreement with published studies. Also, the detected level of metallothionein is in agreement with most published results. In our experiments, increased levels of MTs in PC-3 and PNT1A cell lines were found; published results describe in general similar elevation of MTs when exposed to stress conditions such as heavy metals, reactive oxygen species or hypoxia. We also found differences in the GSH–GSSG system between cell lines – zinc(II) treatment caused elevation of reduced thiols in non-tumorous PNT1A cell lines, and no change of thiols in tumorous PC-3 cell lines. This study also demonstrated a comparison of fluorescence microscopy with precise electrochemical techniques and real-time PCR in the determination of intracellular zinc(II) and thiols with a good agreement in results. If employed together, these methods provide accurate information for zinc(II) fluxes, their buffering by thiol compounds and monitoring of the redox state in cell lines or tissues. Thus, an integrated approach with these methods for detection of thiols and heavy metals may be a powerful tool for understanding the role of oxidative stress in carcinogenesis.

Acknowledgements

This work has been supported by the following projects GACR 301/09/P436, NanoBioTECell GA CR P102/11/1068, IGA VFU 43/2011/FaF and CEITEC CZ.1.05/1.1.00/02.0068.

References

1 (*a*) L. Costello and R. Franklin, The intermediary metabolism of the prostate: a key to understanding the pathogenesis and progression of prostate malignancy, *Oncology*, 2000, **59**, 269–282; (*b*) F. K. Habib, Evaluation of androgen metabolism studies in human prostate cancer–correlation with zinc levels, *Prev. Med.*, 1980, **9**, 650–656; (*c*) V. Y. Zaichick, T. V. Sviridova and S. V. Zaichick, Zinc in human prostate gland: Normal, hyperplastic and cancerous, *J. Radioanal. Nucl. Chem.*, 1997, **217**, 157–161.

2 (*a*) D. Beyersmann and H. Haase, Functions of zinc in signaling, proliferation and differentiation of mammalian cells, *Biometals*, 2001, **14**, 331–341; (*b*) D. E. Baranano, C. D. Ferris and S. H. Snyder, Atypical neural messengers, *Trends Neurosci.*, 2001, **24**, 99–106; (*c*) C. Hogstrand, P. Kille, R. I. Nicholson and K. M. Taylor, Zinc transporters and cancer: a potential role for ZIP7 as a hub for tyrosine kinase activation, *Trends Mol. Med.*, 2009, **15**, 101–111.

3 R. A. Colvin, W. R. Holmes, C. P. Fontaine and W. Maret, Cytosolic zinc buffering and muffling: Their role in intracellular zinc homeostasis, *Metallomics*, 2010, **2**, 306–317.

4 (*a*) P. J. Thornalley and M. Vasak, Possible Role for Metallothionein in Protection against Radiation-Induced Oxidative Stress – Kinetics and Mechanism of Its Reaction with Superoxide and

Hydroxyl Radicals, *Biochim. Biophys. Acta*, 1985, **827**, 36–44; (*b*) T. Eckschlager, V. Adam, J. Hrabeta, K. Figova and R. Kizek, Metallothioneins and Cancer, *Curr. Protein Pept. Sci.*, 2009, **10**, 360–375; (*c*) S. Krizkova, P. Blahova, J. Nakielna, I. Fabrik, V. Adam, T. Eckschlager, M. Beklova, Z. Svobodova, V. Horak and R. Kizek, Comparison of Metallothionein Detection by Using Brdicka Reaction and Enzyme-Linked Immunosorbent Assay Employing Chicken Yolk Antibodies, *Electroanalysis*, 2009, **21**, 2575–2583.

5 S. Krizkova, I. Fabrik, V. Adam, P. Hrabeta, T. Eckschlager and R. Kizek, Metallothionein—a promising tool for cancer diagnostics, *Bratislava Med. J.*, 2009, **110**, 93–97.

6 (*a*) V. Adam, I. Fabrik, T. Eckschlager, M. Stiborova, L. Trnkova and R. Kizek, Vertebrate metallothioneins as target molecules for analytical techniques, *TrAC, Trends Anal. Chem.*, 2010, **29**, 409–418; (*b*) V. Adam, J. Petrlova, J. Wang, T. Eckschlager, L. Trnkova and R. Kizek, Zeptomole Electrochemical Detection of Metallothioneins, *PloS One*, 2010, **5**, 569.

7 (*a*) K. Sigler, J. Chaloupka, J. Brozmanova, N. Stadler and M. Hofer, Oxidative stress in microorganisms – I – Microbial *vs.* higher cells – Damage and defenses in relation to cell aging and death, *Folia Microbiol. (Dordrecht, Neth.)*, 1999, **44**, 587–624; (*b*) P. Storz, Reactive oxygen species in tumor progression, *Front. Biosci.*, 2005, **10**, 1881–1896.

8 K. Kubo, Y. Sakita and T. Minami, Effect of heat treatment on metallothionein isoforms using capillary zone electrophoresis, *Analysis*, 2000, **28**, 366–369.

9 (*a*) D. Potesil, J. Petrlova, V. Adam, J. Vacek, B. Klejdus, J. Zehnalek, L. Trnkova, L. Havel and R. Kizek, Simultaneous femtomole determination of cysteine, reduced and oxidized glutathione, and phytochelatin in maize (*Zea mays L.*) kernels using high-performance liquid chromatography with electrochemical detection, *J. Chromatogr., A*, 2005, **1084**, 134–144; (*b*) J. Petrlova, R. Mikelova, K. Stejskal, A. Kleckerova, O. Zitka, J. Petrek, L. Havel, J. Zehnalek, V. Adam, L. Trnkova and R. Kizek, Simultaneous determination of eight biologically active thiol compounds using gradient elution-Liquid Chromatography with Coul-Array detection, *J. Sep. Sci.*, 2006, **29**, 1166–1173.

10 L. C. Costello and R. B. Franklin, Zinc is decreased in prostate cancer: an established relationship of prostate cancer!, *J. Biol. Inorg. Chem.*, 2011, **16**, 3–8.

11 R. J. Keogh, New technology for investigating trophoblast function, *Placenta*, 2010, **31**, 347–350.

12 K. Kusuzaki, H. Murata, H. Takeshita, S. Hashiguchi, T. Nozaki, K. Emoto, T. Ashihara and Y. Hirasawa, Intracellular binding sites of acridine orange in living osteosarcoma cells, *Anticancer Res.*, 2000, **20**, 971–975.

13 K. Lange, R. Herken, K. Keller and H. Herken, Distribution of Acridine Orange-Stained RNA in Neuroblastoma-Cells during Differentiation, *Naunyn-Schmiedeberg's Arch. Pharmacol.*, 1977, **298**, 259–262.

14 I. Fabrik, S. Krizkova, D. Huska, V. Adam, J. Hubalek, L. Trnkova, T. Eckschlager, J. Kukacka, R. Prusa and R. Kizek, Employment of electrochemical techniques for metallothionein determination in tumor cell lines and patients with a tumor disease, *Electroanalysis*, 2008, **20**, 1521–1532.

15 (*a*) E. Urcan, U. Haertel, M. Styllou, R. Hickel, H. Scherthan and F. X. Reichl, Real-time xCELLigence impedance analysis of the cytotoxicity of dental composite components on human gingival fibroblasts, *Dent. Mater.*, 2010, **26**, 51–58; (*b*) J. J. Quereda, L. Martinez-Alarcon, L. Mendoca, M. J. Majado, J. M. Herrero-Medrano, F. J. Pallares, A. Rios, P. Ramirez, A. Munoz and G. Ramis, Validation of xCELLigence Real-Time Cell Analyzer to Assess Compatibility in Xenotransplantation With Pig-to-Baboon Model, *Transplant. Proc.*, 2010, **42**, 3239–3243; (*c*) L. Vistejnova, J. Dvorakova, M. Hasova, T. Muthny, V. Velebny, K. Soucek and L. Kubala, The comparison of impedance-based method of cell proliferation monitoring with commonly used metabolic-based techniques, *Neuroendocrinol. Lett.*, 2009, **30**, 121–127.

16 (*a*) S. Y. Hess, B. Lonnerdal, C. Hotz, J. A. Rivera and K. H. Brown, Recent advances in knowledge of zinc nutrition and human health, *Food Nutr. Bull. Suppl.*, 2009, **30**, S5–S11; (*b*) M. Hasumi, K. Suzuki, H. Matsui, H. Koike, K. Ito and H. Yamanaka, Regulation of metallothionein and zinc transporter expression in human prostate cancer cells and tissues, *Cancer Lett.*, 2003, **200**, 187–195; (*c*) Z. M. Bataineh, I. H. B. Hani and J. R. Al-Alami, Zinc in normal and pathological human prostate gland, *Saudi Med. J.*, 2002, **23**, 218–220.

17 (*a*) P. Feng, T. L. Li, Z. X. Guan, R. B. Franklin and L. C. Costello, Direct effect of zinc on mitochondrial apoptogenesis in prostate cells, *Prostate*, 2002, **52**, 311–318; (*b*) R. G. Uzzo, P. Leavis, W. Hatch, V. L. Gabai, N. Dulin, N. Zvartau and V. M. Kolenko, Zinc inhibits nuclear factor-kappa B activation and sensitizes prostate cancer cells to cytotoxic agents, *Clin. Cancer Res.*, 2002, **8**, 3579–3583.

18 (*a*) R. B. Franklin, P. Feng, B. Milon, M. M. Desouki, K. K. Singh, A. Kajdacsy-Balla, O. Bagasra and L. C. Costello, hZIP1 zinc uptake transporter down regulation and zinc depletion in prostate cancer, *Mol. Cancer*, 2005, **4**, 1–13; (*b*) T. Kambe, Y. Yamaguchi-Iwai, R. Sasaki and M. Nagao, Overview of mammalian zinc transporters, *Cell. Mol. Life Sci.*, 2004, **61**, 49–68; (*c*) R. B. Franklin, J. Ma, J. Zou, Z. Guan, B. I. Kukoyi, P. Feng and L. C. Costello, Human ZIP1 is a major zinc uptake transporter for the accumulation of zinc in prostate cells, *J. Inorg. Biochem.*, 2003, **96**, 435–442; (*d*) B. C. Milon, A. Agyapong, R. Bautista, L. C. Costello and R. B. Franklin, Ras Responsive Element Binding Protein-1 (RREB-1) Down-regulates hZIP1 Expression in Prostate Cancer Cells, *Prostate*, 2010, **70**, 288–296.

19 J. Vitecek, J. Petrlova, V. Adam, L. Havel, K. J. Kramer, P. Babula and R. Kizek, A fluorimetric sensor for detection of one living cell, *Sensors*, 2007, **7**, 222–238.

20 P. Feng, T. L. Li, Z. X. Guan, R. B. Franklin and L. C. Costello, The involvement of bax in zinc-induced mitochondrial apoptogenesis in malignant prostate cells, *Mol. Cancer*, 2008, **7**, 1–6.

21 H. Wei, M. M. Desouki, S. Lin, D. Xiao, R. B. Franklin and P. Feng, Differential expression of metallothioneins (MTs) 1, 2, and 3 in response to zinc treatment in human prostate normal and malignant cells and tissues, *Mol. Cancer*, 2008, **7**, 1–11Artn 7.

22 (*a*) J. Gumulec, M. Masarik, S. Krizkova, V. Adam, J. Hubalek, J. Hrabeta, T. Eckschlager, M. Stiborova and R. Kizek, Insight to physiology and pathology of zinc(II) ions and their actions in breast and prostate carcinoma, *Curr. Med. Chem.*, 2011, **18**, 5041–5051; (*b*) J. Y. Liang, Y. Y. Liu, J. Zou, R. B. Franklin, L. C. Costello and P. Feng, Inhibitory effect of zinc on human prostatic carcinoma cell growth, *Prostate*, 1999, **40**, 200–207.

23 (*a*) N. Rabiau, H. K. Trraf, M. Adjakly, R. Bosviel, L. Guy, L. Fontana, Y. J. Bignon and D. J. Bernard-Gallon, miRNAs Differentially Expressed in Prostate Cancer Cell Lines after Soy Treatment, *In Vivo*, 2011, **25**, 917–921; (*b*) P. Ostling, S. K. Leivonen, A. Aakula, P. Kohonen, R. Makela, Z. Hagman, A. Edsjo, S. Kangaspeska, H. Edgren, D. Nicorici, A. Bjartell, Y. Ceder, M. Perala and O. Kallioniemi, Systematic Analysis of MicroRNAs Targeting the Androgen Receptor in Prostate Cancer Cells, *Cancer Res.*, 2011, **71**, 1956–1967.

24 (*a*) S. G. Bell and B. L. Vallee, The Metallothionein/Thionein System: An Oxidoreductive Metabolic Zinc Link, *Chembiochem*, 2009, **10**, 55–62; (*b*) S. K. Baird, T. Kurz and U. T. Brunk, Metallothionein protects against oxidative stress-induced lysosomal destabilization, *Biochem. J.*, 2006, **394**, 275–283; (*c*) J. C. Amiard, C. Amiard-Triquet, S. Barka, J. Pellerin and P. S. Rainbow, Metallothioneins in aquatic invertebrates: Their role in metal detoxification and their use as biomarkers, *Aquat. Toxicol.*, 2006, **76**, 160–202; (*d*) M. Ebadi, M. P. Leuschen, H. ElRefaey, F. M. Hamada and P. Rojas, The antioxidant properties of zinc and metallothionein, *Neurochem. Int.*, 1996, **29**, 159–166.

25 J. Gumulec, M. Masarik, S. Krizkova, M. Hlavna, P. Babula, R. Hrabec, A. Rovny, M. Masarikova, J. Sochor, V. Adam, T. Eckschlager and R. Kizek, Evaluation of alpha-methylacyl-CoA racemase, metallothionein and prostate specific antigen as prostate cancer prognostic markers, *Neoplasma*, 2012, **59**, 191–200.

26 (*a*) K. Iguchi, M. Hamatake, R. Ishida, Y. Usami, T. Adachi, H. Yamamoto, K. Koshida, T. Uchibayashi and K. Hirano, Induction of necrosis by zinc in prostate carcinoma cells and identification of proteins increased in association with this induction, *Eur. J. Biochem.*, 1998, **253**, 766–770; (*b*) S. F. Lin, H. Wei, D. Maeder, R. B. Franklin and P. Feng, Profiling of zinc-altered

gene expression in human prostate normal *vs.* cancer cells: a time course study, *J. Nutr. Biochem.*, 2009, **20**, 1000–1012.
27 S. Yamasaki, K. Sakata-Sogawa, A. Hasegawa, T. Suzuki, K. Kabu, E. Sato, T. Kurosaki, S. Yamashita, M. Tokunaga and K. Nishida, Zinc is a novel intracellular second messenger, *J. Cell Biol.*, 2007, **177**, 637.
28 D. Huska, O. Zitka, V. Adam, M. Beklova, S. Krizkova, L. Zeman, A. Horna, L. Havel, J. Zehnalek and R. Kizek, A sensor for investigating the interaction between biologically important heavy metals and glutathione, *Czech J. Anim. Sci.*, 2007, **52**, 37–43.
29 R. N. T. Coffey, R. W. G. Watson, N. J. Hegarty, A. O'Neill, N. Gibbons, H. R. Brady and J. M. Fitzpatrick, Thiol-mediated apoptosis in prostate carcinoma cells, *Cancer (N. Y.)*, 2000, **88**, 2092–2104.
30 R. B. Franklin and L. C. Costello, The Important Role of the Apoptotic Effects of Zinc in the Development of Cancers, *J. Cell. Biochem.*, 2009, **106**, 750–757.

INTERNATIONAL JOURNAL OF ONCOLOGY 44: 923-933, 2014

Cisplatin-resistant prostate cancer model: Differences in antioxidant system, apoptosis and cell cycle

JAROMIR GUMULEC[1,4], JAN BALVAN[1], MARKETA SZTALMACHOVA[1,2], MARTINA RAUDENSKA[1,4], VERONIKA DVORAKOVA[1], LUCIA KNOPFOVA[3], HANA POLANSKA[1], KRISTYNA HUDCOVA[1], BRANISLAV RUTTKAY-NEDECKY[2,4], PETR BABULA[5], VOJTECH ADAM[2,4], RENE KIZEK[2,4], MARIE STIBOROVA[6] and MICHAL MASARIK[1,4]

[1]Department of Pathological Physiology, Faculty of Medicine, Masaryk University, CZ-625 00 Brno; [2]Department of Chemistry and Biochemistry, Mendel University in Brno, CZ-613 00 Brno; [3]Department of Experimental Biology, Faculty of Science, Masaryk University, CZ-625 00 Brno; [4]Central European Institute of Technology, Brno University of Technology, CZ-616 00 Brno; [5]Department of Natural Drugs, Faculty of Pharmacy, University of Veterinary and Pharmaceutical Sciences, CZ-612 42 Brno; [6]Department of Biochemistry, Faculty of Science, Charles University, CZ-128 40 Prague 2, Czech Republic

Received September 24, 2013; Accepted November 11, 2013

DOI: 10.3892/ijo.2013.2223

Abstract. Differences in the antioxidant system, apoptotic mechanism and in cell cycle between prostatic cell lines could partially elucidate the development of cisplatin resistance. The aim of this study was to identify the most characteristic parameter for a particular cell line and/or a particular cisplatin treatment using a general regression model and to assess whether it is possible to use measured parameters as markers of cisplatin resistance. This study integrates the results of viability, antioxidant, flow cytometric and quantitative PCR assays in order to characterize the resistance of prostate cancer to cisplatin. Cell growth using metabolic- (MTT) and impedance-based assays, the expression of key cell death signaling proteins (p53, Bax and Bcl-2), cell cycle, activity of antioxidant system-related proteins (superoxide dismutase, glutathione peroxidase, glutathione reductase and metallothionein) and free radical scavenging capacity assays [free radicals (FR), ferric reducing antioxidant power (FRAP), ABTS] were analyzed in the cell lines 22Rv1, PC-3 and PNT1A with respect to rising concentrations (0-150 μM) and different length of cisplatin treatment (12-72 h). The non-functional-p53 PC-3 cell line showed decreased BAX ($p<0.05$) and, in contrast to PNT1A and 22Rv1, no cisplatin-induced effects on cell cycle. All cell lines showed increasing levels of free radical scavenging activity by ABTS, FRAP and FR assays in a time- and dose-dependent manner ($r>0.76$ at $p<0.001$ for ABTS, FRAP and FR at $p<0.001$). PC-3 showed increased ($p<0.05$) levels of free radical scavenging activity by ABTS and FR methods. These findings, together with significantly elevated MT, decreased p53 and Bax indicate PC-3 to be cisplatin-resistant. The differences in the antioxidant system and apoptotic mechanisms in PC-3 cells may elucidate the development of cisplatin resistance and indicate that this cell line may be further studied as a model of cytostatic resistance.

Correspondence to: Dr Michal Masarik, Department of Pathological Physiology, Faculty of Medicine, Masaryk University, Kamenice 5, CZ-625 00 Brno, Czech Republic
E-mail: masarik@med.muni.cz

Key words: prostate cancer, cell cycle, resistance, cisplatin, oxidative stress

Introduction

Cis-diamminedichloroplatinum or cisplatin is an inorganic compound that is widely used as a therapy of cancers. The biochemical mechanisms of cisplatin cytotoxicity involve the binding of the drug to DNA and non-DNA targets and the subsequent induction of cell death through apoptosis, necrosis, or both (1). It follows that altered expression of regulatory proteins involved in signal transduction pathways that control the apoptosis, necrosis or cell defense mechanisms (Fig. 1) can additionally make certain types of cancer rather insensitive to cytotoxic effects of cisplatin (2,3), which is, among others, case of later stages of prostate cancer. Cellular mechanisms of resistance to cisplatin are multifactorial and result in severe limitations in clinical use (4-6). Therefore, cisplatin resistance model was formed from prostatic cell lines PNT1A, PC-3, and 22Rv1 in this study. The PC-3 cell line was derived from a metastasis of a high grade androgen irresponsive prostate cancer. Cisplatin resistance is presumed in these cells due non-functional p53 (7). Tumor suppressor protein p53 plays a critical role in regulating cell cycle arrest, DNA repair and apoptosis (8). Accordingly, tumor cells lacking functional p53 were found more resistant to cisplatin than cells that contained functional p53 and the resistant cell lines were sensitized to cisplatin upon reconstitution with wild-type p53 (9).

Among other alterations in cellular response to the cisplatin, oxidative stress might be triggered (10,11). In previous studies, the central role of mitochondria damage in the cisplatin-induced toxicity was demonstrated and it is suggested that it probably

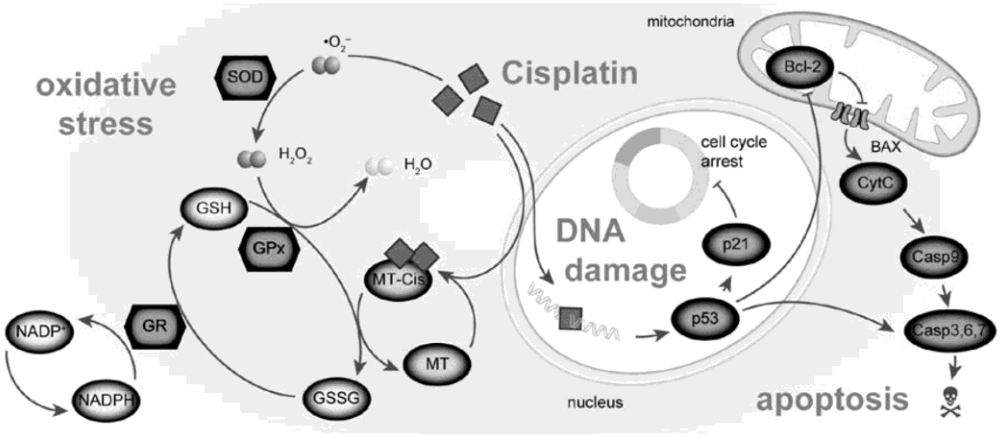

Figure 1. Cisplatin-induced DNA damage, oxidative stress and apoptosis. Cisplatin-cell interaction results in DNA damage, leading to p53 activation. DNA-repair mechanism is allowed due to p21-modulated cell cycle arrest. When damage is irreparable, p53 promotes apoptosis by inhibition of antiapoptic Bcl-2 and consequent caspase activation. Cisplatin binds to metallothionein (MT) and glutathione and thus oxidizes these compounds (GSH, reduced form of glutathione; GSSG, oxidized form of glutathione). Cisplatin generates superoxide radical ($\cdot O_2^-$), transformed by superoxiddismutase (SOD) to hydrogen peroxide, subsequently reduced by GSH in cooperation with glutathione peroxidase (GPx). GSSG is reduced by glutathione reductase (GR) in cooperation with reduced (NADPH).

occurs due to augmented ROS (reactive oxygen species) generation, with consequent impairment of mitochondrial function and structure, depletion of the key components of the mitochondrial antioxidant defense system (GSH and NADPH) and cellular death by apoptosis (12,13). Therefore, understanding the expression of anti- and pro-apoptotic proteins and their relationship to redox system in the cells upon cisplatin treatment will provide valuable insight into the development of cisplatin resistance (11). Therefore, the expression of key apoptosis signaling genes (Bax and Bcl-2) and cell defensive thiol-containing molecule metallothionein (MT) were investigated in this study in different cisplatin concentrations and length of treatment. Additionally, main antioxidant enzymes superoxide dismutase (SOD), glutathione peroxidase (GPx) and glutathione reductase (GR) and antioxidant capacity with respect to the cisplatin treatment were analyzed in this study. MT binds rapidly to platinum and thus sequester cisplatin and remove it from the cells. This binding has primarily been associated with the development of resistance (9). However, there is still a level of inconsistence between studies. In some cases, the levels of MT are higher in cisplatin-resistant cells, but in other cases, the MT levels are unaffected (2).

In summary, differences in antioxidant system, apoptotic mechanism and in cell cycle between prostatic cell lines could partially elucidate the development of cisplatin resistance. Thus, the aim of this study was: i) to identify the most characteristic parameter for particular cell line and/or particular cisplatin treatment using general regression model and ii) to assess, whether it is possible to use measured parameters as markers of cisplatin resistance.

Materials and methods

Chemical and biochemical reagents. RPMI-1640 medium, Ham's F12 medium, fetal bovine serum (FBS) (mycoplasma-free), penicillin/streptomycin and trypsin were purchased from PAA Laboratories GmbH (Pasching, Austria). Phosphate-buffered saline (PBS) was purchased from Invitrogen Corp. (Carlsbad, CA, USA). Ethylenediaminetetraacetic acid (EDTA), cisplatin 0.5 mg/ml solution (Medac, Germany), RIPA buffer and all other chemicals of ACS purity were purchased from Sigma-Aldrich Co. (St. Louis, MO, USA), unless noted otherwise.

Cell cultures. Three human prostatic cell lines were used in this study: i) PNT1A human cell line established by immortalization of normal adult prostatic epithelial cells by transfection with a plasmid containing SV40 genome with a defective replication origin. The primary culture was obtained from the prostate of a 35-year-old male post mortem; ii) 22Rv1 is a human prostate carcinoma epithelial cell line derived from a xenograft that was serially propagated in mice after castration-induced regression and relapse of the parental, androgen-dependent CWR22 xenograft. iii) PC-3 human cell line established from a grade 4 androgen independent and unresponsive prostatic adenocarcinoma from 62-year-old Caucasian male and derived from metastatic site in bone. All cell lines used in this study were purchased from Health Protection Agency Culture Collections (Salisbury, UK).

Culture conditions. PNT1A and 22Rv1 cells were cultured in RPMI-1640 medium with 10% FBS. PC-3 cells were cultured in Ham's F12 medium with 7% FBS. All media were supplemented with penicillin (100 U/ml) and streptomycin (0.1 mg/ml), and the cells were maintained at 37˚C in a humidified incubator (Sanyo, Japan) with 5% CO_2.

Cisplatin treatment. The cisplatin treatment was initiated after cells reached ~50% confluence. The concentration range 0, 10, 25, 50, 100, 150 μmol/l was used for all cell lines. Time points for cell harvest and thus for all subsequent analyses were set subsequently: 12, 24, 48 and 72 h. Thus, 6 (concentrations) x 4 (time points) lyzates were created. Cells were then harvested and washed four times with 1X PBS, pH 7.4.

Cell content quantification. Total cell content was analyzed using Casy model TT system (Roche Applied Science, USA) using following protocol: first, calibration was performed from

samples of viable and necrotic cells. For necrotic cells, 100 µl cell suspension and 800 µl Casy Blue solution was mixed and left for 5 min in room temperature. Subsequently, 9 ml Casy Tone was added. To prepare viable cell standard, 100 µl cell suspension was mixed with 10 ml Casy Tone. All subsequent measurements were performed on 100x diluted 100 µl cell suspension. Prior each measurement, background was subtracted. All samples were measured in duplicates.

Measurements of cell viability - MTT test. The suspension of 5,000 cells was added to each well of standard microtiter plates. Volume of 200 µl was transferred to 2-11 wells. Medium (200 µl) was added to the first and to the last column (1 and 12, control). Plates were incubated for 2 days at 37˚C to ensure cell growth. Medium was removed from columns 2 to 11. Columns 3-10 were filled with 200 µl of medium containing increasing concentration of cisplatin (0-150 µmol/l). As control, columns 2 and 11 were filled with medium without cisplatin. Plates were incubated for 12, 24, 48 and 72 h; then, media were removed and replaced by a fresh medium, three times a day. Columns 1-11 were filled with 200 µl of medium containing 50 µl of MTT (5 mg/ml in PBS) and incubated in a humidified atmosphere for 4 h at 37˚C, wrapped in aluminium foil. After the incubation, MTT-containing medium was replaced by 200 µl of 99.9% dimethyl sulphoxide (DMSO) to dissolve MTT-formazan crystals. Then, 25 µl of glycine buffer was added to all wells and absorbance was immediately determined at 570 nm (VersaMax microplate reader, Molecular Devices, Sunnyvale, CA, USA).

Cell growth and proliferation assay using impedance measurement with xCELLigence system. The xCELLigence system (Roche Applied Science and ACEA Biosciences, San Diego, CA, USA) consists of four main components: the RTCA analyzer, the RTCA station, the RTCA computer with integrated software and disposable E-plate 16. Firstly, the optimal seeding concentration for proliferation and cytotoxic assay was determined. After seeding the total number of cells in 200 µl medium to each well in E-plate 16, the attachment, proliferation and spreading of the cells was monitored every 15 min. All experiments were carried out for 250 h. The results are expressed as relative impedance using the manufacturer's software (Roche Applied Science and ACEA Biosciences).

Flow cytometric analysis of cell cycle. The cells were harvested and fixed with ice-cold 70% ethanol for 30 min. After washing with 1X PBS, the cells were incubated with DNA staining solution consisting of propidium iodide (PI; 50 µg/ml) and RNase (100 µg/ml) for 30 min at 37˚C in the dark. Samples were analyzed with FACSVerse flow cytometer (BD Biosciences, USA) and the data obtained were analyzed using FACSuite software (BD Biosciences).

RNA isolation and reverse transcription. High pure total-RNA isolation kit (Roche, Basel, Switzerland) was used for isolation. The medium was removed and samples were twice washed with 5 ml of ice-cold PBS. Cells were scraped off, transferred to clean tubes and centrifuged at 20,800 x g for 5 min at 4˚C. After this step, lysis buffer was added and RNA isolation was carried out according to manufacturer's instructions. Isolated RNA was used for cDNA synthesis. RNA (600 ng) was transcribed using transcriptor first strand cDNA synthesis kit (Roche, Switzerland) was used according to manufacturer's instructions. Prepared cDNA (20 µl) from total-RNA was diluted with RNase-free water to 100 µl and 5 µl was directly analyzed by 7500 RT-PCR system (Applied Biosystems).

Quantitative polymerase chain reaction (q-PCR). q-PCR was performed in triplicate using the TaqMan gene expression assay system with the 7500 RT-PCR system (Applied Biosystems) and the amplified DNA was analyzed by the comparative Ct method using β-actin as an endogenous control for metallothionein MT2A, Bax, Bcl-2 and p53 gene expression quantification. The primer and probe sets for β-actin (assay ID: Hs99999903_m1), MT2A (Hs02379661_g1) Bcl-2 (Hs99999018_m1), p53 (Hs01034649_m1), and Bax (Hs00180269_m1) were selected from TaqMan gene expression assays (Life Technologies, USA). q-PCR was performed under the following amplification conditions: total volume of 20 µl, initial incubation 50˚C/2 min followed by denaturation 95˚C/10 min, then 45 cycles 95˚C/15 sec, 60˚C/1 min.

Electrochemical detection of metallothionein. Electrochemical detection was used for quantification of metallothionein. Detection was carried out using AUTOLAB Analyser (EcoChemie, The Netherlands) with classical three-electrode arrangement using of differential pulse voltammetry Brdicka reaction. Analysed sample was accumulated on the surface of a working electrode which is represented by hanging mercury drop electrode. After accumulation, detection proceeded in a supporting electrolyte containing cobaltic ($cobalt^{3+}$) salt in ammonia buffer of pH 9.6 (14).

Spectrophotometric measurement. Spectrophotometric measurements were carried out using an automated chemical analyser BS-400 (Mindray, P.R. China). It is composed of cuvette space tempered to 37±1˚C, reagent space with a carousel for reagents (tempered to 4±1˚C), sample space with a carousel for preparation of samples, and an optical detector. Transfer of samples and reagents is provided by robotic arm equipped with a dosing needle (error of dosage up to 5% of volume). Cuvette contents are mixed by an automatic mixer including a stirrer immediately after addition of reagents or samples. Contamination is reduced due to its rinsing system, including rinsing of the dosing needle as well as the stirrer by MilliQ water. For detection itself, the following range of wavelengths can be used - 340, 380, 412, 450, 505, 546, 570, 605, 660, 700, 740, and 800 nm.

Determination of SOD. Kit 19160 SOD (Sigma Aldrich, USA) was used for assay of SOD, EC 1.15.1.1. First, 200 µl volume of reagent R1 (WTS solution 20 times diluted with buffer) was pipetted into a plastic cuvette and agent was incubated at 37˚C for 108 sec. Afterwards, 20 µl volume of sample was pipetted and in 378 sec, the reaction was started by adding 20 µl volume of reagent R2 (enzyme solution 167 times diluted with buffer). It was incubated for 72 sec and then absorbance was measured at λ=450 nm. Kinetic reaction was measured for 108 sec and absorbance was read every 9 sec.

Determination of glutathione reductase and peroxidase. A glutathione reductase and peroxidase cellular activity assay kits

(Sigma Aldrich) were used for GR and GPx activity determination. Reagents R1 and R2 were prepared by dissolving in an assay buffer (100 mmol/l potassium phosphate buffer, pH 7.5, with 1 mmol/l EDTA). The reagent R1 of 260 μl volume (1.15 mmol/l oxidized glutathione in the assay buffer) was poured with 10 μl of sample and 30 μl volume of reagent R2 (1 mmol/l NADPH in GR assay buffer) into a plastic cuvette. The decrease in absorbance was measured at 340 nm using kinetic program for 126 sec.

Determination of antioxidant activity by the FRAP method. The FRAP method (ferric reducing antioxidant power) is based on the reduction of complexes of 2,4,6-tripyridyl-s-triazine with ferric chloride hexahydrate ($FeCl_3 \cdot 6H_2O$); these substances are almost colorless, and eventually slightly brownish. After the reduction, blue ferrous complexes are formed. Procedure for the determination was used as in Sochor *et al* (15). After 150 μl volume of reagent is injected into a plastic cuvette with subsequent addition of a 3-μl sample, absorbance is measured at 605 nm for 12 min. Difference between absorbance at the last (the 12th) min and the 2nd min of the assay procedure was used for calculating of the antioxidant activity.

Determination of antioxidant activity by the free radicals method. This method is based on ability of chlorophyllin (the sodium-copper salt of chlorophyl) to accept and donate electrons with a stable change of maximum absorption. This effect is conditioned by an alkaline environment and the addition of catalyst.

Procedure for the determination was used as in Sochor *et al* (15). Reagent of 150 μl volume is injected into a plastic cuvette with subsequent addition of a 6-μl sample. Absorbance is measured at 450 nm in the second min of assay and the last (the 12th) min. Difference of the two absorbances is considered as an outputting value.

Statistical analysis. First, data were tested for normality using χ^2-test and log-normal fitted data were recalculated to log scale. General regression model method was used to reveal relationships between multiple continuous and categorical variables.

Prior to regression analysis, Pearson's correlation was performed to verify concordant trends among cell lines. Subsequently, partial correlations were used to analyze residuals of time/concentration after adjustment of all other variables. To reveal differences between cell lines, Tukey's post-hoc test within homogeneous groups was employed after adjustment of all other variables. Prior to these analyses, residuals were tested for outliers (no-normally distributed data with outliers was excluded from subsequent analyses). Hierarchical clustering on standardized data was used to determine similar trends within determined parameters. Unless noted otherwise, $p<0.05$ was considered statistically significant. Software Statistica 10 (StatSoft, Inc., USA) was used for analysis.

Results

Effect of treatment on cell viability - comparison of MTT and impedance-based data. To assess the cytotoxic effect of cisplatin on prostate cell lines, and to select concentrations for further analyses, MTT test was performed with concentrations 0 (no drug added), 10, 25, 50, 100, 150, 200 and 250 μmol/l on all cell lines (Fig. 2A). Using logistic regression, IC_{50} concentrations were determined at time points 12, 24, 48 and 72 h. As expected, cisplatin cytotoxicity increases in time-dependent manner (Table I). To understand these temporal changes, real-time cell growth monitoring was employed with the same cisplatin concentrations. Using this method, transient increase in impedance resulting in peaks on growth curves was determined in the first 24 h of treatment (Fig. 2B). This method also showed a similar time-dependent cytotoxicity increase as seen by MTT. However, IC_{50} values calculated by this method were on average 1.3-fold higher compared to MTT and no significant correlation was observed between MTT- and impedance-based IC_{50} values ($r=0.13$ at $p=0.70$).

Flow cytometric analysis of the cell cycle. To reveal the impact of cisplatin on the cell cycle, flow cytometric analysis was performed after the confluence of cells was ~50%. This confluence was reached within 24 to 48 h of treatment. Cisplatin-induced effects on cell cycle is evident in PNT1A and 22Rv1 cell lines (Fig. 2C and D). In these cells, 100 μM cisplatin dose increases the proportion of sub-G1 stage cells; up to 26.7% and 73.2% in PNT1A and 22Rv1, respectively. Flow cytometric analysis of 22Rv1 cells exposed 150 μmol/l cisplatin was below the detection limits due to the low cell counts in the sample. In contrast, PC-3 cell line does not show cell cycle arrest, maintaining <1.3% of cells in sub-G1 in all concentrations without significant increase or decrease.

Effect of treatment on gene expression. Subsequently, dose- and time-dependent response of apoptosis- and oxidative stress-related genes was analyzed. First, the level of metallothionein isoform 2A (RNA and protein), cellular tumor antigen p53 (RNA and protein), apoptosis regulators Bcl-2 and Bcl-2-associated X protein (Bax, RNA only) were analyzed (Fig. 3).

All detected RNAs and proteins were affected in treatment time-, dose- or cell line-dependent manner to some extent. For a more comprehensive understanding, residual analysis of treatment time and cisplatin dose after adjustment of other variables is desirable. Conditions for such residual analysis are met, because all lines showed consistently significant increasing/decreasing trends for all substances, the difference was seen only in the extent of increase/decrease. Partial correlations of time-, cell line-, and dose-adjusted residuals were determined to elucidate the unique contribution of the treatment time and dose individually (Table II). To analyze redundant trends, hierarchical cluster analysis of oxidative markers and RNA and protein was performed. As seen in Fig. 3A and B, Bcl-2, Bax and p53 show similar time- and dose-dependent response are thus clustered together.

First, the unique contribution of cisplatin dose after adjustment of all other variables (treatment time and cell line) is presented here. Significant elevation (i.e., significant partial correlation $r>0$) was determined in Bax (partial $r=0.34$ at $p<0.01$) and metallothionein (partial $r=0.73$ at $p<0.001$ and $r=0.45$ at $p<0.001$ for RNA and protein, respectively). Second, unique contribution of treatment duration was analyzed. p53 and Bcl-2 showed time-dependent increasing trends, $r=0.34$ at $p<0.01$ and $r=0.63$ at $p<0.001$, respectively. The remaining

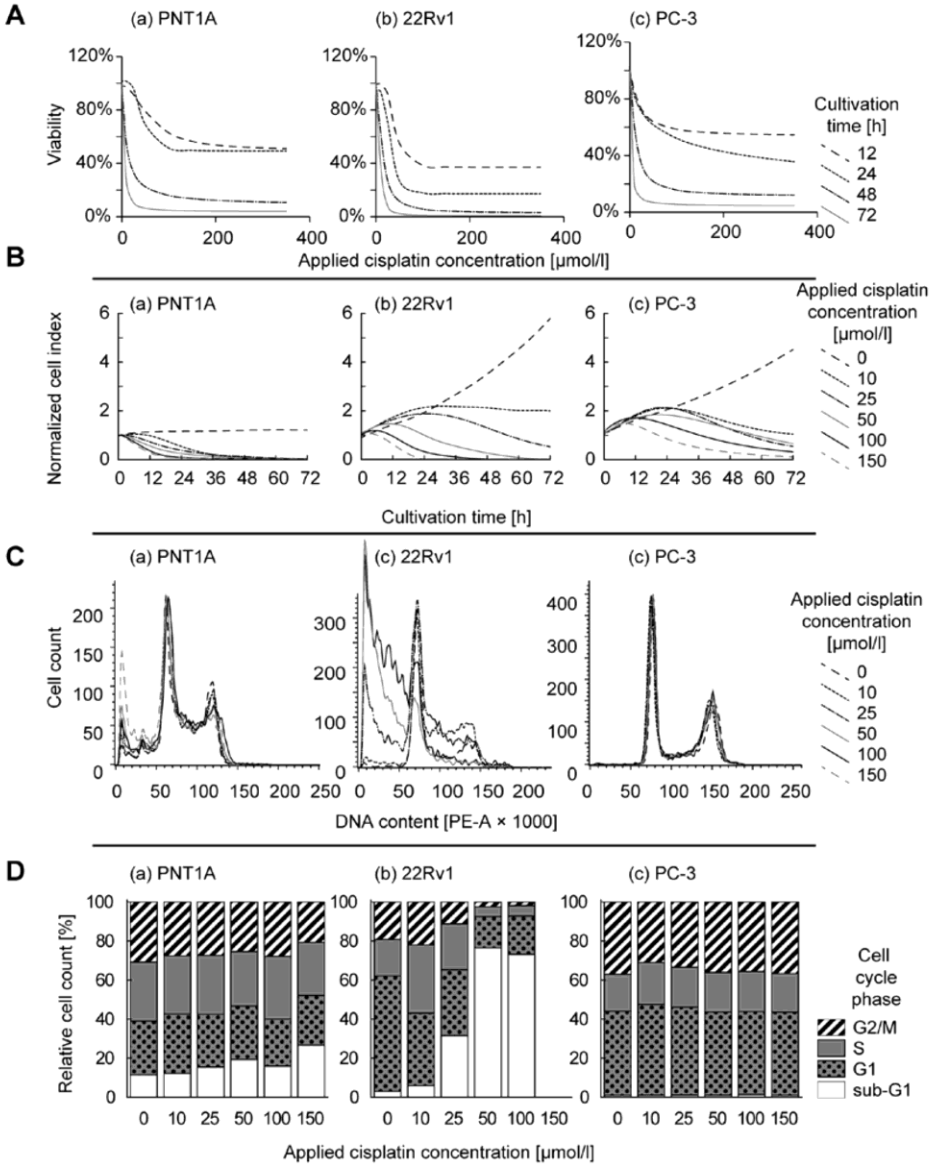

Figure 2. Cisplatin, cell growth and cell cycle. Each column shows one cell line (a-c). A, MTT test: dose-response curves measured in 12, 24, 48 and 72 h. Evident metabolic activity decrease in later measurements. B, Real-time cell growth analysis. The impedance-based signal is represented as a cell index normalized to value 1.0 at the beginning of the treatment. Transient increase in cell index in the first 24 h as a result of cell size and/or adhesivity change following cisplatin treatment. C, Flow cytometric analysis of the cell cycle. Increasing proportion of sub-G1 (increasing peaks) evident in PNT1A and 22Rv1 cells and not in p53-defective PC-3 cells (a, b vs. c). D, Dose-dependent proportion of cells in various stages of the cell cycle. Note cisplatin treatments >150 μM are not shown for better clarity of charts.

Table I. Half-maximal concentrations.[a]

	MTT IC_{50} (μmol/l)				xCELLigence IC_{50} (μmol/l)			
Cell line/time	12 h	24 h	48 h	72 h	12 h	24 h	48 h	72 h
PC-3	18.3	74.9	10.6	1.0	339.6	77.4	25.6	7.0
22Rv1	40.4	30.8	12.7	7.9	Undet.	2413.8	10.5	2.6
PNT1A	61.5	44.0	7.9	3.7	185.7	97.1	12.1	2.7

[a]Time-dependent comparison of IC_{50} determined by MTT and xCELLigence. See evident time-dependent increase of cytotoxicity using both methods. Undet., undeterminable, out of range.

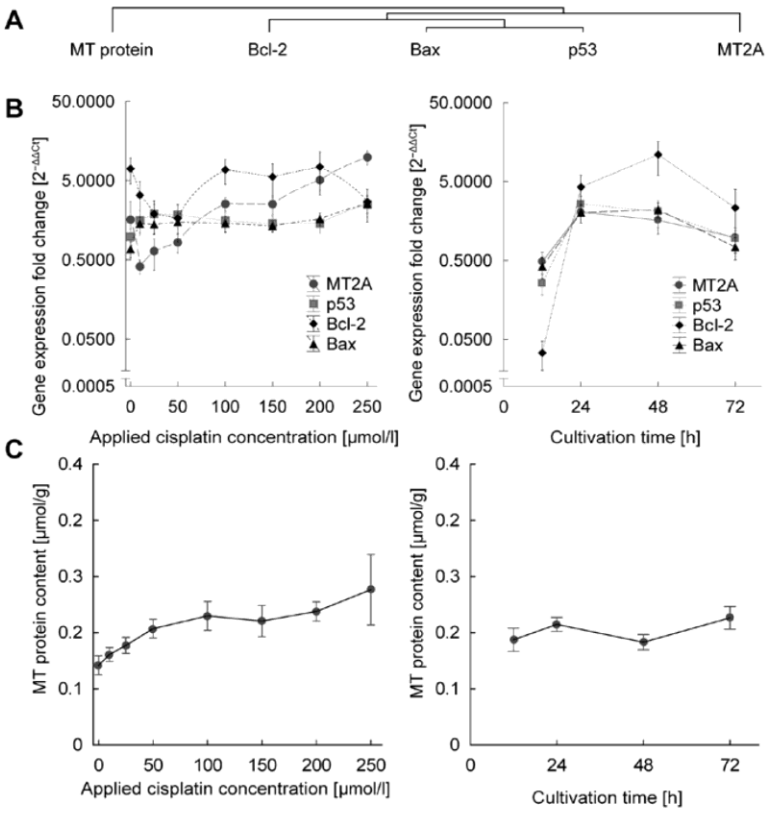

Figure 3. Gene expression and metallothionein protein level following cisplatin treatment. The effect of dosage after adjustment of all other variables shown in the left column, the effect of cultivation time on the right. A, Cluster analysis. See close relation of p53 and Bax in dendrogram resulting in similar trend of these genes in panel B. B, RNA level. There was distinct elevation of gene expression during first 24 h. Note y-axis in log-scale, gene expression fold change relative to PNT1A cell line. MT2A, metallothionein 2A. C, Metallothionein protein level. Distinct cisplatin concentration-related MT increased. For subsequent correlation coefficients see Table II. Data displayed as mean ± SE.

Table II. Dependence of parameters on time, cisplatin concentration and cell lines.[a]

Correlation coefficients (r)	MT protein	MT RNA	p53 RNA	Bcl-2 RNA	Bax RNA	SOD	GR	GPx	FR	FRAP	ABTS
Simple correlation											
Time (h)	0.03	0.09	0.12	0.36[c]	0.05	-0.14	-0.26[b]	0.23[b]	0.22[b]	0.18	0.09
Cisplatin (μmol/l)	0.43[d]	0.71[d]	0.03	0.02	0.24[b]	-0.18	-0.59[d]	0.25[b]	0.82[d]	0.64[d]	0.79[d]
Multiple regression											
Overall	0.59[d]	0.73[d]	0.84[d]	0.69[d]	0.61[d]	0.53[d]	0.82[d]	0.64[d]	0.89[d]	0.76[d]	0.85[d]
Time	0.07	0.22	0.24[b]	0.49[d]	0.13	-0.20	-0.43[d]	0.36[c]	0.52[d]	0.36[c]	0.26[b]
Cisplatin (μmol/l)	0.45[d]	0.73[d]	0.17	0.12	0.34[c]	-0.21	-0.72[d]	0.34[c]	0.88[d]	0.71[d]	0.82[d]
22Rv1 cells	-0.14	0.10	0.34[c]	0.63[d]	0.46[d]	-0.22	0.59[d]	0.48[d]	-0.36[c]	0.40[d]	-0.39[d]
PC-3 cells	0.43[d]	-0.13	-0.82[d]	-0.46[d]	-0.56[d]	-0.29[b]	-0.03	0.06	0.36[c]	-0.01	0.40[d]

[a]Pearson correlation coefficients (R) showing ambiguous results. Second, general regression model is used to show multiple R (see 'Overall' row) and partial correlation coefficients (other parameters). Significant at [b]p<0.05, [c]p<0.01, [d]p<0.001. MT, metallothionein.

RNAs are not dose- or cultivation time-dependent. Despite this fact, time-dependent analysis of all genes exhibit biphasic relation (Fig. 3B). Cisplatin dramatically increases the expression, in particular in first 24 h; up to 60-fold in Bcl-2, 10-fold in p53 and 5-fold in Bax and MT2A genes. However, after 24 h a plateau in expression is observed. As a result, the relation of MT RNA and

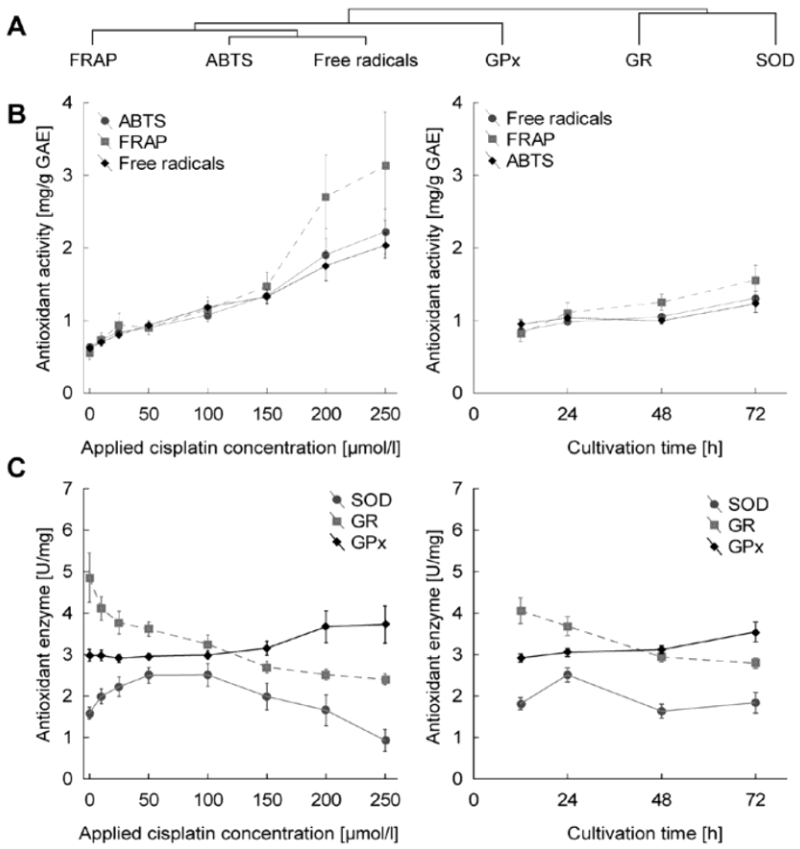

Figure 4. Oxidative stress after cisplatin treatment. The effect of dosage after adjustment of all other variables shown in the left column, the effect of cultivation time on the right. A, Cluster analysis. B, Markers of antioxidant capacity. Note the concordant trend of all three markers. C, Glutathione-related enzymes. Note the dose- and time-dependent GR decrease. Contrary to GR, no distinct cisplatin-related trends were determined in SOD. For subsequent correlation coefficients see Table II. Data displayed as mean ± SE.

protein shows weak, but significant positive correlation (r=0.24 at p=0.016).

Apart from gene expression analysis, protein level of MT was studied (Fig. 3C). Significant positive correlation was observed between MT protein and applied cisplatin dose (r=0.59 at p<0.001) and no correlation was observed in relation to cultivation time.

Effect of treatment on antioxidant capacity. All markers of antioxidant capacity correlate with each other significantly (data not shown). This is well evident in Fig. 4B and corresponds to cluster analysis, where these markers are closely clustered (Fig. 4A). In terms of statistical significance, all markers of antioxidant capacity increased significantly in dose-dependent manner, r=0.88, 0.71 and 0.82 for free radicals, FRAP and ABTS, respectively, at p<0.001. The duration of treatment affects parameters at lower levels of significance with r=0.52, 0.36 and 0.26 for free radicals, FRAP and ABTS (Fig. 4B).

With regard to glutathione-related enzymes, increasing dose- and time-dependent trend is shown only by glutathione peroxidase (r=0.34 and 0.36 for concentration and time at p<0.01), in contrast, glutathione reductase decrease in both time- and dose-dependent manner (at r=-0.72 for concentration and r=-0.43 for time at p<0.001). Superoxide dismutase showed no time- or concentration-dependent trends (Fig. 4C).

Effect of cell lines. Subsequently, the effect of cell lines was analyzed after adjustment of all other variables. Using Tukey's test for homogeneous groups, no significant difference, except in metallothionein RNA, between cell lines was identified. All other parameters showed significantly higher/lower trends between cell lines to some extent.

To identify similar patterns between cell lines, cluster analysis was employed, creating two characteristic branches. The first branch comprises markers of antioxidant capacity, glutathione-related enzymes and metallothionein, in contrast, the second branch includes apoptosis-related genes and SOD (Fig. 5A).

Close similarity is observed between ABTS and FR, showing significant difference between tumorous cell lines only (higher in PC-3). MT, similarly to ABTS and FR, shows significant difference between tumorous lines only. Glutathione peroxidase shows significant difference between all cell lines, while lowest level was observed in healthy cell line, thus, showing similarity to glutathione reductase. Similar trend is observed also in FRAP, where only PNT1A and 22Rv1 differ significantly.

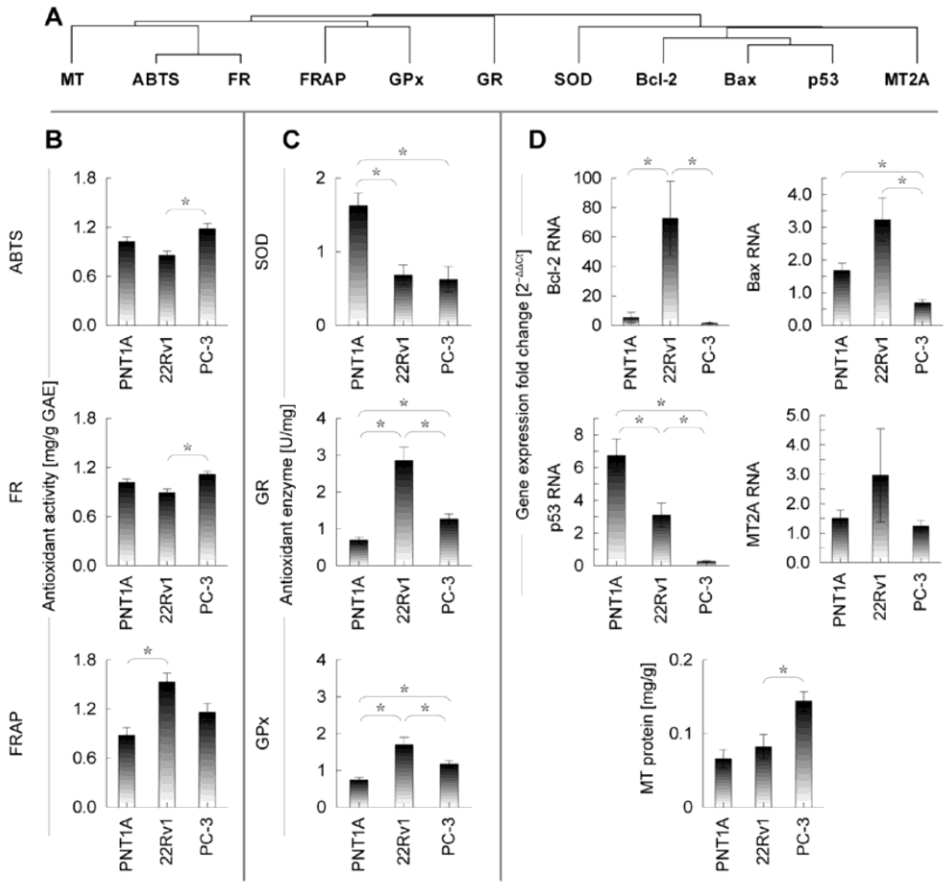

Figure 5. Cell lines and selected markers. The effect of each cell line after adjustment of treatment time and cisplatin dose. A, Cluster analysis. B, Markers of antioxidant capacity. Values displayed in mg/g of galic acid equivalent. FRAP, ABTS - C, Glutathione-related enzymes. D, RNA and protein level of selected genes. RNA level in relative gene expression fold change relative to PNT1A. *Significant at $p<0.05$ using Tukey's post-hoc test. Data displayed as mean ± SE.

With regard to apoptosis-related genes and superoxide dismutase, no difference can be seen in MT mRNA, significantly increased Bax in PC-3 cell line, significantly increased SOD in healthy PNT1A, significant difference between all cell lines in case of p53 (lowest in PC-3, highest in PNT1A) and significantly increased Bcl-2 in tumorous 22Rv1.

Discussion

This study provides time- and dose-dependent description of cisplatin-induced changes in antioxidant properties, apoptosis and cell cycle regulation on prostate cancer cell lines. These approaches clearly illustrate the development of resistance in advanced forms of prostate cancer, represented by the PC-3 cell line.

Cell growth, cell cycle. The results of viability assays distinctly show that the cytostatic effect of cisplatin is unpredictable in first hours of treatment, showing low cytotoxic potential, in particular, when detected using impedance-based method (Fig. 2A). This method provides transient increase in growth curves in particular in the first 24 h of treatment. Inasmuch as this detection method is influenced not only by the number of cells, but also by their size and adhesivity (16,17) and while these transient changes cannot be caused by cell count increase in such a short interval, here we provide evidence of cisplatin-influenced change of cell morphology and/or adhesivity. The steady state stabilization occurs between 24-48 h.

Even after stabilization, high level of disagreement was observed between metabolic-based MTT and impedance-based viability assays. While MTT test demonstrates the most toxic effect on 'aggressive metastatic' PC-3 cells, impedance-based (cell amount-, size- and adhesivity-dependent) technique demonstrates, in contrast, least toxic effects on this cell line (compare MTT- and impedance-based IC_{50} values in Table I, Fig. 2). To find an answer for this seemingly conflicting finding it is appropriate to relate it to the changes in cell cycle and apoptosis in these cell lines.

PC-3 cells are hemizygous for chromosome 17p, and their single copy of the *p53* gene has a deletion at codon 138 that has caused a frameshift and a new in-frame stop codon at position 169 (18). As a result, PC-3 cells do not express p53 protein (19). Our results are in agreement with these findings (20): level of p53 RNA was almost under the detection limits in PC-3 cell line (Fig. 4). P53 acts as a tumor suppressor through the induction of growth arrest and apoptosis (8). PNT1A cell line, which was

used in this experiment as a non-tumor model, was transfected using simian virus 40 (SV40) vector. However, SV40 induces T-antigen expression, which, on the other hand, inhibits the activity of p53 (21). Therefore, cell lines transfected using this vector have limited predictive value in terms of p53-dependent effects. Nevertheless, T-antigen p53 inhibition can be disrupted using oxidants (22), including cisplatin. The objective of the p53 detection in this study was neither to describe subtle concentration-dependent trends in p53 levels nor to describe p53-dependent cascades in detail, but rather to demonstrate a detectable induciblity of p53 expression when exposed to oxidative stress. The fact that detectable p53 content was determined in PNT1A under cisplatin load indicates p53-dependent pathways can be triggered in this cell line. Therefore, PNT1A might be used as model to study p53-dependent pathways, however, only if exposed to oxidative stress. The differences between p53-positive and negative cells are evident in our flow cytometric results: whereas both p53-expressing cells PNT1A and 22Rv1 show cisplatin-induced cell cycle changes accompanied by an increased proportion of sub-G1 phase cells, PC-3 cell does not show similar phenomenon (Fig. 2C and D). Similar phenomenon was demonstrated and linked with cisplatin resistance in non-small cell lung cancer cell line, for instance (23). It has been repeatedly demonstrated that apoptosis is the major mechanism for eliminating damaged cells in cisplatin-induced cells injury (24-26). Thus, PC-3 cells without functional p53 signaling cascade may divide and grow when treated with cisplatin or other p53-targeting cytostatic drug. Because PC-3 is derived from an aggressive metastatic form of prostate cancer, using the description of the monitored genes and parameters, this study provides a good model of cisplatin resistance. In addition, similarly to cisplatin, more pronounced apoptosis in 22Rv1 compared to PC-3 was observed by Gravina *et al* when exposed to 5-azacitine or bicalutamide (27). Taken together, contradictory results of MTT assay and an impedance-based method can be caused by false reduced viability of PC-3, which could be caused by low metabolic activity of cells in autophagy status. The main principle of MTT assay is the tetrazolium salt reduction to formazan, which is quantified photometrically, by mitochondrial succinate dehydrogenase (SDH). SDH is only active in cells with an intact metabolism and respiratory chain. Fasting and oxidative stress, which is present by cisplatin treatment, was associated with a significant decrease of SDH activity, and the reduction was proportional with the decrease in the amount of SDH total protein (28,29). Blocking apoptosis was found to promote autophagy in PC-3 and DU145 cells (30).

In accordance with this finding, we propose an impedance-based method as more reliable for growth monitoring of cytostatic-induced cells. Similar changes between these assays were reported also in our previous study (31).

Cisplatin effects - model of cisplatin resistance? To obtain initial insight into how all the markers and substances mentioned herein change after the exposure to cisplatin, 3-axis dependency graphs were visualized and calculated the simple correlations for each cell line. However, such analysis provides weak correlations and has limited power to emphasize complex multi-dimensional relations (Table II). Based on these graphs it is possible to draw the following conclusions: first, cisplatin concentration or treatment time clearly results in either increase or decrease in the levels of detected substances in all cell lines. Thus, none of the parameters increase in one cell line and decrease in the other in time- or dose-dependent manner. Second, both time and concentration cause more or less distinct changes in the levels of almost all monitored markers and substances. Third, some markers or substances rather increase, while others decrease, depending on the time or concentration.

Inasmuch as representation of graphs with their correlation coefficients would be confusing, statistically insufficiently powerful and, most importantly, such analysis would not refer to the obvious connection between the parameters, general regression model was used to show the effect of cell lines, concentrations of cisplatin and time of measurement simultaneously. This method provides benefits of both multiple linear regression and ANOVA and thus provide a more comprehensive view of all detected substances together. In this context, we focused on the identification of the most characteristic parameter for particular cell line and/or particular cisplatin treatment. Additionally, a hypothesis was verified, whether all measured markers may be used to describe cisplatin resistance.

To evaluate the effect of cisplatin concentration, duration of this cytotoxic effect or combination of these, partial correlations were calculated after the adjustment of all other variables. Partial correlations obtained by general regression model were subsequently compared to initially performed Pearson correlation results. Because significant trends were found mainly after adjusting using general regression model and no parameter correlated only before adjusting (i.e., in Pearson correlations), it is evident, that just variables 'concentration', 'time' and 'cell line' contribute to elucidate the variability (i.e., affect the level of detected substances). This manner explained up to 80% of the variability in data attributing it to the change in detection time, cisplatin concentration or cell line (R^2=0.80 in 'free radicals' method, for instance).

In this context, a hypothesis was formulated, whether all the measured parameters are rather influenced by the duration of the stress conditions (treatment time), or by the stress intensity (drug concentration). Whereas the markers of antioxidant capacity FRAP, ABTS and FR and GPx increase in dose- and time-dependent manner, p53 and Bcl-2 are time-dependent and BAX and MT are dose-dependent only. Interestingly, GR shows a decreasing time- and concentration-dependence. These findings are in agreement with what is inherently predictable: the increased p53 level contributes to apoptosis through Bax-cytochrome C mitochondrial apoptotic pathway by inhibition of Bcl-2 (8,32) (Fig. 1). As a result of such balance, Bax level follows analogous trends in dose-, time- and cell line-dependent manner (Figs. 3 and 5). An agreement with these findings was observed by Kharaziha *et al* (33). Agreement with our data was also provided by Li *et al* demonstrating a simultaneous increase in ROS, p53 and caspases in response to another platinum-based cytostatic drug dicycloplatin (34).

Metallothionein protein level increases with increasing cisplatin concentration due to its (cisplatin-induced) reactive-oxygen-species buffering properties. In contrast, metallothionein is not affected by the duration of cisplatin treatment due to the fact that the concentration of this drug (and thus cisplatin-generated oxidative stress) remain relatively stable after steady state stabilization (Fig. 3). The highest MT levels are determined in an

aggressive, metastasis-derived PC-3 cells. Similar finding was observed by several research teams (35-37). These data suggest MT is an important protective mechanism in cisplatin-induced stress and thus an important mechanism in the development and progression of cytostatic resistance. Such finding was already reported (35). No observed metallothionein RNA-protein match may appear to be a surprising result. However, it cannot be assumed, that significant RNA-protein correlation must be present. A pool of metallothionein capable to buffer limited amounts of oxidative stress is present more or less in all cells and thus RNA-response may not be apparent (38,39).

With regard to the activity of enzymes included in oxidative stress buffering (SOD, GR and GPx), a specific pattern is observed. Whereas non-tumor cell line shows higher activity of SOD and lower activity of GR and GPx, tumorous cells show an inverse trend. When exposed to cisplatin, GPx increases, GR decreases and SOD does not show any significant trend. The decreasing dose- and time-dependent trends in glutathione reductase may seem surprising at first glance. Generally, one would assume that the increase in oxidative stress will also increase oxidized glutathione and thus the activity of glutathione reductase. However, cisplatin causes a depletion of the key components of the mitochondrial antioxidant defense system, including NADPH (13). Because of NADPH oxidation, GR activity is expected to decrease. Similar finding with GR and GPx when treated with cisplatin is reported by Pratibha *et al* in a rat model (40). The authors propose a cisplatin-induced alteration in enzymatic antioxidant status with an increase in lipid peroxidation indicating that these enzymes play an important role in combating oxidative stress induced by free radicals (40).

With regard to markers of antioxidant capacity, it is worth mentioning that all radical scavenging activity detection methods correlate, showing an increase after cisplatin treatment. More pronounced increase is observed in tumorous cell lines particularly in the PC-3. These data suggest an increased ability of tumorous cells to cope with such conditions. There is no evidence on using these methods to describe antioxidant capacity on prostate cancer cell lines. This finding, together with elevated MT, decreased p53 and Bax suggest that the PC-3 cell line has unique features to cope with stress conditions and thus to be resistant to natural regulatory mechanisms such as apoptosis and cell cycle arrest and to stress cytostatics. Thus, this cell line may further be utilized as a model of cytostatic resistance, and markers and substances detected herein illustrate resistance development as well.

In this study, the cell-growth, cell cycle, apoptosis and oxidative stress-related methods were analyzed to describe the development of cisplatin resistance in prostate cancer. In p53-defective PC-3 cells no cisplatin-induced cell cycle arrest and reduced apoptosis was observed. In addition, higher free radical scavenging activity and higher metallothionein was observed in these cells. In contrast to impedance-based real-time cell growth analysis, reduced MTT-based viability suggests reduced metabolic activity and thus cells are expected to turn to autophagy. Thus, we propose an impedance-based method as more reliable for growth monitoring of cytostatic-treated cells.

Taken together, results of this study clearly illustrate, that the prostate cancer cell line PC-3 shows signs of resistance to cytostatics accompanied by an increase in antioxidant capacity, by increased metallothionein expression, by inhibition of cell cycle arrest, and by decreased expression of proapoptic genes. Therefore, PC-3 cell line may be used for further analyses as a model for cytostatic resistance as well as protocols used in this study. However, precise mechanisms affecting the orientation of cells toward autophagy or apoptosis are open topics for further research.

Acknowledgements

The authors gratefully acknowledge financial support from the following projects: the Grant Agency of the Czech Republic (CYTORES GA CR P301/10/0356), Center of Experimental Biomedicine (CZ.1.07/2.3.00/20.0183) and the Central European Institute of Technology (CEITEC CZ.1.05/1.1.00/02.0068).

References

1. Gonzalez VM, Fuertes MA, Alonso C and Perez JM: Is cisplatin-induced cell death always produced by apoptosis? Mol Pharmacol 59: 657-663, 2001.
2. Kartalou M and Essigmann JM: Mechanisms of resistance to cisplatin. Mutat Res 478: 23-43, 2001.
3. Niedner H, Christen R, Lin X, Kondo A and Howell SB: Identification of genes that mediate sensitivity to cisplatin. Mol Pharmacol 60: 1153-1160, 2001.
4. Herraez E, Gonzalez-Sanchez E, Vaquero J, *et al*: Cisplatin-induced chemoresistance in colon cancer cells involves FXR-dependent and FXR-independent up-regulation of ABC proteins. Mol Pharm 9: 2565-2576, 2012.
5. Liu YB, Bernauer AM, Yingling CM and Belinsky SA: HIF1 alpha regulated expression of XPA contributes to cisplatin resistance in lung cancer. Carcinogenesis 33: 1187-1192, 2012.
6. Wu YC, Ling TY, Lu SH, *et al*: Chemotherapeutic sensitivity of testicular germ cell tumors under hypoxic conditions is negatively regulated by SENP1-controlled sumoylation of OCT4. Cancer Res 72: 4963-4973, 2012.
7. Skjoth IHE and Issinger OG: Profiling of signaling molecules in four different human prostate carcinoma cell lines before and after induction of apoptosis. Int J Oncol 28: 217-229, 2006.
8. Faria MHG, Neves EHC, Alves MKS, Burbano RMR, De Moraes MO and Rabenhorst SHB: TP53 mutations in astrocytic gliomas: an association with histological grade, TP53 codon 72 polymorphism and p53 expression. APMIS 120: 882-889, 2012.
9. Fuertes MA, Alonso C and Perez JM: Biochemical modulation of cisplatin mechanisms of action: enhancement of antitumor activity and circumvention of drug resistance. Chem Rev 103: 645-662, 2003.
10. Righetti SC, Perego P, Carenini N, *et al*: Molecular alterations of cells resistant to platinum drugs: role of PKC alpha. Biochim Biophys Acta 1763: 93-100, 2006.
11. Brozovic A, Ambriovic-Ristov A and Osmak M: The relationship between cisplatin-induced reactive oxygen species, glutathione, and BCL-2 and resistance to cisplatin. Crit Rev Toxicol 40: 347-359, 2010.
12. Santos NAG, Catao CS, Martins NM, Curti C, Bianchi MLP and Santos AC: Cisplatin-induced nephrotoxicity is associated with oxidative stress, redox state unbalance, impairment of energetic metabolism and apoptosis in rat kidney mitochondria. Arch Toxicol 81: 495-504, 2007.
13. Martins NM, Santos NAG, Curti C, Bianchi MLP and Santos AC: Cisplatin induces mitochondrial oxidative stress with resultant energetic metabolism impairment, membrane rigidification and apoptosis in rat liver. J Appl Toxicol 28: 337-344, 2008.
14. Kizek R, Trnkova L and Palecek E: Determination of metallothionein at the femtomole level by constant current stripping chronopotentiometry. Anal Chem 73: 4801-4807, 2001.
15. Sochor J, Ryvolova M, Krystofova O, *et al*: Fully automated spectrometric protocols for determination of antioxidant activity: advantages and disadvantages. Molecules 15: 8618-8640, 2010.
16. Quereda JJ, Martinez-Alarcon L, Mendoca L, *et al*: Validation of xCELLigence real-time cell analyzer to assess compatibility in xenotransplantation with pig-to-baboon model. Transplant Proc 42: 3239-3243, 2010.

17. Vistejnova L, Dvorakova J, Hasova M, *et al*: The comparison of impedance-based method of cell proliferation monitoring with commonly used metabolic-based techniques. Neuroendocrinol Lett 30: 121-127, 2009.
18. Carroll AG, Voeller HJ, Sugars L and Gelmann EP: p53 oncogene mutations in 3 human prostate-cancer cell-lines. Prostate 23: 123-134, 1993.
19. Rubin SJ, Hallahan DE, Ashman CR, *et al*: 2 prostate carcinoma cell-lines demonstrate abnormalities in tumor suppressor genes. J Surg Oncol 46: 31-36, 1991.
20. Sztalmachova M, Hlavna M, Gumulec J, *et al*: Effect of zinc(II) ions on the expression of pro- and anti-apoptotic factors in high-grade prostate carcinoma cells. Oncol Rep 28: 806-814, 2012.
21. Schmieg FI and Simmons DT: Characterization of the in vitro interaction between SV40 T-antigen and p53: mapping the p53 binding-site. Virology 164: 132-140, 1988.
22. Gonin S, Diaz-Latoud C, Richard MJ, *et al*: p53/T-antigen complex disruption in T-antigen transformed NIH3T3 fibroblasts exposed to oxidative stress: correlation with the appearance of a Fas/APO-1/CD95 dependent, caspase independent, necrotic pathway. Oncogene 18: 8011-8023, 1999.
23. Barr MP, Gray SG, Hoffmann AC, *et al*: Generation and characterisation of cisplatin-resistant non-small cell lung cancer cell lines displaying a stem-like signature. Plos One 8: 1-19, 2013.
24. Liu J, Liu YP, Habeebu SSM and Klaassen CD: Metallothionein (MT)-null mice are sensitive to cisplatin-induced hepatotoxicity. Toxicol Appl Pharmacol 149: 24-31, 1998.
25. Siddik ZH: Cisplatin: mode of cytotoxic action and molecular basis of resistance. Oncogene 22: 7265-7279, 2003.
26. Wang D and Lippard SJ: Cellular processing of platinum anticancer drugs. Nat Rev Drug Discov 4: 307-320, 2005.
27. Gravina GL, Marampon F, Di Staso M, *et al*: 5-Azacitidine restores and amplifies the bicalutamide response on preclinical models of androgen receptor expressing or deficient prostate tumors. Prostate 70: 1166-1178, 2010.
28. Aitken RJ, Whiting S, De Iuliis GN, McClymont S, Mitchell LA and Baker MA: Electrophilic aldehydes generated by sperm metabolism activate mitochondrial reactive oxygen species generation and apoptosis by targeting succinate dehydrogenase. J Biol Chem 287: 33048-33060, 2012.
29. Komatsu M, Waguri S, Ueno T, *et al*: Impairment of starvation-induced and constitutive autophagy in Atg7-deficient mice. J Cell Biol 169: 425-434, 2005.
30. Cao C, Subhawong T, Albert JM, *et al*: Inhibition of mammalian target of rapamycin or apoptotic pathway induces autophagy and radiosensitizes PTEN null prostate cancer cells. Cancer Res 66: 10040-10047, 2006.
31. Masarik M, Gumulec J, Hlavna M, *et al*: Monitoring of the prostate tumour cells redox state and real-time proliferation by novel biophysical techniques and fluorescent staining. Integr Biol 4: 672-684, 2012.
32. Kuwana T and Newmeyer DD: Bcl-2-family proteins and the role of mitochondria in apoptosis. Curr Opin Cell Biol 15: 691-699, 2003.
33. Kharaziha P, Rodriguez P, Li Q, *et al*: Targeting of distinct signaling cascades and cancer-associated fibroblasts define the efficacy of Sorafenib against prostate cancer cells. Cell Death Dis 3: 1-10, 2012.
34. Li GQ, Chen XG, Wu XP, *et al*: Effect of dicycloplatin, a novel platinum chemotherapeutical drug, on inhibiting cell growth and inducing cell apoptosis. Plos One 7: 1-13, 2012.
35. Kondo Y, Kuo SM, Watkins SC and Lazo JS: Metallothionein localization and cisplatin resistance in human hormone-independent prostatic tumor-cell lines. Cancer Res 55: 474-477, 1995.
36. Suzuki Y, Kondo Y, Himeno S, Nemoto K, Akimoto M and Imura N: Role of antioxidant systems in human androgen-independent prostate cancer cells. Prostate 43: 144-149, 2000.
37. Yamasaki M, Nomura T, Sato F and Mimata H: Metallothionein is up-regulated under hypoxia and promotes the survival of human prostate cancer cells. Oncol Rep 18: 1145-1153, 2007.
38. Costello LC, Fenselau CC and Franklin RB: Evidence for operation of the direct zinc ligand exchange mechanism for trafficking, transport, and reactivity of zinc in mammalian cells. J Inorg Biochem 105: 589-599, 2011.
39. Bell SG and Vallee BL: The metallothionein/thionein system: an oxidoreductive metabolic zinc link. Chembiochem 10: 55-62, 2009.
40. Pratibha R, Sameer R, Rataboli PV, Bhiwgade DA and Dhume CY: Enzymatic studies of cisplatin induced oxidative stress in hepatic tissue of rats. Eur J Pharmacol 532: 290-293, 2006.

PLOS | ONE

RESEARCH ARTICLE

Oxidative Stress Resistance in Metastatic Prostate Cancer: Renewal by Self-Eating

Jan Balvan[1,2], Jaromir Gumulec[1,2], Martina Raudenska[1,2], Aneta Krizova[2,3], Petr Stepka[4], Petr Babula[4], Rene Kizek[2,5], Vojtech Adam[2,5], Michal Masarik[1]*

1 Department of Pathological Physiology, Faculty of Medicine, Masaryk University / Kamenice 5, CZ-625 00, Brno, Czech Republic, **2** Central European Institute of Technology, Brno University of Technology, Technicka 3058/10, CZ-616 00, Brno, Czech Republic, **3** TESCAN Brno, s.r.o., Brno, Czech Republic, **4** Department of Physiology, Faculty of Medicine, Masaryk University / Kamenice 5, CZ-625 00, Brno, Czech Republic, **5** Department of Chemistry and Biochemistry, Mendel University in Brno / Zemedelska 1, CZ-613 00, Brno, Czech Republic

* masarik@med.muni.cz

OPEN ACCESS

Citation: Balvan J, Gumulec J, Raudenska M, Krizova A, Stepka P, Babula P, et al. (2015) Oxidative Stress Resistance in Metastatic Prostate Cancer: Renewal by Self-Eating. PLoS ONE 10(12): e0145016. doi:10.1371/journal.pone.0145016

Editor: Natasha Kyprianou, University of Kentucky College of Medicine, UNITED STATES

Received: September 15, 2015

Accepted: November 25, 2015

Published: December 15, 2015

Data Availability Statement: All relevant data are within the paper and its Supporting Information files.

Funding: This work was supported by funds from the Faculty of Medicine, Masaryk University to junior researcher (Michal Masarik) and by the project MUNI/A/1549/2014 and MUNI/A/1326/2014 with the support of the Specific University Research Grant, as provided by the Ministry of Education, Youth and Sports of the Czech Republic in the year 2015. The funders had no role in study design, data collection and analysis, decision to publish, or preparation of the manuscript. The commercial company (TESCAN) provided support in the form of salary for author

Abstract

Resistant cancer phenotype is a key obstacle in the successful therapy of prostate cancer. The primary aim of our study was to explore resistance mechanisms in the advanced type of prostate cancer cells (PC-3) and to clarify the role of autophagy in these processes. We performed time-lapse experiment (48 hours) with ROS generating plumbagin by using multimodal holographic microscope. Furthermore, we also performed the flow-cytometric analysis and the qRT-PCR gene expression analysis at 12 selected time points. TEM and confocal microscopy were used to verify the results. We found out that autophagy (namely mitophagy) is an important resistance mechanism. The major ROS producing mitochondria were coated by an autophagic membrane derived from endoplasmic reticulum and degraded. According to our results, increasing ROS resistance may be also accompanied by increased average cell size and polyploidization, which seems to be key resistance mechanism when connected with an escape from senescence. Many different types of cell-cell interactions were recorded including entosis, vesicular transfer, eating of dead or dying cells, and engulfment and cannibalism of living cells. Entosis was disclosed as a possible mechanism of polyploidization and enabled the long-term survival of cancer cells. Significantly reduced cell motility was found after the plumbagin treatment. We also found an extensive induction of pluripotency genes expression (*NANOG*, *SOX2*, and *POU5F1*) at the time-point of 20 hours. We suppose, that overexpression of pluripotency genes in the portion of prostate tumour cell population exposed to ROS leads to higher developmental plasticity and capability to faster respond to changes in the extracellular environment that could ultimately lead to an alteration of cell fate.

Aneta Krizova, but did not have any additional role in the study design, data collection and analysis, decision to publish, or preparation of the manuscript. The specific role of this author is articulated in the 'author contributions' section.

Competing Interests: The cooperation with a commercial company (TESCAN) does not alter the authors' adherence to PLOS ONE policies on sharing data and materials.

Introduction

Prostate cancer (PC) is one of the most frequently diagnosed cancer types in men. Most of prostate cancers are initially responsive to androgen deprivation therapy, but later would emerge an aggressive, androgen-independent phenotype resistant to conventional therapies. This advanced type of prostate cancer easily metastasizes. Hematogeneous metastases are usually present in 35% of prostate cancer patients with the most frequent localisation in bones (90%). The widely studied model for androgen-independent, advanced, metastases-producing prostate cancer is the PC-3 cell line established from the lumbar metastasis of a 62 year old Caucasian male with grade 4 of prostatic adenocarcinoma. PC-3 cells are hemizygous for 17p chromosome, and their sole copy of the *p53* gene has a stop codon at position 169 [1]. As a result, PC-3 cells do not express the functional p53 protein, which makes it rather resistant to p53-mediated apoptosis [2]. Furthermore, we chose PC-3 cell line and not DU145, because DU145 prostate cancer cells express PTEN, which is not expressed by PC-3 cells [3, 4]. Multiple functional studies support the role of PTEN as a critical tumour suppressor in prostate cancer [5–7].

In our previous study we demonstrated that the PC-3 cell line showed higher resistance to cisplatin-induced apoptosis and no decreasing proportion of G2/M fraction (4N DNA content) evident in 22Rv1 cells [8]. Cisplatin is primarily considered as a DNA-damaging agent, forming different types of hard-reparable adducts with cellular DNA [9]. Apart from DNA damage, cisplatin also induces reactive oxygen species (ROS) [10]. Due to the fact, we have focused on another ROS-producing reagent, plumbagin [11], which does not form DNA adducts, to assess importance of cell death modulation and dealing with ROS for PC-3 resistance. Plumbagin (5-hydroxy-2-methyl-1,4-naphthoquinone) occurs naturally in the medicinal herb *Plumbago zeylanica L.* and belongs to naphthoquinones. Naphthoquinones display their cytotoxic actions through two ways: as pro-oxidants, reducing oxygen to reactive oxygen species; and as electrophiles, which form covalent bonds with tissue nucleophiles [12]. Furthermore, plumbagin was also shown to suppress the activation of nuclear factor-κB (NF-κB) [13].

In recent studies, ROS generation was associated with the mitochondria as a consequence of impaired mitochondrial protein synthesis [10]. Furthermore, it was pointed out, that cells with a deficit of functional mitochondria are more resilient to cell damage by cisplatin [14]. However, Panov *et al.* found out, that the prostate cancer cell lines LNCaP, PC-3, and DU145 contained 2 to 4 times more mitochondria per gram of cells than normal prostate epithelial cells. Respiratory activities of mitochondria isolated from normal prostate epithelial cells were also 5-20-fold lower than those of mitochondria isolated from prostate cancer cells [15]. Therefore, we presume the existence of some protective mechanisms against ROS in PC-3 cells. Many cell injuries caused by ROS could be sublethal (especially if the studied cells have disrupted apoptosis-triggering mechanisms) and result in an altered steady state in which the damaged cells are able to survive. Even if a damaged cell is driven to oncosis (oncosis is a pre-lethal phase that follows a serious cell injury) or senescence, there are probably some mechanisms to reverse this process [16–18], particularly if the cell is able to get rid of damaging factors and restore ATP production. A possible way to gain enough energy for the survival could be autophagy [19], cannibalism or entosis [20, 21]. Autophagy was at first considered a mechanism that suppresses malignant transformation. However, strong evidences for a dual role of autophagy were discovered [22]. In early tumours, autophagy could be truly a potent tumour suppressor because it can assure organelle and protein quality control and prevent genomic instability and aneuploidy organelle [23]. However, there are significant evidences that autophagy has a cancer-promoting role in established tumours [24].

One of the significant histopathological features of human solid tumours is the occurrence of large atypical cancer cells with multiplicated nuclear DNA that are known as polyploid giant cancer cells (PGCCs). Increased PGCCs numbers usually appear in late disease stages and grades or as a consequence of chemotherapy [25]. An important goal of our study was to explore possible mechanisms of defence against ROS in the advanced type of prostate cancer cells. We tried to assess the role of autophagy and the formation of polyploid giant cancer cells (PGCCs) in the advanced type of prostate cancer. We also attempted to verify a hypothesis that autophagy could be the mechanism of resistance against ROS rather than the mechanism of cell death. This hypothesis is supported by recent findings indicating that well-characterized autophagy activators and mTOR inhibitors (such as rapamycin, PP242, or resveratrol) markedly improve the speed and efficiency of puripotent stem cells generation [26].

Materials and Methods

Chemical and biochemical reagents

Ham's F12 medium, fetal bovine serum (FBS), (mycoplasma free), penicillin/streptomycin and trypsin were purchased from PAA Laboratories GmbH (Pasching, Austria). Phosphate-buffered saline (PBS) was purchased from Invitrogen Corp. (Carlsbad, CA, USA). Ethylenediaminetetraacetic acid (EDTA), plumbagin and other chemicals of ACS purity were purchased from Sigma-Aldrich Co. (St. Louis, MO, USA), unless noted otherwise.

Cell cultures and cultured cell conditions

Human PC-3 prostate cancer cells were used in this study (passage 18–24). The PC-3 cell line was established from grade 4 prostatic adenocarcinoma from 62 years old Caucasian male and derived from the metastatic site in bones. The PC-3 cell line was purchased from HPA Culture Collections (Salisbury, UK).

PC-3 cells were cultured in Ham's F12 medium with 7% FBS. The medium was supplemented with penicilin (100 U/ml) and the cells were maintained at 37°C in humidified incubator with 5% CO_2. Hypoxy/starvation-resistant PC-3 were selected by cultivation without the access of oxygen and with no medium replacement for one month.

Plumbagin treatment

The stock solution of plumbagin was prepared in dimethylsulfoxide (DMSO) and diluted with the medium. An equal volume of DMSO (final concentration $\leq$ 0.1%) was added to the controls. The plumbagin treatment was initialized after the cells reached confluence of ~50%. For cytotoxicity assessment, a range of concentrations 0, 0.5, 1, 1.5, 2, 2.5, 3, 4, 5, and 6 μmol/l of plumbagin was used. Time points for cell harvesting and thus for subsequent analyses were 0 h, 40 min., 1,5, 4, 6, 8, 10, 16, 20, 24, 36, and 48 h.

Cell content quantification

Total cell content was measured using Casy model TT system (Roche Applied Science, USA) and the following protocol: first, calibration was performed from the samples of viable and necrotic cells. For the necrotic cells, 100 μl cell suspension and 800 μl Casy Blue solution were mixed and left for 5 minutes at room temperature. Subsequently, 9 ml CasyTone was added. To prepare a viable cell standard, 100 μl of cell suspension was mixed with 10 ml CasyTone. All subsequent measurements were performed on 100x diluted 100 μl cell suspension. Prior to each measurement, the background was subtracted. All samples were measured in duplicates.

Measurement of cell viability—MTT test

The suspension of 5000 cells was added to each well of standard microtiter plates. Volume of 200 μl was transferred to wells 2–11. The medium (200 μl) was added to the first and to the last column (1 and 12, control). The plates were incubated for 2 days at 37°C to ensure cell growth. The medium was removed from columns 2 to 11. Columns 3–10 were filled with 200 μl of medium containing an increased concentration of plumbagin (0–6 μmol/l). As a control, columns 2 and 11 were filled with the medium without plumbagin. The plates were incubated for 12 and 24 h, then the medium was removed and the cells were washed in PBS. Columns 1–11 were filled with 200 μl of medium containing 50 μl of MTT (5mg/ml in PBS), incubated in humidified atmosphere for 4 h at 37°C, and wrapped in aluminium foil. After the incubation, the MTT-containing medium was replaced with 200 μl of 99.9% dimethylsulfoxide (DMSO) to dissolve MTT-formazan crystals. Subsequently, 25 μl of glycine buffer was added to all wells and absorbance was determined immediately at 570 nm (VersaMax microplate reader, Molecular Devices, Sunnyvale, CA, USA).

Cell growth and proliferation assay using impedance measurement

Cell growth was analyzed using the real-time cell analysis (RTCA) system (xCELLigence; Roche Applied Science and ACEA Biosciences). Firstly, the optimal seeding concentration for proliferation and cytotoxic assay was determined. PC-3 cells were seeded at a density of 7000 cells per well in E-Plates 16. After seeding the total number of cells in 200 μl medium to each well, in E-Plate 16, the attachment, proliferation and spreading of the cells was monitored every 15 min. After 24 hours, plumbagin was added and the cell index (CI), which reflects cell viability, was monitored. All experiments were carried out for 250h. The results are expressed as a cell index using the manufacturer's software (Roche Applied Science and ACEA Biosciences). The experiments were made in duplicates.

Flow cytometric analysis of cell death

Double-staining with fluorescein isothiocyanate (FITC)/propidium iodide (PI) was undertaken using the Annexin V-FLUOS-staining kit (Roche Applied Science) according to the manufacturer's protocol in order to determine percentages of viable, apoptotic and necrotic cells following the exposure to plumbagin. Briefly, the cells were harvested by repetitive pipetting and washed two times with PBS (centrifuged at 2000 rpm for 5 min), resuspended in 100 μl of Annexin-V-FLUOS labelling solution and incubated for 15 min. in the dark at 15–25°C. Annexin V-FITC binding was detected by flow cytometry (Partec GmbH, Münster, Germany) (Ex = 488 nm, Em = 533 nm, FL1 filter for Annexin-V-FLUOS and FL3 filter for PI).

Flow cytometric detection of autophagosomes

Autophagosome formation in PC-3 cells was detected using the CYTO-ID Autophagy Detection Kit (Enzo, PA, USA) following the manufacturer's instruction. The CYTO-ID green fluorescent reagents specifically detect acid autophagic vacuoles formed during autophagy. Briefly, the cells were harvested by gentle repetitive pipetting, spun down and washed twice in RPMI 1640 with 5% fetal bovine serum (FBS). The cells were resuspended in 500 μl of freshly diluted CYTO-ID staining reagent and incubated in the dark at 37°C for 30 min. CYTO-ID fluorescence of cells was immediately analyzed by flow cytometry using the flow cytometr (Partec GmbH, Münster, Germany) (Ex = 480 nm, Em = 530 nm, FL1 filter for CYTO-ID, SSC for cellular granularity). The percentage of cells with CYTO-ID staining was used to represent the formation of autophagosomes.

Flow cytometric analysis of intact healthy cells

The cell pellet was prepared as mentioned above. The cells were resuspended in 500 μl of freshly diluted 1 μM SYTO 16 (Thermo Fisher Scientific, Waltham, MA, USA) staining solution and incubated in the dark at 37°C for 45 min. SYTO 16 fluorescence of cells was immediately analyzed on the same instrument as mentioned above (Ex = 488 nm, Em = 518 nm, FL1 filter for SYTO 16, FSC for cell size). The percentage of SYTO 16-positive cells was analyzed. The data were analyzed using the FloMax software (Partec GmbH, Münster, Germany).

Fluorescence microscopy and cell staining

For fluorescence microscopy, the cells were cultivated directly on microscope glass slides (75x25 mm, thickness 1mm, Menzel Glässer, Braunschweig, Germany) in Petri dishes in the above-described cultivation media (see Cultured cell conditions). The cells were transferred directly onto the slides, which were submerged in the cultivation media. After the treatment, the microscope glass slides with a monolayer of cells were removed from the Petri dishes, rinsed in the cultivation medium without plumbagin supplementation and PBS buffer and directly used for staining and fluorescence microscopy.

The cells were incubated with the following highly specific fluorescent probes: reactive oxygen species were visualized using CellROX Deep Red reagent (Life Technologies, USA, 5 μM, cell-permeant, life-cell stain with absorption/emission maxima of 644/665 nm), mitochondria were visualized using MitoTracker Green FM (Life Technologies, USA, 300 nM, cell-permeant life-cell stain with absorption/emission maxima of 490/516 nm), and endoplasmic reticulum was visualized using ER-Tracker Red (Life Technologies, USA, 1 μM, cell-permeant, life-cell stain with absorption/emission maxima of 587/615 nm). After incubation (45 min, 37°C, dark), the cells were washed three times with PBS buffer (0.05 M, pH 7.0) and observed under the confocal microscope (Leica TCS SP8 X, Germany) using appropriate excitation and emission wavelengths.

TEM visualization of PC-3 ultrastructure

The PC-3 cells were gently harvested by repetitive pipetting and spun down (2000 rpm, 5 min.). Briefly, the cells were fixed with 3% glutaraldehyde in cacodylate buffer for 2 hours and washed three times for 30 minutes in 0.1 M cacodylate buffer. Following this, they were fixed with 0.02 M OsO_4 dissolved in 0.1 M cacodylate buffer, dehydrated in alcohol, and infiltrated with acetone and No. 1 Durcuptan mixture overnight. On the following day, the cells were infiltrated with No. 2 Durcuptan mixture, embedded and polymerized. Ultrathin sections (90 nm, Ultramicrotome LKB, Bromma, Stockholm, Sweden) were transferred onto grids covered with the Formvar membrane (Marivac Ltd., Halifax, Canada). 2% uranyl acetate and Reynold's solution were used for contrast staining. The sections were viewed in the transmission electron microscope (Morgagni 268, FEI Europe B.V., Eindhoven Netherlands). Software AnalySIS (Soft Imaging System, GmbH, Münster, Germany) was used for image analysis of cell ultrastructure.

Quantitative phase imaging

Quantitative phase imaging is a non-invasive technique with high intrinsic contrast even for naturally transparent objects such as live cells. Therefore this method is suitable for long term observations of cell reactions to treatment without any additional staining. In these experiments quantitative phase imaging was performed by Tescan multimodal holographic

microscope Q-PHASE. Q-PHASE is based on the original concept of coherence-controlled holographic microscope [27, 28].

Quantitative phase imaging was initiated immediately after plumbagin treatment. Cells were cultivated in Flow chambers μ-Slide I Lauer Family (Ibidi, Martinsried, Germany) In order to image enough number of cells in one field of view, objectives Nikon Plan 10/0.30 were chosen. Holograms were captured by CCD camera (XIMEA MR4021 MC-VELETA). The entire image reconstruction and image processing were performed in Q-PHASE control software. Quantitative phase images are shown in grayscale with units of pg/μm^2 that were recalculated from original radians according to Barer and Davies [29, 30]. Movies with identification arrows were prepared in ImageJ software.

RNA Isolation and Reverse Transcription

TriPure Isolation Reagent (Roche, Basel, Switzerland) was used for RNA isolation. RNA samples without reverse transcription were used as negative control for qRT-PCR to exclude DNA contamination. The isolated RNA was used for the cDNA synthesis. RNA (1000 ng) was transcribed using the transcriptor first strand cDNA synthesis kit (Roche, Switzerland), which was applied according to manufacturer's instructions. The cDNA (20 μl) prepared from the total-RNA was diluted with RNase-free water to 100 μl and the amount of 5 μl was directly analyzed by using the LightCycler®480 II System (Roche, Basel, Switzerland).

Quantitative real-time polymerase chain reaction

qRT-PCR was performed using TaqMan gene expression assays and the LightCycler®480 II System (Roche, Basel, Switzerland). The amplified DNA was analyzed by the comparative Ct method using β-actin as a reference gene. The primer and probe sets for ACTB (assay ID: Hs99999903_m1), BECN1 (Hs00186838_m1), BIRC5 (Hs00153353_m1), CCL2 (Hs00234140_m1), MAP1LC3 (Hs00797944_s1), SOX2 (Hs01053049_s1), NANOG (Hs04260366_g1), POU5F1 (Hs04260367_gH), and HIF1A (Hs00153153_m1) were selected from the TaqMan gene expression assays (Life Technologies, USA). The qRT-PCR was performed under the following amplification conditions: total volume of 20 μl, initial incubation at 50°C/2 min followed by denaturation at 95°C/10 min, then 45 cycles at 95°C/ 15 sec and at 60°C/1 min.

Statistics

Pearson correlation, principal component analysis and cluster analysis were performed to reveal associations between cases and variables. These analyses were performed on standardized data; the cluster analysis was performed using Ward's method. All charts are depicted with means and standard deviations. Software Statistica (StatSoft, Tulsa, OK, USA) was used for analysis.

Results

Determination of IC50 for plumbagin

To assess the cytotoxic effect of plumbagin on the PC-3 cell line, and to select concentrations for further analyses, MTT test and real time cell analysis (RTCA) impedance based test were performed with concentrations 0 (no drug added), 0.5, 1, 1.5, 2, 2.5, 3, 4, 5, and 6 μmol/l. Using the logistic regression, IC50 concentrations were determined at time-points 6 and 24h (see Fig 1A, 1B, 1C and 1D). The output of RTCA method is a cell index value (CI), see Fig 1A, that reflects the number of cells, as well as morphological parameters, such as the size, shape, and

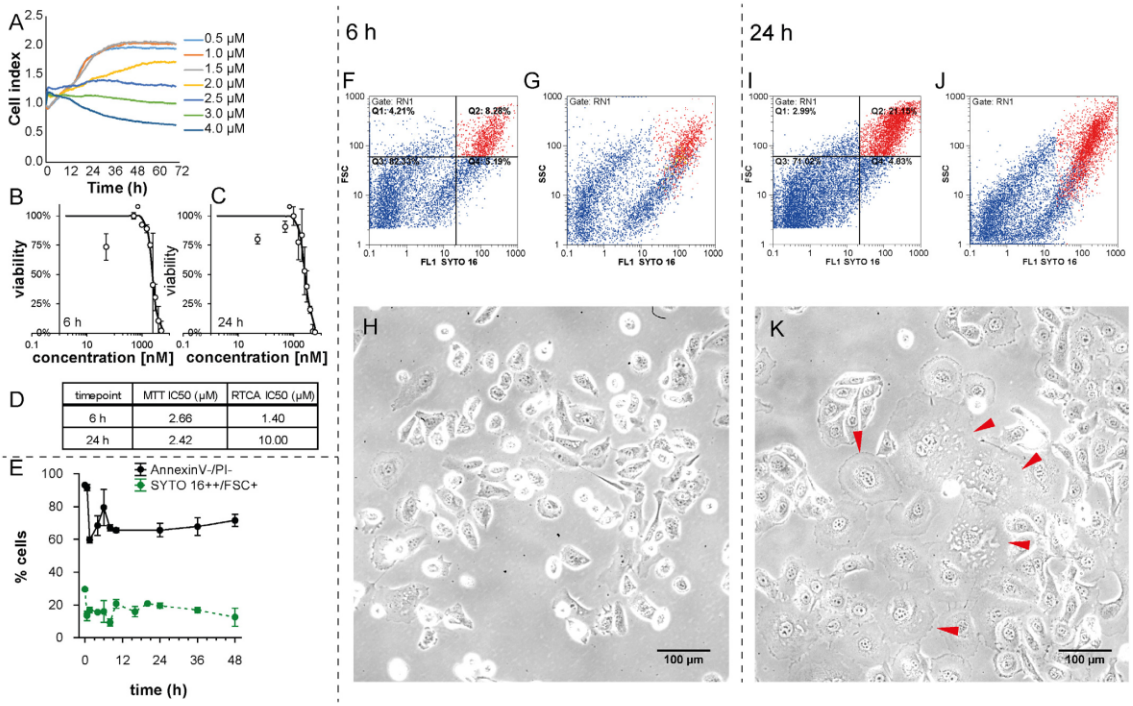

Fig 1. Effect of plumbagin treatment on viability and size of cells. (A) Real-time monitoring of relative cell impedance (showed as a cell index) using the RTCA system. **(B)** MTT-assessed response to 6h plumbagin treatment. **(C)** MTT-assessed response to 24h plumbagin treatment. **(D)** IC50 values according to RTCA and MTT and length of treatment. **(E)** Time-dependent changes in the quantity of large cells with intact nuclei (SYTO 16++/FSC+) and intact cells (AnnexinV-/PI-) assessed by flow-cytometry. **(F)** Numbers of large healthy cells depicted as SYTO 16++ /FSC+ (red) cluster at flow-cytometric dot plot at 6h time-point; Forward-scattered light (FSC) is proportional to cell-surface area or size. **(G)** Granularity of large healthy cells depicted as SYTO 16++ /SSC+ (red) cluster at flow-cytometric dot plot at 6h time-point; Side-scattered light (SSC) is proportional to cell granularity or internal complexity. **(H)** Morphology of PC-3 cells after 6h plumbagin treatment, 20x magnification, phase contrast microscopy. **(I)** Numbers of large healthy cells depicted as SYTO 16++/FSC+ (red) cluster at flow-cytometric dot plot at 24h time-point; Forward-scattered light (FSC) is proportional to cell-surface area or size. **(J)** Granularity of large healthy cells depicted as SYTO 16++/SSC+ (red) cluster at flow-cytometric dot plot at 24h time-point; Side-scattered light (SSC) is proportional to cell granularity or internal complexity. **(K)** Morphology of PC-3 cells after 24h plumbagin treatment; giant PC-3 cells with polyploid giant cancer cell (PGCCs)-like morphology are highlighted by arrows. 20x magnification, phase contrast microscopy.

doi:10.1371/journal.pone.0145016.g001

degree of cell attachment to the substrate. This means that an increase in the average size of surviving cells could affect the CI value and could correlate with higher IC50 values (1.4 µM and 10 µM IC50 after 6h and 24h treatment, respectively). We performed the flow-cytometric analysis by using SYTO 16 double-positivity as a marker of viable cells and forward scatter (FSC) to detect the size of surviving cells after the 2 µM plumbagin treatment. Numbers of large healthy cells depicted as a SYTO 16++ /FSC+ (red) cluster at the flow-cytometric dot plot were elevated at 24h time-point in comparison with 6h time-point; see Fig 1F, 1G, 1I and 1J. This experiment was done in triplicates. The average rate of large SYTO 16++ was 15.92% after 6h of plumbagin treatment and 19.58% after 24h of plumbagin treatment (Fig 1E). As we observed no dividing cells during the treatment (compare treated and untreated time-lapse, S1 and S5 Videos; cell division was apparent only in untreated cells), emergence of larger cancer cells could be assumed namely because no increase in the percentage of annexin V-/propidium iodide (PI)- cells (healthy cells that would result from dividing) was observed between 5h time-

point and 24h time-point of the treatment (Fig 1E). According to these results, the shift in IC50 values identified by the RTCA method may reflect the increased cell size between 6h and 24h time-points, as corroborated by the microscopic analysis; see Fig 1H and 1K.

PC3 cell line is predisposed to mitophagy

To assess the relative intensity of mitophagy related genes expression (*PINK1*, *FUNDC1*, *SMURF1*, and *PARL*) in the PC-3 cell line, we used the CellMiner Database (http://discover.nci.nih.gov/cellminer/). It allows to precisely determine selected genes expression patterns from 5 microarray platforms in 60 cell lines (NCI60 panel) (S1 Appendix). Pro-mitophagic genes *PINK1*, *FUNDC1*, and *SMURF1* were relatively overexpressed in PC-3 as compared with other cell lines; on the other hand, *PARL* (responsible for PINK1 cleavage) was underexpressed. These data suggest that PC-3 cells have possibly a high level of mitochondrial quality control and are able to effectively identify and then degrade damaged mitochondria.

Endoplasmic reticulum-affected mitophagy

In order to establish whether the majority of reactive oxygen species (ROS) in the cell is produced by the mitochondria, we applied fluorescent staining after the plumbagin treatment. General accumulation of ROS was monitored using CellROX Deep Red Reagent. Clear colocalisation of ROS and mitochondria staining was found (see Fig 2B and 2C). Major ROS producing mitochondria (see arrows) were coated by isolation membrane derived from ER (see Fig 2D). This observation was corroborated by transmission electron microscopy (TEM) (see Fig 2F). Swollen and damaged mitochondria were wrapped by engulfing membrane and gradually degraded (see Fig 2G). No coating membrane was found around the healthy mitochondria (see Fig 2E).

Time-lapse imaging

A time-lapse Video was captured by holographic microscope to observe the intensity of cell migration and also to quantify the kinetics of PC-3 cells death in 48 hour period. Many different types of cell-cell interactions were monitored and identified during this period including vesicular transfer (Fig 3F and 3G), eating of dead or dying cells (frequency of observation 2.5%; Fig 3C, S3 Video) and engulfment and cannibalism of living cells (frequency of observation 0.8%; Fig 3B). During the cannibalism of living cell, a cannibalic cell came into contact with a target cell. The next step was a gradual engulfment of target cell. The nucleus of the target cell appeared initially unaltered whereas the engulfing cell's nucleus began to change into a more semilunar shape. Bird eye structure typical for cannibalism was observed (Fig 3B, S2 Video). Finally, the target cell died off. The 2 μM plumbagin treatment had a particular impact on cell motility and on changes in cell-to-cell communication. A significant reduction of cell motility and communication was found after the plumbagin treatment (see Fig 3H and 3I, S1 and S5 Videos).

In oncosis, early changes included marked alterations in the cell shape and volume (Fig 3D, S1 Video). Oncotic cells formed cytoplasmic blebs and showed chromatin clumping followed by necrotic features such as cells membrane rupture and detachment from the surface. Nevertheless, some oncotic cells escaped this fate and were able to reverse processes leading to necrosis. Triggering of oncosis is not an irreversible process; oncosis can be reverted (see Fig 3E, S4 Video).

Moreover, we observed entosis triggering 20 h after the plumbagin treatment in the tumour cell population exposed to plumbagin. During entosis, cells invaded neighbouring cells, which led to the formation of cell-in-cell structure (see Fig 3A, S1 Video), no bird eye structure was

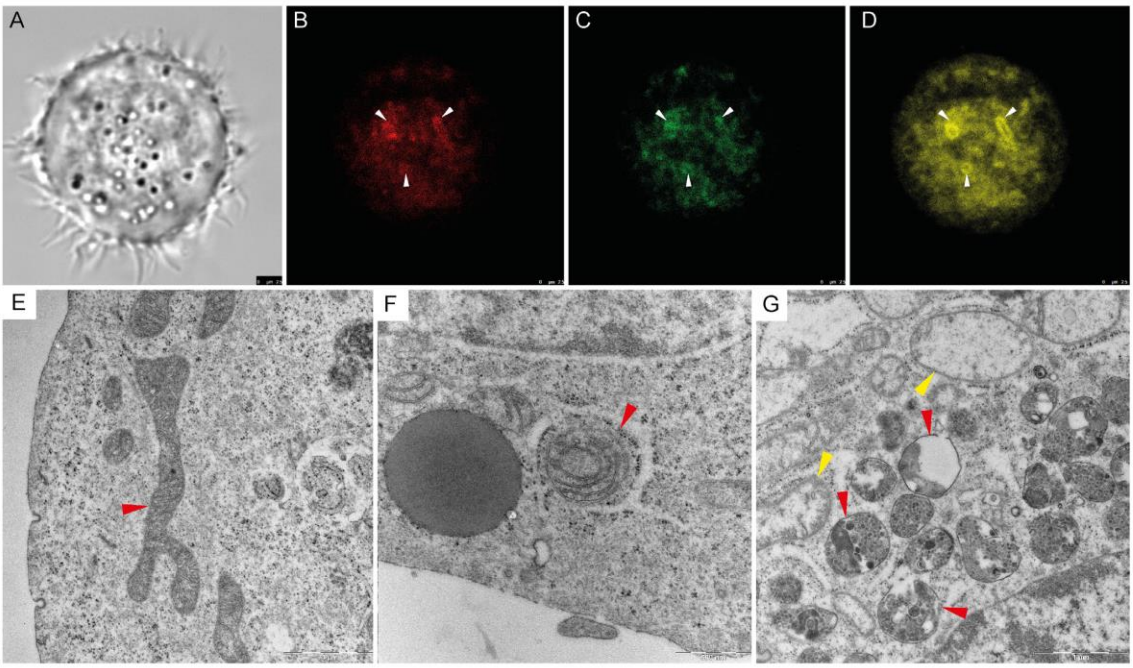

Fig 2. Reactive oxygen species (ROS)-induced mitophagy. (A) Phase contrast microscopy of PC-3 cell after plumbagin treatment. **(B)** General accumulation of ROS after plumbagin treatment monitored by confocal microscopy by using CellROX Deep Red Reagent. Areas with ROS accumulation are highlighted by arrows. **(C)** Mitochondria staining monitored by confocal microscopy using MitoTracker Green; area associated with ROS in Fig 2B are highlighted by arrows. **(D)** Endoplasmic reticulum (ER) staining monitored by confocal microscopy using ERTracker Red; areas associated with ROS in Fig 2B are highlighted by arrows. **(E)** Untreated PC-3 cell, cross-section of undamaged mitochondria (highlighted by red arrow); Transmission Electron Microscope (TEM) visualization. **(F)** plumbagin-treated PC-3 cell, mitochondria coated by ER membrane with ribosomes (highlighted by red arrow); TEM visualization. **(G)** Plumbagin-treated PC-3 cell, gradual degradation of mitochondria in autophagosomes visualised by TEM (red arrows); Swollen mitochondria as a marker of damage (yellow arrow).

doi:10.1371/journal.pone.0145016.g002

observed. Internalized cells played an active role in their engulfment (see Fig 4), which resulted in complete internalization. Cells which have undergone entosis (both engulfing and even engulfed cells) lived about five hours longer than the other observed tumour cells (frequency of this phenomenon was 2.5%). After 48 h of treatment, all PC-3 cells observed by holographic-microscopy were dead.

Time-lapse flow-cytometry

To evaluate the amount of cells positive or negative for typical markers, such as phosphatidyl serine exposure, presence of autophagosomes, or intact cellular membrane and nuclear DNA content, we used flow-cytometry at 12 time points (0h, 40min, 1.5h, 4h, 6h, 8h, 10h, 16h, 20h, 24h, 36h, and 48h). Phosphatidyl serine exposure was detected by Annexin V staining, cell viability by propidium iodide (PI) and SYTO 16 staining, and CYTO-ID Green was used as a marker of autophagosome formation. To determine the proportion of large cells with intact DNA, we used SYTO 16 and FSC. At the beginning of the experiment, about 30% of all cells were large with an intensive SYTO 16++ signal (Fig 1E). A decrease in the amount of SYTO 16 ++ large cells was shown during the first 8 hours of plumbagin treatment (ca. 15% SYTO 16+ + large cells) and an increase in the amount of SYTO 16++ large cells were shown after 10h of

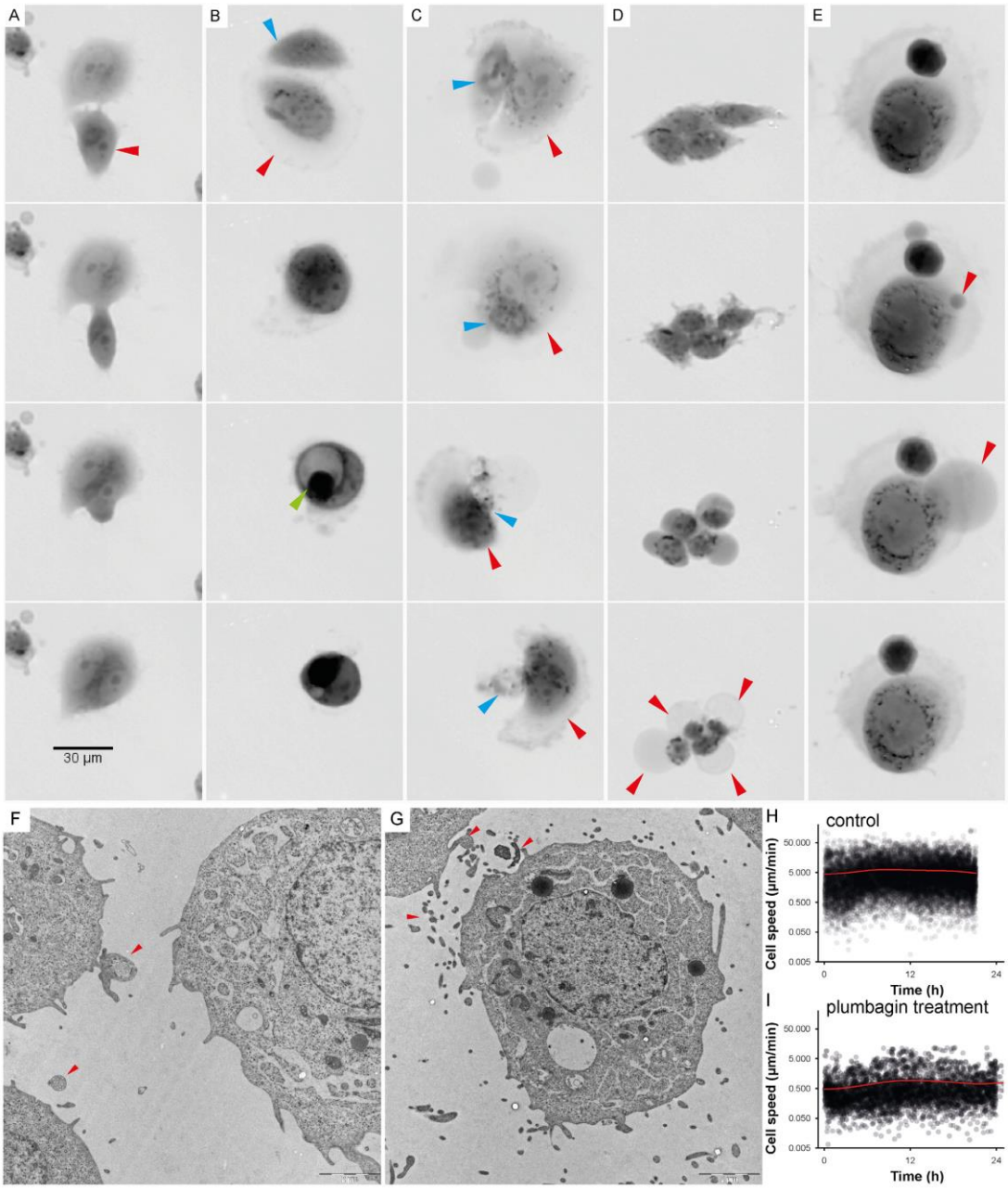

Fig 3. Time-lapse of cell interactions. For detailed time-lapse Videos see S1–S4 Videos. **(A)** Time-lapse imaging of entosis; internalized cell (red arrow) played an active role in its engulfment, which resulted in complete internalization. Both types of cells (engulfing and engulfed) were viable for a long time and lived by about five hours longer than the other observed plumbagin-treated tumour cells. **(B)** Time-lapse imaging of cell fusion with cannibalism (digestion of engulfed cell); during fusion-cannibalism of living cells, the cannibalic cell (red arrow) came in contact with the target cell (blue arrow). The next step was gradual engulfment of the target cell. The nucleus of the target cell appeared initially unaltered whereas the engulfing cell's nucleus began to change into a

semilunar shape. Bird eye structure was observed as a consequence of target cell vacualisation (see green arrow). **(C)** Time-lapse imaging of cannibalism without fusion; the dying cell (blue arrow) was attacked and exploited by the cannibalic cell (red arrow). The target cell was dead after the attack. **(D)** Time-lapse imaging of oncosis; oncotic cells formed typical cytoplasmic blebs that usually lead to necrosis (see red arrow). **(E)** Time-lapse imaging of reverse oncosis; initial forming of oncotic blebs (see red arrow) did not lead to necrosis; the bleb was absorbed and the cell remained viable. (**A-E**) Multimodal holographic microscopy, 10x magnification. **(F)** Communication between PC-3 cells; visualised by TEM (see red arrows). **(G)** Vesicular transfer between PC-3 cells; visualised by TEM (see red arrows). **(H)** Speed of the migration of untreated PC-3 cell population; assessed from holographic microscopy data by CellProfiller software by measurement of "distance travelled"parameter. **(I)** Speed of the migration of PC-3 cell population after 2 μM plumbagin treatment.

doi:10.1371/journal.pone.0145016.g003

treatment (about 20%). As we observed no dividing cells during the treatment (see S1 Video), emergence of giant cancer cells (PGCCs) larger than the average population could be assumed namely because no increase in the percentage of annexin V-/PI- cells (healthy cells that would result from dividing) was observed around the 10h time-point of treatment (Fig 1E).

Furthermore, we used the CYTO-ID Green autophagy dye for autophagy detection. Previously, CYTO-ID was validated by observing co-localization of the dye and RFP-LC3 in HeLa cells using fluorescence microscopy. An increase in CYTO-ID signal indicates the accumulation of autophagosomes [31]. Nevertheless, we detected two cell populations according to the intensity of CYTO-ID signal (CYTO-ID+, CYTO-ID++) (Fig 5A and 5E). The CYTO-ID + population correlated with the LC3-I form assessed by western-blotting (Fig 5F and 5G) ($r = 0.66$; $p = 0.001$) and the CYTO-ID++ population correlated with the LC3-II/LC3-I ratio ($r = 0.49$; $p = 0.016$). A correlation between total CYTO-ID staining and the LC3-II/LC3-I ratio was found, too ($r = 0.70$; $p = 0.0001$). According to our observation, plumbagin functions as an inductor of autophagy in the context of PC-3 cells. We also performed the flow-cytometric CYTO-ID analysis of non-treated PC-3 (Fig 5D), and plumbagin (Fig 5E) and bafilomycin (Fig 5C) (inhibitor of autophagy) treatments. During the plumbagin treatment, a high positive peak of CYTO-ID++ was shown at the time point of 8h. After the 8h peak, signal diminution was observed (probably LC3-II deconjugation and partial degradation of acid autophagic vacuoles);

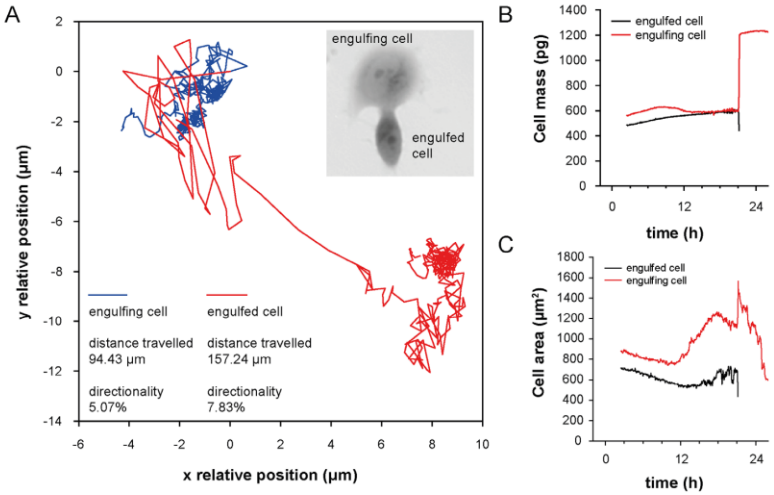

Fig 4. Mechanistic characterization of engulfed and engulfing cells in entosis. (A) Trajectory travelled of both engulfing and engulfed cell until cell fusion. See differences in the travelled distance and in directionality of individual cells. Directionality describes "purposefulness" of the movement where 0% indicate random movement and 100% indicate straight line trajectory between starting and ending position. Position (0.0, 0.0) indicate place of cell fusion. **(B)** Changes in cell mass and **(C)** cell area of engulfed and engulfing cell.

doi:10.1371/journal.pone.0145016.g004

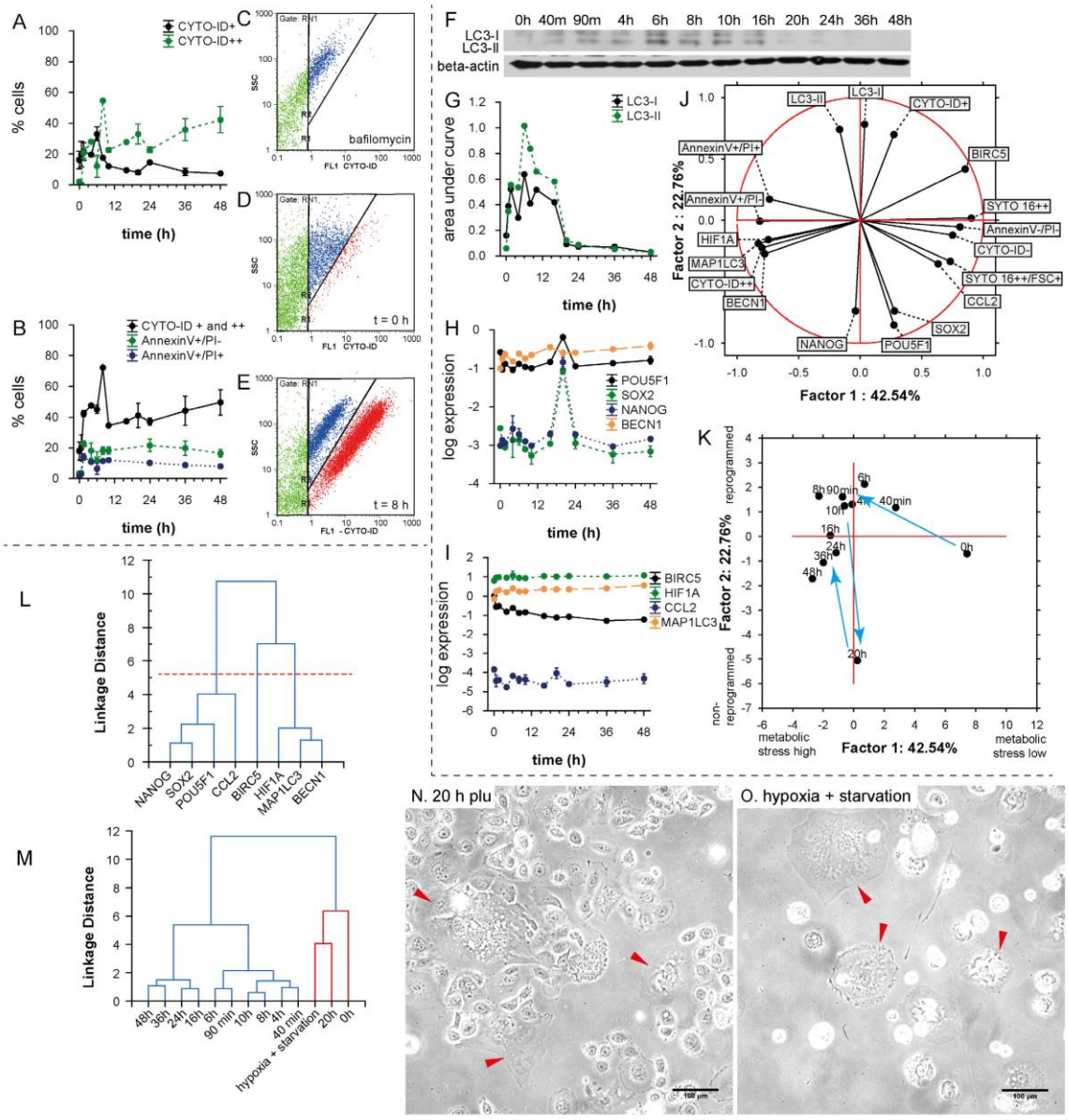

Fig 5. Autophagy and self-renewal after plumbagin treatment. (A) Time dependent dynamics of CYTO-ID Green (CYTO-ID+, CYTO-ID++) after 2 μM plumbagin treatment. See autophagy peak at 8h-time point. **(B)** Time dependent dynamics of cell deaths after 2 μM plumbagin treatment; total CytoID staining (CYTO-ID+ and CYTO-ID++) depicts autophagy, AnnexinV+/PI- depicts apoptosis or early oncosis, and AnnexinV+/PI+ depicts necrosis (raw data and gating strategy in S2 Appendix). **(C)** Amount of autophagic cells after bafilomycin treatment; red cluster depicts CYTO-ID++ population, blue cluster Cyto-ID+ population. **(D)** Amount of autophagic cells in control (not-treated population); red cluster depicts CYTO-ID++ population, blue cluster CYTO-ID + population. **(E)** Amount of autophagic cells after plumbagin treatment; red cluster depicts CYTO-ID++ population, blue cluster CYTO-ID+ population. **(F)** Western blot for LC3-I and LC3-II isoforms at 12 time-points after 2 μM plumbagin treatment (raw data in S3 Appendix). **(G)** Graphic representation of western blot results for LC3-I and LC3-II isoforms at 12 time-points after 2 μM plumbagin treatment. **(H)** Time dependent dynamics of *POU5F*, *SOX2*, *NANOG*, and *BECN1* gene expression after 2 μM plumbagin treatment. **(I)** Time dependent dynamics of *BIRC5*, *HIF1A*, *CCL2*, and *MAP1LC3* gene expression after 2 μM

plumbagin treatments. **(J)** Principal component analysis—projection of variables on the two-factor plane. See distinct clustering of genes with flow-cytometric measurements based on metabolic stress and reprogramming (for details see results). **(K)** Principal component analysis—projection of time-points on the two-factor plane. The first and the second factor are designated as "metabolic stress high-low" and "non-reprogrammed-reprogrammed", respectively (for details see results). **(L)** Cluster analysis of gene expression. The "reprogramming cluster"involved *POU5F*, *SOX2*, *NANOG*, and *CCL2*; the "autophagic and hypoxia cluster"involved *HIF1A*, *MAP1LC3*, and *BECN1*; the third cluster involved *BIRC5* gene. **(M)** Cluster analysis of gene expression of 12 time-points after 2 μM plumbagin treatment and PGCCs selected by hypoxia and starvation; based on correlations of gene expression patterns, similarity between PGCCs and PC-3 cells after 20h plumbagin treatment was found. **(N)** Morphology of cells after 20h plumbagin treatment; cells with polyploid giant cancer cell (PGCCs)-like morphology are highlighted by arrows. **(O)** Morphology of PC-3 cells after 1 month of hypoxia and starvation; cells with PGCCs-like morphology are highlighted by arrows.

doi:10.1371/journal.pone.0145016.g005

see Fig 5A. A decrease in the CYTO-ID++ signal after the time-point of 8h indicates that there is not only the simple accumulation of autophagosomes, but also the degradation of their content. During the whole experiment (48 h), the level of CYTO-ID++ signal was higher than at the zero time-point.

The highest percentage of autophagic cells (according to the accumulation of autophagosomes) was observed 8 hours after the treatment; see Fig 5B. Due to the triggering of autophagic mechanisms, almost no increase of necrotic (AnnexinV+/PI+) and early oncotic or apoptotic (AnnexinV+/PI-) cells was induced (Fig 5B). Almost 40% of cells were autophagic during the 48 h experiment. The quantity of AnnexinV+/PI+ and AnnexinV+/PI- did not exceed 20% at any observed time-point.

Time-lapse gene expression profiling

We isolated RNA (in duplicates) from the PC-3 cells at 12 time-points (0h, 40min, 1.5h, 4h, 6h, 8h, 10h, 16h, 20h, 24h, 36h, and 48h) of plumbagin treatment and performed qRT-PCR. Expression was assessed of *BECN1*, *MAP1LC3A*, *HIF1A*, *BIRC*, *CCL2*, *POU5F1*, *SOX2*, and *NANOG*. During the experiment, we observed a gradual increase in the expression of autophagy-related genes *MAP1LC3A* and *BECN1* and a gradual decrease of *BIRC*. The expression of autophagy-related genes was in a good correlation ($r = 0.92$, $p<0.001$) and correlated also with *HIF1A* ($r = 0.87$, $p<0.001$ and $r = 0.79$, $p<0.001$); see Fig 5L. We also found an extensive induction of pluripotency-associated genes expression (*NANOG*, *SOX2*, and *POU5F1*) at the time-point of 20 h; see Fig 5H. No dramatic changes in *HIF1A* expression were observed during the 12 time-points measurements (Fig 5I). Among the analyzed genes, three different expression clusters were found (see Fig 5L). The most expressed gene cluster was autophagic promoting cluster of genes (*BECN1*, *MAP1LC3A*, and *HIF1A)*. Of all the observed genes, the least expressed one was *CCL2* (Fig 5I).

Principal component analysis

In addition to the correlation analysis, the component analysis made it possible for us to detect the structure of relationships between the observed time-points, thus helping us to assess main variables in the particular time-points. Moreover, this analysis allowed us to classify variables based on the flow-cytometric and expression profiles. To illustrate the model of metabolic stress and self-renewal, two-factor analysis was chosen with a total cumulative variance of 65.3% and eigenvalues 42.54% and 22.76% for factor 1 and factor 2, respectively (Fig 5J). This two-axis model represents both metabolic stress (factor 1) and "self-renewal and reprogramming capacity" (factor 2). These conclusions are based on the following findings: (a) *NANOG*, *SOX2*, and *POU5F1* are genes, which strongly correlate with the pluripotency and self-renewal, (b) annexinV+/PI+ status refers to cell death; (c) PI positivity, Annexin V positivity, CYTO-ID positivity, *BECN1*, *MAP1LC3A*, and *HIF1A* expression are directed to the negative values of factor 1 (high metabolic stress). Taken together, positive values of factor 1 are associated with

the healthy cells rather than with the cell damage, and negative values of factor 2 are associated with cell reprogramming processes, rather than with the naive PC-3 cells. When we accept this model, large cells with the intensive SYTO 16++ signal seem to be further in reprogramming processes than the average SYTO 16++ population of PC-3 cells and naive PC-3 harvested at the zero time-point, and *BIRC* expression is very important for preventing metabolic stress in the naive PC-3, but could also prevent reprogramming mechanisms.

When these factors are used to project cases (time-points), another apparent trend is evident: At the time-point of 20h, PC-3 cells seem to break free from the bondage of metabolic stress by triggering the reprogramming processes. This "reprogrammed" PC-3, are associated with the lower metabolic stress (as represented by positive values of factor 1). However, when the stress continues, the cells are being pushed to higher metabolic stress again, staying partially reprogrammed though; see Fig 5K time-point 48 h. We could assume some cyclic characteristic of stress resistance processes and reprogramming. During these cycles of adaptation, the cells are pushed to a state that is increasingly dedifferentiated.

Polyploid giant cancer cells (PGCCs) expression profiling

When the PC-3 cancer cell line was cultured under normal conditions, some large cells with enlarged nuclei (PGCCs) were sporadically observed. However, the exposure of PC-3 cancer cells to long-term starvation and hypoxia (for at least one month) induced the formation of cells with larger cell and nuclear size, while cells of normal morphology were almost eliminated. PGCCs were highly resistant to oxygen deprivation and could generate regular-sized cancer cells through budding or bursting. The PGCCs induced by starvation and hypoxia were 2–10 times larger than normal cells, and had a distinctive morphology (see Fig 5O).

Next, qRT-PCR gene expression profiling was performed to analyze the specific molecular pattern expressed in PGCCs. Expression profiles of eight genes (*BECN1*, *MAP1LC3A*, *HIF1A*, *BIRC*, *CCL2*, *POU5F1*, *SOX2*, and *NANOG*) were assessed and compared with the normal PC-3 cell expression patterns obtained at the particular time points during the plumbagin treatment by cluster analysis (see Fig 5M). After 20h of plumbagin treatment, the expression pattern of PC-3 cells matched with the PGCCs characteristics as well as the cell morphology (see Fig 5N and 5O).

Discussion

Panov *et al.* found out, that the PC-3 prostate cancer cell line contained 2 to 4 times more mitochondria with enhanced respiratory activity [15], which may cause high sensitivity of PC-3 cells to ROS—produced massively during the plumbagin treatment. However, in cytotoxicity tests we have noticed differences in sensitivity to plumbagin measured by metabolic-based MTT and impedance-based RTCA. The output of RTCA method is a cell index value (CI; see Fig 1A) that reflects the number of cells as well as morphological parameters such as size, shape, and degree of cell attachment to the substrate. This means that an increase in the average size of surviving cells affects CI and could correlate with higher IC50 values (1.4 μM resp. 10 μM IC50 after 6h resp. 24h treatment) As we observed no dividing cells during the 2 μM plumbagin treatment (S1 Video), we assumed that the cells increased their volume between the time-points of 6h and 24h. Accordingly, an increase in the amount of SYTO 16++ large cells was shown at the 20h time-point as compared with the 6h time-point (see Fig 1F and 1I). This might indicate the emergence of giant polyploid cancer cells. SYTO 16 is effective at staining the DNA of cells, because it binds preferentially to DNA over RNA at a ratio of approximately 20:1 [32] and shows specific information about the cell nuclei, such as size and distribution. Furthermore, Manusco *et al.* used SYTO16 staining to enumerate circulating

endothelial cells with a high DNA content [33] and Ibrahim *et al.* identified multinucleate cells during the growth cycle of *Mycobacterium avium* by SYTO 16 staining [34]. Importantly, Wlodkowic *et al.* have recently showed that SYTO dyes do not adversely affect normal cellular physiology. The cytometric detection of SYTO 16 fluorescence loss is even a sensitive marker of early apoptotic events [35].

Unlike the RTCA IC50 values, these values measured by MTT were relatively stable (2.66 μM resp. 2.42 μM IC50 after 6h resp. 24h treatment). The main mechanism of MTT assay is a reduction of tetrazolium salts to formazan by mitochondrial succinate dehydrogenase (SDH). SDH loses its activity by damage of the respiratory chain [36]. According to our results, main reduction of SDH activity takes place during the first 6 hours. As mitochondria are the main producer of ROS, they are an easy target of ROS-mediated damage, too. Thus, the ROS-mediated damage plays a key role in the induction of cellular senescence [37]. In this study we disclosed that the major ROS producing mitochondria in the PC-3 cells are coated by ER membranes. Since the ER mitochondria encounter structure (ERMES) plays a key role in mitophagy in yeast and Boeckler *et al.* showed that successful mitophagy depends on mitochondrial ER tethering, [38], we assume that the major ROS producers in PC-3 are destined for degradation by mitophagy. Mitophagy helps to eliminate damaged mitochondria and maintains their healthy pool [39]. Mitophagy also presents a possible way to gain enough energy for survival [19] and simultaneously removes the ROS producing mitochondria [40]. Accordingly, PC-3 cells express a high amount of pro-mitophagic genes *PINK1*, *FUNDC1*, and *SMURF1* in comparison with the other cell lines of NCI60 panel. On the other hand, *PARL* (responsible for PINK1 cleavage) was underexpressed. The PINK1 protein is connected with the mitochondrial quality control by targeting damaged mitochondria for degradation [41]. The loss of PINK1 also impairs stress-induced autophagy and cell survival [42]. Furthermore, the mitochondrial outer-membrane protein FUNDC1 could mediate hypoxia-induced mitophagy [43]. According to these data, it seems possible that PC-3 cells have a high level of mitochondrial quality control and are able to identify and then degrade the damaged mitochondria. It could seem that getting rid of mitochondria is not much favourable for the tumour cell in the long run, because tumour cells without mitochondrial DNA (mtDNA) show retarded tumour growth [44]. Nevertheless, the tumour formation could be associated with the acquisition of mtDNA from host cells [44] and this temporary handicap could be thus compensated.

Severely damaged cells often exhibit accumulation of autophagosomes and hence seem to be subject to autophagic cell death. Nevertheless, in many cases, this "autophagic cell death" is the cell death during autophagy rather than the cell death by autophagy [45]. In our study, the highest percentage of autophagic cells was observed 8 hours after the treatment (see Fig 5B). Due to the triggering of autophagic mechanisms, almost no increase of necrotic (AnnexinV +/PI+) and early oncotic or apoptotic (AnnexinV+/PI-) cells was induced. It follows that induction of autophagy does not seem to be directly related to cell death. Conversely, our results suggest that autophagy can promote the survival of cells under oxidative stress, which is in accordance with the results of other studies [24, 46]. According to our results, autophagy precedes several mechanisms such as self-renewal and entosis. Sun *et al.* found out that tumour cells with high deformability preferentially engulf neighbouring cells with low deformability in heterogeneous populations. They also found out that downregulation of contractile myosin allows the internalization of neighbouring cells and that a mechanical differential between the engulfing and engulfed cells is required for entosis to progress [47]. Therefore, we would like to present a hypothesis, that reduction in membrane and cell stiffness due to protein catabolism by autophagy could reflect increased entotic activity. Moreover, the entotic vacuole membrane encircling the internalized cells recruits the autophagy protein LC-3 [48]. The initiation of entosis, instead of apoptosis or necrosis, might give the cell additional time to survive the

transient deleterious conditions. The cell in cell structure results in the decreased surface-to-volume ratio, thereby minimizing cell membrane requirements (one membrane for two nuclei) (Fig 4). Furthermore, a live cell internalized by entosis could disrupt host cell division. Subsequently, cytokinesis often fails, which causes the formation of binucleate cells that are able to generate aneuploid cell lineages [49]. It was also shown that the frequency of entotic structures correlates well with the tumour grade [49]. According to this observation, we speculate, that entosis and competition between cells by cannibalism is rather late-stage process in cancer cells and requires activation of mechanisms leading to higher developmental plasticity, changes in cytoskeletal proteins [47] and some kind of de-differentiation of cells accompanied with changes in transcription regulators. All of these could be supported by ROS. For example, transcription factor C/EBPbeta (LIP), is elevated by endoplasmic reticulum stress and oncogenic signalling [50, 51]. Recently, expression of LIP was connected with enhanced autophagy and engulfment of neighbouring cells in the human breast cancer cell line (MDA-MB-468 cell line with mutant p53 [52]) [53]. In our experiment, entotic cells lived by about five hours longer than the other observed tumour cells. Although the all observed PC-3 cells were dead after 48h treatment, it could probably be only the consequence of relatively low numbers of cells (ca. 50 cells) which can be seen in the holographic-microscope field of view. Nevertheless, according to the flow-cytometry results, more than 60% of cells were annexinV-/PI- after 48 h of 2 μM plumbagin treatment. About 18% of these cells were large and SYTO 16++.

Similar to mitophagy, digestion of the cytoplasm of neighbouring cells can provide a source of amino acids, indicating that cannibalism could be a survival mechanism for tumour cells during starvation and other adverse conditions [54]. Significant reduction of cell motility and cannibalism were found after the plumbagin treatment. Furthermore, plumbagin is able to suppress activation of nuclear factor-κB (NF-κB) [13], and therefore could repress anoikis resistance [55], which may be an explanation why plumbagin is probably more toxic for the PC-3 cell line than cisplatin (2.42 μM vs. 75 μM IC50 value after 24h treatment) [8].

We have also found out that specific processes leading to induction of reprogramming to pluripotency (depicted by significant overexpression of *NANOG*, *SOX2*, and *POU5F1* [17, 26, 56]) were triggered 20h after the treatment in the tumour cell population exposed to ROS. These three pluripotency-related transcription factors, Oct 3/4, Nanog, and Sox-2, form a core regulatory network that coordinates the self-renewal and differentiation of stem cells. Transfection of NANOG, SOX2, OCT4, and LIN28 in human fibroblasts induced pluripotency, indicating a key position of these factors in the reprogramming of somatic cells [57]. These self-renewal molecules highly contribute to tumourigenesis [17, 58]. Takahashi *et al.* also showed that the introduction of transcription factors Oct3/4, Sox2, c-Myc, and Klf4 into mouse adult fibroblasts was able to reprogramme differentiated cells to an embryonic-like, pluripotent state [59, 60]. Nanog overexpression was found to be one of the distinctive features of the population of fibroblasts that escaped from Ras-induced senescence [61]. Furthermore, Nanog was found to be promoting the transfer of pluripotency after the cell fusion of reprogrammed and non-reprogrammed cell [62]. Nanog seems to be required during the final stages of somatic cell reprogramming. Once the pluripotent state is established, Nanog is no longer needed [63], which is in accordance with the peak-character of *NANOG* expression observed by us (see Fig 5H). Bambrik *et al.* postulated that the activation of endogenous Oct4 or Nanog may be a marker for fully reprogrammed induced pluripotent stem cells (iPSCs) [64]. We rather suppose, that overexpression of *NANOG*, *SOX2*, and *POU5F* in the prostate tumour cell population (especially in PGCCs; [65]) exposed to ROS leads to higher developmental plasticity and capability to faster respond to changes in the extracellular environment that could ultimately lead to alteration of cell fate (epithelial features vs. mesenchymal character etc.). Similar process was observed in Mitchell et al. study [66]. Expression of pluripotency genes results in

functional reprogramming that could provide to tumour cells higher developmental potency [67] as well as higher stemness [25]. For example, it was observed that differentiated cancer cells and tumor stroma can be originated directly from polyploid giant cancer cells induced by paclitaxel [67].

Here, we hypothesize that autophagy and cell-in-cell structures accompanied with polyploidization could also play an important role in the survival, remodelling and dedifferentiation of cells to a pluripotent state (for summary see Fig 6). Autophagy could cause the degradation of proteins important for the status of differentiation, which could restrain the process of reprogramming, and simultaneously could eliminate proteins that should not be expressed in the pluripotent cells. According to our model arisen from the principal component analysis, *BIRC* expression is very important for preventing metabolic stress in naive PC-3, but could prevent reprogramming mechanisms, too. Protein product of *BIRC* gene (survivin) is able to prevent apoptotic cell death, but also inhibits autophagy [68, 69], which could contribute to the efficiency of puripotent stem cells generation [26]. Furthermore, relatively little expressed in PC-3 cells is another autophagy inhibitor *CCL2* [69].

In our experiment, the expression pattern of PC-3 cells as well as their morphology after 20h of plumbagin treatment matched with the PGCCs characteristics. This observation is in accordance with the idea that entering polyploidy is part of a strictly regulated process that could provide a survival advantage to cells with DNA damage [17]. Notably, the polyploid state can affect the resistance of cancer cells and could also contribute to the generation of cancer stem cells in response to stress [17, 25]. According to our model, large cells with an intensive SYTO 16++ signal (probably PGCCs) seem to be further in reprogramming to pluripotency processes than naive PC-3 cells. Erenpreisa *et al.* discussed, that senescence, polyploidy and self-renewal are three steps to immortality of cancer cells [17]. We predict that autophagy could play an important role in all these three processes, particularly because PC-3 are p53 deficient and hence could be resistant to senescence, which is a natural barrier for reprogramming [26]. PC-3 seem to be predisposed to reprogramming [70–72].

We have already tested other prostate cell lines such as PNT1A and 22Rv1, but they both have partially active p53 and therefore they are not resistant to cell cycle arrest, senescence and cell death [8] triggered due to polyploidization. It is in accordance with other studies where initiation and maintenance of senescence seems to be p53 dependent [37, 73] as well as cell death triggering after polyploidization [74]. According to these results, we supposed, that polyploidization and PGCCs forming as mechanism of resistance is rather typical for cell lines that have p53-deficiency and metastatic potential and is not unique for prostate cancer cell lines. Recent work by Zhang et al. has confirmed the importance of PGCCs in therapy resistance and ovarian cancer progression [25, 75]. In contrast with polyploidization, we supposed that mitophagy is more general principle of coping with cell stress in immortalized cells, which is in accordance with other studies [76–78].

Prostate cancers often show large intra-tumour heterogeneity in almost all measurable characteristics including metabolism, gene expression, cellular morphology, and metastatic potential. Some cell populations inside the tumour seem to be predisposed to resist high levels of metabolic stress. One of the ways how to resist is proper control and degradation of damaged ROS producing mitochondria by mitophagy. Accordingly, autophagy was activated as a protective mechanism and mediated the resistance phenotype of some cancer cells during the ROS-producing treatment in our model of apoptosis-resistant, androgen-independent, metastasis producing prostate cancer (PC-3 cell line). In recent years, it seemed possible that autophagy can execute cell death in cancer cells which are apoptosis defective, but this is not true for the PC-3 cell line. We also assume that autophagy could promote arousal of cell-in-cell structures and thus play a significant role in polyploidization and dedifferentiation of cells to a

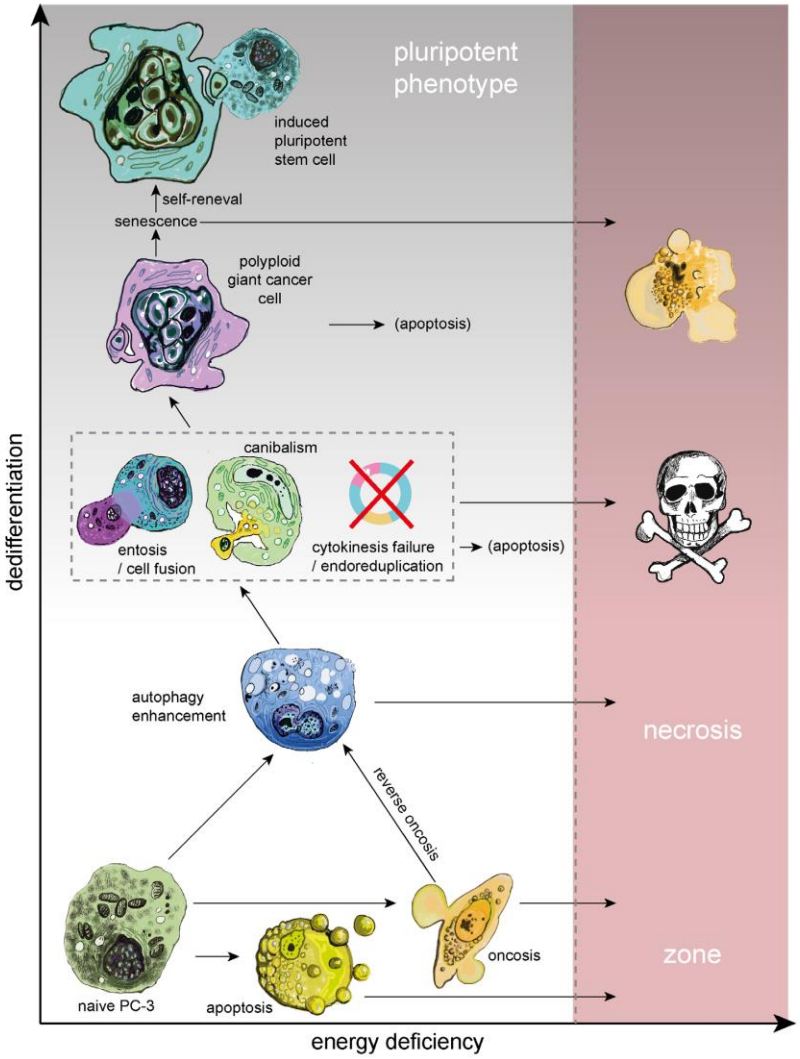

Fig 6. Possible cell fate under oxidative stress. Prolonged oxidative stress (ROS) leads to severe cell damage and depletion of cell energy reserves. Nevertheless, many cell injuries caused by ROS could be sublethal, especially because PC-3 cells have non-functional p53 and therefore disrupt the triggering of apoptosis. Even if a damaged cell is driven to oncosis, reversion of this process is possible, particularly if the cell is able to restore ATP production. A way to gain enough energy for survival could be autophagy. Similar to autophagy, digestion of the cytoplasm of neighbouring cells can provide a source of amino acids. Retention of a foreign nucleic acid by cannibalistic engulfment could result in aneuploid or polyploid state. Furthermore, reduction in membrane and cell stiffness due to protein catabolism by autophagy could reflect increased entotic activity. Cell in cell structure results in the decreased surface-to-volume ratio, thereby minimizing cell membrane requirements. Furthermore, a live cell internalized by entosis could disrupt host cell division. Subsequently, cytokinesis often fails, which can lead to the formation of polyploid giant cancer cells (PGCCs). PGCCs often dye by apoptosis or senescence, but a small fraction of these cells is able to survive and even produce aneuploid progeny. Senescence, polyploidy and self-renewal seem to be three steps to immortality of cancer cells. Autophagy could play an important role in all of them.

doi:10.1371/journal.pone.0145016.g006

pluripotent state. Inasmuch as androgen-independent prostate cancer cells with non-functional p53 are able to quite easy cope with damages caused by ROS producing agents and ROS can even participate in positive selection of resistant PGCCs with some pluripotent characteristics, prostate cancer therapies based on ROS producing agents could be a misleading concept.

Supporting Information

S1 Appendix. Expression of mitophagy-related genes by NCI60 platform. For the assessment of the relative intensity of mitophagy related genes expression (*PINK1*, *FUNDC1*, *SMURF1*, and *PARL*) in the PC3 cell line we used CellMiner Database (http://discover.nci.nih.gov/cellminer/). It allows the determination of selected genes expression patterns from 5 microarray platforms in 60 cell lines (NCI60 panel). The tool output includes relative transcript intensity presented as z-scores and visualized as a bar graph. The bars for each cell line are colour-coded by the tissue of origin.
(TIF)

S2 Appendix. Flow-cytometric analyses. Gating strategy of time-lapse analysis of plumbagin-treated cells using AnnexinV/Propidium iodide, SYTO 16 and CYTO-ID staining and raw data.
(PDF)

S3 Appendix. Western blotting of LC-3. The cropped part of the blot identical to Fig 4 and whole membrane with LC-3 and beta-actin antibodies.
(TIF)

S1 Video. Time-lapse imaging of entosis and oncosis. 2μM plumbagin treatment. **No cell division** appears during 48 hour of plumbagin treatment; red square areas highlight main points of interest; A) during entosis, internalized cell plays an active role in process of internalization. Both, engulfing and engulfed cell live about five hours longer than the other PC-3 cells. B) Oncotic cells formed cytoplasmic blebs and showed chromatin clumping followed by necrotic features such as cell membrane rupture and detaching from the surface.
(MP4)

S2 Video. Time-lapse imaging of cannibalism with the cell fusion (digestion of engulfed cell, detail). Target-cell is gradually engulfed by active cannibalic polynuclear cell. Bird eye structure typical for cannibalism appears. Then the target cell dies off.
(MP4)

S3 Video. Time-lapse imaging of cannibalism without the cell fusion (detail). Weakened target- cell is contacted by cannibalic cell, exploited and left to die.
(MP4)

S4 Video. Time-lapse imaging of reverse oncosis (detail). Recuperation of oncotic cell forming cytoplasmic blebs.
(MP4)

S5 Video. Time-lapse imaging of untreated PC-3 cell line. Unaffected PC-3 cells. Red arrows depict cell division.
(MP4)

Acknowledgments

We thank Dr. Lucia Knopfova for assistance in western blot analysis and Dr. Miroslava Sedlackova for assistance in transmission electron microscopy.

Author Contributions

Conceived and designed the experiments: JB JG MR MM. Performed the experiments: JB JG MR AK PS PB MM. Analyzed the data: JG AK RK VA. Contributed reagents/materials/analysis tools: PB VA RK MM. Wrote the paper: JB JG MR RK VA MM.

References

1. Carroll AG, Voeller HJ, Sugars L, Gelmann EP. P53 oncogene mutations in 3 human prostate-cancer cell-lines. Prostate 1993; 23: 123–34. PMID: 8104329
2. Rubin SJ, Hallahan DE, Ashman CR, Brachman DG, Beckett MA, Virudachalam S, et al. 2 prostate carcinoma cell-lines demonstrate abnormalities in tumor suppressor genes. Journal of Surgical Oncology 1991; 46: 31–6. PMID: 1986144
3. Gustin JA, Maehama T, Dixon JE, Donner DB. The PTEN tumor suppressor protein inhibits tumor necrosis factor-induced nuclear factor kappa B activity. Journal of Biological Chemistry 2001; 276: 27740–4. PMID: 11356844
4. Barbieri CE, Bangma CH, Bjartell A, Catto JW, Culig Z, Gronberg H, et al. The mutational landscape of prostate cancer. Eur Urol 2013; 64: 567–76. doi: 10.1016/j.eururo.2013.05.029 PMID: 23759327
5. Bertram J, Peacock JW, Fazli L, Mui AL, Chung SW, Cox ME, et al. Loss of PTEN is associated with progression to androgen independence. Prostate 2006; 66: 895–902. PMID: 16496415
6. Wu Z, Conaway M, Gioeli D, Weber MJ, Theodorescu D. Conditional expression of PTEN alters the androgen responsiveness of prostate cancer cells. Prostate 2006; 66: 1114–23. PMID: 16637073
7. Choucair K, Ejdelman J, Brimo F, Aprikian A, Chevalier S, Lapointe J. PTEN genomic deletion predicts prostate cancer recurrence and is associated with low AR expression and transcriptional activity. Bmc Cancer 2012; 12.
8. Gumulec J, Balvan J, Sztalmachova M, Raudenska M, Dvorakova V, Knopfova L, et al. Cisplatin-resistant prostate cancer model: Differences in antioxidant system, apoptosis and cell cycle. International Journal of Oncology 2014; 44: 923–33. doi: 10.3892/ijo.2013.2223 PMID: 24366574
9. Sedletska Y, Giraud-Panis MJ, Malinge JM. Cisplatin is a DNA-damaging antitumour compound triggering multifactorial biochemical responses in cancer cells: importance of apoptotic pathways. Curr Med Chem Anticancer Agents 2005; 5: 251–65. PMID: 15992353
10. Marullo R, Werner E, Degtyareva N, Moore B, Altavilla G, Ramalingam SS, et al. Cisplatin Induces a Mitochondrial-ROS Response That Contributes to Cytotoxicity Depending on Mitochondrial Redox Status and Bioenergetic Functions. Plos One 2013; 8.
11. Powolny AA, Singh SV. Plumbagin-induced Apoptosis in Human Prostate Cancer Cells is Associated with Modulation of Cellular Redox Status and Generation of Reactive Oxygen Species. Pharmaceutical Research 2008; 25: 2171–80. doi: 10.1007/s11095-008-9533-3 PMID: 18213451
12. Castro FAV, Mariani D, Panek AD, Eleutherio ECA, Pereira MD. Cytotoxicity Mechanism of Two Naphthoquinones (Menadione and Plumbagin) in Saccharomyces cerevisiae. Plos One 2008; 3.
13. Sandur SK, Ichikawa H, Sethi G, Ahn KS, Aggarwal BB. Plumbagin (5-hydroxy-2-methyl-1,4-naphthoquinone) suppresses NF-kappaB activation and NF-kappaB-regulated gene products through modulation of p65 and IkappaBalpha kinase activation, leading to potentiation of apoptosis induced by cytokine and chemotherapeutic agents. J Biol Chem 2006; 281: 17023–33. PMID: 16624823
14. Qian W, Nishikawa M, Haque AM, Hirose M, Mashimo M, Sato E, et al. Mitochondrial density determines the cellular sensitivity to cisplatin-induced cell death. American Journal of Physiology-Cell Physiology 2005; 289: C1466–C75. PMID: 16107504
15. Panov A, Orynbayeva Z. Bioenergetic and Antiapoptotic Properties of Mitochondria from Cultured Human Prostate Cancer Cell Lines PC-3, DU145 and LNCaP. Plos One 2013; 8.
16. Balvan J, Krizova A, Gumulec J, Raudenska M, Zbysek S, Sedlackova M, et al. Multimodal holographic microscopy: distinction between apoptosis and oncosis. Plos One 2015; 10: e0121674. doi: 10.1371/journal.pone.0121674 PMID: 25803711
17. Erenpreisa J, Cragg MS. Three steps to the immortality of cancer cells: senescence, polyploidy and self-renewal. Cancer Cell International 2013; 13.

18. Trump BF, Berezesky IK, Chang SH, Phelps PC. The pathways of cell death: Oncosis, apoptosis, and necrosis. Toxicologic Pathology 1997; 25: 82–8. PMID: 9061857

19. Singh R, Kaushik S, Wang Y, Xiang Y, Novak I, Komatsu M, et al. Autophagy regulates lipid metabolism. Nature 2009; 458: 1131–5. doi: 10.1038/nature07976 PMID: 19339967

20. Kroemer G, Perfettini J-L. Entosis, a key player in cancer cell competition. Cell Research 2014; 24: 1280–1. doi: 10.1038/cr.2014.133 PMID: 25342563

21. Krajcovic M, Krishna S, Akkari L, Joyce JA, Overholtzer M. mTOR regulates phagosome and entotic vacuole fission. Molecular Biology of the Cell 2013; 24: 3736–45. doi: 10.1091/mbc.E13-07-0408 PMID: 24088573

22. Degenhardt K, Mathew R, Beaudoin B, Bray K, Anderson D, Chen GH, et al. Autophagy promotes tumor cell survival and restricts necrosis, inflammation, and tumorigenesis. Cancer Cell 2006; 10: 51–64. PMID: 16843265

23. Mathew R, Kongara S, Beaudoin B, Karp CM, Bray K, Degenhardt K, et al. Autophagy suppresses tumor progression by limiting chromosomal instability. Genes & Development 2007; 21: 1367–81.

24. Kimmelman AC. The dynamic nature of autophagy in cancer. Genes & Development 2011; 25: 1999–2010.

25. Zhang S, Mercado-Uribe I, Xing Z, Sun B, Kuang J, Liu J. Generation of cancer stem-like cells through the formation of polyploid giant cancer cells. Oncogene 2014; 33: 116–28. doi: 10.1038/onc.2013.96 PMID: 23524583

26. Menendez JA, Vellon L, Oliveras-Ferraros C, Cufi S, Vazquez-Martin A. mTOR-regulated senescence and autophagy during reprogramming of somatic cells to pluripotency: a roadmap from energy metabolism to stem cell renewal and aging. Cell Cycle 2011; 10: 3658–77. doi: 10.4161/cc.10.21.18128 PMID: 22052357

27. Kolman P, Chmelik R. Coherence-controlled holographic microscope. Optics Express 2010; 18: 21990–2003. doi: 10.1364/OE.18.021990 PMID: 20941100

28. Slaby T, Kolman P, Dostal Z, Antos M, Lost'ak M, Chmelik R. Off-axis setup taking full advantage of incoherent illumination in coherence-controlled holographic microscope. Optics Express 2013; 21: 14747–62. doi: 10.1364/OE.21.014747 PMID: 23787662

29. Davies HG, Wilkins MHF. Interference microscopy and mass determination. Nature 1952; 169: 541-. PMID: 14929230

30. Barer R. Refractometry and interferometry of living cells. Journal of the Optical Society of America 1957; 47: 545–56. PMID: 13429433

31. Chan LL-Y, Shen D, Wilkinson AR, Patton W, Lai N, Chan E, et al. A novel image-based cytometry method for autophagy detection in living cells. Autophagy 2012; 8: 1371–82. doi: 10.4161/auto.21028 PMID: 22895056

32. Udovich JA, Besselsen DG, Gmitro AF. Assessment of acridine orange and SYTO 16 for in vivo imaging of the peritoneal tissues in mice. Journal of Microscopy-Oxford 2009; 234: 124–9.

33. Mancuso P, Calleri A, Bertolini F, Tacchetti C, Heymach JV, Shalinsky DR. Quantification of Circulating Endothelial Cells by Flow Cytometry Response. Clinical Cancer Research 2009; 15: 3640–1. doi: 10.1158/1078-0432.CCR-09-0160 PMID: 19451598

34. Ibrahim P, Whiteley AS, Barer MR. SYTO16 labelling and flow cytometry of Mycobacterium avium. Letters in Applied Microbiology 1997; 25: 437–41. PMID: 9449859

35. Wlodkowic D, Skommer J, Darzynkiewicz Z. Rapid quantification of cell viability and apoptosis in B-cell lymphoma cultures using cyanine SYTO probes. Methods Mol Biol 2011; 740: 81–9. doi: 10.1007/978-1-61779-108-6_10 PMID: 21468970

36. Aitken RJ, Whiting S, De Iuliis GN, McClymont S, Mitchell LA, Baker MA. Electrophilic Aldehydes Generated by Sperm Metabolism Activate Mitochondrial Reactive Oxygen Species Generation and Apoptosis by Targeting Succinate Dehydrogenase. Journal of Biological Chemistry 2012; 287: 33048–60. PMID: 22851170

37. Rufini A, Tucci P, Celardo I, Melino G. Senescence and aging: the critical roles of p53. Oncogene 2013; 32: 5129–43. doi: 10.1038/onc.2012.640 PMID: 23416979

38. Boeckler S, Westermann B. Mitochondrial ER Contacts Are Crucial for Mitophagy in Yeast. Developmental Cell 2014; 28: 450–8. doi: 10.1016/j.devcel.2014.01.012 PMID: 24530295

39. Ashrafi G, Schwarz TL. The pathways of mitophagy for quality control and clearance of mitochondria. Cell Death and Differentiation 2013; 20: 31–42. doi: 10.1038/cdd.2012.81 PMID: 22743996

40. Ding W-X, Yin X-M. Mitophagy: mechanisms, pathophysiological roles, and analysis. Biological Chemistry 2012; 393: 547–64. doi: 10.1515/hsz-2012-0119 PMID: 22944659

41. Youle RJ, van der Bliek AM. Mitochondrial Fission, Fusion, and Stress. Science 2012; 337: 1062–5. doi: 10.1126/science.1219855 PMID: 22936770

42. Parganlija D, Klinkenberg M, Dominguez-Bautista J, Hetzel M, Gispert S, Chimi MA, et al. Loss of PINK1 Impairs Stress-Induced Autophagy and Cell Survival. Plos One 2014; 9.

43. Liu L, Feng D, Chen G, Chen M, Zheng Q, Song P, et al. Mitochondrial outer-membrane protein FUNDC1 mediates hypoxia-induced mitophagy in mammalian cells. Nature Cell Biology 2012; 14: 177–85. doi: 10.1038/ncb2422 PMID: 22267086

44. Tan AS, Baty JW, Dong L-F, Bezawork-Geleta A, Endaya B, Goodwin J, et al. Mitochondrial Genome Acquisition Restores Respiratory Function and Tumorigenic Potential of Cancer Cells without Mitochondrial DNA. Cell Metabolism 2015; 21: 81–94. doi: 10.1016/j.cmet.2014.12.003 PMID: 25565207

45. Kroemer G, Levine B. Autophagic cell death: the story of a misnomer. Nature Reviews Molecular Cell Biology 2008; 9: 1004–10. doi: 10.1038/nrm2529 PMID: 18971948

46. Karantza-Wadsworth V, Patel S, Kravchuk O, Chen G, Mathew R, Jin S, et al. Autophagy mitigates metabolic stress and genome damage in mammary tumorigenesis. Genes & Development 2007; 21: 1621–35.

47. Sun Q, Luo T, Ren Y, Florey O, Shirasawa S, Sasazuki T, et al. Competition between human cells by entosis. Cell Research 2014; 24: 1299–310. doi: 10.1038/cr.2014.138 PMID: 25342560

48. Florey O, Kim SE, Sandoval CP, Haynes CM, Overholtzer M. Autophagy machinery mediates macroendocytic processing and entotic cell death by targeting single membranes. Nature Cell Biology 2011; 13: 1335–U118. doi: 10.1038/ncb2363 PMID: 22002674

49. Krajcovic M, Johnson NB, Sun Q, Normand G, Hoover N, Yao E, et al. A non-genetic route to aneuploidy in human cancers. Nature Cell Biology 2011; 13: 324–U07. doi: 10.1038/ncb2174 PMID: 21336303

50. Nakajima S, Kato H, Takahashi S, Johno H, Kitamura M. Inhibition of NF-kappa B by MG132 through ER stress-mediated induction of LAP and LIP. Febs Letters 2011; 585: 2249–54. doi: 10.1016/j.febslet.2011.05.047 PMID: 21627972

51. Li Y, Bevilacqua E, Chiribau CB, Majumder M, Wang CP, Croniger CM, et al. Differential control of the CCAAT/enhancer-binding protein beta (C/EBP beta) products liver-enriched transcriptional activating protein (LAP) and liver- enriched transcriptional inhibitory protein (LIP) and the regulation of gene expression during the response to endoplasmic reticulum stress. Journal of Biological Chemistry 2008; 283: 22443–56. doi: 10.1074/jbc.M801046200 PMID: 18550528

52. Lim LY, Vidnovic N, Ellisen LW, Leong CO. Mutant p53 mediates survival of breast cancer cells. British Journal of Cancer 2009; 101: 1606–12. doi: 10.1038/sj.bjc.6605335 PMID: 19773755

53. Abreu M, Sealy L. Cells Expressing the C/EBPbeta Isoform, LIP, Engulf Their Neighbors. Plos One 2012; 7.

54. Buchheit CL, Weigel KJ, Schafer ZT. Cancer cell survival during detachment from the ECM: multiple barriers to tumour progression. Nat Rev Cancer 2014; 14: 632–41. doi: 10.1038/nrc3789 PMID: 25098270

55. Howe EN, Cochrane DR, Cittelly DM, Richer JK. miR-200c Targets a NF-kappa B Up-Regulated TrkB/NTF3 Autocrine Signaling Loop to Enhance Anoikis Sensitivity in Triple Negative Breast Cancer. Plos One 2012; 7.

56. Loh YH, Wu Q, Chew JL, Vega VB, Zhang WW, Chen X, et al. The Oct4 and Nanog transcription network regulates pluripotency in mouse embryonic stem cells. Nature Genetics 2006; 38: 431–40. PMID: 16518401

57. Yu J, Vodyanik MA, Smuga-Otto K, Antosiewicz-Bourget J, Frane JL, Tian S, et al. Induced pluripotent stem cell lines derived from human somatic cells. Science 2007; 318: 1917–20. PMID: 18029452

58. Ling G-Q, Chen D-B, Wang B-Q, Zhang L-S. Expression of the pluripotency markers Oct3/4, Nanog and Sox2 in human breast cancer cell lines. Oncology Letters 2012; 4: 1264–8. PMID: 23197999

59. Takahashi K, Yamanaka S. Induction of pluripotent stem cells from mouse embryonic and adult fibroblast cultures by defined factors. Cell 2006; 126: 663–76. PMID: 16904174

60. Park IH, Zhao R, West JA, Yabuuchi A, Huo HG, Ince TA, et al. Reprogramming of human somatic cells to pluripotency with defined factors. Nature 2008; 451: 141–U1. PMID: 18157115

61. Kohsaka S, Sasai K, Takahashi K, Akagi T, Tanino M, Kimura T, et al. A population of BJ fibroblasts escaped from Ras-induced senescence susceptible to transformation. Biochemical and Biophysical Research Communications 2011; 410: 878–84. doi: 10.1016/j.bbrc.2011.06.082 PMID: 21703241

62. Silva J, Chambers I, Pollard S, Smith A. Nanog promotes transfer of pluripotency after cell fusion. Nature 2006; 441: 997–1001. PMID: 16791199

63. Saunders A, Faiola F, Wang JL. Concise Review: Pursuing Self-Renewal and Pluripotency with the Stem Cell Factor Nanog. Stem Cells 2013; 31: 1227–36. doi: 10.1002/stem.1384 PMID: 23653415

64. Brambrink T, Foreman R, Welstead GG, Lengner CJ, Wernig M, Suh H, et al. Sequential expression of pluripotency markers during direct reprogramming of mouse somatic cells. Cell Stem Cell 2008; 2: 151–9. doi: 10.1016/j.stem.2008.01.004 PMID: 18371436

65. Salmina K, Jankevics E, Huna A, Perminov D, Radovica I, Klymenko T, et al. Up-regulation of the embryonic self-renewal network through reversible polyploidy in irradiated p53-mutant tumour cells. Experimental Cell Research 2010; 316: 2099–112. doi: 10.1016/j.yexcr.2010.04.030 PMID: 20457152

66. Mitchell R, Szabo E, Shapovalova Z, Aslostovar L, Makondo K, Bhatia M. Molecular Evidence for OCT4-Induced Plasticity in Adult Human Fibroblasts Required for Direct Cell Fate Conversion to Lineage Specific Progenitors. Stem Cells 2014; 32: 2178–87. doi: 10.1002/stem.1721 PMID: 24740884

67. Zhang S, Mercado-Uribe I, Liu J. Tumor stroma and differentiated cancer cells can be originated directly from polyploid giant cancer cells induced by paclitaxel. International Journal of Cancer 2014; 134: 508–18.

68. Roca H, Varsos Z, Pienta KJ. CCL2 Protects Prostate Cancer PC3 Cells from Autophagic Death via Phosphatidylinositol 3-Kinase/AKT-dependent Survivin Up-regulation. Journal of Biological Chemistry 2008; 283: 25057–73. doi: 10.1074/jbc.M801073200 PMID: 18611860

69. Roca H, Varsos ZS, Mizutani K, Pienta KJ. CCL2, survivin and autophagy—New links with implications in human cancer. Autophagy 2008; 4: 969–71. PMID: 18758234

70. Stadtfeld M, Hochedlinger K. Induced pluripotency: history, mechanisms, and applications. Genes & Development 2010; 24: 2239–63.

71. Mali P, Ye ZH, Hommond HH, Yu XB, Lin J, Chen GB, et al. Improved efficiency and pace of generating induced pluripotent stem cells from human adult and fetal fibroblasts. Stem Cells 2008; 26: 1998–2005. doi: 10.1634/stemcells.2008-0346 PMID: 18511599

72. Zhang H, Chi Y, Gao K, Zhang X, Yao J. p53 Protein-mediated Up-regulation of MAP Kinase Phosphatase 3 (MKP-3) Contributes to the Establishment of the Cellular Senescent Phenotype through Dephosphorylation of Extracellular Signal-regulated Kinase 1/2 (ERK1/2). Journal of Biological Chemistry 2015; 290: 1129–40. doi: 10.1074/jbc.M114.590943 PMID: 25414256

73. Beausejour CM, Krtolica A, Galimi F, Narita M, Lowe SW, Yaswen P, et al. Reversal of human cellular senescence: roles of the p53 and p16 pathways. Embo Journal 2003; 22: 4212–22. PMID: 12912919

74. Zemskova M, Lilly MB, Lin Y-W, Song JH, Kraft AS. p53-Dependent Induction of Prostate Cancer Cell Senescence by the PIM1 Protein Kinase. Molecular Cancer Research 2010; 8: 1126–41. doi: 10.1158/1541-7786.MCR-10-0174 PMID: 20647331

75. Zhang L, Ding P, Lv H, Zhang D, Liu G, Yang Z, et al. Number of Polyploid Giant Cancer Cells and Expression of EZH2 Are Associated with VM Formation and Tumor Grade in Human Ovarian Tumor. Biomed Research International 2014.

76. Liu Y-q, Ji Y, Li X-z, Tian K-l, Young CYF, Lou H-x, et al. Retigeric acid B-induced mitophagy by oxidative stress attenuates cell death against prostate cancer cells in vitro. Acta Pharmacologica Sinica 2013; 34: 1183–91. doi: 10.1038/aps.2013.68 PMID: 23892275

77. Basu HS, Schrieber CL, Sperger JM, Naundorf M, Weichman AM, Mehraein-Ghomi F, et al. Abstract 2899: Mitophagy imparts enzalutamide resistance in prostate cancer. Cancer Research 2015; 75: 2899.

78. Zhang HF, Bosch-Marce M, Shimoda LA, Tan YS, Baek JH, Wesley JB, et al. Mitochondrial autophagy is an HIF-1-dependent adaptive metabolic response to hypoxia. Journal of Biological Chemistry 2008; 283: 10892–903. doi: 10.1074/jbc.M800102200 PMID: 18281291

4.2.2 Findings related to the hypothesis 2

***Hypothesis 2**: The previously studied molecule, sarcosine, is associated with changes in antioxidant mechanisms.*

In our earlier studies, we found that amino acids of the sarcosine pathway (glycine, dimethylglycine and sarcosine) significantly affect the ability of cells derived from CaP (22Rv1, PC-3) to migrate, as well as their ability to divide. Sarcosine is thus probably a key metabolite affecting the progression of CaP and may be a suitable target for diagnostic approaches and for possible targeted therapy.

Despite the fact that the sarcosine association with oncogenesis was investigated extensively by a number of other laboratories [79, 87], the mechanism by which sarcosine participates in oncogenesis is not absolutely clear yet. The goal of the following study by Cernei *et al*. [117] was to find out how the sarcosine treatment relates to changes in the cell antioxidant mechanisms.

After the exposure of the PC-3 prostate cells to the increasing concentration of sarcosine, it was found out that this metabolite is not related to the zinc-binding antioxidant metallothionein, the levels of which remained unaffected, though the intracellular concentration of sarcosine has increased dramatically. Taking into account this step, a link between other antioxidant players and sarcosine was searched. From a wide array of antioxidant parameters, none showed a trend changing in dependence on the quantity of delivered sarcosine. At the same time, sarcosine stimulates proliferation of these cells *in vitro* as well as *in vivo* as demonstrated in our previous study [88] (see sec. 3.2.2.). The mechanism affecting the metastatic potential of tumour cells via sarcosine is therefore independent on the metabolic pathways associated with the regulation of reactive oxygen forms.

Conclusion: Sarcosine, a non-coding amino acid, was studied intensively in association with its expected predictive value for the prostate carcinoma diagnosis, affects cancer cells aggression. Based on our experiments, it was confirmed that these mechanisms are related neither to antioxidants nor to the regulation of oxidative stress levels.

Author's publication relevant to this chapter

Cernei N, Zitka O, Skalickova S, et al. Effect of sarcosine on antioxidant parameters and metallothionein content in the PC-3 prostate cancer cell line. Oncology Reports. *2*013; 29(6): 2459-2466.

Available on page 254

ONCOLOGY REPORTS 29: 2459-2466, 2013

Effect of sarcosine on antioxidant parameters and metallothionein content in the PC-3 prostate cancer cell line

NATALIA CERNEI[1], ONDREJ ZITKA[1-3], SYLVIE SKALICKOVA[1], JAROMIR GUMULEC[1,3,4], MARKETA SZTALMACHOVA[1,4], MIGUEL ANGEL MERLOS RODRIGO[1,3], JIRI SOCHOR[1], MICHAL MASARIK[1,3,4], VOJTECH ADAM[1,3], JAROMIR HUBALEK[1,2,3], LIBUSE TRNKOVA[1,3,5], JARMILA KRUSEOVA[6], TOMAS ECKSCHLAGER[6] and RENE KIZEK[1,3]

[1]Department of Chemistry and Biochemistry, Faculty of Agronomy, Mendel University in Brno, CZ-613 00 Brno; [2]Department of Microelectronics, Faculty of Electrical Engineering and Communication, Brno University of Technology, CZ-612 00 Brno; [3]Central European Institute of Technology, Brno University of Technology, CZ-616 00 Brno; [4]Department of Pathological Physiology, Faculty of Medicine, Masaryk University, CZ-625 00 Brno; [5]Department of Chemistry, Faculty of Science, Masaryk University, CZ-625 00 Brno; [6]Department of Paediatric Haematology and Oncology, Second Faculty of Medicine, Charles University in Prague and University Hospital Motol, CZ-150 06 Prague 5, Czech Republic

Received November 9, 2012; Accepted January 29, 2013

DOI: 10.3892/or.2013.2389

Abstract. Sarcosine is currently one of the most discussed markers of prostate cancer. It is involved in amino acid metabolism and methylation processes that occur during the progression of prostate cancer. In this study, we monitored the effect of the addition of sarcosine (0; 10; 250; 500; 1,000 and 1,500 μM) in a time-dependent manner (0-72 h) on the PC-3 prostate cancer cell line. For the assessment of cell viability, the commonly used MTT test was employed. Furthermore, ion-exchange liquid chromatography was used for the determination of sarcosine content in the PC-3 cells. We also determined metallothionein (MT) levels by chip capillary electrophoresis and Brdicka reaction in the cells treated with sarcosine. Sarcosine levels in the cells increased in a concentration-dependent manner levels increased from only 270 nM with the lowest applied concentration of sarcosine (10 μM) to 106 μM with the highest applied concentration of sarcosine (1,500 μM). There was a marginal change observed in the MT concentration. Finally, the antioxidant activity of the PC-3 cells was determined using five different spectrophotometric methods [2,2-diphenyl-1-picrylhydrazyl (DPPH), ferric reducing ability of plasma (FRAP), free radicals, *N*,*N*-dimethyl-*p*-phenylenediamine (DMPD) and 2,2'-azino-bis(3-ethylbenzothiazoline-6-sulphonic acid (ABTS)]. A significant negative correlation was observed between DPPH and FRAP (r=-0.68 at P<0.001) and between DMPD and ABST (r=-0.64 at P<0.001). Additionally, as regards the correlation between MT and DPPH, a significant positive trend (r=0.62 at P<0.001) was observed.

Correspondence to: Professor Rene Kizek, Department of Chemistry and Biochemistry, Faculty of Agronomy, Mendel University in Brno, Zemedelska 1, CZ-613 00 Brno, Czech Republic
E-mail: kizek@sci.muni.cz

Key words: sarcosine, prostate cancer, metallothionein, antioxidant activity, chip electrophoresis, ion-exchange chromatography, Brdicka reaction

Introduction

Prostate cancer (PCa) is characterised as a non-coordinated proliferation of prostatic cells (1). However, the mechanisms behind tumour progression have not yet been elucidated, although the risk factors of cancer initiation have been defined (2). These include primary genetic predispositions, ethnicity, life style and age (3). Old age has been established as a significant risk factor for PCa (4,5). In addition to these factors, a family history of breast or PCa distinctly enhances PCa risk (6). In terms of ethnicity, a distinct gradient between Afro-Americans and Asians is evident (lower incidence in Asian populations) (7). Apart from these factors, androgens also play an important role in cancer development and progression. Therefore, PCa can be classified into either androgen-independent or androgen-dependent (8,9).

Currently, there is no complex test available for the diagnosis of PCa (10). Usually used tests include digital rectal examination, determination of prostate-specific antigen (PSA) levels (11) and transrectal sonography with a biopsy of prostate tissue. In specific cases, computed tomography (12), magnetic resonance (13) and positron emission tomography may be utilised (14). In this context, potential markers of PCa, which may be considered as a useful tool for earlier diagnosis without clinical examinations, are investigated. Currently, PSA, first described in 1977 (15), is the most perspective marker of PCa. However, it is used for diagnosis, for determining the stage of disease and for monitoring the treatment progression; however, its sensitivity (49-91%) and specificity (68-80%) are not sufficient to confirm diagnosis (16). Novel potential markers,

including alpha-methylacyl-CoA racemase (AMACR) (17), prostate cancer antigen 3 (PCA3) and Annexin A3 (18) have been identified. The most discussed marker of early-stage PCa is the amino acid, sarcosine as described by Sreekumar *et al* (19) (Fig. 1). In spite of the controversy in the scientific community and contradicting views on this marker, the role of sarcosine in methylation processes during cancer progression has been shown (19). A recent study demonstrated the effect of sarcosine on the increasing human epidermal growth factor receptor 2 (HER2/neu) expression levels (20). Therefore, it is important to investigate the function and involvement of sarcosine in PCa initiation and progression. The aim of this study was to investigate the effect of sarcosine on PC-3 PCa cells. PC-3 cells were treated with sarcosine at various concentrations (10; 250; 500; 1,000 and 1,500 μM). In addition, the antioxidant capacity of the PC-3 cells following treatment with sarcosine, as well as the metallothionein (MT) concentration were examined.

Materials and methods

Chemical and biochemical reagents. Ham's F12 medium, fetal bovine serum (FBS) (mycoplasma-free), penicillin/streptomycin and trypsin were purchased from PAA Laboratories GmbH (Pasching, Austria). PBS was purchased from Invitrogen Corp. (Carlsbad, CA, USA). Ethylenediaminetetraacetic acid (EDTA) and all other chemicals of ACS purity were purchased from Sigma-Aldrich Co. (St. Louis, MO, USA), unless stated otherwise.

Cell culture conditions. In this study, the highly metastatic PC-3 prostate cancer cell line derived from bone metastasis was used. Cells were cultivated in Ham's F12 medium supplemented with 7% FBS and antibiotics (penicillin and streptomycin). Cells were cultivated in a MCO-18AIC incubator (Sanyo, Osaka, Japan) at 37˚C under 5% CO_2.

Sarcosine treatment of cell cultures. Immediately after the cells grew to 50-60% confluence, the cultivation medium was replaced by fresh medium to synchronise cell growth. Cells were cultivated for 24 h under these conditions. Subsequently, the culture medium was supplemented with sarcosine (N-methylglycine) diluted to a final concentration 10, 150, 250, 500, 1,000 and 1,500 μM. Treatment was carried out for 0, 6, 12, 24 and 72 h, and samples were collected at these strictly defined time points.

Cell content quantification. Total cell number was analysed using a semi-automated image-based cell analyser (CASY, Roche Innovatis, Basel, Switzerland) according to the manufacturer's instructions. The cultivation medium was removed and the samples were washed twice with 5 ml of ice-cold PBS to maintain only viable cells. Cells were scraped and transferred to clean tubes. Trypan blue solution (Roche Innovatis) was diluted to 0.2% prior to use and added to the samples. The following settings were used in the operating software: cell type, standard cells; dilution, none; process type, standard. All samples were measured in duplicate.

Light microscopy of treated cells. For light microscopy, cells were cultivated directly on glass microscope slides (75x25 mm, thickness 1 mm, Fischer Scientific, Pardubice, Czech Republic) in Petri dishes in the abovementioned cultivation medium as described in 'Cell culture conditions'. Cells were transferred directly onto slides, which were submerged in cultivation medium. Following treatment, the glass microscope slides with a monolayer of cells were removed from the Petri dishes, rinsed with cultivation medium without sarcosine supplementation and PBS buffer and directly used for light microscopy under an inverted microscope (Eclipse TS100; Nikon, Tokyo, Japan). Images were taken using a digital camera (Olympus Camedia C-750, Olympus).

MTT assay. To determine cell viability, MTT assay was carried out. MTT is yellow water-soluble stain (3-[4,5-dimethylthiazol-2-yl]-2,5-diphenyltetrazolium bromide) that is reduced by living cells to a non-soluble violet formazan precipitate. Cell suspension was pipetted to a microplate (TPP Techno Plastic Products AG, Trasadingen, Switzerland) according to the following scheme: 1st and 12th well with 200 μl medium and 2nd to 11th well with 200 μl cell suspension. The assay was carried out in duplicate. Furthermore, the cells were incubated for 24 h and the media were exchanged. Subsequently, the columns were fed with 200 μl of medium with 50 μl MTT [5 mg/ml in PBS (Invitrogen)] and incubated for 4 h, wrapped in aluminium foil. Subsequently, medium-MTT was exchanged with 200 μl of 99.9% DMSO to dissolve the MTT-formazan crystals. A total of 25 μl of glycine buffer was then added to the wells with DMSO. Plates were read at λ 570 nm (VersaMax Microplate Reader; Molecular Devices, Sunnyvale, CA, USA).

Ion-exchange chromatography. An AAA 400 liquid chromatography apparatus (Ingos, Prague, Czech Republic) was used for the determination of sarcosine concentration. The system consisted of a glassy filling chromatographic column and a steel precolumn, two chromatographic pumps for the transport of elution buffers and derivatization reagent, a cooled carousel for 25 test tubes of 1.5-2.0 ml volume, a dosing valve, a heat reactor, a Vis detector and a cooled chamber for the derivatization reagent. The glassy chromatographic column (i.d. 3.7 mm and 350 mm length) was filled with LG ANB strong catex in sodium cycle (Spolchemie, Ústí nad Labem, Czech Republic) with particles of average size of 12 μm and a netting of 8%. The glassy column was tempered by a thermostat at a temperature ranging from 35 to 95˚C. The precolumn was filled with LG KS0804 ionex (Ingos). Chromatographic columns for the transfer of elution buffers and derivatization reagent function at a flow of 0.01-10 ml/min under a maximum pressure of 40 MPa. The volume of the injected sample was 100 μl with an application accuracy RSD of ~1%. A two-channel Vis detector with a 5 μl flow volume cuvette was operated at wavelengths of 440 and 570 nm. Ninhydrin solution (Ingos) was used as the derivatization reagent. Ninhydrin was dissolved in solution containing 75% (v/v) of the organic solvent, methyl cellosolve (Ingos), and 25% (v/v) of 4 M acetate buffer (pH 5.5). $SnCl_2$ (Lachema, Brno, Czech Republic) was used as a reducing agent. The derivatization reagent was stored under an inert atmosphere (N_2) with cooling at 4˚C. During the analysis, the mobile phase flow was set at 0.3 ml/min under a pressure range of 4.5 to 6.0 MPa. The reactor temperature was set to 120˚C.

Differential pulse voltammetry for Brdicka reaction. Differential pulse voltammetric measurements were performed with a 747 VA Stand instrument connected to 693 VA Processor and 695 Autosampler (Metrohm, Herisau, Switzerland), using a standard cell with three electrodes and a cooled sample holder (4˚C) for the measurement of cells (Julabo F25; Julabo, Seelbach, Germany). A hanging mercury drop electrode (HMDE) with a drop area of 0.4 mm^2 was used as the working electrode. An Ag/AgCl/3M KCl electrode was the reference and a platinum electrode was the auxiliary electrode. For data processing, the VA Database 2.2 (Metrohm) was employed. The analysed samples were deoxygenated prior to the measurements by purging with argon (99.999%) saturated with water for 120 sec. Brdicka supporting electrolyte containing 1 mM $Co(NH_3)_6Cl_3$ and 1 M ammonia buffer [$NH_3(aq)$ + NH_4Cl, pH 9.6] was used. The supporting electrolyte was exchanged after each analysis. The parameters of the measurement were as follows: initial potential of -0.7 V; end potential of -1.75 V; modulation time, 0.057 sec; time interval, 0.2 sec; step potential, 2 mV; modulation amplitude, -250 mV; E_{ads} 0 V; volume of injected sample, 25 μl; measurement of cell volume, 2 ml (25 μl of sample and 1,975 μl Brdicka solution).

Capillary electrophoresis-Experion system. Analyses on an automated microfluidic Experion electrophoresis system (Bio-Rad Laboratories, Hercules, CA, USA) were carried out according to the manufacturer's instructions with the supplied chemicals (Experion Pro260 Analysis kit; Bio-Rad Laboratories). A sample (4 μl) was mixed with 2 μl of reducing sample buffer (3.3% mercaptoethanol), and after 3 min of boiling, 84 μl of water were added. After the priming of the chip with the gel and gel-staining solution in the diluted priming station sample, the mixture (6 μl) was loaded into the sample wells. The Pro260 Ladder included in the kit was used as a standard. For operation and standard data analysis, Experion software version 3.10 (Bio-Rad Laboratories) was used.

Spectrophotometric analysis. For the determination of antioxidant activity, a BS-400 automated spectrophotometer (Mindray, Shenzhen, China) was used. It is composed of cuvette space tempered to 37±1˚C, reagent space with a carousel for reagents (tempered to 4±1˚C), sample space with a carousel for the preparation of samples and an optical detector. The transfer of samples and reagents was carried out by a robotic arm equipped with a dosing needle (error of dosage up to 5% of volume). Cuvette contents are mixed by an automatic mixer including a stirrer immediately after the addition of reagents or samples. Contamination is reduced due to its rinsing system, including rinsing of the dosing needle as well as the stirrer by Milli-Q water.

Determination of antioxidant activity by the 2,2'-azino-bis(3-ethylbenzothiazoline-6-sulphonic acid (ABTS) test. The ABST test was carried out as previously described by Sochor *et al* (21,22). Briefly, a 150-μl volume of reagent (7 mM $ABTS^{\bullet}$ and 4.95 mM potassium peroxodisulfate) was incubated with 3 μl of sample. Absorbance was measured at λ 660 nm for 12 min. For the calculation of the antioxidant activity, values determined before the decrease of the absorbance (2nd minute of measurement - A_2) and the last measurement value (12th minute of measurement - A_{12}) were used. The resulting value was calculated in accordance with the following formula: differential absorbance $A = A_{12} - A_2$.

Determination of antioxidant activity by the 2,2-diphenyl-1-picrylhydrazyl (DPPH) test. The DPPH test was carried out as described by Sochor *et al* (21,22). Briefly, a 150-μl volume of reagent (0.095 mM $DPPH^{\bullet}$) was incubated with 15 μl of sample. Absorbance was measured at 505 nm for 10 min and the output ratio was achieved by the difference of absorbance at the 10th and 2nd minute of the assay procedure.

Determination of antioxidant activity by the N,N-dimethyl-p-phenylenediamine (DMPD) method. The DMPD test was carried out as previously described by Sochor *et al* (21,22). Briefly, a 160 μl volume of reagent (200 mM DMPD, 0.05 M $FeCl_3$, 0.1 M acetate buffer pH 5.25) was injected into a plastic cuvette with the subsequent addition of 4 μl of sample. Absorbance was measured at 505 nm. The difference between absorbance at the 10th and 2nd minute of the assay procedure was used for the calculation of the antioxidant activity.

Determination of antioxidant activity by the free radical method. The determination of antioxidant activity using the free radical method was carried out as previously described by Pohanka *et al* (23). Briefly, a 150 μl volume of reagent was injected into a plastic cuvette with the subsequent addition of a 6 μl of sample. Absorbance was measured at 450 nm in the 2nd minute of the assay and the 10th minute. The difference of the two absorbances was considered as an output value.

Determination of antioxidant activity by the ferric reducing ability of plasma (FRAP) method. The determination of antioxidant activity using the FRAP method was carried out as previously described by Sochor (21,22). Briefly, a 150 μl volume of reagent was injected into a plastic cuvette with the subsequent addition of 3 μl of sample. Absorbance was measured at 605 nm for 10 min. The difference between the absorbance at the final 10th minute and the 2nd minute of the assay procedure was used for the calculation of the antioxidant activity.

Statistical analysis. Software Statistica 10 (StatSoft, Tulsa, OK, USA) was used for statistical evaluation. T-tests were used to compare levels across groups and correlations were performed to reveal trends between variables. A P-value <0.05 was considered to indicate a statistically significant difference, unless stated otherwise.

Results and Discussion

Cell treatment and viability test. The PC-3 PCa cell line was derived from a metastatic site in the bone and represents a highly aggressive metastatic form of PCa. Compared to the widely used prostate cancer cell lines, DU145 and LNCaP, PC-3 is androgen-independent and does not express PSA (24,25). As mentioned in the Introduction, sarcosine is considered a tumour marker for the diagnosis of PCa. A schematic diagram of the role of sarcosine in the biochemistry of PCa cells adopted from a previous study (26) is shown in (Fig. 1).

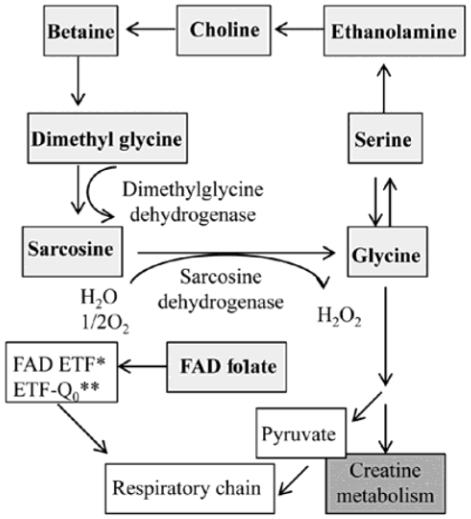

Figure 1. Sarcosine metabolism in the mitochondria. Formed FAD folate is involved in the respiratory chain and glycine is involved in creatine metabolism. *ETF, electron transfer flavoprotein; **ETF-Q_0, ubiquinone oxidoreductase (26).

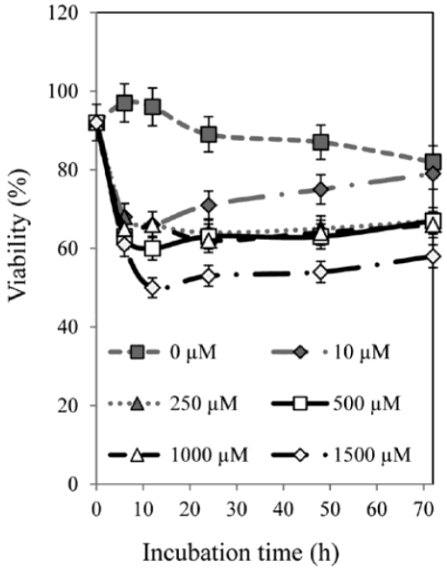

Figure 2. Viability of prostate cancer cells treated with various concentrations of sarcosine (0, 10, 100, 250, 500, 1,000 and 1,500 μM). Influence of selected markers, values are recalculated to determine viability. For measurements, the MTT assay was used as described in 'MTT assay'.

Therefore, the first experiments focused on the determination of cell viability and proliferation following treatment with sarcosine. The commonly used 3-[4,5-dimethylthiazol-2-yl]-2,5-diphenyl tetrazolium bromide (MTT) assay was employed for these tests. For MTT assay, the cells were harvested and re-cultivated in a 96-well plate (5,000 cells/well). After 24 h of growth synchronization, the cells were treated with sarcosine at various concentrations ranging from 10 to 1,500 μM. The cells were further cultivated under these conditions, and samples were taken in the strictly defined time points (6, 12, 24, 48 and 72 h), when viability was evaluated. The results are shown in Fig. 2. Compared to the viability of the control cells (i.e., those not treated with sarcosine), the viability of the sarcosine-treated cells was significantly reduced. The determined IC_{50} value at all the time points was ~325.5 μM. In all the applied concentrations, cell viability was reduced by 30-40% after 10 h of treatment; subsequently, a moderate increase in cell viability (65-80%) compared to the initial viability values was recorded. As shown in Fig. 2, the increasing sarcosine concentration (10-1,500 μM) led to a reduction in cell viability (significance level $P<0.05$) during the first 6-24 h of treatment (34% on average). After 12 h, the decreasing trend in cell proliferation slowly increased compared to the untreated control cells, where the decrease was only moderate and was characteristic of the growth curve of the PC-3 PCa cell line. These results confirm the microscopic observations, where the toxic effect of sarcosine at a high concentration (1,500 μM) was evident. At this concentration, changes in cell morphology (loss of typical shape, formation of round cells and loss of adherence) were determined. At lower concentrations, sarcosine reduced cell viability, although non-significant cellular morphological changes were observed (data not shown).

Sarcosine determination. In the following experiment, both the culture medium and sarcosine-treated cells were analysed for sarcosine content by ion-exchange chromatography (27). In the sarcosine-treated cells, sarcosine content was recalculated to the percentage of viable cells. The sarcosine content in the cells significantly increased until 24 h of treatment at all concentrations (10-1,500 μM). However, after 24 h of treatment, only a moderate sarcosine content increase was recorded. The untreated cells showed a similar tendency compared to the treated cells. These results indicate the possibility of sarcosine biosynthesis by PC-3 cells (19). The obtained results indicated a contrary tendency compared to the sarcosine content in PC-3 cells, i.e., that the concentration of sarcosine in the culture medium increased at all concentrations (10-1,500 μM). This increase is characterised by the directional slopes from each applied concentration (Fig. 3). The most significant increase in sarcosine content was recorded at the highest applied sarcosine concentrations (500-1,500 μM). As regards statistical significance, a significant change in the sarcosine content was observed at the concentrations between 0-1,000 μM vs. 1,500 μM ($P=0.02$). On the other hand, the sarcosine content increased in the culture medium in the case of the untreated control cells.

Determination of MT levels. MT is considered as a possible marker of PCa (28-34). As certain studies have indicated, its levels are elevated in the blood serum of patients suffering from PCa, independent of their state of health (35,36). Chip capillary electrophoresis (Experion) was used for the determination of MT levels. The assumed molecular weight of MT varies from 6 to 15 kDa (37); however, this depends on the type of isoform and the rate of oxidation (38,39). From the Experion records, it is evident that PC-3 cells cultivated for 12 h synthesised MT with molecular weights of 11, 15

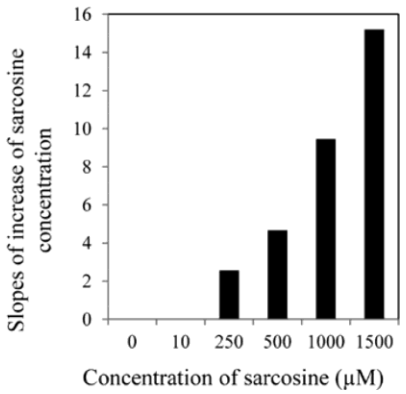

Figure 3. Slopes of increase of sarcosine concentrations (0; 10; 100; 250; 500; 1,000 and 1,500 μM) on the sarcosine concentrations determined in the culture medium.

and 19 kDa (see MT peaks, Fig. 4A). These results are also visible on virtual output (Fig. 4B). The height of these peaks increased depending on the applied sarcosine concentration up to 1,000 μM. On the other hand, a distinct increase in all three peaks was determined for the highest applied concentration of sarcosine (1,500 μM); however, this increase was below the level of statistical significance. This trend is shown in Fig. 4C. Furthermore, PC-3 cells affected by sarcosine were investigated electrochemically using the Brdicka reaction, which is a highly sensitive method for the determination of MT levels (40,41). As shown in Fig. 5A, the MT level was reduced with the highest applied sarcosine concentration (1,500 μM) in a time-dependent manner. This trend confirmed the results obtained by the chip capillary electrophoresis method. As regards the dependence of mentioned variables, we revealed a significant positive correlation between sarcosine and MT (r=0.41 at P=0.03, Fig. 5B). Moreover, no other significant dependencies were identified across variables, including markers of oxidative capacity.

Antioxidant capacity determination. A number of methods have been introduced for the determination of antioxidant activity in the field of chemical and biological analysis (23,42-44). The methods differ according the molecular mechanisms of the particular group of antioxidants (45-47). These mechanisms usually involve the quenching/trapping of the radicals; however, the strictly specific mechanisms of the majority of these antioxidants remain unclear. Therefore, the approaches for the determination of antioxidant capacity are based on various techniques with different chemical principles. In our study, for the determination of the antioxidant capacity of PC-3 cells, we used five different methods, DPPH, TEAC, FRAP, DMPD and free radicals.

The DPPH test is based on the ability of the stable 2,2-diphenyl-1-picrylhydrazyl free radical to react with hydrogen donors and it is still one of the most commonly used methods. In this test, a radical solution is decolourised after reduction with antioxidant (AH) or a radical (R$^{\bullet}$) in accordance with the following scheme: DPPH$^{\bullet}$ + AH→DPPH-H + A$^{\bullet}$, DPPH$^{\bullet}$ + R$^{\bullet}$ → DPPH-R (48). The ABTS radical method is based on the quenching of substances which acts as a hydrogen radical cation created as one electron oxidation of synthetic chromophore ABTS$^{\bullet}$ which is thus reduced and changes its colour, which is monitored as a decrease in absorbance at a preferable wavelength (49). The FRAP method is based on the principle of redox reaction using Fe(III) complexes which are colourless and following reduction, it generates violet-coloured products. DMPD radical cation (DMPD$^{\bullet+}$) is generated through a reaction between DMPD and potassium persulfate and is subsequently reduced in the presence of hydrogen-donating antioxidants, similar to the DPPH test. After the addition of a sample containing antioxidants, DMPD$^{\bullet+}$ radicals are scavenged and as a result of this scavenging, the coloured solution is decolourised (50). The FRAP method is based on the ability of chlorophyllin (the sodium-copper salt of chlorophyl) to accept and donate electrons with a stable change of maximum absorption. This effect is conditioned by an alkaline environment and the addition of a catalyst (21).

All methods were calibrated using the standard compound, Trolox. The obtained results were recalculated to the viable

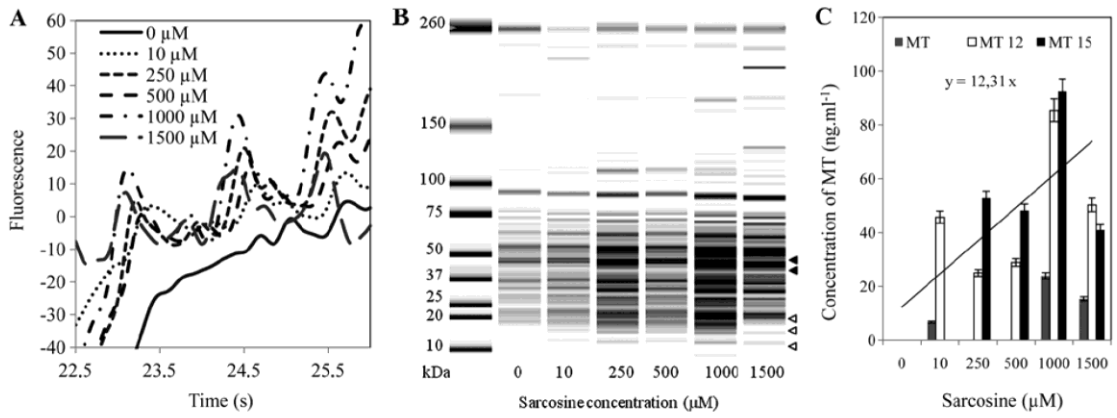

Figure 4. (A) Intensity of metallothionein (MT) peaks with the increasing sarcosine concentration. Capillary electrophoresis was used for all measurements as described in 'Capillary electrophoresis-Experion system'. (B) Virtual gel output. Arrows indicate further analysed peaks corresponding to molecular weight of 9.5 kDa labelled as MT, respectively. (C) Intensity of MT peaks with the increasing sarcosine concentration.

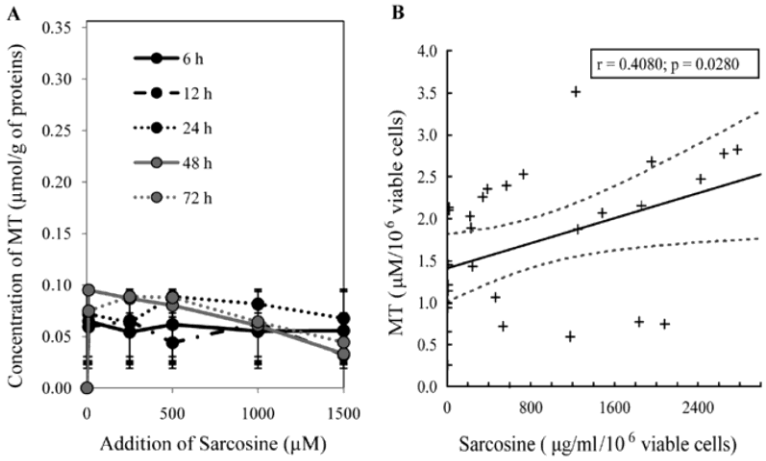

Figure 5. (A) Influence of sarcosine addition on metallothionein (MT) concentration (converted to whole protein concentration). (B) Correlation between sarcosine and MT values obtained by analysis of cells treated with applied concentrations of sarcosine (0, 10, 100, 250, 500, 1,000 and 1,500 μM) (r=0.41 at P=0.03).

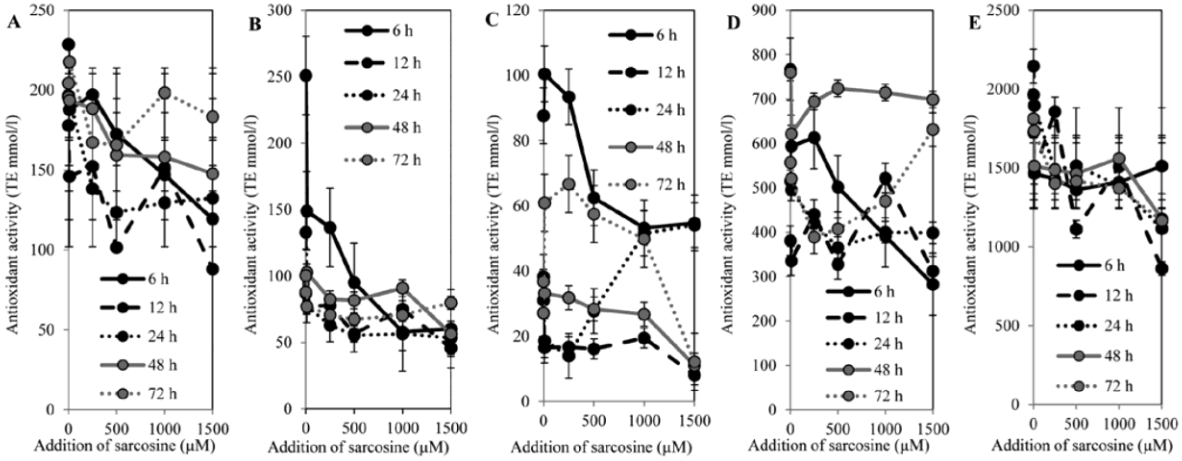

Figure 6. Influence of sarcosine treatment (0, 250, 500, 1,000 and 1,500 μM) on antioxidant capacity [expressed as Trolox equivalent (TE)]. Values were recalculated to determine cell viability. The spectrophotometric methods: (A) free radicals; (B) FRAP; (C) DPPH; (D) ABTS; (E) DMPD was used.

cells (% of viability) that were determined in as described above in 'Spectrophotometric analysis'. The antioxidant capacity determined by the free radical method (Fig. 6A) showed a decreasing tendency in a concentration-dependent manner within the time interval of 0 to 48 h. Subsequently, the antioxidant capacity increased in a time-dependent manner. The highest antioxidant capacity was determined after 72 h of sarcosine treatment in a concentration-dependent manner. However, the antioxidant capacity was reduced by 10% compared to the untreated control cells. The results obtained using the FRAP method correlated with the results obtained by the free radical method (Fig. 6B). A decrease in antioxidant capacity in a concentration-dependent manner was evident. The highest antioxidant capacity was determined in the cells treated with sarcosine for 6 h; subsequently, a decrease was recorded. After 48 h of incubation, an increase in antioxidant capacity in the PC-3 cells treated with high sarcosine concentrations (500-1,000 μM) was observed. On the other hand, the highest sarcosine concentration (1,500 μM) led to a significant reduction in antioxidant capacity. Different results were obtained after 72 h of treatment. The lower sarcosine concentrations (up to 500 μM) led to a reduction in antioxidant capacity, and the higher concentrations led to a significant increase in antioxidant capacity. The DPPH method confirmed the results obtained by the previous two methods (Fig. 6C). The most evident increase in antioxidant capacity was recorded in the untreated PC-3 cells and in the PC-3 cells treated with sarcosine in the concentration of 250 μM at the time points of 6, 12, 48 and 72 h. High sarcosine concentrations (500-1,500 μM) led to a significant reduction in antioxidant capacity. However, the obtained results indicate the role of the duration of the treatment. PC-3 cells incubated for 24 h showed an increasing tendency in antioxidant capacity in a concentration-dependent manner. This fact is particularly

evident in the PC-3 cells treated with 1,000 μM sarcosine. The ABTS method revealed similar results to those obtained by the DPPH method in both the untreated control (0 μM of sarcosine) and treated cells (Fig. 6D). On the other hand, the increasing antioxidant capacity with the increasing sarcosine concentrations in the treated cells for 48 h was evident. The DMPD method showed a decreasing tendency in antioxidant capacity with the increasing sarcosine concentrations within the time points of 12 to 72 h (Fig. 6E). On the other hand, the increase in antioxidant capacity is evident in the cells treated with sarcosine for 6 h. The results indicate the involvement of the compounds with antioxidant activity in the metabolism of the PC-3 cells following sarcosine treatment. The changes in antioxidant capacity demonstrate the rapid response to sarcosine treatment in a time-dependent manner. As regards the correlation of markers of oxidative capacity, we revealed a significant negative trend between DPPH and FRAP ($r=-0.68$ at $P<0.001$) and between DMPD and ABST ($r=-0.64$ at $P<0.001$). In addition, significant positive trends were observed only between MT and DPPH ($r=0.62$ at $P<0.001$).

In conclusion, non-invasive markers for PCa, through which it would be possible to diagnose PCa by urine analysis, are required. The non-protein amino acid, sarcosine, is one of the substances with potential for use in the diagnosis of PCa by urine analysis. However, the exact function of this amino acid in tumour cells is not yet fully understood. In this study, we attempted to cast light on the effects of various sarcosine doses on PC-3 PCa cells and discovered that this compound significantly influences various determined markers.

Acknowledgements

The present study was financially supported by CEITEC CZ.1.05/1.1.00/02.0068, NanoBioTECell GACR P102/11/1068, CYTORES GAČR P301/10/0356 and project for conceptual development of research organization 00064203.

References

1. Boyd LK, Mao XY, Xue LY, *et al*: High-resolution genome-wide copy-number analysis suggests a monoclonal origin of multifocal prostate cancer. Gene Chromosomes Cancer 51: 579-589, 2012.
2. Shimojo H, Kobayashi M, Kamigaito T, Shimojo Y, Fukuda M and Nakayama J: Reduced glycosylation of alpha-dystroglycans on carcinoma cells contributes to formation of highly infiltrative histological patterns in prostate cancer. Prostate 71: 1151-1157, 2011.
3. Chang HH, Chen BY, Wu CY, *et al*: Hedgehog overexpression leads to the formation of prostate cancer stem cells with metastatic property irrespective of androgen receptor expression in the mouse model. J Biomed Sci 18:6 2011.
4. Song LM, Zhu YC, Han P, *et al*: A retrospective study: correlation of histologic inflammation in biopsy specimens of Chinese men undergoing surgery for benign prostatic hyperplasia with serum prostate-specific antigen. Urology 77: 688-692, 2011.
5. Astigueta JC, Abad MA, Morante C, Pow-Sang MR, Destefano V and Montes J: Characteristics of metastatic prostate cancer ocurring in patients under 50 years of age. Actas Urol Esp 34: 327-332, 2010 (In Spanish).
6. Lindstrom S, Schumacher FR, Cox D, *et al*: Common genetic variants in prostate cancer risk prediction - results from the NCI Breast and Prostate Cancer Cohort Consortium (BPC3). Cancer Epidemiol Biomarkers Prev 21: 437-444, 2012.
7. Hall MJ, Ruth K and Giri VN: Rates and predictors of colorectal cancer screening by race among motivated men participating in a prostate cancer risk assessment program. Cancer 118: 478-484, 2012.
8. Vindrieux D, Reveiller M, Chantepie J, *et al*: Down-regulation of DcR2 sensitizes androgen-dependent prostate cancer LNCaP cells to TRAIL-induced apoptosis. Cancer Cell Int 11: 42, 2012.
9. Paquet S, Fazli L, Grosse L, *et al*: Differential expression of the androgen-conjugating UGT2B15 and UGT2B17 enzymes in prostate tumor cells during cancer progression. J Clin Endocrinol Metab 97: E428-E432, 2012.
10. Armstrong AJ, Eisenberger MA, Halabi S, *et al*: Biomarkers in the management and treatment of men with metastatic castration-resistant prostate cancer. Eur Urol 61: 549-559, 2012.
11. Prensner JR, Rubin MA, Wei JT and Chinnaiyan AM: Beyond PSA: the next generation of prostate cancer biomarkers. Sci Transl Med 4: 127rv3, 2012.
12. Lattanzi J, McNeely S, Hanlon A, Das I, Schultheiss TE and Hanks GE: Daily CT localization for correcting portal errors in the treatment of prostate cancer. Int J Radiat Oncol Biol Phys 41: 1079-1086, 1998.
13. van Vugt HA, Roobol MJ, Busstra M, *et al*: Compliance with biopsy recommendations of a prostate cancer risk calculator. BJU Int 109: 1480-1488, 2012.
14. Schoder H and Larson SM: Positron emission tomography for prostate, bladder, and renal cancer. Semin Nucl Med 34: 274-292, 2004.
15. Fukushima K, Satoh T, Baba S and Yamashita K: alpha 1,2-Fucosylated and beta-N-acetylgalactosaminylated prostate-specific antigen as an efficient marker of prostatic cancer. Glycobiology 20: 452-460, 2010.
16. Page ST, Hirano L, Gilchriest J, *et al*: Dutasteride reduces prostate size and prostate specific antigen in older hypogonadal men with benign prostatic hyperplasia undergoing testosterone replacement therapy. J Urol 186: 191-197, 2011.
17. Luo J, Zha S, Gage WR, *et al*: Alpha-methylacyl-CoA racemase: a new molecular marker for prostate cancer. Cancer Res 62: 2220-2226, 2002.
18. Cao DL, Ye DW, Zhang HL, Zhu Y, Wang YX and Yao XD: A multiplex model of combining gene-based, protein-based, and metabolite-based with positive and negative markers in urine for the early diagnosis of prostate cancer. Prostate 71: 700-710, 2011.
19. Sreekumar A, Poisson LM, Rajendiran TM, *et al*: Metabolomic profiles delineate potential role for sarcosine in prostate cancer progression. Nature 457: 910-914, 2009.
20. Dahl M, Bouchelouche P, Kramer-Marek G, Capala J, Nordling J and Bouchelouche K: Sarcosine induces increase in HER2/neu expression in androgen-dependent prostate cancer cells. Mol Biol Rep 38: 4237-4243, 2011.
21. Sochor J, Ryvolova M, Krystofova O, *et al*: Fully automated spectrometric protocols for determination of antioxidant activity: advantages and disadvantages. Molecules 15: 8618-8640, 2010.
22. Sochor J, Salas P, Zehnalek J, *et al*: An assay for spectrometric determination of antioxidant activity of a biological extract. Listy Cukrov Reparske 126: 416-417, 2010.
23. Pohanka M, Sochor J, Ruttkay-Nedecky B, *et al*: Automated assay of the potency of natural antioxidants using pipetting robot and spectrophotometry. J Appl Biomed 10: 155-167, 2012.
24. Ghosh A, Wang YN, Klein E and Heston WD: Novel role of prostate-specific membrane antigen in suppressing prostate cancer invasiveness. Cancer Res 65: 727-731, 2005.
25. Tai S, Sun Y, Squires JM, *et al*: PC3 is a cell line characteristic of prostatic small cell carcinoma. Prostate 71: 1668-1679, 2011.
26. Moolenaar SH, Poggi-Bach J, Engelke UF, *et al*: Defect in dimethylglycine dehydrogenase, a new inborn error of metabolism: NMR spectroscopy study. Clin Chem 45: 459-464, 1999.
27. Cernei N, Zitka O, Ryvolova M, *et al*: Spectrometric and electrochemical analysis of sarcosine as a potential prostate carcinoma marker. Int J Electrochem Sci 7: 4286-4301, 2012.
28. Eckschlager T, Adam V, Hrabeta J, Figova K and Kizek R: Metallothioneins and cancer. Curr Protein Pept Sci 10: 360-375, 2009.
29. Krizkova S, Fabrik I, Adam V, Hrabeta J, Eckschlager T and Kizek R: Metallothionein - a promising tool for cancer diagnostics. Bratisl Lek Listy 110: 93-97, 2009.
30. Krizkova S, Adam V, Eckschlager T and Kizek R: Easy-to-use and rapid detection of potential tumour disease marker metallothionein by using of PVDF membranes and chicken antibodies. FEBS J 276: 317-317, 2009.
31. Krizkova S, Fabrik I, Huska D, *et al*: An adsorptive transfer technique coupled with Brdicka reaction to reveal the importance of metallothionein in chemotherapy with platinum based cytostatics. Int J Mol Sci 11: 4826-4842, 2010.

32. Krizkova S, Masarik M, Majzlik P, *et al*: Serum metallothionein in newly diagnosed patients with childhood solid tumours. Acta Biochim Pol 57: 561-566, 2010.
33. Krejcova L, Fabrik I, Hynek D, *et al*: Metallothionein electrochemically determined using Brdicka reaction as a promising blood marker of head and neck malignant tumours. Int J Electrochem Sci 7: 1767-1784, 2012.
34. Sochor J, Hynek D, Krejcova L, *et al*: Study of metallothionein role in spinocellular carcinoma tissues of head and neck tumours using Brdicka reaction. Int J Electrochem Sci 7: 2136-2152, 2012.
35. Gumulec J, Masarik M, Krizkova S, *et al*: Evaluation of alpha-methylacyl-CoA racemase, metallothionein and prostate specific antigen as prostate cancer prognostic markers. Neoplasma 59: 191-201, 2012.
36. Krizkova S, Ryvolova M, Gumulec J, *et al*: Electrophoretic fingerprint metallothionein analysis as a potential prostate cancer biomarker. Electrophoresis 32: 1952-1961, 2011.
37. Hamer DH: Metallothionein. Annu Rev Biochem 55: 913-951, 1986.
38. Krizkova S, Adam V and Kizek R: Study of metallothionein oxidation by using of chip CE. Electrophoresis 30: 4029-4033, 2009.
39. Krizkova S, Masarik M, Eckschlager T, Adam V and Kizek R: Effects of redox conditions and zinc(II) ions on metallothionein aggregation revealed by chip capillary electrophoresis. J Chromatogr A 1217: 7966-7971, 2010.
40. Adam V, Fabrik I, Eckschlager T, Stiborova M, Trnkova L and Kizek R: Vertebrate metallothioneins as target molecules for analytical techniques. TrAC Trends Anal Chem 29: 409-418, 2010.
41. Ryvolova M, Krizkova S, Adam V, *et al*: Analytical methods for metallothionein detection. Curr Anal Chem 7: 243-261, 2011.
42. Sochor J, Pohanka M, Ruttkay-Nedecky B, *et al*: Effect of selenium in organic and inorganic form on liver, kidney, brain and muscle of Wistar rats. Cent Eur J Chem 10: 1442-1451, 2012.
43. Jurikova T, Sochor J, Rop O, *et al*: Evaluation of polyphenolic profile and nutritional value of non-traditional fruit species in the Czech Republic - a comparative study. Molecules 17: 8968-8981, 2012.
44. Rop O, Reznicek V, Mlcek J, *et al*: Antioxidant and radical oxygen species scavenging activities of 12 cultivars of blue honeysuckle fruit. Hort Sci 38: 63-70, 2011.
45. Sochor J, Babula P, Krska B, *et al*: Evaluation of output signals from CoulArray detector for determination of antioxidant capacity of apricots samples. In: Analysis of Biomedical Signals and Images. Jan J, Jirik R, Kolar R, Kolarova J, Kozumplik J and Provaznik I (eds). Brno University of Technology VUT v Brně Press, Brno, pp209-214, 2010.
46. Krauth-Siegel RL and Leroux AE: Low-molecular-mass antioxidants in parasites. Antioxid Redox Signal 17: 583-607, 2012.
47. Pohanka M, Karasova JZ, Musilek K, Kuca K, Jung YS and Kassa J: Changes of rat plasma total low molecular weight antioxidant level after tabun exposure and consequent treatment by acetylcholinesterase reactivators. J Enzyme Inhib Med Chem 26: 93-97, 2011.
48. Parejo L, Codina C, Petrakis C and Kefalas P: Evaluation of scavenging activity assessed by Co(II)/EDTA-induced luminol chemiluminescence and DPPH· (2,2-diphenyl-1-picrylhydrazyl) free radical assay. J Pharmacol Toxicol Methods 44: 507-512, 2000.
49. Nilsson J, Pillai D, Onning G, Persson C, Nilsson A and Akesson B: Comparison of the 2,2'-azinobis-3-ethylbenzotiazoline-6-sulfonic acid (ABTS) and ferric reducing antioxidant power (FRAP) methods to asses the total antioxidant capacity in extracts of fruit and vegetables. Mol Nutr Food Res 49: 239-246, 2005.
50. Asghar MN, Khan IU, Arshad MN and Sherin L: Evaluation of antioxidant activity using an improved DMPD radical cation decolorization assay. Acta Chim Slov 54: 295-300, 2007.

5 PART IV: Novel approaches to the analysis of prostate cancer markers

5.1 Theoretical basis

CaP has a variable biological potential with different options of therapy. For the successful treatment, it is necessary to identify and distinguish aggressive forms of this pathology from the clinically latent forms with the low metastatic potential and slow growth rate. Therefore, a personalized approach is needed to define men with a higher risk of CaP progression, to distinguish indolent and aggressive disease and to improve the stratification of post-treatment risks. Such approach can facilitate clinical decisions, improve selection for active monitoring protocols and minimize side effects of the therapy.

Research of new biomarkers associated with CaP carcinogenesis is considered an opportunity to provide patients with new possibilities, to understand the risk of CaP development better and to predict the clinical course of the disease. None of the currently used diagnostic methods is able to distinguish the aggressive and the latent tumour forms. All biopsy-verified carcinomas are therefore treated as the life-threatening forms. Therefore, a significant proportion of patients has no benefit from treatment [118]. Such an approach leads to a significant decrease in life quality because radical prostatectomy results in erectile dysfunction in up to 70% of patients and incontinence in 10% of them [119]. It is therefore desirable to find such CaP markers that would be able to distinguish between aggressive and latent tumour forms at initial stages [120, 121].

Measurement of serum concentration of the prostate-specific antigen (PSA) is the most common current screening assay for CaP, but it is neither sensitive nor specific sufficiently [122]. The total PSA (tPSA) circulating in serum has two components. The first component is PSA bound to α1-antichymotrypsin (ACT) and the second component is free PSA (fPSA) [123-125]. To improve the specificity of the total PSA (tPSA), the fPSA/tPSA ratio, which in some cases is able to distinguish benign prostatic hyperplasia (BPH) from CaP, was tested [126]. However, the percentage of fPSA was shown to increase with the age and prostate size [127]. fPSA was able to distinguish between CaP and BPH only in patients with a small prostate size (less than 40 cm^3) [128, 129]. To take into account the prostate size, Benson et al. have introduced the term PSA density (PSAD). It is assumed that CaP releases more PSA per unit volume of the prostate into circulation than BPH [130]. To distinguish between the two diseases, a limit PSAD value from 0.1 to 0.2 ng/mL/cm^3 is currently used. However, the threshold should vary according to the amount of total tPSA (0.05 ng/mL/ cm^3 at tPSA 2-4 ng/mL; 0.1 at tPSA 4-10 ng/mL and 0.19 at

10-20 ng/mL). Particularly in the patients with a low tPSA concentration, additional use of PSAD may improve the selection of the patients who may benefit from the prostate biopsy [131]. As the absolute PSA values are unable to predict the presence of the prostate carcinoma and its aggressiveness accurately, a great attention is paid to PSA kinetics (change in PSA levels). PSA kinetics describes PSA changes over time. To describe changes in PSA levels, such features like PSA velocity (PSAV) and PSA doubling time (PSADT, i.e. the time necessary for PSA doubling) are applied. Increase by 0.75 ng/ml/year is considered the threshold PSAV value. The value of 0.75 ng/ml/year, based on at least three samplings in two-year intervals as a minimum, seems to be useful for determining the increased risk of CaP [132]. Guidelines for CaP diagnostics recommend that males with the PSAV value higher than 0.35 ng/ml should consider biopsy every year, though their total PSA is low [133]. Nevertheless, many studies report that PSAV and PSADT did not improve the specificity of the PSA itself [134-136].

Because of the non-specificity of the PSA-based diagnostics, other markers and approaches are examined, such as non-coding RNA PCA3 expression, prostate health index (PHI), kallikrein panel (4k-panel), TMPRSS2: ERG fusion detection, loss of tumour suppressor PTEN and detection of circulating tumour cells [137, 138]. Possible CaP management with the use of biomarkers is proposed in **Fig. 5.**

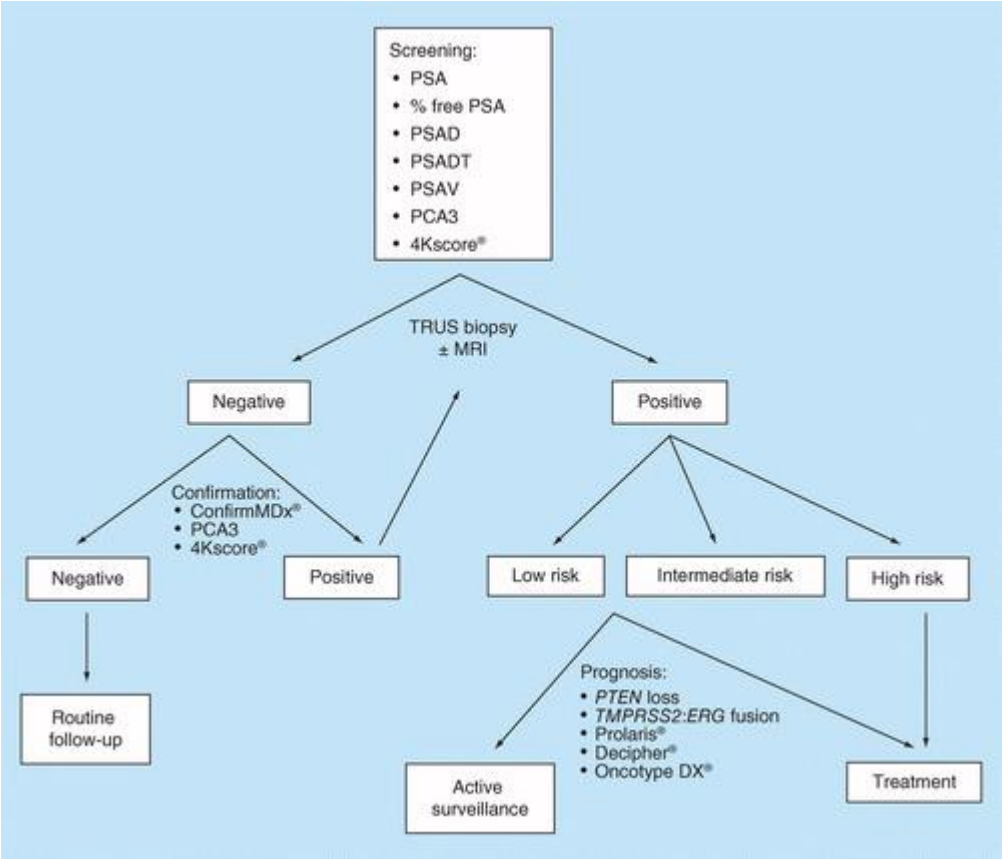

Figure 5 | Algorithms for CaP diagnostics management. MRI: Magnetic resonance imaging; PCA3: Prostate cancer antigen 3; PSA: Prostate specific antigen; PSAD: PSA density; PSADT: PSA doubling time; PSAV: PSA velocity; TRUS: Transrectal ultrasound.

The markers studied by us included metallothionein, caveolin-1 and alpha-methylacyl CoA-racemase (AMACR). Significance and functions of metallothioneins were discussed in the previous text, and therefore we will focus on the theory concerning caveolin-1 and AMACR. Alpha-methylacyl CoA-racemase is a peroxisomal and mitochondrial enzyme involved in β-oxidation of branched fatty acids, catabolism of bile acid metabolites and metabolism of certain drugs. Increase in AMACR protein levels was reported in most adenocarcinomas and in high grade prostatic intraepithelial neoplasia [139, 140]. Low levels of this marker are described in benign hyperplasia and in atypical adenomatous hyperplasia [141]. Overexpression of AMACR may play a role in stimulating CaP cell growth by the pathway independent of androgen signalling [142].

Caveolin-1 (Cav-1) is a membrane protein and an important structural component of caveolae. The group of these proteins plays an important role in cholesterol degradation, but also takes an important part in transmembrane signalling. The effect of Cav-1 on the progression of tumour diseases and the increase of Cav-1 serum levels in prostate carcinoma was described recently [143, 144]. Cav-1 is reported to be overexpressed in CaP cells and is associated with the

disease progression. Specific oncogenic activities of Cav-1 were associated with the Akt activation. However, the Cav-1 protein can also be secreted by the CaP cells. Results of recent studies showed that the secreted Cav-1 can stimulate cell survival and angiogenic activity in the CaP microenvironment. Pre-operative Cav-1 concentrations in serum had prognostic potential in the males who underwent radical prostatectomy [145].

5.2 Hypothesis verified under PART IV

The following hypotheses were formulated based on the above theoretical starting points:

Hypothesis 1: Metallothionein, caveolin-1, AMACR and sarcosine are suitable biomarkers of CaP progression and their expression is correlated with the clinical and pathological characteristics of the CaP patients.

Hypothesis 2: Metallothionein is also detectable in other biological materials - blood, tumour tissue; the procedure of metallothionein analysis is automated thanks to using the isolation of this protein by means of paramagnetic particles.

Hypothesis 3: Sensitivity of sarcosine detection can be increased using advanced techniques such as FRET.

5.2.1 Findings related to the hypothesis 1

***Hypothesis 1*: Metallothionein, caveolin-1, AMACR and sarcosine are suitable biomarkers of CaP progression and their expression is correlated with the clinical and pathological characteristics of the CaP patients.**

Metallothionein, caveolin-1 and AMACR were selected for detection in the blood serum of the patients and volunteers included in this study, because these proteins (as reported) leave the prostatic tissue during the cancerogenesis, thus penetrating into the serum. A statistically significant increase in the level of metallothionein ($p < 0.001$) was found, with caveolin-1 and AMACR levels not changing significantly between the control and the tumour groups (**Fig. 6**). No statistically significant correlations between the age and all three monitored markers were found. Protein levels of Cav-1 and AMACR were distinctly higher in the Gleason score 9 in the serum of CaP patients [146, 147]. Metallothionein levels were grading independent. No statistically significant differences between the localized (T1,2) and spreading (T3,4) tumours were found in all three examined markers (data not shown). However, the serum level of Cav-1 was higher in patients with T4 tumours (**Fig. 6C**). Level of none of the examined markers changed in patients with hypertension, ischemic heart disease and hyperlipoproteinemia, ischemic disease of

lower limbs and gastroduodenal ulcer disease. Similarly, level of the examined markers did not differ in the group of smokers and non-smokers.

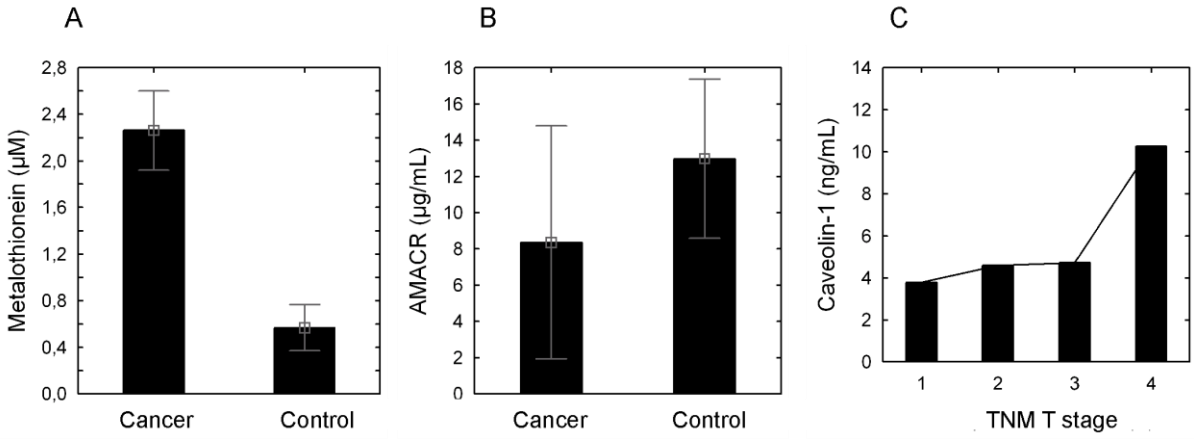

Figure 6 | Level of tumour markers in patients' serum. (A) metallothionein level, (B) level of alpha methylacyl-CoA- racemase (AMACR), (C) level of Caveolin-1 depending on disease staging.

Serum metallothionein level is increased significantly in the patients with the prostate carcinoma. The fact puts it in the position of a possible tumour marker of this disease, affected minimally by the clinical status of the patient, as its level is affected neither by smoking, age, grading of the disease, nor by the presence of comorbidities common in the population.

Though the level of caveolin-1 did not differ between the tumour and non-tumour groups, its higher serum level was found in the patients with affected surrounding tissues and organs (TNM stage T4) compared with the lower stages. Similarly, as in metallothionein, the level of caveolin-1 was affected neither by the presence of comorbidities nor by smoking and was not age-dependent. The alpha-methyl CoA-racemase level did not differ between the patients and the controls either.

None of the substances studied therein meets criteria for being a marker of the aggressive disease form. This statement dwells on the assumption that a majority of prostate tumours is latent and slowly growing (i.e. stages T1 and T2), and only a minor part of them behave aggressively (reaching stages T3 and T4). There was no statistically significant difference in the level of monitored proteins between these two groups. However, the level of caveolin-1 was significantly higher in the serum of patients with tumours of stage 4. Therefore, the level of this marker should be tested on a larger set of patients with the aggressive tumour form. Although not meeting the criteria for being a marker of the aggressive form of the disease, metallothionein as the only one showed a significantly increased level in the serum of patients suffering from prostate

tumours in this study. Thus, it can be used as a supplement to PSA screening. However, its application has to be verified on a significantly larger set of data.

Furthermore, sarcosine as a potential tumour marker was determined. After the optimization and validation of the ion exchange chromatography, the use of this method for the determination of sarcosine in biological samples was tested. Results of sarcosine determination in the urine of the patients with diagnosed CaP (n = 11), patients with BPH (n = 3) and healthy volunteers (n = 23) are shown in Heger *et al.* on page 315. It can be seen from the diagram that while the average sarcosine content in the urine of volunteers was 0.1 ± 0.3 μmol/l, the average sarcosine content in the CaP patients was 470 ± 70 μmol/l. These results suggest that sarcosine is potentially a suitable marker for the prostate carcinoma diagnostics. Our results show that the average content of sarcosine in the urine specimens of prostate carcinoma patients is significantly higher than in the control samples.

Conclusion: None of the substances studied therein meets criteria for being a marker of the aggressive disease form. There was no statistically significant difference in the level of monitored proteins between the localized (T1, 2) and spreading (T3, 4) tumours. However, the level of caveolin-1 was significantly higher in the serum of patients with tumours of stage 4 and AMACR and Cav-1 levels were higher in patients with Gleason grade 9. Metallothionein as the only one showed a significantly increased level in the serum of CaP patients compared with control samples. The determination of sarcosine in connection with the determination of other CaP biomarkers has a potential to improve the prostate carcinoma diagnostics and to eliminate false positive and false negative cases.

Author's publications relevant to this chapter

1. Gumulec J, Sochor J, Hlavna M, et al. Caveolin-1 as a potential high-risk prostate cancer biomarker. Oncology Reports. 2012;27(3):831-841.
   Available on page 269
2. Gumulec J, Masarik M, Krizkova S, et al. Evaluation of alpha-methylacyl-CoA racemase, metallothionein and prostate specific antigen as prostate cancer prognostic markers. Neoplasma. 2012;59(2):191-200.
   Available on page 280

ONCOLOGY REPORTS 27: 831-841, 2012

Caveolin-1 as a potential high-risk prostate cancer biomarker

JAROMIR GUMULEC[1,2], JIRI SOCHOR[2,3], MARIAN HLAVNA[1], MARKETA SZTALMACHOVA[1,2], SONA KRIZKOVA[2,3], PETR BABULA[2,3], ROMAN HRABEC[4], ARNE ROVNY[4], VOJTECH ADAM[2,3], TOMAS ECKSCHLAGER[5], RENE KIZEK[2,3] and MICHAL MASARIK[1]

[1]Department of Pathological Physiology, Faculty of Medicine, Masaryk University, CZ-625 00 Brno; [2]Department of Chemistry and Biochemistry, Mendel University in Brno, CZ-613 00 Brno; [3]Central European Institute of Technology, Brno University of Technology, CZ-616 00 Brno; [4]Department of Urology, St. Anne's University Hospital Brno, CZ-656 91 Brno; [5]Department of Paediatric Haematology and Oncology, 2nd Faculty of Medicine Charles University, CZ-150 06 Prague 5, Czech Republic

Received October 4, 2011; Accepted November 7, 2011

DOI: 10.3892/or.2011.1587

Abstract. Current diagnostic techniques of prostate cancer cannot efficiently distinguish the latent and low-risk forms from the high-risk significant forms of prostate cancer. Caveolin-1 (Cav-1), except other functions, plays an important role in cell transformation and the process of tumorigenesis. Furthermore, Cav-1 is involved in metastatic processes. It has also been shown that Cav-1 expression is induced under stress conditions, such as oxidative stress. The present study focused on the determination of prognostic markers of aggressive (high-grade) forms of prostate cancer. We determined serum Cav-1 and serum markers of antioxidant activity-glutathione (GSH), 2,2-diphenyl-1-picrylhydrazyl (DPPH), Trolox equivalent antioxidant capacity (TEAC), ferric-reducing antioxidant power (FRAP), N,N-dimethyl-1,4-diaminobenzene (DMPD), free radicals method (FRK) and blue chromium peroxide (Cro) in 97 serum samples (82 prostate cancer patients and 15 controls). We found insignificant differences in Cav-1 between the sera of patients and controls (5.69 in the cancer group vs. 5.42 ng/ml in the control group). However, we found a significant ($p<0.004$) 2.8-fold elevation of Cav-1 in high tumour stages (TNM T4) compared to lower stages and a significant positive association with histological grading ($r=0.29$, $p=0.028$). We also found that in patients with high serum Cav-1 the antioxidant capacity of the body is reduced. These findings indicate that Cav-1 may be an interesting tool for the prediction of disease burden.

Correspondence to: Dr Michal Masarik, Department of Pathological Physiology, Faculty of Medicine, Masaryk University, Kamenice 5, CZ-625 00 Brno, Czech Republic
E-mail: masarik@med.muni.cz

Key words: prostate cancer, tumour marker, prognostic marker, immunodetection, electrochemistry, polymerase chain reaction, molecular biology techniques

Introduction

Discovering and definition of new biochemical markers, which are specifically connected with grave pathological states including tumour diseases, are among the most important objectives of biomedical research. Identification of highly specific and sensitive biomarkers represents the main aim of modern research, because only such biomarkers may be applied towards the early diagnosis of malignant disease, prediction of prognosis and eventually development of an appropriate treatment strategy in clinical practice (1). Malignant tumours occupy the first position among diagnosed diseases due to the improvement of health care. The process of genesis of a tumour cell includes accumulation of alterations in a cell genome, which may develop for decades. Mechanisms of the cell cycle and apoptosis regulation play a crucial role in the protection against these changes.

Prostate carcinoma is the most frequent malignant disease among men in the Czech Republic. Global data about the incidence of prostate carcinoma are not too exact, especially due to fact that a lot of men die due to this disease without its clinical manifestations (2). Substantial progress in the diagnosis of tumour diseases has been observed along with the development of proteomics due to the identification of new tumour markers (3-8). These markers, usually proteins, are closely connected with the development and eventually the progression of the disease and are present in tumour cells in altered concentrations.

Due to the introduction of prostate-specific antigen (PSA) screening in prostate cancer diagnosis, the incidence of this disease has increased by >50% in the recent years. At present, its incidence is higher in comparison with bronchogenic carcinoma with almost half of the men at the age of 80 suffering from prostate carcinoma. PSA represents the routinely used diagnostic marker of prostate carcinoma (9-11). Measurements of PSA blood serum levels began in the early 1980s. There are plenty of methods used for determination of PSA blood serum levels (10,12). However, determination of PSA is not specific and sensitive in the blood serum and its positive predictive value is only about 35%. PSA may also be elevated in various

non-tumour conditions in healthy men. Its level is increased in other prostate diseases (benign prostatic hyperplasia, prostatitis and prostate infections) or with physical activity including cycling. Almost two thirds of men with increased PSA are healthy. Contrariwise, 20% of men suffering from prostate carcinoma have normal PSA levels.

Therefore, it is not surprising that searching for new markers for this type of tumour disease is still a focus of research. Caveolin is a protein, which is often associated with tumour disease as a potential tumour marker. It is an integral membrane protein and important integral part of caveolae membranes. Its presence was already discovered in caveolae membranes in 1953 (13). These membranes are involved in receptor-independent endocytosis. Caveolae are microdomains of lipid rafts, which are rich in sphingolipids and cholesterol and play an essential role in the degradation of cholesterol (14). However, they also participate in transmembrane signalling. There are three known types of caveolin, which differ in their molecular structure and tissue distribution. Caveolin-1 is profusely present in adipocytes, epithelial cells, pneumocytes and fibroblasts. Caveolin-2 is expressed in the cells of mesenchyma, epithelial cells and neuroglia. Caveolin-3 occurs predominantly in muscle cells (15,16). All types of caveolins are investigated in view of the pathogenesis of some diseases (17-20). The connection between caveolin-1 and tumorigenesis has been investigated in many studies (21-24). Caveolin-1 has been demonstrated to regulate cell proliferation, so, it can play an important role in cell transformation and the process of tumorigenesis (23,25,26). Caveolin-1 is also involved in metastatic processes (25). The reason for the participation of caveolin-1 in these processes is the fact that normal epithelial cells are characterized by cell adhesion and the cell is closely connected through the membrane with its surroundings and is able to respond to changes in cell surroundings. Caveolin-1 directly participates in these cell processes, especially due to its connection with integrins. Changes in protein function lead to the lapse of cell functions (adhesion) and cell mobility and the development of metastatic processes (22). Furthermore, it has been demonstrated that caveolin-1 expression is induced under stress conditions, such as oxidative stress (27,28).

Metallothioneins (MT) as a metal-binding proteins represent other promising tumour markers, which are intensely studied in connection with prostate carcinoma among other diseases (29-31). It has been recently demonstrated that metallothioneins play an important role in the development and progression of some tumour diseases (32-42). Enhanced levels of MT in tumour cells are probably closely connected with cell proliferation (43,44). Recent studies point at the overexpression of MT in relation to the metal-based cytostatic agents (45,46). Other potential tumour markers include α-methylacyl-CoA-racemase (AMACR). This substance is a peroxisomal and mitochondrial enzyme involved in β-oxidation of branched fatty acids and in catabolism of bile acids metabolites (47). Increased levels of these proteins have been described in adenocarcinomas and high grade prostatic intraepithelial neoplasia (48). On the other hand, only low levels of this marker are described in benign hyperplasia and in atypical adenomatous hyperplasia (47,49,50).

It is well evidenced that the total antioxidant capacity of the human body is reduced, when patients suffer from a serious disease such as cancer, particularly when the disease is long-term and the patients are of higher age (51-53). Thus, we aimed to determine most of the common markers of antioxidant capacity and to put them into the context with caveolin-1. The originality of this study consists in the analysis and mutual correlation between the above-mentioned tumour markers and the markers of oxidative stress in blood sera of patients suffering from prostate carcinoma. Our results show the necessity for the determination of more tumour markers to aid in the knowledge of the disease stage of the patient and for the identification of optimal treatments.

Materials and methods

Chemical and biochemical reagents. All chemicals of ACS purity were purchased from Sigma-Aldrich (St. Louis, Mo, USA) unless otherwise noted. The primary mouse metallothionein antibody and the secondary anti-mouse horseradish peroxidase (HRP)-conjugated antibody were purchased from Abcam (Cambridge, MA, USA). The primary rabbit PSA and caveolin-1 antibody and the secondary anti-rabbit HRP-conjugated antibody were purchased from Santa Cruz Biotechnology, Inc. (Santa Cruz, CA, USA). The primary rabbit AMACR antibody was purchased from Clonestar (Czech Republic). For chemiluminiscent detection of Western blot membranes the ECL Western blot detection reagents system from Bio-Rad Laboratories (USA) was used.

Sample preparation for electrochemical analysis. The samples of blood serum were denatured at 99˚C in a thermomixer (Eppendorf 5430, Germany) for 15 min with shaking and centrifuged at 15,000 x g at 4˚C for 30 min (Eppendorf 5402). Heat treatment effectively denatures and removes thermolabile and high-molecular-weight proteins from samples. The prepared samples were used for MT and glutathione (GSH) analyses.

Differential pulse voltammetry-Brdicka reaction. Differential pulse voltammetric measurements were performed with the 747 VA Stand instrument connected to the 746 VA Trace Analyzer and the 695 Autosampler (Metrohm, Switzerland), using a standard cell with three electrodes and cooled sample holder (4˚C). A hanging mercury drop electrode (HMDE) with a drop area of 0.4 mm^2 was the working electrode. An Ag/AgCl/3M KCl electrode was the reference and glassy carbon electrode was auxiliary. For data processing GPES 4.9 supplied by EcoChemie was employed. The analysed samples were deoxygenated prior to measurements by purging with argon (99.999%) and saturated with water for 120 sec. Brdicka supporting electrolyte containing 1 mM $Co(NH_3)_6Cl_3$ and 1 M ammonia buffer [NH_3(aq) + NH_4Cl, pH 9.6] was used. The supporting electrolyte was exchanged after each analysis. The parameters of the measurement were as follows: initial potential of -0.7 V, end potential of -1.75 V, modulation time 0.057 sec, time interval 0.2 sec, step potential 2 mV, modulation amplitude -250 mV, E_{ads} = 0 V, volume of injected sample: 20 μl (x100 diluted sample with 0.1 M phosphate-buffer pH 7.0). All experiments were carried out at a temperature of 4˚C employing the thermostat Julabo F25 (Labortechnik GmbH, Germany).

Determination of low-molecular-mass thiols. High performance liquid chromatography with an electrochemical detection (HPLC-ED) system consisted of two solvent delivery pumps operating in the range of 0.001-9.999 ml/min (Model 582 ESA Inc., Chelmsford, MA), Zorbax Eclipse AAA Column (4.6 x 150 mm 3.5-μm particle size; Varian Inc., CA, USA), and a CoulArray electrochemical detector (Model 5600A, ESA, USA). The sample (30 μl) was injected using an autosampler (Model 540 Microtiter HPLC; ESA, USA). HPLC-ED experimental conditions were as follows. The compositions of the mobile phases were: A, 80 mM trifluoroacetic acid and B, methanol. They were mixed in gradient from 3% B in the first minute, 10 % B in the second to the sixth minute and 98% B from the seventh minute of the separation; flow of the mobile phase was 0.8 ml/min, temperature of the separation was 40˚C; working electrodes potential was 900 mV; detector temperature was 30˚C; each measurement was done in triplicates. Retention time of the reduced GSH was 5 min. GSH concentration was calculated from a calibration curve (0.5-100 μM). The signal was quantified as a sum of current responses from all working electrodes (54,55). In the case of real sample measurements, the shift of the retention time was of about ±2%.

Determination of antioxidant activity. For determination of antioxidant activity a BS-400 automated spectrophotometer (Mindray, China) was used. It is composed of cuvette space tempered to 37±1˚C, reagent space with a carousel for reagents (tempered to 4±1˚C), sample space with a carousel for preparation of samples and an optical detector. Transfer of samples and reagents is provided by robotic arm equipped with a dosing needle (error of dosage up to 5% of volume). Cuvette contents are mixed by an automatic mixer including a stirrer immediately after addition of reagents or samples. Contamination is reduced due to its rinsing system, including rinsing of the dosing needle as well as the stirrer by MilliQ water. For detection itself, the following range of wave lengths can be used - 340, 380, 412, 450, 505, 546, 570, 605, 660, 700, 740 and 800 nm. Experimental details on all used spectrometric assays have been previously described (56).

Sodium dodecyl sulphate polyacrylamide gel electrophoresis (SDS-PAGE). The electrophoresis was performed according to Laemmli using a Mini Protean Tetra apparatus with a gel dimension of 8.3 x 7.3 cm (Bio-Rad Laboratories) (57). Firstly we poured 10% (m/V) running gel and then 5% (m/V) stacking gel. The gels were prepared from 30% (m/V) acrylamide stock solution with 1% (m/V) bisacrylamide (SERVA, Germany). The polymerization of the running or stacking gels was carried out at room temperature for 45 min. Prior to analysis the samples were mixed with reducing (DTT, final concentration 400 mM) sample buffer in 4:1 ratio. The samples were boiled for 5 min and then the sample was loaded onto the gel. For determination of molecular mass, the protein ladder, broad or lower range (Bio-Rad Laboratories) was used. The electrophoresis ran at 80 V for 20 min subsequently increased to 120 V for 1 h (Power Basic, Bio-Rad Laboratories) in Tris-glycine buffer (0.025 M Trizma-base, 0.19 M glycine and 0.0035 M SDS, pH 8.3). Silver staining of the gels was performed using the Bio-Rad Silver stain kit according to Merril *et al* (58).

Western blot analysis. After the electrophoretic separation, the proteins were transferred onto a nitrocellulose membrane (Bio-Rad Laboratories) in a Bio-Rad apparatus. The blotting was carried out for 1 h at a constant current of 0.9 mA for 1 cm^2 of the membrane. After the transfer, the membrane was blocked in 5% non-fat milk in PBS (137 mM NaCl, 2.7 mM KCl, 1.4 mM NaH_2PO_4, and 4.3 mM Na_2HPO_4; pH 7.4) for 2 h. The incubation with mouse primary antibody in dilution of 1:750 in PBS with 5% non-fat milk was carried out for 12 h at 4˚C. After three washing with PBS containing 0.05 % (v/v) Tween-20 (PBS-T) for 5 min the membrane was incubated with secondary antibody (anti-mouse labelled with HRP, Sigma-Aldrich, diluted 1:5,000) for 1 h at room temperature. Then, the membrane was washed three times with PBS-T for 5 min and incubated with the ECL WB detection reagents (Santa Cruz Biotechnology Inc.).

Dot-immunobinding assay. For immunobinding assays PVDF membranes (Bio-Rad Laboratories) were used. The sample (1 μl) was applied and dried. Further the membrane was blocked in 2% bovine serum albumin (BSA) in PBS for 0.5 h with constant shaking. The incubation with the primary antibody (1:500 diluted) was carried out for 1 h at 37˚C. After three times repeated washing in PBS containing 0.05% (v/v) Tween-20 (0.05% PBS-T) for 5 min, the membrane was incubated in the presence of secondary antibody at a dilution 1:5,000 for 1 h at 37 C. Then the membrane was washed three times in 0.05% PBS-T for 5 min and incubated in chromogenic substrate [0.4 mg/ml AEC (3-aminoethyl-9-carbazole) in 0.5 M acetate buffer with 0.1% H_2O_2, pH 5.5]. After sufficient colouring the reaction was stopped by rinsing in water.

tPSA and fPSA determination. Total PSA (tPSA) and free PSA (fPSA) contents were determined by the immunochemistry analyser AIA 600 II (Tosoh, Japan). AIA 600 II is specifically designed for measurement of immunochemistry parameters in biological fluids using reagents of AIA-PACK series. Analyses were carried out according to the manufacturer's instructions. The instrument was calibrated using the AIA-PACK Calibrator set using a 6-point calibration (Tosoh). All reactions were performed in the special disposable test cups containing dried and lyophilized reagents. The immunochemical antigen-antibody reaction employed magnetic particles (1.5 mm). Samples were incubated at 37˚C. 4-Methylumbelliferyl phosphate was used as a substrate and fluorescence corresponding to enzymatic activity on magnetic particles was measured.

Determination of serum caveolin-1 protein. For determination of the serum levels of caveolin-1 protein the Human caveolin-1 ELISA Kit (Uscn Life Science, Inc., Wuhan, China; detection range 0.24-15 ng/ml) was used according to the manufacturer's manual. To detect the concentration of serum caveolin-1 level using the ELISA kit, the 60 ng/ml caveolin-1 standard was diluted to the concentration range 0.24-16 ng/ml in duplicates and absorption was measured.

Densitometric and statistical analysis. The signal intensity of bands after immunochemistry analysis was determined using the ImageJ 1.45 software (NIH, USA) as an area under the curve and concentration was calculated according to the protein

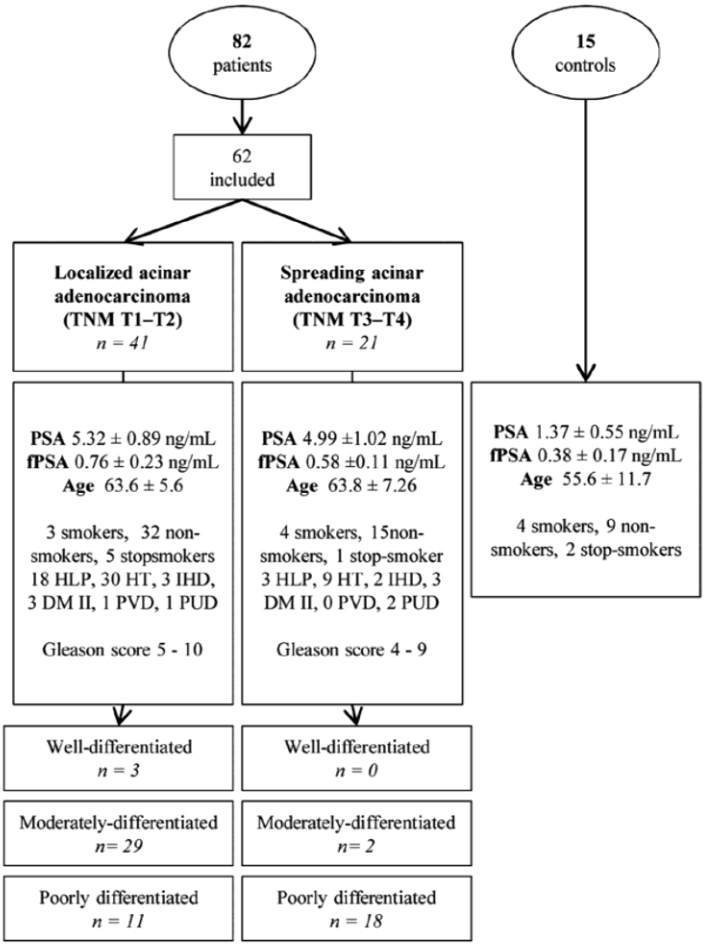

Figure 1. Characterisation of patients and controls. Categorization by tumour localization and differentiation. HLP, hyperlipoproteinaemia; HT, hypertension; IHD, ischaemic heart disease; DMII, diabetes mellitus type II; PVD, peripheral vascular diseas; PUD, peptic ulcer disease.

standard. Software Statistica 9.1 (StatSoft, USA) was used for statistical analysis. To test the normal distribution of data and thus usability of parametric tests, the Kolmogorov-Smirnov test was used. The Student's t-test for independent values was used to evaluate differences between the two groups. Simple linear correlations were performed to reveal the relationships between variables. To characterize data, associations were visualized using tree clustering with Euclidean distances measurement and single linkage. Subsequently, patients divided into clusters using K-means clustering analysis. Unless noted otherwise, a level of statistical significance was designated to p=0.05.

Results

Blood serum caveolin-1 levels were statistically evaluated in groups of controls and histologically verified tumours. Consequently, caveolin-1 level was related to data in the patient's history, such as age, smoking habits, associated diseases, clinical tumour stage and histological grade (Fig. 1). Subsequently, caveolin-1 was related to the level of serum PSA in order to evaluate the use of caveolin-1 as an auxiliary marker along with a PSA. Cluster analysis of PSA and caveolin-1 levels was performed to divide the patients into the groups characterised with high or low caveolin-1 or PSA. In these groups tumour stage and grade was evaluated.

Because tumour pathogenesis and growth are tightly associated with oxidative stress, we also determined serum markers of antioxidant activity, GSH, 2,2-diphenyl-1-picrylhydrazyl (DPPH), Trolox® equivalent antioxidant capacity (TEAC), ferric reducing antioxidant power (FRAP), N,N-dimethyl-1,4-diaminobenzene (DMPD), free radicals method (FRK) and blue chromium peroxide (Cro). We have previously described these methods in detail in study by Sochor *et al* (56). In addition, it has been shown that caveolin-1 is associated with oxidative stress in cancer progression. Thus, we correlated caveolin-1 levels with markers of oxidation and performed cluster analysis to elucidate possible associations. We also associated caveolin-1 with other previously determined potential prostate cancer serum tumour markers, namely α-methylacyl-CoA racemase (AMACR) and metallothionein (MT) which we have previously demonstrated as a high specificity and sensitivity diagnostic tool for prostate cancer diagnosis (59).

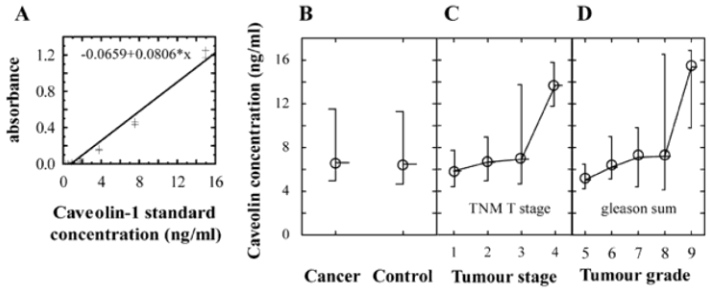

Figure 2. Caveolin-1 in patients. (A) Calibration curve. Absorbance of caveolin-1 standard in concentrations 0.24-16 ng/ml, obtained calibration curve at correlation r=0.98. (B) Serum caveolin-1 in patients and controls. No significant difference between groups was observed. (C) Caveolin-1 in relation to TNM tumour stage. Significantly higher ($p<0.004$) caveolin-1 level was determined in tumour exceeding seminal vesicles (T4) compared to lower stages of tumour. (D) Caveolin-1 grouped by histological tumour grade (Gleason sum). Higher caveolin-1 level was in high grade tumours (correlation r=0.29 at $p=0.028$).

Table I. Caveolin-1 and PSA levels in relation to tumour stage (TNM T stage), histological differentiation and tumour grade (Gleason sum score).

	n	PSA (ng/ml)	Free PSA (ng/ml)	Caveolin-1 (ng/ml)
Tumour stage				
T1	1	3.12	0.54	4.19
T2	40	5.41±3.44	0.77±0.44	5.25±2.62
T3	18	5.18±3.96	0.58±0.38	6.60±3.69
T4	3	5.58±4.01	0.57±0.33	14.25±2.19[a]
Tumour differentiation				
Well	3	4.15±1.40	0.63±0.42	4.13±1.27
Moderately	23	4.83±3.50	0.66±0.40	5.64±3.02
Poorly	28	5.95±4.66	0.72± 0.48	6.28±3.32
Tumour grade (Gleason sum score)				
5	5	3.69±1.43	0.46±0.02	3.86±1.11
6	20	5.03±2.56	0.82±0.39	5.11±2.42
7	32	4.85±3.22	0.58±0.37	5.75±2.98
8	3	10.12±8.17	1.02±0.82	6.96±4.83
9	4	6.87±5.03	0.64±0.42	9.99±4.04
10	1	3.90	-[b]	-[b]
Total	62	4.83±3.56	0.66±0.39	5.65±3.02

[a]Significant at $p<0.004$; [b]insufficient data for Gleason sum score 10 patients.

Tested cohort characteristics. We have analysed sera of 82 patients with histologically verified acinar adenocarcinoma of the prostate and 15 controls (Fig. 1). Out of these patients only 62 patients were selected for further analysis due to the lack of complete history data or insufficient quality of samples (haemolysis and/or extreme values detected). The average age of the patients was 63.7 years and ranged from 48 to 78 years. Of the 62 patients, 49 were non-smokers, 9 were smokers and the rest were former smokers. Forty-two patients (68%) had localized tumours (T1-2) and 20 patients had spreading tumours of higher stage. The tumour differentiation ranged from well differentiated (3 tumours) to poorly differentiated (27 tumours) (Table I). The Gleason sum score ranged within 5-10. Patients had the following associated illnesses: hypertension (39 patients) hyperlipoproteinaemia (21 patients), ischaemic heart disease (5 patients), diabetes mellitus type II (6 patients), peripheral vascular disease (1 patient), peptic ulcer disease (3 patients), and tumour in history (1 patient). Of 62 patients, 15% did not suffer from any associated disease.

Caveolin-1 in patients and controls. Caveolin-1 standard in the concentration range from 0.24 to 16 ng/ml was used for determining the calibration dependence shown in Fig. 2A. Using linear regression we obtained strictly linear dependence with $R^2>0.99$. The serum caveolin-1 concentration ranged within 1.12-14.15 ng/ml and 1.74-14.97 ng/ml in the patients group and controls, respectively. The mean serum concentrations were 5.69 ng/ml in the cancer group and 5.42 ng/ml

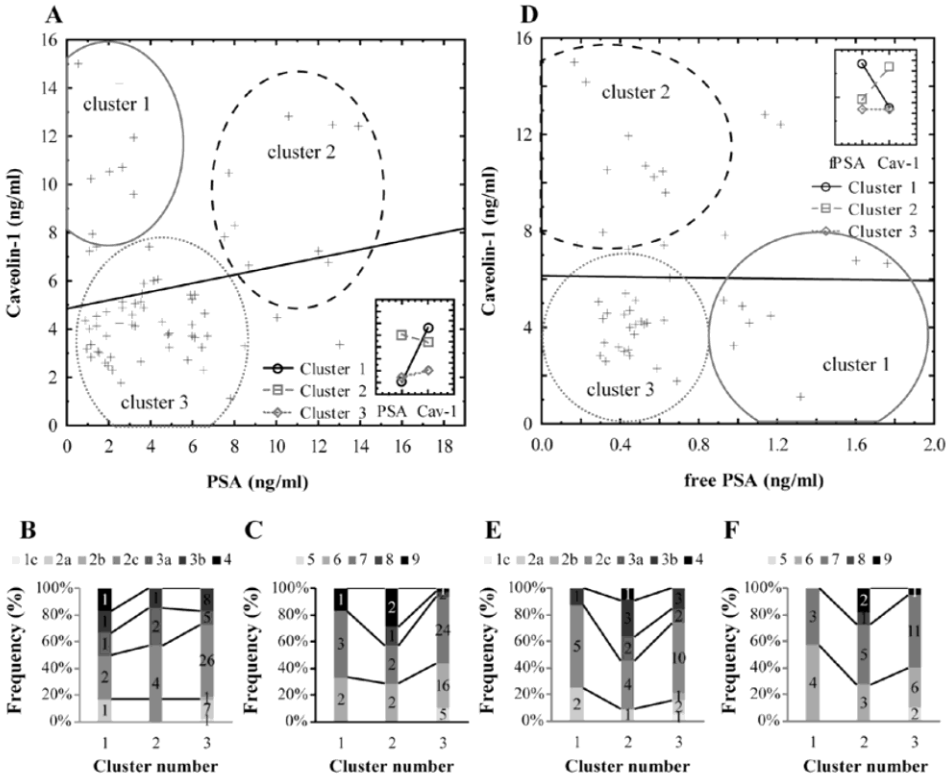

Figure 3. Caveolin-1 and prostate specific antigen (PSA). (A) Caveolin-1-PSA relation weak insignificant correlation was observed (see inset). Three clusters were apparent: patients with low PSA and high caveolin-1 (grey cluster 1), patients with high PSA and high caveolin-1 (dashed cluster 2) and patients with low PSA and low caveolin-1 (dotted grey cluster 3). (B) Tumour stage (TNM T) in three determined PSA/caveolin-1 clusters. Patients with low caveolin-1 and low PSA (cluster 3) had mostly lower grade tumours compared to clusters 1 and 2. (C) Tumour grade (Gleason sum) in PSA/caveolin-1 clusters of patients. Larger proportion of patients with higher PSA and higher caveolin-1 had higher grade (GS 8,9) tumours compared to patients with high caveolin-1 only (cluster 1) and low PSA and low caveolin-1 (cluster 3). (D) Caveolin-1 and free PSA no significant dependence revealed. Three clusters were apparent: patients with high free PSA and low caveolin-1 (grey cluster 1), patients with high caveolin-1 and low free PSA (dashed cluster 2) and patients with low caveolin-1 and low free PSA (dotted grey cluster 3). (E) Tumour stage (TNM T) in fPSA/caveolin-1 clusters. Patients with low fPSA and high caveolin-1 (cluster 2) had distinctly higher stage tumours compared to other clusters. (F) Tumour grade (Gleason sum) in fPSA/caveolin-1 clusters of patients. Patients with high caveolin-1 and low free PSA (cluster 2) had distinctly higher grade tumours.

in the control group. To verify the normality and thus suitability of parametric methods, the Kolmogorov-Smirnov test was performed. We found caveolin-1 levels were distributed normally ($p<0.1$), thus, independent t-test was used. No significant change between group of controls and patients was determined (Fig. 2B). Cluster analysis revealed statistically significant variance of values in a group of cancer sera and led to classification of patients into two groups: high caveolin-1 and low caveolin-1 (data are not shown). Serum caveolin-1 was subsequently related to tumour stage (TNM T stage) and tumour grade (Gleason score sum) to clarify the differences in values. A similar trend was observed in both relations: caveolin-1 levels remained low in low stage and low grade tumours and distinctly increased in the highest stage and grade tumours (Fig. 2C and D). Patients with tumour spreading beyond the seminal vesicle (TNM T4 stage) had significantly ($p<0.004$) 2.8-fold increased serum caveolin-1 levels compared to T1-3 stages (Table I). However, no statistically significant differences between localised (T1-2) tumours and those that extend through the prostate capsule (T3-4) were detected. In terms of tumour grade and its relation to caveolin-1, patients with Gleason sum 9 had distinctly higher caveolin-1 levels. This trend was significant ($r=0.29$ at $p=0.028$); however, the difference between Gleason sum 9 patients and others was below the threshold of statistical significance.

In addition, other correlations with data obtained from history were carried out. No statistically important correlations between age of patients and caveolin-1 were found. Level of caveolin-1 was not significantly changed in connection with associated disease-hypertension, ischemic heart disease and hyperlipidaemia, ischemic disease of lower extremities and duodenal ulcer. Similarly, no differences in monitored markers between group of smokers and non-smokers were evident (data not shown).

Caveolin-1 and PSA correlation. Correlation analysis of serum caveolin-1 levels to PSA levels, found that no correlation exists between these proteins ($p=0.13$). When cluster analysis was performed, three groups were found: patients with low caveolin-1 and low PSA (grey dotted ellipse, cluster 3 in Fig. 3A), patients with low PSA and high caveolin-1 (grey cluster 1) and patients with high caveolin-1 and PSA (black dashed cluster 2).

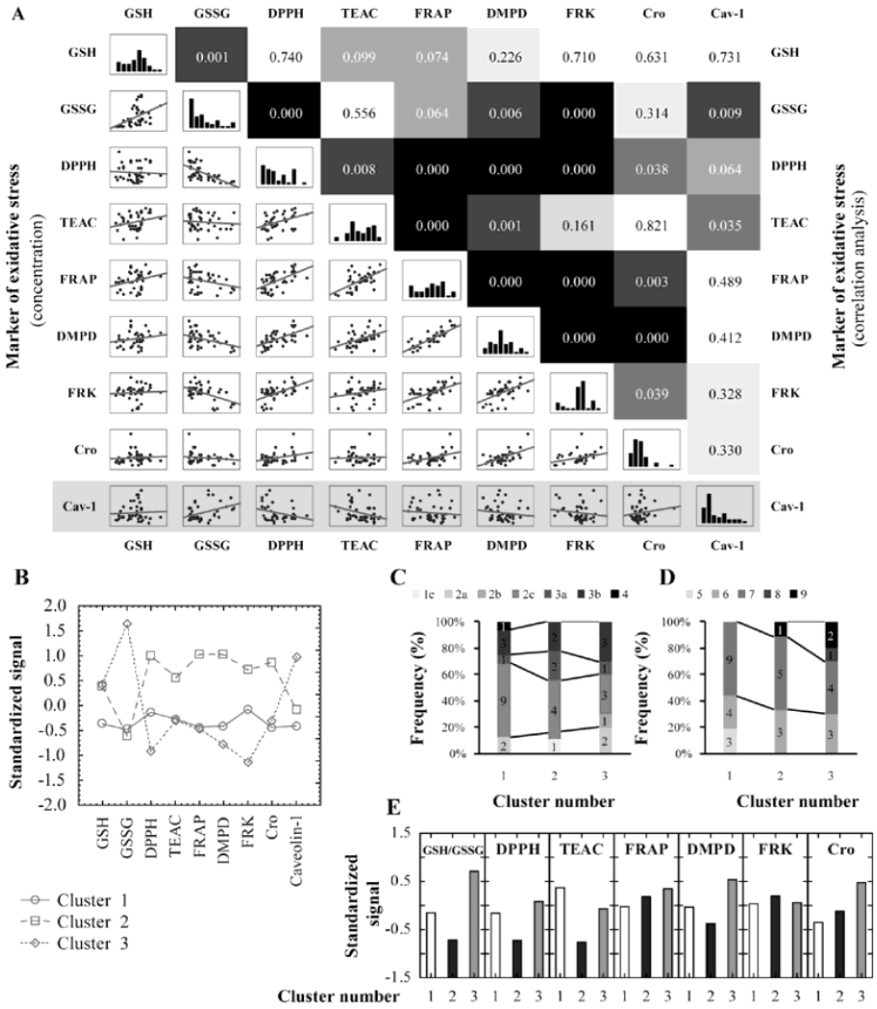

Figure 4. Caveolin-1 and markers of oxidation. (A) Correlations of markers of oxidation and caveolin-1 with each other with distribution histograms (diagonally). Bottom left part displays relations of markers/proteins, the top right part displays statistical significance of correlation (black, more significant trend; white, less significant). Evident significant correlations of caveolin-1 with reduced glutathione (GSH), 2,2-diphenyl-1-picrylhydrazyl (DPPH) and Trolox® equivalent antioxidant capacity (TEAC). (B) Cluster analysis of markers of oxidation together with caveolin-1. Inverse association of caveolin-1 and markers is obvious: the first cluster is characterized by no relations in caveolin-1 and markers of oxidation. The second cluster represents patients with high antioxidative potential (low GSSG and high antioxidative markers) and high caveolin-1. The third cluster represents patients with lower oxidative/antioxidant markers and low caveolin-1. (C) Tumour stage in subsequent clusters. No distinct differences in tumour staging within clusters of high or low caveolin-1/markers of oxidation were evident. (D) Tumour grade (represented as Gleason sum) in subsequent clusters. In the 'low antioxidative potential' cluster 3 are patients of distinctly higher content of high grade tumours compared to other patients. (E) Markers of antioxidant capacity in clusters by PSA/caveolin-1 characterized in Fig. 3A. We found significantly lower levels of the GSH/GSSG ratio, DPPH, TEAC and DMPD in the 'high PSA-high caveolin-1' cluster compared to the other clusters.

To characterize patients within those clusters, stage and grade was plotted in Fig. 3B and C. It is well evident that patients with high caveolin-1 and PSA (cluster 2) had lower proportions of localized tumours T1 and T2 compared to patients where only caveolin-1 is high and the PSA remains low (cluster 1), or where both proteins were low (cluster 3). A similar trend was evident in tumour grading (Fig. 3C), whereas in cluster 3 there was only a minimal proportion of high grade Gleason sum 8 and 9 tumours. In the 'both markers high cluster 2' the proportion of these high grades was about 40%.

A similar association was also observed with caveolin-1 and the free PSA fraction (Fig. 3D). Similarly to the total PSA, in a group of low free PSA and low caveolin-1 (cluster 3) the proportion of low stage and low grade tumours was higher (Fig. 3E and F). Patients characterised with high serum free PSA and low caveolin-1 were of marginally higher stage and grade compared to the 'low free PSA-low caveolin-1' cluster 3 group, whereas, patients with high serum caveolin-1 and low free PSA were of significant proportion of T3-4 and grade Gleason sum 8 and 9 tumours.

Association of caveolin-1 and oxidative stress. Markers of antioxidant activity were determined in the sera of patients and correlated with serum caveolin-1 level to elucidate

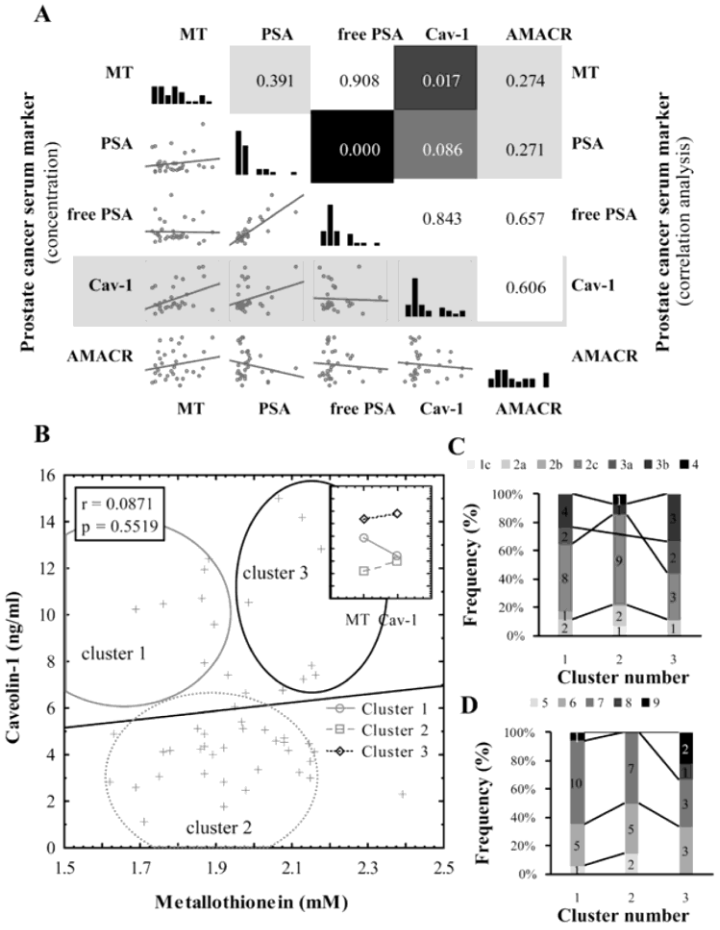

Figure 5. Relation of caveolin-1 to other potential prostate cancer markers. (A) Correlation matrix. A weak significant trend was observed between caveolin-1 and metallothionein (MT), no significant relation between caveolin-1 and PSA and α-methylacyl CoA-racemase (AMACR). (B) Caveolin-1 and MT clustering analysis of clinical data. Three clusters were apparent: patients with higher MT and lower caveolin-1 (grey cluster 1), patients with low MT and low caveolin-1 (grey dotted cluster 2) and patients with high caveolin-1 and high MT (black cluster 3). (C) Tumour stage (TNM T) in MT/caveolin-1 clusters. Higher proportion of high-stage tumours are apparent in cluster 3 compared to cluster 2. (D) Tumour grade (Gleason sum) in clusters of patients. In the cluster with higher MT and higher caveolin-1 (cluster 3) a higher proportion of patients with high-grade tumours is apparent compared to the other clusters.

potential connections. Association between those markers is displayed in Fig. 4A. We observed significant trends between caveolin-1 and reduced GSH, TEAC and borderline significance with DPPH. Among others, our results show that most of the markers of antioxidant capacity correlate more with each other compared to with caveolin-1. Strongest correlations were observed between ferric reducing antioxidant power and N,N-dimethyl-1,4-diaminobenzene and free radical method. In order to elucidate the connections between markers of (anti)oxidation, cluster analysis was performed. Using this procedure, patients were divided into three distinct clusters (Fig. 4B) as follows. Cluster 2 which consists of patients with high antioxidant capacity, low caveolin-1 and low reduced GSH (Fig. 4B); cluster 3 which consists of patients with low antioxidative capacity, high caveolin-1 and high reduced glutathione and cluster 1 which shows no apparent dependencies compared to the previous clusters, and in which the markers of (anti)oxidation are of rather lower levels. In Fig. 4C and D we identified the tumour grade and tumour stage within these clusters. It is clear from these results that patients with lower antioxidative potential and higher caveolin-1 level (cluster 3) had a higher proportion of high grade (Gleason sum 8,9) tumours compared to others (compare clusters 2 and 3 in Fig. 4D). No similar trend was however observed, if we highlighted tumour stage within these clusters (Fig. 4C).

Then, we aimed our attention at the markers of antioxidative capacity from a different perspective. We related markers of antioxidation to caveolin-1 and PSA together. Three clusters of PSA have been described: high PSA and caveolin-1, high caveolin-1, and low PSA and caveolin-1. In these clusters, the levels of individual antioxidative markers were visualized. We found a significantly lower ($p<0.05$) level GSH/GSSG ratio, DPPH, TEAC and DMPD in the group of patients with high caveolin-1 and high PSA compared to the group of patients with low serum caveolin-1 and low PSA.

Association of caveolin-1 with other potential tumour markers. We subsequently performed correlation analyses

between caveolin-1 and other potential serum markers of prostate cancer, which we have determined in our previous studies on the same sample set of patients (59). Thus, regarding PSA, which is mentioned in this table for overall complexity, here we show associations of caveolin-1 with MT and AMACR (Fig. 5A). In our previous study we have shown that metallothionein may be utilized as a marker of prostate cancer with high level of sensitivity and specifity (59). We found no major relationships between serum caveolin-1 level and serum MT levels (r=0.08, Fig. 5B). No trend was also observed when associated with AMACR. When cluster analysis on MT and caveolin-1 was carried out in the same way as with PSA or markers of oxidation (Fig. 5A), we found that when both of these serum markers are of high level, worse prognosis is expected, because greater proportion high grade (30 vs. 0% of GS 8-9 tumours in cluster 3 vs. cluster 2) and high stage (30 vs. 14% of T3b and T4 tumours in cluster 3 vs. cluster 2) tumours are present in these patients (Fig. 5C and D).

Discussion

In this study, we may clearly conclude that caveolin-1 is associated with worse prognosis. This we may evidence by three findings: first, higher serum caveolin-1 levels are associated with higher stage and grade tumours (which are of worse prognosis); second, caveolin-1 positively correlates with PSA levels, and third, patients with high serum caveolin-1 have a lower antioxidant capacity of the body. It is highly desirable to differentiate high-risk 'significant' forms of prostate cancer from latent, 'non-significant' forms. We expect that the prediction of high-risk tumours may be estimated when more cancer markers are determined concurrently. Utilization of caveolin-1 together with free and total PSA and possibly also with metallothionein may provide more accurate results in the estimation of prostate cancer risk when determined together. Based on our results we may conclude that patients with low free PSA, high caveolin-1 and high total PSA have worse prognosis compared to patients with lower serum caveolin-1 levels. Similarly, patients, who have high caveolin-1 and low PSA have better prognosis (lower stage and lower grade tumours) compared to patients with high PSA and caveolin-1 together. The similar benefit is also provided by the combined utilization of metallothionein and caveolin-1 as tumour markers, where patients with high metallothionein and low caveolin-1 are of better prognosis compared to patients with high levels of both markers. The merit of the use of fPSA, tPSA, caveolin-1 together as a marker of worse prognosis tumour may be underplayed by this finding. In cancers, the antioxidant capacity is reduced (51-53). Furthermore, patients with reduced antioxidant capacity are of worse prognosis when compared to patients with higher antioxidant potential. We may clearly confirm that the antioxidant capacity is associated with the severity of disease in this experiment by findings shown in Fig. 4D, from which it is apparent that patients with low antioxidative markers are of higher tumour grade.

An important finding of our study is the fact that high caveolin-1 levels are associated with patients of low antioxidative potential. Cluster analysis shown in Fig. 4B clearly points to the relationship between caveolin-1 and the antioxidative capacity of the patient's body. Patients with low caveolin-1 are of better prognosis because their antioxidative capacity is apparently higher (cluster 2 in Fig. 4B), whereas patients with high serum caveolin-1 have apparently lower antioxidative capacity. Due to the fact that caveolin-1 positively correlates with reduced glutathione and negatively correlates with markers of antioxidant capacity (even below the level of significance), we may speculate that caveolin-1 reflects the burden of the disease. This relation has not been published yet. The relationship of caveolin-1 with oxidative stress can also be viewed from another point of view. Recent studies have demonstrated that caveolin-1 is a target molecule in p38 MAPK mediated response to stress conditions such as oxidative stress (27,28). After such stimuli, caveolin-1 is phosphorylated and thus contributes to various signalling pathways (60) resulting most likely in processes, such as premature cellular senescence (27). Thus, the connection of low antioxidant capacity and high caveolin-1 found in our study may be explained as consequence of caveolin-1 mediated response to high oxidative burden. In such long-term high oxidative stress conditions the resulting antioxidant capacity may be reduced, nevertheless, caveolin-1 remains higher. Utilization of multiple protocols for the determination of antioxidative capacity or free radical quenching activity, as performed in this study, may be useful because of discrepancies between the activity measured *in vitro*, and the antioxidative effects observed *in vivo* (61). Each technique is based on different principles and enables determination of the antioxidant activity of specific groups of compounds (56,62,63).

In the recent decade, caveolin-1 was linked with various types of cancers, of which it was most extensively studied in the cancers of the breast and prostate. It was found that tumour tissue and/or serum caveolin-1 levels vary in a cancer-dependent manner and these changes in caveolin-1 levels may be associated with tumour protection or progression (25). When focused on prostate cancer, elevated caveolin-1 expression was observed in tumour tissue and in mice when compared to non-tumour tissue (64-66). According to Thompson *et al*, caveolin-1 is also elevated in the serum of patients with localized tumours compared to healthy controls and patients with benign prostatic hyperplasia (67,68). These findings are inconsistent with ours; we found no significant difference between controls and cancers. However, it has also been revealed that caveolin-1 is connected with tumour progression and metastatic dissemination and is distinctly elevated in androgen resistant tumours. Thus this molecule was suggested as a tissue marker of an aggressive form of cancer (68-74). It has also been shown that suppression of caveolin-1 expression can restore the sensitivity to androgens in androgen-insensitive tumours (65). Higher expression of caveolin-1 was also identified in tissue samples of patients of higher grade tumours and of higher PSA (75). This is in good agreement with our results, where we also identified associations with high stage and high grade tumours with high PSA. Also, according to a study by Karam *et al* on patients before and after radical prostatectomy, patients of higher caveolin-1 are in risk of higher postoperative PSA and thus of worse postoperative prognosis (75). Although we did not compare patients before and after treatment procedures, we similarly observed correlation of caveolin-1 with PSA. Furthermore, worse prognosis could be expected from higher oxidative stress in high caveolin-1 patients.

Our findings together with data from recent studies suggest that caveolin-1 is involved in disease pathogenesis and progression. Clarification can contribute to the understanding of this disease with potential novel targeted therapeutic approaches. Although associations between caveolin-1 and high-risk tumours were identified in this study, we still cannot infer that caveolin-1 may serve as a high-risk aggressive tumour marker even in a phase when tumours are localized in the prostate and thus are still curable. To confirm this, it is necessary to monitor caveolin-1 levels in a follow-up study during the course of prostate cancer progression from its initial stages. It is necessary to verify these facts in the extensive group of patients including those with disseminated disease.

Acknowledgements

Financial support from IGA MZ NS10200-3 and CEITEC CZ.1.05/1.1.00/02.0068 is greatly acknowledged.

References

1. Gannot G, Tangrea MA, Richardson AM, *et al*: Layered expression scanning: multiplex molecular analysis of diverse life science platforms. Clin Chim Acta 376: 9-16, 2007.
2. Bensalah K, Montorsi F and Shariat SF: Challenges of cancer biomarker profiling. Eur Urol 52: 1601-1609, 2007.
3. Duffy MJ: PSA as a marker for prostate cancer: a critical review. Ann Clin Biochem 33: 511-519, 1996.
4. Matsumoto K, Irie A, Satoh T, Kuruma H, Arakawa T and Baba S: Occupational bladder cancer: from cohort study to biologic molecular marker. Med Sci Monitor 11: RA311-RA315, 2005.
5. Sargent DJ, Conley BA, Allegro C and Collette L: Clinical trial designs for predictive marker validation in cancer treatment trials. J Clin Oncol 23: 2020-2027, 2005.
6. Sarrazin S, Adam E, Lyon M, *et al*: Endocan or endothelial cell specific molecule-1 (ESM-1): a potential novel endothelial cell marker and a new target for cancer therapy. Biochim Biophys Acta 1765: 25-37, 2006.
7. Tuxen MK: Tumor marker CA125 in ovarian cancer. J Tumor Marker Oncol 16: 49-68, 2001.
8. Zehentner BK and Carter D: Mammaglobin: a candidate diagnostic marker for breast cancer. Clin Biochem 37: 249-257, 2004.
9. Barry MJ: Prostate-specificy-antigen testing for early diagnosis of prostate cancer. N Engl J Med 344: 1373-1377, 2001.
10. Catalona WJ, Smith DS, Ratliff TL, *et al*: Measurement of prostate-specific antigen in serum as a screening test for prostate cancer. N Engl J Med 324: 1156-1161, 1991.
11. Thompson IM, Pauler DK, Goodman PJ, *et al*: Prevalence of prostate cancer among men with a prostate-specific antigen level ≤4.0 ng per milliliter. N Engl J Med 350: 2239-2246, 2004.
12. Schmid HP, McNeal JE and Stamey TA: Observations on the doubling time of prostate-cancer: the use of serial prostate-specific antigen in patients with untreated disease as a measure of increasing cancer volume. Cancer 71: 2031-2040, 1993.
13. Palade GE: Fine structure of blood capillaries. J Appl Phys 24: 1424-1424, 1953.
14. Patra SK and Bettuzzi S: Epigenetic DNA-methylation regulation of genes coding for lipid raft-associated components: A role for raft proteins in cell transformation and cancer progression (Review). Oncol Rep 17: 1279-1290, 2007.
15. Gould ML, Williams G and Nicholson HD: Changes in caveolae, caveolin, and polymerase 1 and transcript release factor (PTRF) expression in prostate cancer progression. Prostate 70: 1609-1621, 2010.
16. Couet J, Belanger MM, Roussel E and Drolet MC: Cell biology of caveolae and caveolin. Adv Drug Deliv Rev 49: 223-235, 2001.
17. Frank PG, Pavlides S and Lisanti MP: Caveolae and transcytosis in endothelial cells: role in atherosclerosis. Cell Tissue Res 335: 41-47, 2009.
18. Zheng YZ and Foster LJ: Biochemical and proteomic approaches for the study of membrane microdomains. J Proteomics 72: 12-22, 2009.
19. Volonte D, Galbiati F and Lisanti MP: Visualization of caveolin-1, a caveolar marker protein, in living cells using green fluorescent protein (GFP) chimeras. The subcellular distribution of caveolin-1 is modulated by cell-cell contact. FEBS Lett 445: 431-439, 1999.
20. UniProt knowledgebase for Q03135 (Cav1_Human). http://www.uniprot.org/uniprot/Q03135.
21. Shatz M and Liscovitch M: Caveolin-1: a tumor-promoting role in human cancer. Int J Radiat Biol 84: 177-189, 2008.
22. Burgermeister E, Liscovitch M, Rocken C, Schmid RM and Ebert MPA: Caveats of caveolin-1 in cancer progression. Cancer Lett 268: 187-201, 2008.
23. Ando T, Ishiguro H, Kimura M, *et al*: The overexpression of caveolin-1 and caveolin-2 correlates with a poor prognosis and tumor progression in esophageal squamous cell carcinoma. Oncol Rep 18: 601-609, 2007.
24. Zhang Q, Furukawa K, Chew HH, *et al*: Down-regulation of caveolin-1 in mouse Lewis lung cancer P29 is a causal factor for the malignant properties in a high-metastatic subline. Oncol Rep 16: 289-294, 2006.
25. Williams TM and Lisanti MP: Caveolin-1 in oncogenic transformation, cancer, and metastasis. Am J Physiol Cell Physiol 288: C494-C506, 2005.
26. Conde MC, Ramirez-Lorca R, Lopez-Jamar JME, *et al*: Genetic analysis of caveolin-1 and eNOS genes in colorectal cancer. Oncol Rep 16: 353-359, 2006.
27. Dasari A, Bartholomew JN, Volonte D and Galbiati F: Oxidative stress induces premature senescence by stimulating caveolin-1 gene transcription through p38 mitogen-activated protein kinase/Sp1-mediated activation of two GC-rich promoter elements. Cancer Res 66: 10805-10814, 2006.
28. Chen DB, Li SM, Qian XX, Moon CS and Zheng J: Tyrosine phosphorylation of caveolin 1 by oxidative stress is reversible and dependent on the c-src tyrosine kinase but not mitogen-activated protein kinase pathways in placental artery endothelial cells. Biol Reprod 73: 761-772, 2005.
29. Krizkova S, Adam V, Petrlova J, *et al*: A suggestion of electrochemical biosensor for study of platinum(II)-DNA interactions. Electroanalysis 19: 331-338, 2007.
30. Popiela TJ, Rudnicka-Sosin L, Dutsch-Wicherek M, *et al*: The metallothionein and RCAS1 expression analysis in breast cancer and adjacent tissue regarding the immune cells presence and their activity. Neuro Endocrinol Lett 27: 786-794, 2006.
31. Zelena J, Potesil D, Vacek J, *et al*: Metallothionein as a prognostic marker of tumor disease. Klin Onkol 17: 190-195, 2004.
32. Ebert MPA, Günther T, Hoffmann J, *et al*: Expression of metallothionein II in intestinal metaplasia, dysplasia, and gastric cancer. Cancer Res 60: 1995-2001, 2000.
33. Kasahara K, Fujiwara Y, Nishio K, *et al*: Metallothionein content correlates with the sensitivity of human small cell lung cancer lines to cisplatin. Cancer Res 51: 3237-3242, 1991.
34. Theocharis SE, Margeli AP, Klijanienko JT and Kouraklis GP: Metallothionein expression in human neoplasia. Histopathology 45: 103-118, 2004.
35. Adam V, Baloun J, Fabrik I, Trnkova L and Kizek R: An electrochemical detection of metallothioneins at the zeptomole level in nanolitre volumes. Sensors 8: 2293-2305, 2008.
36. Adam V, Blastik O, Krizkova S, *et al*: Application of the Brdicka reaction in determination of metallothionein in patients with tumours. Chem Listy 102: 51-58, 2008.
37. Fabrik I, Krizkova S, Huska D, *et al*: Employment of electrochemical techniques for metallothionein determination in tumour cell lines and patients with a tumor disease. Electroanalysis 20: 1521-1532, 2008.
38. Eckschlager T, Adam V, Hrabeta J, Figova K and Kizek R: Metallothioneins and cancer. Curr Protein Pept Sci 10: 360-375, 2009.
39. Adam V, Fabrik I, Eckschlager T, Stiborova M, Trnkova L and Kizek R: Vertebrate metallothioneins as target molecules for analytical techniques. TrAC-Trends Anal Chem 29: 409-418, 2010.
40. Adam V, Petrlova J, Wang J, Eckschlager T, Trnkova L and Kizek R: Zeptomole electrochemical detection of metallothioneins. PLoS One 5: e11441, 2010.
41. Ryvolova M, Krizkova S, Adam V, *et al*: Analytical methods for metallothionein detection. Curr Anal Chem 7: 243-261, 2011.
42. Kizek R, Trnkova L and Palecek E: Determination of metallothionein at the femtomole level by constant current stripping chronopotentiometry. Anal Chem 73: 4801-4807, 2001.

43. Cherian MG, Jayasurya A and Bay BH: Metallothioneins in human tumors and potential roles in carcinogenesis. Mutat Res 533: 201-209, 2003.
44. Jin R, Huang J, Tan PH and Bay BH: Clinicopathological significance of metallothioneins in breast cancer. Pathol Oncol Res 10: 74-79, 2004.
45. Kelly SL, Basu A, Teicher BA, Hacker MP, Hamer DH and Lazo JS: Overexpression of metallothionein confers resistance to anticancer drugs. Science 241: 1813-1815, 1988.
46. Theocharis S, Karkantaris C, Philipides T, *et al*: Expression of metallothionein in lung carcinoma: correlation with histological type and grade. Histopathology 40: 143-151, 2002.
47. Kuefer R, Varambally S, Zhou M, *et al*: α-methylacyl-CoA racemase: expression levels of this novel cancer biomarker depend on tumor differentiation. Am J Pathol 161: 841-848, 2002.
48. Luo J, Zha S, Gage WR, *et al*: α-methylacyl-CoA racemase: a new molecular marker for prostate cancer. Cancer Res 62: 2220-2226, 2002.
49. Xu J, Stolk JA, Zhang X, *et al*: Identification of differentially expressed genes in human prostate cancer using subtraction and microarray. Cancer Res 60: 1677-1682, 2000.
50. Evans AJ: α-methylacyl CoA racemase (P504S): overview and potential uses in diagnostic pathology as applied to prostate needle biopsies. J Clin Pathol 56: 892, 2003.
51. Buttke TM and Sandstrom PA: Oxidative stress as a mediator of apoptosis. Immunol Today 15: 7-10, 1994.
52. Droge W: Free radicals in the physiological control of cell function. Physiol Rev 82: 47-95, 2002.
53. Valko M, Rhodes CJ, Moncol J, Izakovic M and Mazur M: Free radicals, metals and antioxidants in oxidative stress-induced cancer. Chem Biol Interact 160: 1-40, 2006.
54. Potesil D, Petrlova J, Adam V, *et al*: Simultaneous femtomole determination of cysteine, reduced and oxidized glutathione, and phytochelatin in maize (*Zea mays L.*) kernels using high-performance liquid chromatography with electrochemical detection. J Chromatogr A 1084: 134-144, 2005.
55. Petrlova J, Mikelova R, Stejskal K, *et al*: Simultaneous determination of eight biologically active thiol compounds using gradient elution-liquid chromatography with Coul-Array detection. J Sep Sci 29: 1166-1173, 2006.
56. Sochor J, Ryvolova M, Krystofova O, *et al*: Fully automated spectrometric protocols for determination of antioxidant activity: advantages and disadvantages. Molecules 15: 8618-8640, 2010.
57. Laemmli UK: Cleavage of structural proteins during assembly of head of bacteriophage-T4. Nature 227: 680-685, 1970.
58. Merril CR, Dunau ML and Goldman D: A rapid sensitive silver stain for polypeptides in polyacrylamide gels. Anal Biochem 110: 201-207, 1981.
59. Krizkova S, Ryvolova M, Gumulec J, *et al*: Electrophoretic fingerprint metallothionein analysis as a potential prostate cancer biomarker. Electrophoresis 32: 1952-1961, 2011.
60. Volonte D, Galbiati F, Pestell RG and Lisanti MP: Cellular stress induces the tyrosine phosphorylation of caveolin-1 (Tyr(14)) via activation of p38 mitogen-activated protein kinase and c-Src kinase - Evidence for caveolae, the actin cytoskeleton, and focal adhesions as mechanical sensors of osmotic stress. J Biol Chem 276: 8094-8103, 2001.
61. Duplancic D, Kukoc-Modun L, Modun D and Radic N: Simple and rapid method for the determination of uric acid-independent antioxidant capacity. Molecules 16: 7058-7067, 2011.
62. Bartosz G: Non-enzymatic antioxidant capacity assays: limitations of use in biomedicine. Free Radic Res 44: 711-720, 2010.
63. Prior RL and Cao GH: In vivo total antioxidant capacity: comparison of different analytical methods. Free Radic Biol Med 27: 1173-1181, 1999.
64. Tahir SA, Ren CZ, Timme TL, *et al*: Development of an immunoassay for serum caveolin-1: a novel biomarker for prostate cancer. Clin Cancer Res 9: 3653-3659, 2003.
65. Nasu Y, Timme TL, Yang G, *et al*: Suppression of caveolin expression induces androgen sensitivity in metastatic androgen-insensitive mouse prostate cancer cells. Nat Med 4: 1062-1064, 1998.
66. Yang G, Truong LD, Wheeler TM and Thompson TC: Caveolin-l expression in clinically confined human prostate cancer: a novel prognostic marker. Cancer Res 59: 5719-5723, 1999.
67. Tahir SA, Frolov A, Hayes TG, *et al*: Preoperative serum caveolin-1 as a prognostic marker for recurrence in a radical prostatectomy cohort. Clin Cancer Res 12: 4872-4875, 2006.
68. Thompson TC, Tahir SA, Li L, *et al*: The role of caveolin-1 in prostate cancer: clinical implications. Prostate Cancer Prostatic Dis 13: 6-11, 2010.
69. Watanabe M, Yang G, Cao GW, *et al*: Functional analysis of secreted caveolin-1 in mouse models of prostate cancer progression. Mol Cancer Res 7: 1446-1455, 2009.
70. Tahir SA, Yang G, Ebara S, *et al*: Secreted caveolin-1 stimulates cell survival/clonal growth and contributes to metastasis in androgen-insensitive prostate cancer. Cancer Res 61: 3882-3885, 2001.
71. Yang G, Truong LD, Timme TL, *et al*: Elevated expression of caveolin is associated with prostate and breast cancer. Clin Cancer Res 4: 1873-1880, 1998.
72. Thompson TC, Timme TL, Li L and Goltsov A: Caveolin-1, a metastasis-related gene that promotes cell survival in prostate cancer. Apoptosis 4: 233-237, 1999.
73. Li LK, Yang G, Ebara S, *et al*: Caveolin-1 mediates testosterone-stimulated survival/clonal growth and promotes metastatic activities in prostate cancer cells. Cancer Res 61: 4386-4392, 2001.
74. Mouraviev V, Li LK, Tahir SA, *et al*: The role of caveolin-1 in androgen insensitive prostate cancer. J Urol 168: 1589-1596, 2002.
75. Karam JA, Lotan Y, Roehrborn CG, Ashfaq R, Karakiewicz PI and Shariat SF: Caveolin-1 overexpression is associated with aggressive prostate cancer recurrence. Prostate 67: 614-622, 2007.

Neoplasma 59, 2, 2012 191

doi:10.4149/neo_2012_025

Evaluation of alpha-methylacyl-CoA racemase, metallothionein and prostate specific antigen as prostate cancer prognostic markers

J. GUMULEC[1,2,3], M. MASARIK[1,2,3], S. KRIZKOVA[2,3], M. HLAVNA[1], P. BABULA[2,3], R. HRABEC[4], A. ROVNY[4], M. MASARIKOVA[2,3], J. SOCHOR[2,3], V. ADAM[2,3], T. ECKSCHLAGER[5], R. KIZEK[2,3,*]

[1]Department of Pathological Physiology, Faculty of Medicine, Masaryk University,Kamenice 5, CZ-625 00 Brno, Czech Republic; [2]Department of Chemistry and Biochemistry, Mendel University in Brno,Zemedelska 1, CZ-613 00 Brno, Czech Republic; [3]Central European Institute of Technology, Brno University of Technology, Technicka 3058/10, CZ-616 00 Brno, Czech Republic; [4]Department of Urology, St. Anne's University Hospital Brno,Pekarska 53/55, CZ-656 91 Brno, Czech Republic; [5]Department of Paediatric Haematology and Oncology, 2nd Faculty of Medicine Charles University, and University Hospital Motol, V Uvalu 84, CZ-150 06 Praha 5, Czech Republic

Correspondence: kizek@sci.muni.cz

Received September 20, 2011 / Accepted October 17, 2011

Current diagnostic techniques are inefficient in distinguishing latent and low-risk forms of prostate cancer from high-risk forms. The present study is focused on determination of putative tumor markers of aggressive high-grade forms of prostate cancer. Potential markers were determined in blood sera of 133 patients (82 cases and 51 controls) and in cell lines (Gleason score 9-derived 22Rv1 and normal tissue derived PNT1A) on mRNA and protein levels. Alpha-methylacyl-CoA racemase (AMACR), metallothionein classes 1A and 2A (MT1A and MT2A) were determined and compared to prostate specific antigen (PSA) levels. On mRNA level, significantly increased expression of MT2A (2.4-fold), PSA (2.6-fold) and AMACR (8.4-fold) and insignificantly (1.9-fold) elevated MT1A in 22Rv1 compared to non-tumor PNT1A were determined. On protein level, significant enhancement of free PSA and total PSA in tumor cell line was evident. AMACR protein was 1.5-fold elevated in tumor line (below the level of significance). Contrary to mRNA, significantly ($p = 0.01$) reduced level of MT protein in tumor lines was determined. In the case of serum level, significantly enhanced MT level (4.5-fold) in patients' sera was found. No significant changes were observed in the case of AMACR. These findings indicate possible alternative role of MT to PSA prostate cancer marker. In addition, level of AMACR is distinctly higher in the Gleason score 9 in serum of patients and MT shows a descending trend in relation to Gleason score.

Keywords: cancer, tumor marker, immunodetection, electrochemistry, polymerase chain reaction, mRNA

Prostate carcinoma is one of the most studied oncological diseases due to its high incidence in male population. It represents one of the most frequent cancers in developed countries and common cause of cancer-related death[1,2]. Recently significantly increased number of newly diagnosed patients suffering from this malignant disease is directly related to introduction of prostatic specific antigen (PSA) evaluation to the clinical practice [3-7]. This marker enabled detection of early stages of disease, undetectable when commonly used rectal investigation is employed. PSA screening contributed towards 20% reduction of mortality. It is well evident from the study focused on the European medical institutes published in the prestigious New England Journal of Medicine [8]. Ascertained reduction of mortality is caused by the fact that PSA screening is able to detect early stages T1 and T2 of prostate carcinoma, otherwise non-detectable by the conventional methods, such as digital rectal investigation. Tumors of stage T3 and T4, which are usually associated with tissue invasion or metastasizing, are often incurable and the therapeutic approach is based on a palliative treatment only. Despite the evident benefit of PSA evaluation, digital rectal investigation has its importance in the diagnostics and it should not be neglected by a general practitioner [9,10]. Besides PSA, there have been identified and tested other markers [11-16], including those detected in urine [17].

On the other hand, it is necessary to accentuate that a large amount of tumors is asymptomatic (up to 80 %).They are usually evidenced only at dissection of departed in connection with other cause of disease or at surgery [17]. Based of above mentioned facts, it is proper to sub-classify prostate tumors into two groups: 1. significant tumor swith direct risk

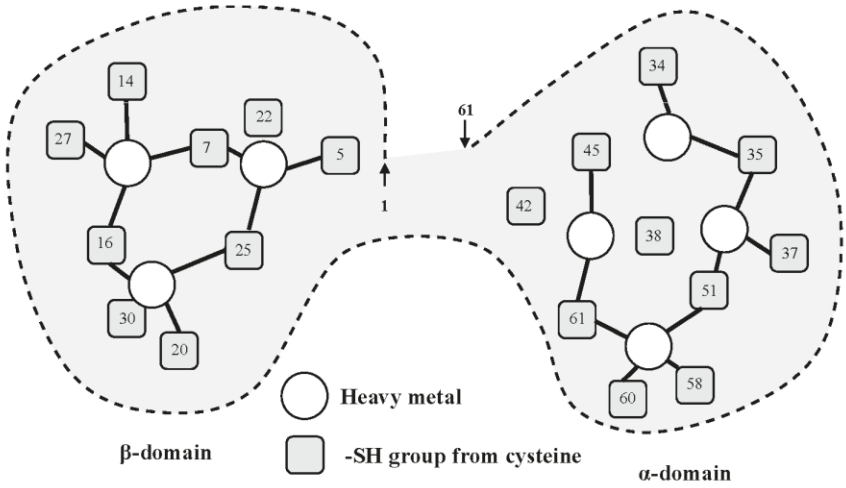

Figure 1. Structure of human metallothionein containing seven divalent ions.

to a life; 2. non-significant tumors, where risk to a life is highly improbable. Currently used diagnostic methods including PSA determination, digital rectal examination, transrectal ultrasonography or biopsy, are not able to differentiate between aggressive and latent forms of tumor. All bioptically (histologically) verified prostate carcinomas are treated as significant, dangerous tumors with direct risk. This therapeutic approach leads to the significant reduction of quality of life because of important side effects of the treatment. Erectile dysfunction is detected in more than 70% and urinary incontinence in approximately 10 % of patients after radical prostatectomy. However, there is significant rate of patients who are treated in vain[18]. Due to these facts, it is quite necessary to find such prostate carcinoma markers that are useful for distinction of aggressive and latent tumor forms already at early stages of the disease[19-30]. Metallothionein (MT) and alpha-methyl CoA-racemase (AMACR) belong to the possible markers of prostate carcinoma at early stages, but their clinical potential must be still investigated.

Metallothioneins (MT) represent proteins of low molecular weight (6–10 kDa) with high rate of cysteine (Fig. 1). Presence of –SH group-containing amino acids is directly connected with the ability of these proteins to bind various metal ions [31-33]. Therefore, metallothioneins play a crucial role in transport of metal ions, their detoxification and protection of cells against oxidative stress connected with effects of the metal ions [34]. These proteins are involved also in regulation of apoptosis; their increased levels have antiapoptotic effect. In addition, metallothioneins regulate level, activity and cellular localisation of transcriptional factor NF-κB, which activates antiapoptotic genes Bcl-2, c-myc and TRAF-1 that belong to the group of prooncogenes. This antiapoptotic cascade can be efficient as the protective mechanism of prostate carcinoma cells against apoptotic signals at their proliferation [35,36].

Alpha-methyl CoA-racemase (AMACR) is peroxisomal and mitochondrial enzyme involved in beta oxidation of branched fatty acids, catabolism of bile acids metabolites and ibuprofen metabolism [37]. Ibuprofen belongs to a class of drugs called non-steroidal anti-inflammatory drugs, such as aspirin. They are used for the management of mild to moderate pain, fever, and inflammation. Increased levels of AMACR have been described in adenocarcinomas and high grade prostatic intraepithelial neoplasia [38]. On the other hand, low levels of this marker have been described in benign hyperplasia and in atypical adenomatous hyperplasia [39-41]. Thus, AMACR is well established tissue prostate cancer biomarker [41]. Moreover, it has been demonstrated that high level of AMACR affects progression of prostate cancer due to 1. more energy-efficient utilization of fatty acids [39], 2. AMACR-substrate-mediated oxidative stress, and 3. affection of nuclear hormone receptors.

Cellular processes in prostate carcinoma cells were investigated especially using cell lines LNCaP (androgen-sensitive), PC-3 (androgen-resistant), and DU 145 (androgen-resistant). These lines don't represent ideal model because they differ from in vivo state and they are derived not from primary tumor but from metastatic dissemination in bones (PC-3), brain (DU 145), and lymphatic nodes (LNCaP). Cell line 22Rv1 represents poorly differentiated primary prostate adenocarcinoma of Gleason grading score 9. Cell line expresses androgen receptor (AR) and synthesizes high amounts of PSA [42]. Cell line 22Rv1 is more suitable model of prostate adenocarcinoma because of reduced genetic variability and lower rate of aneuploidy – karyotype 50 XY (trisomy of 7, 8, 12), DNA index 1.30 (PC-3: 1.84 and LNCaP: 2.09) in comparison with other cell lines [42].

Aim of the present study was to compare the level of putative prostate cancer markers in sera of patients with prostate cancer and healthy volunteers and to compare the expression

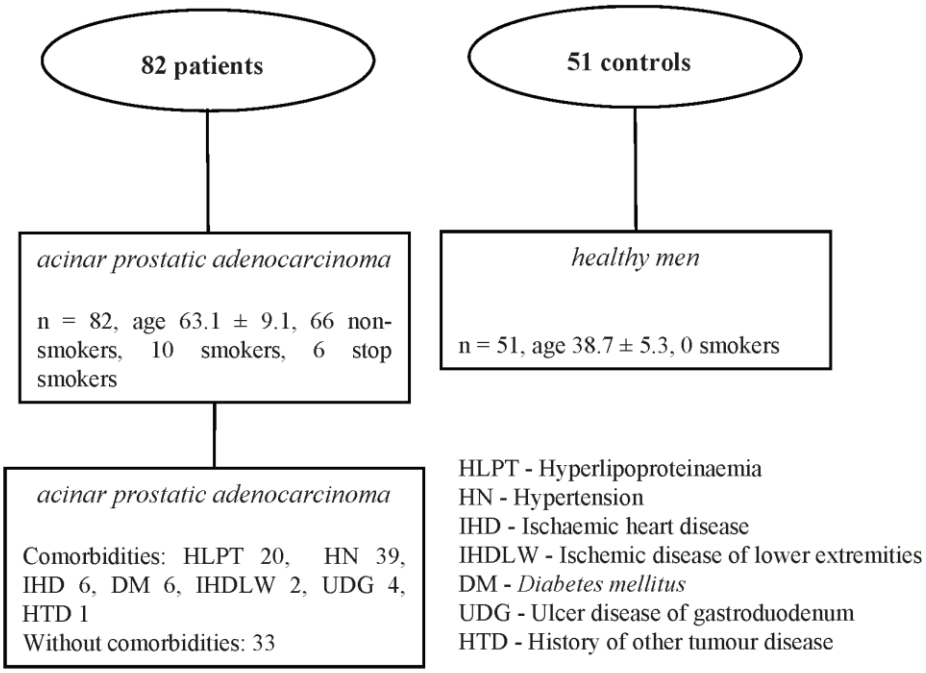

Figure 2. Characteristics of patients and healthy men included in the study.

of these markers and other proteins connected with tumor behaviour (apoptosis regulation, invasivity and zinc metabolism) on mRNA and protein level in 22Rv1 prostate cancer cell line and control prostate cell line.

Material and Methods

Cell lines, blood sera. Control cell line derived by immortalisation of normal prostatic epithelial cells of 35-year old man obtained post mortem (PNT1A) and 22Rvl cell line derived from xenograft passaged on castrated mice were used in this study. These cell lines were purchased from the HPA Culture Collections (Salisbury, UK). 22Rv1 and PNT1A cells were cultured in RPMI-1640 medium with 10% FBS. Medium was supplemented with penicillin and streptomycin (1U/mL), and the cells were maintained at 37 °C in a humidified incubator with 5% CO_2. Sub-cultivations of the cells were carried out after 21 days. Once the cells grew up to ~ 75% confluence of the culture, the cultivation medium was replaced by fresh medium for 24 h to synchronize cell growth. Proteins from these cell lines and from tested blood sera of patients were isolated by the use of RIPA buffer by the mechanical homogenisation or heat denaturation (99 °C) of obtained material. Heat lysates were subsequently subjected to electrochemical determination of MT, PSA and AMACR was determined in RIPA lysates.

Patients with diagnosed prostate carcinoma. Blood sera of patients with histologically verified prostate adenocarcinoma (82 samples) were compared to 51 controls (Fig. 2). Average age of patients was 63 years (40–78). Tumors were classified from high to low differentiated tumors with Gleason score, describing rate of tumor differentiation, in the range between 5 and 10. Pathological staging of samples varied from 1c to 4, all patients were without dissemination into adjacent lymphatic nodes or organs. There were 80 % of non-smokers, 12 % of smokers and 8 % of stop-smokers in the set. Forty percent of patients were without co-morbidities, 37 % of patients suffered from one co-morbidity, 7 % of patients had 2 and the rest of patients had 3 and more co-morbidities. Hyperlipoproteinaemia was diagnosed in 24 % of patients, hypertension in 47 %, ischemic heart disease in 7 %, *diabetes mellitus* of the second type in 7 %, ischemic disease of lower extremities in 2 %, ulcer disease of gastroduodenum in 5%, and history of other tumor disease in 1 % of patients. In the control group, there were 51 tested probands. Age of control group varied from 18 to 55 (38 at average). Tested blood sera were obtained from Urology clinic, St. Anne´s University Hospital in Brno, Czech Republic. Enlistment of patients into realised clinical study was approved by the Ethic commission of the Faculty of medicine, Masaryk University, Brno, Czech Republic.

Polymerase chain reaction. High pure total mRNA isolation kit (Roche, Switzerland) was used for mRNA isolation from cell lines. Isolated mRNA was transcribed into cDNA by the use of Transcriptor first strand cDNA synthesis kit (Roche, Switzerland) in accordance with manufacturer's propositions.

Real-time PCR was carried out by the system TaqMan using apparatus 7500 real-time PCR system (Applied Biosystems, USA). Results were evaluated in triplicates by the comparative Ct method ($2^{-\Delta\Delta Ct}$) and standardized against β-actin. The primer and probe sets for β-actin (Assay ID: Hs00185826_m1), MT1A (Assay ID: Hs00185826_m1), MT2A (Hs00794796_m1), AMACR (Hs01091294_m1), and PSA (Hs02576345_m1) were selected from TaqMan gene expression assay. Real-time PCR was performed under the following amplification conditions: total volume of 20 μL, initial denaturation 95 °C/10 min, than 45 cycles 95 °C/15 sec, 60 °C/1 min. Samples were examined in quadruplicates.

Electrochemical detection of metallothionein. Electrochemical detection was used for quantification of metallothionein[43]. Detection was carried out using AUTOLAB Analyser (EcoChemie, Netherlands) with classical three-electrode arrangement using of differential pulse voltammetry Brdicka reaction. Analysed sample was accumulated on the surface of a working electrode which is represented by hanging mercury drop electrode. After accumulation, detection proceeded in a supporting electrolyte containing cobaltic (cobalt(III)) salt in ammonia buffer of pH = 9.6 [33,44].

Gel electrophoresis, western blotting. Samples were separated on 10 % SDS-PAGE gels (BioRad, USA) and stained by silver nitrate (kit BioRad, USA, under manufacturer´s propositions) and simultaneously blotted on a nitrocellulose membrane and immunodetected by specific antibodies. Dot-blots were used for rapid orientation. Serum samples were 8-fold diluted. Membranes were incubated for 1 h in 5% milk and for 12 h in primary antibody (1:500), washed and incubated in secondary antibody (1:2000). Polyclonal rabbit antibody (Santa Cruz Biotechnology, USA) was used against metallothionein, isoforms 1 and 2, polyclonal rabbit antibody (Clonestar, CZ) was used against AMACR. Monoclonal mouse antibody (Santa Cruz Biotechnology, USA) was used for detection of PSA.

Descriptive statistics. Obtained results were evaluated using software Statistica 9 (StatSoft, USA). For better comparison of data sets, measured protein data were normalized to the range 0–1. To disprove null hypothesis that cell line mRNA, protein and serum levels of specified genes are equal, t-tests were used. Correlation matrices were used for finding of correlations between tested compounds. Cluster analysis (K-means) was employed for orientation in the set of patients. Significance level $p = 0.05$ was established for determination of significantly different value.

Results

Molecular-biological analysis of cell lines. Model of tumor tissue is represented by the cell line 22Rv1. The potential markers on the mRNA and protein levels were determined. mRNA level is expressed as a relative fold change of expression in comparison with non-malignantcell line PNT1A. Elevated expression of all studied markers in tumor cell line was observed. Statistically significant enhancement was detected in case of metallothionein – class 2A (MT2A, 2.4-fold expression in 22Rv1 compared to PNT1A, $p = 0.006$, Fig. 3A), AMACR (8.4-fold, $p = 0.0004$, Fig. 3B) and PSA (2.6-fold, $p = 0.008$, Fig. 3C) in the cancer line. Metallothionein class 1A expression level was only 1.9-fold higher in the tumor cell line (insignificant, $p = 0.29$). In addition to mRNA level, the protein level of all three observed markers was also determined (Fig. 3D-F). Enhancement of free PSA and total PSA in tumor cell line was well evident at the protein level. AMACR was insignificantly elevated in the tumor line (1.5-fold, $p = 0.132$). Interestingly, significantly ($p = 0.01$) reduced level of metallothionein protein in tumor cells was observed (Fig. 3D).

Clinical study in patients suffering from malignant disease. Metallothionein, AMACR, free PSA and total PSA levels were detected in the blood serum of prostate cancer patients and volunteers to assess their applicability as markers of prostate cancer. Our group has previously shown that serum MT levels are elevated with high level of specificity and sensitivity in prostate cancer patients with possible application as an additional tool for prostate cancer diagnosis [23]. Compared to previous study, in this paper the group of tested samples has been enlarged. The levels of potential tumor markers were compared between each other to reveal potential relationship, which has never been done before for this combination of genes.

PSA was determined as a widely used marker to compare potential markers to it. Significantly higher PSA level ($p = 0.001$) and significantly ($p < 0.001$) lower free/total PSA ratio in patients were observed. In addition, higher metallothionein content with high level of significance ($p < 0.0001$, Fig. 4A) was well evident. This fact also supports the hypothesis that metallothionein is increasingly transported from prostate cancer cells to the extracellular space. Interestingly, metallothionein levels varied distinctly less than PSA levels in control group (displayed as a variation coefficient 14.1 % and 75 % for MT and PSA, respectively, Fig. 4B).This finding suggests that MT level is faintly affected by the tumor stage, grade, or clinical data. In terms of serum AMACR levels, no significant changes between patients and controls were detected in blood serum (Fig. 4C). No significant correlations between AMACR, MT and PSA were observed. Hierarchical tree clustering analysis of genes did not reveal any specific groups of patients (not shown).

In addition, correlations and t-tests were carried out with data obtained from clinical records. Subsequently, patients were divided into groups by presence of various common diseases, smoking habit, tumor size and its differentiation. No statistically significant differences between localised tumors (T1, 2) and tumors that extend through the prostate capsule (T3, 4), and monitored markers have been detected (data are not shown). As the tumor differentiation (good vs. medium vs. poorly differentiated) is concerned, significantly higher (1.8-fold, $p = 0.005$) total PSA was determined in poorly differentiated tumors as compared to the others (data not shown). However, no similar correlation

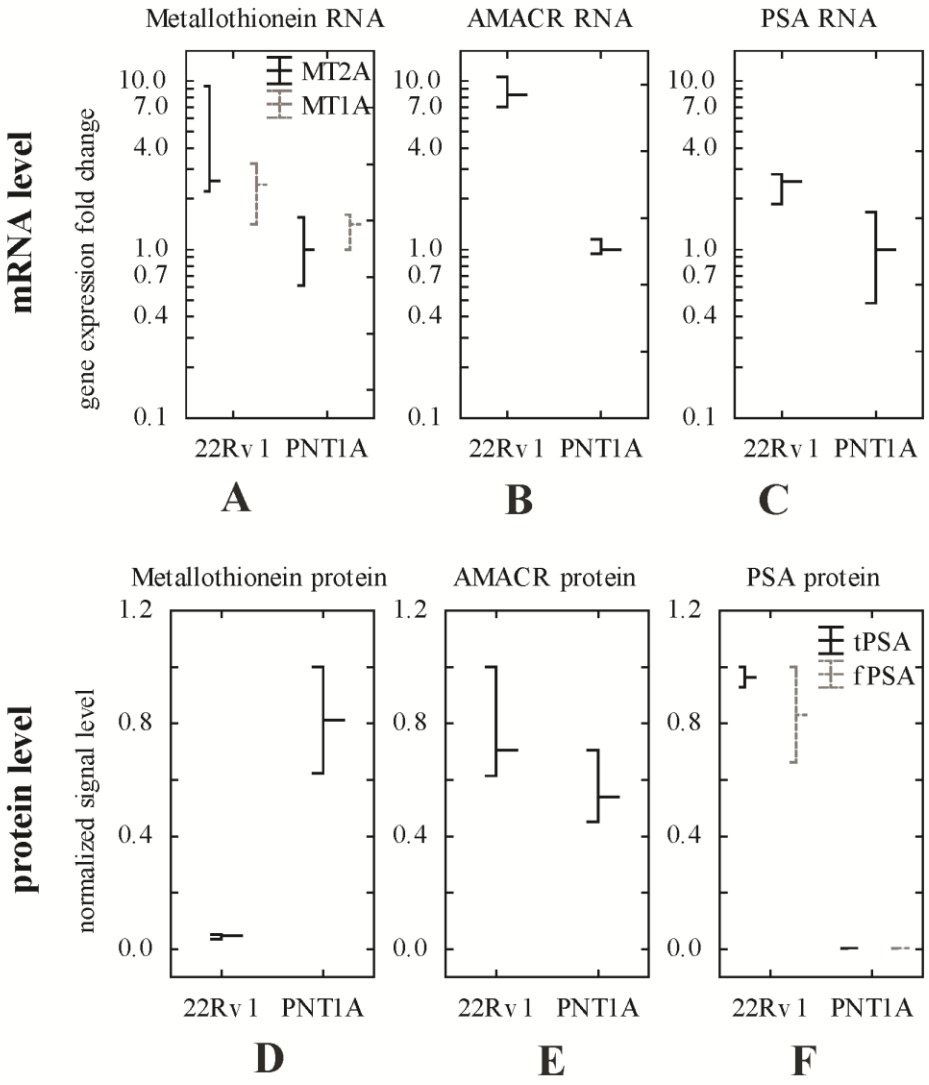

Figure 3. Levels of gene expression in cell lines. Level of mRNA genes expressed as relative fold change of expression ($2^{-\Delta\Delta Ct}$ method) of tumor cell line (22Rv1) in comparison with non-tumor cell line PNT1A. (a) mRNA level of metallothionein classes 1A and 2A (MT1A, MT2A) in cell lines 22Rv1 (tumor) and PNT1A (non-tumor), (b) mRNA level of AMACR in cell lines, (c) mRNA level of PSA in cell lines, (d) metallothionein (protein content) in cell lines, (e) level of AMACR (protein content) in cell lines, (f) level of total (tPSA) and free PSA (fPSA) protein in cell lines.

was observed in AMACR and MT. Levels of monitored markers were not changed in connection with associated disease – hypertension, ischemic heart disease and hyperlipemia and duodenal ulcer. Significantly higher (2-fold) AMACR level in group of patients with ischemic disease of lower extremities was observed. However, due to the limited number of participants with this disease in this study (N = 3) the robustness of this finding is limited and needs to be verified on larger file. No differences in monitored markers between smokers and non-smokers have been evident in all studied genes (data not shown).

Metallothionein showed an inverse, decreasing trend depending on Gleason grading (Fig. 4D). Increased level of metallothionein makes this protein possible candidate of tumor marker of prostate adenocarcinoma that is minimally influenced by the clinical status of the patient. Its level is not affected by smoking, age, and co-morbidities. Observed descending trend of serum MT in relation to Gleason grading score is interestingly an inverse one as compared to similar trend in PSA, and needs to be elucidated in further studies. No statistically important correlations between the age of

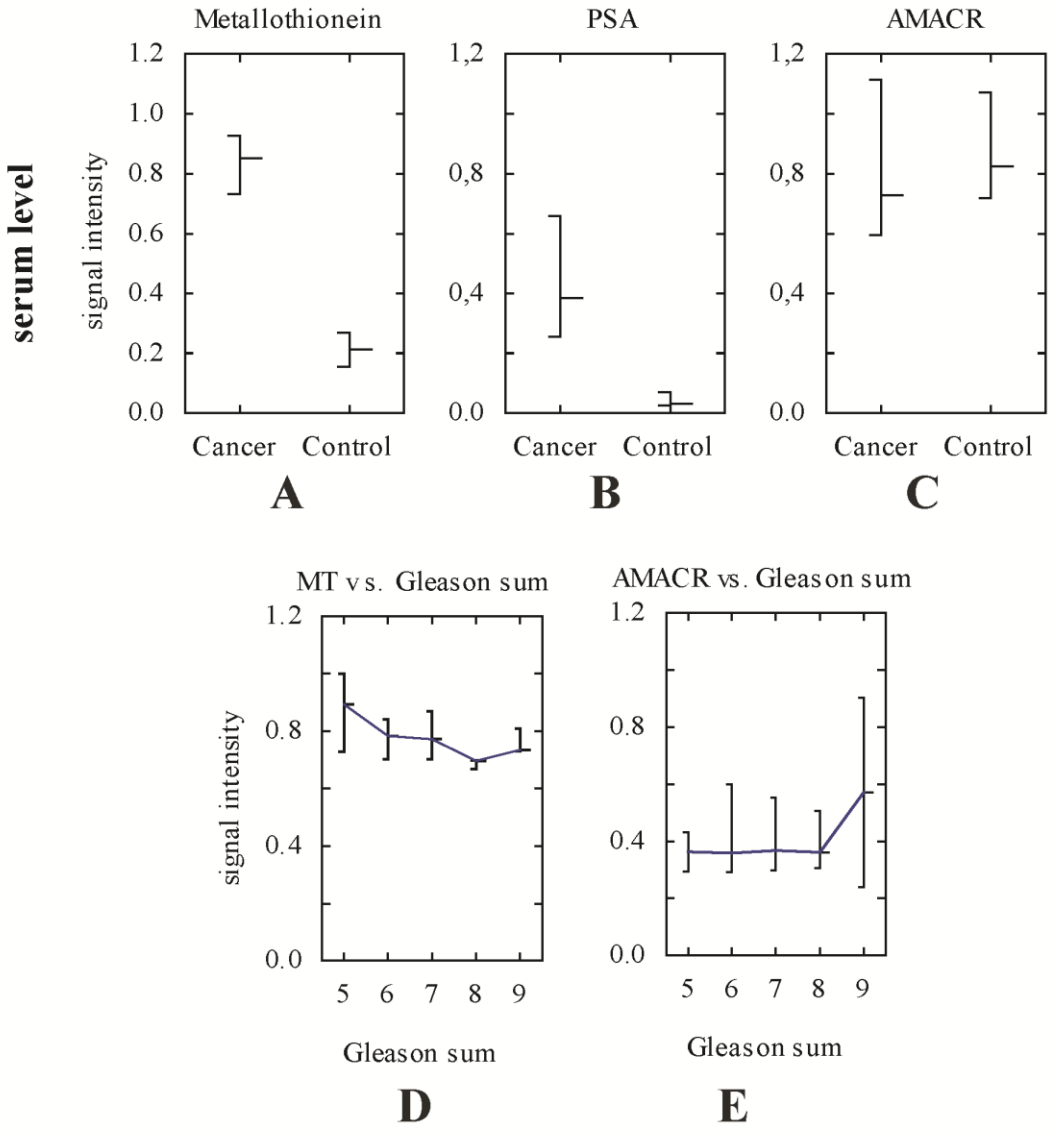

Figure 4. Level of tumor markers in blood serum of patients. (a) metallothionein, (b) PSA, (c) Alpha-methylacyl-CoA racemase (AMACR), (d) dependence of metallothionein level on the Gleason score, (e) dependence of AMACR on the Gleason score.

patients and all monitored proteins in serum were proved. In the dependence on Gleason grading score of malignant disease, AMACR did not show significant trend, however, was distinctly higher at T4 stage of TNM classification (Fig. 4E).

Discussion

The finding shown in Fig. 3 is in the contradiction with MT mRNA level. This fact suggests a conclusion that metallothionein is transported to the extracellular space by still unknown mechanisms (increased MT on mRNA and reduced MT on the protein level). Due to the transport of MT out of the cells, its level is significantly reduced in intracellular space. With respect to the MT relation to zinc ions, whose metabolism is abnormal in the prostate tumor tissue, MT participation on pathogenesis of malignant disorder can be expected [45-53]. To date, there is no evidence in the literature determining metallothionein level in 22Rv1 and PNT1A cell lines, however, there were done some experiments describing behaviour of RWPE-1 cell line, which revealed similarities of

behaviour of this cell line with prostate tissue [54] as well as in the case of PC-3 cell line [55]. Moreover, it was found that MT was up-regulated under hypoxia in prostate cancer cells (LNCaP and PC-3) and overexpressed in prostate cancer tissue and residual cancer cells after androgen ablation therapy [56]. Besides other published studies, our finding is in agreement with results determining MT content in tissue samples. MT reduction in tumor tissue was reported by Suzuki et al. [57]. Similarly, Wong et al. presented lower MT content in the tumor tissue compared to benign prostatic hyperplasia [58,59]. The association between cadmium coming from smoking and MT on protein level and prostate carcinoma risk was also found [60], but the mRNA level of MT could be decreased in prostate carcinoma patients compared to benign hyperplasia ones both associated with smoking [59].The clinical importance of MT on protein level was also shown by Athanassiadou et al. [61]. It has been shown that MT1 and MT2 tissue levels vary in individual prostate cancers to that found in the normal prostate gland, while higher MT content correlates with tumor grade. As mentioned previously, AMACR may be utilized immunohistochemically as a prostate cancer tissue biomarker [41]. In this study, we demonstrated similar results on mRNA and protein as previously shown in biopsies [62].

None of the studied markers meets requirements of marker of aggressive form of malignant disease. This predication is based on the presumption that a majority of prostate tumors is latent and slowly-growing (stages T1 and 2) and only a minority of them demonstrates aggressive growth (stages T3 and 4). No significant differences in monitored proteins have been determined between these two groups. However, level of patients´ blood serum AMACR is of in the Gleason score 9 distinctly higher and level of MT shows a descending trend in relation to Gleason score. Although AMACR does not differ between patients and controls, this preliminary data suggest that these markers are somehow related to tumor grade. It was previously shown that AMACR, as a tissue marker for prostate cancer [41,63], is higher in high-risk forms of cancer such as untreated metastases or hormone refractory cancer [38]. Wright et al. explored the potential relationship between AMACR polymorphisms, red meat/dairy intake, and prostate cancer risk. They found that no effect modification of AMACR polymorphisms by either dietary red meat or dairy intake on PCa risk was observed [64]. Besides AMACR itself, there were identified other promising markers correlated with the presence of a tumor[65]. One may speculate that similar trend could be reflected in the serum level of AMACR as well. In conclusion, it is necessary to verify these facts in the extensive group of patients including those with disseminated (metastasizing) disease in a follow-up study. Although metallothionein does not fulfil the conditions for marker of aggressive form of disease, it is the only compound distinctively enhanced in the blood serum of patients suffering from prostate tumors in this study. It can be concluded that MT may be as the only from monitored markers used as a supplement or addition to PSA screening. However, its application must be further verified on more extensive group of patients.

Conclusions. Metallothionein has been previously demonstrated by our group as a prostate cancer tumor marker with high sensitivity and specificity [23]. In this study, we demonstrate that alpha-methylacyl-CoA racemase does not differ in serum of prostate cancer patients and controls, however, AMACR is distinctly higher in high-grade (Gleason score 9) tumors and level of MT shows a descending trend in relation to Gleason score. These preliminary data suggest that these markers are somehow related to tumor grade. At the level of tumor tissue (represented by cell line model in this study), it was demonstrated that although AMACR protein level does not differ significantly, tissue mRNA differ distinctly presented by higher levels of AMACR. In the case of metallothionein, contradictory findings on mRNA and protein level were observed. At the mRNA level, MT is higher in tumor cell line; however, MT is higher in non-tumor cell line at the protein level. Probable explanation of this assumed discrepancy is excretion of metallothionein from prostate cancer cells. These data suggest that MT and AMACR are in some way involved in disease pathogenesis or progression. Clarification of this way might contribute to understanding of this prostate cancer with potential novel targeted therapeutic approaches.

From the point of view of clinical significance of our results it can be concluded that metallothionein can be considered as a promising marker of prostate cancer. Moreover, this marker has been found elevated even in other types of cancers such as breast carcinoma [66], head and neck cancer [67], medulloblastoma[35], melanoma [68,69] and other [70-74]. Nevertheless, combination of MT and PSA levels could be of prognostic significance due to possible revealing of false positive results, but this assumption needs to be investigated in greater details. We can also suggest using AMACR, which could be used in diagnostics for some relations to Gleason score.

Acknowledgements: Financial support from IGA MZ NS10200-3 is greatly acknowledged.

References

[1] FH SCHRODER, I VAN DER CRUIJSEN-KOETER, HJ DE KONING, AN VIS, RF HOEDEMAEKER et al. Prostate cancer detection at low prostate specific antigen. J Urol 2000; 163: 806-811. http://dx.doi.org/10.1016/S0022-5347(05)67809-3

[2] P JANTSCHEFF, N ESSER, A GEIPEL, P WOIAS, V ZIROLI et al. Metastasizing, Luciferase Transduced MAT-Lu Rat Prostate Cancer Models: Follow up of Bolus and Metronomic Therapy with Doxorubicin as Model Drug. Cancers 2011; 3: 2679-2695. http://dx.doi.org/10.3390/cancers3022679

[3] G SARDANA, B DOWELL, EP DIAMANDIS. Emerging Biomarkers for the Diagnosis and Prognosis of Prostate Cancer. Clin Chem 2008; 54: 1951-1960. http://dx.doi.org/10.1373/clinchem.2008.110668

[4] L COLLETTE, T BURZYKOWSKI, FH SCHRODER. Prostate-specific antigen (PSA) alone is not an appropriate surrogate marker of long-term therapeutic benefit in prostate cancer trials. Eur J Cancer 2006; 42: 1344-1350. http://dx.doi.org/10.1016/j.ejca.2006.02.011

[5] IP GARRAWAY, WY SUN, CP TRAN, S PERNER, B ZHANG et al. Human Prostate Sphere-Forming Cells Represent a Subset of Basal Epithelial Cells Capable of Glandular Regeneration In Vivo. Prostate 2010; 70: 491-501.

[6] KL PENNEY, JA SINNOTT, K FALL, Y PAWITAN, Y HOSHIDA et al. mRNA Expression Signature of Gleason Grade Predicts Lethal Prostate Cancer. J Clin Oncol 2011; 29: 2391-2396. http://dx.doi.org/10.1200/JCO.2010.32.6421

[7] A SBONER, F DEMICHELIS, S CALZA, Y PAWITAN, SR SETLUR et al. Molecular sampling of prostate cancer: a dilemma for predicting disease progression. BMC Med Genomics 2010; 3: 8. http://dx.doi.org/10.1186/1755-8794-3-8

[8] FH SCHROEDER, J HUGOSSON, MJ ROOBOL, TLJ TAMMELA, S CIATTO et al. Screening and Prostate-Cancer Mortality in a Randomized European Study. N Engl J Med 2009; 360: 1320-1328. http://dx.doi.org/10.1056/NEJMoa0810084

[9] DV MAKAROV, S LOEB, RH GETZENBERG, AW PARTIN. Biomarkers for Prostate Cancer. Annu Rev Med 2009; 60: 139-151.

[10] J TOSOIAN, S LOEB. PSA and Beyond: The Past, Present, and Future of Investigative Biomarkers for Prostate Cancer. TheScientificWorldJOURNAL 2010; 10: 1919-1931. http://dx.doi.org/10.1100/tsw.2010.182

[11] R RAAIJMAKERS, SH DE VRIES, BG BLIJENBERG, MF WILDHAGEN, R POSTMA et al. hK2 and free PSA, a prognostic combination in predicting minimal prostate cancer in screen-detected men within the PSA range 4-10 ng/ml. Eur Urol 2007; 52: 1358-1364. http://dx.doi.org/10.1016/j.eururo.2007.04.037

[12] LG ZHANG, CY WANG, R YANG, JD SHI, R FU et al. Real-time quantitative RT-PCR assay of prostate-specific antigen and prostate-specific membrane antigen in peripheral blood for detection of prostate cancer micrometastasis. Urol Oncol-Semin Orig Investig 2008; 26: 634-640. http://dx.doi.org/10.1016/j.urolonc.2007.07.016

[13] MA ROWLANDS, D GUNNELL, R HARRIS, LJ VATTEN, JMP HOLLY et al. Circulating insulin-like growth factor peptides and prostate cancer risk: A systematic review and meta-analysis. Int J Cancer 2009; 124: 2416-2429. http://dx.doi.org/10.1002/ijc.24202

[14] SK BATABYAL, R MAJHI, RS BASU. Clinical utility of the interaction between lectin and serum prostate specific antigen in prostate cancer. Neoplasma 2009; 56: 68-71. http://dx.doi.org/10.4149/neo_2009_01_68

[15] T JAMASPISHVILI, A SCORILAS, M KRAL, I KHOMERIKI, D KURFURSTOVA et al. Immunohistochemical localization and analysis of kallikrein-related peptidase 7 and 11 expression in paired cancer and benign foci in prostate cancer patients. Neoplasma 2011; 58: 298-303.

[16] B DJAVAN, A KAZZAZI, L DULABON, M MARGREITER, A FARR et al. Diagnostic Strategies for Prostate Cancer. Eur Urol Suppl 2011; 10: E26-E37. http://dx.doi.org/10.1016/j.eursup.2011.03.010

[17] T JAMASPISHVILI, M KRAL, I KHOMERIKI, V STUDENT, Z KOLAR et al. Urine markers in monitoring for prostate cancer. Prostate Cancer Prostatic Dis 2010; 13: 12-19. http://dx.doi.org/10.1038/pcan.2009.31

[18] L HUMBERT, M CHEVRETTE Somatic Molecular Genetics of Prostate Cancer, in: W.D. Foulkes and K.A. Cooney (Eds.), Male Reproductive Cancers Epidemiology, Pathology and Genetics, Springer Verlag, New York, Dordrecht, Heidelberg, London, 2009.

[19] S PUNNEN, RK NAM. Indications and timing for prostate biopsy, diagnosis of early stage prostate cancer and its definitive treatment: A clinical conundrum in the PSA era. Surg Oncol-Oxf 2009; 18: 192-199. http://dx.doi.org/10.1016/j.suronc.2009.02.006

[20] EI CANTO, KM SLAWIN. Early management of prostate cancer: How to respond to an elevated PSA? Annu Rev Med 2002; 53: 355-368.

[21] S KRIZKOVA, M MASARIK, J KUKACKA, R PRUSA, T Eckschlager et al. Study of zinc-dependent aggregation of metallothionein from human prostatic cancer cell lines. EJC Suppl 2010; 8: 49-49. http://dx.doi.org/10.1016/S1359-6349(10)70993-9

[22] S KRIZKOVA, M MASARIK, P MAJZLIK, J KUKACKA, J KRUSEOVA et al. Serum metallothionein in newly diagnosed patients with childhood solid tumors. Acta Biochim Pol 2010; 57: 561-566.

[23] S KRIZKOVA, M RYVOLOVA, J GUMULEC, M MASARIK, V ADAM et al. Electrophoretic fingerprint metallothionein analysis as a potential prostate cancer biomarker. Electrophoresis 2011; 32: 1952-1961. http://dx.doi.org/10.1002/elps.201000519

[24] M MASARIK, N CERNEI, J GUMULEC, O ZITKA, P BABULA et al. Immunological determination of serum prostate specific antigen in cancer patients and tumor cell lines – New perspective. Int J Mol Med 2010; 26: S47-S47.

[25] M MASARIK, N CERNEI, P MAJZLIK, D HUSKA, H BINKOVA et al. Level of metallothionein, glutathione and heat-stable proteins in tumors from patients with head and neck cancer. Int J Mol Med 2010; 26: S46-S46.

[26] M MASARIK, J GUMULEC, S KUCHTICKOVA, V ADAM, S KRIZKOVA et al. Detection of metallothionein and alpha-methylacyl CoA racemase as potential new markers for prostate carcinoma. Int J Mol Med 2009; 24: S48-S48.

[27] M MASARIK, J GUMULEC, S KUCHTICKOVA, V KUDLACKOVA, N CERNEI et al. Determination of metallothioneins and alpha-methylacyl-CoA racemase in patients with prostate carcinoma. Int J Mol Med 2010; 26: S47-S47.

[28] M MASARIK, J GUMULEC, S KUCHTICKOVA, V KUDLACKOVA, M JURAJDA et al. Determination of novel tumor markers in prostate carcinoma. FEBS J 2010; 277: 188-188.

[29] M MASARIK, J GUMULEE, N CERNEI, O ZITKA, P BABULA et al. Sarcosine as a new marker for prostate tumors. Int J Mol Med 2010; 26: S47-S47.

[30] ME MCDOWELL, S OCCHIPINTI, RA GARDINER, PD BAADE, SK STEGINGA. A review of prostate-specific

antigen screening prevalence and risk perceptions for first-degree relatives of men with prostate cancer. Eur J Cancer Care 2009; 18: 545-555. http://dx.doi.org/10.1111/j.1365-2354.2008.01046.x

[31] J PETRLOVA, D POTESIL, R MIKELOVA, O BLASTIK, V ADAM et al. Attomole voltammetric determination of metallothionein. Electrochim Acta 2006; 51: 5112-5119. http://dx.doi.org/10.1016/j.electacta.2006.03.078

[32] R KIZEK, L TRNKOVA, E PALECEK. Determination of metallothionein at the femtomole level by constant current stripping chronopotentiometry. Anal Chem 2001; 73: 4801-4807. http://dx.doi.org/10.1021/ac010126u

[33] V ADAM, I FABRIK, T ECKSCHLAGER, M STIBOROVA, L TRNKOVA et al. Vertebrate metallothioneins as target molecules for analytical techniques. TRAC-Trends Anal Chem 2010; 29: 409-418. http://dx.doi.org/10.1016/j.trac.2010.02.004

[34] T ECKSCHLAGER, V ADAM, J HRABETA, K FIGOVA, R KIZEK. Metallothioneins and Cancer. Curr Protein Pept Sci 2009; 10: 360-375. http://dx.doi.org/10.2174/138920309788922243

[35] S KRIZKOVA, V ADAM, T ECKSCHLAGER, R KIZEK. Using of chicken antibodies for metallothionein detection in human blood serum and cadmium-treated tumor cell lines after dot- and electroblotting. Electrophoresis 2009; 30: 3726-3735. http://dx.doi.org/10.1002/elps.200900201

[36] S KRIZKOVA, I FABRIK, V ADAM, P HRABETA, T Eckschlager et al. Metallothionein – a promising tool for cancer diagnostics. Bratisl Med J 2009; 110: 93-97.

[37] R KUEFER, S VARAMBALLY, M ZHOU, PC LUCAS, M LOEFFLER et al. alpha-Methyl acyl-CoA racemase: Expression levels of this novel cancer biomarker depend on tumor differentiation. Am J Pathol 2002; 161: 841-848. http://dx.doi.org/10.1016/S0002-9440(10)64244-7

[38] J LUO, S ZHA, WR GAGE, TA DUNN, JL HICKS et al. alpha-Methylacyl-CoA racemase: A new molecular marker for prostate cancer. Cancer Res 2002; 62: 2220-2226.

[39] JC XU, JA STOLK, XQ ZHANG, SJ SILVA, RL HOUGHTON et al. Identification of differentially expressed genes in human prostate cancer using subtraction and microarray. Cancer Res 2000; 60: 1677-1682.

[40] AJ EVANS. alpha-Methylacyl CoA racemase (P504S): overview and potential uses in diagnostic pathology as applied to prostate needle biopsies. J Clin Pathol 2003; 56: 892-897. http://dx.doi.org/10.1136/jcp.56.12.892

[41] MA RUBIN, M ZHOU, SM DHANASEKARAN, S VARAMBALLY, TR BARRETTE et al. alpha-methylacyl coenzyme A racemase as a tissue biomarker for prostate cancer. JAMA-J Am Med Assoc 2002; 287: 1662-1670.

[42] RM SRAMKOSKI, TG PRETLOW, JM GIACONIA, TP PRETLOW, S SCHWARTZ et al. A new human prostate carcinoma cell line, 22Rv1. In Vitro Cell Dev Biol-Anim 1999; 35: 403-409.

[43] V ADAM, J PETRLOVA, J WANG, T ECKSCHLAGER, L TRNKOVA et al. Zeptomole Electrochemical Detection of Metallothioneins. PLoS One 2010; 5.

[44] V ADAM, O BLASTIK, S KRIZKOVA, P LUBAL, J KUKACKA et al. Application of the Brdicka reaction in determination of metallothionein in patients with tumors. Chem Listy 2008; 102: 51-58.

[45] Y OGRA, KT SUZUKI. Targeting of tetrathiomolybdate on the copper accumulating in the liver of LEC rats. J Inorg Biochem 1998; 70: 49-55. http://dx.doi.org/10.1016/S0162-0134(98)00012-9

[46] M KATO, W LIU, AA AKHAND, Y DAI, M OHBAYASHI et al. Linkage between melanocytic tumor development and early burst of Ret protein expression for tolerance induction in metallothionein-I ret transgenic mouse lines. Oncogene 1999; 18: 837-842. http://dx.doi.org/10.1038/sj.onc.1202329

[47] I NAKAGAWA, M SUZUKI, N IMURA, A NAGANUMA. Involvement of oxidative stress in paraquat-induced metallothionein synthesis under glutathione depletion. Free Radic Biol Med 1998; 24: 1390-1395. http://dx.doi.org/10.1016/S0891-5849(98)00008-2

[48] K SUZUKI, K NAKAZATO, K NAKAJIMA Cadmium-induced metallothionein expression and metallothionein mRNA in mice, 1999.

[49] Y SUZUKI, Y KONDO, S HIMENO, K NEMOTO, M AKIMOTO et al. Role of antioxidant systems in human androgen-independent prostate cancer cells. Prostate 2000; 43: 144-149. http://dx.doi.org/10.1002/(SICI)1097-0045(20000501)43:2<144::AID-PROS9>3.0.CO;2-H

[50] K TAKABA, K SAEKI, K SUZUKI, H WANIBUCHI, S FUKUSHIMA. Significant overexpression of metallothionein and cyclin D1 and apoptosis in the early process of rat urinary bladder carcinogenesis induced by treatment with N-butyl-N-(4-hydroxybutyl)nitrosamine or sodium L-ascorbate. Carcinogenesis 2000; 21: 691-700. http://dx.doi.org/10.1093/carcin/21.4.691

[51] BX ZHANG, M SATOH, N NISHIMURA, JS SUZUKI, H SONE et al. Metallothionein deficiency promotes mouse skin carcinogenesis induced by 7,12-dimethylbenz a anthracene. Cancer Res 1998; 58: 4044-4046.

[52] C TOHYAMA, N NISHIMURA, JS SUZUKI, M KARASAWA, H NISHIMURA. Metallothionein messenger-rna in the testis and prostate of the rat detected by digoxigenin-labeled riboprobe. Histochemistry 1994; 101: 341-346. http://dx.doi.org/10.1007/BF00268995

[53] S KOIZUMI, K SUZUKI, F OTSUKA. A nuclear factor that recognizes the metal-responsive elements of human metallothionein-iia gene. J Biol Chem 1992; 267: 18659-18664.

[54] AL ALBRECHT, RK SINGH, S SOMJI, MA SENS, DA SENS et al. Basal and metal-induced expression of metallothionein isoform 1 and 2 genes in the RWPE-1 human prostate epithelial cell line. J Appl Toxicol 2008; 28: 283-293. http://dx.doi.org/10.1002/jat.1277

[55] H WEI, MM DESOUKI, S LIN, D XIAO, RB FRANKLIN et al. Differential expression of metallothioneins (MTs) 1, 2, and 3 in response to zinc treatment in human prostate normal and malignant cells and tissues. Mol Cancer 2008; 7: 1-7. http://dx.doi.org/10.1186/1476-4598-7-7

[56] M YAMASAKI, T NOMURA, F SATO, H MIMATA. Metallothionein is up-regulated under hypoxia and promotes the survival of human prostate cancer cells. Oncol Rep 2007; 18: 1145-1153.

[57] T SUZUKI, H YAMANAKA, Y TAMURA, K NAKAJIMA, K KANATANI et al. Metallothionein of prostatic tissues and fluids in rats and humans. Tohoku J Exp Med 1992; 166: 251-257. http://dx.doi.org/10.1620/tjem.166.251

[58] YC WONG, YZ WANG, JSK LEE, NNC TAM, D LEE. Changes in serum and tissue zinc levels in sex hormone-induced prostatic carcinogenesis in the Noble rat. Tumor Biol 2000; 21: 328-336. http://dx.doi.org/10.1159/000030138

[59] JD LEE, SM WU, LY LU, YT YANG, SY JENG. Cadmium Concentration and Metallothionein Expression in Prostate Cancer and Benign Prostatic Hyperplasia of Humans. J Formos Med Assoc 2009; 108: 554-559. http://dx.doi.org/10.1016/S0929-6646(09)60373-9

[60] J SCHOPFER, G DRASCH, GN SCHRAUZER. Selenium and Cadmium Levels and Ratios in Prostates, Livers, and Kidneys of Nonsmokers and Smokers. Biol Trace Elem Res 2010; 134: 180-187. http://dx.doi.org/10.1007/s12011-010-8636-y

[61] P ATHANASSIADOU, A BANTIS, M GONIDI, P ATHANASSIADES, E AGELONIDOU et al. The expression of metallothioneins on imprint smears of prostate carcinoma: Correlation with clinicopathologic parameters and tumor proliferative capacity. Tumori 2007; 93: 189-194.

[62] Z JIANG, BA WODA. Diagnostic utility of alpha-methylacyl CoA racemase (P504S) on prostate needle biopsy. Adv Anat Pathol 2004; 11: 316-321. http://dx.doi.org/10.1097/01.pap.0000146924.14246.be

[63] C XIE, HJ KIM, JG HAW, A KALBASI, BK GARDNER et al. A novel multiplex assay combining autoantibodies plus PSA has potential implications for classification of prostate cancer from non-malignant cases. J Transl Med 2011; 9.

[64] JL WRIGHT, ML NEUHOUSER, DW LIN, EM KWON, ZD FENG et al. AMACR Polymorphisms, Dietary Intake of Red Meat and Dairy and Prostate Cancer Risk. Prostate 2011; 71: 498-506. http://dx.doi.org/10.1002/pros.21267

[65] XJ WU, M ZAYZAFOON, XZ ZHANG, O HAMEED. Is There a Role for Fatty Acid Synthase in the Diagnosis of Prostatic Adenocarcinoma? A Comparison With AMACR. Am J Clin Pathol 2011; 136: 239-246. http://dx.doi.org/10.1309/AJCP0Y5QWWYDKCJE

[66] V ADAM, J BALOUN, I FABRIK, L TRNKOVA, R KIZEK. An electrochemical detection of metallothioneins at the zeptomole level in nanolitre volumes. Sensors 2008; 8: 2293-2305. http://dx.doi.org/10.3390/s8042293

[67] I FABRIK, S KRIZKOVA, D HUSKA, V ADAM, J HUBALEK et al. Employment of electrochemical techniques for metallothionein determination in tumor cell lines and patients with a tumor disease. Electroanalysis 2008; 20: 1521-1532. http://dx.doi.org/10.1002/elan.200704215

[68] S KRIZKOVA, I FABRIK, V ADAM, J KUKACKA, R PRUSA et al. Utilizing of adsorptive transfer stripping technique Brdicka reaction for determination of metallothioneins level in melanoma cells, blood serum and tissues. Sensors 2008; 8: 3106-3122. http://dx.doi.org/10.3390/s8053106

[69] S KRIZKOVA, I FABRIK, V ADAM, J KUKACKA, R PRUSA et al. Effects of reduced glutathione, surface active agents and ionic strength on the detection of metallothioneins by using of Brdicka reaction. Electroanalysis 2009; 21: 640-644. http://dx.doi.org/10.1002/elan.200804406

[70] RA GOYER, J LIU, MP WAALKES. Cadmium and cancer of prostate and testis. Biometals 2004; 17: 555-558. http://dx.doi.org/10.1023/B:BIOM.0000045738.59708.20

[71] MO PEDERSEN, A LARSEN, M STOLTENBERG, M PENKOWA. The role of metallothionein in oncogenesis and cancer prognosis. Prog Histochem Cytochem 2009; 44: 29-64.

[72] OJK TAN, BH BAY, VTK CHOW. Differential expression of metallothionein isoforms in nasopharyneal cancer and inhibition of cell growth by antisense down-regulation of metallothionein-2A. Oncol Rep 2005; 13: 127-131.

[73] B WERYNSKA, B PULA, B MUSZCZYNSKA-BERNHARD, A PIOTROWSKA, A JETHON et al. Correlation between Expression of Metallothionein and Expression of Ki-67 and MCM-2 Proliferation Markers in Non-Small Cell Lung Cancer. Anticancer Res 2011; 31: 2833-2839.

[74] D LAUKENS, A WAEYTENS, P DE BLESER, C CUVELIER, M DE VOS. Human Metallothionein Expression under Normal and Pathological Conditions: Mechanisms of Gene Regulation Based on In silico Promoter Analysis. Crit Rev Eukaryot Gene Expr 2009; 19: 301-317.

5.2.2 Findings related to the hypothesis 2

***Hypothesis 2*: Metallothionein is also detectable in other biological materials - blood, tumour tissue; the procedure of metallothionein analysis is automated thanks to using the isolation of this protein by means of paramagnetic particles.**

The micro detection systems based on electrochemical determination undoubtedly belong among the new biophysical approaches that can contribute significantly to the study of information macromolecules. Electrochemical detection is based on studying oxidation/ reduction and adsorption of biologically important polymers such as nucleic acids (NA) and proteins on the surface of the working electrode. Moreover, electrochemistry can be applied to determine structural changes, denaturation processes, physical or chemical damage of NA. In the case of proteins, a considerable attention is paid to the exchange of electrons in their redox centres and to monitor protein adsorption to solid surfaces. Besides the analyses of physical and chemical properties of NA and proteins, the electrochemical methods are used with a great success to determine low concentrations of both NA, peptides and proteins. A great attention is also paid to the electrochemical detection of protein - NA interaction and their chemical modifications, such as binding of intercalating agents and interaction of drugs with their structure [148-156]. A possibility of applying the electrochemical methods in the analyses of such adducts directly in the tumour cells or using these techniques in the construction of simple biosensors also follows from the facts above.

Earlier studies demonstrated the diagnostic potential of metallothionein in the prediction of prostate carcinoma. Thanks to its chemical properties (high cysteine content, low molecular weight), this molecule is hardly detectable by the western blotting, commonly used to detect proteins. The electrochemical detection allows a high degree of sensitivity, at the same time requiring a rather complex sample preparation. The aim of the following works was to create an automated method for the detection of metallothionein at RNA and protein levels.

Detection of mRNA serum levels has been recently an attractive issue, particularly from the perspective of carcinoma biomarkers. In the work of Fojtu et al [157] (available on page 292), paramagnetic particles modified with streptavidin were used to optimize serum isolation of mRNA. Moreover, one-step modality of separation was proposed to further accelerate the protocol. In the final phase, this protocol was verified on serum samples of the patients suffering from prostate carcinomas.

Paramagnetic particles also contributed to optimizing detection at a protein level from the cell line lysate samples. In the work by Masarik et al. [158] (see p. 301), the immuno-separation protocol was optimized using paramagnetic particles with conjugated antibody via the G protein. Subsequently, metallothionein was determined by electrochemistry - Brdička reaction and also using the SDS-PAGE electrophoresis, and the protocol was compared with a conventional procedure.

Conclusion: The procedures based on paramagnetic nanoparticles allow to isolate both RNA and proteins from complex samples, thereby increasing detection specificity and at the same time reducing amounts of consumed chemicals. This procedure was optimized for metallothionein in serum and cell lysate samples.

Author's publications relevant to this chapter

1. Fojtu M, Gumulec J, Balvan J, et al. Utilization of paramagnetic microparticles for automated isolation of free circulating mRNA as a new tool in prostate cancer diagnostics. Electrophoresis. 2014;35(2-3):306-315.
   Available on page 292
2. Masarik M, Gumulec J, Sztalmachova M, et al. Isolation of metallothionein from cells derived from aggressive form of high-grade prostate carcinoma using paramagnetic antibody-modified microbeads off-line coupled with electrochemical and electrophoretic analysis. Electrophoresis. 2011;32(24):3576-3588.
   Available on page 301

306 *Electrophoresis* 2014, *35*, 306–315

Michaela Fojtu[1]*
Jaromir Gumulec[1,2]*
Jan Balvan[1]
Martina Raudenska[1]
Marketa Sztalmachova[1,3]
Hana Polanska[1]
Kristyna Smerkova[3]
Vojtech Adam[2,3]
Rene Kizek[2,3]
Michal Masarik[1,2]

[1]Department of Pathological Physiology, Faculty of Medicine, Masaryk University, Brno, Czech Republic
[2]Central European Institute of Technology, Brno University of Technology, Brno, Czech Republic
[3]Department of Chemistry and Biochemistry, Mendel University in Brno, Brno, Czech Republic

Received April 19, 2013
Revised May 15, 2013
Accepted May 16, 2013

Research Article

Utilization of paramagnetic microparticles for automated isolation of free circulating mRNA as a new tool in prostate cancer diagnostics

Determination of serum mRNA gained a lot of attention in recent years, particularly from the perspective of disease markers. Streptavidin-modified paramagnetic particles (SMPs) seem an interesting technique, mainly due to possible automated isolation and high efficiency. The aim of this study was to optimize serum isolation protocol to reduce the consumption of chemicals and sample volume. The following factors were optimized: amounts of (i) paramagnetic particles, (ii) oligo(dT)$_{20}$ probe, (iii) serum, and (iv) the binding sequence (SMPs, oligo(dT)$_{20}$, serum vs. oligo(dT)$_{20}$, serum and SMPs). RNA content was measured, and the expression of metallothionein-2A as possible prostate cancer marker was analyzed to demonstrate measurable RNA content with ability for RT-PCR detection. Isolation is possible on serum volume range (10–200 μL) without altering of efficiency or purity. Amount of SMPs can be reduced up to 5 μL, with optimal results within 10–30 μL SMPs. Volume of oligo(dT)$_{20}$ does not affect efficiency, when used within 0.1–0.4 μL. This optimized protocol was also modified to fit needs of automated one-step single-tube analysis with identical efficiency compared to conventional setup. One-step analysis protocol is considered a promising simplification, making RNA isolation suitable for automatable process.

Keywords:
Metallothionein / Microseparation / Paramagnetic microparticles / Prostate cancer / Serum mRNA
DOI 10.1002/elps.201300190

1 Introduction

Extracellular mRNA was found in the circulation [1]. Such RNA can be detected in plasma, serum, and other body fluids, as well as from cell-free supernatants of in vitro cultivated cells [2, 3]. Based on the fact that the ubiquitous concentration of RNases is relatively high, and that RNA-degrading enzymes are extremely stable, it seems likely that RNA is complexed with other molecules, which makes it resistant to digestion [4].

The extracellular mRNA is thought to be released into the circulation from intact and viable cells as well as necrotic cells [5]. An increasing amount of evidence suggests that liberation of cell-free nucleic acids into plasma from organs or compartments is likely due to cell death [6, 7]. The formation of apoptotic bodies, which contain either DNA or RNA, was observed in tumor patients, especially during and after therapy [8].

The biological roles of circulating mRNA are still unclear, although its physiological significance has been investigated during the last several years. Cell-free DNA, mRNA, and microRNA seem to be promising molecular biomarkers for clinical applications, and also signaling molecules for intercellular communication. The secretion and transfer of macromolecular RNA between mammalian cells has been described [9–11]. Garcia-Olmo et al. even concluded that metastases are the result of a transformation of susceptible cells by circulating nucleic acids [12, 13]. According to their observations, the hematogenous dissemination is closely associated with the detection of circulating nucleic acids than with circulating tumor cells [14, 15].

Prostate cancer is one of the most common cancers [16]. To date, prostate specific antigen (PSA) is routinely used biomarker for this disease. However, contradictory results were published regarding the PSA screening in 2009. While European Randomized Study of Screening for Prostate Cancer reported 20% reduction of risk [17], no such benefit of screening was determined in Prostate, Lung, Colorectal

Correspondence: Dr. Michal Masarik, Department of Pathological Physiology, Faculty of Medicine, Masaryk University, Kamenice 5, CZ-625 00 Brno, Czech Republic
E-mail: masarik@med.muni.cz
Fax: +420-5-4949-4340

Abbreviations: **FBS**, fetal bovine serum; **MT2A**, metallothionein-2A; **PSA**, prostate specific antigen; **ROC**, receiver operating characteristic; **SMP**, streptavidin-modified paramagnetic microparticle

*These authors contributed equally to this work.

Colour Online: See the article online to view Fig. 4 in colour.

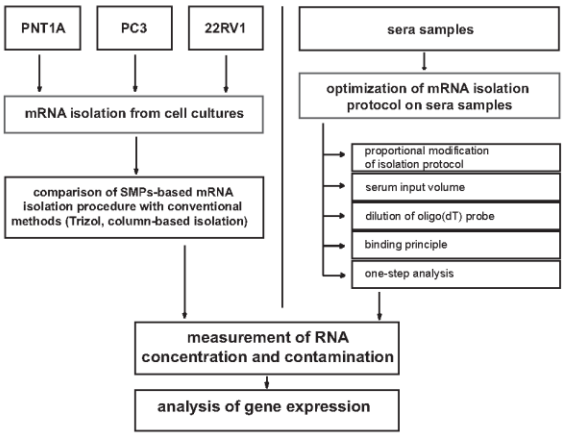

Figure 1. Scheme of study design. RNA contamination by proteins measured by absorbance ratio 260/280.

and Ovary Study [18]. Therefore, development of alternative biomarkers is desirable. Due to the fact that nucleic acids in plasma/serum may be a suitable source for the development of noninvasive diagnostic, prognostic, and follow-up tests for cancer and other types of diseases, we focused on isolation and detection of mRNA as well as determining the level of metallothionein-2A (MT2A) expression by RT-PCR. MT can indeed serve as a new prognostic marker of cancer progression, as it is clear from numerous recent publications [19–22]. The detection of circulating RNA offers certain advantages over the detection of circulating DNA [23]. First, if both plasma RNA and DNA were derived from the same cell population, the released RNA would likely be quantitatively more abundant than DNA [24]. This is because multiple copies of an RNA transcript may be present in each cell, depending on the gene's expression, whereas each cell contains only a single diploid genome equivalent of DNA. Second, some cancer researchers reported that a greater proportion of cancer cases was positive for the investigated plasma RNA markers than DNA markers [25]. The number of protocols applied for the isolation of extracellular mRNA is probably as numerous as the laboratories using them. Even if most researchers use commercially available kits, there is no accepted "standard" method so far. Fast, easily automatable, and simple procedure for isolating circulating mRNA from limited amounts of plasma/serum is highly required. Promising in this regard could be the use of paramagnetic microparticles, streptavidin-modified paramagnetic microparticles (SMPs) in particular. SMPs can be modified with biotinylated oligo(dT) fragment and therefore can bind mRNAs. In this study, we compared the isolation of mRNA made by SMPs with methods commonly used for mRNA isolation (Trizol Reagent, silica columns) and assessed the applicability of these methods for the isolation of circulating MT2A mRNA transcript for prostate cancer diagnostics. The basic scheme of the study is shown in Fig. 1.

2 Materials and methods

2.1 Chemical and biochemical reagents

RPMI-1640 medium, Ham's F12 medium, fetal bovine serum (FBS, mycoplasma-free), penicillin/streptomycin, and trypsin were purchased from PAA Laboratories (Pasching, Austria). PBS was purchased from Invitrogen Corporation (Carlsbad, CA, USA). EDTA and all other chemicals of ACS purity were purchased from Sigma-Aldrich (St. Louis, MO, USA), unless noted otherwise.

2.2 Cell cultures and culture conditions

Three human prostatic cell lines were used in this study: (i) PNT1A human cell line established from normal adult prostatic epithelium; (ii) 22Rv1, human prostatic epithelial cell line derived from androgen-dependent primary tumor; and (iii) PC-3 human cell line established from a grade 4 androgen-independent cancer from metastatic site in bone. All cell lines used in this study were purchased from Health Protection Agency Culture Collections (Salisbury, UK).

PNT1A and 22RV1 cells were cultured in RPMI-1640 medium with 10% FBS. PC-3 cells were cultured in Ham's F12 medium with 7% FBS. All media were supplemented with penicillin (100 U/mL) and streptomycin (0.1 mg/mL), and the cells were maintained at 37°C in a humidified incubator (Sanyo, Japan) with 5% CO_2.

2.3 Cell-content quantification

Cell content was analyzed using Casy model TT system (Roche Applied Science, USA) using protocol recommended by manufacturer. For each cell type, new calibration was prepared and all subsequent measurements were performed on 100 × diluted 100 μL cell suspension. All samples were measured in duplicates.

2.4 Set of patients with diagnosed prostate carcinoma

Serum samples of patients with histologically verified prostate adenocarcinoma (35 samples) were used in our study and compared to 14 controls. Average age of patients was 62.1 years, range 53–71 years. Tumors were classified histologically with Gleason score, ranging 6–9. Pathological staging of samples varied from T2a to T4, all patients were without nodal or metastatic dissemination. In the control group, all probands were without neoplastic disease. Age of control group of volunteers varied 23–37 years, mean age was 30.1 years. Tested serum samples were obtained from Urology clinic, St. Anne's University Hospital in Brno, Czech Republic. Inclusion of patients into realized clinical study was approved by the Ethic commission of the Faculty of

Medicine, Masaryk University, and St. Anne's University Hospital, Brno, Czech Republic.

2.5 RNA isolation from cell cultures

Three different procedures were used to extract RNA from cell cultures to evaluate isolation efficiency and RNA yield. For this purpose, we used High Pure RNA Isolation Kit (Roche, Basel, Switzerland) employing silica columns (further referred to as "column-based"), Trizol RNA Isolation using TriPure reagent (Roche), and mRNA Isolation Kit (Roche) utilizing streptavidin-modified paramagnetic microparticles (SMPs). The medium was removed and samples were washed with 5 mL of ice-cold PBS twice. Cells were scraped off, transferred to clean tubes, and centrifuged at 20 800 × *g* for 5 min at 4°C. A total of 5×10^6 cells were used for each isolation procedure. Column-based isolation and isolation utilizing SMPs were used according to manufacturer's instruction starting the lysis step. Trizol isolation was performed using TriPpure reagent (monophasic solution of phenol and guanidine isothiocyanate) by incubating samples for 5 min at 25°C to permit the complete dissociation of nucleoprotein complexes. Then, 40 μL of chloroform per 200 μL of TriPure was added. Samples were centrifuged at 10 600 rpm for 15 min at 2–6°C. Following centrifugation, RNA remains exclusively in the aqueous phase. The aqueous phase was transferred into a clean tube. RNA was precipitated by mixing with isopropyl alcohol (0.1 mL of isopropyl alcohol per 200 μL TriPure). Samples were incubated at 25°C for 10 min and centrifuged at 10 600 rpm for 10 min at 4°C. Then, the supernatant was removed and RNA pellet was washed once with 75% ethanol. Two hundred microliters of ethanol per 200 μL of TriPure reagent was added. Samples were vortexed and subsequently centrifuged at 8400 rpm for 5 min at 4°C. Then, dry RNA pellet was dissolved in 50 μL of RNase-free water for 18 min at 58°C.

2.6 Extracellular RNA isolation from serum samples

All three above-mentioned isolation methods were used in order to extract extracellular mRNA from serum samples. Since the SMPs isolation protocol is not primarily intended by manufacturer for this purpose, individual steps were optimized to find out what volumes of reagents are the most effective for obtaining extracellular mRNA. Briefly, basic SMPs isolation was carried out by resuspending microbeads in 70 μL of PBS and removed by magnetic separator. Total 0.5 μL of oligo$(dT)_{20}$ probe was added to 200 μL of serum to form hybridization mix. It was mixed with SMPs and incubated for 5 min at 37°C. SMPs with bound mRNA were then separated and washed three times with SMP washing buffer. To dissociate mRNA from SMPs, 10 μL redistilled water was added and samples were incubated for 3 min at 65°C. Optimizations of isolation protocol were then carried out (Table 1).

First, volumes of reagents were proportionally modified and serum volume was gradually decreased. Consequently, effectiveness of two different binding principles was evaluated. Oligo$(dT)_{20}$ probe was first mixed with serum sample, then it was added to SMPs and incubated 5 min at 37°C. The second binding principle was based on hybridization oligo$(dT)_{20}$ probe first with SMPs; subsequently, after 5-min incubation, serum sample was added.

Dilution of oligo$(dT)_{20}$ probe was also carried out, since the amount of extracellular mRNA in serum sample is definitely much lower than in cell cultures. Probe was 10 × diluted for easy handling and its volume was gradually decreased.

2.7 One-step analysis

One-step analysis was performed using 50 μL SMPs and 200 μL serum sample. Elution step was skipped and reverse transcription followed by analysis of gene expression was carried out in the presence of SMPs. For details of individual optimization steps, see Section 3.

2.8 RNA content and purity measurement

RNA and mRNA concentrations and purities were determined by NanoDrop spectrophotometer (Thermo Fisher Scientific, Wilmington, DE, USA). Optical density ratio at $\lambda = 260/280$ nm was calculated to evaluate protein contamination of RNA. While product of column-based isolation and Trizol isolation protocols is total RNA, SMPs isolation enable to obtain mRNA directly. In order to compare efficiency of these isolation methods, mRNA concentrations were calculated with an assumption that mRNA content in typical mammalian cell is 5% of total RNA at most. The same recount was applied on serum samples, where we assumed 50% of total RNA to be mRNA [26].

2.9 RNA reverse transcription

Isolated RNA was used for cDNA synthesis. From all isolation protocols, 6 μL (of total 10 μL isolated using SMPs, 50 μL using Trizol, and 50 μL using column-based isolation) of RNA was used for each transcription. RNA was transcribed using Transcriptor First Strand cDNA Synthesis Kit (Roche) according to the manufacturer's instructions. Five microliters of prepared cDNA (of total 20 μL transcribed) from total RNA (High Pure Isolation Kit, Trizol RNA Isolation) and mRNA (mRNA Isolation Kit) was subsequently analyzed by 7500 real-time PCR system (Applied Biosystems).

2.10 Quantitative PCR (q-PCR)

After reverse transcription, q-PCR was performed with 5 μL of cDNA from each sample using the TaqMan gene

Table 1. Optimization steps for serum RNA isolation using SMPs

Optimization step	SMPs (μL)	Serum (μL)	Oligo(dT)$_{20}$ probe (μL)	cRNA (ng/μL)	$A_{260/280}$	Threshold cycle (C_t)
Proportional modification	5	20	0.05	1.5	1.31	–
	10	40	0.10	3.8	1.14	–
	15	60	0.15	4.3	1.26	–
	20	80	0.20	8.3	1.11	–
	30	120	0.30	5.2	1.30	–
	40	160	0.40	9.7	1.31	–
	50	200	0.50	12.9	1.20	–
Serum volume	20	10	0.20	6.5	1.10	39.38
	20	30	0.20	6.6	1.15	38.65
	20	50	0.20	6.8	0.94	38.81
	20	80	0.20	7.7	1.08	40.01
	20	100	0.20	7.6	1.10	38.40
	20	150	0.20	6.3	1.06	38.86
Binding principle "A"	20	80	0.20	8.6	1.17	–
Binding principle "B"	20	80	0.20	7.6	1.10	–
Oligo(dT)$_{20}$ probe	20	80	0.40	5.3	0.91	38.44
	20	80	0.30	4.9	0.94	37.94
	20	80	0.20	3.1	1.18	37.06
	20	80	0.10	5.0	1.08	37.29

Volumes of reagents isolated RNA content, RNA contamination and metallothionein gene expression analysis by qRT-PCR. $A_{260/280}$ ratio designates protein contamination of RNA. Threshold cycle represents metallothinein qRT-PCR measurement. Binding principle "A" indicates first oligo(dT)$_{20}$ binding to sample following binding to SMPs; "B" indicates first oligo(dT)$_{20}$ binding to SMPs, following incubation with sample.

expression assay with the 7500 real-time PCR system. The primer and probe set for MT2A (Hs02379661_g1) was selected from TaqMan gene expression assay libraries (Life Technologies, USA). q-PCR was performed under the following amplification conditions: total volume of 20 μL, initial incubation 50°C/2 min followed by denaturation 95°C/10 min, and then 45 cycles at 95°C/15 s, 60°C/1 min.

2.11 Statistical analysis

To reveal differences between groups, one way and factorial ANOVA were employed. Pearson correlations were performed to reveal dependencies between continuous variables. Unless noted otherwise, p level <0.05 was considered significant. Receiver operating characteristic (ROC) analysis was used to calculate sensitivity and specificity. Software Statistica 10 (StatSoft, USA) and MedCalc 12 (MedCalc Software, Belgium) were used for analysis.

3 Results

3.1 Comparison of RNA isolation assays on cell lines

First, the RNA isolation efficiency of three widely used isolation assays as column-based (High Pure Isolation Kit), paramagnetic micro particle based (mRNA Isolation Kit, Roche, further designated as SMPs), and Trizol-based (TriPure, Roche) were compared. Because of the lack of standardized RNA isolation procedures for serum or plasma, this optimization step was performed on well-characterized prostate cell lines as PNT1A, PC-3, and 22Rv1 according to manufacturer's recommended protocol. While column-based and TriPure isolation assays isolate total RNA content indiscriminately (i.e. including mRNAs, tRNAs rRNAs, miRNAs, and other forms), SMPs isolate only mRNA molecules selectively. Inasmuch as mRNA comprises at most 5 and 50% of total cellular and extracellular RNA, respectively, detected amounts were converted to this percentage (see Section 4 for details).

Using SMPs, significantly largest amount of total mRNA from an equal number of cells (500 000 cells) was isolated (mRNA ranged 17.6–59.5 ng/μL; up to sevenfold, $p = 0.035$ and threefold, $p = 0.066$, for column- and Trizol-based isolation assays, respectively, Fig. 2A). However, the isolation using SMPs led to significantly lowest purity (mean 260/280 = 1.74 vs. 1.90 and 2.10 for TriPure and column-based isolation assays). Although distinct differences were observed between cell lines, it is beyond the scope of this study and is not widely discussed. To verify these results, the expression of MT2A level was analyzed (Fig. 2B). Insignificantly higher C_t values (i.e. lower MT2A level) were detected using paramagnetic particle assay. In addition, no significant differences were observed between cell lines.

3.2 Comparison of RNA isolation assays on serum samples

Consequently, mRNA was isolated from 200 μL of sera from prostate cancer patients. Three random samples were analyzed, all three isolation protocols were used under identical conditions as for cellular RNA isolation (30 μL SMPs,

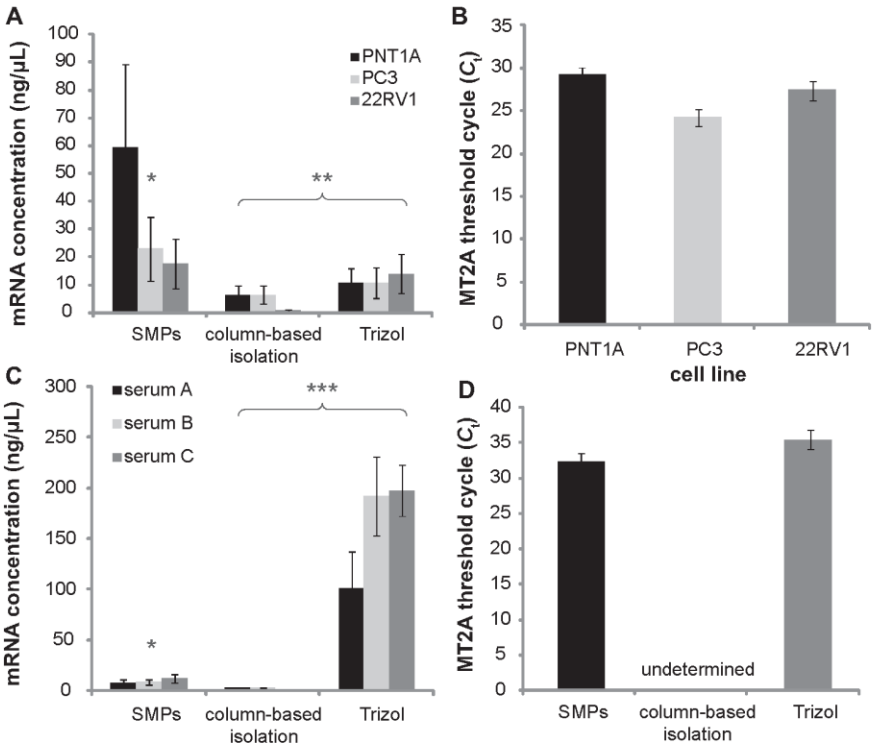

Figure 2. Comparison on isolation protocols on cellular and extracellular RNA. (A) Comparison of RNA isolation efficiency from prostate cell lines. (B) MT2A gene expression using SMP isolation protocol isolated from prostate cell lines. (C) Comparison of RNA isolation efficiency from serum. *, SMPs isolate mRNA selectively, other protocols isolate whole RNA content. **, An approximate calculation, mRNA comprises up to 5% of total cellular RNA. ***, Approximate extracellular mRNA content, up to 50% of RNA. (D) Analysis of MT2A gene expression using SMPs, Trizol- and column-based isolation from serum from prostate cancer patients. No significant difference between SMP and Trizol-based isolation. Data are displayed as mean ± SD.

0.5 μL oligo(dT)$_{20}$). Compared to cellular isolation, more distinct differences between methods were observed (Fig. 2C). Column-based method did not lead to satisfactory results with insufficient RNA content isolated. Seemingly high Trizol efficiency is caused by approximate "50% recalculation." In the next step, serum MT RNA level was detected (Fig. 2D). However column-based detection was below detection limits, no significant difference was observed between Trizol- and SMP-based isolation.

3.3 Optimization of serum RNA isolation

Based on the Section 3.2, we proved that RNA isolation from sera was possible using Trizol- and SMP-based technique. In this step, the aim was to optimize serum isolation protocol using SMPs and to reduce the need of chemicals and sample volume. Thus, the amounts of (i) paramagnetic particles, (ii) oligo(dT)$_{20}$ probe, (iii) serum volume, and (iv) the binding sequence (first anchoring paramagnetic particles with oligo(dT)$_{20}$ probe following serum addition vs. first oligo(dT)$_{20}$ probe + serum binding following addition of paramagnetic particles) were manipulated. Consequently, RNA content was measured, the expression of MT2A was analyzed to demonstrate measurable RNA content and ability for real-time PCR detection.

First, the paramagnetic particle amount was optimized. The following SMP amounts were used: 50 (recommended by manufacturer), 40, 30, 20, 15, 10, 10, and 5 μL. Together with decreasing SMP content, all components were changed ratiometrically (Table 1). RNA was isolated using whole listed SMP volume range, significant strong correlation between SMP and mRNA concentrations was detected ($r = 0.91$, $p = 0.004$, Fig. 3A). Using 5 μL SMPs, 1.5 ng/μL mRNA was isolated from 20 μL serum volume. With regard to purity of isolated mRNA, no correlation was observed; mean 260/280 ratio was 1.22 ± 0.08. To evaluate the use of this volume for qRT-PCR detection, the PCR efficiency of MT expression was calculated [27]. Thus, five dilutions were prepared and the efficiency 1.96 ± 0.12 (of max. 2.0) was determined ($r = -0.97$, Fig. 3B). Thus, isolation using 5 μL SMPs and 10 μL serum is feasible. Nevertheless, isolation using 20 μL SMPs showed slight increase in effectiveness. Thus, this concentration was used for further optimization steps.

Second, amount of serum amount was optimized (Fig. 3C). The following volumes of serum were used: 10, 30, 50, 80, 100, and 150 μL. Although relatively low purity of isolated samples was observed (260/280 nm = 1.07 ± 0.06), no significant correlation between SMP volume and mRNA concentration was observed ($r = 0.13$ at $p = 0.81$). Thus, whole concentration range may be used for RNA isolation.

In the next step, the effectiveness of binding sequence of individual components (sample, MP, oligo(dT)$_{20}$) was

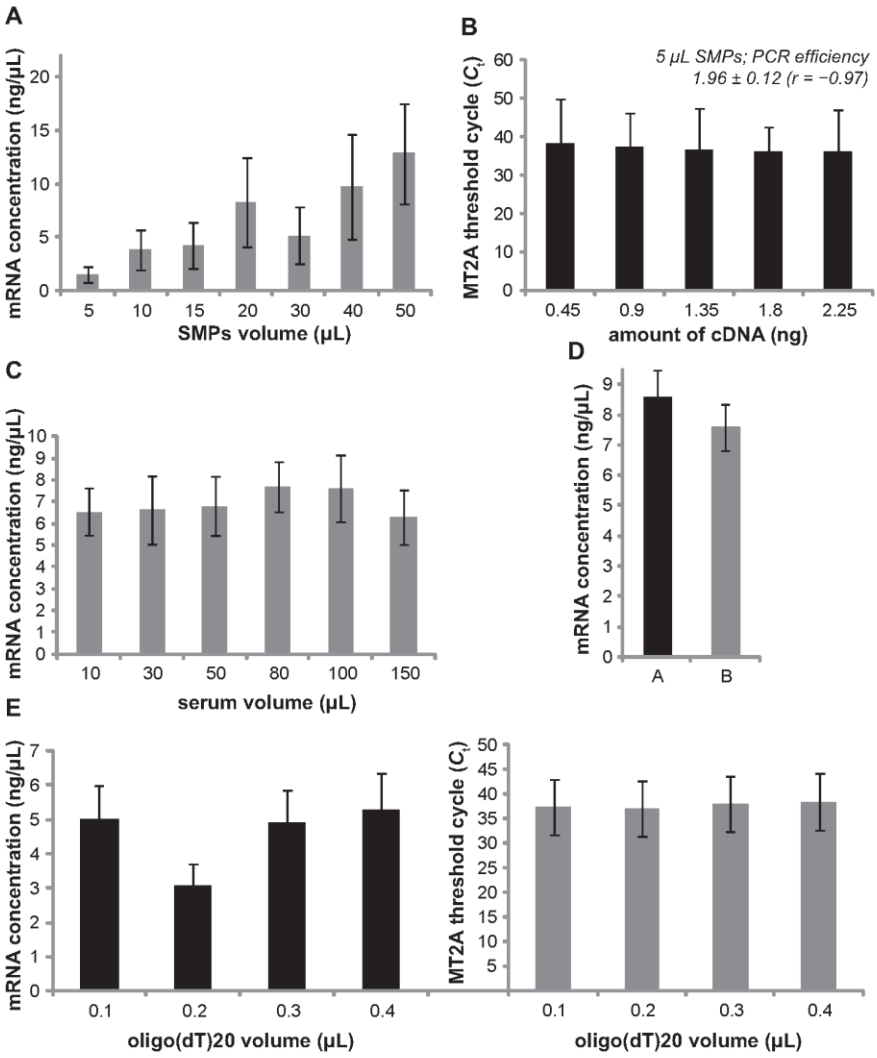

Figure 3. Optimization steps of serum RNA isolation using SMPs. (A) Amount of isolated mRNA versus volume of SMPs. (B) PCR efficiency calculation prepared from RNA isolated using lowest used (5 µL) SMP volume. (C) Optimization of sample volume, no relation was observed. (D) Optimization of binding principle. Binding principle "A" indicates first oligo(dT)$_{20}$ binding to sample following binding to SMPs; "B" indicates first oligo(dT)$_{20}$ binding to SMPs, following incubation with sample. No significant difference was observed. (E) Optimization of oligo(dT)$_{20}$ volume. Left: mRNA content, right: MT2A expression. For details, see Table 1. Data are displayed as mean ± SD.

analyzed. Using three randomly selected sera, the following variants were tested: (i) oligo(dT)$_{20}$ was first incubated with sample and this complex was subsequently bound to SMPs (also recommended by manufacturer); (ii) oligo(dT)$_{20}$ was first bound to SMPs, following incubation with sample. No significant difference between those binding sequences was detected (8.56 ± 2.05 and 7.6 ± 2.06 for first and second binding principle, Fig. 3D). Consequently, amount of oligo(dT)$_{20}$ probe was optimized (Fig. 3E). Based on the previous steps, 20 µL SMPs and 80 µL serum were used, and oligo(dT)$_{20}$ ranged 0.1–0.4 µL. No significant correlation was determined ($r = 0.35$ at $p = 0.65$). In addition, although low sample purity was detected, no significant relation with oligo(dT)$_{20}$ volume was detected (absorbance ratio 1.02 ± 0.12 for 260/280). Despite this fact, MT expression is detectable in all oligo(dT)$_{20}$ volumes, with its qRT-PCR threshold cycle (C_t) ranging 36.2–39.2. Thus, the oligo(dT)$_{20}$ volume is not an important factor influencing the effectiveness of isolation.

3.4 One-step analysis

Simple approach is desirable for automated RNA isolation, in which all the steps take place in a single tube. Therefore, previously optimized protocol was modified where SMPs were left in same tube for subsequent analyses (for details, see Section 2) and those variants were compared on three randomly selected sera (Fig. 4A).

Although lower threshold cycle values for MT expression were detected using modified one-step analysis, differences were below the level of statistical significance ($p = 0.77$, $C_t = 36.2 \pm 1.6$ and 34.7 ± 1.4 for conventional and one-step analysis, Fig. 4B).

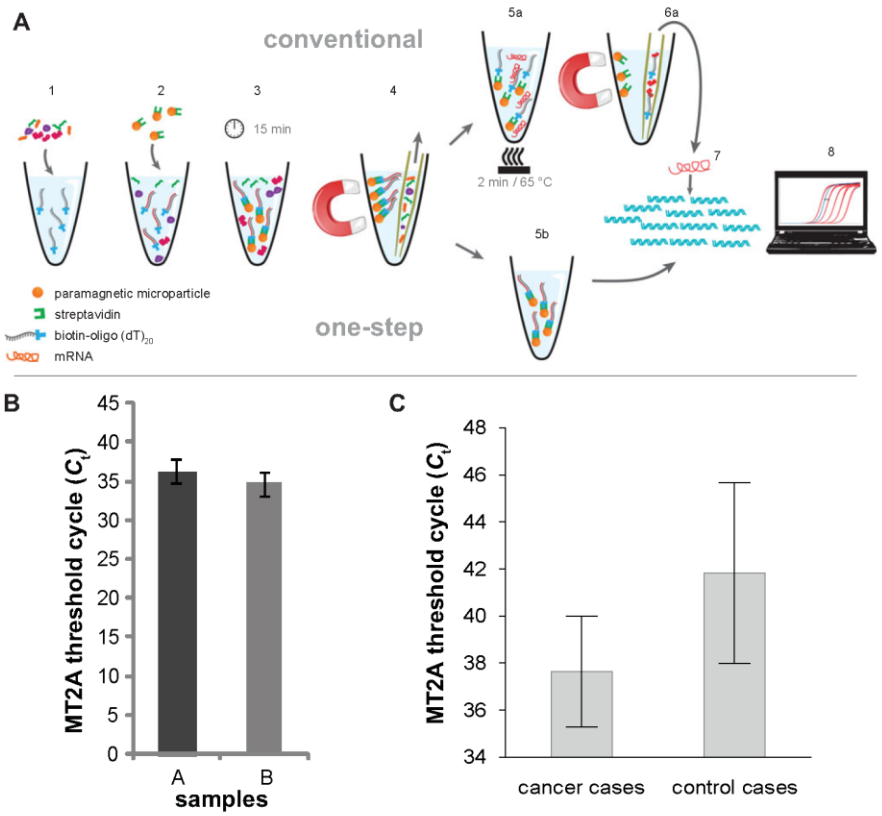

Figure 4. One-step analysis and application for prostate cancer detection. (A) Comparison of conventional and one-step isolation. (1) Addition of sample, anchorage of biotinylated oligo(dT)$_{20}$ to serum mRNA; (2) addition of streptavidin-modified paramagnetic particle; (3) incubation of RNA–oligo(dT)$_{20}$ SMP complex; (4) 3× washing; (5a) Conventional isolation, releasing streptavidin-biotin binding; (6a) Transferring RNA and oligo(dT)$_{20}$ to PCR reaction; (7) cDNA transcription and amplification using PCR; (8) Real-time PCR detection; (5b) One-step analysis, direct transfer of SMP–oligo(dT)$_{20}$–RNA to PCR reaction. (B) Comparison of one-step versus conventional analysis, expression of MT2A. No significant difference was observed. (C) Analysis of serum metallothionein 2A mRNA level in healthy individuals and prostate cancer patients isolated using one-step analysis. Significantly lower MT levels observed in healthy individuals ($p < 0.001$). Data are displayed as mean ± SD.

3.5 Serum MT mRNA as a cancer marker

To outline possible applications of serum RNA detection, serum MT2A expression was analyzed using qRT-PCR on 35 patients suffering from prostate cancer and compared to 14 healthy controls. Using optimized protocol, a significantly higher MT level was observed in patients suffering from cancer ($p < 0.001$, mean $C_t = 41.83 \pm 3.85$ vs. 37.64 ± 2.36 for controls and cases, respectively; Fig. 4C). Based on ROC analysis, 65.7% sensitivity and 85.7% specificity were determined on a threshold $C_t = 37$.

4 Discussion

In this study, we subjected serum samples to RNA extraction protocols in order to analyze their benefits in extracellular RNA isolation and in subsequent determination of free circulating mRNA transcript of MT2A in prostate cancer patients. In particular, column-based isolation, Trizol RNA isolation, and protocol employing SMPs were confronted for the first time. Consequently, an isolation protocol was optimized and the optimization efficiency was analyzed using RNA content and RNA purity measurement and verified by real-time PCR. Though relative gene expression analysis calls for standardization using housekeeping gene, no such step was employed in this study and raw C_t values are shown. It was assumed that serum composition is relatively constant and thus the predictive value of raw C_t values is sufficient for this report. In addition, reliable and unambiguous housekeeping gene for standardization of MT2A expression or appearance of MT2A transcript in serum samples is still missing.

Initially, these methods were applied on cell cultures to determine their efficiency by RNA content measurement. Afterward, identical protocols were compared on serum samples. Because SMPs isolate mRNA directly, it was necessary to convert amount of (total) RNA extracted by column-based and Trizol method to mRNA in order to compare RNA yields. It is generally known that mRNA covers 5% of total RNA in cell cultures at most. On the other hand, some reports indicate that the mRNA proportion of the total RNA extracted from serum samples could be considerably bigger (around 50%) [26]. These percentages were used to provide rough estimates.

4.1 Optimized serum isolation protocol

Moreover, our goal was also to optimize isolation protocol using SMPs on sera, because there are few reports describing utilization of SMPs in extracellular RNA isolation. Circulating RNA detection is particularly promising from the perspective of disease markers; higher percentage of detectable tumors

found with DNA markers was repeatedly reported [25]. According to our results, SMPs appear to be highly effective method for mRNA isolation from cell cultures. Compared to Trizol, isolation from serum samples is seemingly not as effective as from intracellular material. However, SMP specificity to mRNA must be taken into account compared to other isolation protocols. Furthermore, with purification being affinity-based, cDNA contamination by genomic DNA is avoided [28], and no DNase I treatment is necessary.

Due to the fact that SMP isolation protocol is designed for mRNA isolation from cell cultures with distinctly higher RNA content compared to serum, pronounced reduction of reagent volumes is possible. Optimizations validate that analysis of gene expression can be performed from 20 μL of sample using 5 μL SMPs, or even from 10 μL of serum using 20 μL of SMPs (i.e. tenfold reduction). Moreover, fivefold reduction of oligo(dT)$_{20}$ probe volume is possible. Volume reductions described herein are still far from detection limits and further reductions are feasible.

Efficiency of two different binding principles was compared. Isolation utilizing SMPs is grounded on highly specific and strong streptavidin-biotin interaction. Streptavidin is coated on the surface of microbead, whereas oligo(dT)$_{20}$ probe is labeled with biotin. Conventional binding principle (marked as principle "A") lies in initially mixing biotinyled oligo(dT)$_{20}$ probe with serum sample and following incubation of this hybridization mix with streptavidin-coated microparticles. On the other hand, modified principle (marked as "B") was based on the incubation of oligo(dT)$_{20}$ probe first with microbeads. Serum sample was added after incubation. Since in principle "A" is reduction of mRNA yield more likely owing to lesser steric constraints, this principle was assumed to be more effective. However, distinctions between two principles were not statistically significant.

In order to examine potential for further automation, one-step analysis was performed, where all procedures from extracellular mRNA isolation, reverse transcription up to gene expression analysis are run in one flow without removing SMPs. Our results are in agreement with previous reports [28] that prove no significant influence on fluorescence signal during RT-PCR analysis. Data also indicate that SMPs do not cause quenching of fluorescence signal and that their autofluorescence is negligible [28]. Here, we show that this method is reliable, sensitive and exhibit at least equally well results as conventional methods. In combination with reduction of reagents volumes, this analysis represents reproducible and economic high-throughput method for gene expression analysis from extracellular mRNA. Although there are several commercial isolation kits, adjusted for extracellular RNA extraction, they mostly require high input volume of serum (range, 250 μL–5 mL). Our goal was, therefore, to minimize input volume of biological material, which might in the upshot lead to reduction of screening invasivity. Here, we demonstrated isolation of extracellular RNA even from 10 μL of serum with no undesirable effect on analysis of gene expression by RT-PCR. The extra benefit of this method is direct mRNA isolation, whereas other procedures provide total RNA.

However, this protocol has certain disadvantages. Compared to other isolation protocols, RNA isolation using SMPs distinctly reduces purity of isolated nucleic acids. Plasma and serum are biospecimens that have a very high concentration of proteins that could potentially interfere with sample preparation and detection assay. Similar findings were also demonstrated by study dealing with optimization of microRNA isolation protocol from serum samples [29]. It was demonstrated that certain proteins and proteolipid complexes might even directly protect extracellular RNA from degradation by serum RNases [30]. More specifically, circulating RNA may be packed into apoptotic bodies, which considerably decrease susceptibility to nucleases in serum. These protein structures are obviously not removed by SMPs isolation protocol and additional purification of RNA should be performed. Despite this fact, no changes in qRT-PCR were observed.

4.2 Circulating miRNAs as cancer biomarker

Due to the controversy of prostate cancer screening using PSA [17], novel prostate tumor biomarkers are desirable. To date, various compounds and protocols were evaluated, including DNA sequence variations, genetic aberrations, and various tissue-, blood-, and urine-based markers [31–33]. From this perspective, MT seems to be a promising tool for cancer diagnostics. Use of MT as a prostate cancer marker was evaluated on both serum and protein level. Immunohistochemical analyses reported both significant decrease [21] and elevation [34] with no associations with tumor grade [21, 35–37]. On serum level, we previously reported significantly higher MT protein level [22, 38]. It should be noted that proper selection of controls is crucial when assessing the suitability of MT as a cancer biomarker. It was reported that MT levels differ between benign hyperplasia and cases significantly [39]. In addition, histological hyperplasia increases linearly with age, being detectable in 50% of 40-year-old male subjects [40]. Taken together, selection of controls younger than 40 years is desirable when assessing the difference between "healthy" and "tumorous" cases. Additionally, sera of cancer patients appear to be valuable source of useful molecular markers on both extracellular RNA and DNA level. Amplification of extracellular mRNA from serum samples may offer a new approach to cancer diagnostics, monitoring, and pharmacogenomic evaluation. There are numerous reports describing the connection of extracellular mRNA in connection with cancer diagnostics. For instance, Koperski et al. described detection of tumor-related tyrosinase mRNA in melanoma patients [41], Fleischhacker et al. referred similar findings with hnRNP-B1 and HER2/neu-specific mRNA from sera of patients with malignant lung tumor [42], and results of study of March-Villalba et al. indicate that hTERT mRNA is an effective molecular marker for the diagnosis of prostate cancer [43]. Based on our results, although serum MT2A mRNA appears to be a prospective marker for the diagnosis of

prostate cancer, further studies including higher number of patients are required to validate its diagnostic value.

To conclude, taking into consideration specific mRNAs as specific disease markers, automatable SMP-based mRNA isolation is a promising tool for high-throughput analyses. This study outlines the possibility of serum mRNA isolation using this technique, compares it with other isolation protocols, points to its relative easy miniaturization, automation, and shows possible utilization in the detection of prostate cancer.

The work has been supported by NanoBioTECell GACR P102/11/1068, CEITEC CZ.1.05/1.1.00/02.0068, and CEITEC doc 02/2012 (JG). The authors wish to express their thanks to Dr. Roman Hrabec for serum samples collection.

The authors have declared no conflict of interest.

5 References

[1] Swaminathan, R., Butt, A. N., in: Swaminathan, R., Butt, A., Gahan, P. (Eds.), *Circulating Nucleic Acids in Plasma and Serum Iv*, Blackwell Publishing, Oxford 2006, pp. 1–9.

[2] Rosi, A., Guidoni, L., Luciani, A. M., Mariutti, G., Viti, V., *Cancer Lett.* 1988, *39*, 153–160.

[3] Fleischhacker, M., Schmidt, B., *Biochimica et biophysica acta* 2007, *1775*, 181–232.

[4] Reddi, K. K., Holland, J. F., *Proc. Natl. Acad. Sci. USA* 1976, *73*, 2308–2310.

[5] Fleischhacker, M., in: Swaminathan, R., Butt, A., Gahan, P. (Eds.), *Circulating Nucleic Acids in Plasma and Serum Iv*, Blackwell Publishing, Oxford 2006, pp. 40–49.

[6] Fournie, G. J., Courtin, J. P., Laval, F., Chale, J. J., Pourrat, J. P., Pujazon, M. C., Lauque, D., Carles, P., *Cancer Lett.* 1995, *91*, 221–227.

[7] Jahr, S., Hentze, H., Englisch, S., Hardt, D., Fackelmayer, F. O., Hesch, R. D., Knippers, R., *Cancer Res.* 2001, *61*, 1659–1665.

[8] Halicka, H. D., Bedner, E., Darzynkiewicz, Z., *Exp. Cell Res.* 2000, *260*, 248–256.

[9] Kolodny, G. M., *Exp. Cell Res.* 1971, *65*, 313–324.

[10] Kolodny, G. M., Rosentha, L. J., Culp, L. A., *Exp. Cell Res.* 1972, *73*, 65–72.

[11] de la Taille, A., Chen, M. W., Burchardt, M., Chopin, D. K., Buttyan, R., *Cancer Res.* 1999, *59*, 5461–5463.

[12] Garcia-Olmo, D., Ontanon, J., Martinez, E., *Blood* 2000, *95*, 724–725.

[13] Garcia-Olmo, D., Garcia-Olmo, D. C., Ontanon, J., Martinez, E., Vallejo, M., *Histol. Histopathol.* 1999, *14*, 1159–1164.

[14] Garcia-Olmo, D. C., Gutierrez-Gonzalez, L., Samos, J., Picazo, M. G., Atienzar, M., Garcia-Olmo, D., *Ann. Surg. Oncol.* 2006, *13*, 1136–1144.

[15] Garcia-Olmo, D. C., Gutierrez-Gonzalez, L., Ruiz-Piqueras, R., Picazo, M. G., Garcia-Olmo, D., *Cancer Lett.* 2005, *217*, 115–123.

[16] Siegel, R., Naishadham, D., Jemal, A., *CA Cancer J. Clin.* 2013, *63*, 11–30.

[17] Schroeder, F. H., Hugosson, J., Roobol, M. J., Tammela, T. L. J., Ciatto, S., Nelen, V., Kwiatkowski, M., Lujan, M., Lilja, H., Zappa, M., Denis, L. J., Recker, F., Berenguer, A., Maattanen, L., Bangma, C. H., Aus, G., Villers, A., Rebillard, X., van der Kwast, T., Blijenberg, B. G., Moss, S. M., de Koning, H. J., Auvinen, A., Investigators, E., *N. Engl. J. Med.* 2009, *360*, 1320–1328.

[18] Andriole, G. L., Grubb, R. L., Buys, S. S., Chia, D., Church, T. R., Fouad, M. N., Gelmann, E. P., Kvale, P. A., Reding, D. J., Weissfeld, J. L., Yokochi, L. A., Crawford, E. D., O'Brien, B., Clapp, J. D., Rathmell, J. M., Riley, T. L., Hayes, R. B., Kramer, B. S., Izmirlian, G., Miller, A. B., Pinsky, P. F., Prorok, P. C., Gohagan, J. K., Berg, C. D., Team, P. P., *N. Engl. J. Med.* 2009, *360*, 1310–1319.

[19] Masarik, M., Gumulec, J., Sztalmachova, M., Hlavna, M., Babula, P., Krizkova, S., Ryvolova, M., Jurajda, M., Sochor, J., Adam, V., Kizek, R., *Electrophoresis* 2011, *32*, 3576–3588.

[20] Nakayama, A., Fukuda, H., Ebara, M., Hamasaki, H., Nakajima, K., Sakurai, H., *Biol. Pharm. Bull.* 2002, *25*, 426–431.

[21] Wei, H., Desouki, M. M., Lin, S., Xiao, D., Franklin, R. B., Feng, P., *Mol. Cancer* 2008, *7*, 7.

[22] Krizkova, S., Ryvolova, M., Gumulec, J., Masarik, M., Adam, V., Majzlik, P., Hubalek, J., Provaznik, I., Kizek, R., *Electrophoresis* 2011, *32*, 1952–1961.

[23] Lambrechts, A. C., van't Veer, L. J., Rodenhuis, S., *Ann. Oncol.* 1998, *9*, 1269–1276.

[24] Chan, R. W. Y., Wong, J., Chan, H. L. Y., Mok, T. S. K., Lo, W. Y. W., Lee, V., To, K. F., Lai, P. B. S., Rainer, T. H., Lo, Y. M. D., Chiu, R. W. K., *Clin. Chem.* 2010, *56*, 82–89.

[25] Anker, P., Mulcahy, H., Stroun, M., *Int. J. Cancer* 2003, *103*, 149–152.

[26] Garcia, J. M., Garcia, V., Pena, C., Dominguez, G., Silva, J., Diaz, R., Espinosa, P., Citores, M. J., Collado, M., Bonilla, F., *RNA* 2008, *14*, 1424–1432.

[27] Pfaffl, M. W., *Nucleic Acids Res.* 2001, *29*, e45.

[28] Jost, R., Berkowitz, O., Masle, J., *Biotechniques* 2007, *43*, 206–211.

[29] Sergueeva, Z., Dow, S., Collins, H., Parrish, M. L., *19th International Molecular Med Tri-Con*, Cambridge Healthtech Institute, San Francisco, USA 2012.

[30] Hasselmann, D. O., Rappl, G., Tilgen, W., Reinhold, U., *Clin. Chem.* 2001, *47*, 1488–1489.

[31] Choudhury, A. D., Eeles, R., Freedland, S. J., Isaacs, W. B., Pomerantz, M. M., Schalken, J. A., Tammela, T. L. J., Visakorpi, T., *Eur. Urol.* 2012, *62*, 577–587.

[32] Parekh, D. J., Ankerst, D. P., Troyer, D., Srivastava, S., Thompson, I. M., *J. Urol.* 2007, *178*, 2252–2259.

[33] Roobol, M. J., Schroder, F. H., Crawford, E. D., Freedland, S. J., Sartor, A. O., Fleshner, N., Andriole, G. L., *J. Urol.* 2009, *182*, 2112–2120.

[34] Yamasaki, M., Nomura, T., Sato, F., Mimata, H., *Oncol. Rep.* 2007, *18*, 1145–1153.

[35] Athanassiadou, P., Bantis, A., Gonidi, M., Athanassiades, P., Agelonidou, E., Grapsa, D., Nikolopoulou, P., Patsouris, E., *Tumori* 2007, *93*, 189–194.

3576 *Electrophoresis* 2011, *32*, 3576–3588

Michal Masarik[1]
Jaromir Gumulec[1]
Marketa Sztalmachova[1,2]
Marian Hlavna[1]
Petr Babula[2,3]
Sona Krizkova[2,3]
Marketa Ryvolova[2,3]
Michal Jurajda[1]
Jiri Sochor[2,3]
Vojtech Adam[2,3]
Rene Kizek[2,3]

[1]Department of Pathological Physiology, Faculty of Medicine, Masaryk University, Brno, Czech Republic
[2]Department of Chemistry and Biochemistry, Mendel University in Brno, Brno, Czech Republic
[3]Central European Institute of Technology, Brno University of Technology, Brno, Czech Republic

Received June 5, 2011
Revised June 30, 2011
Accepted July 2, 2011

Research Article

Isolation of metallothionein from cells derived from aggressive form of high-grade prostate carcinoma using paramagnetic antibody-modified microbeads off-line coupled with electrochemical and electrophoretic analysis

Prostate cancer with altered zinc(II) cell metabolism is the second most frequently diagnosed cancer in developed countries. The alterations of zinc(II) metabolism can influence metabolism of other metal ions and can also be associated with the expression and translation of metal-binding proteins including metallothioneins. The aim of this article was to optimize immunoseparation protocol based on paramagnetic beads conjugated with protein G for the isolation of metallothionein. Isolated metallothionein was determined by differential pulse voltammetry Brdicka reaction and SDS-PAGE. Optimal conditions: antigen-binding time – 60 min, temperature – 70°C, and buffer composition and pH – acetate buffer, pH 4.3, were determined. Under the optimized conditions, lysates from 22Rv1 prostate cancer cells treated with various concentrations of cadmium(II) and copper(II) ions were analyzed. We observed strong correlation in all experimental groups and all lysate types (r>0.83 at p<0.041) between metallothionein concentration related to viability and concentration of copper(II) ions and cadmium(II) ions in medium. Moreover, the results were compared with standard sample preparation as heat treatment and SDS-PAGE analysis.

Keywords:
Immunoprecipitation / Metallothionein / Microparticles / Microseparation / Prostate cancer
DOI 10.1002/elps.201100301

1 Introduction

Prostate cancer is the second most frequently diagnosed cancer in developed countries and the third most common cancer causing death in men. It is not surprising that numerous researchers focus on studying the origin and progression of this type of cancer. Based on the current research, alterations in zinc(II) cell metabolism belong to the most interesting findings. This feature is associated with the changing expression of major zinc-protein-transporter called ZIP1 [1]. However, there are other proteins connected with metal homeostasis in a cell including metallothioneins (MTs). These proteins belonging to the group of intracellular and low-molecular-mass proteins (from 2 to 16 kDa) were discovered in 1957 when Margoshes and Vallee isolated them from a horse renal cortex tissue [2, 3].

Based on their metal-inducible properties and their high affinity for metal ions, homeostasis of heavy metal levels is probably MT's most important biological function. MT can also serve as "maintainers" of the cell redox pool [4]. In mammals, these proteins may serve as a reservoir of metals (mainly zinc and copper) for the synthesis of apoenzymes and zinc-finger transcription regulators. Moreover, new roles of these proteins have been discovered including those needed in the carcinogenic process [5–10]. Isolation, separation, detection, and/or quantification of MT are not easy tasks for modern bioanalytical chemistry. From the point of view of MT separation, electrophoretic methods have several advantages [11–24].

Numerous methods and approaches have been developed to shorten the time of isolation and to obtain biologically important molecules with sufficient purity to be

Correspondence: Dr. Michal Masarik, Department of Pathological Physiology, Faculty of Medicine, Masaryk University, Kamenice 5, CZ-625 00 Brno, Czech Republic
E-mail: masarik@med.muni.cz
Fax: +420-5-4949-4340

Abbreviations: AO, Acridine orange; **MP,** paramagnetic or superparamagnetic particle/bead; **MT,** metallothionein; **MTT,** 3-(4,5-dimethylthiazol-2-yl)-2,5-diphenyltetrazolium bromide

Colour Online: See the article online to view Figs. 1, 3, 4 and 6 in colour.

analyzed by ultra-sensitive analytical tools [25–28]. Paramagnetic or superparamagnetic particles/beads (MPs) represent promising tool for this purpose [29–31]. MPs, whose size is ranging from nanometer to millimeter, respond to external magnetic field and facilitate bioactive molecules binding because of their affinity for the MP-modified surface made of biological components [32–35]. The time needed to get target biomolecule is also reduced due to the fact that binding of the biomolecule by MPs can protect it against physical and biological damage, e.g. denaturation [36]. Physico-chemical properties of MPs (e.g. their size, surface topography) are important to evaluate their usage in biology [37–45]. The mostly used MPs in biosensors applications are superparamagnetic nanoparticles composed of ferrous oxide or ferric oxide [46]. Nanoparticles from ferric oxide also provide surface suitable for biomolecule binding.

The aim of this article is to optimize immunoseparation protocol based on paramagnetic beads with protein G for the isolation of MT. Isolated MT is determined by differential pulse voltammetry Brdicka reaction and SDS-PAGE. Further, the optimized protocol is used for the isolation of MT in lysates of 22Rv1 prostate cancer cells treated with cadmium(II) and copper(II) ions, due to the fact that prostate cancer cell has altered metal ions metabolism.

2 Materials and methods

2.1 Chemicals

RPMI-1640 medium, fetal bovine serum (FBS)-mycoplasma free, *penicillin/streptomycin*, and trypsin EDTA were purchased from PAA Laboratories GmbH (Austria). Magnetizable microparticles modified with protein G were purchased from Invitrogen (Carlsbad, CA, USA). EDTA, copper (II) sulfate pentahydrate ($CuSO_4 \cdot 5H_2O$), cadmium (II) nitrate tetrahydrate ($Cd(NO_3)_2 \cdot 4H_2O$) and bovine serum albumin (BSA), acetic acid, sodium acetate, citric acid, sodium citrate, DTT, and all other chemicals of ACS purity were used and purchased from Sigma Aldrich (St. Louis, MO, USA), unless noted otherwise. Polyclonal rabbit antibody against MT1A/MT2A was purchased from Santa Cruz Biotechnology (Santa Cruz, CA, USA). Monoclonal mouse antibody against MT was purchased from DAKO (Carpinteria, CA, USA).

2.2 Cell culture and cultivation conditions

Human prostate carcinoma epithelial cell line 22Rv1 derived from a xenograft that was serially propagated in mice after castration was used in this study. The cell line was obtained from HPA Culture Collections, Salisbury, UK. 22Rv1 cells were cultured in RPMI-1640 medium with 10% FBS. Medium was supplemented with *penicillin* and *streptomycin* (1 U/mL), and the cells were maintained at 37°C in a humidified incubator with 5% CO_2. Subcultivations of the cells were carried out after 21 days. Once the cells grew up to ~75% confluence of the culture, the cultivation medium was replaced by fresh medium for 24 h to synchronize cell growth. The cells were then exposed to copper sulfate (0–800 μM) or cadmium nitrate (0–150 μM) for 48 h.

2.3 Measurements of cell viability – 3-(4,5-dimethylthiazol-2-yl)-2,5-diphenyltetrazolium bromide assay

The 3-(4,5-Dimethylthiazol-2-yl)-2,5-diphenyltetrazolium bromide (MTT) assay was used to determine cell viability. MTT is a yellow water-soluble tetrazolium dye that is reduced by living cells to a purple formazan. Cell suspension in cultivation medium was diluted to obtain cell density of 5×10^3 cells/mL and transferred with a multichannel pipette to wells of sterile 96-well microtitter plates. Then, plates were incubated for 2 days at 37°C to ensure cell growth. Then, copper(II) and cadmium(II) solutions were prepared in the concentration range of 0–150 μM for cadmium(II) ions and 0–800 μM for copper(II) ions. The highest applied concentrations have lethal effect for all cells and the lowest has no effect on cell growth. Plates were incubated for 24 h. All medium was removed and new was added three times per 24 h. Then, wells were fed with 200 μL of medium with 50 μL of MTT (5 mg/mL in PBS) and incubated for 4 h in a humidified atmosphere at 37°C, wrapped in aluminium foil. Subsequently, medium-MTT was exchanged with 200 μL of DMSO (Sigma-Aldrich) to dissolve MTT–formazan crystals. Finally, 25 μL of glycine buffer was added to all wells and absorbance was recorded at 570 nm by VersaMax microplate reader (Molecular Devices, Sunnyvale, CA, USA).

2.4 Cell growth and proliferation assay using impedance measurement with xCELLigence system

The xCELLigence system was used according to the instructions of the supplier (Roche Applied Science and ACEA Biosciences) [47]. The xCELLigence system consists of four main components: the RTCA analyzer, the RTCA DP station, the RTCA computer with integrated software, and disposable E-plate 16. First, we determined the optimal seeding concentration for proliferation and cytotoxic assay. After seeding the total number of cells in 200 μL medium to each well in E plate 16, the attachment, proliferation, and spreading of the cells were monitored every 15 min. Approximately, 20 h after seeding, when the cells were in log growth phase, the cells were exposed to copper(II) ions (0–800 μM) and cadmium(II) ions (0–150 μM). Control wells contained cultivation medium only without additions of metal ions. All experiments were carried out for 200 h.

2.5 RNA isolation, cDNA preparation

For RNA isolation, High pure total RNA isolation kit (Roche, Switzerland) was used. Cell line medium was removed and the samples were washed twice with 5 mL of ice-cold PBS. Cells were scraped, transferred to clean tubes, and centrifuged at 20 800 × *g* for 5 min at 4°C. Subsequently, lysis buffer was added and RNA isolation was carried out according to the manufacturer's instructions. Isolated RNA was used for cDNA synthesis. Total RNA (app. 600 ng) was transcribed using Transcriptor first strand cDNA synthesis kit (Roche, Switzerland) according to the manufacturer's instructions. Prepared cDNA (20 μL) was diluted with RNase-free water to 100 μL and directly analyzed by real-time polymerase chain reaction (PCR).

2.6 Real-time reverse-transcription PCR (RT-PCR)

Real-time reverse-transcription PCR was performed in triplicates using the TaqMan gene expression assay system with the 7500 real-time PCR system (Applied Biosystems, USA). The amplified DNA was analyzed by the comparative Ct method using β-actin as an endogenous control. The primer and probe sets for β-actin (Assay ID: Hs00185826_m1), for MT1A (Assay ID: Hs00185826_m1), and for MT2A (Hs00794796_m1) were selected from TaqMan gene expression assay. Real-time PCR was performed under the following amplification conditions: total volume, 20 μL; initial denaturation, 95°C/10 min; then followed by 45 cycles at 95°C/15 s, 60°C/1 min.

2.7 Preparation of cell lysates

2.7.1 RIPA lysates

Cell line medium was removed and the samples were washed twice with 500 μL of ice-cold PBS. Cells were transferred to new tubes and centrifuged at 2500 rpm for 5 min at room temperature. Then, the cell pellet was transferred to 1.5-mL tubes and washed twice with PBS and centrifuged at 2500 rpm for 5 min again. RIPA buffer (Cell Signaling Technology, Boston, MA, USA) was added and the tubes were vortexed for 15 min on ice. Then, the samples were centrifuged at 14 000 rpm for 15 min at 4°C and the obtained supernatant was used for subsequent microbead-based measurements.

2.7.2 Heat denatured lysates

Approximately, 0.01 g of the cells in 500 μL of PBS was mechanically disintegrated using the Ultra-Turrax T8 homogenizer (Ika, Germany) and placed in an ice bath for 3 min at 25 000 rpm. The cell homogenate was kept at 99°C in a thermomixer (Eppendorf 5430, Germany) for 15 min with shaking. The denatured homogenates were centrifuged at 15 000 × *g* for 30 min at 4°C (Eppendorf 5402, Germany). Heat treatment effectively denatures and removes thermolabile and high-molecular-mass proteins from the samples [48].

2.8 Total protein quantification – Biuret method

Total proteins in the samples of human carcinoma prostate cell line 22Rv1 were determined using the automated biochemical analyzer BS-200 (Mindray, China). Reagent and sample handling was controlled by BS-200 software (Mindray, China). The commercially available kit from Medesa (Czech Republic) was used. The standard calibration curve was prepared from BSA by diluting the stock solution (1 mg/mL) with 0.1 M phosphate buffer, pH 7.0. The concentration range from 0.97 to 1000 μg/mL was prepared. To the 180 μL of the Biuret kit solution, 45 μL of the sample was added. The solution was mixed and incubated for 10 min at 37°C. The absorbance was measured by spectrophotometer at 510 nm (BS-200, Mindrays P. R. China).

2.9 Immunoprecipitation protocol

The immunoprecipitation protocol with subsequent electrochemical analysis is shown in Fig. 1. The magnetic beads conjugated with protein G (DB-G) (10 μL) were washed twice in 100 μL of PBS buffer. Polyclonal rabbit antibody against MT 1A/2A (1 μg) was added to DB-G and the Ab–DB-G complex was incubated for 60 min at room temperature using thermomixer at approx. 800 rpm to avoid bead sedimentation. During this incubation, the antibody is bound to the Dynabeads via its Fc region. Subsequently, tubes were placed on a magnet, and thus, the beads were migrated to the side of the tube facing the magnet and allowed to remove the supernatant easily. Unbound antibody solution was removed and the samples were washed with 100 μL of PBS. Then, 10 μL of the sample was added and the tubes were kept at room temperature in a shaker for 60 min for MT immunoprecipitation. Tubes were placed on the magnet, the supernatant was removed, and beads were washed three times with 100 μL of PBS. Then, 10 μL of acetate buffer, pH 4.3, was added to the bead–sample complex and incubated at 70°C for 15 min using thermomixer at approx. 800 rpm. Subsequently, the supernatant with released MT was removed and transferred to new tubes prior to the following measurements.

2.10 Differential pulse voltammetry – Brdicka reaction

Differential pulse voltammetric measurements were performed with 747 VA Stand instrument connected to 746 VA Trace Analyzer and 695 Autosampler (Metrohm,

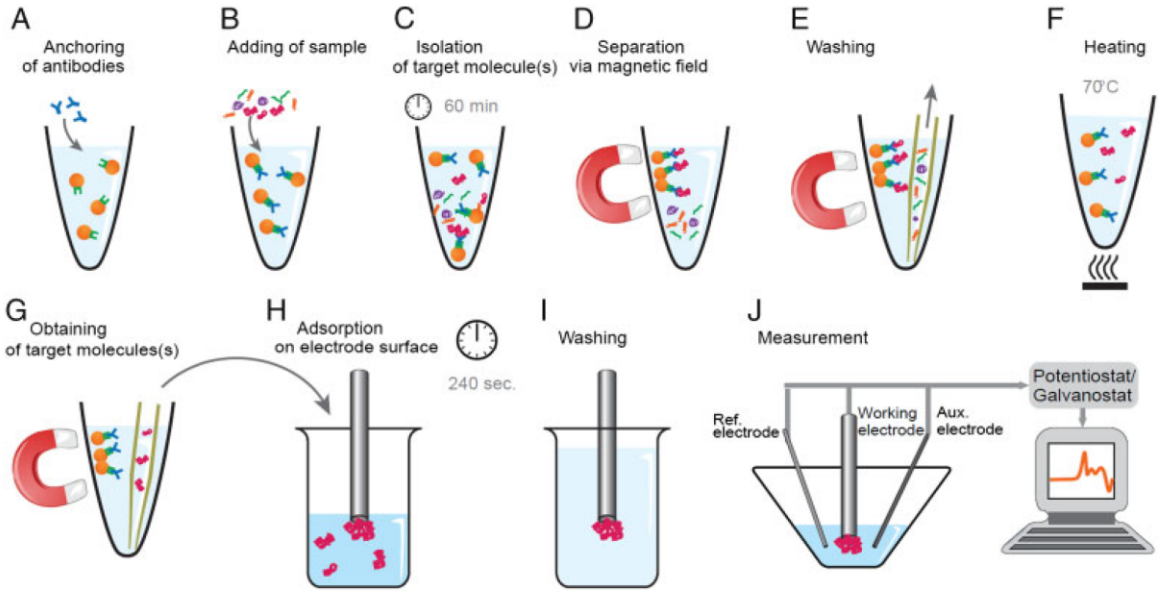

Figure 1. Paramagnetic particles separation and detection. (A) First, protein-G particles are being anchored with rabbit anti-MT IgG. (B) Sample is added to complex antibody-protein-G particle and (C) incubated for 1 h. (D) Further, tube is placed on the magnet, complex MT-IgG-particle is fixed on a side of test tube and (E) sample is washed by PBS, pure complex MT-IgG-particle remains in the tube. (F) Sample is heated to 70°C for 15 min, and MT is released from complex of IgG-particle. (G) Sample is placed on magnet, supernatant with MT (H) is transferred to vessel containing acetate buffer (pH = 4.3) and hanging mercury drop electrode is immersed. (H) Sample is being adsorbed onto working electrode for 240 s. (I) Electrode with the adsorbed protein is washed and transferred into electrochemical cell. (J) Differential pulse voltammetry Brdicka reaction measurement is carried out.

Switzerland), using a standard cell with three electrodes and cooled sample holder (4°C). A hanging mercury drop electrode (HMDE) with a drop area of 0.4 mm^2 was the working electrode. An Ag/AgCl/3M KCl electrode was the reference and glassy carbon electrode was auxiliary electrode. For data processing, GPES 4.9 software supplied by EcoChemie was employed. Brdicka supporting electrolyte containing 1 mM $Co(NH_3)_6Cl_3$ and 1 M ammonia buffer ($NH_3(aq)+NH_4Cl$, pH = 9.6) was used. The supporting electrolyte was exchanged after each analysis. The parameters of the measurement were as follows: initial potential, −0.7 V; end potential, −1.75 V; modulation time, 0.057 s; time interval, 0.2 s; step potential, 2 mV; modulation amplitude, −250 mV; E_{ads} = 0 V; volume of injected sample, 20 μL (100 × diluted sample with 0.1 M phosphate buffer, pH 7.0). All experiments were carried out at 4°C. Temperature was reached using thermostat Julabo F25 (Labortechnik GmbH, Germany) [49–53].

2.11 SDS-PAGE

The electrophoresis was performed according to Laemmli using a Mini Protean Tetra apparatus with a gel dimension of 8.3 × 7.3 cm (Bio-Rad, USA) [54]. First, we poured 10% *m/V* running gel and then 5% *m/V* stacking gel. The gels were prepared from 30% *m/V* acrylamide stock solution with 1% *m/V* bisacrylamide (SERVA, Germany). The polymerization of the running or stacking gels was carried out at room temperature for 45 min. Prior to analysis, the samples were mixed with reducing (DTT – final concentration, 400 mM) sample buffer in 4:1 ratio. The samples were boiled for 5 min and then the sample was loaded onto the gel. For the determination of molecular mass, the protein ladder, broad, or lower range (Bio-Rad) was used. The electrophoresis ran at 80 V for 20 min subsequently increased to 120 V for 1 h (Power Basic, Bio-Rad) in tris-glycine buffer (0.025 M Trizma-base, 0.19 M glycine, and 0.0035 M SDS, pH = 8.3). Silver staining of the gels was performed using Bio-Rad Silver stain kit (Bio-Rad) according to Merril et al. [55].

2.12 Fluorescence microscopy and cell staining

For fluorescence microscopy, cells were cultivated directly on microscope glass slides (75 × 25 mm, thickness 1 mm, Fischer Scientific, Czech Republic) in Petri dishes in cultivation media, which are described above (Section 2.2). Cells were transferred directly onto the slides, which were submerged in cultivation media, and further cultivated. After treatment, microscope glass slides with monolayer of cells were removed from Petri dishes, rinsed with cultivation medium and PBS buffer, and used for staining and fluorescence microscopy.

Acridine orange (AO, Sigma-Aldrich) was used as a general cytological stain, which is suitable for the determination of lysozomal proton pump activity, changes in the

pH and detection of DNA/RNA. A working solution (5 μg/mL) was prepared by diluting the stock solution (1 mg/mL) with the PBS buffer (pH = 7.2). Cells were stained and incubated for 30 min at 37°C and dark. Further, the cells on microscope glass slide were washed with PBS buffer (pH = 7.2) and observed using fluorescence microscope (Axioskop 40, Carl Zeiss, Germany) equipped with a broadband excitation and a set of filters (FITC-DAPI, Carl Zeiss). Photographs were taken using digital camera (Olympus Camedia 750, Olympus, Japan).

For the detection of apoptotic and death cells, double staining by Hoechst 33342 and propidium iodide (both Sigma-Aldrich) was used. Hoechst 33342 stains condensed chromatin of apoptotic cells, whereas propidium iodide stains dead cells only. Hoechst 33342 stains chromatin of normal cells weakly only. Working solutions of both stains were prepared by diluting the stock solutions (Hoechst 33342, 5 mg/mL; propidium iodide, 1 mg/mL) with the PBS buffer (pH = 7.2) to the final concentrations of 5 μg/mL (Hoechst 33342) and 1 μg/mL (propidium iodide). After incubation (30 min at 37°C and dark), the cells were washed with PBS buffer (pH = 7.2) and observed under a fluorescence microscope (Axioskop 40, Carl Zeiss) equipped by FITC and DAPI filters (Carl Zeiss). Photographs were taken using digital camera (Olympus Camedia 750, Olympus).

2.13 Determination of cadmium(II) and copper(II) ions

To prepare the samples, a microwave digestion was used according to the recently published article [56]. Briefly, the mineralization of samples took place in a microwave system Multiwave3000 (Anton-Paar GmbH, Austria). Cells (100 μL) were placed into glass vials MG5 and 900 μL of nitric acid (w/w, 65%) was added. Prepared samples were sealed and placed into the rotor 64MG5 (Anton-Paar GmbH). Rotor with the samples was inserted into the microwave system and the microwave digestion was carried out under the following conditions: power, 100 W; ramp, 10 min; hold, 99 min, cooling, 10 min; maximum temperature, 80°C. The sample preparation for subsequent electrochemical measurements was as follows: 15 μL mineralized sample was pipetted into Eppendorf tubes with 985 μL acetate buffer (pH = 5.00). A blank digestion was simultaneously carried out the same way.

Electrochemical analyzer (Metrohm AG, Switzerland) was used for the determination of Cd(II) and/or Cu(II) [57]. The analyzer (757 VA Computrace, Metrohm, Switzerland) employs a conventional three-electrode configuration with a hanging mercury drop electrode working electrode: 0.4 mm^2, Ag/AgCl/3M KCl as reference electrode, and a platinum auxiliary electrode. Differential pulse voltammetric measurements were carried out under the following parameters: deoxygenating with argon, 60 s; deposition potential, −1.3 V; time of deposition, 240 s; start potential, −1.3 V; end potential, 0.15 V; pulse amplitude, 0.025 V; pulse time, 0.04 s; step potential, 5.035 mV; time of step potential, 0.3 s.

2.14 Statistical data analysis

Software Excel 2007 (Microsoft, USA) was used to arrange the data set. Software Statistica 9.1 (StatSoft, USA) was used to perform statistical analysis and chart construction. Viability was determined by linear regression from linear part of MTT ("MTT viability") and by fitting real-time impedance chart in $t = 120$ h, data transposition and regression from linear part of curve ("Normalized impedance"). MT, free, and total metal content are expressed as a relative ratio of electrochemically determined signal peak/MTT assay viability normalized to the range of 0–100%. The signal intensity of silver-stained gels was determined using ImageJ 1.45 software (NIH, USA) as an area under the curve normalized to the range of 0–100%. Simple linear correlations were performed to reveal the relationships between variables. Unless noted otherwise, a level of statistical significance was designated to $p = 0.05$. In all charts, whisker bars represent one standard deviation.

3 Results and discussion

So-called double surface techniques, where the binding of antigen (in case of proteins) or hybridization process (in case of nucleic acids) is carried on the (first) surface of magnetic beads and the determination is performed on the second surface (surface of the electrode), have many advantages. In the last decade, they were applied for many purposes [35, 58–67]. Our article demonstrates immunoseparation of MT using paramagnetic beads conjugated to the protein G, which has not been performed before. Our paramagnetic bead-based immunoassay for MT determination combines the features of specific immunoseparation with subsequent very sensitive voltammetric detection (Fig. 1). Advantages of both steps are discussed in the previously published articles [7, 51]. The MT antibody is immobilized with high affinity on protein G-conjugated paramagnetic particles via its Fc fragment and then MT is selectively isolated. After the release from the particles, MT was electrochemically determined. The sensitivity of paramagnetic bead immunoseparation assay is strongly dependent on various conditions such as the concentration of antibody–antigen complex; therefore, we carried out several experiments to optimize experimental conditions such as the amount of paramagnetic beads, the type of anti-MT antibody, and others for the most sensitive and selective determination of MT.

3.1 Optimization of immunoseparation protocol

It is well known that the sensitivity and effectiveness of the immunoprecipitation technique can be easily improved if

the optimal conditions of individual steps of the protocol are chosen. To combine the magnetic bead-based immunoprecipitation procedure with electrochemical detection of isolated MT, we first studied the optimal type of MT antibody (Fig. 2A). The isolated MT was subsequently determined using differential pulse voltammetry Brdicka reaction and verified using SDS-PAGE.

In the previous experiments, we have shown that chicken egg yolk IgY anti-MT antibody (HENA, Czech Republic) led to significantly higher signal in Western blot assay as compared with other anti-MT antibodies [7]. However, according to the paramagnetic beads' manual, protein G or protein A beads do not bind to the chicken IgY antibodies. Therefore, we decided to test binding affinity of a mouse monoclonal antibody (DAKO) and rabbit polyclonal antibody (Santa Cruz Biotechnology). Subsequently, we measured signal of mouse antibody- and rabbit antibody-separated MT using differential pulse voltammetry. Only small differences in the intensity of positive samples 1 and 2 (RIPA cell lysate of 22Rv1) containing a high amount of MT, measured using both antibodies, were observed. Usage of rabbit polyclonal antibody gave slightly, but not significantly, higher results compared with mouse monoclonal antibody. This could be associated with some nonspecific interactions of polyclonal antibodies with the sample. Samples 3 and 4 are blank controls of BSA in the concentration of 50 μg/mL. White boxes in Fig. 2A correspond to the mouse monoclonal antibody and the grey ones correspond to rabbit polyclonal antibody. Due to slightly higher signal, rabbit polyclonal antibody was used in the following experiments.

Further, the best antigen-binding time (Fig. 2B) was optimized. We used MT standard in the concentration of 100 μg/mL as an antigen. The time interval from 15 to 90 min was tested and no significant differences were observed in tested time intervals. Moreover, electrochemical experiments were verified by SDS-PAGE technique as it is shown in the inset of Fig. 2B. We can see bands at 7 kDa corresponding to MT monomer. Based on SDS-PAGE, no significant change was found in the amount of the isolated MT. Based on the fact that the method can be used for the analysis of real samples, 60 min long time interval was used.

Finally, we tested optimal temperature (Fig. 2C) and pH (Fig. 2D) to release MT from the surface of paramagnetic beads. For both optimization steps, 100 μg/mL MT standard was used and the samples were measured using differential pulse voltammetry. The temperature was tested within the range from 0 to 70°C. The highest signal intensity was obtained at 70°C, which is in good agreement with other articles, where elevated temperature was optimal for releasing MuTS protein from the surface paramagnetic beads [60, 64]. Further, we studied the influence of pH. The tested pH range was from 1.2 to 10.5. The optimal pH was determined as 4.3 based on the results shown in Fig. 2D.

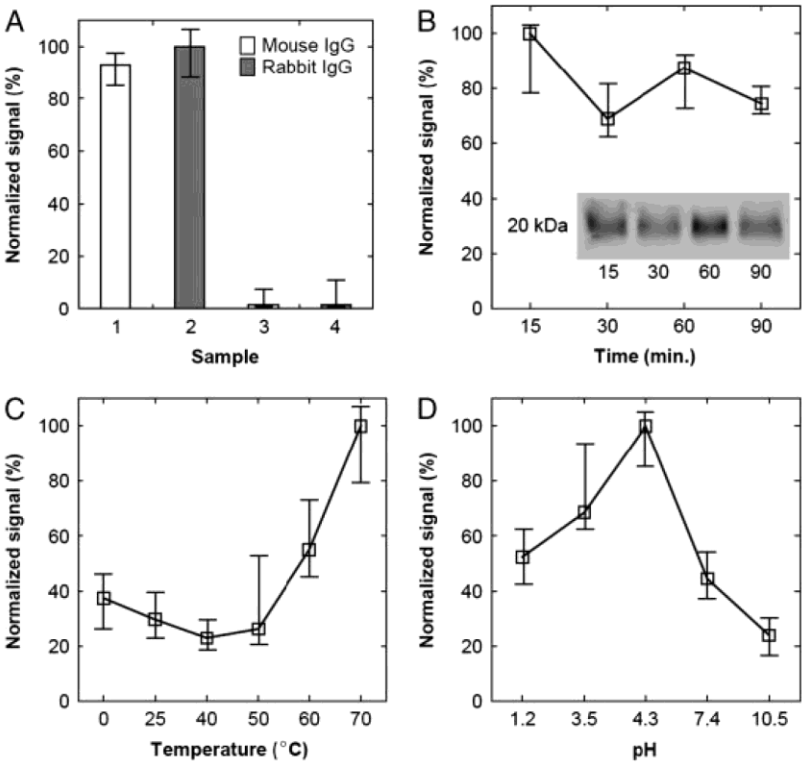

Figure 2. Optimization steps. (A) Antibody optimization. Samples 1 and 3 are 22Rv1 cell lines separated with mouse polyclonal IgG. Samples 2 and 4 are blank controls (BSA, 50 μg/mL) separated with rabbit polyclonal IgG. (B) Binding time optimization. After antibody binding to protein G at paramagnetic beads, we tested binding times (15, 30, 60, and 90 min) for antigen (MT standard, 50 μg/mL). (C) Denaturation temperature optimization (Fig. 1F). Testing of optimal releasing temperatures (0, 25, 40, 50, 60, and 70°C) for the isolation of MT. (D) Releasing pH optimization. Testing of optimal pH in releasing step (1.2, 3.5, 4.3, 7.4, and 10.5) for the isolation of MT.

Temperature of 70°C and pH value of 4.3 were used for the release of MT by immunoprecipitation procedure (Fig. 1). Under these optimized conditions, we observed 98% MT standard yield (determined MT concentration, 98.5 ± 6.5 μg/mL; MT standard concentration, 100 μg/mL), which shows that rabbit polyclonal IgG is as an effective tool for MT isolation under these conditions.

The usage of IgG-modified particles has been reviewed several times [37, 68–73]. Chu et al. reported an electrochemical immunoassay based on silver on colloidal gold labels, which, after silver metal dissolution in an acidic solution, was indirectly determined by ASV at a glassy-carbon electrode [74]. The method was evaluated for a noncompetitive heterogeneous immunoassay of using IgG as a model analyte. The anodic stripping peak current of silver depended linearly on the IgG concentration over the range of 1.66–27.25 ng/mL in a logarithmic plot. A detection limit as low as 1 ng/mL human IgG was achieved. The method was applied to detect *Schistosoma japonicum* antibodies (SjAb) in rabbit serum [75]. A detection limit as low as 3.0 ng/mL *S. japonicum* antibodies was achieved. A potentiometric immunosensor based on gold nanoparticle labels and an ion-selective microelectrode was reported by Chumbimuni-Torres et al. [76]. This immunosensor is based on a sandwich immunoassay where the target mouse IgG antigen is captured by the primary anti-mouse gold substrate modified by IgG antibodies, followed by adding a secondary anti-mouse IgG antibody conjugated to gold nanoparticle tags and by catalytic silver enlargement onto the gold labels. Silver-enhanced gold nanoparticle labels were also used to develop conductive immunosensors with ultrasensitive detection of human IgG down to the 0.2 pM level [76]. The method holds promise for creating miniaturized on-chip protein arrays. An electrochemical immunoassay method based on Au nanoparticle-labeled immunocomplex enlargement was reported by Zhou et al. [77]. When the aggregates formed from nano-Au-labeled goat-anti-human C-3 and nano-Au-labeled rabbit-anti-goat IgG were immobilized on the electrode surface by the sandwich method (antibody/antigen/aggregate), the electrochemical signal of the electrode was enlarged greatly. The reported immunosensor could quantitatively determine complement C-3 in the range of 0.12, similar to 117.3 ng/mL, and the detection limit was 0.02 ng/mL.

3.2 Viability and impedance assays

After the optimization of experimental conditions, we were interested to test the system on real samples as cell extracts. Cell lines derived from metastatic dissemination as PC-3, LNCaP, or DU-145 belong to the most widely used models of prostate cancer cells. In contrast, newly created cell line 22Rv1 is derived from high-grade primary tumor from patient with bone metastases [78]. 22Rv1 cell line among others has fewer chomosomes and simpler chromosome with low level of variation. Therefore, this cell line represents more precisely high-risk form of tumor, in which it is desirable to focus on understanding the pathogenesis of a disease and development of targeted therapeutic strategies [79–81].

To follow the biochemical changes in cells, a method for measuring their viability is needed. Real time and continuous monitoring using xCELLigence system allows label-free assessment of cell proliferation, viability, and cytotoxicity, revealing the physiological state of the cells and decreases the costs in comparison to the conventional cell analysis. The xCELLigence system utilizes impedance readout to noninvasively quantify cellular status in real time [82–84]. The cells are seeded in E-plates that are integrated with gold microelectrode arrays. Due to the application of a low potential, alternating current signal leads to the generation of an electric field between the electrodes, which interacts with the ionic environment of the cultivation medium inside the wells and is differentially modulated by the numbers of cells covering the electrodes, the morphology of those cells, and the strength of cell attachment. The impedance readout detects and quantifies discrete changes in cell morphology and adhesion, allowing for an unbiased detection of specific cellular processes in real time [85, 86].

We compared this xCELLigence system with one of the commonly used methods called MTT viability end-point assay. This assay is widely used for the determination of cytotoxic effect of chemicals. Primarily, it was necessary to determine the optimal cell concentration for proliferation and viability assays (MTT test). Cells in count of 5000, 10 000, 15 000, 20 000, 30 000, and 40 000 per well were seeded in E-plate 16 or sterile 96-well microtiter plate and the measurement of relative impedance in case of xCELLigence system or absorbance in case of MTT was carried out (data not shown). It was found out that the response determined in the well containing 5000 cells was the best for the analysis of proliferation and cytotoxic assay of heavy metals. 22Rv1 cells were then treated with cadmium(II) (Fig. 3A and C) and copper(II) ions (Fig. 3B and D) in concentrations: 0 (control), 25, 50, 100, and 150 μM for cadmium(II) and 0 (control), 100, 300, 500, and 800 μM for copper(II). The observed changes in adhesion, spreading, and proliferation were recorded as relative impedance. We observed linear increase of the relative impedance in control samples of cells (cells without cadmium or copper – red line), which were in logarithmic growth phase. Then, the growing cells reached the stationary phase, where the impedance values remain nonchanged. After this, the impedance value decreased due to cells decay. After addition of heavy metal ions, slight increase in the impedance values was observed. This phenomenon is caused by morphological changes in cell structure. The xCELLigence system is able to detect not only the number of cells or proliferation potential but also spreading and morphology changes of cells [82, 84]. After 50 h long cadmium(II) treatment, a decrease in impedance of all experimental groups was determined due to the cytotoxic effect of metal. On the other hand, the copper(II) (100 and 300 μM) treatment lead to the further increase of impedance, which can be associated with the

Electrophoresis 2011, *32*, 3576–3588 **Proteomics and 2-DE** 3583

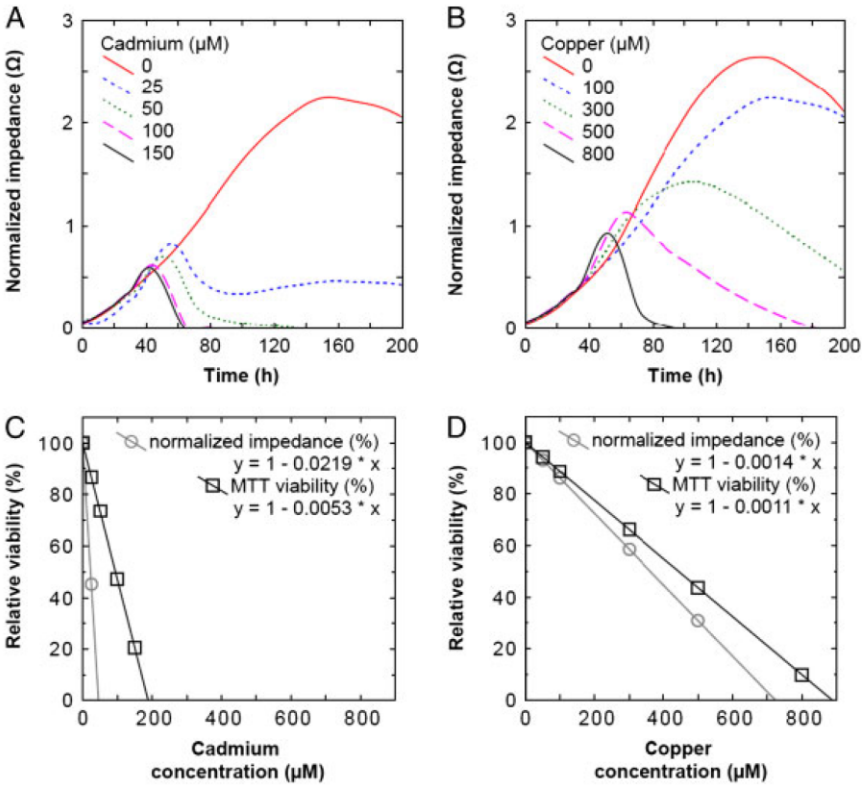

Figure 3. (A) Real-time cell growth monitoring, impedance measurement. Normalized impedance (cell index) reflects cell content in time. In cadmium treatment, clearly visible is its toxic effect on cells in the concentration of $<50\,\mu M$. In contrast, copper influences the cell line growth significantly less; visible inhibitory effect is present in the concentrations of $>300\,\mu M$. (B) Comparison of MTT viability assay versus real-time cell growth monitoring system. Equations are created by regression from linear part of MTT ("MTT viability") and by fitting real-time impedance chart in $t = 120$ h, data transposing and regression from linear part of curve ("Normalized impedance"). Steeper function represents data calculated from real-time impedance monitoring, similar trend is observed in both metals.

essentiality of copper(II) ions and their positive effect on cell growth.

Figure 3C and D shows the dependence of metal concentration on relative viability. The changes between the MTT and the xCELLigence assay are caused by different evaluations of the results. The MTT assay is the so-called end-analysis and we determined the absorbance intensity after 72 h from seeding, whereas using xCELLigence system we can monitor cell proliferation in real time. To obtain very similar results, 800 cell samples per replicate would need to be prepared and analyzed by MTT assay, which would be very laborious, high-cost, and time-consuming. Compared with MTT-based viability assay, the real-time monitoring of cell proliferation, spreading, and morphology using xCELLigence system gives us the possibility to detect minor changes in the cell structure and in the response of cells to chemical treatment, impossible to achieve by the currently established end-point analysis.

3.3 Fluorescence microscopy of 22Rv1 cells treated by copper(II) and cadmium(II) ions

Based on the previously mentioned facts, we also aimed our attention on morphology of the treated cells. Treatment of 22Rv1 cells with cadmium(II) ions led not only to significant changes in cell viability and changes in growth (formation of clusters of densely packed cells) but also to biochemical changes including activity of lysozomal proton pump and intracellular pH (Fig. 4). Control cells formed the clusters of densely packed cells with average activity of lysozomal proton pump. The ion concentrations of 25 and 50 μM caused the formation of very compact clusters; peripheral cells of these clusters demonstrated higher activity of lysozomal proton pump as well as changes in pH in comparison with control cells, whereas cells localized in the center of the clusters exhibited only average activity of lysozomal proton pump and minimal changes in pH. High Cd(II) concentrations as 100 and 150 μM caused significant changes in viability with only a low percentage of living cells with enhanced activity of lysozomal proton pump, which is responsible for lysozome acidification. AO is useful not only for staining of lysozomes, demonstrating the activity of lysozomal proton pump and pH, but also for the detection of nucleic acids due to intercalation. DNA is stained in green (green emission), RNA electrostatically binds AO exhibiting the red emission. Under the highest Cd(II) concentrations, only green-emitting nuclei were observable. These cells were dead; the emission was based on the direct interaction between DNA and AO. Propidium iodide/Hoechst 33342 double staining is used to discriminate between dead (red emission) and apoptotic (blue emission) cells. Treatment of 22Rv1 cells with cadmium(II) ions led to the increase of dead cells. In addition, apoptotic and preapoptotic cells were

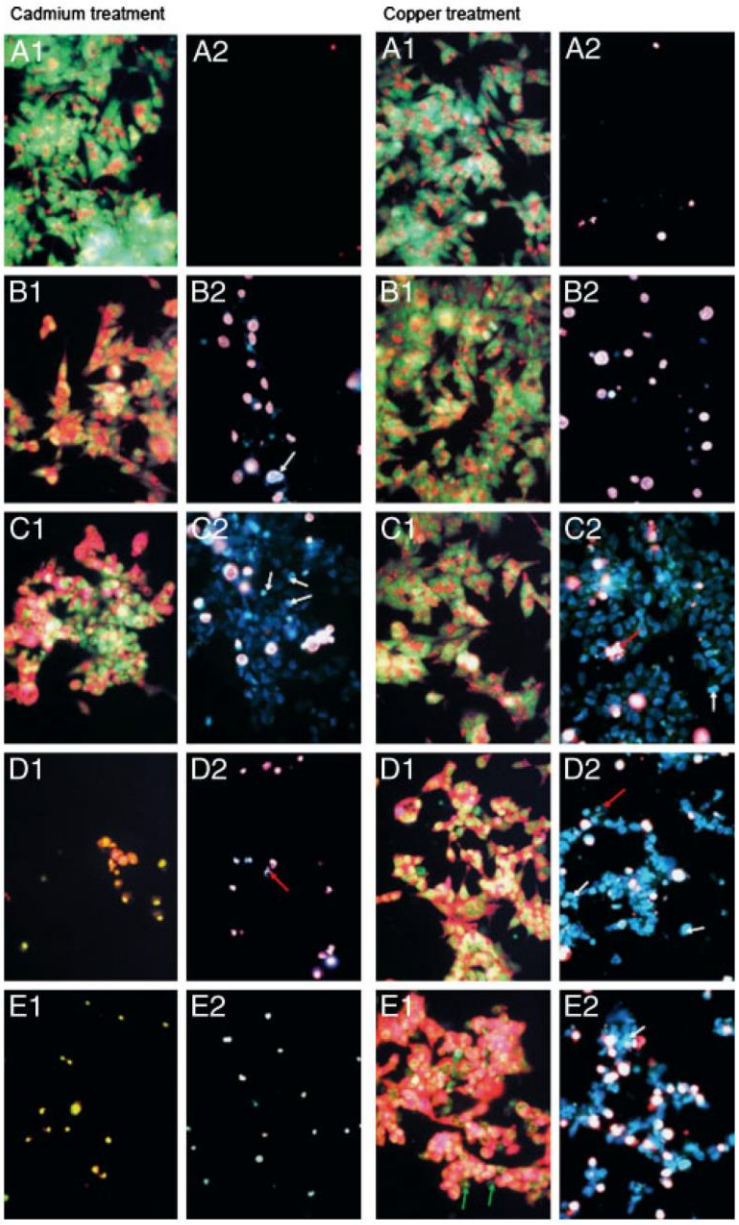

Figure 4. Fluorescence microscopy observation of the 22Rv1 cells after cadmium (II) and copper(II) ions treatment. *Effect of cadmium (II) ions* on 22Rv1 cells (left part). (A) Control, (B) 25 μM, (C) 50 μM, (D) 100 μM, and (E) 150 μM. (**1**) AO staining and (**2**) propidium iodide/Hoechst 33342 staining. White arrows indicate chromatin condensation – apoptotic cells, red arrows DNA fragmentation as a typical sign of apoptosis. Red-emitting cells are death. Only weak blue emission indicates normal cells. *Effect of copper(II) ions* on 22Rv1 cells (right part). (A) Control, (B) 100 μM, (C) 300 μM, (D) 500 μM, and (E) 800 μM. (**1**) AO staining and (**2**) propidium iodide/Hoechst 33342 staining. White arrows indicate chromatin condensation as a typical feature of apoptotic cells, and red arrow indicates DNA fragmentation as a result of apoptotic processes. Green arrows indicate death cells. See intensive acidification of 22Rv1 cells under treatment by Cu(II) ions in the highest concentration (800 μM).

well evident in lower concentrations (25 and 50 μM), whereas dead cells were prevailing in the two highest concentrations. Abovementioned findings point out that the high toxicity of cadmium(II) ions was able to induce apoptosis under very low concentration and necrosis under higher concentrations (Fig. 4).

Treatment of 22Rv1 cells with copper(II) ions led especially to significant changes in the activity of lysozomal proton pump, which is responsible for lysozome acidification and pH changes (low pH values cause the orange/red emission). Control cells formed the clusters of densely packed cells with normal activity of lysozomal proton pump. Lowest copper(II) concentrations caused only minimal changes in the activity of lysozomal proton pump. In addition, cell acidification was not observable. Two highest Cu(II) concentrations (500 and 800 μM) caused an intensive acidification of lysozomes and cytoplasm, and enhanced the activity of lysozomal proton pump. Dead cells are also well evident. These cells lack red emission of lysozomes and demonstrate only green emission of DNA. Treatment of 22Rv1 cells with copper(II) ions led to the increase of dead cells. Dead cells were observable under the lowest Cu(II) concentration, increasing Cu(II) concentration caused increasing number of apoptotic and preapoptotic cells. In

comparison with cadmium(II) ions, copper(II) ions demonstrated significantly lower toxicity. In addition, the lowest Cd(II) concentrations caused predominantly induction of apoptosis and the highest Cd(II) concentration necrosis, whereas increasing Cu(II) concentration led to increasing rate of apoptotic cells (Fig. 4).

3.4 MT separation and detection in cell lysates treated with copper(II) and cadmium(II) ions

It can be concluded that metal ion treatment caused marked changes in the cells from point of view of their viability and morphology. Further, the determination of MT was carried out in cell extracts. Primarily, we compared the above-optimized immunoseparation protocol with a standard heat-denaturation protocol. Both fractions were analyzed by SDS-PAGE with silver staining and electrochemical detection (Fig. 5A). On the silver-stained gels, a difference between unseparated RIPA lysates (Fig. 5B) and immunoseparated lysates (Fig. 5C) was clearly visible. In unseparated lysate, a broad range of proteins is visible, whereas in immunoseparated sample, three bands are present: antibody heavy chain band, antibody light chain band, and MT band (12 kDa). In RIPA lysate gel (Fig. 5B), MT band is barely visible in designated range, whereas in MP-separated gel (Fig. 5C, lines 1–10), MT band is significantly more distinctive. Furthermore, we electrochemically determined MT content in both unseparated and immunoseparated samples. We provided the evidence that immunoseparation protocol did not affect the protein content and immunoseparated MT content correlated with the previously optimized MT analysis [53]. To prove that MP separation step did not affect protein yield, we determined electrochemically MT level in heat and RIPA lysates in cadmium and copper treatment before and after MP-separation procedure (Fig. 5A). We found a strong correlation between MT unseparated and separated ($r>0.98$ at $p<0.014$) in both metal treatments and lysate types except RIPA lysate after cadmium treatment, in which we observed close-to-significant correlation. Therefore, we may conclude that MP-separation step does not affect protein yield. From the perspective of comparing the methods of cell lysis, we yielded slightly higher MT content in heat lysates treated by cadmium. In copper(II)-treated cells, we observed no significant differences in MT yield between lysate types. This difference is most likely due to the variation in cell growth and therefore we may conclude that lysis protocol does not significantly affect MT yield.

In heat lysates, free and total cadmium and copper content was determined. In cadmium(II)-treated cells, the total/free cadmium content ratio does not differ significantly (Fig. 6A). Moreover, under high cadmium(II) doses (100 μM, i.e. more than half of the inhibitory concentration according to MTT assay), free and total cadmium content decreased significantly. This is most likely due to severe alterations of cellular functions under these conditions. In copper(II)-treated cells (Fig. 6B), we found an increasing trend in both free and total copper, whereas the ratio of total/free copper increases with increasing copper concentration in medium, suggesting that copper is being tightly bound under the conditions of high copper doses.

In terms of MT content in cells treated with copper(II) and cadmium(II) ions, we observed elevation of MT level

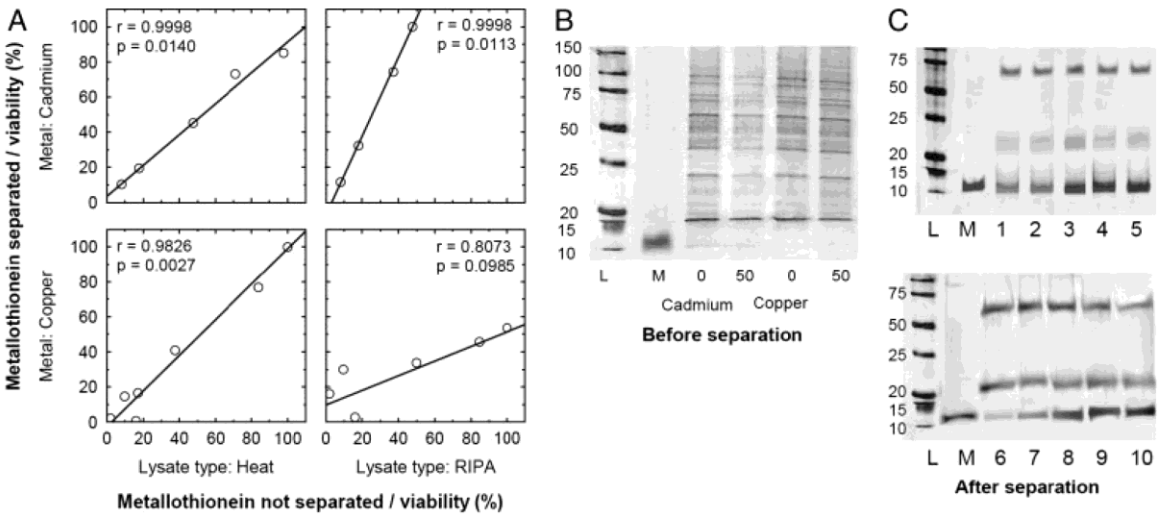

Figure 5. Comparison of separation and nonseparation technique. (A) *X*-axis represents electrochemically determined MT normalized to viability, *Y*-axis represents MT paramagnetically separated and electrochemically determined, normalized to viability. Except RIPA lysate in copper treatment, everything correlates at $p<0.01$. (B) SDS-PAGE analysis. Silver staining RIPA lysate. L, ladder; M, MT marker (50 μg/mL). In cadmium and copper treatment, MT band is low apparent. (C) SDS-PAGE analysis. Silver staining, after MP-separation. Lines 1–5 represent increasing copper concentration, and lines 6–10 represent increasing cadmium treatment concentration. In both gels, MT band is visible at 12 kDa range.

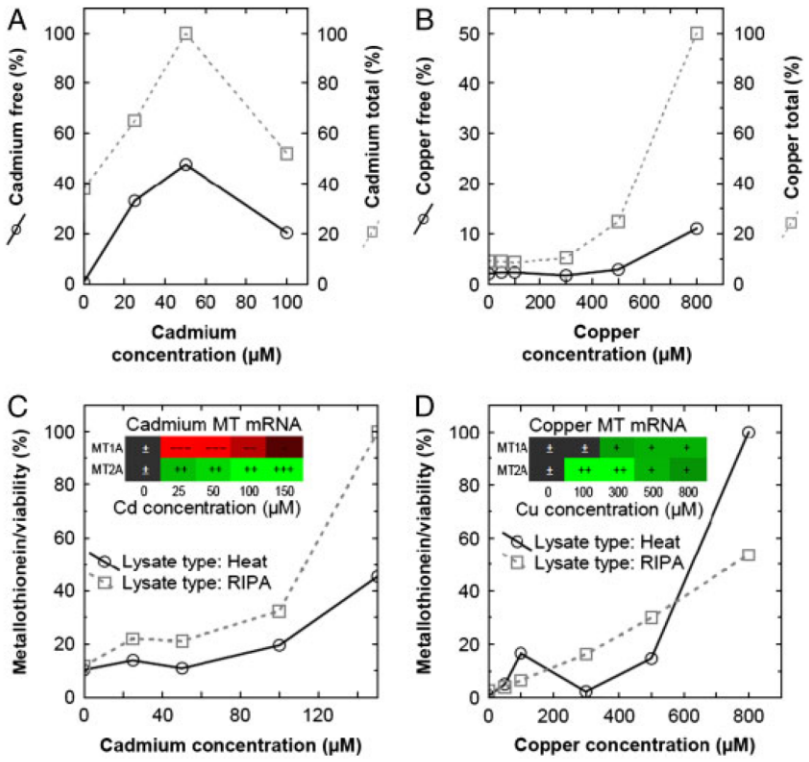

Figure 6. (A) Free and total metal content in metal treatment. *X*-axis represent amount of copper/cadmium in medium, left *Y*-axis represent free copper/cadmium, right *Y*-axis represent total copper/cadmium content. (B) MT content in cadmium- and copper-treated cells. In both cell lines and both lysate types, the MT content increases and correlates with metal treatment concentration (see text for details) Inset: MT RNA content in metal treatment. MT1A and MT2A major MT classes were determined. In cadmium treatment, MT1A isoform decreases with increasing cadmium content, whereas MT2A distinctly increases its expression. In contrast, in copper treatment, MT1A and MT2A classes' expressions increase with increasing copper content.

depending on metal concentration added (Fig. 6A). In 150 μM cadmium(II)-treated cells, we observed up to 10-fold elevation. In 800 μM copper(II)-treated cells, up to 20-fold elevation of MT level under high metal doses was found. We observed a strong correlation between MT concentration related to viability and concentration of copper(II) ions and cadmium(II) ions in the medium in all treatments and all lysate types ($r>0.83$ at $p<0.041$). These results indicate that MT is copper- and cadmium-inducible, but copper is able to induce the expression of MT more effectively than cadmium. This may be associated with lower toxicity of copper(II) ions compared with cadmium(II) ones. Under high copper(II) dose, MT system is still inducible, whereas the high cadmium load does not permit these systems to work properly and lead the cells to apoptosis/necrosis. Second explanation may be related to the fact, which we observed on the RNA level. We were interested in the dynamics of MT expression and because it is not possible to distinguish different isoforms of MT using electrochemical approach, we determined RNA level of MT. It was observed that copper(II) induces both major MT isoforms (MT-1A and MT-2A), whereas cadmium induces MT-2A isoform only (Fig. 6C and D, inset). Interestingly, the highest MT-2A isoform expression was observed after 100 μM copper(II) treatment. On the contrary, after cadmium(II) treatment, we observed distinctive decrease of MT-1A isoform expression and much more distinct elevation of MT-2A compared with MT-2A elevation after copper(II) treatment. This is in contrary with MT protein level, in which we observed no transient elevation of MT protein after cadmium(II) or copper(II) treatment. This fact may be evidenced by no correlation observed between RNA and protein level in both lyzate types and metal treatments except statistically significant trend in MT-2A RNA – MT protein isoform after cadmium(II) treatment in RIPA and heat lyzates ($r>0.98$ at $p<0.002$, data not shown). Based on the results obtained, we assume that there are more complex regulations of MT protein level in cells treated with copper(II) or cadmium(II) ions.

4 Concluding remarks

Moreover, we suggested new immuno-protocol based on antibody-modified microbeads for the isolation of MT. This protocol is coupled with electrochemical detection as the most sensitive one for the determination of this protein. Besides this, we show the applicability of this method for the analysis of real samples represented by cell lines treated with cadmium(II) and copper(II) ions. Together with other methods used for the determination of metal ions content, cell viability and growth, cell morphology, and some RNA assays, we can give a picture about biochemical pathways even at intracellular level. Based on the results, it can be concluded that copper(II) induces both major MT isoforms (MT-1A and MT-2A), whereas cadmium induces MT-2A

isoform only. This may implicate that some MT isoforms have higher affinities to some metal types. However, the correlation between mRNA and protein as MT was not found.

Financial support from the grants CEITEC CZ.1.05/1.1.00/02.0068, GACR 301/09/P436, and IGA MZ NS10200-3 is highly acknowledged.

The authors have declared no conflict of interest.

5 References

[1] Hogstrand, C., Kille, P., Nicholson, R. I., Taylor, K. M., *Trends Mol. Med.* 2009, *15*, 101–111.

[2] Margoshes, M., Vallee, B. L., *J. Am. Chem. Soc.* 1957, *79*, 4813–4814.

[3] Coyle, P., Philcox, J. C., Carey, L. C., Rofe, A. M., *Cell. Mol. Life Sci.* 2002, *59*, 627–647.

[4] Viarengo, A., Burlando, B., Ceratto, N., Panfoli, I., *Cell. Mol. Biol.* 2000, *46*, 407–417.

[5] Eckschlager, T., Adam, V., Hrabeta, J., Figova, K., Kizek, R., *Curr. Protein Pept. Sci.* 2009, *10*, 360–375.

[6] Babula, P., Kohoutkova, V., Opatrilova, R., Dankova, I., Masarik, M., Kizek, R., *Chim. Oggi-Chem. Today* 2010, *28*, 18–21.

[7] Krizkova, S., Adam, V., Eckschlager, T., Kizek, R., *Electrophoresis* 2009, *30*, 3726–3735.

[8] Krizkova, S., Fabrik, I., Adam, V., Hrabeta, P., Eckschlager, T., Kizek, R., *Bratisl. Med. J.* 2009, *110*, 93–97.

[9] Krizkova, S., Fabrik, I., Adam, V., Kukacka, J., Prusa, R., Chavis, G. J., Trnkova, L., Strnadel, J., Horak, V., Kizek, R., *Sensors* 2008, *8*, 3106–3122.

[10] Krizkova, S., Masarik, M., Majzlik, P., Kukacka, J., Kruseova, J., Adam, V., Prusa, R., Eckschlager, T., Stiborova, M., Kizek, R., *Acta Biochim. Pol.* 2010, *57*, 561–566.

[11] Krizkova, S., Adam, V., Kizek, R., *Electrophoresis* 2009, *30*, 4029–4033.

[12] Krizkova, S., Ryvolova, M., Gumulec, J., Masarik, M., Adam, V., Majzlik, P., Hubalek, J., Provaznik, I., Kizek, R., *Electrophoresis* 2011, in press.

[13] Zitka, O., Krizkova, S., Huska, D., Adam, V., Hubalek, J., Eckschlager, T., Kizek, R., *Electrophoresis* 2011, *32*, 857–860.

[14] Benavente, F., Andon, B., Gimenez, E., Barbosa, J., Sanz-Nebot, V., *Electrophoresis* 2008, *29*, 2790–2800.

[15] Benavente, F., Andon, B., Gimenez, E., Olivieri, A. C., Barbosa, J., Sanz-Nebot, V., *Electrophoresis* 2008, *29*, 4355–4367.

[16] Moini, M., *Rapid Commun. Mass Spectrom.* 2010, *24*, 2730–2734.

[17] Perez-Rama, M., Abalde, J., Herrero, C., Suarez, C., Torres, E., *J. Sep. Sci.* 2009, *32*, 2152–2158.

[18] Shariati, F., Shariati, S., *Biol. Trace Elem. Res.* 2011, *141*, 340–366.

[19] Kubo, K., Sakita, Y., Okazaki, Y., Otaki, N., Kimura, M., Minami, T., *J. Chromatogr. B* 1999, *736*, 185–190.

[20] Kubo, K., Sakita, Y., Otaki, N., Kimura, M., Minami, T., *J. Chromatogr. B* 2000, *742*, 193–198.

[21] Minami, T., Kubo, K., Ichida, S., *J. Chromatogr. B* 2002, *779*, 211–219.

[22] Minami, T., Matsubara, H., Ohigashi, M., Kubo, K., Okabe, N., Okazaki, Y., *Electrophoresis* 1996, *17*, 1602–1606.

[23] Adam, V., Fabrik, I., Eckschlager, T., Stiborova, M., Trnkova, L., Kizek, R., *Trends Anal. Chem.* 2010, *29*, 409–418.

[24] Ryvolova, M., Krizkova, S., Adam, V., Beklova, M., Trnkova, L., Hubalek, J., Kizek, R., *Curr. Anal. Chem.* 2011, *7*, 243–261.

[25] Archer, M. J., Lin, B. C., Wang, Z., Stenger, D. A., *Anal. Biochem.* 2006, *355*, 285–297.

[26] Cler, L., Bu, D. W., Lewis, C., Euhus, D., *Mol. Cell. Probes* 2006, *20*, 191–196.

[27] Dubus, S., Gravel, J. F., Le Drogoff, B., Nobert, P., Veres, T., Boudreau, D., *Anal. Chem.* 2006, *78*, 4457–4464.

[28] Ki, J. S., Chang, K. B., Roh, H. J., Lee, B. Y., Yoon, J. Y., Jang, G. Y., *J. Biosci. Bioeng.* 2007, *103*, 242–246.

[29] Becker, C., Hodenius, M., Blendinger, G., Sechi, A., Hieronymus, T., Muller-Schulte, D., Schmitz-Rode, T., Zenke, M., *J. Magn. Magn. Mater.* 2007, *311*, 234–237.

[30] Cao, Z. J., Li, Z. X., Zhao, Y. J., Song, Y. M., Lu, J. Z., *Anal. Chim. Acta* 2006, *557*, 152–158.

[31] Chiou, C. H., Huang, Y. Y., Chiang, M. H., Lee, H. H., Lee, G. B., *Nanotechnology* 2006, *17*, 1217–1224.

[32] Jaffrezic-Renault, N., Martelet, C., Chevolot, Y., Cloarec, J. P., *Sensors* 2007, *7*, 589–614.

[33] Kim, D. K., Zhang, Y., Voit, W., Rao, K. V., Muhammed, M., *J. Magn. Magn. Mater.* 2001, *225*, 30–36.

[34] Kinoshita, T., Seino, S., Mizukoshi, Y., Nakagawa, T., Yamamoto, T. A., *J. Magn. Magn. Mater.* 2007, *311*, 255–258.

[35] Palecek, E., Fojta, M., *Talanta* 2007, *74*, 276–290.

[36] Yeung, S. W., Hsing, I. M., *Biosens. Bioelectron.* 2006, *21*, 989–997.

[37] Gijs, M. A. M., *Microfluid. Nanofluid.* 2004, *1*, 22–40.

[38] Heer, R., Eggeling, M., Schotter, J., Nohammer, C., Pichler, R., Mansfeld, M., Bruckl, H., *J. Magn. Magn. Mater.* 2007, *311*, 244–248.

[39] Hsing, I. M., Xu, Y., Zhao, W. T., *Electroanalysis* 2007, *19*, 755–768.

[40] Lagae, L., Wirix-Speetjens, R., Liu, C. X., Laureyn, W., Borghs, G., Harvey, S., Galvin, P., Ferreira, H. A., Graham, D. L., Freitas, P. P., Clarke, L. A., Amaral, M. D., *IEE Proc. Circuit Device Syst.* 2005, *152*, 393–400.

[41] Minc, N., Futterer, C., Dorfman, K., Bancaud, A., Gosse, C., Goubault, C., Viovy, J. L., *Anal. Chem.* 2004, *76*, 3770–3776.

[42] Mykhaylyk, O., Vlaskou, D., Tresilwised, N., Pithayanukul, P., Moller, W., Plank, C., *J. Magn. Magn. Mater.* 2007, *311*, 275–281.

[43] Nikitin, P. I., Vetoshko, P. M., Ksenevich, T. I., *J. Magn. Magn. Mater.* 2007, *311*, 445–449.

[44] Pichl, L., Heitmann, A., Herzog, P., Oster, J., Smets, H., Schottstedt, V., *Transfusion* 2005, *45*, 1106–1110.

[45] Revyakin, A., Ebright, R. H., Strick, T. R., *Nat. Methods* 2005, *2*, 127–138.

[46] Ngomsik, A. F., Bee, A., Draye, M., Cote, G., Cabuil, V., *C. R. Chim.* 2005, *8*, 963–970.

[47] ACEA Bioscience, RTCA DP Instrument Operator's Manual, Inc. Roche Diagnostic GmbH. 2008, pp. 10–20.

[48] Profrock, D., Prange, A., Schaumloffel, D., Ruck, W., *Spectroc. Acta Pt. B Atom. Spectr.* 2003, *58*, 1403–1415.

[49] Fabrik, I., Krizkova, S., Huska, D., Adam, V., Hubalek, J., Trnkova, L., Eckschlager, T., Kukacka, J., Prusa, R., Kizek, R., *Electroanalysis* 2008, *20*, 1521–1532.

[50] Fabrik, I., Ruferova, Z., Hilscherova, K., Adam, V., Trnkova, L., Kizek, R., *Sensors* 2008, *8*, 4081–4094.

[51] Krizkova, S., Blahova, P., Nakielna, J., Fabrik, I., Adam, V., Eckschlager, T., Beklova, M., Svobodova, Z., Horak, V., Kizek, R., *Electroanalysis* 2009, *21*, 2575–2583.

[52] Krizkova, S., Fabrik, I., Adam, V., Kukacka, J., Prusa, R., Trnkova, L., Strnadel, J., Horak, V., Kizek, R., *Electroanalysis* 2009, *21*, 640–644.

[53] Petrlova, J., Potesil, D., Mikelova, R., Blastik, O., Adam, V., Trnkova, L., Jelen, F., Prusa, R., Kukacka, J., Kizek, R., *Electrochim. Acta* 2006, *51*, 5112–5119.

[54] Laemmli, U. K., *Nature* 1970, *227*, 680–685.

[55] Merril, C. R., Dunau, M. L., Goldman, D., *Anal. Biochem.* 1981, *110*, 201–207.

[56] Majzlik, P., Strasky, A., Adam, V., Nemec, M., Trnkova, L., Zehnnalek, J., Hubalek, J., Provaznik, I., Kizek, R., *Int. J. Electrochem. Sci.* 2011, *6*, in press.

[57] Adam, V., Fabrik, I., Kohoutkova, V., Babula, P., Hubalek, J., Vrba, R., Trnkova, L., Kizek, R., *Int. J. Electrochem. Sci.* 2010, *5*, 429–447.

[58] Adam, V., Huska, D., Hubalek, J., Kizek, R., *Microfluid. Nanofluid.* 2010, *8*, 329–339.

[59] Gai, Q. Q., Qu, F., Zhang, T., Zhang, Y. K., *J. Chromatogr. A* 2011, *1218*, 3489–3495.

[60] Masarik, M., Cahova, K., Kizek, R., Palecek, E., Fojta, M., *Anal. Bioanal. Chem.* 2007, *388*, 259–270.

[61] Nemcova, K., Havran, L., Sebest, P., Brazdova, M., Pivonkova, H., Fojta, M., *Anal. Chim. Acta* 2010, *668*, 166–170.

[62] Palecek, E., Fojta, M., Jelen, F., *Bioelectrochemistry* 2002, *56*, 85–90.

[63] Palecek, E., Kizek, R., Havran, L., Billova, S., Fojta, M., *Anal. Chim. Acta* 2002, *469*, 73–83.

[64] Palecek, E., Masarik, M., Kizek, R., Kuhlmeier, D., Hassmann, J., Schulein, J., *Anal. Chem.* 2004, *76*, 5930–5936.

[65] Tudorache, M., Tencaliec, A., Bala, C., *Talanta* 2008, *77*, 839–843.

[66] Marszall, M. P., Bucinski, A., Gorynski, K., Proszowska, A., Kaliszan, R., *J. Chromatogr. A* 2011, *1218*, 229–236.

[67] Qing, L. S., Xue, Y., Zheng, Y., Xiong, J., Liao, X., Ding, L. S., Li, B. G., Liu, Y. M., *J. Chromatogr. A* 2010, *1217*, 4663–4668.

[68] Hartwell, S. K., Grudpan, K., *Microchim. Acta* 2010, *169*, 201–220.

[69] Kuramitz, H., *Anal. Bioanal. Chem.* 2009, *394*, 61–69.

[70] Liu, G. D., Lin, Y. H., *Talanta* 2007, *74*, 308–317.

[71] Ng, A. H. C., Uddayasankar, U., Wheeler, A. R., *Anal. Bioanal. Chem.* 2010, *397*, 991–1007.

[72] Diaz-Gonzalez, M., Gonzalez-Garcia, M. B., Costa-Garcia, A., *Electroanalysis* 2005, *17*, 1901–1918.

[73] Lim, C. T., Zhang, Y., *Biosens. Bioelectron.* 2007, *22*, 1197–1204.

[74] Chu, X., Fu, X., Chen, K., Shen, G. L., Yu, R. Q., *Biosens. Bioelectron.* 2005, *20*, 1805–1812.

[75] Chu, X., Xiang, Z. F., Fu, X., Wang, S. P., Shen, G. L., Yu, R. Q., *J. Immunol. Methods* 2005, *301*, 77–88.

[76] Chumbimuni-Torres, K. Y., Dai, Z., Rubinova, N., Xiang, Y., Pretsch, E., Wang, J., Bakker, E., *J. Am. Chem. Soc.* 2006, *128*, 13676–13677.

[77] Zhou, G. Z., Li, J. S., Jiang, J. H., Shen, G. L., Yu, R. Q., *Acta Chim. Sin.* 2005, *63*, 2093–2097.

[78] Sramkoski, R. M., Pretlow, T. G., Giaconia, J. M., Pretlow, T. P., Schwartz, S., Sy, M. S., Marengo, S. R., Rhim, J. S., Zhang, D. S., Jacobberger, J. W., *In Vitro Cell. Dev. Biol. Anim.* 1999, *35*, 403–409.

[79] Liu, T., Xu, F. H., Du, X. L., Lai, D. M., Liu, T. J., Zhao, Y. R., Huang, Q., Jiang, L. Z., Huang, W. B., Cheng, W. W., Liu, Z. X., *Mol. Cell. Biochem.* 2010, *340*, 265–273.

[80] Marcias, G., Erdmann, E., Lapouge, G., Siebert, C., Barthelemy, P., Duclos, B., Bergerat, J. P., Ceraline, J., Kurtz, J. E., *Hum. Mutat.* 2010, *31*, 74–80.

[81] Sardana, G., Jung, K., Stephan, C., Diamandis, E. P., *J. Proteome Res.* 2008, *7*, 3329–3338.

[82] Abassi, Y. A., Xi, B., Zhang, W. F., Ye, P. F., Kirstein, S. L., Gaylord, M. R., Feinstein, S. C., Wang, X. B., Xu, X., *Chem. Biol.* 2009, *16*, 712–723.

[83] Holthausen, F., *Cell Analysis 2010*, Springer Medizin, Heidelberg 2010.

[84] Urcan, E., Haertel, U., Styllou, M., Hickel, R., Scherthan, H., Reichl, F. X., *Dent. Mater.* 2010, *26*, 51–58.

[85] Vistejnova, L., Dvorakova, J., Hasova, M., Muthny, T., Velebny, V., Soucek, K., Kubala, L., *Neuroendocrinol. Lett.* 2009, *30*, 121–127.

[86] Zajickova, Z., Rubi, E., Svec, F., *J. Chromatogr. A* 2011, *1218*, 3555–3558.

5.2.3 Findings related to the hypothesis 3

***Hypothesis 3*: Sensitivity of sarcosine detection can be increased using advanced techniques such as FRET.**

Chromatographic approaches with mass spectrometry detection are the most commonly used methods for the detection of sarcosine in biological materials [79, 159]. However, precise determination of sarcosine in complex biological samples is still a matter of concern - mainly due to the presence of other amino acids [160]. Therefore, the detection method using the Förster resonance energy transfer (FRET) principle between the quantum dots and the green fluorescence protein, facilitated by a sandwich arrangement with sarcosine antibodies, was optimized.
We successfully synthesized nanomaghemite core- based paramagnetic nanoparticles, containing the binding sites for sarcosine antibodies and thiol moieties of oligonucleotide linker, bearing GFP functionalized with AuNPs. Abs@PMPs conjugate was able to bind sarcosine in biological samples as prostatic cell lines and urinary samples of onco-patients. Using HWR heptapeptide, Abs@QDs acceptor molecule was constructed and using sandwich binding of antibodies FRET was observed, and this was dependent on sarcosine concentration. We were able to discriminate sarcosine in both prostatic cells and urinary samples with very good sensitivity and without undesired interference.
Conclusion: The FRET-based sarcosine detection method is a highly sensitive and specific detection method with the detection limit of 50 μM.

Author's publication relevant to this chapter

Heger Z, Cernei N, Krizkova S, et al. Paramagnetic Nanoparticles as a Platform for FRET-Based Sarcosine Picomolar Detection. Scientific Reports. 2015;5.
Available on page 315

SCIENTIFIC REPORTS

OPEN

SUBJECT AREAS:
CANCER
DIAGNOSTIC MARKERS

Received
28 October 2014

Accepted
6 February 2015

Published
9 March 2015

Correspondence and requests for materials should be addressed to R.K. (kizek@sci.muni.cz)

Paramagnetic Nanoparticles as a Platform for FRET-Based Sarcosine Picomolar Detection

Zbynek Heger[1,2], Natalia Cernei[1,2], Sona Krizkova[1,2], Michal Masarik[3], Pavel Kopel[1,2], Petr Hodek[4], Ondrej Zitka[1,2], Vojtech Adam[1,2] & Rene Kizek[1,2]

[1]Department of Chemistry and Biochemistry, Faculty of Agronomy, Mendel University in Brno, Zemedelska 1, CZ-613 00, Czech Republic, European Union, [2]Central European Institute of Technology, Brno University of Technology, Technicka 3058/10, CZ-616 00 Brno, Czech Republic, European Union, [3]Department of Pathological Physiology, Faculty of Medicine, Masaryk University, Kamenice 5, CZ-612 00 Brno, Czech Republic, European Union, [4]Department of Biochemistry, Faculty of Science, Charles University in Prague, Hlavova 2030, CZ-128 40 Prague 2, Czech Republic, European Union.

Herein, we describe an ultrasensitive specific biosensing system for detection of sarcosine as a potential biomarker of prostate carcinoma based on Förster resonance energy transfer (FRET). The FRET biosensor employs anti-sarcosine antibodies immobilized on paramagnetic nanoparticles surface for specific antigen binding. Successful binding of sarcosine leads to assembly of a sandwich construct composed of anti-sarcosine antibodies keeping the Förster distance (*Ro*) of FRET pair in required proximity. The detection is based on spectral overlap between gold-functionalized green fluorescent protein and antibodies@quantum dots bioconjugate (λ_{ex} 400 nm). The saturation curve of sarcosine based on FRET efficiency (F_{604}/F_{510} ratio) was tested within linear dynamic range from 5 to 50 nM with detection limit down to 50 pM. Assembled biosensor was then successfully employed for sarcosine quantification in prostatic cell lines (PC3, 22Rv1, PNT1A), and urinary samples of prostate adenocarcinoma patients.

Prostate carcinoma (CaP) was determined to be the most common cause of cancer-related deaths in men in USA in 2013[1]. Early diagnostic of CaP is of great importance for successful elimination of metastatic expansion. Commonly used biomarker as prostate specific antigen (PSA) has been shown to have less sensitivity and specificity leading to both false-negative and/or false-positive results in some cases[2,3], hence novel potential biomarkers have been searching. In 2009, sarcosine (Sar) was highlighted as a potential CaP biomarker enabling us to distinguish benign, localized or metastatic tumours with very high accuracy. This marker can be detected not only in blood, but also in urine, which allows a simple and non-invasive diagnostics[4].

Gas chromatography mass spectrometry[4] and liquid chromatography mass spectrometry[5] are the most commonly utilized analytical methods for sarcosine determination. Using of sarcosine-oxidase as a part of (nano)-biosensors allows specific determination of sarcosine by using photoelectrochemical[6], fluorescent[7] or colorimetric detection[8] with limits of detection in nanomolar range. However, the accurate Sar identification in complex biological matrices as urine is still challenging, particularly its determination in the presence of other amino acids[9]. Thus, the development of novel and sensitive methods for precise determination of sarcosine is necessary for both confirmation of its potential to be used as valid CaP biomarker, and its application for screening purposes.

Herein we describe the method for sarcosine determination based on Förster resonance energy transfer (FRET) between quantum dots (QDs) and green fluorescent protein (GFP) enabled by sandwich arrangement using anti-sarcosine antibodies (Abs) in patient urinary samples and in prostatic cell lines (PC3, 22Rv1, PNT1A).

Results and Discussion

Characterization of the nanoconstruct. The superparamagnetic iron oxide nanoparticles (SPIONs - γ-Fe_2O_3 and Fe_3O_4) are versatile nanoscaled materials that have been applied in various fields of the interest[10–12]. They can be simply functionalized to provide binding sites towards various molecules and, moreover, they can be conveniently immobilized *via* external magnetic field. Hence, we exploited these nanostructures as a platform for FRET-based sarcosine biosensing.

www.nature.com/scientificreports

The morphology of prepared nanoparticles was determined by scanning electron microscopy. As it can be seen in Fig. 1A (scale bar 200 nm), nanoparticles form aggregates, due to their low zeta potential, determined as - 7.09 ± 0.13 mV (upper inset in Fig. 1B). Generally, iron oxide nanoparticles exhibit their absolute zeta potential within the pH range 4–10[13], and thus using PBS (pH = 7.4) leads to aggregation of nanometric particles that was partially reduced using ultrasonic homogenizer (Bandelin electronic, Berlin, Germany) to form suspension containing particles with relatively uniform size (d = 23 ± 5 nm, Fig. 1B).

X-ray fluorescence spectra revealed that iron originating from nanomaghemite (γ-Fe_2O_3), which was used to constitute a paramagnetic core, formed almost one half of present elements (particularly 482 $\mu g.mg^{-1}$). Gold, used for nanoparticles surface modification allowing their conjugation with antibodies or binding thiol-containing compounds, was identified as the second most abundant element (137 $\mu g.mg^{-1}$, Fig. 1C).

Paramagnetic properties of the nanoparticles were also evidenced by SECM. It is shown in Figs. 1D–E that placement of a neodymium magnet under the detection electrode led nanoparticles attraction to one place, which was observed as local increasing of current response. Reduction of nanoparticles layer rapidly decreased the relative current response (from basic −0.70 nA to app. −1.33 nA).

To prepare sarcosine-sensing nanoparticles we employed anti-sarcosine antibodies isolated from egg yolks of sarcosine-immunized hens[14]. We examined the absorption of antibodies (electrostatic and/or hydrophobic interactions) on a surface of nanoparticles modified with gold. Primarily, the bioconjugation capacity was evaluated by SDS-PAGE of unbound Abs (original concentrations 0–10 $mg.mL^{-1}$). The optimal coating of nanoparticles was achieved using antibodies dilution of 1–1.2 $mg.mL^{-1}$ (Fig. 1F). For nanoparticles covered with 1 $mg.mL^{-1}$ Abs, the recovery of sarcosine isolation from 2 μM standard solution was 25%, as calculated from determination of nanoparticles-attached sarcosine (Fig. 1F). Moreover, it was revealed that no sarcosine was bound to nanoparticles without Abs and therefore, there is no need to block their surface before their use for sarcosine isolation.

FRET. The design of the suggested paramagnetic nanoparticles-based structure is schematically shown in Fig. 2. The main purpose of this biosensor is the isolation and detection of sarcosine with high specificity and sensitivity. By using preliminary ELISA experiments it was evaluated that sandwich assay with anti-sarcosine antibodies reached limit of detection of 8 nM for sarcosine (data not shown). Hence, we employed sarcosine as a linker, connecting two fluorophores to perform FRET, localized on paramagnetic nanoparticles.

Due to the fact that both, donor (GFP) and acceptor (QDs) have to be modified to enable specific binding to the target structures, we evaluated the possible changes of their fluorescence properties upon their modification. As a donor we employed GFP that was previously described to provide sufficient quantum yield for detection and moreover, it is sufficiently stable to be imaged during the experiment[15]. For GFP functionalization we utilized its modification with gold nanoparticles (AuNPs). Similarly to Bale *et al.*[16] we employed a simple procedure comprising a mixing of GFP (in final concentration of 1 $mg.mL^{-1}$) with AuNPs both in PBS.

As it is shown in Fig. 3A, the modified GFP retained 78.9% of its fluorescence, indicating favorable retention of protein structure after functionalization. As gold binds thiols with high affinity and it does not undergo any unusual reactions with them[17], we were able to use dsDNA with thiol moieties on both ends to form a linker between modified GFP and conjugate of Abs@PMPs. The resulting structure retained 12.3% of initial fluorescence of unmodified GFP exhibited

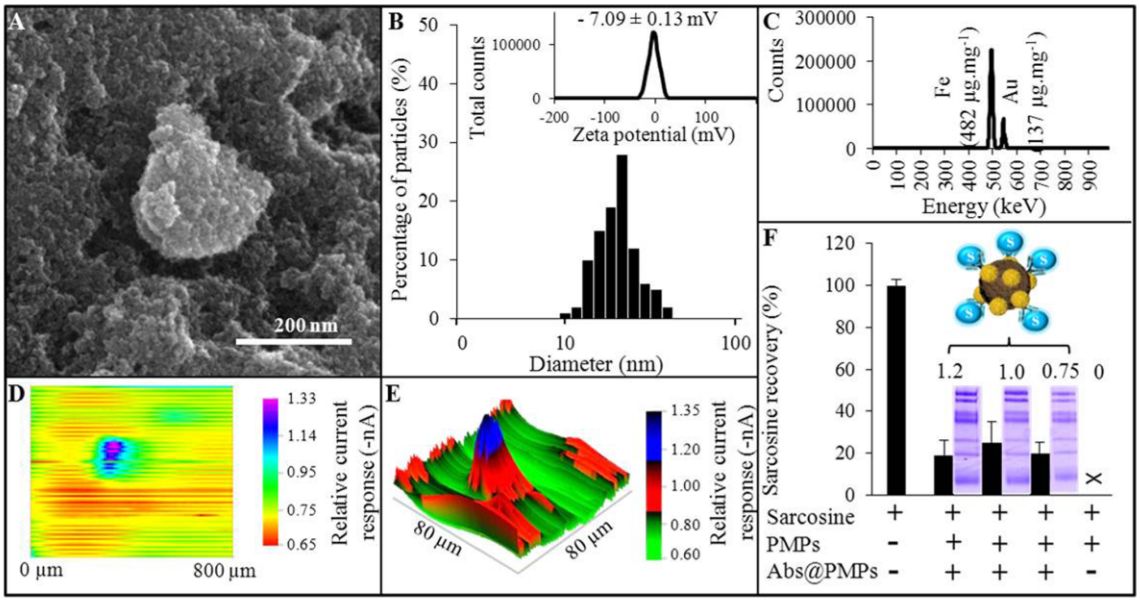

Figure 1 | The characterization of paramagnetic microparticles, composed of nanomaghemite core, modified with polyvinylpyrrolidone and gold expressed as: (A) SEM micrograph (length of scale bar is 200 nm). (B) Particles size distribution, with expression of their zeta potential (determined in PBS, pH 7.4). (C) XRF spectrum showing the most abundant elements in paramagnetic particles. (D) SECM scans expressing the electrochemical current response behavior of immobilized nanoparticles (800 × 800 μm). (E) Scan was further converted to more detailed 3D scan (80 × 80 μm) that shows the decrease of relative current response influenced by nanoparticles presence. (F) Results of recoveries of sarcosine (2 μM) binding to antibodies at nanoparticles, obtained from IEC analyses. Values are means of three independent replicates (n = 3). Vertical bars indicate standard error. SDS-PAGE showing the binding capacity of nanoparticles towards sarcosine antibodies (0.75–1.2 $mg.mL^{-1}$ of Abs) are illustrated too.

www.nature.com/scientificreports

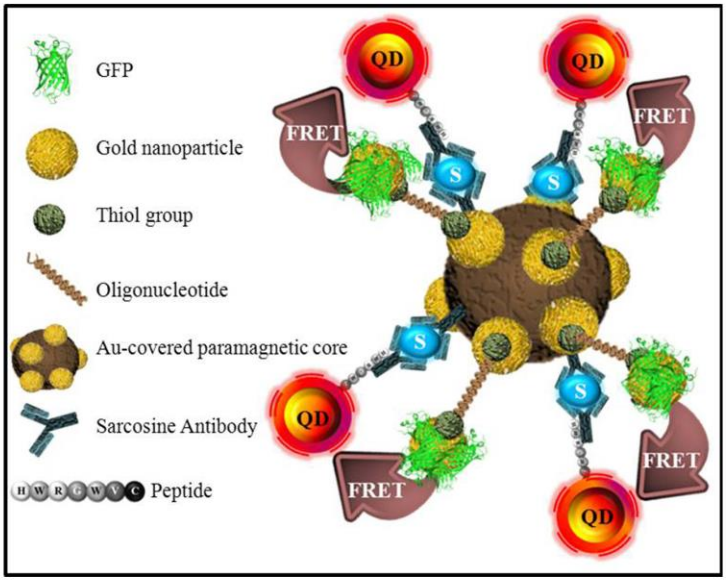

Figure 2 | A schematic expression of FRET between green fluorescent proteins (green) and quantum dots (QD, red-yellow) on surface of paramagnetic nanoparticle modified with polyvinylpyrrolidone and gold. Spectral overlap is enabled by binding of sarcosine (S, blue) and provided by sandwich of its antibodies (all components shown in left part of figure).

paramagnetic properties and contained specific binding sites for sarcosine (Fig. 3A). Using atomic absorption spectrometry, the content of gold, originating from both protein functionalization and modification of nanoparticles, was determined as 0.0037 $\mu g.mL^{-1}$.

QDs were shown to be one of the most suitable fluorophores in FRET configuration due to their exceptional brightness, high quantum yields and characteristic excitation and emission spectra[18]. A basic fluorescence characterization of our CdTe QDs revealed excitation maxima at λ_{exc} 520 nm with emission peak at λ_{em} 604 nm. Using excitation of GFP (λ_{exc} 400 nm), very weak fluorescence was obtained (4.2% when compared with 100%, determined in QDs excitation maxima, Fig. 3B). To obtain the acceptor molecules with the required parameters as high fluorescence and specificity, we employed peptide to connect QDs with anti-sarcosine antibodies. Synthetic heptapeptide HWRGWVC was previously exploited for bioconjugation of QDs with human immunoglobulin by us[19]. Hence, we employed the natural ability of its *N*-terminus composed of histidine followed by aromatic and positively charged amino acids to recognize and bind antibodies through their Fc region. The major advantage is that peptide-mediated conjugation controls the orientation of antibody to face the antigen binding site outward. Moreover, cysteine at the peptide *C*-terminus serves as a stabilization agent of colloidal nature of CdTe QDs solution. As it can be seen in Fig. 3B, the conjugation resulted in decrease of fluorescence of QDs to 71.3%

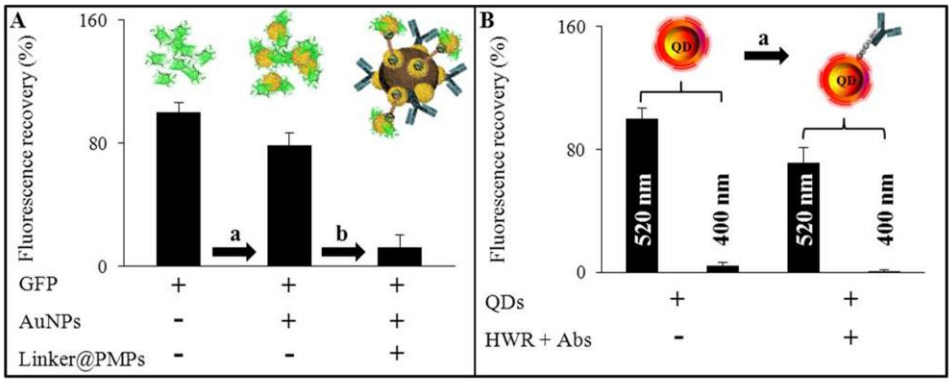

Figure 3 | To provide the binding sites for oligonucleotide linker, GFP was modified with gold nanoparticles (AuNPs). During the whole workflow, (a) process of GFP conjugation and (b) subsequent binding to a surface on nanomaghemite through oligonucleotide linker, (A) fluorescence recovery was evaluated (λ_{exc} 400 nm and λ_{em} 510 nm). As the acceptors for fluorescent resonance transfer there were employed quantum dots with λ_{exc} 520 nm and λ_{em} 604 nm. (B) Their fluorescent properties were tested both in their optimal excitation and in the excitation of GFP (λ_{exc} 400 nm). (a) Fluorescence of bare QDs and fluorescence after their conjugation with HWR heptapeptide, carrying sarcosine antibodies was determined at λ_{em} 604 nm. Values are means of three independent replicates ($n = 3$). Vertical bars indicate standard error.

www.nature.com/scientificreports

of initial value while maintaining their excitation and emission maxima (λ_{exc} 520 nm; λ_{em} 604 nm).

Close contact of two fluorophores and their spectral overlap allows the desired Förster/fluorescence resonance emission transfer. We mixed together both donor (GFP connected to paramagnetic nanoparticle bearing Abs with bound sarcosine), and acceptor (Abs@QDs conjugate). After the incubation (37°C, 800 rpm, 1 h) the surplus of liquid was removed while complex was immobilized in vial using external magnetic field and washed with PBS with 0.5% Tween-20 and 1% bovine serum albumin (BSA), which protects QDs against quenching, caused by induction of their colloidal instability, resulting from interaction with buffer components. The size of assembled biosensor was established to be relatively uniform within 3 different batches (d = 103 ± 11 nm) with standard deviation of 6%. Further characterization revealed that GFP content in assembled biosensor was app. 224 $\mu g.mL^{-1}$, while the level of the major component of QDs as cadmium was found to be 58 $\mu g.mL^{-1}$. Based on these fact and protocol published by Casanova et al.[20], we found that the number of FRET pair(s) per nanoparticle was 0.25. which is cause mainly due to the excess of the particles to GFP and QDs. Finally, a fluorescence behavior was studied.

Detection of sarcosine. Sarcosine was shown to be crucial for FRET, while its absence led to detection of donor fluorescence (λ_{em} 510 nm) only with no effect on FRET (Fig. 4A). Importantly, it was confirmed that the acceptor (Abs@QDs conjugate) has no ability to join the paramagnetic complex *via* an unspecific bond. In the case of sarcosine captured in antibodies sandwich, it was observed that donor excitation triggers spectral overlap leading to "lighting up" of the acceptor. Hence, it was shown that our construct can assemble a spatial orientation enabling a FRET and moreover, it was revealed that FRET efficiency (F_{604}/F_{510} ratio, which describes the relationship between an increase of acceptor fluorescence intensity at the expense of the fluorescence intensity of donor upon its excitation) is dependent on antigen concentration. As it can be seen in inset in Fig. 4A, the acceptor emission intensity is proportional to concentration of antigen and spectral overlap is observed till 50 pM sarcosine, which is more sensitive than other described biosensors[6–8]. This phenomenon is caused by saturation of certain number of antibodies, resulting in propagation of sandwich binding sites on sarcosine molecule towards limited amount of acceptors. On the other hand, using concentrations higher than 50 nM, the antibodies reach saturation plateau disallowing quantification of antigen. Determination of sarcosine was tested within linear dynamic range (5–50 nM) of the saturation curve (Fig. 4B), based on FRET efficiency (F_{604}/F_{510} ratio), with the parameters of y = 0.024x + 0.665, R^2 = 0.993). Due to the fact that sarcosine amount in clinical samples of the prostatic onco-patients varies widely; sarcosine quantification is fundamentally dependent on a proper dilution of analyzed sample. The accomplishment of this requirement leads to very sensitive and specific detection.

As mentioned above, sarcosine analyses are difficult due to presence of many interfering compounds complicating the most commonly used analyses separation (GC/LC) hyphenated to mass detection[9]. The amino acids commonly present in urine were tested for their interfering potential (Fig. 4C). It was revealed that our sensor is able to distinguish sarcosine in the presence of various urinary amino acids including alanine. Negligible FRET efficiency was determined as a result of a background fluorescence of solution (F_{604}/F_{510} ratio 0.01–0.02 compared with 0.58 of sarcosine).

Based on obtained results we hypothesized that our approach can be applicable also for evaluation of sarcosine levels in prostatic cell lines and clinical urinary samples. Firstly, Abs@PMPs conjugate was employed to quantify sarcosine in disrupted prostatic cells. It was shown that sarcosine is present in all types of prostatic cells, including normal prostatic epithelial cells (PNT1A) - 0.03 nmol per 10^6 cells, human carcinoma epithelial cells derived from a xenograft propagated in mice (22Rv1) - 0.07 nmol per 10^6 cells, and human cell line from androgen independent prostatic adenocarcinoma derived from metastatic site in bone (PC3) - 0.11 nmol per 10^6 cells (Fig. 5A). These results are in agreement with results published by Khan and colleagues used glycine-*N*-methyl transferase (GNMT) knockdown cell lines for sarcosine assessment[21].

The primary purpose of our sarcosine sensor was the isolation and quantification of urinary sarcosine as the non-invasive biomarker. Urine is one of the most accessible and stable body fluids however, it is rather complex biological matrix containing interfering compounds, which may reduce the effectiveness of analytical assays[22]. Hence, to observe the influence of this matrix, we diluted control urinary sample (0×; 10×; 100×; and 1000×) and all of diluted aliquots were spiked with 40 nM sarcosine. Sarcosine (5.4 nM) was determined also in control non-spiked samples (Fig. 5B).

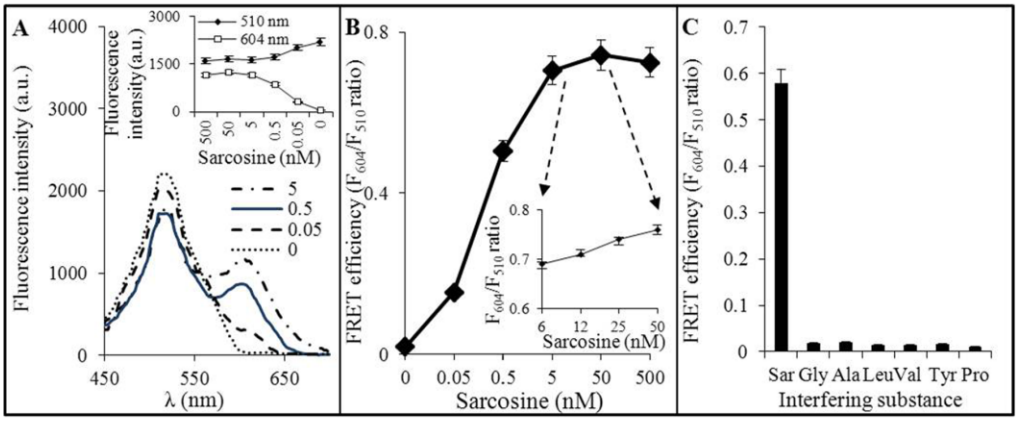

Figure 4 | (A) Fluorescence emission spectra of FRET were recorded for 0–5 nM sarcosine at 25°C. The excitation wavelength was set to 400 nm. In inset: there is the expression of fluorescence (λ_{exc} 400 nm) dependence on sarcosine concentration evaluated in both emission maxima of GFP (λ_{em} 510 nm) and QDs (λ_{em} 604 nm). (B) Saturation curve of sarcosine (0–500 nM, diluted in PBS, pH 7.4). In inset: the calibration curve determined within linear range 5–50 nM. (C) The expression of interfering potential of various amino acids (all of them diluted in PBS, pH 7.4 to the final 50 nM concentrations) on FRET efficiency. Values are means of three independent replicates (n = 3). Vertical bars indicate standard error.

www.nature.com/scientificreports

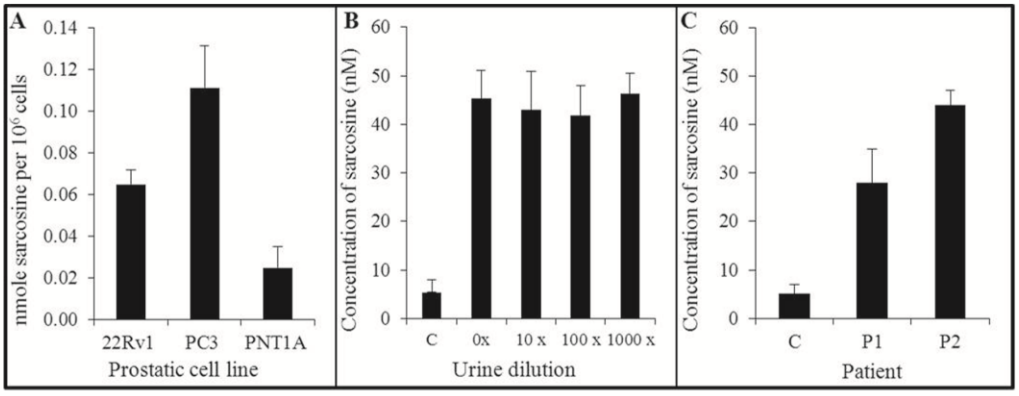

Figure 5 | An utilization of antibodies for sarcosine isolation from the real samples of urine. (A) Sarcosine amount isolated from prostatic cell lines (PC3, 22Rv1, PNT1A). (B) Urinary samples were spiked with 40 nM sarcosine and various dilution were tested (0×; 10×; 100×; and 1000×) and compared to control (C) without sarcosine spike. Analyses were performed using FRET at λ_{exc} 400 nm and concentrations were calculated according to calibration curve. (C) Sarcosine concentration determined in real samples of patients suffering from acinar adenocarcinoma of prostate. The urinary samples were diluted 100× prior to isolation. Values are means of three independent replicates ($n = 3$) analyzed with different batches of system. Vertical bars indicate standard error.

Furthermore, it was revealed that the urine dilution does not influence sarcosine binding to Abs and all of the diluted aliquots show comparable content of antigen determined *via* FRET (41.9–46.3 nM).

Presented data allow us to proceed with real clinical samples obtained from prostate adenocarcinoma patients. Regarding to results obtained using IEC we diluted two analyzed urinary samples 100× with water. For comparison one undiluted control was employed too (Fig. 5C). The use of Abs@PMPs conjugate and subsequent assembly of entire FRET construct resulted in sarcosine identification in both urinary samples. FRET quantification of antigen in 100× diluted urine showed that the content of the target analyte was 28 and 44 nM in sample 1 and 2. If we calculate the dilution and compare the results with those found by IEC (3.3 and 5.2 μM), we can conclude that these methods are in very good agreement. Moreover, three different batches of FRET system were tested with standard deviation of 2–7%. Hence, it can be stated that isolation of sarcosine through Abs followed by FRET analysis may provide very specific and sensitive bioanalytical approach. Particularly, the sensitive determination of sarcosine changes during the disease progression may provide useful prognostic and diagnostic tool able to increase the successful diagnostic rate of prostate carcinoma[23], leading to decrease of mortality associated with this disease.

In conclusion, we successfully synthesized nanomaghemite core-based paramagnetic nanoparticles, containing the binding sites for sarcosine antibodies and thiol moieties of oligonucleotide linker, bearing GFP functionalized with AuNPs. Abs@PMPs conjugate was able to bind sarcosine in biological samples as prostatic cell lines and urinary samples of onco-patients. Using HWR heptapeptide, Abs@QDs acceptor molecule was constructed and using sandwich binding of antibodies FRET was observed, and this was dependent on sarcosine concentration. We were able to discriminate sarcosine in both prostatic cells and urinary samples with very good sensitivity and without undesired interference. Our approach may be exploited for quantification of sarcosine fluctuations in time for prognostic approaches.

Methods

Chemicals. All reagents for syntheses, native oligonucleotides, standards, and other chemicals were purchased from Sigma-Aldrich (St. Louis, MO, USA) in ACS purity, unless noted otherwise.

Synthesis of nanomaghemite, gold nanoparticles, quantum dots and HWR peptide. Nanometric maghemite was prepared by $NaBH_4$ reduction of $FeCl_3 \cdot 6H_2O$ according to protocol as follows: 1 g of $FeCl_3 \cdot 6\ H_2O$ (3.7 mM) was dissolved in 80 mL of MilliQ water and a solution of 0.2 g of $NaBH_4$ (5.3 mM) in ammonia (3.5%, 10 mL) was poured into the first solution under vigorous stirring. The obtained solution was boiled for 2 h. After cooling down the magnetic nanoparticles were separated by external magnetic field and washed with water for several times. Subsequently, nanomaghemite particles were suspended in water solution of 20 mL of 7.5% polyvinylpyrrolidone (PVP) (40 μM) and modified with 1 mM $HAuCl_4$, followed by addition of 0.75 mL of 0.1 M trisodium citrate. The resulting mixture was stirred overnight, separated using an external magnetic force field and dried at 40°C.

Gold nanoparticles were prepared by "citrate" method. Aqueous solution of sodium citrate (0.5 mL, 40 mM) was added to a solution of $HAuCl_4 \cdot 3\ H_2O$ (10 mL, 1 mM). The mixture was stirred overnight.

CdTe quantum dots were prepared by mixing of 10 mL of 20 mM solution of cadmium acetate dihydrate in MiliQ water (76 mL) with 1 mL of 4 mM mercapto-succinic acid dissolved in water, followed by addition of 1.8 mL of 1 M NH_3. Finally, 1.5 mL of 10 mM solution of Na_2TeO_3 was added and after few minutes 50 mg of $NaBH_4$ (1.3 mM) was poured to the stirred solution. After 1 hour stirring, the volume of reaction mixture was adjusted to 100 mL using water and the solution was heated in microwave reactor Multiwave 300 (Anton Paar, Graz, Austria) at 300 W and 120°C for 10 min.

The heptapeptide with the amino acid sequence HWRGWVC (943.0912 Da) was prepared on Liberty Blue peptide synthesizer (CEM, Matthews, NC, USA) by standard Fmoc solid-phase synthesis using 20% piperidine in dimethylformamide (*v/v*). Purity of crude peptide was analysed using high performance liquid chromatography with UV detection (ESA Inc., Chelmsford, MA, USA) and matrix-assisted laser ionization/desorption time-of-flight mass spectrometry (Bruker ultrafleXtreme, Bruker Daltonik GmbH, Germany).

Characterization of modified nanometric maghemite particles. Firstly, the morphology of nanoparticles was observed using scanning electron microscope MIRA3 LMU (Tescan, a.s., Brno, Czech Republic). An accelerating voltage of 15 kV and beam current about 1 nA were used with satisfactory results regarding to maximum throughput.

Particles size and zeta potential was measured by Particle Size Analyzer (Zetasizer Nano ZS90, Malvern instruments, Malvern, UK). For this purpose, particles were dispersed in phosphate buffered saline (PBS, 137 mM NaCl, 2.7 mM KCl, 1.4 mM NaH_2PO_4, and 4.3 mM Na_2HPO_4, pH 7.4) and incubated at 25°C for 15 min prior the measurement.

Elemental composition was evaluated using X-ray fluorescence spectrometer Xepos (SPECTRO GmbH, Kleve, Germany), with parameters set as follows - measurement duration: 300 seconds, tube voltage from 24.81 to 47.72 kV, tube current from 0.55 to 1.0 mA.

Scanning electrochemical microscopy was employed to obtain data on electrochemical behavior of nanoparticles layer. Microscope Model 920D (CH instruments, Inc., Austin, TX, USA) consisted of 10 mm measuring platinum disc probe electrode with potential of 0.2 V. The measurement was performed in Teflon cell with volume of 1.5 mL under the following setting: amperometric mode, vertical scan was carried out in the area 500 × 500 μm with rate of 30 $\mu m.s^{-1}$.

Binding capacity of nanoparticles was determined using sodium dodecyl sulfate polyacrylamide gel electrophoresis (SDS-PAGE) in 12.5% (*w/w*) separation gel and 5% (*w/w*) focusing gel. Separation was conducted at 120 V for 80 min.

Table 1 | Overview of the information of the acinar adenocarcinoma patients

Patient	PSA*	fPSA**	cT***	pT****	GS*****
1	7.07	0.22	T1c	pT2c	3 + 4
2	8.78	-	T2c	pT3a	3 + 3

*Prostate specific antigen (ng.mL^{-1}), **free prostate specific antigen (free/total PSA ratio), ***clinical stage: *T1c* - tumor identified by needle biopsy, PSA elevated, *T2c* – both lobes affected. ****Pathological stage: *pT2c* - tumor affects both lobes, *pT3a* - tumor extends beyond the prostate. *****Gleason score.

Production of sarcosine antibodies. Leghorn hens were immunized weekly by three subcutaneous injections (0.1 mg/dose/animal) with Sar immunogen (Sar-beta-Ala-beta-Ala-Cys-NH_2) conjugated to maleimide-activated keyhole limpet haemocyanin (KLH) (Imject Maleimide-Activated mcKLH, Thermo Scientific, Rockford, IL, USA). The conjugation of hapten to carrier protein (KLH) was performed according to manufacturer's instructions. Preparation of antibodies and their immunoreactivity tests were carried out according to previously optimized protocol[14]. The entire process was conducted in accordance with the Regulations for the Care and Use of Laboratory Animals (311/1997, Ministry of Agriculture, Czech Republic).

Bioconjugation of antibodies on paramagnetic nanoparticles and isolation of sarcosine. Prior to a bioconjugation, paramagnetic nanoparticles were washed with PBS to remove impurities. For bioconjugation, sarcosine antibodies were mixed with paramagnetic nanoparticles (0.5 mg.100 μL^{-1}) in ratio 1 : 1. The resulting mixture was incubated for 60 minutes under shaking (800 rpm) at 37°C in thermoblock ThermomixerR (Eppendorf AG, Hamburg, Germany). After the incubation, the conjugate of antibodies at nanoparticles (Abs@PMPs) was washed three times with PBS and prepared for sarcosine binding. The binding of Sar with Abs@PMPs was carried out simply through the addition of conjugate to a sample (standard, urine, and/or cell lines), containing Sar. The conditions of isolation were as follows: 60 min, 800 rpm, 37°C, thermoblock ThermomixerR (Eppendorf AG, Hamburg, Germany). The bioconjugate with bound sarcosine was removed using an external magnetic field and three times washed with PBS and stored for further experiments.

Preparation of donor - green fluorescent protein functionalized with AuNPs. For *Escherichia coli* transformation, the pGLO plasmid (Bio-Rad, Philadelphia, PA, USA), containing the reporter gene for green-fluorescent protein (GFP) was employed. *GFP* gene was under control of the arabinose-induced promoter araBAD and the *araC* gene encoding regulator protein. Bacteria transformed with pGLO plasmid were selected according to their ampicillin resistance. The positive transformants were grown in Luria-Bertani broth with 100 mg.L^{-1} of ampicillin and 0.2% arabinose (*w*/*w*) and incubated at 32°C overnight. The cells were harvested using centrifuge type 5340R (Eppendorf AG, Hamburg, Germany) at 4000 rpm for 10 min. The pellets were resuspended using TE buffer (1 mM EDTA with pH 8, 10 mM TRIS-HCl pH 7.5). To initiate the enzymatic digestion of the bacterial cell wall 10 mg.mL^{-1} of fresh lysozyme was added. The protein fractions were collected by centrifugation for 10 minutes at 14 000 rpm and 4°C. GFP was further purified from the bacterial lysate using fast protein liquid chromatography system Biologic DuoFlow (Bio-Rad, Philadelphia, PA, USA) and gel filtration column (Macro-Prep Methyl HIC support, Bio-Rad, Philadelphia, PA, USA). GFP separation was done by isocratic elution with ammonium sulfate. The presence of GFP was confirmed using matrix-assisted laser desorption/ionization time-of-flight mass spectrometry (MALDI-TOF MS) Bruker Ultraflextreme (Bruker Daltonik GmbH, Bremen, Germany) and SDS-PAGE. After the purification, GFP was functionalized with gold nanoparticles (AuNPs) through simple attachment of protein (1 mg.mL^{-1}) on AuNPs dissolved in PBS. The suspension was shaken overnight at 25°C and the resulting one was filtered through Amicon Ultra Centrifugal Filters with ultracel-3 membrane (Merck Millipore, Darmstadt, Germany) to remove the excess of unbound AuNPs.

Atomic absorption spectrometry. Gold in GFP and cadmium originating from QDs was determined on 280Z Agilent Technologies AAS (Agilent, Santa Clara, CA, USA) with electrothermal atomization. As the radiation source gold/cadmium ultrasensitive hollow cathode lamp (lamp current of 4 mA) was employed. The spectrometer was operated at 242.8/228.8 nm resonance line with spectral bandwidth of 1.0/0.5 nm. The pyrolysis temperature 500°C for 8 s and the atomization temperature 2600°C for 3 s were applied. The flow of argon was 300 mL.min^{-1}. Zeeman background correction was used with field strength of 0.8 T. Cadmium was determined in the presence of palladium (1 g.L^{-1}) chemical modifier.

Preparation of acceptor – quantum dot-heptapeptide-antibody conjugate. To control the proper orientation of antibodies localized on acceptor molecule (QDs), the synthetic heptapeptide was employed as a linker between Abs and QD according to our previous study[19].

Prostatic cell lines types and growth conditions. Three human prostatic cell lines purchased from Health Protection Agency Culture Collection (Salisbury, UK) were used for experiments as follows: i) PNT1A established by immortalization of normal adult prostatic epithelial cells by transfection with a plasmid containing SV40 genome with a defective replication origin, ii) 22Rv1 a human prostate carcinoma epithelial cells derived from a xenograft serially propagated in mice after castration-induced regression and relapse of the parental, androgen-dependent CWR22 xenograft, and iii) PC-3 human cell line established from a grade 4 androgen independent and unresponsive prostatic adenocarcinoma obtained from 62-year-old Caucasian male and derived from metastatic site in bone. PNT1A and 22Rv1 were cultured in RPMI-1650 medium with 10% fetal bovine serum (FBS). PC-3 cells were cultured in Ham's F12 medium with 7% FBS. The media were supplemented with penicillin (100 U.mL^{-1}) and streptomycin (0.1 mg.mL^{-1}) and the cells were maintained at 37°C in a humidified incubator (Sanyo, Japan) with 5% CO_2.

Preparation of prostatic cell lines prior to sarcosine isolation. The prostatic cells were harvested and washed with PBS. Prior to isolation the cells were frozen by liquid nitrogen to disrupt their structure. The frozen sample was further homogenized using ultrasonic homogenizer SONOPLUS mini20 (Bandelin electronic, Berlin, Germany). Then, 1 mL of 0.2 M phosphate buffer (pH = 7.0) was added and the sample was homogenized for 5 minutes. The cell homogenates were then treated with Abs@PMPs bioconjugate.

Real urinary samples. To determine the interference of substances occurred in urine, real samples of urine were diluted (0×, 10×, 100×, 1000×) and spiked with sarcosine to final concentration of 40 nM. These samples (250 μL) were incubated with Abs@PMPs (0.5 mg) under the following: 60 min, 800 rpm and 37°C. Particles were removed from urine using external magnetic field (Chemagen, Baesweiler, Germany) and Abs@PMPs with bound sarcosine was processed for FRET assay. Sarcosine was also isolated from urinary samples of patients suffering from acinar adenocarcinoma of prostate (obtained from St. Anne's University Hospital, Department of Urology in Brno). Detailed information about patients is shown in Table 1. Enrolment of patients into realized clinical study was approved by the Ethic committee of the Faculty of medicine, Masaryk University, Brno, Czech Republic. As a control sample, urinary samples obtained from healthy individual (25 years) were used. Informed consent was obtained from all subjects, healthy and patient ones.

Sarcosine determination using ion-exchange liquid chromatography. For determination of sarcosine an ion-exchange liquid chromatography (Model AAA-400, Ingos, Prague, Czech Republic) with post column derivatization by ninhydrin and absorbance detector in visible light range (VIS) was used. Glass column with inner diameter of 3.7 mm and 350 mm length was filled manually with strong cation exchanger (Ostion LG ANB, Ingos, Prague, Czech Republic) 12 μm particles, 8% porosity in sodium cycle. Double channel VIS detector with inner cell of 5 μL was set to two wavelengths: 440 and 570 nm. Recovery of sarcosine was determined according to our previous study[24].

Fluorescence measurements. Fluorescence analyses were performed using multifunctional microplate reader Tecan Infinite 200 PRO (TECAN, Maennedorf, Switzerland). Samples (50 μL) were applied into UV-transparent 96 well microplate with flat bottom Costar® (Corning, NY, USA). All measurements were performed at 25°C controlled by Tecan Infinite 200 PRO. Fluorescence attributes were evaluated at two excitations (λ_{exc} 400 nm for GFP and λ_{exc} 520 nm for QDs) and two emission wavelengths (λ_{em} 510 nm for GFP and λ_{em} 604 nm for QDs).

1. Siegel, R., Naishadham, D. & Jemal, A. Cancer statistics, 2013. *CA-Cancer J Clin* **63**, 11–30 (2013).
2. Cernei, N. *et al.* Sarcosine as a Potential Prostate Cancer Biomarker-A Review. *Int J Mol Sci* **14**, 13893–13908 (2013).
3. Heger, Z. *et al.* Determination of common urine substances as an assay for improving prostate carcinoma diagnostics. *Oncol Rep* **31**, 1846–1854 (2014).
4. Sreekumar, A. *et al.* Metabolomic profiles delineate potential role for sarcosine in prostate cancer progression. *Nature* **457**, 910–914 (2009).
5. Jiang, Y. Q., Cheng, X. L., Wang, C. A. & Ma, Y. F. Quantitative Determination of Sarcosine and Related Compounds in Urinary Samples by Liquid Chromatography with Tandem Mass Spectrometry. *Anal Chem* **82**, 9022–9027 (2010).
6. Riedel, M. *et al.* Photoelectrochemical Sensor Based on Quantum Dots and Sarcosine Oxidase. *ChemPhysChem* **14**, 2338–2342 (2013).
7. Burton, C., Gamagedara, S. & Ma, Y. F. A novel enzymatic technique for determination of sarcosine in urine samples. *Anal Methods* **4**, 141–146 (2012).
8. Lan, J. M. *et al.* Colorimetric determination of sarcosine in urine samples of prostatic carcinoma by mimic enzyme palladium nanoparticles. *Anal Chim Acta* **825**, 63–68 (2014).
9. Chen, J., Zhang, J., Zhang, W. P. & Chen, Z. L. Sensitive determination of the potential biomarker sarcosine for prostate cancer by LC-MS with N,N '-dicyclohexylcarbodiimide derivatization. *J Sep Sci* **37**, 14–19 (2014).
10. Haviv, A. H., Greneche, J. M. & Lellouche, J. P. Aggregation Control of Hydrophilic Maghemite (gamma-Fe2O3) Nanoparticles by Surface Doping Using Cerium Atoms. *J Am Chem Soc* **132**, 12519–12521 (2010).
11. Guo, Q. J., Teng, X. W., Rahman, S. & Yang, H. Patterned Langmuir-Blodgett films of monodisperse nanoparticles of iron oxide using soft lithography. *J Am Chem Soc* **125**, 630–631 (2003).

12. El-Boubbou, K., Gruden, C. & Huang, X. Magnetic glyco-nanoparticles: A unique tool for rapid pathogen detection, decontamination, and strain differentiation. *J Am Chem Soc* **129**, 13392–13393 (2007).
13. Schwegmann, H., Feitz, A. J. & Frimmel, F. H. Influence of the zeta potential on the sorption and toxicity of iron oxide nanoparticles on S. cerevisiae and E. coli. *J Colloid Interface Sci* **347**, 43–48 (2010).
14. Hodek, P. *et al.* Optimized Protocol of Chicken Antibody (IgY) Purification Providing Electrophoretically Homogenous Preparations. *Int J Electrochem Sci* **8**, 113–124 (2013).
15. Shaner, N. C., Steinbach, P. A. & Tsien, R. Y. A guide to choosing fluorescent proteins. *Nat Methods* **2**, 905–909 (2005).
16. Bale, S. S. *et al.* Nanoparticle-Mediated Cytoplasmic Delivery of Proteins To Target Cellular Machinery. *ACS Nano* **4**, 1493–1500 (2010).
17. Love, J. C. *et al.* Self-assembled monolayers of thiolates on metals as a form of nanotechnology. *Chem Rev* **105**, 1103–1169 (2005).
18. Qu, L. H. & Peng, X. G. Control of photoluminescence properties of CdSe nanocrystals in growth. *J Am Chem Soc* **124**, 2049–2055 (2002).
19. Janu, L. *et al.* Electrophoretic study of peptide-mediated quantum dot-human immunoglobulin bioconjugation. *Electrophoresis* **34**, 2725–2732 (2013).
20. Casanova, D. *et al.* Single lanthanide-doped oxide nanoparticles as donors in fluorescence resonance energy transfer experiments. *J Phys Chem B* **110**, 19264–19270 (2006).
21. Khan, A. P. *et al.* The Role of Sarcosine Metabolism in Prostate Cancer Progression. *Neoplasia* **15**, 491–501 (2013).
22. Ryan, D., Robards, K., Prenzler, P. D. & Kendall, M. Recent and potential developments in the analysis of urine: A review. *Anal Chim Acta* **684**, 17–29 (2011).
23. Abate-Shen, C. & Shen, M. M. Diagnostics The prostate-cancer metabolome. *Nature* **457**, 799–800 (2009).
24. Zitka, O. *et al.* Microfluidic chip coupled with modified paramagnetic particles for sarcosine isolation in urine. *Electrophoresis* **34**, 2639–2647 (2013).

Acknowledgments

The financial support by CEITEC CZ.1.05/1.1.00/02.0068 is greatly acknowledged.

Author contributions

Z.H. participated on FRET measurements and prepared the draft of the manuscript. N.C. performed the chromatographic detection of sarcosine and processed and discussed the results. S.K. performed antibodies based experiments and participated on the preparation of the nano-construct. M.M. performed the cell experiments and prepared cell and urinary samples prior to analysis. P.K. synthesized quantum dots and particles. P.H. prepared the antibodies and participated on the preparation of the nano-construct. O.Z. participated in the preparation of the manuscript. V.A. helped with the results discussion and conceived the study. R.K. designed experiments, discussed the results and submitted the manuscript.

Additional information

Competing financial interests: The authors declare no competing financial interests.

How to cite this article: Heger, Z. *et al.* Paramagnetic Nanoparticles as a Platform for FRET-Based Sarcosine Picomolar Detection. *Sci. Rep.* **5**, 8868; DOI:10.1038/srep08868 (2015).

6 Summary

Cancer is the leading cause of mortality in Western countries and the second leading cause of death in developed countries. The burden of cancer is rising in economically developed countries: their population is growing and ageing and it adopts cancer-associated lifestyle choices including smoking, physical inactivity, and “westernized” diets. Prostate cancer is the second most frequently diagnosed cancer and the sixth leading cause of cancer death in males. The prevalence of prostate cancer increases with age. It does, however, usually respond to treatment and, if localized, may be curable. The tempo of tumour growth varies from very slow to moderately rapid, and some patients may have prolonged survival, even after cancer has metastasized to distant sites. It is therefore obvious that research in cancer field and therefore CaP should be given due attention.

This habilitation thesis summarizes new findings in the field of biochemistry, pathogenesis and diagnostics of prostate cancer. It has been divided into four parts depending on their specific focus.

We can summarize our findings by individual PARTS:

PART I - Zinc, metallothionein and prostate cancer progression

Zinc ions and metallothionein are important players in pathogenesis of CaP. We found out that decreased concentration of zinc was demonstrated both in the model tumour cell line and in the patients’ tumour tissue. This reduction was not accompanied by a decrease in the concentration of zinc-binding metallothionein. Gene and protein expression of the most frequently represented MT form, i.e. MT2A, was increased in the prostate tumour lines compared to the non-tumour line PNT1A. Based on zinc and MT concentrations it is possible to say that the selected prostate tumour cell lines are a relatively good model of the real CaP status. Furthemore, zinc ions can significantly alter expression of the genes involved in CaP carcinogenesis. The primary prostate tumour derived cells were shown to have a higher cell resistance to the zinc-induced apoptosis. This higher resistance was reflected by changes in gene expression of pro- and anti-apoptotic BAX and BCL2 and in the expression of the MKI67 proliferation marker. This increased tolerance to zinc did not appear in the PC-3 cells derived from CaP bone metastasis. PC-3 cells tolerate zinc much less than the non-tumour epithelial prostate cells PNT1A. In the

next part of this work, zinc was therefore monitored as a possible inhibitor of CaP carcinogenesis and its progression to the castration-resistant prostate cancer (CRPC) phase. Furthermore, the significance of miR-375 in CaP and its possible relationship with resistance to docetaxel (which is used as one of few chemotherapeutics to treat metastatic CaP) was revealed. Finally, we found out that long-term exposure of CaP-derived tumour cells to high zinc concentrations leads to increased accumulation of zinc inside the cells, but on the other side also contributes to activation of the signalling pathways leading to resistance and increased aggressiveness of cells.

PART II - Metabolism of amino acids and prostate carcinoma progression

Metabolism of prostate gland cells is unique and different from metabolism of other cells in human body. Changes in amino acid levels induced by carcinogenesis and/or resistance to zinc could be relevant for diagnostic purposes and may also potentially lead to new therapeutic options. Ratios of certain logically related amino acids may be a sensitive indicator of the malignant phenotype. Inhibition of aspartate synthesis could also become a promising approach. We have also dealt with amino acids accumulated in tumour cells or tissues that are able to affect substantially the events associated with CaP carcinogenesis. Amino acids of the sarcosine pathway (glycine, dimethylglycine and sarcosine) affect the ability of cells derived from CaP (22Rv1, PC-3) to migrate, as well as their ability to divide. The tumour-supporting effect of sarcosine could be observed on the rate of tumour growth in mice. Sarcosine is thus probably a key metabolite affecting the progression of CaP and is a suitable target for diagnostic approaches as well as for possible targeted therapy.

PART III - Redox status and oxidative stress of prostatic cells

In this part of habilitation thesis, we have devoted ourselves mainly to the effect of external factors on the change of the cellular redox status and thus on the potential development of oxidative stress state in the prostate tumour cells. The importance of zinc ions associated with the development and progression of prostate carcinoma was clarified sufficiently in PART I. However, the zinc ions play a role of exogenous stimulators of ROS production and increase the level of oxidative stress in cells. We demonstrated that the sensitivity of individual prostate cell lines to the increasing concentrations of zinc ions differs considerably. After the application of zinc ions, different behaviour of the tumour and non-tumour cells and their antioxidant systems was demonstrated. Based on the integrative approaches we were able monitoring of the redox

status in the individual cell lines. These methods were then used for the evaluation of cisplatin effects. Cisplatin belongs to commonly used cytostatic drugs. We focused on the analysis of oxidative stress, cell cycle, apoptosis and selected cytotoxic analyses. Our attention was directed to the PC3 line, representing a model of the aggressive prostate carcinoma. After the application of cisplatin, we could not see in this line a typical cell cycle arrest in the G1/G0 phase, and at the same time, we observed a decreased tendency for apoptosis. Moreover, we demonstrated that this cell line exhibits a higher antioxidant activity and higher metallothionein content after the administration of cisplatin and thus can be used as a model of cisplatin resistance. Finally, non-coding amino acid sarcosine was studied intensively in association with its expected predictive value for the prostate carcinoma diagnosis, affects cancer cells aggression. Based on our experiments, it was confirmed that these mechanisms are related neither to antioxidants nor to the regulation of oxidative stress levels.

PART IV - Novel approaches to the analysis of prostate cancer markers

Discovering and definition of new biochemical markers, which are specifically connected with grave pathological states including tumour diseases, are among the most important objectives of biomedical research. Identification of highly specific and sensitive biomarkers represents the main aim of modern research, because only such biomarkers may be applied towards the early diagnosis of malignant disease, prediction of prognosis and eventually development of an appropriate treatment strategy in clinical practice. We have decided to study MT, Cav-1 and AMACR in connection with the progression of CaP. None of the substances studied therein meets criteria for being a marker of the aggressive disease form. There was no statistically significant difference in the level of monitored proteins between the localized (T1, 2) and spreading (T3, 4) tumours. However, the level of caveolin-1 was significantly higher in the serum of patients with tumours of stage 4 and AMACR and Cav-1 levels were higher in patients with Gleason grade 9. MT as the only one showed a significantly increased level in the serum of CaP patients compared with control samples. The determination of sarcosine in connection with the determination of other CaP biomarkers has a potential to improve the prostate carcinoma diagnostics and to eliminate false positive and false negative cases.

Furthermore, we have decided to introduce new methodologies based on paramagnetic nanoparticles and Förster resonance energy transfer (FRET). Paramagnetic nanoparticles allow to isolate both RNA and proteins from complex samples, thereby increasing detection specificity and at the same time reducing amounts of consumed chemicals. This procedure was optimized for metallothionein in serum and cell lysate samples. In case of the FRET assay we describe the

method for sarcosine determination based on this methodology between quantum dots and green fluorescent protein enabled by sandwich arrangement using anti-sarcosine antibodies in prostate cancer patient urinary samples and in prostatic cell lines (PC3, 22Rv1, PNT1A).

7 Abstrakt

Předložená habilitační práce je kompilací vybraných vědeckých publikací, ke kterým jsem přispěl jako první autor, korespondující autor či spoluautor v průběhu mé vědecké kariéry. Tyto články byly zveřejněny v letech 2011 až 2017. Všechny zde uvedené publikace mají společné téma týkající se karcinomu prostaty. Habilitační práce především shrnuje nové poznatky v oblasti biochemie a patogeneze karcinomu prostaty a je rozdělena na čtyři části podle jejich specifických zaměření. První část je věnována problematice zinečnatých iontů a jejich vztahu ke vzniku a progresi karcinomu prostaty. Druhá část se zabývá metabolismem aminokyselin u karcinomu prostaty. Část třetí je věnována monitorování redoxního stavu nádorových buněk prostaty a poslední část je zaměřena na detekci nových nádorových markerů. Doprovodný text zdůrazňuje můj příspěvek k novým poznatkům v oblasti patogeneze karcinomu prostaty a také stručný vhled do zkoumané problematiky. Součástí habilitační práce jsou i originální publikace, kde je možné nalézt komplexní informace o jednotlivých experimentálních studiích.

8 Abstract

Cancer is the leading cause of mortality in Western countries and the second leading cause of death in developed countries. The burden of cancer is rising in economically developed countries: their population is growing and ageing and it adopts cancer-associated lifestyle choices including smoking, physical inactivity, and “westernized” diets. Prostate cancer is the second most frequently diagnosed cancer and the sixth leading cause of cancer death in males. The prevalence of prostate cancer increases with age. It does, however, usually respond to treatment and, if localized, may be curable. The tempo of tumour growth varies from very slow to moderately rapid, and some patients may have prolonged survival, even after cancer has metastasized to distant sites. It is therefore obvious that research in cancer field and therefore CaP should be given due attention. This habilitation summarizes new findings in the field of biochemistry and pathogenesis of prostate cancer. It has been divided into four parts depending on their specific focus. The first part is devoted to the issue of the zinc ions and their relation to prostate cancer development and progression. Part two deals with the amino acid metabolism in prostate cancer. Part three is dedicated to monitoring of the redox status of the prostate tumour cells and the last part is focused on the newly investigated prostate cancer markers and their determination.

9 References

1. Ellem, S.J. and G.P. Risbridger, *Treating prostate cancer: A rationale for targeting local oestrogens.* Nature Reviews Cancer, 2007. **7**(8): p. 621-627.
2. Raudenská, M., J. Balvan, J. Gumulec, M. Sztalmachová, H. Polanská, V. Adam, M. Stiborová, T. Eckschlager, R. Kizek, and M. Masarík, *Molecular mechanisms of anti-cancer treatment resistance in prostate tumours.* Prakticky Lekar, 2014. **94**(2): p. 88-93.
3. Waltregny, D. and V. Castronovo, *Recent advances in prostate cancer metastasis.* Tumori, 1996. **82**(3): p. 193-204.
4. Williams, S.A., P. Singh, J.T. Isaacs, and S.R. Denmeade, *Does PSA play a role as a promoting agent during the initiation and/or progression of prostate cancer?* Prostate, 2007. **67**(3): p. 312-329.
5. Telang, J.M., B.R. Lane, M.L. Cher, D.C. Miller, and J.M. Dupree, *Prostate cancer, family history, and eligibility for active surveillance: A systematic review of the literature.* BJU Int, 2017.
6. Bergin, A.R.T., E. Hovey, A. Lloyd, G. Marx, P. Parente, T. Rapke, and P. de Souza, *Docetaxel-related fatigue in men with metastatic prostate cancer: a descriptive analysis.* Support Care Cancer, 2017.
7. Bubendorf, L., A. Schopfer, U. Wagner, G. Sauter, H. Moch, N. Willi, T.C. Gasser, and M.J. Mihatsch, *Metastatic patterns of prostate cancer: an autopsy study of 1,589 patients.* Hum Pathol, 2000. **31**(5): p. 578-83.
8. Denmeade, S.R. and J.T. Isaacs, *A history of prostate cancer treatment.* Nature Reviews Cancer, 2002. **2**(5): p. 389-396.
9. Yap, T.A., A.D. Smith, R. Ferraldeschi, B. Al-Lazikani, P. Workman, and J.S. de Bono, *Drug discovery in advanced prostate cancer: translating biology into therapy.* Nature Reviews Drug Discovery, 2016. **15**(10): p. 699-718.
10. Feldman, B.J. and D. Feldman, *The development of androgen-independent prostate cancer.* Nature Reviews Cancer, 2001. **1**(1): p. 34-45.
11. Foltyn, I., *Active search for prostate cancer by PSA testing in GP surgery.* Prakt. Lekar, 2007. **87**(2): p. 117-118.
12. Mlcochova, P., C. Barinka, J. Tykvart, P. Sacha, and J. Konvalinka, *Prostate-specific membrane antigen and its truncated form PSM'.* Prostate, 2009. **69**(5): p. 471-479.
13. Hankey, B.F., E.J. Feuer, L.X. Clegg, R.B. Hayes, J.M. Legler, P.C. Prorok, L.A. Ries, R.M. Merrill, and R.S. Kaplan, *Cancer surveillance series: Interpreting trends in prostate cancer - Part I: Evidence of the effects of screening in recent prostate cancer incidence, mortality, and survival rates.* Journal of the National Cancer Institute, 1999. **91**(12): p. 1017-1024.
14. Thompson, I.M., *Prevalence of prostate cancer among men with a prostate-specific antigen level <= 4.0 ng per milliliter (vol 350, pg 2239, 2004).* New England Journal of Medicine, 2004. **351**(14): p. 1470-1470.
15. Baillargeon, J., B.H. Pollock, A.R. Kristal, P. Bradshaw, J. Hernandez, J. Basler, B. Higgins, S. Lynch, T. Rozanski, D. Troyer, and I. Thompson, *The association of body*

mass index and prostate-specific antigen in a population-based study. Cancer, 2005. **103**(5): p. 1092-1095.
16. Sharrard, R.M. and N.J. Maitland, *Regulation of protein kinase B activity by PTEN and SHIP2 in human prostate-derived cell lines.* Cell Signal, 2007. **19**(1): p. 129-38.
17. Hartel, A., A. Didier, S.E. Ulbrich, M. Wierer, and H.H.D. Meyer, *Characterisation of steroid receptor expression in the human prostate carcinoma cell line 22RV1 and quantification of androgen effects on mRNA regulation of prostate-specific genes.* Journal of Steroid Biochemistry and Molecular Biology, 2004. **92**(3): p. 187-197.
18. Horoszewicz, J.S., S.S. Leong, E. Kawinski, J.P. Karr, H. Rosenthal, T.M. Chu, E.A. Mirand, and G.P. Murphy, *LNCaP model of human prostatic-carcinoma.* Cancer Research, 1983. **43**(4): p. 1809-1818.
19. Fraser, M., H. Zhao, K.R. Luoto, C. Lundin, C. Coackley, N. Chan, A.M. Joshua, T.A. Bismar, A. Evans, T. Helleday, and R.G. Bristow, *PTEN deletion in prostate cancer cells does not associate with loss of RAD51 function: implications for radiotherapy and chemotherapy.* Clin Cancer Res, 2012. **18**(4): p. 1015-27.
20. Skjoth, I.H. and O.G. Issinger, *Profiling of signaling molecules in four different human prostate carcinoma cell lines before and after induction of apoptosis.* Int J Oncol, 2006. **28**(1): p. 217-29.
21. Mitchell, S., P. Abel, M. Ware, G. Stamp, and E. Lalani, *Phenotypic and genotypic characterization of commonly used human prostatic cell lines.* BJU Int, 2000. **85**(7): p. 932-44.
22. Gumulec, J., J. Balvan, M. Sztalmachova, M. Raudenska, V. Dvorakova, L. Knopfova, H. Polanska, K. Hudcova, B. Ruttkay-Nedecky, P. Babula, V. Adam, R. Kizek, M. Stiborova, and M. Masarik, *Cisplatin-resistant prostate cancer model: Differences in antioxidant system, apoptosis and cell cycle.* Int J Oncol, 2014. **44**(3): p. 923-33.
23. Grattan, B.J. and H.C. Freake, *Zinc and cancer: implications for LIV-1 in breast cancer.* Nutrients, 2012. **4**(7): p. 648-75.
24. Franklin, R.B. and L.C. Costello, *The Important Role of the Apoptotic Effects of Zinc in the Development of Cancers.* Journal of Cellular Biochemistry, 2009. **106**(5): p. 750-757.
25. Coyle, P., J.C. Philcox, L.C. Carey, and A.M. Rofe, *Metallothionein: The multipurpose protein.* Cellular and Molecular Life Sciences, 2002. **59**(4): p. 627-647.
26. Franklin, R.B., P. Feng, B. Milon, M.M. Desouki, K.K. Singh, A. Kajdacsy-Balla, O. Bagasra, and L.C. Costello, *hZIP1 zinc uptake transporter down regulation and zinc depletion in prostate cancer.* Molecular Cancer, 2005. **4**: p. 13.
27. Vallee, B.L. and K.H. Falchuk, *The biochemical basis of zinc physiology.* Physiological Reviews, 1993. **73**(1): p. 79-118.
28. Elliott, J.L., *Zinc and copper in the pathogenesis of amyotrophic lateral sclerosis.* Progress in Neuro-Psychopharmacology & Biological Psychiatry, 2001. **25**(6): p. 1169-1185.
29. Cousins, R.J., J.P. Liuzzi, and L.A. Lichten, *Mammalian zinc transport, trafficking, and signals.* J Biol Chem, 2006. **281**(34): p. 24085-9.
30. Gunther, V., U. Lindert, and W. Schaffner, *The taste of heavy metals: Gene regulation by MTF-1.* Biochimica Et Biophysica Acta-Molecular Cell Research, 2012. **1823**(9): p. 1416-1425.
31. Gaither, L.A. and D.J. Eide, *Eukaryotic zinc transporters and their regulation.* Biometals, 2001. **14**(3-4): p. 251-270.
32. Chang, C.C. and P.C. Huang, *Semi-empirical simulation of Zn/Cd binding site preference in the metal binding domains of mammalian metallothionein.* Protein Engineering, 1996. **9**(12): p. 1165-1172.

33. Ruttkay-Nedecky, B., L. Nejdl, J. Gumulec, O. Zitka, M. Masarik, T. Eckschlager, M. Stiborova, V. Adam, and R. Kizek, *The Role of Metallothionein in Oxidative Stress.* International Journal of Molecular Sciences, 2013. **14**(3): p. 6044-6066.
34. Lee, B.Y., D.H. Shin, S. Cho, K.S. Seo, and H. Kim, *Genome-wide analysis of copy number variations reveals that aging processes influence body fat distribution in Korea Associated Resource (KARE) cohorts.* Human Genetics, 2012. **131**(11): p. 1795-1804.
35. Seibold, P., R. Hein, P. Schmezer, P. Hall, J.J. Liu, N. Dahmen, D. Flesch-Janys, O. Popanda, and J. Chang-Claude, *Polymorphisms in oxidative stress-related genes and postmenopausal breast cancer risk.* International Journal of Cancer, 2011. **129**(6): p. 1467-1476.
36. Ricote, M., M. Royuela, I. Garcia-Tunon, F.R. Bethencourt, R. Paniagua, and B. Fraile, *Pro-apoptotic tumor necrosis factor-alpha transduction pathway in normal prostate, benign prostatic hyperplasia and prostatic carcinoma.* Journal of Urology, 2003. **170**(3): p. 787-790.
37. Royuela, M., G. Rodriguez-Berriguete, B. Fraile, and R. Paniagua, *TNF-alpha/IL-1/NF-kappa B transduction pathway in human cancer prostate.* Histology and Histopathology, 2008. **23**(10): p. 1279-1290.
38. Raudenska, M., J. Gumulec, O. Podlaha, M. Sztalmachova, P. Babula, T. Eckschlager, V. Adam, R. Kizekb, and M. Masarik, *Metallothionein polymorphisms in pathological processes.* Metallomics, 2014. **6**(1): p. 55-68.
39. Costello, L.C., R.B. Franklin, Y. Liu, and M.C. Kennedy, *Zinc causes a shift toward citrate at equilibrium of the m-aconitase reaction of prostate mitochondria.* Journal of Inorganic Biochemistry, 2000. **78**(2): p. 161-165.
40. Costello, L.C. and R.B. Franklin, *Novel role of zinc in the regulation of prostate citrate metabolism and its implications in prostate cancer.* Prostate, 1998. **35**(4): p. 285-296.
41. Costello, L.C., R.B. Franklin, P. Feng, M. Tan, and O. Bagasra, *Zinc and prostate cancer: a critical scientific, medical, and public interest issue (United states).* Cancer Causes & Control, 2005. **16**(8): p. 901-915.
42. Franz, M.C., P. Anderle, M. Burzle, Y. Suzuki, M.R. Freeman, M.A. Hediger, and G. Kovacs, *Zinc transporters in prostate cancer.* Molecular Aspects of Medicine, 2013. **34**(2-3): p. 735-741.
43. Costello, L.C. and R.B. Franklin, *A comprehensive review of the role of zinc in normal prostate function and metabolism; and its implications in prostate cancer.* Archives of Biochemistry and Biophysics, 2016. **611**: p. 100-112.
44. Feng, P., T.L. Li, Z.X. Guan, R.B. Franklin, and L.C. Costello, *The involvement of bax in zinc-induced mitochondrial apoptogenesis in malignant prostate cells.* Molecular Cancer, 2008. **7**.
45. Costello, L.C. and R.B. Franklin, *The clinical relevance of the metabolism of prostate cancer; zinc and tumor suppression: connecting the dots.* Molecular Cancer, 2006. **5**.
46. Kambe, T., Y. Yamaguchi-Iwai, R. Sasaki, and M. Nagao, *Overview of mammalian zinc transporters.* Cellular and Molecular Life Sciences, 2004. **61**(1): p. 49-68.
47. Costello, L.C. and R.B. Franklin, *The intermediary metabolism of the prostate: a key to understanding the pathogenesis and progression of prostate malignancy.* Oncology, 2000. **59**.
48. Gumulec, J., M. Masarik, S. Krizkova, V. Adam, J. Hubalek, J. Hrabeta, T. Eckschlager, M. Stiborova, and R. Kizek, *Insight to Physiology and Pathology of Zinc(II) Ions and Their Actions in Breast and Prostate Carcinoma.* Current Medicinal Chemistry, 2011. **18**(33): p. 5041-5051.
49. He, L. and G.J. Hannon, *Microrna: Small RNAs with a big role in gene regulation.* Nature Reviews Genetics, 2004. **5**(7): p. 522-531.

50. Chen, X., Y. Ba, L.J. Ma, X. Cai, Y. Yin, K.H. Wang, J.G. Guo, Y.J. Zhang, J.N. Chen, X. Guo, Q.B. Li, X.Y. Li, W.J. Wang, Y. Zhang, J. Wang, X.Y. Jiang, Y. Xiang, C. Xu, P.P. Zheng, J.B. Zhang, R.Q. Li, H.J. Zhang, X.B. Shang, T. Gong, G. Ning, K. Zen, J.F. Zhang, and C.Y. Zhang, *Characterization of microRNAs in serum: a novel class of biomarkers for diagnosis of cancer and other diseases.* Cell Research, 2008. **18**(10): p. 997-1006.
51. Pekarik, V., J. Gumulec, M. Masarik, R. Kizek, and V. Adam, *Prostate Cancer, miRNAs, Metallothioneins and Resistance to Cytostatic Drugs.* Current Medicinal Chemistry, 2013. **20**(4): p. 534-544.
52. Kratochvilova, M., M. Raudenska, Z. Heger, L. Richtera, N. Cernei, V. Adam, P. Babula, M. Novakova, M. Masarik, and J. Gumulec, *Amino Acid Profiling of Zinc Resistant Prostate Cancer Cell Lines: Associations With Cancer Progression.* Prostate, 2017. **77**(6): p. 604-616.
53. Masarik, M., J. Gumulec, M. Hlavna, M. Sztalmachova, P. Babula, M. Raudenska, M. Pavkova-Goldbergova, N. Cernei, J. Sochor, O. Zitka, B. Ruttkay-Nedecky, S. Krizkova, V. Adam, and R. Kizek, *Monitoring of the prostate tumour cells redox state and real-time proliferation by novel biophysical techniques and fluorescent staining.* Integrative Biology, 2012. **4**(6): p. 672-684.
54. Gumulec, J., M. Masarik, V. Adam, T. Eckschlager, I. Provaznik, and R. Kizek, *Serum and Tissue Zinc in Epithelial Malignancies: A Meta-Analysis.* Plos One, 2014. **9**(6).
55. Gumulec, J., M. Raudenska, V. Adam, R. Kizek, and M. Masarik, *Metallothionein - Immunohistochemical Cancer Biomarker: A Meta-Analysis.* Plos One, 2014. **9**(1).
56. Hlavna, M., M. Raudenska, K. Hudcova, J. Gumulec, M. Sztalmachova, V. Tanhauserova, P. Babula, V. Adam, T. Eckschlager, R. Kizek, and M. Masarik, *MicroRNAs and zinc metabolism-related gene expression in prostate cancer cell lines treated with zinc(II) ions.* International Journal of Oncology, 2012. **41**(6): p. 2237-2244.
57. Holubova, M., M. Axmanova, J. Gumulec, M. Raudenska, M. Sztalmachova, P. Babula, V. Adam, R. Kizek, and M. Masarik, *KRAS NF-kappa B is involved in the development of zinc resistance and reduced curability in prostate cancer.* Metallomics, 2014. **6**(7): p. 1240-1253.
58. Sztalmachova, M., M. Hlavna, J. Gumulec, M. Holubova, P. Babula, J. Balvan, J. Sochor, V. Tanhauserova, M. Raudenska, S. Krizkova, V. Adam, T. Eckschlager, R. Kizek, and M. Masarik, *Effect of zinc(II) ions on the expression of pro- and anti-apoptotic factors in high-grade prostate carcinoma cells.* Oncology Reports, 2012. **28**(3): p. 806-814.
59. Wang, Y., R. Lieberman, J. Pan, Q. Zhang, M.J. Du, P. Zhang, M. Nevalainen, M. Kohli, N.K. Shenoy, H. Meng, M. You, and L. Wang, *miR-375 induces docetaxel resistance in prostate cancer by targeting SEC23A and YAP1.* Molecular Cancer, 2016. **15**.
60. Franklin, R.B. and L.C. Costello, *Zinc as an anti-tumor agent in prostate cancer and in other cancers.* Archives of Biochemistry and Biophysics, 2007. **463**(2): p. 211-217.
61. Ho, E., *Zinc deficiency, DNA damage and cancer risk.* Journal of Nutritional Biochemistry, 2004. **15**(10): p. 572-578.
62. Uzzo, R.G., P. Leavis, W. Hatch, V.L. Gabai, N. Dulin, N. Zvartau, and V.M. Kolenko, *Zinc inhibits nuclear factor-kappa B activation and sensitizes prostate cancer cells to cytotoxic agents.* Clinical Cancer Research, 2002. **8**(11): p. 3579-3583.
63. Gallus, S., R. Foschi, E. Negri, R. Talamini, S. Franceschi, M. Montella, V. Ramazzotti, A. Tavani, L. Dal Maso, and C. La Vecchia, *Dietary zinc and prostate cancer risk: A case-control study from Italy.* European Urology, 2007. **52**(4): p. 1052-1057.

64. Lagiou, P., J. Wuu, A. Trichopoulou, C.C. Hsieh, H.O. Adami, and D. Trichopoulos, *Diet and benign prostatic hyperplasia: A study in Greece.* Urology, 1999. **54**(2): p. 284-290.
65. Lawson, K.A., M.E. Wright, A. Subar, T. Mouw, A. Hollenbeck, A. Schatzkin, and M.F. Leitzmann, *Multivitamin use and risk of prostate cancer in the national institutes of health-AARP diet and health study.* Journal of the National Cancer Institute, 2007. **99**(10): p. 754-764.
66. Weinrich, S.P., J.H. Priest, M.A. Moyad, and M.C. Weinrich, *Intake of selected nutritional supplements by African-American men.* Urology, 2004. **64**(6): p. 1094-1097.
67. Maxwell, P.J., R. Gallagher, A. Seaton, C. Wilson, P. Scullin, J. Pettigrew, I.J. Stratford, K.J. Williams, P.G. Johnston, and D.J.J. Waugh, *HIF-1 and NF-kappa B-mediated upregulation of CXCR1 and CXCR2 expression promotes cell survival in hypoxic prostate cancer cells.* Oncogene, 2007. **26**(52): p. 7333-7345.
68. Tafani, M., B. Pucci, A. Russo, L. Schito, L. Pellegrini, G. Perrone, L. Villanova, L. Salvatori, L. Ravenna, E. Petrangeli, and M. Russo, *Modulators of HIF1α and NFkB in Cancer Treatment: Is it a Rational Approach for Controlling Malignant Progression?* Frontiers in Pharmacology, 2013. **4**(13).
69. Whitaker, H.C. and D.E. Neal, *RAS pathways in prostate cancer - mediators of hormone resistance?* Curr Cancer Drug Targets, 2010. **10**(8): p. 834-9.
70. Ananieva, E., *Targeting amino acid metabolism in cancer growth and anti-tumor immune response.* World J Biol Chem, 2015. **6**(4): p. 281-9.
71. Costello, L.C., Y.Y. Liu, R.B. Franklin, and M.C. Kennedy, *Zinc inhibition of mitochondrial aconitase and its importance in citrate metabolism of prostate epithelial cells.* Journal of Biological Chemistry, 1997. **272**(46): p. 28875-28881.
72. DeFeo, E.M., C.L. Wu, W.S. McDougal, and L.L. Cheng, *A decade in prostate cancer: from NMR to metabolomics.* Nat Rev Urol, 2011. **8**(6): p. 301-11.
73. Giskeodegard, G.F., H. Bertilsson, K.M. Selnaes, A.J. Wright, T.F. Bathen, T. Viset, J. Halgunset, A. Angelsen, I.S. Gribbestad, and M.B. Tessem, *Spermine and Citrate as Metabolic Biomarkers for Assessing Prostate Cancer Aggressiveness.* Plos One, 2013. **8**(4).
74. Cheng, L.L., C.L. Wu, M.R. Smith, and R.G. Gonzalez, *Non-destructive quantitation of spermine in human prostate tissue samples using HRMAS H-1 NMR spectroscopy at 9.4 T.* Febs Letters, 2001. **494**(1-2): p. 112-116.
75. Eidelman, E., J. Twum-Ampofo, J. Ansari, and M.M. Siddiqui, *The Metabolic Phenotype of Prostate Cancer.* Frontiers in Oncology, 2017. **7**.
76. Huang, G., X.R. Liu, L. Jiao, C.L. Xu, Z.X. Zhang, L.H. Wang, Y. Li, C. Yang, W.D. Zhang, and Y.H. Sun, *Metabolomic evaluation of the response to endocrine therapy in patients with prostate cancer.* European Journal of Pharmacology, 2014. **729**: p. 132-137.
77. Lloyd, S.M., J. Arnold, and A. Sreekumar, *Metabolomic profiling of hormone-dependent cancers: a bird's eye view.* Trends in Endocrinology and Metabolism, 2015. **26**(9): p. 477-485.
78. Massie, C.E., A. Lynch, A. Ramos-Montoya, J. Boren, R. Stark, L. Fazli, A. Warren, H. Scott, B. Madhu, N. Sharma, H. Bon, V. Zecchini, D.M. Smith, G.M. DeNicola, N. Mathews, M. Osborne, J. Hadfield, S. MacArthur, B. Adryan, S.K. Lyons, K.M. Brindle, J. Griffiths, M.E. Gleave, P.S. Rennie, D.E. Neal, and I.G. Mills, *The androgen receptor fuels prostate cancer by regulating central metabolism and biosynthesis.* Embo Journal, 2011. **30**(13): p. 2719-2733.
79. Sreekumar, A., L.M. Poisson, T.M. Rajendiran, A.P. Khan, Q. Cao, J.D. Yu, B. Laxman, R. Mehra, R.J. Lonigro, Y. Li, M.K. Nyati, A. Ahsan, S. Kalyana-Sundaram, B. Han, X.H. Cao, J. Byun, G.S. Omenn, D. Ghosh, S. Pennathur, D.C. Alexander, A. Berger,

J.R. Shuster, J.T. Wei, S. Varambally, C. Beecher, and A.M. Chinnaiyan, *Metabolomic profiles delineate potential role for sarcosine in prostate cancer progression.* Nature, 2009. **457**(7231): p. 910-914.

80. Khan, A.P., T.M. Rajendiran, B. Ateeq, I.A. Asangani, J.N. Athanikar, A.K. Yocum, R. Mehra, J. Siddiqui, G. Palapattu, J.T. Wei, G. Michailidis, A. Sreekumar, and A.M. Chinnaiyan, *The Role of Sarcosine Metabolism in Prostate Cancer Progression.* Neoplasia, 2013. **15**(5): p. 491-+.
81. Lucarelli, G., M. Rutigliano, V. Galleggiante, A. Giglio, S. Palazzo, M. Ferro, C. Simone, C. Bettocchi, M. Battaglia, and P. Ditonno, *Metabolomic profiling for the identification of novel diagnostic markers in prostate cancer.* Expert Review of Molecular Diagnostics, 2015. **15**(9): p. 1211-1224.
82. Dasgupta, S., N. Putluri, W.W. Long, B. Zhang, J.H. Wang, A.K. Kaushik, J.M. Arnold, S.K. Bhowmik, E. Stashi, C.A. Brennan, K. Rajapakshe, C. Coarfa, N. Mitsiades, M.M. Ittmann, A.M. Chinnaiyan, A. Sreekumar, and B.W. O'Malley, *Coactivator SRC-2-dependent metabolic reprogramming mediates prostate cancer survival and metastasis.* Journal of Clinical Investigation, 2015. **125**(3): p. 1174-1188.
83. Franklin, R.B., J. Zou, Z. Yu, and L.C. Costello, *EAAC1 is expressed in rat and human prostate epithelial cells; functions as a high-affinity L-aspartate transporter; and is regulated by prolactin and testosterone.* BMC Biochemistry, 2006. **7**(1): p. 10.
84. Cutruzzola, F., G. Giardina, M. Marani, A. Macone, A. Paiardini, S. Rinaldo, and A. Paone, *Glucose Metabolism in the Progression of Prostate Cancer.* Frontiers in Physiology, 2017. **8**.
85. Testa, C., C. Pultrone, D.N. Manners, R. Schiavina, and R. Lodi, *Metabolic imaging in Prostate Cancer: where we Are.* Frontiers in Oncology, 2016. **6**.
86. Liu, Q., C.T. Harvey, H. Geng, C.H. Xue, V. Chen, T.M. Beer, and D.Z. Qian, *Malate dehydrogenase 2 confers docetaxel resistance via regulations of JNK signaling and oxidative metabolism.* Prostate, 2013. **73**(10): p. 1028-1037.
87. Ferro, M., C. Buonerba, D. Terracciano, G. Lucarelli, V. Cosimato, D. Bottero, V.M. Deliu, P. Ditonno, S. Perdona, R. Autorino, I. Coman, S. De Placido, G. Di Lorenzo, and O. De Cobelli, *Biomarkers in localized prostate cancer.* Future Oncology, 2016. **12**(3): p. 399-411.
88. Heger, Z., J. Gumulec, N. Cernei, H. Polanska, M. Raudenska, M. Masarik, T. Eckschlager, M. Stiborova, V. Adam, and R. Kizek, *Relation of exposure to amino acids involved in sarcosine metabolic pathway on behavior of non-tumor and malignant prostatic cell lines.* Prostate, 2016. **76**(7): p. 679-690.
89. Lucarelli, G., P. Ditonno, C. Bettocchi, M. Spilotros, M. Rutigliano, A. Vavallo, V. Galleggiante, M. Fanelli, A.M.V. Larocca, C.A. Germinario, E. Maiorano, F.P. Selvaggi, and M. Battaglia, *Serum sarcosine is a risk factor for progression and survival in patients with metastatic castration-resistant prostate cancer.* Future Oncology, 2013. **9**(6): p. 899-907.
90. Heger, Z., M.A.M. Rodrigo, P. Michalek, H. Polanska, M. Masarik, V. Vit, M. Plevova, D. Pacik, T. Eckschlager, M. Stiborova, and V. Adam, *Sarcosine Up-Regulates Expression of Genes Involved in Cell Cycle Progression of Metastatic Models of Prostate Cancer.* Plos One, 2016. **11**(11).
91. Park, K., Z.M. Chen, T.Y. MacDonald, J. Siddiqui, H.H. Ye, A. Erbersdobler, M.M. Shevchuk, B.D. Robinson, M.G. Sanda, A.M. Chinnaiyan, H. Beltran, M.A. Rubin, and J.M. Mosquera, *Prostate cancer with Paneth cell-like neuroendocrine differentiation has recognizable histomorphology and harbors AURKA gene amplification.* Human Pathology, 2014. **45**(10): p. 2136-2143.

92. Meraldi, P., R. Honda, and E.A. Nigg, *Aurora-A overexpression reveals tetraploidization as a major route to centrosome amplification in p53-/- cells.* EMBO J, 2002. **21**(4): p. 483-92.
93. Au, K.M., A. Satterlee, Y.Z. Min, X. Tian, Y.S. Kim, J.M. Caster, L.Z. Zhang, T. Zhang, L. Huang, and A.Z. Wang, *Folate-targeted pH-responsive calcium zoledronate nanoscale metal-organic frameworks: Turning a bone antiresorptive agent into an anticancer therapeutic.* Biomaterials, 2016. **82**: p. 178-193.
94. Hattori, Y. and Y. Maitani, *Folate-linked nanoparticle-mediated suicide gene therapy in human prostate cancer and nasopharyngeal cancer with herpes simplex virus thymidine kinase.* Cancer Gene Therapy, 2005. **12**(10): p. 796-809.
95. Zhao, D.M., X.H. Zhao, Y.G. Zu, J.L. Li, Y. Zhang, R. Jiang, and Z.H. Zhang, *Preparation, characterization, and in vitro targeted delivery of folate-decorated paclitaxel-loaded bovine serum albumin nanoparticles.* International Journal of Nanomedicine, 2010. **5**: p. 669-677.
96. Pollock, S., R. Antrobus, L. Newton, B. Kampa, J. Rossa, S. Latham, N.B. Nichita, R.A. Dwek, and N. Zitzmann, *Uptake and trafficking of liposomes to the endoplasmic reticulum.* Faseb Journal, 2010. **24**(6): p. 1866-1878.
97. Tisman, G. and A. Garcia, *Control of prostate cancer associated with withdrawal of a supplement containing folic acid, L-methyltetrahydrofolate and vitamin B12: a case report.* J Med Case Rep, 2011. **5**: p. 413.
98. Kalyanaraman, B., *Teaching the basics of cancer metabolism: Developing antitumor strategies by exploiting the differences between normal and cancer cell metabolism.* Redox Biol, 2017. **12**: p. 833-842.
99. Owen, O.E., S.C. Kalhan, and R.W. Hanson, *The key role of anaplerosis and cataplerosis for citric acid cycle function.* J Biol Chem, 2002. **277**(34): p. 30409-12.
100. Marnett, L.J., *Lipid peroxidation-DNA damage by malondialdehyde.* Mutat Res, 1999. **424**(1-2): p. 83-95.
101. Birben, E., U.M. Sahiner, C. Sackesen, S. Erzurum, and O. Kalayci, *Oxidative Stress and Antioxidant Defense.* World Allergy Organ J, 2012. **5**(1): p. 9-19.
102. Conklin, K.A., *Chemotherapy-associated oxidative stress: impact on chemotherapeutic effectiveness.* Integr Cancer Ther, 2004. **3**(4): p. 294-300.
103. Shacter, E., J.A. Williams, R.M. Hinson, S. Senturker, and Y.J. Lee, *Oxidative stress interferes with cancer chemotherapy: inhibition of lymphoma cell apoptosis and phagocytosis.* Blood, 2000. **96**(1): p. 307-13.
104. Khandrika, L., B. Kumar, S. Koul, P. Maroni, and H.K. Koul, *Role of Oxidative Stress in Prostate Cancer.* Cancer Lett, 2009. **282**(2): p. 125-36.
105. Hayes, J.D. and D.J. Pulford, *The glutathione S-transferase supergene family: regulation of GST and the contribution of the isoenzymes to cancer chemoprotection and drug resistance.* Crit Rev Biochem Mol Biol, 1995. **30**(6): p. 445-600.
106. Zhu, M. and W.E. Fahl, *Functional characterization of transcription regulators that interact with the electrophile response element.* Biochem Biophys Res Commun, 2001. **289**(1): p. 212-9.
107. Frohlich, D.A., M.T. McCabe, R.S. Arnold, and M.L. Day, *The role of Nrf2 in increased reactive oxygen species and DNA damage in prostate tumorigenesis.* Oncogene, 2008. **27**(31): p. 4353-62.
108. Nelson, W.G., A.M. De Marzo, T.L. DeWeese, and W.B. Isaacs, *The role of inflammation in the pathogenesis of prostate cancer.* J Urol, 2004. **172**(5 Pt 2): p. S6-11; discussion S11-2.
109. Fiaschi, T. and P. Chiarugi, *Oxidative Stress, Tumor Microenvironment, and Metabolic Reprogramming: A Diabolic Liaison.* Int J Cell Biol, 2012. **2012**.

110. Arcucci, A., M.R. Ruocco, G. Granato, A.M. Sacco, and S. Montagnani, *Cancer: An Oxidative Crosstalk between Solid Tumor Cells and Cancer Associated Fibroblasts.* Biomed Res Int, 2016. **2016**: p. 4502846.
111. Toullec, A., D. Gerald, G. Despouy, B. Bourachot, M. Cardon, S. Lefort, M. Richardson, G. Rigaill, M.C. Parrini, C. Lucchesi, D. Bellanger, M.H. Stern, T. Dubois, X. Sastre-Garau, O. Delattre, A. Vincent-Salomon, and F. Mechta-Grigoriou, *Oxidative stress promotes myofibroblast differentiation and tumour spreading.* EMBO Mol Med, 2010. **2**(6): p. 211-30.
112. Prakash, A., K. Bharti, and A.B. Majeed, *Zinc: indications in brain disorders.* Fundamental & Clinical Pharmacology, 2015. **29**(2): p. 131-49.
113. Kondoh, M., K. Kamada, M. Kuronaga, M. Higashimoto, M. Takiguchi, Y. Watanabe, and M. Sato, *Antioxidant property of metallothionein in fasted mice.* Toxicology Letters, 2003. **143**(3): p. 301-306.
114. Gonzalez, V.M., M.A. Fuertes, C. Alonso, and J.M. Perez, *Is cisplatin-induced cell death always produced by apoptosis?* Mol. Pharmacol., 2001. **59**(4): p. 657-663.
115. Balvan, J., J. Gumulec, M. Raudenska, A. Krizova, P. Stepka, P. Babula, R. Kizek, V. Adam, and M. Masarik, *Oxidative Stress Resistance in Metastatic Prostate Cancer: Renewal by Self-Eating.* Plos One, 2015. **10**(12).
116. Erenpreisa, J. and M.S. Cragg, *Three steps to the immortality of cancer cells: senescence, polyploidy and self-renewal.* Cancer Cell International, 2013. **13**(1): p. 92.
117. Cernei, N., O. Zitka, S. Skalickova, J. Gumulec, M. Sztalmachova, M.A.M. Rodrigo, J. Sochor, M. Masarik, V. Adam, J. Hubalek, L. Trnkova, J. Kruseova, T. Eckschlager, and R. Kizek, *Effect of sarcosine on antioxidant parameters and metallothionein content in the PC-3 prostate cancer cell line.* Oncology Reports, 2013. **29**(6): p. 2459-2466.
118. Takahashi, S., S. Suzuki, S. Inaguma, M. Asamoto, and T. Shirai, *Differences between latent and clinical prostate carcinomas: Lower cell proliferation activity in latent cases.* Prostate, 2006. **66**(2): p. 211-217.
119. Lein, M., I. Stibane, R. Mansour, C. Hege, J. Roigas, A. Wille, K. Jung, G. Kristiansen, D. Schnorr, S.A. Loening, and S. Deger, *Complications, urinary continence, and oncologic outcome of 1000 laparoscopic transperitoneal radical prostatectomies - Experience at the Charite Hospital Berlin, Campus Mitte.* European Urology, 2006. **50**(6): p. 1278-1284.
120. Kido, M., M. Hitosugi, K. Ishii, S. Kamimura, and K. Joh, *Latent Prostate Cancer in Japanese Men Who Die Unnatural Deaths: A Forensic Autopsy Study.* Prostate, 2015. **75**(9): p. 917-922.
121. Mundy, G.R., *Metastasis to bone: Causes, consequences and therapeutic opportunities.* Nature Reviews Cancer, 2002. **2**(8): p. 584-593.
122. Labrie, F., A. Dupont, R. Suburu, L. Cusan, M. Tremblay, J.L. Gomez, and J. Emond, *Serum prostate specific antigen as pre-screening test for prostate cancer.* J Urol, 1992. **147**(3 Pt 2): p. 846-51; discussion 851-2.
123. Lilja, H., A. Christensson, U. Dahlen, M.T. Matikainen, O. Nilsson, K. Pettersson, and T. Lovgren, *Prostate-specific antigen in serum occurs predominantly in complex with alpha-1-antichymotrypsin.* Clinical Chemistry, 1991. **37**(9): p. 1618-1625.
124. Lilja, H., D. Ulmert, and A.J. Vickers, *Prostate-specific antigen and prostate cancer: prediction, detection and monitoring.* Nature Reviews Cancer, 2008. **8**(4): p. 268-278.
125. Stenman, U.H., J. Leinonen, H. Alfthan, S. Rannikko, K. Tuhkanen, and O. Alfthan, *A complex between prostate-specific antigen and alpha-1-antichymotrypsin is the major form of prostate-specific antigen in serum of patients with prostatic-cancer - assay of the complex improves clinical sensitivity for cancer.* Cancer Research, 1991. **51**(1): p. 222-226.

126. Abrahamsson, P.A., H. Lilja, and J.E. Oesterling, *Molecular forms of serum prostate-specific antigen - The clinical value of percent free prostate-specific antigen.* Urologic Clinics of North America, 1997. **24**(2): p. 353-+.
127. Partin, A.W., W.J. Catalona, P.C. Southwick, E.N.P. Subong, G.H. Gasior, and D.W. Chan, *Analysis of percent free prostate-specific antigen (PSA) for prostate cancer detection: Influence of total PSA, prostate volume, and age.* Urology, 1996. **48**(6A): p. 55-61.
128. Haese, A., M. Graefen, J. Noldus, P. Hammerer, E. Huland, and H. Huland, *Prostatic volume and ratio of free-to-total prostate specific antigen in patients with prostatic cancer or benign prostatic hyperplasia.* Journal of Urology, 1997. **158**(6): p. 2188-2192.
129. Stephan, C., M. Lein, K. Jung, D. Schnorr, and S.A. Loening, *The influence of prostate volume on the ratio of free to total prostate specific antigen in serum of patients with prostate carcinoma and benign prostate hyperplasia.* Cancer, 1997. **79**(1): p. 104-109.
130. Benson, M.C., I.S. Whang, A. Pantuck, K. Ring, S.A. Kaplan, C.A. Olsson, and W.H. Cooner, *Prostate specific antigen density: a means of distinguishing benign prostatic hypertrophy and prostate cancer.* J Urol, 1992. **147**(3 Pt 2): p. 815-6.
131. Stephan, C., G. Stroebel, M. Heinau, A. Lenz, A. Roemer, M. Lein, D. Schnorr, S.A. Loening, and K. Jung, *The ratio of prostate-specific antigen (PSA) to prostate volume (PSA density) as a parameter to improve the detection of prostate carcinoma in PSA values in the range of < 4 ng/mL.* Cancer, 2005. **104**(5): p. 993-1003.
132. Carter, H.B., J.D. Pearson, Z. Waclawiw, E.J. Metter, D.W. Chan, H.A. Guess, and P.C. Walsh, *Prostate-specific antigen variability in men without prostate cancer: effect of sampling interval on prostate-specific antigen velocity.* Urology, 1995. **45**(4): p. 591-6.
133. Mohler, J., R.R. Bahnson, B. Boston, J.E. Busby, A. D'Amico, J.A. Eastham, C.A. Enke, D. George, E.M. Horwitz, R.P. Huben, P. Kantoff, M. Kawachi, M. Kuettel, P.H. Lange, G. Macvicar, E.R. Plimack, J.M. Pow-Sang, M. Roach, 3rd, E. Rohren, B.J. Roth, D.C. Shrieve, M.R. Smith, S. Srinivas, P. Twardowski, and P.C. Walsh, *NCCN clinical practice guidelines in oncology: prostate cancer.* J Natl Compr Canc Netw, 2010. **8**(2): p. 162-200.
134. Ross, A.E., S. Loeb, P. Landis, A.W. Partin, J.I. Epstein, A. Kettermann, Z. Feng, H.B. Carter, and P.C. Walsh, *Prostate-specific antigen kinetics during follow-up are an unreliable trigger for intervention in a prostate cancer surveillance program.* J Clin Oncol, 2010. **28**(17): p. 2810-6.
135. Vickers, A.J., T. Wolters, C.J. Savage, A.M. Cronin, M.F. O'Brien, K. Pettersson, M.J. Roobol, G. Aus, P.T. Scardino, J. Hugosson, F.H. Schroder, and H. Lilja, *Prostate-specific antigen velocity for early detection of prostate cancer: result from a large, representative, population-based cohort.* Eur Urol, 2009. **56**(5): p. 753-60.
136. Wolters, T., M.J. Roobol, C.H. Bangma, and F.H. Schroder, *Is prostate-specific antigen velocity selective for clinically significant prostate cancer in screening? European Randomized Study of Screening for Prostate Cancer (Rotterdam).* Eur Urol, 2009. **55**(2): p. 385-92.
137. Gaudreau, P.O., J. Stagg, D. Soulières, and F. Saad, *The Present and Future of Biomarkers in Prostate Cancer: Proteomics, Genomics, and Immunology Advancements.* Biomark Cancer, 2016. **8**(Suppl 2): p. 15-33.
138. Sharma, P., K. Zargar-Shoshtari, and J.M. Pow-Sang, *Biomarkers for prostate cancer: present challenges and future opportunities.* Future Science Oa, 2016. **2**(1).
139. Luo, J., S. Zha, W.R. Gage, T.A. Dunn, J.L. Hicks, C.J. Bennett, C.N. Ewing, E.A. Platz, S. Ferdinandusse, R.J. Wanders, J.M. Trent, W.B. Isaacs, and A.M. De Marzo, *alpha-Methylacyl-CoA racemase: A new molecular marker for prostate cancer.* Cancer Research, 2002. **62**(8): p. 2220-2226.

140. Rubin, M.A., M. Zhou, S.M. Dhanasekaran, S. Varambally, T.R. Barrette, M.G. Sanda, K.J. Pienta, D. Ghosh, and A.M. Chinnaiyan, *alpha-methylacyl coenzyme A racemase as a tissue biomarker for prostate cancer.* Jama-Journal of the American Medical Association, 2002. **287**(13): p. 1662-1670.
141. Jiang, N., S. Zhu, J. Chen, Y. Niu, and L. Zhou, *A-methylacyl-CoA racemase (AMACR) and prostate-cancer risk: a meta-analysis of 4,385 participants.* Plos One, 2013. **8**(10): p. e74386.
142. Zha, S., S. Ferdinandusse, S. Denis, R.J. Wanders, C.M. Ewing, J. Luo, A.M. De Marzo, and W.B. Isaacs, *alpha-Methylacyl-CoA racemase as an androgen-independent growth modifier in prostate cancer.* Cancer Research, 2003. **63**(21): p. 7365-7376.
143. Williams, T.M. and M.P. Lisanti, *Caveolin-1 in oncogenic transformation, cancer, and metastasis.* American Journal of Physiology-Cell Physiology, 2005. **288**(3): p. C494-C506.
144. Yang, G., L.D. Truong, T.L. Timme, C.Z. Ren, T.M. Wheeler, S.H. Park, Y. Nasu, C.H. Bangma, M.W. Kattan, P.T. Scardino, and T.C. Thompson, *Elevated expression of caveolin is associated with prostate and breast cancer.* Clinical Cancer Research, 1998. **4**(8): p. 1873-1880.
145. Thompson, T., S. Tahir, L. Li, M. Watanabe, K. Naruishi, G. Yang, D. Kadmon, C. Logothetis, P. Troncoso, C. Ren, A. Goltsov, and S. Park, *The role of caveolin-1 in prostate cancer: clinical implications.* Prostate Cancer Prostatic Dis, 2010. **13**(1): p. 6-11.
146. Gumulec, J., M. Masarik, S. Krizkova, M. Hlavna, P. Babula, R. Hrabec, A. Rovny, M. Masarikova, J. Sochor, V. Adam, T. Eckschlager, and R. Kizek, *Evaluation of alpha-methylacyl-CoA racemase, metallothionein and prostate specific antigen as prostate cancer prognostic markers.* Neoplasma, 2012. **59**(2): p. 191-200.
147. Gumulec, J., J. Sochor, M. Hlavna, M. Sztalmachova, S. Krizkova, P. Babula, R. Hrabec, A. Rovny, V. Adam, T. Eckschlager, R. Kizek, and M. Masarik, *Caveolin-1 as a potential high-risk prostate cancer biomarker.* Oncology Reports, 2012. **27**(3): p. 831-841.
148. Kizek, R., L. Trnkova, and E. Palecek, *Determination of metallothionein at the femtomole level by constant current stripping chronopotentiometry.* Anal. Chem., 2001. **73**(20): p. 4801-4807.
149. Kizek, R., J. Vacek, V. Adam, and B. Vojtesek, *Metallothionein - Cisplatine and anticancer therapy.* Klin. Biochem. Metab., 2004. **12**(2): p. 72-78.
150. Palecek, E., *Oscillographic polarography of highly polymerized deoxyribonucleic acid.* Nature, 1960. **188**: p. 656-657.
151. Palecek, E., *Electroactivity of proteins and its possibilities in biomedicine and protemics.*, in *Electrochemistry of nucleic acids and proteins. Towards electrochemical sensors for genomics and proteomics.*, E. Palecek, F. Scheller, and J. Wang, Editors. 2005, Elsevier: Amsterdam. p. 690-750.
152. Palecek, E. and M. Fojta, *Detecting DNA Hybridization and Damage.* Anal. Chem., 2001. **73**: p. 74A-83A.
153. Palecek, E., M. Fojta, F. Jelen, and V. Vetterl, *Electrochemical analysis of nucleic acids*, in *The encyclopedia of electrochemistry*, A.J. Bard and M. Stratsmann, Editors. 2002, Wiley-VCH. p. 365-429.
154. Palecek, E. and I. Postbieglová, *Adsorptive stripping voltammetry of bimacromolecules with transfer of the adsorbed layer.* J. Electroanal. Chem., 1986. **214**: p. 359-371.
155. Petrlova, J., O. Blastik, O. Zitka, V. Adam, D. Potesil, R. Mikelova, R. Prusa, M. Stiborova, L. Trnkova, J. Zehnalek, and R. Kizek, *An electrochemical study of*

metallothionein as a potential tumour disease marker. Annals the Polisch Chemical Society, 2005. **in press**.

156. Petrlova, J., D. Potesil, R. Mikelova, O. Blastik, V. Adam, L. Trnkova, F. Jelen, R. Prusa, J. Kukacka, and R. Kizek, *Attomole voltammetric determination of metallothionein.* Electrochim. Acta, 2006. **in press**.
157. Fojtu, M., J. Gumulec, J. Balvan, M. Raudenska, M. Sztalmachova, H. Polanska, K. Smerkova, V. Adam, R. Kizek, and M. Masarik, *Utilization of paramagnetic microparticles for automated isolation of free circulating mRNA as a new tool in prostate cancer diagnostics.* Electrophoresis, 2014. **35**(2-3): p. 306-315.
158. Masarik, M., J. Gumulec, M. Sztalmachova, M. Hlavna, P. Babula, S. Krizkova, M. Ryvolova, M. Jurajda, J. Sochor, V. Adam, and R. Kizek, *Isolation of metallothionein from cells derived from aggressive form of high-grade prostate carcinoma using paramagnetic antibody-modified microbeads off-line coupled with electrochemical and electrophoretic analysis.* Electrophoresis, 2011. **32**(24): p. 3576-3588.
159. Jiang, Y.Q., X.L. Cheng, C.A. Wang, and Y.F. Ma, *Quantitative Determination of Sarcosine and Related Compounds in Urinary Samples by Liquid Chromatography with Tandem Mass Spectrometry.* Analytical Chemistry, 2010. **82**(21): p. 9022-9027.
160. Chen, J., J. Zhang, W.P. Zhang, and Z.L. Chen, *Sensitive determination of the potential biomarker sarcosine for prostate cancer by LC-MS with N,N '-dicyclohexylcarbodiimide derivatization.* Journal of Separation Science, 2014. **37**(1-2): p. 14-19.